physics and chemistry of fission

NDS LIBRARY COPY

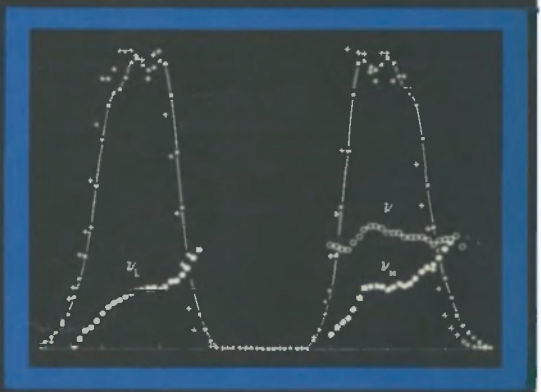

PROCEEDINGS
OF A SYMPOSIUM,
SALZBURG,
22-26 MARCH 1965

vol. II

NDS Library Copy

INTERNATIONAL ATOMIC ENERGY AGENCY, VIENNA, 1965

PHYSICS AND CHEMISTRY OF FISSION

VOL. II

The following States are Members of the International Atomic Energy Agency:

AFGHANISTAN
ALBANIA
ALGERIA
ARGENTINA
AUSTRALIA
AUSTRIA
BELGIUM
BOLIVIA
BRAZIL
BULGARIA
BURMA
BYELORUSSIAN SOVIET SOCIALIST REPUBLIC
CAMBODIA
CAMEROON
CANADA
CEYLON
CHILE
CHINA
COLOMBIA
CONGO, DEMOCRATIC REPUBLIC OF
COSTA RICA
CUBA
CYPRUS
CZECHOSLOVAK SOCIALIST REPUBLIC
DENMARK
DOMINICAN REPUBLIC
ECUADOR
EL SALVADOR
ETHIOPIA
FINLAND
FRANCE
FEDERAL REPUBLIC OF GERMANY
GABON
GHANA
GREECE
GUATEMALA
HAITI
HOLY SEE
HONDURAS
HUNGARY
ICELAND
INDIA
INDONESIA
IRAN
IRAQ
ISRAEL
ITALY
IVORY COAST
JAPAN
REPUBLIC OF KOREA
KUWAIT
LEBANON
LIBERIA
LIBYA
LUXEMBOURG
MADAGASCAR
MALI
MEXICO
MONACO
MOROCCO
NETHERLANDS
NEW ZEALAND
NICARAGUA
NIGERIA
NORWAY
PAKISTAN
PARAGUAY
PERU
PHILIPPINES
POLAND
PORTUGAL
ROMANIA
SAUDI ARABIA
SENEGAL
SOUTH AFRICA
SPAIN
SUDAN
SWEDEN
SWITZERLAND
SYRIA
THAILAND
TUNISIA
TURKEY
UKRAINIAN SOVIET SOCIALIST REPUBLIC
UNION OF SOVIET SOCIALIST REPUBLICS
UNITED ARAB REPUBLIC
UNITED KINGDOM OF GREAT BRITAIN AND NORTHERN IRELAND
UNITED STATES OF AMERICA
URUGUAY
VENEZUELA
VIET-NAM
YUGOSLAVIA

The Agency's Statute was approved on 23 October 1956 by the Conference on the Statute of the IAEA held at United Nations Headquarters, New York; it entered into force on 29 July 1957. The Headquarters of the Agency are situated in Vienna. Its principal objective is "to accelerate and enlarge the contribution of atomic energy to peace, health and prosperity throughout the world".

Printed by the IAEA in Austria
July 1965

PROCEEDINGS SERIES

PHYSICS AND CHEMISTRY OF FISSION

PROCEEDINGS OF THE SYMPOSIUM ON
PHYSICS AND CHEMISTRY OF FISSION
HELD BY THE
INTERNATIONAL ATOMIC ENERGY AGENCY
IN SALZBURG, 22 - 26 MARCH 1965

In two volumes

VOL.II

INTERNATIONAL ATOMIC ENERGY AGENCY
VIENNA, 1965

Symposium on Physics and Chemistry of Fission,
Salzburg, 22 - 26 March 1965.
Proceedings . . . held by the International Atomic
Energy Agency . . . Vienna, the Agency, 1965.
2 vols. (IAEA Proceedings series)

539.173
541.28

PHYSICS AND CHEMISTRY OF FISSION
IAEA, VIENNA, 1965
STI/PUB/101

FOREWORD

In recognition of recent significant developments in nuclear fission, the International Atomic Energy Agency convened this first International Symposium on the Physics and Chemistry of Fission at Salzburg, Austria, from 22 to 26 March, 1965. Nearly 200 delegates from 29 countries and 5 international organizations participated in the Symposium in which all aspects of the fission process and its products were considered.

Each of the nine technical sessions of the Symposium was opened with a survey paper intended to provide an up-to-date picture of the current status of the session topic. Contributed original papers were then presented during the remainder of each session. The first two sessions were concerned with dynamics in the neighbourhood of the saddle point and the descent from saddle point to scission point, and the interpretation of angular distribution and fission cross-section data. The remaining seven sessions were concerned largely with experimental studies of post-scission phenomena. These sessions were marked by reports of truly impressive advances in new experimental techniques such as solid-state detectors in conjunction with ultra-fast time-of-flight and coincidence methods, on-line mass separators, detailed studies of nuclear gamma rays, X-rays and conversion electrons, and the increasing use of big computers for ever more elaborate (and, it is to be hoped, more accurate) data processing and analysis.

It was clear at the Salzburg Symposium that the long-standing gap between empirical knowledge and theoretical understanding of fission is still widening. The fission theorists nevertheless have welcomed this flood of new information as additional material for a systematic approach that must ultimately lead to fuller theoretical understanding of the process of nuclear fission.

EDITORIAL NOTE

The papers and discussions incorporated in the proceedings published by the International Atomic Energy Agency are edited by the Agency's editorial staff to the extent considered necessary for the reader's assistance. The views expressed and the general style adopted remain, however, the responsibility of the named authors or participants.

For the sake of speed of publication the present Proceedings have been printed by composition typing and photo-offset lithography. Within the limitations imposed by this method, every effort has been made to maintain a high editorial standard; in particular, the units and symbols employed are to the fullest practicable extent those standardized or recommended by the competent international scientific bodies.

The affiliations of authors are those given at the time of nomination.

The use in these Proceedings of particular designations of countries or territories does not imply any judgement by the Agency as to the legal status of such countries or territories, of their authorities and institutions or of the delimitation of their boundaries.

The mention of specific companies or of their products or brand-names does not imply any endorsement or recommendation on the part of the International Atomic Energy Agency.

CONTENTS OF VOL. II

PROMPT NEUTRONS FROM FISSION (Session VI)

Prompt neutrons from fission (SM-60/43) (Review Paper) 3
J. Terrell (United States of America)
Discussion 23
Boron-pile $\bar{\nu}$ measurements (SM-60/44) 25
D. W. Colvin and M. G. Sowerby (United Kingdom)
Discussion 37
The energies, angular distribution and yields of the prompt neutrons from individual fragments in the thermal-neutron fission of U^{233} and U^{235} (SM-60/45) 39
J. C. D. Milton and J. S. Fraser (Canada)
Discussion 53
$\bar{\nu}$ in neutron-induced fission of U^{235} and Th^{232}, and in photofission of U^{238} (SM-60/46) 57
H. Condé and M. Holmberg (Sweden)
Prompt-neutron emission from U^{235} fission fragments (SM-60/47) 67
T. Cornell, E. E. Maslin and A. L. Rodgers (United Kingdom)
The energy balance in fission and Monte Carlo calculations on prompt-neutron emission (SM-60/48) 73
G. E. Gordon and N. K. Aras (United States of America)
Discussion 91
Fission-neutron spectra of U^{235}, Pu^{239} and Cf^{252} (SM-60/49) 93
H. Condé and G. During (Sweden)
Discussion 102
A liquid scintillator experiment for measuring $\bar{\nu}$ for Pu^{241} (SM-60/77) 103
J. W. Boldeman (Australia)
General discussion 109

PROMPT AND DELAYED GAMMA-RAYS, DELAYED NEUTRONS, BETA-ACTIVITY (Sessions VII and VIII)

Prompt and delayed gamma-rays from fission (SM-60/52) (Review Paper) 113
H. Maier-Leibnitz, P. Armbruster and H. J. Specht (Federal Republic of Germany)
The prompt gamma-ray, prompt electron and prompt X-ray spectra associated with fission fragments of specific mass (SM-60/53) 125
H. R. Bowman, S. G. Thompson, R. L. Watson, S. S. Kapoor and J. O. Rasmussen (United States of America)

Average number and energy of gamma-rays emitted as a function of fragment mass in U^{235} thermal-neutron-induced fission (SM-60/54) 143
H. Maier-Leibnitz, H. W. Schmitt and P. Armbruster (United States of America)
The angular distribution of gamma-rays from the fission of U^{235} (SM-60/55) 163
G. Graff, A. Lajtai and L. Nagy (Hungary)
Discussion 169
Delayed neutrons and photoneutrons from fission products (SM-60/58) (Review Paper) 171
S. Amiel (Israel)
Comparison of observed delayed-neutron abundances with calculated fission yields of neutron precursors (SM-60/59) 197
G. Hermann, J. Fiedler, G. Benedict, W. Eckhardt, G. Luthardt, P. Patzelt and H. D. Schüssler (Federal Republic of Germany)
Измерение относительных выходов запаздывающих нейтронов (SM-60/84 215
Б.П. Максютенко (СССР)
Discussion 221
Search for delayed-neutron precursors in antimony and arsenic fission products (SM-60/74) 225
P. del Marmol, M. Nève de Mevergnies and A. Speecke (Belgium)
Short-lived antimony and arsenic isotopes formed in fission (SM-60/62) 233
L. Tomlinson (United Kingdom)
Discussion 241
Indirect determination of half-lives of short-lived fission gases using a gas flow method (SM-60/60) 243
P. Patzelt and G. Herrmann (Federal Republic of Germany)
Recent experiments on the beta activity of fission products from the thermal-neutron fission of U^{233}, U^{235} and Pu^{239} (SM-60/61) 253
H. J. Specht and H. Seyfarth (Federal Republic of Germany)
Discussion 261

FISSION AT INTERMEDIATE AND HIGH EXCITATION ENERGIES
(Session VIII)

Fission of heavy elements by high-energy protons (SM-60/63) (Review Paper) 265
G. Friedlander (United States of America)
О делении ядер при средних и высоких энергиях возбуждения (SM-60/97) 283
Н.А. Перфилов (СССР)

Mesures de sections efficaces absolues de fission induite par des protons de 156 MeV, utilisant le mica comme détecteur de fragments de fission (SM-60/64) 307
M. Maurette et C. Stephan (France)
Discussion 315
Fission yields in the iodine region (SM-60/65) 323
G. Rudstam (CERN)
Ranges of iodine and bromine isotopes produced in the interaction of high-energy protons with uranium (SM-60/67) 329
R. Brandt (CERN)
Angular distributions of U^{238} fission fragments produced by mono-energetic gamma rays (SM-60/78) 343
H. G. de Carvalho, A. G. de Silva, R. N. Alves, R. Bösch and W. Wölfli (Brazil)
Сечения деления Ta^{181}, Re, Pt, Au^{197}, Pb, Bi^{209}, Th^{232}, U^{235} и U^{238} протонами с энергией 150–660 Мэв (SM-60/83) 349
В. А. Коньшин, Е. С. Матусевич и В. И. Регушевский (СССР)

LIGHT PARTICLES EMITTED IN FISSION: TERNARY FISSION (Session IX)

Variation of fission-fragment kinetic energy distribution, mass distribution, and yield of long-range alpha particles in the resonance-neutron-induced fission of U^{235} and Pu^{239} (SM-60/68) 355
E. Melkonian and G. K. Mehta (United States of America)
Alpha particle emission in fission (SM-60/69) 369
I. Halpern (United States of America)
The emission of long-range alpha particles in fission (SM-60/70) 387
N. Feather (United Kingdom)
Long-range alpha particle emission in the fission of U^{235} by 3-MeV neutrons (SM-60/71) 397
V. A. Hattangadi, T. Methasiri, D. M. Nadkarni, R. Ramanna and P. N. Rama Rao (India)
Discussion 407
Ternary fission (SM-60/73) 409
M. L. Muga (United States of America)
Discussion 428
Variation of the binary-to-ternary fission ratio for U^{235} in the thermal-neutron-energy region (SM-60/75) 429
A. J. Deruytter and M. Nève de Mevergnies (Belgium)
Тройное деление урана-235 на резонансных нейтронах (SM-60/87) 439
И. Квитек, Ю. П. Попов и Ю. В. Рябов (СССР)
Discussion 446
Summary Talk 447
J. J. Griffin

List of Chairmen of Sessions and Secretariat of Symposium 453
List of Participants 454
Author Index 467

PROMPT NEUTRONS FROM FISSION

(Session VI)

Review Paper

PROMPT NEUTRONS FROM FISSION*

J. TERRELL
LOS ALAMOS SCIENTIFIC LABORATORY,
UNIVERSITY OF CALIFORNIA,
LOS ALAMOS, N. MEX., UNITED STATES OF AMERICA

Abstract — Résumé — Аннотация — Resumen

PROMPT NEUTRONS FROM FISSION. A survey is given of the present state of knowledge of the spectrum, angular distribution and number of prompt fission neutrons, as functions of incident neutron energy and individual fragment mass, for low-energy fission.

The energy spectrum of prompt neutrons has been found to be of the same form (nearly Maxwellian) for many different types of fission. It has been shown that this type of spectrum is to be expected on the basis of evaporation from moving fragments, and theoretical predictions of the spectrum agree very accurately with experimental data. Some data are now available on the variation of the neutron spectrum with fragment mass and angle of emission.

Only recently has it become possible to take accurate data on the angular distribution of the neutrons. It appears that the neutrons have the angular distribution to be expected if emitted almost isotropically from the moving fragments, with a possibility that some small fraction are not emitted in this way, but directly from the fissioning nuclide.

Much work has been done on the variation of fission neutron number $\bar{\nu}$ with incident neutron energy for neutron-induced fission. The neutron number increases roughly linearly with energy, with a slope of about 0.15 n/MeV. There is now evidence that this slope changes somewhat with energy. This change must be associated with other changes in the fission process.

The most interesting recent discovery concerning fission neutrons is the strong dependence of neutron number on individual fragment mass. The data are being rapidly improved by means of the newer techniques of determining fragment mass yields from velocity and pulse-height data, and of determining neutron yields from cumulative mass yields. There is evidence of similar dependence of neutron yield on fragment mass in a number of cases. It has been suggested that this property is directly connected with the deformability of the fragments, and in particular with the near-spherical shapes of magic-number fragments. On the basis of a simple fragment-deformation theory, the deformation parameter is calculated directly from experimental data, and is seen to have a very similar dependence on mass for four types of fission. These ideas seem likely to lead to a more basic understanding of the fission process, including the mass yields and energies of the fragments.

NEUTRONS INSTANTANÉS PROVENANT DE LA FISSION. L'auteur passe en revue l'état actuel des connaissances concernant le spectre, la distribution angulaire et le nombre des neutrons instantanés, en fonction de l'énergie des neutrons incidents et de la masse des divers fragments, pour la fission à basse énergie.

Il a été constaté que, pour beaucoup de types de fission différents, le spectre énergétique des neutrons instantanés a la même forme, à peu près maxwellienne, et prouvé que l'on peut s'attendre à ce genre de spectre d'après l'évaporation émanant de fragments en mouvement: les résultats des études théoriques sur *le spectre sont en bon accord avec les données de l'expérience. On dispose maintenant de données sur la variation* du spectre des neutrons selon la masse du fragment et l'angle d'émission.

C'est seulement assez récemment qu'il a été possible d'obtenir des données précises sur la distribution angulaire des neutrons. Il semble que les neutrons ont bien la distribution angulaire à laquelle on peut s'attendre s'ils sont émis de façon à peu près isotrope par des fragments en mouvement, et il se peut qu'une petite fraction ne soit pas émise de cette manière, mais directement par le nucléide qui subit la fission.

On a beaucoup étudié la variation du nombre des neutrons de fission $\bar{\nu}$ selon l'énergie des neutrons incidents dans la fission par neutrons. L'augmentation du nombre de neutrons selon l'énergie est à peu près linéaire, la pente de la droite étant de l'ordre de 0,15 neutron/MeV. Il est à présent démontré que cette pente varie

* Work performed under the auspices of the United States Atomic Energy Commission.

légèrement en fonction de l'énergie. Cette variation doit être associée à d'autres variations qui se produisent dans le processus de fission.

Parmi les récentes découvertes touchant les neutrons de fission, la plus intéressante est le fait que le nombre de neutrons dépend étroitement de la masse des divers fragments. On améliore les données assez rapidement au moyen des techniques modernes qui permettent de déterminer les rendements en fragments selon la masse à partir des données relatives à la vitesse et à l'amplitude d'impulsion, et les rendements en neutrons à partir des rendements cumulatifs selon la masse. Des indications montrent que, dans certains cas, le rendement en neutrons dépend d'une façon analogue de la masse des fragments. Il a été suggéré que cette propriété est directement liée à la déformabilité des fragments, plus particulièrement à la forme à peu près sphérique des fragments ayant un nombre magique.

Sur la base d'une théorie simple fragment-déformation, l'auteur calcule le paramètre de déformation directement à partir des données expérimentales; on s'aperçoit que ses variations selon la masse sont très analogues pour quatre types de fission. Il semble que ces idées permettront de mieux comprendre les bases du processus de fission, y compris les rendements selon la masse et les énergies des fragments.

МГНОВЕННЫЕ НЕЙТРОНЫ ДЕЛЕНИЯ. Дается обзор имеющихся в настоящее время данных о распределении спектров, угловом распределении и числе мгновенных нейтронов деления как функций энергии бомбардирующих нейтронов и масс отдельных осколков для делений, вызванных частицами низких энергий.

Установлено, что энергетический спектр мгновенных нейтронов имеет одинаковую форму (почти Максвелловскую) для многих различных видов деления. Показано, что эту форму спектра следовало ожидать, исходя из эмиссии нейтронов из движущихся осколков; теоретические расчеты этого спектра очень точно согласуются с экспериментальными данными. В настоящее время имеются некоторые данные вариации нейтронного спектра в зависимости от масс осколков и угла эмиссии.

Лишь в последнее время оказалось возможным получить точные данные об угловом распределении нейтронов. Представляется, что нейтроны имеют такое угловое распределение, которого следует ожидать в том случае, если они испускаются почти изотропически из движущихся осколков, при этом существует возможность того, что некоторая небольшая часть испускается не таким путем, а непосредственно из делящегося ядра.

Проделана большая работа по изучению вариации числа нейтронов деления $\bar{\nu}$ при изменении энергии бомбардирующих нейтронов в случае деления, вызванного нейтронами. Число нейтронов увеличивается примерно линейно с увеличением энергии со склоном порядка 0,15 нейтрона на 1 Мэв. В настоящее время имеются доказательства того, что этот склон несколько меняется с изменением энергии. Это изменение должно быть связано с другими изменениями в процессе деления.

Наиболее интересным *открытием последнего времени, касающимся нейтронов деления*, является зависимость числа нейтронов от масс отдельных осколков. Эти данные в настоящее время очень заметно улучшаются благодаря применению новых методов определения выхода масс осколков по данным о скорости и амплитуде импульсов и благодаря определению выходов нейтронов по совокупным выходам масс. В ряде случаев имеются доказательства аналогичной зависимости выхода нейтронов от масс осколков. Было высказано предположение, что это свойство непосредственно связано с деформируемостью осколков и, в частности, с почти *сферическими формами осколков*, соответствующих ядрам с магическими числами. На основе теории деформации простого осколка вычисляется параметр деформации непосредственно из экспериментальных данных, и видно, что он имеет ту же самую зависимость от массы для четырех типов деления. Представляется вероятным, что эти предположения могут привести к более фундаментальному пониманию процесса деления, включая выходы масс и энергии осколков.

NEUTRONES INMEDIATOS DE FISION. El autor expone los conocimientos actuales sobre el espectro, la distribución angular y el número de neutrones inmediatos de fisión, considerados en función de la energía de los neutrones incidentes y de la masa de cada fragmento, en el caso de la fisión de baja energía.

Se ha comprobado que el espectro energético de los neutrones inmediatos presenta una forma cuasi maxwelliana, para muchos tipos de fisiones diferentes. Se ha demostrado que cabe esperar un espectro de este tipo basándose en la evaporación neutrónica por los fragmentos en movimiento; las previsiones teóricas de dicho espectro concuerdan muy satisfactoriamente con los datos experimentales. En la actualidad se dispone de algunos datos sobre la variación del espectro neutrónico con la masa y el ángulo de emisión de los fragmentos.

Sólo en fecha reciente se han podido obtener datos precisos sobre la distribución angular de los neutrones. Al parecer, tal distribución es plausible cuando los neutrones son emitidos cuasi isotrópicamente por los fragmentos en movimiento, existiendo la posibilidad de que una pequeña fracción no sea emitida de esta forma, sino directamente por el núclido durante la fisión.

Se han realizado considerables trabajos sobre la variación del número de neutrons de fisión $\bar{\nu}$ en función de la energía de los neutrones incidentes, en el caso de la fisión inducida por éstos. El número de neutrones aumenta de modo prácticamente proporcional a la energía, siendo la pendiente de la recta del orden de 0,15 neutrón/MeV. Existen pruebas de que esta pendiente varía ligeramente con la energía; esta variación debe ir asociada a otras modificaciones del proceso de fisión.

El descubrimiento reciente de mayor interés acerca de los neutrones de fisión es la estrecha relación de dependencia existente entre el número de neutrones y la masa de cada fragmento. La precisión de los datos aumenta en forma rápida gracias a la aplicación de nuevas técnicas de determinación del rendimiento másico de los fragmentos, basándose en datos relativos a la velocidad y la amplitud de impulsos, y de determinación del rendimiento neutrónico partiendo del rendimiento másico acumulado. En buen número de casos existen pruebas de una análoga relación de dependencia entre el rendimiento neutrónico y la masa de los fragmentos: se ha sugerido que esta propiedad está directamente vinculada a la capacidad de deformación de los fragmentos, y en particular la forma cuasi esférica de los fragmentos de número mágico. Si se aplica una teoría de la deformación simple de los fragmentos, el parámetro de deformación puede calcularse directamente a partir de los datos experimentales y se observa que su variación en función de la masa es análoga en cuatro tipos de fisión. Estos conceptos contribuirán sin duda a perfeccionar nuestro conocimiento del proceso de fisión, y, en particular, del rendimiento másico y de la energía de los fragmentos.

INTRODUCTION

There is so much now known about the prompt neutrons emitted from fission [1, 2] that it would be impossible to cover all the topics in this paper. I shall deal briefly with the energy spectrum and other matters that are covered in other papers in this Symposium. The last part of my paper is on what seems to me the most interesting phenomenon – the variation of neutron numbers with fragment mass.

NEUTRON ENERGY SPECTRA

The energy spectrum of prompt fission neutrons is now known with some accuracy for many cases. The best-known spectrum, and a typical one, is that from neutron-induced fission of U^{235} (Fig. 1). Experimental data [3, 4] are shown here as the number per unit energy, N(E), divided by $\sqrt{E}$, with arbitrary normalization. When presented in this way the spectra appear to be linear on a logarithmic scale, which suggests that they may be represented as Maxwellian distributions,

$$N(E) = (\sqrt{4}/\pi T^3)\sqrt{E}\, e^{-E/T}. \qquad (1)$$

A spectrum of this general type is to be expected for neutrons emitted from moving fission fragments [5]. The laboratory energy spectrum should be proportional to $\sqrt{E}$ at low energies, regardless of the form of the centre-of-mass emission spectrum. At high energies both the emission spectrum and the laboratory spectrum are expected to be of exponentially decreasing form. If the emission spectrum should be of Maxwellian type the laboratory

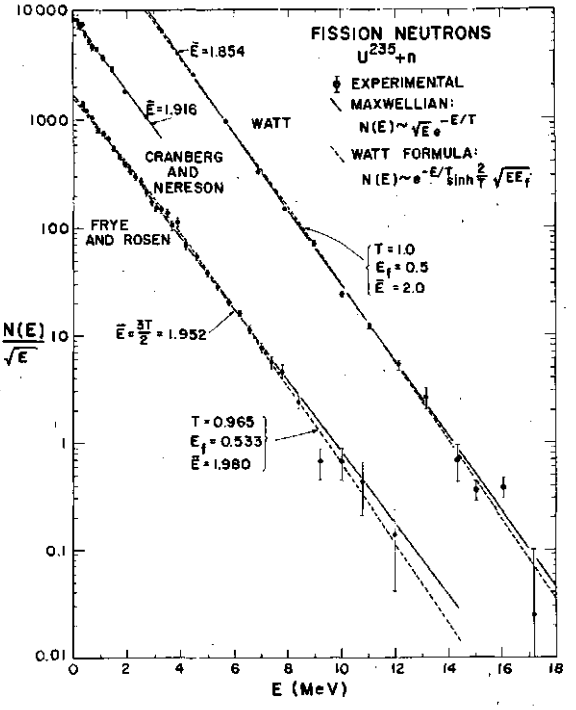

Fig. 1

Experimental fission neutron spectra for thermal-neutron fission of U^{235}. Standard deviations are indicated in this and other figures.

spectrum for given fragment velocity would be a Watt distribution [3],

$$N(E) = (e^{-E_f/T} / \sqrt{\pi E_f T})\, e^{-E/T} \sinh(2\sqrt{E E_f}/T). \tag{2}$$

Here E_f is the energy of a neutron having the velocity of the fragment, and T is the parameter characterizing the emission spectrum, equal to 2/3 of its average energy.

As can be seen in Fig. 1, there is not a great deal of difference between the Watt and Maxwellian distributions, and both can be made to fit the data well. However, the Watt distribution does not fit quite as well if the energy E_f is given the actual average value, about 0.75 MeV. This indicates that the centre-of-mass emission spectrum is broader than a Maxwellian distribution. Both evaporation-theory calculations [5] and experimental evidence [6 – 9] indicate that the variance of the emission energy E_{cm} is given by

$$\sigma^2(E_{cm}) \cong 0.80\,(\bar{E}_{cm})^2. \tag{3}$$

The numerical factor 0.80 would be 2/3 if the emission spectrum were accurately Maxwellian. Apparently the spectrum is better represented by the sum of two Maxwellian distributions of different average energy [5, 6]. Thus the laboratory spectrum can be viewed as the sum of perhaps four Watt

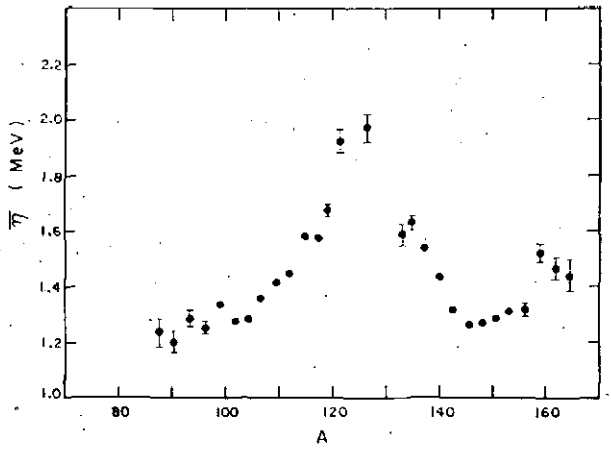

Fig. 2

Average centre-of-mass neutron kinetic energy for Cf^{252} as a function of fragment mass; from BOWMAN, MILTON, THOMPSON and SWIATECKI [8].

distributions, the result of which is close to a Maxwellian distribution. All fission neutron spectra seem to fit this same pattern.

Knowledge of the emission spectrum has been raised to a more sophisticated plane recently by the study of this spectrum as a function of fragment mass. Figure 2 shows the results of BOWMAN, MILTON, THOMPSON and SWIATECKI [8] for Cf^{252}. The average centre-of-mass energy is shown as a function of the fragment mass. The nuclear temperature of the fragments, as measured by the emission energies of neutrons, is seen to be maximum for symmetrical fission, and always to be similar in corresponding light and heavy fragments. A similar result has been obtained by MILTON and FRASER [10] for neutron-induced fission of U^{233}. This should probably not be interpreted as related to the two fragments being in thermal equilibrium at the scission point. The rather low temperature at this point, when most of the fragment energy is tied up in unavailable deformation energy, should have little to do with the temperatures of the fragments following separation and the emission of neutrons. Rather we should expect the neutron emission energies to follow the trend of the average neutron number curve, $\nu_f(M)$, perhaps to be proportional to $\sqrt{(\nu_f+1/2)/M}$. This is what simple evaporation theory would predict [5], allowing 3 or 4 MeV for gamma-ray emission.

Actually the average emission energy in Fig. 2 does seem to have this sort of dependence on ν_f and M [8], except in the vicinity of mass 135, near the magic numbers Z = 50 and N = 82. Here the fragment temperature is higher than would be expected on the basis of excitation per nucleon, but magic or near-magic nuclei are well-known to have unusually high temperatures for low excitations. This simply means that for magic fragments the level density increases only slowly with increasing excitation.

Evaporation and nuclear temperature theory have been quite successful in accounting for the energy spectra of fission neutrons, even with essentially no adjustment of theoretical constants. Figure 3 shows the experimental

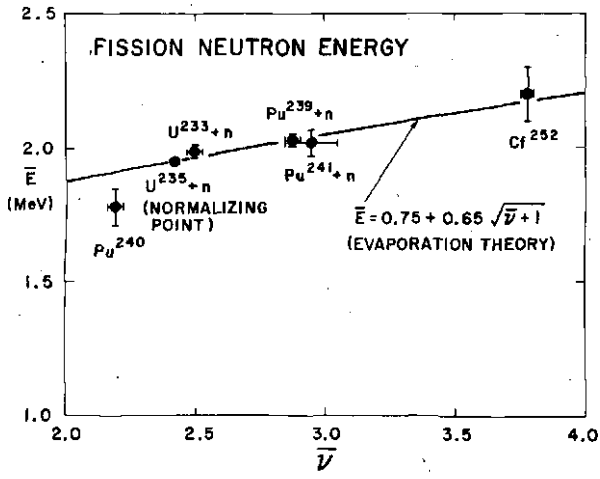

Fig. 3

Average energy of prompt fission neutrons as a function of the average number $\bar{\nu}$ of neutrons emitted. The curve predicted by evaporation theory has been fitted to the U^{235} + n point by choice of the coefficient 0.65. Experimental points are from many sources (see text and Ref. [6]).

results on average laboratory energy $\bar{E}$ of fission neutrons (as summarized in [5] and [6]). This average energy, which is about 2 MeV, has a tendency to increase with increasing neutron number $\bar{\nu}$. The prediction of evaporation theory [5, 6] is given by

$$\bar{E} = \bar{E}_f + \bar{E}_{cm}$$

$$\cong 0.75 + 0.65\sqrt{\bar{\nu}} + 1 \text{ (MeV)}. \qquad (4)$$

The value of 0.75 ± 0.02 MeV is the experimental figure, based on the work of many people, for the average of the neutron energy E_f corresponding to fragment velocity. It does not change appreciably over a wide range of fissioning nuclides. It is assumed, in arriving at this average, that the ratio of neutrons emitted from light and heavy fragments is $\bar{\nu}_L/\bar{\nu}_H = 1.1 \pm 0.1$. The other numerical factor, 0.65 MeV, is chosen so that the theoretical curve will pass through the U^{235} point ($\bar{\nu} = 2.42$, $\bar{E} = 1.95$ MeV). This corresponds to the choice $a \cong 11$ MeV^{-1} for the nuclear temperature constant in the equation $E = aT^2$, which is more or less precisely what statistical mechanics would predict for fission fragments [5].

The theoretical curve agrees fairly well with the other experimental points in Fig. 3. For some of these cases the value of $\bar{E}$ is not known with great precision, but for U^{233} and Pu^{239} the method of activation ratios has allowed rather precise comparison of the various fission spectra [11, 12]. This is also true for Bonner's sphere detectors [13]. The results for U^{233} and Pu^{239} agree well with the predicted curve.

Since there is an increase in $\bar{\nu}$ with increasing excitation energy of a given fissioning nuclide, one would expect the average fission spectrum ener-

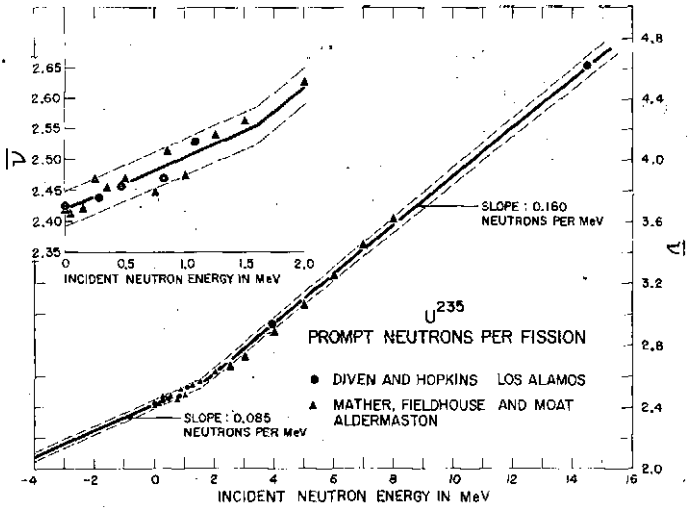

Fig. 4

Average number $\overline{\nu}$ of prompt neutrons emitted per neutron-induced fission of U^{235} as a function of incident neutron energy.
The solid line is a "universal curve" fitted to the data points, with standard deviations shown by the dashed line; from HOPKINS and DIVEN [14].

gy $\overline{E}$ to increase also, at the rate of about 0.025 MeV per MeV of incident neutron energy. The experimental evidence so far does not seem to be sufficiently accurate to determine whether this is so.

VARIATION OF NEUTRON NUMBER WITH EXCITATION

In recent years the data on average neutron numbers have become increasingly accurate. Figure 4 shows the data on $\overline{\nu}$ for neutron-induced fission of U^{235}, as determined by DIVEN and HOPKINS [14] and by MATHER, FIELDHOUSE and MOAT [15]. The data points cover the range of incident neutron energy from thermal to 14 MeV. Over almost all this range the value of $\overline{\nu}$ increases at the rate of about 0.16 n/MeV, which is close to what would be expected if all the added energy went into the production of neutrons; each neutron requires about 6.7 MeV to produce, including binding energy and centre-of-mass kinetic energy. However, there is apparently a lower slope of $\overline{\nu}$ from thermal to 1 or 2 MeV incident neutron energy; Hopkins and Diven have chosen a figure of 0.085 n/MeV for this range, thus fitting all the data here with two straight lines, joining at E = 1.60 MeV, $\overline{\nu}$ = 2.548. Other choices of curves can be and have been made [15].

There is no particular evidence here for a kink in the curve near 7 MeV, when second-chance fission becomes possible. Actually one would not expect much of an effect here, since whether or not a neutron is emitted before fission should not make more than perhaps 0.1 n difference in the total $\overline{\nu}$, and the change would be spread over several MeV because of the energy spectrum of emitted neutrons.

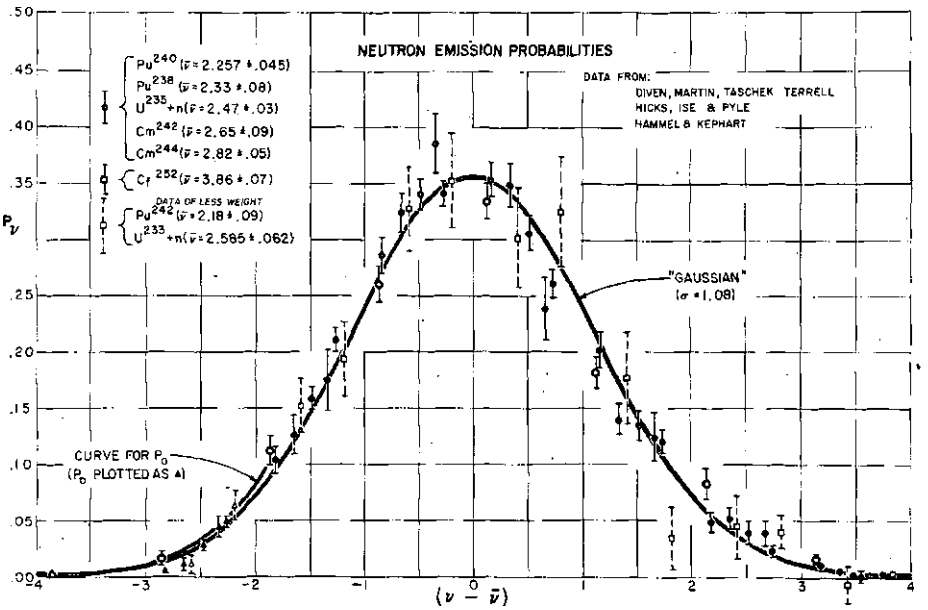

Fig. 5

Experimental neutron emission probabilities P_ν for emitting ν neutrons.
The horizontal scale is the difference of ν from the average $\bar{\nu}$ for each case.
The continuous curves are for a cumulative Gaussian distribution, as described in the text.

This particular dependence of $\bar{\nu}$ on excitation may be viewed as a sort of "universal curve" [14], with the excitation adjusted by addition of a constant to allow for different thermal values of $\bar{\nu}$. The data for $U^{233}+n$ can be fitted to this curve by adding 0.456 MeV [14] to the excitation. The data are less complete, however, and do not clearly indicate a change in slope. The $Pu^{239}+n$ data need to be shifted by 3.286 MeV [14], so that the break would come below thermal energy. The difference in values of $\bar{\nu}$ for thermal fission of Pu^{239} and spontaneous fission of Pu^{240} (which has 6.3 MeV less excitation) corresponds to a slope of only 0.11 n/MeV, so that a change of slope somewhere is necessary in this case.

It seems clear then that the dependence of $\bar{\nu}$ on excitation shows a change of slope, at least for the cases of U^{235} and Pu^{239} neutron-induced fission. It is not hard to think of reasons for this, such as changes in the mass distribution with excitation, or a change of 1 or 2 MeV in the total kinetic energy of the fragments. Small as this effect is, it seems to be clear evidence that something is changing in the fission process. Perhaps the fission barrier is making itself felt in some way at very low excitations.

DISTRIBUTION OF NEUTRON NUMBERS

There is also considerable experimental data now on the variation of the neutron number ν for fixed excitation of the fissioning nuclide, as seen in Fig. 5. An average $\bar{\nu}$ of, say, 2.42 for U^{235} fission does not, of course, im-

ply that every fission produces 2.42 neutrons. Sometimes none are emitted; sometimes 5 or 6 come out. Shown in this figure are the experimental data of DIVEN, MARTIN, TASCHEK and TERRELL [16], of HICKS, ISE and PYLE [17], and of HAMMEL and KEPHART [18], for eight different types of fission. The probabilities P_ν for emission of exactly ν neutrons are shown as functions of $(\nu - \bar{\nu})$. This shift of the horizontal scale by the average number of neutrons $\bar{\nu}$ makes all the experimental points fall fairly well on a single Gaussian curve [19]. I should point out that the $\bar{\nu}$ values indicated in Fig. 5 are now known to be about 2% high, but this has almost no effect on the calculated variances. All the neutron number distributions have variances σ^2 of the order of 1.25, except for Cf^{252}, which has $\sigma^2 = 1.55 \pm 0.04$.

The emission probabilities P_ν may be represented quite accurately [19] as the integrals over equal ranges of a Gaussian distribution with width $\sigma_0 = 1.08$, so that

$$\sum_0^\nu P_n = (2\pi)^{-1/2} \int_{-\infty}^{(\nu - \bar{\nu} + 1/2 + b)/\sigma_0} e^{-t^2/2}\, dt. \tag{5}$$

The quantity b is a small correction ($b < 0.01$) due to the fact that negative values of ν are not allowed here. The continuous Gaussian distribution may be considered to represent the distribution of total excitation energy of the fission fragments. If E_0, approximately 6.7 MeV, is the average excitation energy change caused by the emission of one neutron, then the excitation energy distribution must have an rms width of $\sigma_0 E_0$, about 7 or 8 MeV [19]. This agrees fairly well with the width of fragment kinetic energy distributions, as would be expected.

It must be kept in mind that σ_0^2 is the variance of the continuous Gaussian distribution, not of the discrete neutron number distribution. When a discrete distribution is represented as the integral over steps of width h of a continuous distribution, the two variances are related [6] by Sheppard's grouping correction,

$$\sigma^2 \cong \sigma_0^2 + h^2/12. \tag{6}$$

In this case $h = 1$, so that $\sigma_0 = 1.08$ corresponds to $\sigma^2 = 1.25$.

We see then that the distribution of neutron numbers gives fairly directly the distribution of fragment excitation energy. This result does not depend appreciably on how the excitation energy is divided between the two fragments. However, we must know this division if we wish to know the excitation energy distribution for a single fragment. If the excitations in the two fragments emitted in fission have equal distributions and are not correlated, each has a variance of $1/2\ \sigma_0^2 E_0^2$. If the excitations are correlated, then the widths could be either greater or smaller than given by this. We do not yet have experimental knowledge of this important matter, although it could be obtained [6].

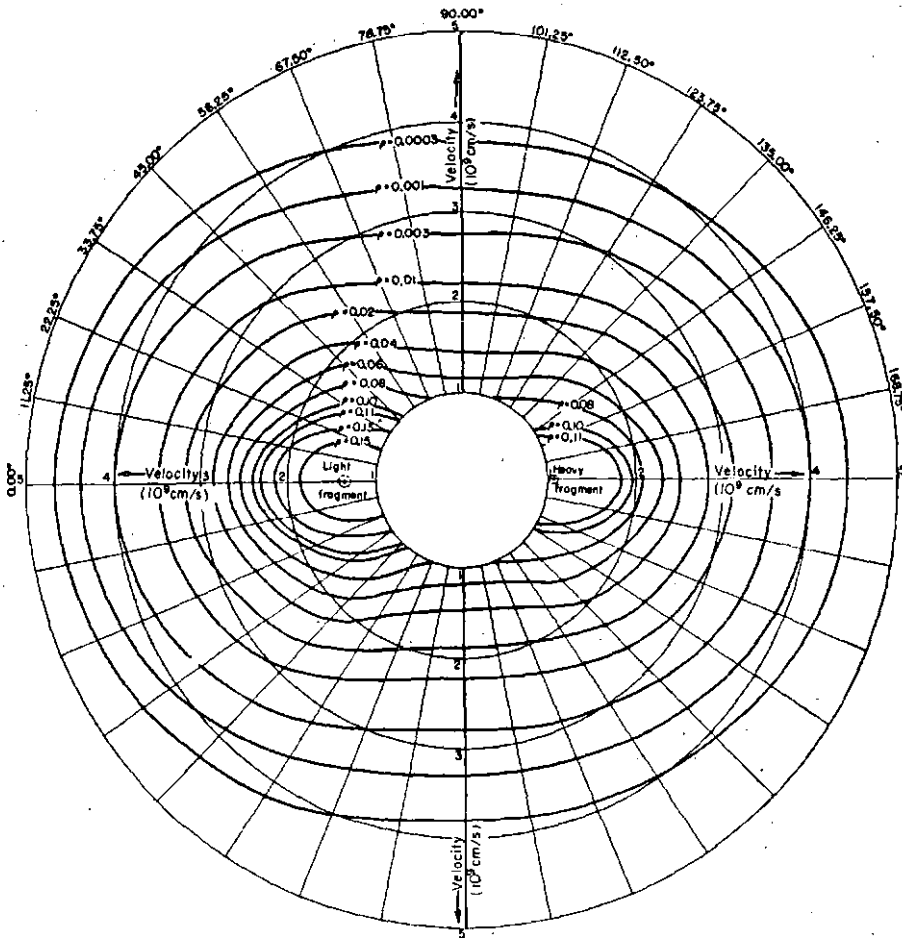

Fig. 6

Fission-neutron density distribution $\rho(V, \theta)$ in velocity space, as observed for Cf^{252}. The contour lines represent constant neutron density. Average velocities of light and heavy fragments are also shown; from BOWMAN, THOMPSON, MILTON and SWIATECKI [7].

NEUTRON ANGULAR DISTRIBUTION

Knowledge of the angular distribution of fission neutrons, relative to the fragment directions, has improved remarkably in recent years. Figure 6 shows some of the results obtained by BOWMAN, THOMPSON, MILTON and SWIATECKI [7] in their remarkable experiment on Cf^{252}. What is shown is the neutron density distribution in velocity space, with contour lines of constant neutron density, somewhat smoothed. This distribution is the same as that produced in ordinary space by plotting the positions of all neutrons at a fixed time following fission, say at 1 ns. The data points lie along the

radical lines, except that no data were taken at 0° and 180°, the fragment directions.

The average velocities of light and heavy fragments are shown as points in the figure. No neutron data are shown below a velocity of 1 cm/ns, approximately the heavy fragment velocity, because of the poorly known efficiencies of the neutron counters in this region. The results show a strong correlation between neutron velocities and fragment velocities, indicating that at least most of the neutrons are emitted from the fragments. The isotropic emission of neutrons from one fragment would produce in velocity space a spherically symmetric set of constant-density surfaces. The experimental results seen in Fig. 6 indicate that both Cf^{252} fragments emit similar numbers of neutrons, with perhaps 10% more coming from the light fragments. The emission is nearly isotropic; the emission spectrum and laboratory energy spectrum are consistent with other data and have been discussed earlier. Some rather similar results have been obtained for thermal-neutron fission of U^{235}, by SKARSVÅG and BERGHEIM [20].

According to BOWMAN et al. [7], and also Skarsvåg and Bergheim, their results are consistent with the emission of 10% or 15% of the neutrons from the fissioning nuclide, and not from the fragments. No definite answer is possible here because of lack of data at low neutron velocities, and the usual experimental uncertainties. The data [7, 9, 20, 21] are consistent with the emission of 100% of the neutrons from the fragments [9], with perhaps a slight anisotropy favouring 0° and 180°.

One other interesting result that may be obtained from Fig. 6 has to do with the form of the neutron emission spectrum at low velocities in the centre of mass. If the emission spectrum has the general form of a Maxwellian distribution (Eq. (1)), or of a sum of Maxwellian distributions with the factor $\sqrt{E}$ dominating at low energies, the distribution in velocity space should have a flat maximum at zero emission velocity, i.e. at the point corresponding to fragment velocity. An emission spectrum dominated by a higher power of E would produce a deep minimum at the same point. The data seem to imply that the factor is not very different from $E^{1/2}$, although it would be good to have data points a little closer to the fragment velocity point.

VARIATION OF NEUTRON NUMBER WITH FRAGMENT MASS

Experimental

The most interesting fission phenomenon now under investigation is the variation of neutron emission with fragment mass. It is not exactly a new phenomenon, since it was first seen by FRASER and MILTON in 1953 for thermal-neutron fission of U^{233} [22], established for Cf^{252} by WHETSTONE in 1958 [23] and verified for U^{235} by APALIN et al. [24] in 1959. FRASER and MILTON have recently improved on their earlier work, with results [10] seen in Fig. 7. The dependence of the number of neutrons ν_f emitted by individual fission fragments on the fragment mass is seen to follow the now well-known sawtooth curve. Also shown for comparison are the fission-fragment mass yields. There are curious bumps and wiggles in the neutron yield curve, which are probably real. The sum of the neutrons emitted from

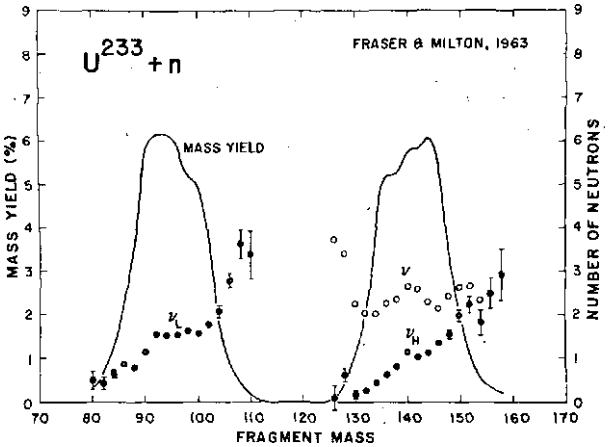

Fig. 7

Neutron yields for thermal-neutron-induced fission of U^{233} as functions of fragment mass. Also shown is the mass yield for this experiment; from data of FRASER and MILTON [10].

both fragments, $\nu = \nu_L + \nu_H$, is seen to have a more nearly constant value, with a sharp increase near symmetrical fission. Here ν increases from the average of ~ 2.5 to a peak of ~ 4, or possibly more after correction for spurious symmetrical fission events that actually correspond to higher mass ratios. We observe that in this case, as apparently in all other cases, the minimum values of ν_f correspond closely to the regions of rapidly vanishing fragment mass yields.

Very similar results have been obtained by APALIN et al. [25] for thermal-neutron fission of U^{235}. They were the first to obtain good evidence for the maximum in ν for symmetrical fission, and have obtained similar results for U^{233}, U^{235} and Pu^{239} [24, 25].

Turning now to spontaneous fission of Cf^{252}, we see in Fig. 8, from the work of STEIN [26], the same sort of sawtooth neutron yield dependence. Stein's data (the points with standard deviations) are taken by a new method, which does not involve counting neutrons at all, but consists of simultaneous measurement of the velocities and energies of the fragments. The two velocities are essentially unchanged by neutron emission and yield the initial fragment masses; the knowledge of both velocity and energy for one fragment gives the final fragment mass. The neutron number is determined for each event by the difference between these two masses. The two mass distributions are shown below, not corrected for scattering losses.

Also shown in Fig. 8 are the Cf^{252} data of BOWMAN et al. [8] (the dashed line) and my own results [6] (the solid line). Not shown are WHETSTONE's early results [23], which are similar, except for the effects of mass dispersion. Similar results have also been obtained by SCHMITT, KIKER and WILLIAMS [27] using mass yield data only. All the results shown agree rather well and indicate that Cf^{252} has the same sawtooth neutron yield dependence as other types of fission. Notice the minimum in neutron yield near mass 100, which appears to be a real phenomenon. The total

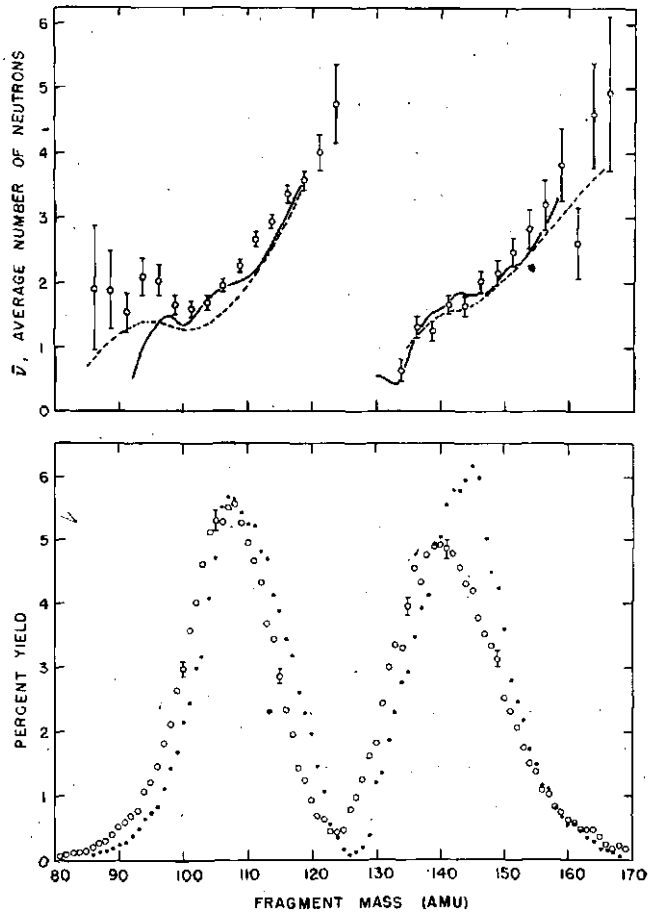

Fig. 8

Neutron yields (upper figure) as functions of fragment mass, for Cf^{252} fission. The points with standard deviations represent the neutron yields of Stein, the continuous curve the data of TERRELL [6], and the dashed line the data of BOWMAN et al. [8]. In the lower figure are shown Stein's initial (solid points) and final (open points) mass yield; from STEIN [26].

neutron yield ν, not shown here, apparently has a small but not spectacular peak for symmetrical fission.

My own results on neutron emission were obtained by an independent method also not involving neutron counting, which was first used in 1959 and 1960 [28]. The most accurate data have been determined for thermal-neutron fission of U^{235}, and are shown in Fig. 9. The method [6] is basically that of a comparison of initial and final mass yields. The results may be seen to be similar to those obtained by direct counting, with perhaps less uncertainty. Estimated standard deviations are shown by dotted lines. Essentially the same method has also been used by FARRAR and TOMLINSON [29]. It may be shown that if the mass distributions are treated as continuous

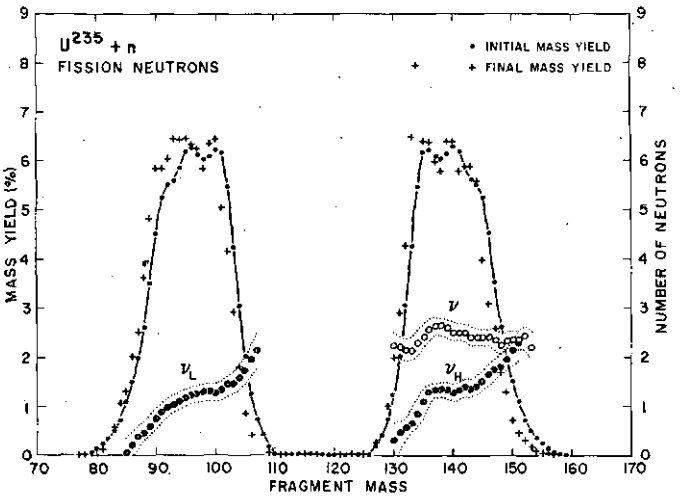

Fig. 9

Neutron yields as functions of mass for thermal-neutron-induced fission of U^{235} as determined from initial and final mass yields, which are also shown. Standard deviations of the neutron yields are indicated by dotted lines.

distributions, the initial and final mass yields, y(M) and Y(M), are related by

$$\int_0^{M_0 - \nu_f(M_0)} Y(M)dM = \int_0^{M_0} y(M)dM + \tfrac{1}{2}(dy/dM)\langle\sigma^2(\nu_f; M)\rangle + \ldots \qquad (7)$$

Here $\nu_f(M_0)$ is the average number of neutrons emitted by fragments of initial mass M_0, and the slope and conditional variance in the small correction term [6] are to be evaluated at the same initial mass M_0.

The continuous final mass distribution used in Eq. (7) may be obtained from the discrete radiochemical and mass spectrometric yields by interpolation on the cumulative yields $\Sigma_0^{M_0} Y(M)$. The initial mass yield, determined by double time-of-flight methods, is automatically obtained as a continuous distribution because of the small but unavoidable experimental mass dispersion.

It is necessary to correct this mass distribution for the dispersion, and the easiest way is to fold in an operator consisting of a distribution having negative variance. Such an operator [6] can consist of the three-element distribution, at unit mass steps, $-\sigma^2/2$, $1+\sigma^2$, $-\sigma^2/2$, where σ^2 is the variance to be removed. If the data are good enough for a higher-order correction, a symmetrical five-element operator can be chosen having second central moment (variance) equal to $-\sigma^2$, and fourth central moment the same as the dispersion function, if this is Gaussian ($\mu_4 = 3\sigma^4$), and so on to higher orders if desired. If it is necessary to smooth the experimental yields, it is useful to know that the five-element operator producing minimum fluctuations has the second and fourth elements equal to zero.

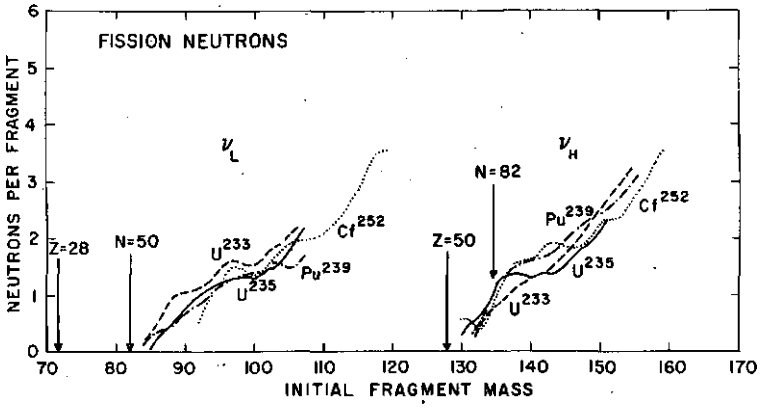

Fig. 10

Neutron yields as functions of mass for four types of fission as determined from mass-yield data. Also indicated are the approximate fragment masses corresponding to magic numbers for unchanged charge-to-mass ratio of the fragments.

Although the concept of negative variance may be unfamiliar to statisticians, it may be shown that this operator method of unfolding dispersion is precisely equivalent to somewhat more tedious methods involving fitting polynomials or Fourier series, or correcting by such terms [27] as $\frac{1}{2}\sigma^2(d^2y/dM^2)$.

The neutron number results obtained by such methods for four different types of fission [6] are shown in Fig. 10, as functions of initial fragment mass. The initial mass distributions were the work of STEIN [30], WHETSTONE [31], and of MILTON and FRASER [32, 33]. The final mass distributions, radiochemical or mass-spectrometric, were the work of many people (see Ref. [6]).

It is remarkable that the results for these different types of fission look so much alike when shown as functions of fragment mass. It suggests that the excitation of the fragments depends more on properties of the fragments than on the mass ratio, and leads to the idea of a universal neutron yield curve [6]. The number of neutrons emitted approaches zero at the magic numbers N = 50 and Z = 50, and perhaps N = 82 has an effect also. Even Z = 40 may be responsible for the slight dip in the vicinity of mass 100. It should be realized that the locations of magic numbers shown here are only approximate, and based on unchanged charge ratios. It is probable that Z = 50 actually occurs a few mass units higher, as the heavy fragments tend to have a smaller proton-to-neutron ratio than the light fragments [34].

There is little known about the neutron yield from individual fragments in the range of mass numbers from 110 to 130, except for Cf^{252}. If the yields for Cf^{252} are typical, then one would expect a total of about six neutrons to be emitted from symmetrical neutron-induced fission of U^{233}, U^{235} and Pu^{239}. This is in fairly good agreement with experimental data.

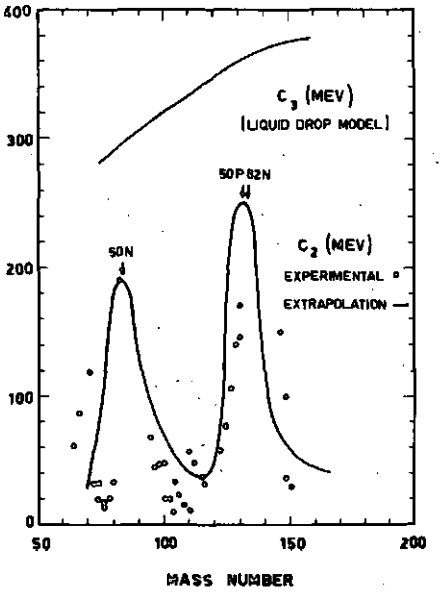

Fig. 11

Deformation parameter C_2 as a function of mass number; the points are from Coulomb-excitation data [43], and the continuous line is an extrapolation for fission fragments. Also shown for comparison is the liquid drop prediction for C_3; from FONG [38].

Theoretical

It is noteworthy that the fragment yields and the neutron yields tend to vanish at the same points, and that these correspond to the magic numbers N = 50 and Z = 50. I suggested in 1962 that these phenomena were due to a special property of magic nuclides, their resistance to deformation [6]. Magic and near-magic nuclides are well known to prefer spherical shapes and to be unusually stiff against deformation. Thus fission into a pair of fragments, one magic and one non-magic, would obviously require the least total of Coulomb interaction and deformation energies if most of the deformation at scission occurred in the less stiff non-magic fragment. This would result in very little excitation of the magic fragment following scission, and the emission of almost no neutrons. The stiffness of the magic fragment would also result in a higher Coulomb interaction energy, or fission barrier, and thus probably a lower fragment yield. This would account [6] for the cutoff of mass yields at magic numbers, the presence of three mass peaks for radium fission, and the single mass peak for bismuth fission. All these mass peaks are bounded by the magic numbers N = 50 and Z = 50. Many other predictions can be made from the same basic idea, which might be called the fragment-shell, or fragment-deformation, theory of fission.

Essentially the same idea has been arrived at by BLINOV and EISMONT [35], by MILTON and SWIATECKI [33, 36] and by VANDENBOSCH [37]. This theory has also been used by FONG [38], by HONDA [39], by BOWMAN

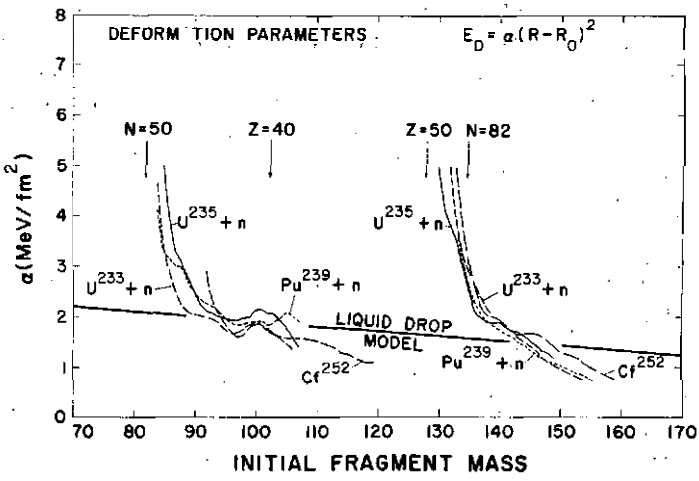

Fig. 12

Deformation parameter α as a function of fission-fragment mass for four types of fission, determined from neutron-yield and fragment-energy data on the basis of fragment-deformation theory. The approximate masses corresponding to magic numbers are indicated for unchanged charge-to-mass ratio. Shown for comparison is the prediction from liquid drop theory by BOHR and WHEELER [47]. The relation between α and C_2 is (for spherical fragments): $C_2 = (5/2\pi)\alpha R_0^2 \simeq 30\,\alpha$.

et al. [8] and by THOMAS et al. [40]. Actually, BRUNNER and PAUL in 1960 and 1961 [41] were developing very similar ideas about deformation and magic fragments, though not in connection with the emission of neutrons.

The expected dependence of fission-fragment stiffness on fragment mass is shown in Fig. 11, taken from the work of FONG [38]. The deformation parameter shown in the lower part of the figure is C_2, which is defined in terms of spheroidal deformations of fission fragments [42]. The deformation energy is given by $\frac{1}{2} C_2 \beta_2^2$, with β_2 defined as the coefficient of the second-order spherical harmonic.

The coefficient C_2 has been evaluated from Coulomb excitation studies by ALDER, BOHR, HUUS, MOTTELSON and WINTHER [43]; their values are shown as points in this figure. The stiffness shows large peaks at magic numbers, and low values in regions of permanently-deformed nuclides. However, fission fragments, which do not have the same neutron/proton ratio as ordinary nuclides, should have rather different values of C_2, requiring an extrapolation from known values. Fong's extrapolated values of C_2 are shown as a heavy line in Fig. 11. The two peaks correspond to N = 50, and to the combination of Z = 50 and N = 82. The upper curve is the third-order deformation parameter C_3, based on liquid drop theory and used by Fong in earlier calculations [44]. Using the extrapolated values of C_2, FONG [36] has had some success in accounting for neutron emission.

It is of great interest, however, to derive the deformation parameters of fragments directly from fission data, rather than to depend on extrapolations. Figure 12 shows the results I have obtained in this way solely from fission data, based on a rather simple theory worked out some years ago. The two fragments are assumed, in this theory, to be of roughly

spheroidal form, just touching at the scission point, with their long axes along the direction of separation. The parameter α, which is shown as a function of fragment mass, is defined in terms of the deformation energy E_D and the change in the fragment maximum radius, or major semi-axis, from the value R_0 at zero excitation to the value R when excited. It is assumed that the deformation energy is quadratic in the radius change, so that

$$E_D = \alpha (R - R_0)^2. \tag{8}$$

The relation between α and C_2 is not simple except for spherical fragments, for which we have

$$C_2 = (5/2\pi)\alpha R_0^2 \cong 30\,\alpha, \tag{9}$$

for the units used here.

The deformation parameter α is seen, in Fig. 12, to have very similar dependence on mass for all four types of fission shown. It rises to high values for the stiff fragments near N = 50, Z = 50 and perhaps N = 82. It even seems to have a small peak at the semi-magic number Z = 40. In other mass regions the low value of α corresponds to easily deformed nuclides, such as for symmetrical fission of the three neutron-induced types of fission (but not for Cf^{252}). VANDENBOSCH has obtained a similar dependence of stiffness on fragment mass, on a somewhat different basis [37]. The "universal deformation parameter curve" shown here is based on the ν_f data shown in Fig. 10, and on kinetic energy data taken from the work of MILTON and FRASER [33] and of WHETSTONE [31].

In this theory the fragments are not assumed to be spherical at zero excitation, but may have permanent deformations. Both the values of α and R_0 are obtained directly from the experimental fission data, which consist of the neutron numbers ν_L and ν_H for the two fragments and the total kinetic energy E_K of the same fragments. The deformation energy is assumed to be essentially given by the excitation energy which leads to emission of neutrons and gamma rays, so that, for one fragment,

$$E_D \cong 6.7\,(\nu_f + \tfrac{1}{2})\ \text{(MeV)}. \tag{10}$$

Thus we are assuming that fission is taking place near threshold, and that there is very little extra excitation in the form of a high temperature at the scission point. It is also assumed, for simplicity, that the fragment kinetic energy E_K is the same as the Coulomb interaction energy between two charges ($Z_L e$ and $Z_H e$) effectively located at the centres of the fragments, so that

$$E_K = Z_L Z_H e^2/(R_L + R_H). \tag{11}$$

The subscripts L and H, as usual, refer to light and heavy fragments.

The classical principle of minimizing the potential energy, $E_K + E_{DL} + E_{DH}$, then leads to the set of equations,

$$\alpha_L = E_K^4/4E_{DL}\, Z_L^2 Z_H^2 e^4 \tag{12}$$

$$\alpha_H = E_K^4/4E_{DH}\, Z_L^2 Z_H^2 e^4 \tag{13}$$

$$R_{L0} + R_{H0} = Z_L Z_H e^2 (E_K - 2E_{DL} - 2E_{DH})/E_K^2. \tag{14}$$

These allow us to calculate α_L, α_H and $R_{L0} + R_{H0}$ from E_K, E_{DL} and E_{DH}. Naturally the calculation can be reversed, and E_K, E_{DL} and E_{DH} calculated from the deformation parameters. The value of $R_{L0} + R_{H0}$ remains in the vicinity of 12 to 13 fermis for the data shown, which is perhaps what would be expected for fragments in their ground states.

One interesting result of this theory is that there is only one set of values E_K, E_{DL} and E_{DH} resulting from given values of the deformation parameters α_L, α_H and $R_{L0} + R_{H0}$. This implies that fission at a higher energy would not give different values of these three energies. It is apparently true that E_K changes little with increasing energy supplied to the fissioning nuclide, and the changes that are seen may be due to changes in the type of fission fragments produced (such as in their values of Z). As to E_D, it should be kept in mind that this is the energy of deformation only, and additional energy supplied to the fissioning nuclide will presumably result in hotter fragments of similar deformation but higher excitation energy.

A refinement of this theory has been considered, in which the Coulomb interaction energy is taken to be the slightly greater value for two spheroids in contact, as calculated by COHEN and SWIATECKI [45] and by MILTON and WILBER [46]. Because this spheroidal effect may be comparable to, and partly cancelled by, the effects of polarization and non-quadratic dependence of E_D on R, it has not been incorporated in these calculations. It should be kept in mind that if the quadratic relation of Eq. (8) is not precise the values calculated for α and R_0 will be effective values, which could vary with excitation.

As to the liquid-drop-model deformation parameter line shown in Fig. 12, this is the 1939 prediction of BOHR and WHEELER [47] for spherical nuclides. Their choice of surface tension and radius constant leads to the equation

$$\alpha = 2.86 - 0.0630\,(Z^2/A)\ (\mathrm{MeV/fm^2}). \tag{15}$$

They predicted that the deformation parameter would vanish at a critical value of Z^2/A, 45.4 from this equation, and of course corresponding to a mass far above the fission-fragment range. It is satisfying that this classical prediction agrees reasonably well with the values of α determined from fission-fragment data. The differences seem to be just what would be expected for magic fragments and permanently deformed fragments.

Because of the results shown here, and other predictions of fragment deformation theory, we can hope that the variation of neutron number with fragment mass has at last given us a real key to the understanding of many of the still puzzling features of fission.

REFERENCES

[1] HYDE, E.K., The Nuclear Properties of the Heavy Elements III: Fission Phenomena, Prentice-Hall Inc., Englewood Cliffs, N.J., (1964) 211.

[2] KEEPIN, G.R., Physics of Nuclear Kinetics, Addison-Wesley Publishing Co., Inc., Reading, Mass. (1965) 37.

[3] WATT, B.E., Phys. Rev. 87 (1952) 1037.

[4] CRANBERG, L., FRYE, G., NERESON, N. and ROSEN, L., Phys. Rev. 103 (1956) 662.

[5] TERRELL, J., Phys. Rev. 113 (1959) 527.

[6] TERRELL, J., Phys. Rev. 127 (1962) 880.

[7] BOWMAN, H.R., THOMPSON, S.G., MILTON, J.C.D. and SWIATECKI, W.J., Phys. Rev. 126 (1962) 2120.

[8] BOWMAN, H.R., MILTON, J.C.D., THOMPSON, S.G. and SWIATECKI, W.J., Phys. Rev. 129 (1963) 2133.

[9] SARGENT, C.P., BERTOZZI, W., DEMOS, P.T., MATTHEWS, J.L. and TURCHINETZ, W., Phys. Rev. 137 (1965) B89.

[10] MILTON, J.C.D. and FRASER, J.S., unpublished (1963).

[11] GRUNDL, J.A. and NEUER, J.R., Bull. Am. phys. Soc. 1 (1956) 95; GRUNDL, J.A., unpublished (1963).

[12] KOVALEV, V.P., ANDREEV, V.N., NIKOLAEV, M.N. and GUSEINOV, A.S., Ž. eksp. teor. Fiz. 33 (1957) 1069.

[13] BONNER, T.W., Nucl. Phys. 23 (1961) 116.

[14] HOPKINS, J.C. and DIVEN, B.C., Nucl. Phys. 48 (1963) 433.

[15] MATHER, D.S., FIELDHOUSE, P. and MOAT, A., Phys. Rev. 133 (1964) B1403.

[16] DIVEN, B.C., MARTIN, H.C., TASCHEK, R.F. and TERRELL, J., Phys. Rev. 101 (1956) 1012.

[17] HICKS, D.A., ISE, J., Jr. and PYLE, R.V., Phys. Rev. 101 (1956) 1016.

[18] HAMMEL, J.E. and KEPHART, J.F., Phys. Rev. 100 (1955) 190.

[19] TERRELL, J., Phys. Rev. 108 (1957) 783.

[20] SKARSVÅG, K. and BERGHEIM, K., Nucl. Phys. 45 (1963) 72.

[21] KAPOOR, S.S., RAMANNA, R. and RAMA RAO, P.N., Phys. Rev. 131 (1963) 283.

[22] FRASER, J.S. and MILTON, J.C.D., Phys. Rev. 93 (1954) 818.

[23] WHETSTONE, S.L., Jr., Phys. Rev. 114 (1959) 581.

[24] APALIN, V.F., DOBRYNIN, Yu.P., ZAKHAROVA, V.P., KUTIKOV, I.E. and MIKAELYAN, L.A., Atomnaja Energiya 8 (1960) 15.

[25] APALIN, V.F., GRITSYUK, Yu.N., KUTIKOV, I.E., LEBEDEV, V.I. and MIKAELYAN, L.A., Nucl. Phys. 38 (1962) 193; ibid. 41 (1963) ibid. 92 55 (1964) 249.

[26] STEIN, W.E., "Simultaneous velocity and energy measurement of fission fragments", these Proceedings I.

[27] SCHMITT, H.W., KIKER, W.E. and WILLIAMS, C.W., Phys. Rev. 137 (1965) B837.

[28] TERRELL, J., Bull. Am. phys. Soc. 6 (1961) 16.

[29] FARRAR, H. and TOMLINSON, R.H., Canad. J. Phys. 40 (1962) 943.

[30] STEIN, W.E., Phys. Rev. 108 (1957) 94.

[31] WHETSTONE, S.L. Jr., Phys. Rev. 131 (1963) 1232.

[32] MILTON, J.C.D. and FRASER, J.S., Phys. Rev. 111 (1958) 877.

[33] MILTON, J.C.D. and FRASER, J.S., Canad. J. Phys. 40 (1962) 1626; ibid. 41 (1963) 817.

[34] WAHL, A.C., "Mass and charge distribution in low-energy fission", these Proceedings I.

[35] BLINOV, M.V. and EISMONT, V.P., Ž. eksp. teor. Fiz. 42 (1962) 180.

[36] MILTON, J.C.D. and SWIATECKI, W., unpublished (1962).

[37] VANDENBOSCH, R., Nucl. Phys. 46 (1963) 129.

[38] FONG, P., Phys. Rev. Lett. 11 (1963) 375.

[39] HONDA, T., J. Phys. Soc. Japan 18 (1963) 1697.

[40] THOMAS, T.D., GIBSON, W.M. and SAFFORD, G.J., "Thermal-neutron-induced fission of U^{235}, U^{233} and Pu^{239}", these Proceedings I.

[41] BRUNNER, W. and PAUL, H., Ann. Phys., Lpz. 6 (1960) 267; ibid. 7 (1961) 326, 333; ibid. 8 (1961) 146.

[42] BOHR, A., Mat.-fys. Meddr. 26 (1952) No. 14.

[43] ALDER, K., BOHR, A., HUUS, T., MOTTELSON, B. and WINTHER, A., Rev. mod. Phys. 28 (1956) 432.

[44] FONG, P., Phys. Rev. 102 (1956) 434.
[45] COHEN, S. and SWIATECKI, W.J., Ann. Phys. 19 (1962) 67.
[46] MILTON, J.C.D. and WILBER, B.M., unpublished (1961).
[47] BOHR, N. and WHEELER, J.A., Phys. Rev. 56 (1939) 426.

DISCUSSION

M. PETRASCU: I have a question in connection with Fig. 8 in Dr. Terrell's paper. The points with standard deviation were obtained by Dr. Stein when, for calibrating the solid-state detectors, he used the data represented by the dashed curve obtained by Bowman et al. Now the general trend of the points follows that of the dashed curve. Is that because they are, to a certain extent, dependent on each other?

J. TERRELL: Perhaps Dr. Stein would like to answer that question.

W. STEIN: With regard to the data shown in Fig. 8, I should merely like to draw attention to the variation of $\bar{\nu}$ with fragment mass. The absolute neutron numbers were restricted to the values given by Bowman et al. at fragment masses 99.1 and 147.7.

S.S. KAPOOR: You mentioned, Dr. Terrell, that the data on angular distributions of the neutrons given by various groups show that about 10% or 15% of the neutrons are not emitted from the moving fragments. But afterwards you said that all the data were consistent with the emission of 100% of the neutrons from the moving fragments. How do you arrive at this conclusion?

J. TERRELL: After a careful examination of all the data, I have found no convincing evidence that any neutrons are emitted other than from the moving fragments. The possibility is not excluded, of course, but the lack of data for very low-energy neutrons in the laboratory angular distribution makes it difficult to establish whether there is emission from the fissioning nuclide. Sargent, Bertozzi et al. (Ref. [9] in my paper) have arrived at a somewhat similar conclusion.

S. S. KAPOOR: You pointed out that the fragments with Z = 50 and N = 82 are emitted with a lower yield because of the higher barrier, but this is certainly not the region of lowest fission yield. Therefore the high barrier for emission of the magic fragments is certainly not the only reason for the asymmetry observed in the mass distributions.

J. TERRELL: It seems to me that the magic numbers Z = 50 and N = 50 (and perhaps N = 82) do correspond very closely to the regions of lowest mass yield, or at least rapidly decreasing yield. This is true in many types of fission, including that for lower-mass nuclides such as radium and bismuth, and is probably not just coincidence. However, the complete theory of mass yields has not yet been worked out, as far as I know.

M. NÈVE de MEVERGNIES: If part of the prompt fission neutrons was not emitted by the moving fragments but was emitted isotropically at scission, would this phenomenon produce an effect on the neutron emission spectrum in the laboratory system?

J. TERRELL: Yes, in principle. One might expect that the emission spectrum of the neutrons emitted from the fissioning nuclide would be different from the laboratory spectrum produced by the emission of neutrons

from moving fragments. It might not be proportional to $E^{1/2}$ at low energies, and the sum of the two spectra would then also not be proportional to $E^{1/2}$ at low energies, but it might be difficult to detect if the fraction of non-fragment neutrons were small. Moreover, the velocity-space representation of fission neutrons would show a "hill" near V = 0 if such neutrons were emitted.

U.V. RYABOV: In slow-neutron fission, fission takes place via $J = I \pm \frac{1}{2}$ states that are appreciably separated in energy. Could you state the order of magnitude that might be expected for uranium and plutonium fission?

J. TERRELL: I believe Dr. Moore would like to answer that question.

M.S. MOORE: One can estimate the variation in $\bar{\nu}$ from resonance to resonance by using the correlation for p-wave fission (noted by Blyumkina et al.) between $\bar{\nu}$ and the total fragment kinetic energy. From fragment kinetic energy variations observed from resonance to resonance one might expect variations in $\bar{\nu}$ of 1-2%.

BORON PILE $\bar{\nu}$ MEASUREMENTS

D. W. COLVIN AND M. G. SOWERBY
ATOMIC ENERGY RESEARCH ESTABLISHMENT, HARWELL, BERKS.,
UNITED KINGDOM

Abstract — Résumé — Аннотация — Resumen

BORON PILE $\bar{\nu}$ MEASUREMENTS. Accurate absolute measurements of $\bar{\nu}$, the average number of neutrons per fission, have been made with the boron pile. The experimental method is described and results are presented of the $\bar{\nu}$ values obtained for the thermal-neutron-induced fission of U^{233}, U^{235}, Pu^{239} and Pu^{241}, the spontaneous fission of Pu^{240} and Cf^{252}, and the fast neutron-induced fission of U^{235} in the energy range 100 keV to 2.6 MeV.

MESURES DE $\bar{\nu}$ A L'AIDE DE L'ASSEMBLAGE BORE. Les auteurs ont procédé, au moyen de l'assemblage bore, à des mesures absolues très exactes du nombre moyen, $\bar{\nu}$, de neutrons par fission. Ils exposent la méthode expérimentale utilisée et présentent les résultats des valeurs de $\bar{\nu}$ obtenues pour la fission de ^{233}U, ^{235}U, ^{239}Pu et ^{241}Pu par neutrons thermiques, la fission spontanée de ^{240}Pu et de ^{252}Cf, et la fission de ^{235}U par neutrons rapides dans la gamme d'énergie allant de 100 keV à 2,6 MeV.

ИЗМЕРЕНИЯ $\bar{\nu}$ НА РЕАКТОРЕ "БОРОН". На реакторе "Борон" были произведены точные абсолютные измерения числа нейтронов на акт деления ($\bar{\nu}$). Описывается метод проведения эксперимента и приводятся полученные значения $\bar{\nu}$ для деления урана-233, урана-235, плутония-239 и плутония-241, вызванного тепловыми нейтронами, для спонтанного деления плутония-240 и калифорния-252 и для вызванного быстрыми нейтронами деления урана-235 в диапазоне энергий от 100 кэв до 2,6 Мэв.

MEDICIONES DE $\bar{\nu}$ EN EL REACTOR BORON. En el reactor Boron se han efectuado mediciones absolutas exactas del parámetro $\bar{\nu}$, o sea, el número medio de neutrones emitidos por fisión. Se describe el método experimental y se indican los valores de $\bar{\nu}$ obtenidos para la fisión del ^{233}U, ^{235}U, ^{239}Pu y ^{241}Pu inducida por neutrones térmicos, la fisión espontánea del ^{240}Pu y del ^{252}Cf, y la fisión, inducida por neutrones rápidos, del ^{235}U en el intervalo de energía 100 keV-2,6 MeV.

INTRODUCTION

The accurate measurement of $\bar{\nu}$, the average number of neutrons per fission, is required for reactor physics calculations. If the reproduction factor for a thermal reactor, K_{eff}, has to be calculated to $\pm \frac{1}{2}\%$, then it is necessary to demand that $\bar{\nu}$ be measured to $\pm \frac{1}{2}\%$ or better. For fast reactors an accuracy of $\pm$ 1% is desired in the energy range 1 keV to 5 MeV.

The measurements of $\bar{\nu}$ can be divided into two categories, absolute measurements and relative measurements. Most experiments on $\bar{\nu}$ have been of the latter type and they are only of great value (neglecting the least-squares fitting of 2200 m/s data) if the standard $\bar{\nu}$ used is accurately known. Until recently most absolute $\bar{\nu}$ measurements were made using standard neutron sources to calibrate the neutron detector. This method suffers from the following disadvantages:

(i) Until recently standard neutron sources have not been calibrated to better than $\pm$ 1.5%.

(ii) The variation of neutron detection efficiency with neutron energy

cannot be measured accurately with sources. This is particularly important if the standard source has an energy spectrum markedly different from the fission spectrum.

(iii) Standard sources that have a fission spectrum, e.g. the spontaneous fission sources of Harwell and the Atomic Weapon Research Establishment (A.W.R.E.), contain sufficient fissile material for neutrons reflected from the moderator of a neutron detector to cause appreciable multiplication. FIELDHOUSE and CULLIFORD [1] calculate an increase of 4.2 ± 0.5% when the A.W.R.E. source is placed in an oil tank.

The boron pile experiment was designed to measure $\bar{\nu}$ accurately and absolutely without the use of a standard source. Most of the measurements are for thermal and spontaneous fission but some results have been obtained for fast neutron-induced fission. As a full description of the boron pile has been given previously [2] this paper will concentrate on the results and their errors.

EXPERIMENTAL METHOD

The boron pile, which is shown in Fig. 1, consists of a graphite stack with a cubic core of side 220 cm in which there is an 11 × 11 lattice of holes. In each of these holes, except the central one, there are two 5-cm diam. $B^{10}F_3$ counters. Round this core there is a 35-cm-thick graphite reflector and a neutron shield consisting of 0.4 mm of cadmium inside 61 cm of concrete. The central hole is key-hole shaped with the circular part 10.1-cm diam. This assembly has a counting efficiency of approximately 64% for a neutron source placed at the centre; when the pile was designed it was expected that the efficiency would vary by approximately 2% over the fission neutron spectrum.

To measure $\bar{\nu}$ a fission chamber was placed in the central hole of the pile and, for neutron-induced fission, a collimated beam of neutrons passed through it. For thermal fissions the neutron beam was obtained from the reactor GLEEP and for fast fissions the neutrons were produced by the Harwell 5-MeV Van de Graaff accelerator using T(p, n) and Li^7(p, n) reactions. The fission pulses were used to trigger a gating system that measured ($\bar{R}$) the average number of neutrons detected per event. When corrected for the effects described in the next section $\bar{R}$ is proportional to the number of prompt neutrons per fission. Measurements have been made on the thermal fission of U^{235}, Pu^{239}, U^{233} and Pu^{241}, the fast neutron-induced fission of U^{235}, and the spontaneous fission of Pu^{240} and Cf^{252}.

The pile was calibrated by replacing the fission chamber with a gridded fast ionization chamber containing tetra-deutero-methane, and making use of the deuteron photodisintegration reaction in which "$\bar{\nu}$" is one and the energy of the neutron is known from the γ-ray energy. Using the same gating system $\bar{R}$ was measured as a function of neutron energy using the γ-rays of different energies given in Table I. The proton beam required for the (p, γ) reactions was obtained from the Harwell 5-MeV Van de Graaff accelerator.

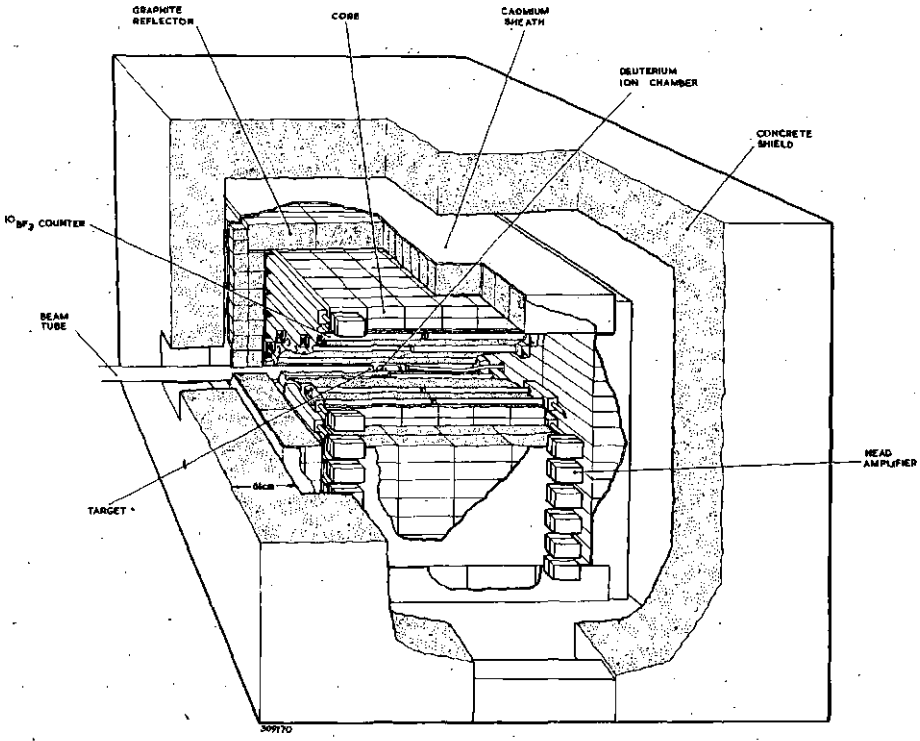

Fig.1

The boron pile

TABLE I

CALIBRATION γ-RAYS

Gamma-ray	Gamma-ray energy (MeV)	Approximate neutron energy (MeV)
ThC"	2.618	0.190
Na^{24}	2.757	0.265
$F^{19}(p,\alpha\gamma)$	6.14, 6.92, 7.12	2.0
$Al^{27}(p,\gamma)$	11.135, 12.915	4.9

The gating system consisted of two gates of the same length, the "prompt" and "background" gates, separated by a delay. The "prompt" gate was opened by either the photoproton or fission pulse and the "background" gate was usually opened 15 ms later. The difference between the average neutron counts through the two gates gave the average number of neutrons ($\bar{R}$) detected per event for the gate length used. The choice of gate length depended upon the experiment being performed; for a typical value of 4 ms approxi-

mately 4% of the neutrons were captured after the prompt gate had closed and the cosmic ray neutron background was 0.2 n per gate. A feature of this system, essential for precise measurements, is the sampling of the background close to each event.

Throughout the experiment frequent measurements of $\bar{R}$ for either Pu^{240} or Cf^{252} have been made. In this way it was possible to use these elements as standards and make the other measurements relative to them. This was necessary because firstly, the boron pile had to be moved from GLEEP to the 5-MeV Van de Graaff accelerator, when its properties might have changed slightly, and secondly, to overcome possible long-term changes in the performance of the electronics and the counters. (In practice there is no evidence of efficiency changes greater than the experimental error (0.13%) during a period of 2 yr.)

CORRECTIONS TO EXPERIMENTAL DATA

Seven corrections have to be applied to the experimental values of $\bar{R}$:

(i) The count-rate effect.
(ii) The overlap correction.
(iii) The effect of fission chamber, ion chamber and beam tube on efficiency.
(iv) The correction for neutrons captured after the "prompt" gate has closed.
(v) The variation of efficiency with position in the central channel.
(vi) The effects of impurities in the fission foils.
(vii) The correction for delayed neutrons.

The count-rate correction exists because the gating system has a dead-time circuit that does not allow the "prompt" gate to reopen until the "background" gate has closed. Since the "prompt" gate is opened by the first event after the end of the dead time there is less background in the prompt gate due to events occurring before the gate than there is in the "background" gate. It can be shown that if the neutrons are captured exponentially after the event with a mean lifetime of τ s, a good approximation for the boron pile, then the ratio of the true to measured values of $\bar{R}$ is $1 + x\tau$ (x is the event count-rate per second). This correction has been verified experimentally and is 2.5% for x equal to 20. In practice the effect was rendered negligible by replicating the twin gates n times and triggering each "twin" in turn, thus using all the events. The above ratio then becomes $1/[1 - (x\tau/1 + x\tau)^n]$.

The overlap correction, which must be applied to the value of $\bar{R}$ to allow for the dead time of the scalers used to record the neutron counts through the gates, is small. Typically a dead time of 5 μs is used (3.5 μs is the minimum set by the pulses from the $B^{10}F_3$ counters). It can be shown that if first order overlap is considered and if the cosmic-ray background comes in bursts then the overlap losses in the "prompt" and "background" gates, $\Delta(P)$ and $\Delta(B)$ respectively, are given as follows:

$$\Delta(B) = \delta T \left(\frac{b^2}{T^2} + \frac{N\epsilon^2}{2\tau} (\sigma^2 + \bar{\nu}^2 - \bar{\nu}) + 2.3 \times 10^4 \right) \quad (1)$$

$$\Delta(P) = \frac{\delta}{2\tau} (1 - e^{-2T/\tau}) \epsilon^2 (\sigma^2 + \bar{\nu}^2 - \bar{\nu}) + 2\delta\epsilon\bar{\nu} (1 - e^{-T/\tau}) \frac{b}{T} + \Delta(B) \quad (2)$$

where δ is the dead time in seconds
τ is the gate length in seconds
b is the background per gate
ϵ is the efficiency of the pile
N is the number of events (i.e. fissions) occurring per second
σ^2 is the variance of the distribution in ν.

The third term in $\Delta(B)$ (δ T 2.3 $\times$ 10^4) is due to the burst nature of the cosmic-ray background. For Cf^{252}, which has the largest overlap correction, $\Delta(P) - \Delta(B)$ is 0.35% for a 4-ms gate and a 3.5-μs dead time.

Any material placed in the central hole in the pile, e.g. the fission chamber, reduces the efficiency of the pile. Care was taken to minimize this effect by using, as far as possible, materials with low thermal-absorption cross-sections but even so it is important because the maximum of the thermal-neutron distribution occurs at the centre of the pile. The effect has been measured by introducing the materials into the central hole and observing the reduction in the counts due to radio thorium D_2O, Pu^{240} (spontaneous fission) and plutonium-beryllium neutron sources placed at the centre of the pile. The results were used to calculate the effect as a function of absorber position and source neutron energy by assuming that it was proportional to the thermal neutron density at the position of the absorber. Table II shows the values of F, the factor by which the efficiency is reduced when the absorbers were in their normal operating positions.

A small fraction of the neutrons are captured after the "prompt" gate has closed. It is found experimentally that for times greater than 2 ms after the opening of the gate the rate of capture is exponential in form with a characteristic mean life that depends slightly upon the initial neutron energy spectrum and the equipment in the central hole. This correction can be made in most runs to an accuracy of $\pm$ 0.1% in $\bar{R}$.

There are two $B^{10}F_3$ counters, end to end, in all the lattice holes in the pile core except the central one. Because of counter construction all the neutrons captured in the B^{10} within the first 3 cm of the end of the counter are not recorded. This causes a dip in pile efficiency at the centre, which, though small, must be allowed for in all runs. It is found for instance that the efficiency increases by 0.2% if a fission source is moved 3 in away from the centre of the pile.

In the thermal fission measurements on GLEEP it was necessary to correct for the isotopic composition of the foils. For the Pu^{239} foils it was necessary to allow for the spontaneous fission of Pu^{240}, and for the Pu^{241} foils similar corrections were required for the Pu^{240} and Pu^{242} as well as for the Pu^{239}. No corrections were required for the U^{233} and U^{235} foils.

TABLE II

REDUCTION IN PILE EFFICIENCY PRODUCED BY EQUIPMENT IN THE CENTRAL CHANNEL

Equipment	Neutron spectrum or energy (MeV)	Reduction of efficiency by factor F	
Fission chamber used for thermal fission	Fission spectrum	1.0097	± 0.1%
Fission chamber used for fast fission	Fission spectrum	1.014	± 0.14%
Deuterium ion chamber	0.190 (Rd Th D_2O)	1.0200	± 0.1%
Deuterium ion chamber	0.265 (Na^{24})	1.0197	± 0.1%
Deuterium ion chamber and beam tube	2.0 ($F^{19}(p,\alpha\gamma)$)	1.0273	± 0.1%
Deuterium ion chamber and beam tube	4.9 ($Al^{27}(p,\gamma)$)	1.0195	± 0.1%

The delayed neutrons from fission are not counted in this experiment because the gate lengths are much shorter than the delayed neutron periods. The corrected values of $\bar{R}$ are therefore proportional to the number of prompt neutrons ($\bar{\nu}p$) per fission. The data of KEEPIN et al. [3], COX et al. [4] and COX [5] on delayed neutron fractions have been used to correct $\bar{\nu}_p$ to $\bar{\nu}$.

EXPERIMENTAL DIFFICULTIES AND POSSIBLE ERRORS

Electrical interference caused great difficulty during the calibration of the pile. The effect on the neutron counters and fission chambers was not serious but for the deuterium ion chamber much trouble was experienced particularly when ThC" and Na^{24} γ-rays were being used. The problem was reduced by accepting only those pulses from the ion chamber in anti-coincidence with pulses from an aerial and by making frequent "no-source" runs. This technique introduces a small correction because there is then likely to be less "pick-up" in the "prompt" gate than in the "background" gate.

During the experiment it was found that the Van de Graaff beam was modulated at 50 Hz because of the interaction of the beam with the magnetic field of the belt motors. Since the beam produces neutrons (for the calibration runs by (γ, n) reactions) the pile-neutron count is modulated. Since the events triggering the gating system are most likely to occur in the peaks of the current a background measured after a delay of 15 ms will be incorrect. This error can easily be eliminated by using a 20 ms delay between the opening of the "prompt" and "background" gates.

One of the most important effects that must be investigated is the possible anisotropy in the boron pile efficiency. It is possible to imagine that because of streaming down the lattice that neutrons starting out parallel

to the lattice will be detected less efficiently than those starting perpendicular to the lattice. Experiments have been done with Na^{24} γ-rays making use of the anisotropy of the photo-disintegration reaction. No evidence of any anisotropy in efficiency was found within the experimental error of 0.4%. It is believed that any anisotropy in efficiency cannot affect the efficiency calibration for an isotropic source by more than 0.2%.

The neutron beam used for the thermal $\bar{\nu}$ measurements contains fast neutrons. Cadmium difference runs were made to check that the effect of these was negligible.

The neutrons emitted in the fission process can cause a further fission if they interact with the fissile material either before they leave the fission chamber or after they have been thermalized. Experiments have been performed that show that the probabilities of such reactions are so small that the effects are negligible. The effect of thermalized neutrons causing fission is important in the fast fission measurements where the large neutron fluxes incident on the fission chamber result in many scattered neutrons producing a background of thermal fissions. This effect has been measured and typically gives a correction of 0.3%.

A possible systematic error in all $\bar{\nu}$ measurements is the loss of fissions due to the foil thickness. Since $\bar{\nu}$ is correlated with the total fragment kinetic energy the fissions that are missed are likely to have low kinetic energy and a high $\bar{\nu}$. This effect is unimportant for Cf^{252} because the foils are essentially "mass-less" and therefore Cf^{252} is a very good material for a standard. In the boron pile experiment the possible error due to this effect was considered by checking that $\bar{\nu}$ was not affected by variations of the fission chamber bias near the operating point. DIVEN [6] considered the problem by uniformly dispersing Cf^{252} in a uranium foil (1.2 mg/cm^2) and comparing the values of $\bar{\nu}$ (Cf^{252}) for this and a "mass-less" Cf^{252} foil. The results of these two experiments agree that there is no error greater than 0.3% introduced by foil thickness.

ANALYSIS OF DATA

Most of the data obtained in this experiment have been analysed using an IBM 7090 computer. The analysis was done in two stages. In the first stage the raw data were corrected for the effects as described above, and the results for each run written on to magnetic tape. (Approximately 700 runs were analysed and each run had up to nine gating circuits.) In the second stage of the analysis the runs were selected from the tape so that all similar runs (e.g. Cf^{252} data) could be averaged together and subjected to statistical tests. These tests verified that the errors assigned to the individual runs were reasonable and that no unknown systematic changes took place between the groups of runs obtained at different times. The data were also divided into day and night runs so as to verify that the effects of interference, which were much more serious for day runs, had been overcome. Two errors were obtained for any group of averaged runs; the error obtained from the errors of the individual runs (internal error) and the error obtained from the spread in values (external error). The larger of these two errors has always been used.

RESULTS

Table III gives the values of the thermal $\bar{\nu}$-ratios obtained. Table IV gives the values of $\bar{\nu}_p$ (E) for U^{235} relative to $\bar{\nu}_p$ for the spontaneous fission of Cf^{252}. Table V gives the values of $\bar{R}'$ which must be used to obtain the

TABLE III

$\bar{\nu}$-RATIOS FOR THERMAL AND SPONTANEOUS FISSION

Isotopes	$\bar{\nu}$-ratio	Error
U^{233}/U^{235}	1.020	0.006
Pu^{239}/U^{235}	1.182	0.008
Pu^{240}/U^{235}	0.888	0.005
Cf^{252}/U^{235}	1.557	0.007
Pu^{241}/U^{235}	1.210	0.011

TABLE IV

$\bar{\nu}_p$ (E) FOR U^{235} RELATIVE TO $\bar{\nu}_p(Cf^{252})$

Energy (MeV)	$\bar{\nu}_p(E)(U^{235})/\bar{\nu}_p(Cf^{252})$
0.101 ± 0.060	0.6566 ± 0.0126
0.514 ± 0.054	0.6679 ± 0.0118
0.571 ± 0.156	0.6648 ± 0.0069
0.572 ± 0.015	0.6625 ± 0.0077
0.604 ± 0.053	0.6660 ± 0.0060
0.946 ± 0.128	0.6695 ± 0.0052
1.497 ± 0.109	0.6851 ± 0.0052
2.123 ± 0.095	0.7092 ± 0.0057
2.572 ± 0.085	0.7209 ± 0.0063

absolute values of $\bar{\nu}$ for Cf^{252} and U^{235} ($\bar{R}'$ is the value of $\bar{R}$ corrected for effects (a) to (f) given in Section 3). The $\bar{\nu}$-values for other isotopes can be obtained by using the ratios given in Table III. The errors given are those due to statistics, pile stability and the error in F.

PENDLEBURY [7] has calculated the variation of the pile efficiency with energy by the Carlson S_n method assuming that the pile is a spherical homogeneous assembly with a reflector. A correction has been made to this calculation to allow for the end effects of the counters and the resulting curve is shown in Fig. 2 normalized so that the efficiency at 2 MeV is 1.0. Also shown are the normalized experimental values of efficiency and the

TABLE V

$\bar{R}'$ VALUES

Experiment	Neutron energy	$\bar{R}'$	Error (%)
Cf^{252}	Fission	2.3811	0.11
U^{235}	Fission	1.5230	0.40
ThC"	190 keV	0.6440	0.60
Na^{24}	265 keV	0.6457	0.21
$F^{19}(p\alpha\gamma)$	2.0 MeV	0.6433	0.25
$Al^{27}(p\gamma)$	4.9 MeV	0.6500	1.24

Cf^{252} fission-neutron energy spectrum. It can be seen that the calculated curve does not fit the experimental data very well (which is perhaps not

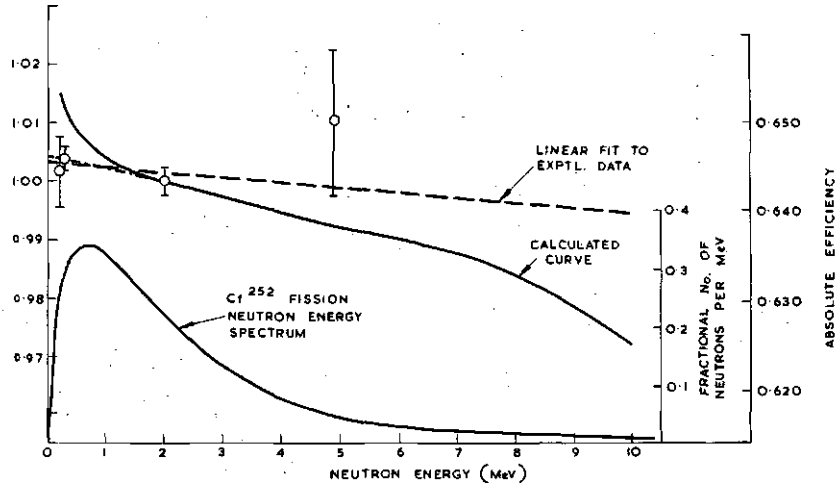

Fig.2

Variation of boron pile efficiency with energy

surprising because of the assumptions made) and so it is difficult to obtain a "best value" for the pile efficiency for a fission spectrum. Table VI lists the values of efficiency obtained for various assumptions. It is assumed that the second assumption gives the correct efficiency and this gives a value of 0.6428 ± 0.0020 for both the U^{235} and Cf^{252} fission spectra. Using this value of the efficiency and applying the corrections for delayed neutrons the absolute $\bar{\nu}$ values for Cf^{252} and U^{235} are

$$\bar{\nu}\ (Cf^{252}) = 3.713 \pm 0.015$$

$$\bar{\nu}\ (U^{235}) = 2.385 \pm 0.015.$$

Table VII gives the contributions to the final errors.

TABLE VI

EFFICIENCY FOR A Cf^{252} FISSION SPECTRUM

Assumed variation of efficiency with neutron energy	Efficiency
Linear least-squares fit to experimental data	0.6438
Straight line through 265-keV and 2-MeV data for energies < 2 MeV. Above 2 MeV the calculated curve.	0.6428
Calculated curve normalized as 1 at 2 MeV	0.6442
Calculated curve normalized at 265 keV	0.6401
Best fit of calculated curve to experimental data (2-MeV efficiency = 0.9955)	0.6413
Independent of neutron energy (weighted mean of experimental data)	0.6447

TABLE VII

ERRORS IN $\bar{\nu}$ VALUES

Error	Contribution to error in $\bar{\nu}$ (%)	
	Cf^{252}	U^{235}
Efficiency	0.31	0.31
Value of $\bar{R}'$ for fission	0.11	0.40
Loss of fissions below bias	-	0.30
Effect of electrical pick-up	0.03	0.03
Van de Graaf beam modulation	0.05	0.05
Anisotropy in efficiency	0.20	0.20
Correction for neutrons captured after the gate	0.10	0.10
Total error	0.40	0.63

DISCUSSION

Tabulations of the results of the many experiments made to determine $\bar{\nu}$ have been given by LEACHMAN [8] and ASPLUND-NILSSON [9]. Recently accurate data, which can be compared with the present measurements, have been obtained with large liquid scintillators by HOPKINS and DIVEN [10], ASPLUND-NILSSON et al. [11] and MATHER et al. [12, 13]. The values of $\bar{\nu}$ ratios obtained in this experiment are in good agreement with the other

measurements and therefore the discussion will be concentrated on the absolute $\bar{\nu}$-values.

Three accurate absolute measurements of $\bar{\nu}$ have now been made using the associated particle technique for calibration. The results of these measurements for $\bar{\nu}$ (Cf^{252}) are 3.780 ± 0.030 (HOPKINS and DIVEN [10]), 3.808 ± 0.034 (ASPLUND-NILSSON et al. [11]) and 3.713 ± 0.015 (boron pile). The equivalent U^{235} $\bar{\nu}$-values are 2.441 ± 0.030, 2.447 ± 0.030 and 2.385 ± 0.015. The two liquid scintillator measurements agree within one standard error and are appreciably higher than the boron pile datum. In order to get the boron pile value as high as 3.78 the efficiency would have to be approximately 0.632 (assuming the efficiency measurement to be in error). Such an efficiency appears to be unreasonable when one considers the efficiency measurements, particularly since one of the important features about this experiment is that the corrections to the data have either been measured or, if calculated, verified experimentally.

Absolute values of $\bar{\nu}$ can also be obtained from measurements of η and α (η is the number of neutrons per neutron captured and α is the ratio of the capture and fission cross-sections). Taking the U^{235} input data used by WESTCOTT et al. [14] in their recent compilation (η = 2.0761 ± 0.0084 α = 0.1733 ± .002) one obtains $\bar{\nu}$ (U^{235}) = 2.436 ± 0.011 ($\bar{\nu}$ (Cf^{252}) obtained by using Cf^{252}/U^{235} ratio in Table III is 3.780 ± 0.024). The only other measurements of absolute $\bar{\nu}$ values which have sufficient accuracy to be considered in this discussion are those made by KENWARD et al. [15] and MOAT et al. [16] and which used the Harwell spontaneous fission source for calibration. In both these experiments the neutron detectors consisted of BF_3 counters embedded in paraffin wax and such systems are sensitive to neutron energy spectrum differences. FIELDHOUSE [17] has recently reconsidered the strength of the Harwell spontaneous fission source and suggests that the source strength should be (1.989 ± 0.016) × 10^4 n/s. This is 2.3% lower than the value used in these two experiments. Using this new value the absolute $\bar{\nu}$ values obtained are (assuming the errors can be reduced because of the increased accuracy in the source strength) $\bar{\nu}$(U^{235}) = 2.363 ± 0.021 (Kenward et al.) $\bar{\nu}$ (Cf^{252}) = 3.69 ± 0.052 (Moat et al.). These values are consistent with the boron pile data though the Moat et al. value is also consistent with the other data. It would therefore appear that there is some discrepancy in the absolute $\bar{\nu}$ measurements; the measurements made with the liquid scintillators and the value deduced from η and α are appreciably higher (1 - 2%) than the boron pile values and the values obtained using the Harwell standard spontaneous fission source.

The $\bar{\nu}$ (E) data given in Table IV agree very well with the data of MATHER et al. [12], HOPKINS and DIVEN [10] and MEADOWS and WHALEN [18] for energies greater than 1 MeV. Below 1 MeV the data are higher than expected on the assumption of a linear variation of $\bar{\nu}_p$(E) through the thermal value and data above 1 MeV. The data are consistent with the conclusions of BLYUMKINA et al. [19] who for U^{235} suggest that because of channel effects ν_p(E) is not linear with energy in this energy region.

CONCLUSIONS

The following conclusions can be made about the results of the boron pile experiment:

(i) Absolute accurate values of $\bar{\nu}$ have been measured with an accuracy varying between 0.4% (Cf^{252}) and 1.11% (Pu^{241}).

(ii) These $\bar{\nu}$-values do not depend upon calculated corrections. All corrections have either been measured or, if calculated, verified experimentally.

(iii) The absolute $\bar{\nu}$ values obtained in this experiment are about 2% lower than the absolute values produced by the large liquid scintillator technique though the $\bar{\nu}$ ratios and the relative $\bar{\nu}$ (E) measurements are in reasonable agreement. The values obtained from the measurements of η and α agree with the liquid scintillator data and the values obtained using the Harwell spontaneous fission neutron source agree with the boron pile data.

(iv) The boron pile experiment is fundamentally different from the liquid scintillator experiments and the differences between the results could well be due to systematic errors that will be different for the two types of measurement.

ACKNOWLEDGEMENTS

The authors are indebted to Mr. R.I. Macdonald and Mr. J.R. Johnson for their excellent assistance during this experiment. The support and encouragement of Dr. E. Bretscher is gratefully acknowledged.

REFERENCES

[1] FIELDHOUSE, P. and CULLIFORD, E.R., Neutron Dosimetry 2 IAEA, Vienna (1963) 565.
[2] COLVIN, D.W. and SOWERBY, M.G., Proc. 2nd UN Int. Conf. PUAE 16 (1958) 121.
[3] KEEPIN, G.R., WIMMETT, T.F. and ZEIGLER, R.K., Phys. Rev. 107 (1957) 1044.
[4] COX, S., FIELDS, P., FRIEDMAN, A., SJOBLOM, R. and SMITH, A., Phys. Rev. 112 (1958) 960.
[5] COX, S., Phys. Rev. 123 (1961) 1735.
[6] DIVEN, B.C., private communication.
[7] PENDLEBURY, E., private communication.
[8] LEACHMAN, R.B., Proc. 2nd UN Int. Conf. PUAE 15 (1958) 229.
[9] ASPLUND-NILSSON, I., FOA4 Rapport A 4200-411 (1963).
[10] HOPKINS, J. and DIVEN, B.C., Nucl. Phys. 48 (1963) 433.
[11] ASPLUND-NILSSON, I., CONDÉ, H. and STARFELT, N., Nucl. Sci. Engng 16 (1963) 124.
[12] MATHER, D.S., FIELDHOUSE, P. and MOAT, A., Phys. Rev. 133 (1964) B1403.
[13] MATHER, D.S., FIELDHOUSE, P. and MOAT, A., private communication.
[14] WESTCOTT, C.H., EKBERG, K., HANNA, G.C., PATTENDEN, N.J. and SANATANI, S., Proc. 3rd UN Int. Conf. PUAE (1964) Paper 717.
[15] KENWARD, C.J., RICHMOND, R. and SANDERS, J.E., AERE R/R 2212 (1958).
[16] MOAT, A., MATHER, D.S. and McTAGGART, M.H., Reactor Sci. Technol. 15 (1961) 102.
[17] FIELDHOUSE, P., private communication.
[18] MEADOWS, J.W. and WHALEN, J.F., Phys. Rev. 126 (1962) 197.
[19] BLYUMKINA, YuA., BONDARENKO, I.I., KUZNETSOV, V.F., NESTEROV, V.G., OKOLOVITCH, V.N., SMIRENKIN, G.N. and USACHEV, L.N., Nucl. Phys. 52 (1964) 648.

DISCUSSION

G. HANNA: Was the standard neutron source you referred to a spontaneous fission neutron source?

M. SOWERBY: No. The agreement in neutron source calibration between the N.P.L. and the boron pile that I described was for a Ra-γ-Be source. Similar agreement is obtained for the Atomic Weapons Research Establishment spontaneous fission source.

THE ENERGIES, ANGULAR DISTRIBUTION AND YIELDS OF THE PROMPT NEUTRONS FROM INDIVIDUAL FRAGMENTS IN THE THERMAL-NEUTRON FISSION OF U^{233} AND U^{235}

J.C.D. MILTON AND J.S. FRASER
CHALK RIVER NUCLEAR LABORATORIES
CHALK RIVER, ONT., CANADA

Abstract — Résumé — Аннотация — Resumen

THE ENERGIES, ANGULAR DISTRIBUTION AND YIELDS OF THE PROMPT NEUTRONS FROM INDIVIDUAL FRAGMENTS IN THE THERMAL-NEUTRON FISSION OF U^{233} AND U^{235}. An apparatus for simultaneously recording the velocities of both fission fragments and the velocity of a neutron at any one of four angles to the fragment direction has been used to investigate the neutron-emission properties of individual fragments. Early results for U^{233} exhibit the saw-tooth variation of ν, the neutron yield per fragment, observed in the spontaneous fission of Cf^{252}. The yields in the vicinity of mass 130 are consistent with no neutrons being emitted from these fragments. Unlike the neutron yields, the average neutron kinetic energy is symmetric about the symmetric mass point, being high near this point and low at the most probable mass division. The paradox between very small yields and high apparent nuclear temperatures has been qualitatively explained on the basis of a model that takes account of shell structure in the level densities and assumes that at the time of scission the fragments are cold but in some cases highly deformed, in others nearly spherical. The model is supported by the fact that in fissions with more than the average total excitation energy, the fragments near mass 130 and 80 receive much less than half the increase in energy and the other fragment of the pair much more.

The experiment is now being conducted with U^{235} under considerably improved conditions. The background per channel under the neutron spectrum has been reduced by nearly a factor of three, so that 0.39 of all recorded events in the 10° detector are useful neutron events with a corresponding increase in statistical accuracy. Better time resolution in the fragment system (1.5 ns, full width at half maximum) has allowed the flight paths to be shortened to 125 and 100 cm (formerly 145-145 cm) with a concomitant higher counting-rate.

RENDEMENTS EN NEUTRONS INSTANTANÉS ÉMIS PAR LES FRAGMENTS DE LA FISSION DE ^{233}U ET ^{235}U PAR DES NEUTRONS THERMIQUES — ÉNERGIES ET DISTRIBUTION ANGULAIRE DE CES NEUTRONS. Pour étudier les propriétés des fragments de fission relatives à l'émission de neutrons, les auteurs ont utilisé un appareil permettant d'enregistrer simultanément les vitesses des deux fragments de fission et la vitesse d'un neutron faisant l'un quelconque des quatre angles donnés avec la direction du fragment. Les premiers résultats dans le cas de ^{233}U montrent que ν, rendement en neutrons par fragment, subit les variations en dents de scie déjà observées dans la fission spontanée de ^{252}Cf. Au voisinage de la masse 130, les rendements sont compatibles avec le fait qu'aucun neutron n'est émis par ces fragments. Contrairement aux rendements en neutrons, la moyenne de l'énergie cinétique des neutrons est symétrique par rapport au point de masse symétrique; elle est haute au voisinage de ce point et basse au point correspondant à la répartition la plus probable des masses. Les auteurs expliquent qualitativement le paradoxe existant entre les très petits rendements et les hautes températures nucléaires apparentes en se fondant sur un modèle qui tient compte de la structure en couches dans les densités du niveau et qui suppose qu'au moment de la scission les fragments sont froids mais parfois fortement déformés et parfois à peu près sphériques. L'hypothèse de ce modèle est confirmée par le fait que, dans les fissions où l'énergie d'excitation totale est supérieure à la moyenne, les fragments dont les masses sont voisines de 130 et 80 reçoivent beaucoup moins que la moitié de l'accroissement en énergie, tandis que l'autre fragment de la paire en reçoit beaucoup plus.

A l'heure actuelle, les auteurs font une expérience sur ^{235}U dans des conditions sensiblement améliorées. Le bruit de fond par canal en dessous du spectre des neutrons a été réduit d'un facteur de presque trois, de sorte que 39% de tous les événements enregistrés dans le détecteur à 10° sont des événements neutroniques utiles et qu'on observe une augmentation correspondante de l'exactitude statistique. Une meilleure résolution en temps dans le système des fragments (1,5 ns, largeur entière à mi-hauteur du maximum) a permis de ramener

les trajectoires de vol à 125 et 100 cm (précédemment 145 et 145 cm) et d'augmenter concurremment le taux de comptage.

ЭНЕРГИИ, УГЛОВЫЕ РАСПРЕДЕЛЕНИЯ И ВЫХОДЫ МГНОВЕННЫХ НЕЙТРОНОВ ИЗ ОТДЕЛЬНЫХ ОСКОЛКОВ ПРИ ДЕЛЕНИИ УРАНА-233 И УРАНА-235 ТЕПЛОВЫМИ НЕЙТРОНАМИ. Для изучения характеристик эмиссии нейтронов отдельными осколками использовался прибор для одновременной регистрации скоростей осколков деления и скоростей нейтронов для любого из четырех углов по направлению движения осколков. Предварительные результаты для урана-233 показывают пилообразную вариацию выхода нейтронов на каждый осколок (ν), наблюдавшуюся при спонтанном делении калифорния-252. Выходы вблизи массы 130 совместимы с отсутствием эмиссии нейтронов из этих осколков. В отличие от выходов нейтронов средняя кинетическая энергия нейтронов является симметричной около симметричной точки массы, является высокой вблизи этой точки и низкой в точке наиболее вероятного деления массы. Парадокс между очень небольшими выходами и высокими ядерными температурами был качественно объяснен на основании модели, которая учитывает структуру оболочки при плотностях уровней и предполагает, что во время деления осколки являются холодными, но в некоторых случаях они сильно деформированы, а в других случаях имеют почти сферическую форму. Правильность этой модели подтверждается тем фактом, что при делениях с более чем средними общими энергиями возбуждения осколки, имеющие массы, близкие к 130 и 80, получают гораздо меньше половины увеличения энергии, а другой осколок пары получает значительно большую энергию.

В настоящее время проводится эксперимент с ураном-235 при значительно улучшенных условиях. Фон на каждый канал при наличии спектра нейтронов уменьшен почти в три раза, так что 0,39 всех зарегистрированных явлений в 10° детекторе являются полезными нейтронными явлениями, что соответствует повышению статистической точности. Более хорошая разрешающая способность по времени в системе осколков (1,5 наносек на полной ширине половины максимума) позволила сократить траектории полета до 125 и 100 см (раньше эти расстояния составляли 145—145 см) при одновременном повышении скорости счета.

ENERGIAS, DISTRIBUCIONES ANGULARES Y RENDIMIENTOS DE LOS NEUTRONES INMEDIATOS EMITIDOS POR LOS DISTINTOS FRAGMENTOS EN LA FISION DEL ^{233}U Y DEL ^{235}U INDUCIDA POR NEUTRONES TERMICOS. Para investigar las propiedades de emisión neutrónica de los distintos fragmentos de fisión se ha utilizado un aparato que registra simultáneamente la velocidad de los dos fragmentos y la velocidad de los neutrones en uno cualquiera de cuatro ángulos formados con la dirección de los fragmentos. Los resultados iniciales correspondientes al ^{233}U indican que ν, esto es, el rendimiento neutrónico por fragmento observado en la fisión espontánea del ^{252}Cf, varía según una función en dientes de sierra. A juzgar por los rendimientos en las proximidades de la masa 130, los fragmentos correspondientes no emiten neutrones. A diferencia de los rendimientos neutrónicos, la energía cinética media de los neutrones es simétrica respecto del punto de simetría másica, siendo elevada en las proximidades de dicho punto y reducida en el de división másica más probable. La paradoja que suponen los muy reducidos rendimientos y las elevadas temperaturas nucleares aparentes se explica, desde el punto de vista cualitativo, mediante un modelo que refleja la estructura de capas de la densidad de los niveles y se funda en la hipótesis de que, en el momento de la escisión, los fragmentos están fríos, pero muy deformados en algunos casos, mientras que en otros su forma es casi esférica. La validez del modelo es confirmada por el hecho de que en las fisiones con energías de excitación superiores a la total media, los fragmentos cuya masa es del orden de 130 y de 80 reciben mucho menos de la mitad del incremento de energía, mientras que el fragmento complementario adquiere una proporción mucho mayor.

En la actualidad, el experimento se suele realizar con ^{235}U en condiciones considerablemente perfeccionadas. La actividad de fondo por canal de fisión en el espectro neutrónico se ha reducido casi a un tercio, de forma que pueden aprovecharse 39 de cada cien sucesos registrados en el detector de 10°, con el consiguiente aumento de la precisión estadística. En el sistema de análisis de los fragmentos, la mejora del poder resolutivo en cuanto al tiempo (1,5 ns, de anchura total a la mitad del máximo) ha permitido acortar las trayectorias de vuelo, que son ahora de 125 y 100 cm (antes de 145 y 145 cm), con la consiguiente elevación del índice de recuento.

INTRODUCTION

In recent years several experiments [3, 7, 11, 12] on the prompt fission neutrons have gathered much information on the division of excitation energy between the fragments. The experiment reported here is similar to one already reported for Cf^{252} [3]. It attempts to measure the velocity and angular distributions of the neutrons for fragments of a given mass and energy. The mass resolution obtained is slightly less than two mass units.

EXPERIMENTAL ARRANGEMENT

The energies and masses of the fragments and the energies of the neutrons are all defined by time-of-flight using the apparatus shown in Fig. 1. In the present arrangement the fragment flight paths are 125 and 99 cm. The method of timing the fragments has been described in detail elsewhere [1, 2]. The neutrons are detected in cylinders of NE 102 plastic 5-in diam. × 2-in thick after transversing a 106-cm flight path. The over-all time resolution of both systems is 1.5 ns (full width at half maximum (FWHM)). With the present flight paths this leads to a fragment mass resolution of 1.8 mass units and energy resolution of 4.2% or 7 MeV. A calculation of neutron energy resolution must include the spread, estimated as 3 cm [3], due to the detector thickness as well as the time spread. The result depends markedly on neutron velocity, e.g.

$$\frac{\Delta V}{V} = \frac{1}{D}\left[(\Delta t V)^2 + (\Delta x)^2\right]^{1/2} = \begin{cases} 3.2\% \text{ at } V = 1 \text{ cm/ns} \\ 7.6\% \text{ at } V = 5 \text{ cm/ns.} \end{cases}$$

These two velocities, corresponding to neutron energies of 0.52 and 13.1 MeV, are chosen in the present experiment as limits of the useful energy range.

The neutron beam from the NRU reactor is filtered through 6 in of bismuth and 8 in of quartz maintained at liquid nitrogen temperature to give a thermal flux of $\sim 2 \times 10^8$ n/cm^2.s at the position of the source. Under these conditions a thin source of about 40 μg/cm^2 of U^{235} gives a coincidence fission rate in the 4-in detectors of 460 counts/min. The bias on the neutron detectors is set somewhat below the Am^{241} 60-keV gamma peak. At this low bias setting of about 30-keV electron energy, in addition to the good beam quality achieved by filtering, the neutron counters must be heavily shielded to reduce the background counting-rate. The present shielding consists of 2 in of lead surrounding the outside of the detector-photomultiplier assembly, 9/16 in of lead and 3/16 in of borated polythene in front of the detectors, and laminated iron and borated polythene sheets placed between the source and the detectors (see Fig. 1). This combination of shielding and filtering reduced the rate in the neutron detectors to 50 000 - 100 000 counts/min. The total event rate for all four counters is about 6/min, about half of which are acceptable neutron events. About 7 weeks running-time was required to garner the 150 000 events reported for U^{235} in this paper.

All flight times are converted to pulse amplitudes in six time-to-amplitude converters, two for the fragments and four for the neutrons (see Fig. 1), and subsequently digitized in three 256 channel encoders, one for

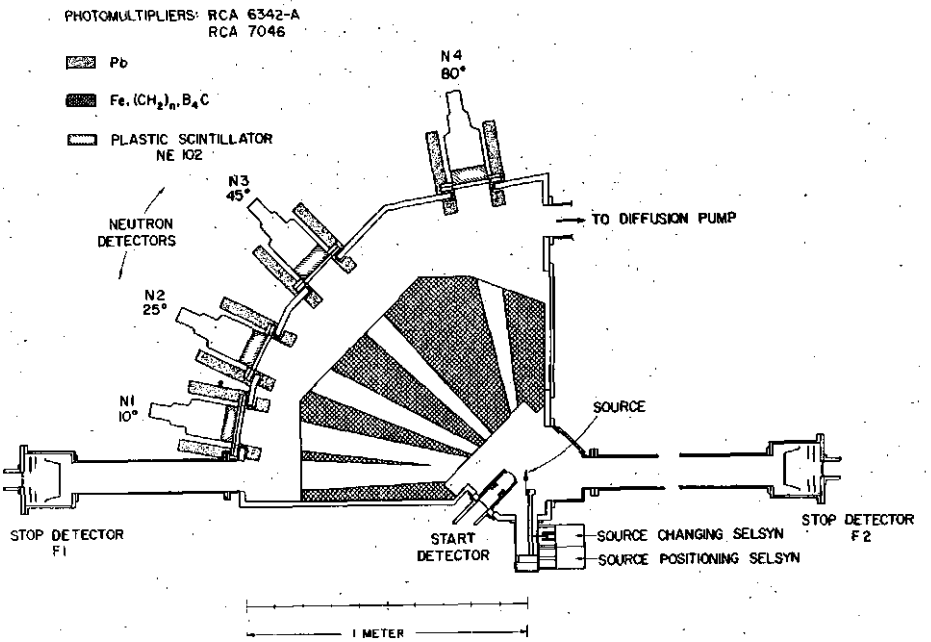

Fig. 1

Neutron-fragment time-of-flight apparatus.
The fission detector distances are not to scale,
and the lead and borated polythene shields in front of the detectors are not specifically shown.

each of the fragments, and one for all four neutron detectors. An event then consists of two fragment flight times, a neutron flight time and a neutron counter number punched on five-channel paper tape. If pulses arrive in two or more neutron counters within 1 μs the event is rejected. Time calibrations are punched on the tapes about every 10 000 events and distinguished from neutron events by a special code. The calibrations cover a range of 100 ns, and are done automatically by a motor-driven, air-cored, helical delay line [4], and give the slope of the time versus channel number line. The zero of the fragment time scale was determined by placing the stop detectors, one by one, as close as possible to the source. The zero of the neutron time scale is obtained by observing the position of the prompt gamma-ray peak.

The efficiency of the neutron detectors is obtained by comparing the observed time-of-flight spectrum in each of the four counters with the accurately known U^{235} neutron spectrum [5]. In order to make the comparison, it is necessary to average over all fragment directions. This is done with a U^{235} source on a stainless steel backing in a 2π solid-angle gas scintillation counter that replaced the source and start foil assembly (see Fig. 1). A mixture of about 25% nitrogen, 75% argon flowing through the counter optimized the pulse height. A typical neutron detector efficiency, shown in Fig. 2, goes to zero at about 200 keV, has an average value of 50% for the fission spectrum, and goes to very high values at high energies. The increase in ap-

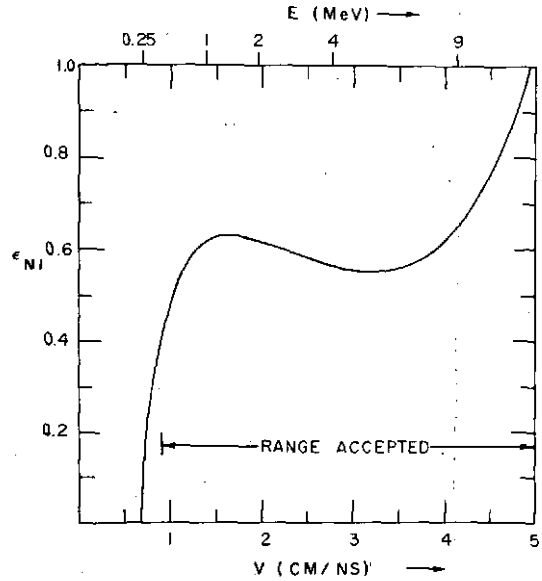

Fig. 2

Representative apparent efficiency of the neutron detectors in situ.
The rise at high energies is attributed to detection of the gamma ray following inelastic scattering.

parent efficiency above 4 MeV does not occur when the measurement is done with source and detector moved into the air, well removed from large amounts of material, and is therefore attributed to inelastic scattering (n, n'γ), especially in the iron of the interior shielding, with subsequent detection of the gamma ray. The curve in Fig. 2 does not imply that detection efficiencies of over 100% are obtained. But if the curve obtained in this way is used as an apparent efficiency, a zeroeth order correction for resolution and spectral distortion due to scattering is made automatically. The correction would be exact if the spectral shapes during calibration and actual runs were the same. They are not, however, and further corrections must be made.

DATA PROCESSING

Local, and temporary, pecularities of the computing facilities demand that the punched paper tape be converted to punched cards for final loading on magnetic tape. This gives us the opportunity of removing the calibration cards. Daily checks on the calibration are made, and at the end of a run all calibration events are fitted by least squares to obtain the slopes of the calibration lines.

While the data are being loaded on to Bendix G-20 compatible tape they are sorted into four groups corresponding to the four neutron counters. Further data processing starts from this point with the four angles treated separately.

After a preliminary inspection, the neutron time-of-flight spectrum is divided into four regions. In order these are: background, gamma, neutron

and background. In the first pass-through of the tape, fission fragments associated with the two background regions are sorted to determine the "normal" distribution, i.e. the number of fissions as a function of mass and energy without reference to neutron emission. This distribution should be the same as that obtained previously [1] but the method has the advantage of providing the normal distribution under identical conditions to those obtaining when the neutrons are actually being measured. To use this method it is important that the random background is not too low in order to get reasonable statistical accuracy.

On the second pass, gamma events are sorted and a Gaussian fitted to the peak to obtain the zero of the neutron time scale. Proper attention to the fragment initiating the coincidence is necessary here and subsequently, because of the separation of 4.5 cm between the source and start foils (Fig. 1). Every event is corrected exactly for this effect.

On the third pass, events in the two background regions are folded into the neutron region in such a way that there is a one-to-one correspondence between a channel in the neutron region and one in the background region. The event is then treated as a background event with the new channel number. The four velocity moments $\langle V^0 \rangle$, $\langle V^1 \rangle$, $\langle V^2 \rangle$ and $\langle V^4 \rangle$ in both the laboratory and centre-of-mass co-ordinate systems are then calculated. In so doing the "weight" attached to each event is computed from the known total number of fissions, and the detector efficiency, solid angle and inefficiency due to neutron recoil. The latter effect is a loss of counts caused by the non-collinearity of the fragments. In making the correction, the proper angle and velocity of the observed neutron is used, the number of unobserved neutrons as a function of fragment mass and energy is guessed at, and the direction and energy of the unobserved neutrons is assumed to be uncorrelated with the observed one. At the same time the fragment velocity is corrected for the neutron recoil. Each event is then sorted, with its proper weight, into each of eight two-dimensional arrays (for the eight velocity moments) whose co-ordinates are the mass and total kinetic energies of the fragments. In addition, two further two-dimensional arrays keep track of quantities necessary in estimating the statistical errors. At the end of this pass the moments of the background are stored as negative numbers.

The treatment of the neutron region in the fourth pass is identical to that described above, except for the sign of the weights and the conversion of the channel numbers, which is now superfluous.

In addition to the moment information for all fragment masses and energies, the computer also stores the complete velocity spectrum for the two major fragment groups, light and heavy. All the processing so far described requires roughly 12 ms/neutron event. At the conclusion of this stage, which requires about 24 min for the 120 000 events at 10°, the computer plots and prints a large number of summaries under various options. Some of these will now be described.

RESULTS

At the time of writing, the data were still being acquired and the results must therefore be considered provisional. This paper reports on about

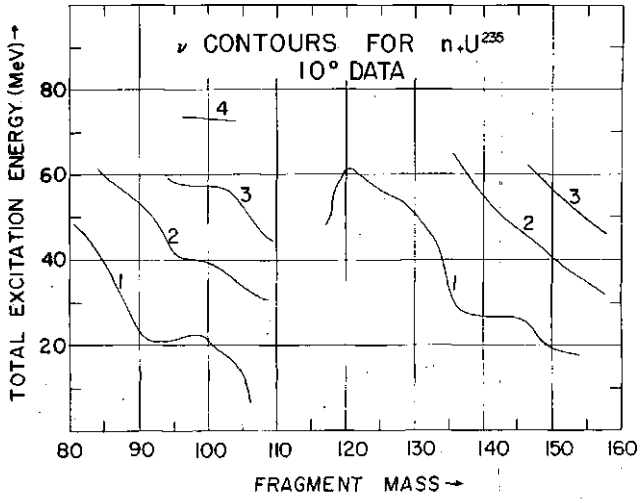

Fig. 3

Contours of the $\nu(M, E^*)$ surface for thermal-neutron fission of U^{235} as observed in the 10° counter. The numbers attached to the contours are number of neutrons per fragment. No corrections have been made to the data and considerable smoothing has been done, so that the exact location and shape of the contour lines should not be taken too seriously.

150 000 neutron events obtained for U^{235} between early November and late January 1965.

The curves in Figs. 3 and 4 are traced directly from plots made by the computer. Figure 3 shows the contours of the $\nu(M, E^*)$ surface (ν is the number of neutrons per fragment, M is the fragment mass and E^* is the total excitation energy calculated from the energy releases of reference [6] and the known kinetic energies). Clearly the surface is not a simple one, but has considerable structure. Some of this structure is brought out more clearly in Fig. 4, in which the number of neutrons per fragment, ν, and $\langle V^2 \rangle$ (proportional to their average centre-of-mass energy) is plotted versus fragment mass as deduced from the 10° data. The mass yield is shown for comparison. (The relatively lower heavy fragment mass yield is not yet understood.) The over-all saw tooth nature of the curve is readily apparent. Detailed comparisons of this curve with that of APALIN et al. [7] have not been attempted for reasons that will be stated later. It is clear, however, that our results show considerably more structure than Apalin's. In particular, the statistically significant peaks at masses 90, 96 and 101 correlate exactly with the fine structure in the mass yields noted earlier [2]. The greater statistical scatter in the average centre-of-mass energy E_{CM} curves (middle of Fig. 4), precludes any definite statement about corresponding fine structure, but in its over-all appearance, the variation of E_{CM} with fragment mass is similar to that of U^{233} (see Fig. 5) and Cf^{252} [3]. The most striking effect is the increase in E_{CM} in the region of mass 134, where the number of neutrons is nearly zero. In fact, unlike the ν curve, the E_{CM} curve is very nearly symmetric about the equal mass split point, 118.

Qualitative explanations of the ν and E_{CM} variation with mass have been discussed by MILTON [8] and it is shown that both the statistical model of

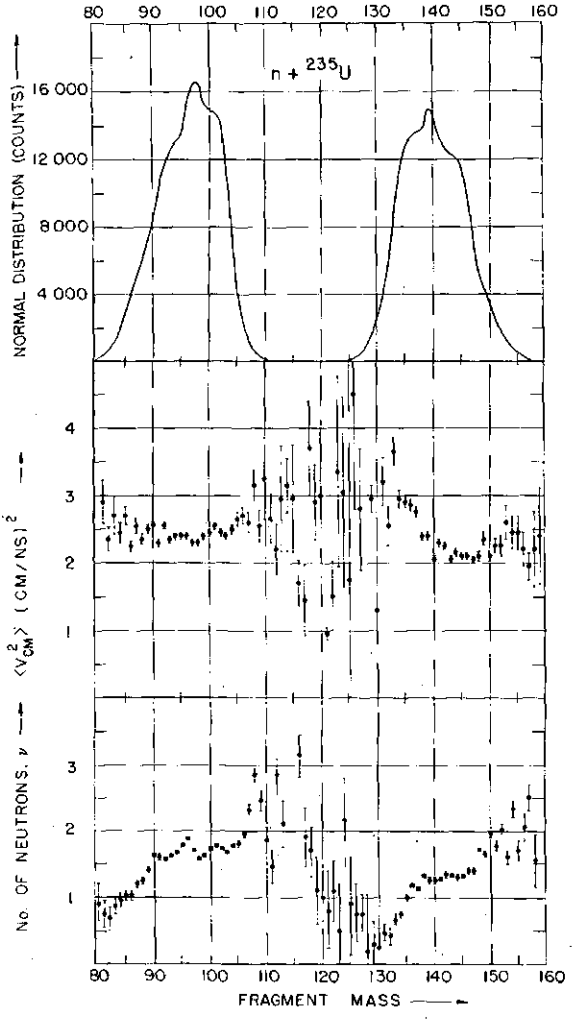

Fig. 4

Bottom.

Number of neutrons per fragment ν versus fragment mass for U^{235}.

No correction has been made for "scission" neutrons or for the contribution of one fragment to the other member of the pair.

This correction will be largest near mass 80 because of the relatively low velocity of, and large number of neutrons emitted by, the heavy fragments.

Middle.

Average centre-of-mass moment $\langle v^2 \rangle = \langle E_{CM} \rangle / 0.5228$.

Corrections for neutrons from the other fragment should be small here.

Top.

Mass yield shown for orientation. In a perfect experiment the peaks should be symmetric about mass 118.

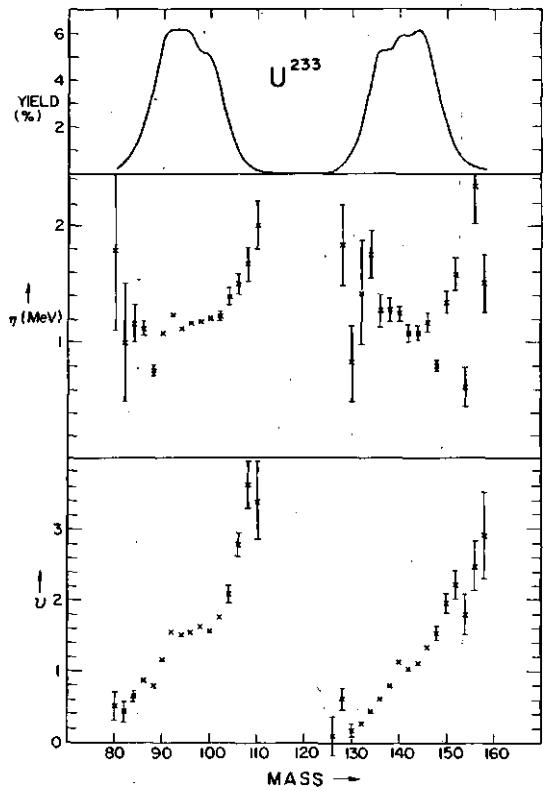

Fig. 5

As in Fig. 4 but for n + U^{233}. The symbol η is used for E_{CM}.

hot fragments in contact, and the "fragment-shell" model of cold fragments at scission, sometimes distorted, sometimes not, lead to similar predictions. However they differ qualitatively in their prediction of the rate of change of ν with total excitation energy, $d\nu/dE^*$. It is shown in Ref. [8] that the statistical model predicts a variation of $d\nu/dE^*$ with fragment mass that generally increases with mass but is extra large near the closed shells at masses 80 and 132. TERRELL [9] has pointed out that average values of $\langle d\nu/dE^* \rangle$ may be obtained from data such as ours by calculating the conditional co-variances $C(\nu, E;M) = \langle \nu E \rangle_M - \langle \nu \rangle_M \langle E \rangle_M$ and variances $\sigma^2 (E;M) = \langle E^2 \rangle_M - \langle E \rangle_M^2$. The method is identical to a suitably weighted least-squares fit of the data to straight lines with slopes $\langle d\nu/dE^* \rangle$. This quantity is plotted in Fig. 6. This figure has not yet been corrected for fragment energy resolution and the corrections are likely to be large. However they will not alter the fact that for the fragment pair 104-132 $\langle d\nu/dE^* \rangle$ is large for the light fragment and small for the heavy, in contradiction to the prediction of the statistical model. If ν is taken as a measure of the excitation energy going into an individual fragment, this means that for the pair 104 - 132 any increase in total excitation energy to be shared is taken preferentially by the light fragment. This is exactly what would be expected if the light fragment

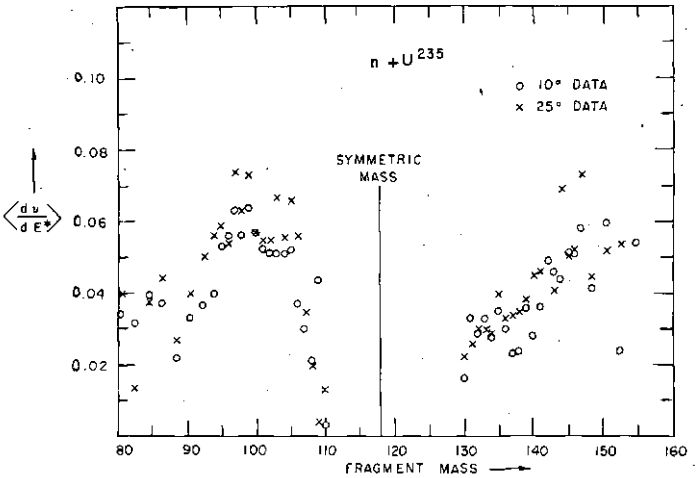

Fig. 6

Average slopes $\langle d\nu/dE^* \rangle$ of the curves of ν versus E^* as a function of fragment mass. The points are not corrected for experimental fragment energy resolution. This correction will be large. The weighted average of $\langle d\nu/dE^* \rangle$ over all fragments should be 1/6.6 = 0.15 neutrons/MeV. As in Figs. 4 and 5 all neutrons are assumed to come from the fragment heading towards the indicated counter.

in this pair were easily deformable, and the heavy very stiff, as predicted by the fragment shell theories [5, 8, 10].

Turning now to a slightly different point, that of the energy deficit at symmetric fission [1], the present experiment confirms the conclusion of APALIN et al. [11] that the missing energy appears as neutrons. In Fig. 7 the total excitation energy, as deduced from the number of neutrons and their energies plus 7.5 MeV of gamma-ray energy, is compared with the same quantity calculated from the energy released [6] and the measured total kinetic energy. The agreement appears to be within the errors associated with the measurements.

ORIGIN OF THE NEUTRONS

Apart from the remarks of the last paragraph, all the results of the previous section are based upon the assumption that neutrons are emitted more or less isotropically from moving fragments. So far we have not investigated this point as critically as previous workers [3, 12]. We have, however, made quite a large number of least-squares fits to the neutron density $\rho(v, \theta)$ in the laboratory system (see Ref. [3] for definitions). In all cases, good fits could not be obtained by assuming that all the neutrons were emitted from the moving fragments, even allowing for anisotropies of the $P_2(\cos\psi)$-type in the centre-of-mass system. On the other hand, considerably better fits could be obtained by assuming a component that is isotropic in the laboratory system. The results of some of these fits are summarized in Tables I and II, and illustrated in Fig. 8.

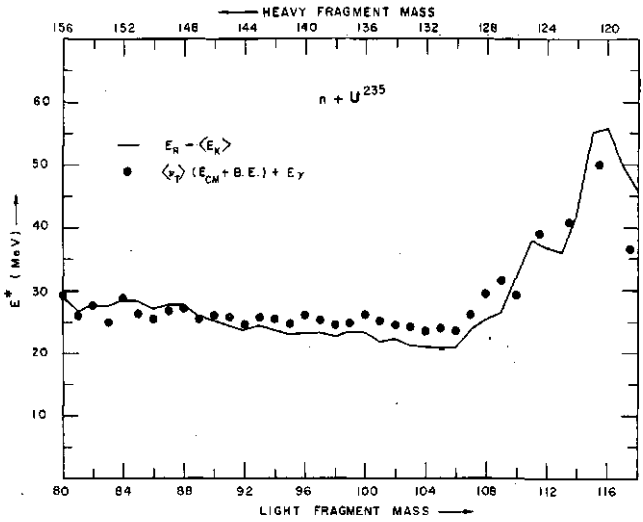

Fig. 7

Comparison of the total excitation energy E* calculated from the known energy release and the measured kinetic energies, and from the measured prompt radiations. E_γ was assumed constant at 7.5 MeV for all masses. Data from all four angles included.

In all cases, the neutrons were assumed to be evaporated from the moving fragments with "evaporation" spectra

$$\phi(E_{CM}) = (E_{CM}/T^2)\exp(-E_{CM}/T) \tag{1}$$

but two rather different temperature distributions were assumed. The first was a superposition of the spectra, Eq. (1), for one to four discrete temperatures assumed to be the same for both fragments as was done in Ref. [3]. Unlike Cf^{252}, three temperature components were no better than two for U^{235}; two were, however, better than one (see Table I). The second temperature distribution was a continuous one specified by

$$\alpha(T) = \begin{cases} bT & T < T_{max} \\ 0 & T \geq T_{max} \end{cases} .$$

The only parameter now is T_{max}, since b is specified by normalization. However in this case T_{max} was allowed to be different for the light and heavy fragments. The central component in both cases was assumed to be given by $\phi(E_c) = (E_c/T_c^2)\exp(-E_c/T_c)$. The continuous temperature distribution fits are somewhat better than the superposition fits. This is principally because the continuous distribution does not have such a large dip at small angles near neutron velocities equal to the fragment velocities. This suggests that a centre-of-mass spectrum of the type $\phi(E_{CM}) = (2/\pi^{1/2}T^{3/2})E^{1/2}\exp(-E_{CM}/T)$ would also give a good fit [12]. However, even the best fits so far obtained including a central, or scission component, are not good in the sense that all disagreements between the fitted and experimental points can be ascribed to statistical fluctuations. One way of seeing this is to look at χ in Table I.

TABLE I

LEAST-SQUARES FITS TO $n + U^{235}$ DATA

(a) Superposition of evaporation components

Fit No.	$\left\{\begin{matrix} T_c \\ \alpha \end{matrix}\right\}$		$\left\{\begin{matrix} T_c \\ \nu_c \end{matrix}\right\}$	$\begin{matrix} \nu_L \\ \nu_H \end{matrix}$	ν_{TOT}	A_2	$\langle E_{CM} \rangle$ (MeV)	$\langle E_{LAB} \rangle$ (MeV)	χ
2	0.288	0.842 --	--	1.228	2.20	≅0	1.34	2.15	3.44
	0.308	0.692 --	≅0	0.909					
3	0.291	0.844 --	--	1.332	2.28	-0.105	1.35	2.16	3.07
	0.304	0.696 --	≅0	0.951					
5	0.310	0.857 --	0.942	1.196	2.44	≅0	1.34	2.11	2.33
	0.339	0.661 --	0.491	0.751					
6	0.309	0.856 --	0.946	1.211	2.44	-0.025	1.34	2.11	2.32
	0.336	0.664 --	0.460	0.769					

(b) Triangular temperature distribution with sharp cut-off

	T_{max}		$\left\{\begin{matrix} T_c \\ \nu_c \end{matrix}\right\}$	$\left\{\begin{matrix} \nu_L \\ \nu_H \end{matrix}\right\}$	ν_{TOT}	$\langle E_{CM} \rangle$	$\langle E_{LAB} \rangle$	χ
	Light	Heavy						
7	0.993	0.982	--	1.284	2.19	1.32	2.13	2.40
			≅0	0.907				
8	0.992	0.943	1.070	1.190	2.14	1.30	2.12	1.78
			0.474	0.743				

TABLE II

LEAST-SQUARES FITS TO $n + Pu^{239}$ DATA

Fit No.	T_{max}		$\begin{Bmatrix} T_c \\ \nu_c \end{Bmatrix}$	$\begin{Bmatrix} \nu_L \\ \nu_H \end{Bmatrix}$	ν_{TOT}	$\langle E_{CM} \rangle$	$\langle E_{LAB} \rangle$	χ
	Light	Heavy						
9	1.001	1.076	-- ≡0	1.384 1.157	2.54	1.38	2.13	2.46
10	1.008	1.071	0.985 0.796	1.225 0.888	2.91	1.38	2.12	1.66

Note:

All All temperatures and energies are in MeV.

α is the amount of evaporation component with Temperature $T \cdot \Sigma_\alpha = 1$.

ν_c and T_c are the amount and temperature of the central component.

ν_L and ν_H are the number of neutrons from the light and heavy fragments.

$\nu_{TOT} = \nu_L + \nu_H + \nu_c$.

E_{CM} is the average energy of the neutrons arising from the fragments in the fragment system.

E_{LAB} is the average energy of all the neutrons.

See text for definitions of A_2, χ and T_{max}.

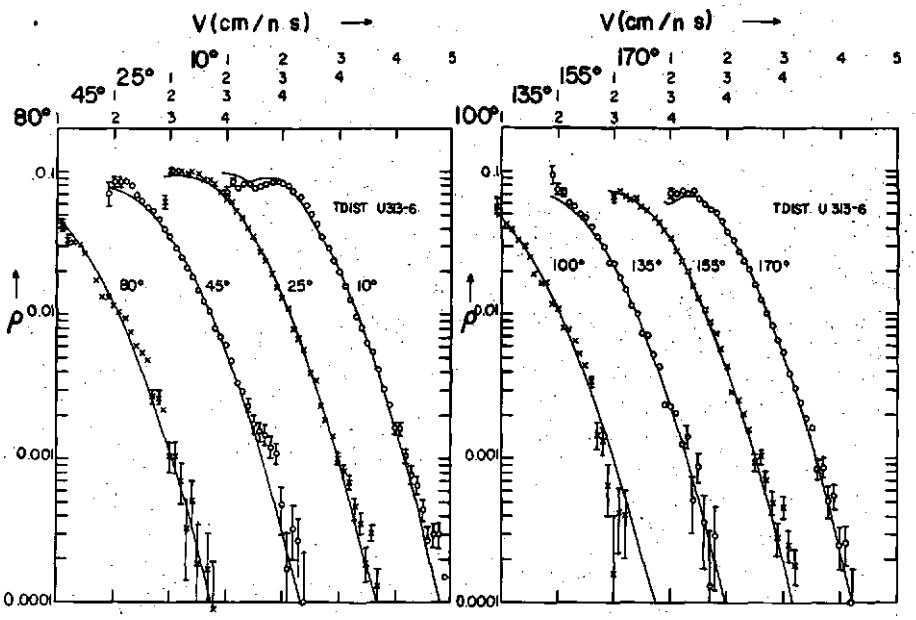

Fig. 8

Least-squares fits

As here defined, χ should have a mean value of unity and an rms deviation $\approx 1/\sqrt{f} \approx 1/\sqrt{360}$, where f is the number of degrees of freedom, in our case f = 365 − (number of parameters). In this sense, all the χ's in Table I are significantly different from one.

In closing we note that T_{max} is nearly the same for light and heavy fragments. This is also apparent in a detailed comparison of the centre-of-mass spectra, and is in agreement with previous observations [3, 12].

CONCLUSION

As in the case of Cf^{252} [3], it is not possible to obtain good agreement with the U^{235} neutron distributions by assuming that all the neutrons arise from the moving fragments. Some neutrons more nearly isotropic in the laboratory system are needed. A similar conclusion was reached by SKARSVAG and BERGHEIM [12] and by KAPOOR, RAMANNA and RAMA RAO [13] for U^{235}. There is yet no theoretical justification for any particular type of energy distribution for this central component, but it is unlikely that its presence will seriously alter conclusions so far reached about neutron emission from individual fragments, as in Figs. 2–6. Some corrections yet to be made will, however, alter the detailed appearance of these figures.

REFERENCES

[1] MILTON, J.C.D. and FRASER, J.S., Canad. J. Phys. 40 (1962) 1626.
[2] FRASER, J.S., MILTON, I.C.D., BOWMAN, H.R. and THOMPSON, S.G., Canad. J. Phys. 41 (1963) 2080.
[3] BOWMAN, H.R., THOMPSON, S.G., MILTON, J.C.D. and SWIATECKI, W.J., Phys. Rev. 126 (1962) 2120, Phys. Rev. 129 (1963) 2133.
[4] GRAHAM, R.L., GEIGER, J.S., BELL, R.E. and BARTON, R., Nucl. Instrum. Meth. 15 (1962) 40.
[5] TERRELL, J., Phys. Rev. 113 (1959) 527.
[6] MILTON, J.C.D., Univ. Calif. Radiation Lab. Rpt. UCRL-9883-Rev.
[7] APALIN, V.F., GRITZYUK, Yu.N., KUTIKOV, I.E., LEBEDEV, V.I. and MIKHAELYAN, L.A., Kurchatov Atomic Energy Institute IAE-710; see also Nucl. Phys. 55 (1964) 249.
[8] MILTON, J.C.D., Advanced Course on Nuclear Physics with Thermal Neutrons, Kjeller Report KR-64 (1963).
[9] TERRELL, J., Phys. Rev. 127 (1962) 880.
[10] VANDENBOSCH, R., Nucl. Phys. 46 (1963) 129.
[11] APALIN, V.F., GRITZYUK, Y.N., KUTIKOV, I.E., LEBEDEV, V.I. and MIKHAELYAN, L.A., Kurchatov Atomic Energy Institute IAE-709.
[12] SKARSVAG, K. and BERGHEIM, K., Nucl. Phys. 45 (1963) 72.
[13] KAPOOR, S.S., RAMANNA, R., and RAMA RAO, D.N., Phys. Rev. 131 (1963) 283.

DISCUSSION

J. TERRELL: How many temperatures were used in fitting the sum of evaporation spectra to the centre-of-mass emission spectrum? In my own work, when I calculated the centre-of-mass spectrum at very low energies, the computer went crazy and had to be guided gently by hand. If the computed emission spectrum had a dependence on E closer to the evaporation spectrum value (first power of E) than the Maxwellian $E^{1/2}$, this might give too low a neutron density near the fragment velocity points and require the addition of the neutrons not emitted from the fragments. It is possible that such a purely computational difficulty could bring about the need for non-fragment neutrons.

As to the two peaks in the 10° spectrum, one was near the fragment velocity and the other was at 2 cm per ns, about twice the fragment velocity. This does not seem to me to constitute evidence for emission of neutrons from the fissioning nuclide, rather than from the fragments.

J.C.D. MILTON: Two rather different methods of fitting were employed, as explained in the paper. There appears to be no difference in the results. The first method was the superposition of discrete evaporation components, as described in the paper by Bowman et al. (Ref. [3]). In the second method a continuous distribution was used. The particular distribution used was one proportional to temperature up to a maximum value, T_{max}, and zero thereafter. In this case the power of E is effectively between 1/2 and 1, but closer to 1/2. The fits to the experimental values that I showed were obtained by this method. Values for the temperatures and the number of temperatures used are given in the tables. As we have no angle smaller than 10°, very small centre-of-mass energies are never encountered. While much remains to be done, of course, to put the data in final form, I do not believe the poor fits obtained without a central component are caused by computational inadequacies.

There is a faint suggestion of a dip at the light fragment velocity in the 10° data. Angular resolution corrections would tend to enhance such a dip. If it should turn out to be real, it would imply a power of E greater than the Maxwellian 1/2. If the power is substantially greater than 1/2, then very large central components would be required to obscure the dip; if it is equal to 1/2, no dip would appear. Thus I think the existence or non-existence of a dip is not closely connected with a central component. In addition, as mentioned in the paper, it is impossible to have a peak in the 25° data higher than that in the 10° data if the neutron emission is isotropic in the centre of mass.

R. RAMANNA: In the laboratory spectrum of the prompt neutrons one would expect a dip at energies corresponding to the fragment velocities. I notice a small dip in your curves, and we also noted this in a paper published in 1963.[1] There is also a Soviet paper in which this is shown. In your Kjeller lecture notes you state that it is not possible to get this dip. Can you please clarify?

J.C.D. MILTON: I cannot conceive of making such a statement. There must be an ambiguity in the printed text to give rise to such an interpretation.

P. ARMBRUSTER: Did you consider the possibility that the neutrons are emitted from nuclei with high spins aligned perpendicular to the direction of flight? This alignment could give rise to anisotropy in the system of the moving fragments.

J.C.D. MILTON: If the spins are aligned perpendicular to the direction of motion of the fragments, one would expect an angular distribution in the centre-of-mass system with a P_2 ($\cos \theta_{LAB}$) term. Such a term was allowed for in the fits with a coefficient A_2 to be determined. The result of so doing was indicated by the crosses (x) in the slides. In no case was the improvement in the fit sufficient to remove the large excess at 90° in the laboratory system. The effect of a positive A_2 is to produce relative peaking at 0° in the laboratory system, while a negative A_2 produces peaking at 45°. Skarsvag and Bergheim have also considered the effect of spins aligned along the direction of motion (Ref. [12] in the paper) and they too could not obtain good fits without the use of a central component for the thermal-neutron fission of U^{235}.

S.S. KAPOOR: How much uncertainty in the data do you expect as a result of the uncertainty in the estimation of the background, which, I gather, is quite large in your experiment?

J.C.D. MILTON: The statistical uncertainty in the background is included in the errors shown in the figures. The background is not large. As a matter of fact we have recently removed some of the shielding to increase the random background so that we can obtain better statistics for the normal fission distribution (without reference to neutrons). If I remember correctly, the total number of neutron events in the useful energy region was greater than 10 times the total background in the 10° counter.

G. HERRMANN: It appears to me that the numbers of neutrons emitted from a given fragment are quite similar in each of the three cases you studied, with one interesting exception. That is the region around mass number 135.

---

[1] KAPOOR, S.S., RAMANNA, R. and RAMA RAO, P.N., Emission of Prompt Neutrons in the Thermal Neutron Fission of U^{235}, Phys. Rev. 131 (1963) 283.

There, the U^{235} and Pu^{239} curves rise steeply, levelling off in a plateau at mass 136, whereas the U^{233} curve rises much more slowly and shows almost no plateau. Thus, at a fragment mass 136, for example, fragments from U^{235} and Pu^{239} emit about 1.2 n and those from U^{233} 0.5 n. Can you explain this difference? I ask this because neutron evaporation from those fragments has been considered as an explanation for the fine structure observed in the radiochemical mass-yield curves.

J.C.D. MILTON: Although I pointed out some fine structure in the figures, I would not like to make too much of the details at present. As I mentioned, the experiment is still in progress. Several important corrections, e.g. resolution corrections, have not yet been made. In addition, the experimental conditions were considerably different during the U^{233} runs.

$\bar{\nu}$ IN NEUTRON-INDUCED FISSION OF U^{235} AND Th^{232}, AND IN PHOTOFISSION OF U^{238}

H. CONDÉ AND M. HOLMBERG
RESEARCH INSTITUTE OF NATIONAL DEFENCE,
STOCKHOLM, SWEDEN

Abstract — Résumé — Аннотация — Resumen

$\bar{\nu}$ IN NEUTRON-INDUCED FISSION OF U^{235} AND Th^{232}, AND IN PHOTOFISSION OF U^{238}. The average number of prompt neutrons ($\bar{\nu}$) emitted in the neutron-induced fission of U^{235} and Th^{232} and in the photofission of U^{238} has been measured with a large liquid scintillator as the fission neutron detector. The measurements were made relative to $\bar{\nu}$ for the spontaneous fission of Cf^{252}.

The $\bar{\nu}$-values of U^{235} were measured at some different incident energies between 30 keV and 15 MeV, and the results are in agreement with measurements by Moat et al., and Hopkins and Diven.

The measurements of Th^{232} were made for several incident neutron energies from the fission threshold at about 1.4 MeV to 15 MeV. Special interest was concentrated on the energy region near the fission threshold where the fission cross-section and the fragment angular distribution show strong variations with neutron energy. The measurements indicate that the energy dependence of $\bar{\nu}$ in this region may be non-linear.

A measurement of $\bar{\nu}$ in the photofission of U^{238} at a gamma-ray energy of 7 MeV has been made. The result is not in agreement with measurements by Prokohorova et al. and Lazareva et al. The spontaneous fission of Pu^{240} and the thermal-neutron-induced fission of Pu^{239} give a difference in $\bar{\nu}$ corresponding to 0.10 n/MeV. The result of the present investigation combined with the $\bar{\nu}$-value for the spontaneous fission of U^{238} gives 0.10 ± 0.02 in agreement with the data obtained for the compound nucleus of Pu^{240}.

VARIATION DE $\bar{\nu}$ DANS LA FISSION DE ^{235}U ET ^{232}Th PAR DES NEUTRONS ET DANS LA PHOTOFISSION DE ^{238}U. Le nombre des neutrons instantanés ($\bar{\nu}$) émis dans la fission de ^{235}U et ^{232}Th par des neutrons et dans la photofission de ^{238}U a été mesuré au moyen d'un grand scintillateur liquide comme détecteur des neutrons de fission. Les mesures ont été effectuées par rapport à $\bar{\nu}$ pour la fission spontanée de ^{252}Cf.

Les valeurs de $\bar{\nu}$ pour ^{235}U ont été mesurées à différentes énergies incidentes comprises entre 30 keV et 15 MeV; les résultats sont en accord avec les mesures de Moat et al. ainsi qu'avec celles de Hopkins et Diven.

Les mesures pour ^{232}Th ont été faites à plusieurs énergies des neutrons incidents comprises entre le seuil de fission voisin de 1,4 MeV et 15 MeV. Les auteurs se sont spécialement intéressés à la région d'énergie voisine du seuil de fission, où la section efficace de fission et la distribution angulaire des fragments accusent de fortes variations en fonction de l'énergie des neutrons. D'après les mesures, il se peut que, dans cette région, la variation de $\bar{\nu}$ en fonction de l'énergie ne soit pas linéaire.

Les auteurs ont mesuré $\bar{\nu}$ pour la photofission de ^{238}U à une énergie gamma de 7 MeV. Le résultat n'est pas en accord avec les mesures faites par Prokohorova et al. ou avec celles faites par Lazaréva et al. La fission spontanée de ^{240}Pu et la fission de ^{239}Pu par neutrons thermiques donnent une différence dans les valeurs de $\bar{\nu}$ qui correspond à 0,10 neutron par MeV. Le résultat de l'étude actuelle, combiné à la valeur de $\bar{\nu}$ pour la fission spontanée de ^{238}U, donnent $0,10 \pm 0,02$, ce qui est en accord avec les données obtenues pour le noyau composé ^{240}Pu.

ЭНЕРГЕТИЧЕСКАЯ ЗАВИСИМОСТЬ $\bar{\nu}$ ПРИ ВЫЗВАННОМ НЕЙТРОНАМИ ДЕЛЕНИИ УРАНА-235 И ТОРИЯ-232 И ФОТОДЕЛЕНИИ УРАНА-238. Среднее число мгновенных нейтронов ($\bar{\nu}$), испускаемых при вызванном нейтронами делении урана-235 и тория-232 и при фотоделении урана-238 было измерено с помощью большого жидкого сцинтиллятора, используемого в качестве детектора нейтронов деления. Результаты измерений были увязаны с величиной для спонтанного деления калифорния-252.

Значения $\bar{\nu}$ для урана-235 были измерены при некоторых различных энергиях бомбардирующих частиц между 30 кэв и 15 Мэв; эти результаты согласуются с результатами измерений, выполненных Моатом и другими, а также Гопкинсом и Дайвеном.

Измерения для тория-232 были выполнены для нескольких энергий бомбардирующих нейтронов, начиная с порога деления, составляющего примерно 1,4—15 Мэв. Особое внимание

было обращено на область энергий вблизи порога деления, где сечение деления и угловое распределение осколков сильно колеблются в зависимости от энергии нейтронов. Результаты измерений показывают, что энергетическая зависимость $\bar{\nu}$ в этой области может быть нелинейной.

Были произведены измерения $\bar{\nu}$ для фотоделения урана-238 при энергии гамма-лучей 7 Мэв. Полученные результаты не согласуются с результатами, полученными Прохоровой и другими и Лазаревой и другими. Спонтанное деление плутония-240 и вызванное тепловыми нейтронами деление плутония-239 дают разницу в $\bar{\nu}$, соответствующую 0,10 нейтрона на Мэв. Результат настоящего исследования в сочетании со значением $\bar{\nu}$ для спонтанного деления урана-238 дает 0,10 ± 0,02, что согласуется с данными, полученными для составных ядер плутония-240.

VARIACION DE $\bar{\nu}$, EN FUNCION DE LA ENERGIA, EN LA FISION NEUTRONICA DEL ^{235}U Y DEL ^{232}Th Y EN LA FOTOFISION DEL ^{238}U. Los autores han medido, empleando como detector de los neutrones de fisión un contador de centelleador líquido de gran volumen, el promedio de neutrones inmediatos ($\bar{\nu}$) emitidos en la fisión neutrónica del ^{235}U y del ^{232}Th así como en la fotofisión del ^{238}U. También realizaron mediciones con respecto a $\bar{\nu}$ en la fisión espontánea del ^{252}Cf.

Determinaron los valores de $\bar{\nu}$ en la fisión del ^{235}U correspondientes a diversas energías incidentes, comprendidas entre 30 keV y 15 MeV, comprobando que los resultados obtenidos concuerdan con los de las mediciones realizadas por Moat y sus colaboradores y por Hopkins y Diven.

En el caso del ^{232}Th las mediciones se realizaron para diversas energías de los neutrones incidentes, comprendidas entre 1,4 y 15 MeV aproximadamente, partiendo del umbral de fisión. Se prestó especial atención a la región energética próxima a dicho umbral, en la que la sección eficaz de fisión y la distribución angular de los fragmentos varían muy considerablemente con la energía neutrónica. Las mediciones indicaron que la variación de $\bar{\nu}$ en función de la energía puede muy bien no ser lineal en esta región.

También se procedió a medir $\bar{\nu}$ en la fotofisión del ^{238}U para una energía de los rayos gamma de 7 MeV. El resultado obtenido no concuerda con los valores determinados por Prokoborova y por Lazareva con sus respectivos colaboradores. Entre los valores de $\bar{\nu}$ correspondientes a la fisión espontánea del ^{240}Pu y a la fisión del ^{239}Pu inducida por neutrones térmicos, se obtuvo una diferencia de 0,10 n/MeV. El resultado de la presente investigación, combinado con el valor de $\bar{\nu}$ obtenido para la fisión espontánea del ^{238}U, da un valor de 0,10 ± 0,02, que concuerda con los datos obtenidos para el núcleo de compuesto ^{240}Pu.

INTRODUCTION

The measurements of the $\bar{\nu}$-values from neutron-induced fission of U^{233}, U^{235}, U^{238} and Pu^{239} have given a $\bar{\nu}$-dependence of incident neutron energy, E_n, which is not essentially changed in going from one isotope to another [1-4]. Thus 2 MeV above the fission thresholds the measured $\bar{\nu}$-values can be fitted by a straight line with a slope of about 0.155 n/MeV. This corresponds well to the calculated value of about 6.7 MeV for emitting 1 n from the fission fragments.

However, in certain isotopes (U^{233}, U^{235}) the increase of $\bar{\nu}$ in the neighbourhood of the fission threshold is not so rapid. HOPKINS and DIVEN [1] fit their data in this region with a straight line with a slope of 0.085 n/MeV. Furthermore, BLYUMKINA et al. [5] have found irregularities in the $\bar{\nu}$-values of U^{233} and U^{235}, which are related to fission channel effects. There may be a correlation between these channel effects and the different values of $d\bar{\nu}/dE_n$ = 0.085 and 0.15 observed below and above 2 MeV respectively.

Another problem related to these considerations is the transition between sub-barrier and super-barrier fission. OKOLOVICH and SMIRENKIN [6] have suggested that the total kinetic energy of the fission fragments is changed in the transition between the two states. This also implies that the

$\bar{\nu}$-values from spontaneous and induced fission in the same compound nucleus are related to a change in the kinetic energy of the fragments.

In the present investigation the $\bar{\nu}$-value of U^{235} has been measured at 60 keV and 7.5 MeV. The $\bar{\nu}$-values of Th^{232} have been measured with special interest in the threshold region. The $\bar{\nu}$-value in the fission of U^{238} induced by 7-MeV gamma rays has also been measured, and the result is compared with the spontaneous value of U^{238}.

Large liquid scintillators, 100 l in volume, were used as fission neutron detectors. A description of the experimental arrangement and procedure has been given previously [3]. The measurements have been made relative to $\bar{\nu}$ of the spontaneous fission of Cf^{252}. This $\bar{\nu}$-value was taken as a weighted average of the values measured by HOPKINS and DIVEN [1], COLVIN and SOWERBY [4], and ASPLUND-NILSSON et al. [7]. The average value was 3.775 ± 0.020.

$\bar{\nu}$ OF U^{235}

The present measurement was made with 60-keV neutrons from the $Li^7(p, n)$-reaction and the thermal $\bar{\nu}$-value was calculated by an extrapolation to thermal energy assuming a linear energy dependence of $\bar{\nu}$ with a slope of 0.085 n/MeV. The error given for the relative value includes counting statistics and uncertainties in the corrections. The corrections applied to the experimental relative value were:

(i) Overlap correction
(ii) False gates
(iii) Fission spectra differences
(iv) Anisotropy of fission neutron emission
(v) Fission foil thickness
(vi) Fission induced by background neutrons
(vii) Impurities in the fissile deposit
(viii) Uncertainty in the primary neutron energy.

The total correction was estimated to be 0.013 ± 0.007. The result is $\bar{\nu}_{th}(U^{235}) = 2.417 \pm 0.015$.

If the delayed neutrons are added [8], the result will be $\bar{\nu}(U^{235}) = 2.433 \pm 0.015$.

With the same experimental technique and data handling as described in Ref. [3], a $\bar{\nu}$-value for U^{235} at 7.5 MeV of incident neutron energy was estimated. The result was $\bar{\nu} = 3.47 \pm 0.06$, which is in agreement with measurements by MATHER et al. [2].

$\bar{\nu}$ OF Th^{232}

The $\bar{\nu}$-values of Th^{232} have been measured at several neutron energies between 1.4 and 14.8 MeV in order to compare the dependence of $\bar{\nu}$ with the linear dependence obtained for other fissile isotopes. The fission cross-section of Th^{232} [9] and the angular distribution of the fission fragments [10] vary strongly in the energy region around the fission threshold. Several $\bar{\nu}$-measurements close in energy were made in this energy region to investigate possible irregularities also in the energy dependence of the $\bar{\nu}$-values.

TABLE I

FULLY CORRECTED EXPERIMENTAL $\bar{\nu}$-VALUES OF Th^{232}

The $\bar{\nu}$-values are based on $\bar{\nu}$ = 3.775 ± 0.000 for the spontaneous fission of Cf^{252}.
The stated uncertainties are due to counting statistics only.

Neutron energy (MeV)	$\bar{\nu}$
1.42 ± 0.02	2.205 ± 0.060
1.61 ± 0.01	2.084 ± 0.037
1.80 ± 0.01	2.119 ± 0.055
2.23 ± 0.01	2.180 ± 0.049
2.64 ± 0.01	2.273 ± 0.052
3.6 ± 0.3[a]	2.41 ± 0.10
7.45 ± 0.05	3.028 ± 0.060
14.8 ± 0.2	4.065 ± 0.060
14.9 ± 0.3[a]	4.32 ± 0.13

[a] Corrected data of Ref. [11], assuming the same corrections as in the present investigation

The results of the $\bar{\nu}$-measurements of Th^{232} are given in Table I together with the corrected $\bar{\nu}$-values at 3.6 and 14.9 MeV measured by CONDÉ and STARFELT [11]. The error in the $\bar{\nu}$-value due to uncertainties in the corrections is estimated to be less than 0.5%.

In Fig. 1 the present data on prompt $\bar{\nu}$ of Th^{232} fission are shown together with the corrected $\bar{\nu}$-values at 3.6 and 14.9 MeV of Ref. [11]. The data of KUZMINOV and LEROY [12, 13] at about 15 MeV are also shown. The straight line represents a least mean square fit to the data in Table I from 1.6 MeV to 14.9 MeV of incident neutron energy. The equation of the line is $\bar{\nu}(E_n) = 1.849 + 0.154\ E_n$.

The $\bar{\nu}$-values versus incident neutron energy for induced fission of U^{235} can, according to HOPKINS and DIVEN [1], be fitted by two straight lines of slopes 0.085 n/MeV up to about 1.6 MeV and 0.16 n/MeV above 1.6 MeV. By adjusting the energy scale of the $\bar{\nu}$ versus incident neutron-energy curve for U^{233} [1], U^{238} [3] and Pu^{239} [1] one can fit the data by the same straight lines, "the universal curve", as for U^{235}. The present data cannot be fitted to the "universal curve" with only an adjustment of the energy scale. If 1.75 MeV is subtracted from the actual incident neutron energy for Th^{232} the intersection of the two straight lines in the "universal curve" will be at about 3.4 MeV. The line with the slope of 0.160 n/MeV will then give a good fit to the measured $\bar{\nu}$-values but not the line with the slope of 0.085/MeV.

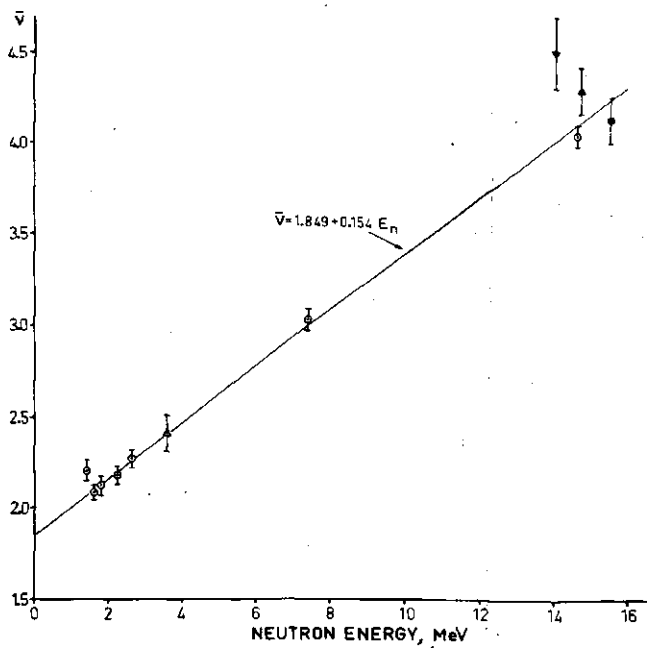

Fig. 1

Number of prompt neutrons emitted per fission for neutron-induced fission of Th^{232} as function of incident neutron energy. The open circles are the present investigation, the open triangles are data of CONDÉ and STARFELT [11], the filled triangle is from LEROY [13], and the filled square is from KUZMINOV [12]. The line represents a least mean square fit to present results.

In the energy region at the fission threshold the present investigation agrees with a linear relationship of energy dependence of $\bar{\nu}$ down to 1.6 MeV. Figure 2 shows the experimental points of $\bar{\nu}$ from 1.4 to 4 MeV of incident neutron energy and also the fission cross-section [9] and the anisotropy of the fission fragments [10] in the same region. The $\bar{\nu}$-values measured by BUTLER and MEADOWS [14], KUZMINOV [12], MATHER et al. [15] and SMITH et al. [16] are also shown in Fig. 2.

At 1.4 MeV the three actual measurements have given a comparatively high $\bar{\nu}$-value. This rise in $\bar{\nu}$ just at the fission threshold has made it reasonable to exclude the $\bar{\nu}$-value at 1.4 MeV in the calculation of the linear dependence of $\bar{\nu}$ on the incident neutron energy.

At 1.6 MeV the measurement by BUTLER and MEADOWS [14] disagrees with the present investigation. The very marked anisotropy at this energy (see Fig. 2) may be a source of error and therefore the correction due to fission foil thickness is of importance. The present measurement was made by using two different types of fission chambers. The parallel plate chamber had a coating thickness of 4 mg/cm² and the fissile layer perpendicular to the incident neutron beam. Here the corrected $\bar{\nu}$-value is 2.08 ± 0.04 with a correction of 1.3% for the fission foil thickness. The cylindrical chamber had a coating thickness of 2 mg/cm² and the fissile layer parallel to the

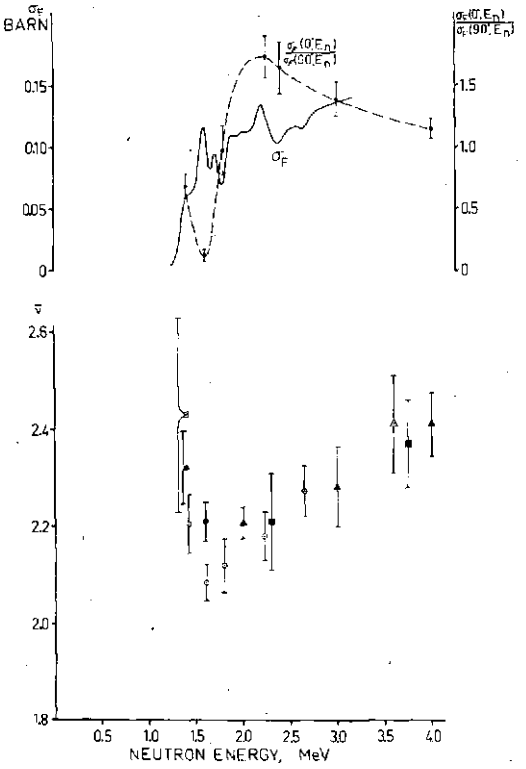

Fig. 2

Number of prompt neutrons emitted per fission, $\bar{\nu}$, for neutron-induced fission of Th^{232} as a function of incident neutron energy. The open circles are the present investigation, the filled circle is from BUTLER and MEADOWS [14], the open triangle is from CONDÉ and STARFELT [11], the filled triangles are data of MATHER et al. [15], the open square is from SMITH et al. [16], and the filled squares are data of KUZMINOV [12]. The upper curves represent the energy dependence of the anisotropy of fission fragments and the total fission cross-section of Th^{232} [10, 11].

beam. The correction for the foil thickness is 0.45% and the $\bar{\nu}$-value is 2.08 ± 0.09.

The present investigation of Th^{232} is in good agreement with measurements by MATHER et al. [15] and KUZMINOV [12].

BLYUMKINA et al. [5] observed a non-linear energy dependence of $\bar{\nu}$ for neutron-induced fission of U^{233} and U^{235}. The irregularities observed are considered to be a consequence of the large spacing (0.8 MeV) between the first rotational bands in the energy gap of the even compound nuclei at the threshold region. Another irregularity was observed in the energy region above the first two rotational bands, which they connected with the opening of one-particle fission channels. They estimated an appreciable change in the average kinetic energy of the fission fragments in the transition to the new channels.

In the case of Th^{232} the compound nucleus is odd and several one-particle states are available also in the threshold region. The observed $\bar{\nu}$-value at

1.4 MeV deviates by more than twice the statistical error from the value given by the straight line fitting the data from 1.6 to 15 MeV. In accordance with the effects observed by BLYUMKINA et al., the decrease in $\bar{\nu}$ for Th^{232} at 1.4 to 1.6 MeV may indicate the opening of a new one-particle fission channel.

$\bar{\nu}$ OF U^{238}

There are only a few direct measurements of the $\bar{\nu}$-values for photofission. LAZAREVA et al. [17] have measured $\bar{\nu} = 1.6 \pm 0.5$ for U^{238} fission induced by gamma rays from bremsstrahlung with $E_{max} = 5.5$ MeV, and PROKHOROVA and SMIRENKIN [18] reported $\bar{\nu} = 4.2 \pm 0.2$ for gamma rays of 6.7 MeV in the same nucleus. These values are to be compared with a weighted mean value of $\bar{\nu} = 2.00 \pm 0.05$ for spontaneous fission of U^{238} [19]. The reported $\bar{\nu}$-values are not in agreement with the data for the compound nucleus Pu^{240}. Prokhorova and Smirenkin also suggest that the fragment deformation in photofission is greater than in neutron-induced fission.

In the present investigation the $\bar{\nu}$-value from fission of U^{238} with 7-MeV mono-energetic gamma rays is measured with somewhat greater accuracy than in the two previous works to determine if there is such a difference.

The gamma rays were produced by the reaction $F^{19}(p,\alpha\gamma)O^{16}$. At a proton energy of 2.0 MeV the two gamma rays at about 7 MeV are most intense. A thin CaF_2 target was placed at the centre of the axial channel of the scintillator tank, and the fission chamber was mounted in such a way that the target was at the central point of the chamber (Fig. 3). A proton

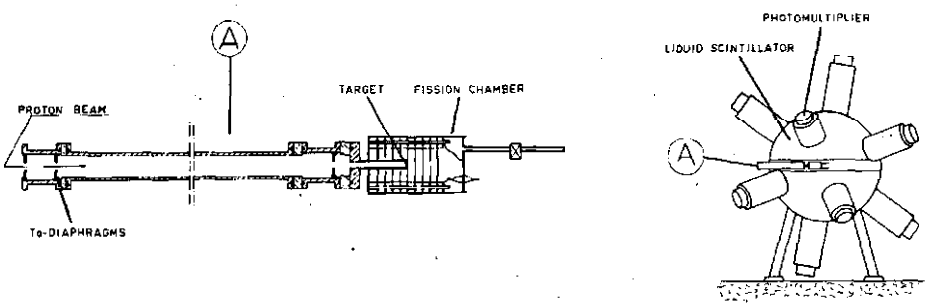

Fig. 3

Experimental arrangement for the measurement of $\bar{\nu}$ in the photofission of U^{238} at 7 MeV

current of about 0.1 μA was needed in this 4π target arrangement. A pulsed proton beam was used together with time-of-flight technique. This arrangement made it possible to avoid counting most of the spontaneous fission of U^{238}.

The $\bar{\nu}$-value obtained in the present measurement is $\bar{\nu} = 2.77 \pm 0.13$. This value is not in agreement with the results referred to above. However, the difference between the measured $\bar{\nu}$-value at 7 MeV and the spontaneous one corresponds to 0.11 ± 0.02 n/MeV, which may be compared with the difference in $\bar{\nu}$-values between the thermal-neutron-induced fission of Pu^{239}

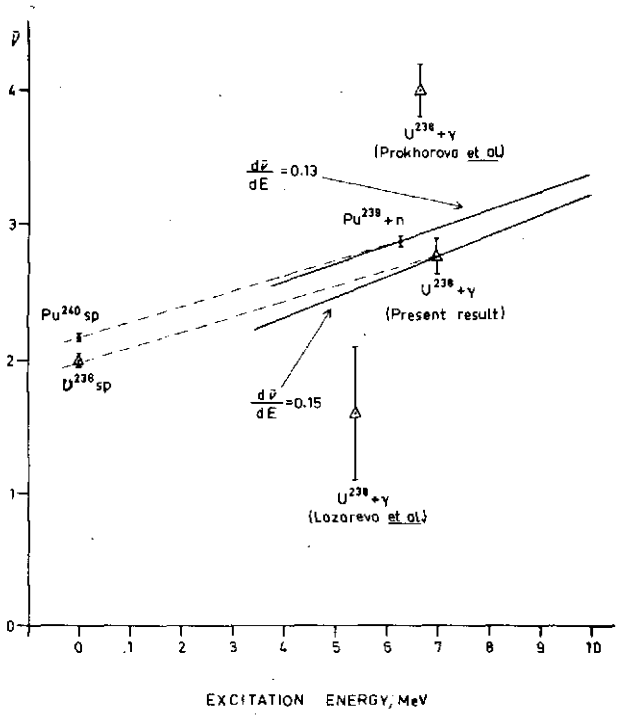

Fig. 4

$\bar{\nu}$-values in the fission of the compound nuclei of U^{238} and Pu^{240}. The data of the spontaneous fissions of U^{238} and Pu^{240}, and of the thermal fission of Pu^{239}, are weighted average values [1, 15, 19]. The straight full lines with the slopes of 0.13 and 0.15 neutrons per MeV represent the energy dependence of $\bar{\nu}$ above MeV of excitation energy for Pu^{240} and U^{238} respectively.

and the spontaneous fission of Pu^{240}, which also will be 0.11 n/MeV [1] (Fig. 4).

Assuming $d\bar{\nu}/dE = 0.15 \pm 0.01$ down to zero excitation energy and $\bar{\nu} = 2.77$ at 7 MeV, one obtains $\bar{\nu} = 1.70$ for spontaneous fission of U^{238}. To explain the measued value of $\bar{\nu} = 2.00$ the decrease in fragment kinetic energy must be 2 ± 1 MeV. OKOLOVICH and SMIRENKIN [6] reported a value of 4.8 ± 1.0 MeV as the difference between fragment kinetic energy in photofission of U^{238} at 7 MeV and spontaneous fission of the same nucleus.

ACKNOWLEDGEMENT

The authors wish to thank Dr. N. Starfelt for his constant interest in the investigation and for many fruitful discussions.

REFERENCES

[1] HOPKINS, J.C. and DIVEN, B.C., Nucl. Phys. 48 (1963) 433.

[2] MATHER, D.S., FIELDHOUSE, P. and MOAT, A., Phys. Rev. 133 (1964) B1403.

[3] ASPLUND-NILSSON, I., CONDÉ, H. and STARFELT, N., to be published in Nucl. Sci. Engng.

[4] COLVIN, D.W. and SOWERBY, M.G., private communication.

[5] BLYUMKINA, Yu. A., BONDARENKO, I.I., KUZNETSOV, V.F., NESTEROV, V.G., OKOLOVITCH, V.N., SMIRENKIN, G.N. and USACHEV, L.N., Nucl. Phys. 52 (1964) 648.

[6] OKOLOVICH, V.N. and SMIRENKIN, G.N., Soviet Phys.-JETP 16 (1963) 1313.

[7] ASPLUND-NILSSON, I., CONDE, H. and STARFELT, N., Nucl. Sci. Engng 16 (1963) 124.

[8] COX, S., FIELDS, P., FRIEDMAN, A., SJOBLOM, R. and SMITH, A., Phys. Rev. 112 (1958) 960.

[9] HUGHES, D.J. and SCHWARTZ, R.B., Neutron Cross Sections, BNL-325, 2nd ed., Brookhaven National Laboratory (1958).

[10] HENKEL, R.L. and BROLLEY, J.E., Phys. Rev. 103 (1956) 1292.

[11] CONDÉ, H. and STARFELT, N., Nucl. Sci. Engng 11 (1961) 397.

[12] KUZMINOV, B.D., AEC-tr-3944 (1959).

[13] LEROY, M.J., C.R. Acad. Sci., Paris 247 (1958) 200.

[14] BUTLER, D. and MEADOWS, J.W., private communication.

[15] MATHER, D.S., FIELDHOUSE, P. and MOAT, A., private communication.

[16] SMITH, A.B., NOBLES, R.G. and COX, S.A., Phys. Rev. 115 (1959) 1242.

[17] LAZAREVA, L.E., GAVRILOV, B.I., VALUEV, B.N., ZATSEPINA, G.N., STAVINSKII, V.S., conference of the Academy of Sciences of the USSR on the Peaceful Uses of Atomic Energy (1955) 217 (AEC-tr-2435).

[18] PROKHOROVA, L.I. and SMIRENKIN, G.N., Soviet J. atomic Energy 8 (1961) 390.

[19] ASPLUND-NILSSON, I., CONDE, H. and STARFELT, N., Nucl. Sci. Engng 15 (1963) 213.

PROMPT-NEUTRON EMISSION FROM U^{235} FISSION FRAGMENTS

T. CORNELL*, E.E. MASLIN AND A.L. RODGERS
ATOMIC WEAPONS RESEARCH ESTABLISHMENT,
ALDERMASTON, BERKS., UNITED KINGDOM
(presented by D. Vallis)

Abstract — Résumé — Аннотация — Resumen

PROMPT-NEUTRON EMISSION FROM U^{235} FISSION FRAGMENTS. A gadolinium-loaded large liquid scintillation counter is being used in conjunction with a neutron beam from the HERALD reactor at the Atomic Weapons Research Establishment, Aldermaston, to study neutron emission in the fission process. In particular, the neutron emission from individual fission fragments is observed.

A fission-fragment detector comprising two gold-silicon surface barrier counters operating in coincidence is situated at the edge of a 1-m-diam. spherical scintillation tank. The solid-state counters are placed on opposite sides of an evaporated fissile deposit on a thin nickel backing. A system of collimators selects for measurement only those fission events that have fragments travelling in the direction along the incident neutron beam and along the axis of the scintillator. Numbers of neutrons detected within 10 μs of a fission event are recorded.

The angular correlation of neutron emission with fragment direction is used to associate the neutrons with the particular fission fragment that emitted them. Energies of both fragments are available from the solid-state counters, and identification of fragment mass and of the total kinetic energy of the fragment pair is made. The number of neutrons emitted by each fragment of the pair has been measured as a function of both the fragment mass and the total kinetic energy of the pair for thermal neutrons incident on U^{235}. The usual asymmetry in the distribution of excitation energy between the heavy and light fragments is observed. The variation of the number of neutrons from the pair as a function of mass ratio is also determined.

NEUTRONS INSTANTANÉS ÉMIS PAR LES FRAGMENTS DE LA FISSION DE ^{235}U. A l'établissement de recherche sur les engins nucléaires d'Aldermaston, on utilise un grand compteur à scintillateur liquide chargé de gadolinium, conjointement avec un faisceau de neutrons émis par le réacteur HERALD pour étudier l'émission de neutrons dans le processus de fission et pour observer plus particulièrement l'émission des neutrons par les divers fragments de fission.

Un détecteur de fragments de fission, qui comporte deux compteurs à barrière de surface Au-Si fonctionnant en coïncidence, est installé au bord d'un réservoir sphérique de 1 mètre de diamètre contenant le scintillateur liquide. Les compteurs à semi-conducteurs sont placés de part et d'autre du produit fissile déposé par évaporation sur un mince support en nickel. Un ensemble de collimation permet de ne choisir pour les mesurer que les fissions dont les fragments se déplacent dans la direction du faisceau des neutrons incidents et dans l'axe du scintillateur. On enregistre les nombres des neutrons détectés dans les 10 μs qui suivent une fission.

La corrélation angulaire de l'émission de neutrons avec la direction des fragments permet de rattacher les neutrons au fragment de fission qui les a émis. Les compteurs à semi-conducteurs fournissent les énergies des deux fragments et on identifie la masse des fragments et l'énergie cinétique totale de la paire de fragments. Le nombre de neutrons émis par chaque fragment de la paire a été mesuré en fonction de la masse des fragments et de l'énergie cinétique totale de la paire pour la fission de ^{235}U par neutrons thermiques. On observe l'asymétrie habituelle dans la répartition de l'énergie d'excitation entre le fragment lourd et le fragment léger. Les auteurs déterminent également la variation du nombre des neutrons émis par la paire, en fonction du rapport des masses.

ЭМИССИЯ МГНОВЕННЫХ НЕЙТРОНОВ ИЗ ОСКОЛКОВ ДЕЛЕНИЯ УРАНА-235. Заполненный гадолинием большой жидкостный сцинтилляционный счетчик используется в Исследовательском центре атомного оружия в Олдермастоне вместе с пучком нейтронов из реак-

* Now at Rolls Royce, Derby

тора "Геральд" для изучения эмиссии нейтронов в процессе деления. В частности, рассматривается эмиссия нейтронов из отдельных осколков деления.

Детектор осколков деления, включающий два счетчика с поверхностными барьерами из золота и кремния, действующие в совпадении, расположен на грани сферического сцинтилляционного бака диаметром 1 м.

Счетчики твердых тел расположены на противоположных сторонах выпаренного делящегося осадка на тонкой никелевой основе. Система коллиматоров отбирает для измерения только те явления деления, которые имеют осколки, движущиеся вдоль направления пучка бомбардирующих нейтронов и вдоль оси сцинтиллятора. Регистрируются количества нейтронов, обнаруженных в течение десяти микросекунд, приходящихся на явление деления.

Угловая корреляция эмиссии нейтронов с направлением осколков используется для увязки этих нейтронов с конкретным осколком деления, который их испускает. Счетчики твердых тел измеряют энергии обоих осколков, и производится определение масс осколков и общей кинетической энергии пары осколков. Для тепловых нейтронов, бомбардирующих уран-235, было измерено количество нейтронов, испускаемых каждым осколком пары, как функция массы осколка и общей кинетической энергии пары. Между тяжелыми и легкими осколками наблюдается обычная асимметрия распределения энергии возбуждения. Определяется также вариация количества нейтронов, испускаемых парой осколков, как функция отношения масс.

EMISION DE NEUTRONES INMEDIATOS POR FRAGMENTOS DE FISION DEL ^{235}U. En el Atomic Weapons Research Laboratory (Aldermaston) se utiliza un contador grande de centelleador líquido activado por gadolinio, juntamente con un haz de neutrones producido por el reactor HERALD, para estudiar la emisión de neutrones en el proceso de fisión. Se investiga en particular la emisión de neutrones por los distintos fragmentos de fisión.

En la periferia de un depósito de centelleador de forma esférica, de 1 m de diámetro, se ha montado un detector de fragmentos de fisión, que comprende dos contadores de Au-Si de barrera superficial, que funcionan en coincidencia. Los contadores de estado sólido se colocan en las caras opuestas de una muestra de material fisionable, depositada por evaporación en un soporte delgado de níquel. Un sistema de colimadores selecciona, para su medición, exclusivamente aquellos procesos de fisión que producen fragmentos que se desplazan en la dirección del haz de neutrones incidentes y del eje del centelleador. Se registra el número de neutrones detectado en un lapso de 10 μs a partir del momento en que ocurre la fisión.

Para vincular los neutrones al fragmento de fisión que los emite, se utiliza la correlación angular de la emisión neutrónica con la dirección de los fragmentos. La energía de los dos fragmentos se determina por medio de los contadores de estado sólido, y los fragmentos se identifican sobre la base de su masa y de la energía cinética total del par de fragmentos. El número de neutrones emitidos por cada uno de los componentes del par de fragmentos, en el caso de la fisión del ^{235}U inducida por neutrones térmicos, se ha medido en función de la masa de los fragmentos y de la energía cinética total del par. Se observa la asimetría habitual en la distribución de la energía de excitación entre el fragmento pesado y el ligero. Se determina también la variación del número de neutrones emitidos por el par en función de la razón másica.

A gadolinium-loaded spherical liquid scintillation counter of 80-cm diam. is being used in conjunction with a neutron beam from the HERALD reactor to study prompt-neutron emission in the fission process. In this paper measurements of the neutron emission from individual fragments are reported.

A fission-fragment detector, comprising two gold-silicon surface barrier counters operating in coincidence, is situated at the periphery of the scintillation tank. The counters are placed on opposite sides of a 20-μg cm^{-2} evaporated deposit of U^{235} on 70-μg cm^{-2} nickel backing. Only those fission events that have fragments travelling within ± 23° of the axis of the scintillation counter, viz. the direction of the incident neutron beam, are selected for measurement. The angular correlation of the prompt neutrons with the fragment direction is used to associate the neutrons with the particular fragments that emitted them.

The scintillation counter contains approximately 250 l of commerical scintillant type NE 323 with 0.5% by weight of gadolinium loading. Fission neutrons entering the scintillant are thermalized mainly by proton recoils

in an average time of 10 μs and are finally captured preferentially (98%) by the gadolinium nuclei. The 9 MeV of gamma radiation released from each capture event produces scintillations that are detected by 12, 5-in-diam., EMI photomultiplier tubes, type 9618B, which are isotropically disposed over the surface of the sphere and in intimate contact with the liquid. Losses in neutron counting-rate by pulse overlap are less than 1%. The photomultipliers are operated in three banks of four tubes in a triple coincidence arrangement to eliminate detection of noise pulses. The neutron pulses are recorded within a specified period following a fission event, defined as a coincidence between pulses from the two surface barrier counters.

The arrangement has a high intrinsic efficiency (85%) for detecting fast neutrons from a fission event. However, in the present work it was necessary to operate with a gating period of 10 μs to minimize the background counting-rate that arose mainly from the direct scatter of the incident neutron beam by the surface barrier counters. Under these conditions the intrinsic efficiency falls to approximately 30% and the background is one count per gate.

The heights of coincident pulses from the surface barrier counters represent the kinetic energy of each fragment and these, together with the number of scintillation pulses detected during the 10-μs gating period, were digitized and stored on paper tape.

The analysis of the data proceeds entirely with the aid of a large off-line digital computer. Firstly the raw data are sorted into two energy channel spectra and a spectrum representing the frequency distribution of pulses from the scintillation counter. Long-term drifts in pulse height from the surface barrier counters are corrected for by the computer, and graphical printouts of each spectra are available to ascertain that no sudden changes of pulse height have occurred during the data collection. In the second stage of the analysis the data is corrected for background and for the efficiency of the scintillation counter by normalizing the average number of detected neutrons to 2.43 per fission event. The data are then sorted into two matrices giving both the number of events and the measured average number of fission neutrons for each value of fragment mass and combined fragment kinetic energy. In this experiment linear response is assumed for the pulse-height versus energy characteristic of the surface barrier counters.

The data from pairs of complementary masses are taken in conjunction with a matrix of calculated coefficients that define the probability of emission of a fission neutron from the fragment into the detector. This gives a corrected value of $\bar{\nu}$, the average number of prompt neutrons emitted per fragment of each value of mass and total kinetic energy. The matrix of coefficients are calculated transforms, assuming isotropic emission of neutrons in the fragment frame of reference and a neutron emission spectrum of two Maxwellian terms; the resulting probabilities are integrated over the range of angles of fragment emission defined by the fragment collection geometry.

The number and neutron-number matrices enable information on the mass and total kinetic energy spectra, and on the neutron emission, to be obtained. In particular by summing and averaging the matrix of neutron values along the total kinetic energy co-ordinate, average values of neutron emission as a function of fragment mass are obtained. Also sums of pairs

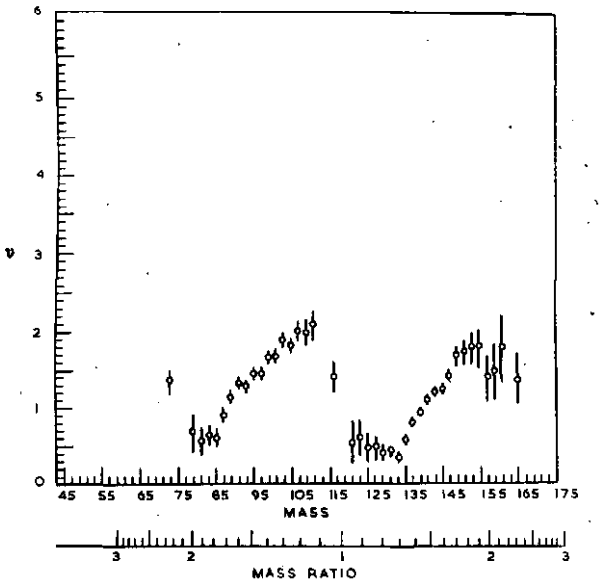

Fig. 1

Number of neutrons emitted from individual fission fragments as a function of the mass of the fragment (Series 1 data)

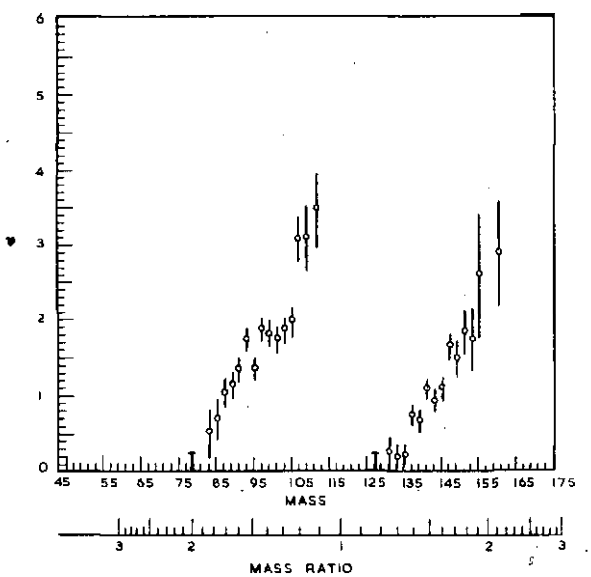

Fig. 2

Number of neutrons emitted from individual fission fragments as a function of the mass of the fragment (Series 2 data)

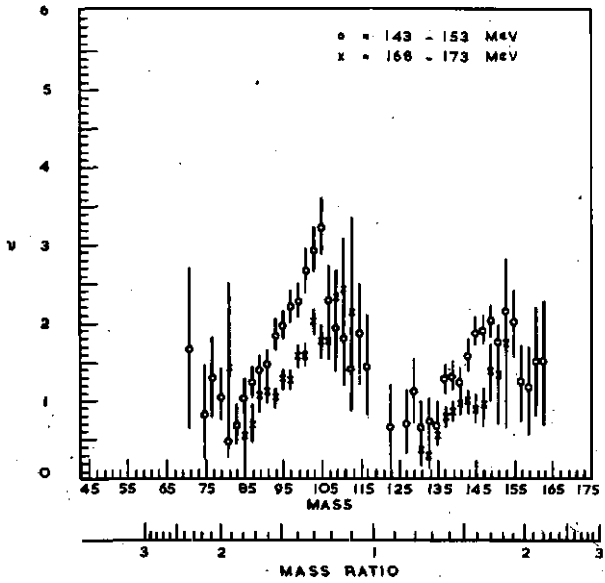

Fig. 3

The prompt-neutron-emission curve for two total kinetic energy groups

of neutron emission values for complementary masses provide the total average ν for the pair of fragments as a function of mass ratio.

Two sets of data were taken. In the first set of data, in which 1.6×10^5 events were recorded at a coincidence rate of 1 event s^{-1}, the fragment collimation was defined by the barrier-counter extremities. This resulted in a peak-to-valley ratio in the mass spectrum of only 30 :1. The data form the Series 1 data shown in the Fig. 1. Series 2 data use better collimation loading to a peak-to-valley in the mass spectrum of $\sim 150:1$ and 3×10^4 total events were recorded (See Fig. 2). In both series the half width of the total kinetic energy spectrum is 22 MeV. Mass spectra were observed to change with total kinetic energy; symmetric modes become less frequent, with the probable mass ratio decreasing, as the energy is increased.

The neutron-emission data in Series 1 were in good agreement with other measurements on U^{235} [1] and the "saw-tooth" variation with fragment mass is clearly exhibited. Of particular interest in this series is evidence for minima in the neutron emission in the regions of nuclide masses associated with the closed neutron shell N = 50 and the doubly closed shell N = 80 Z = 50. However the details of the behaviour near the N = 50 closed shell are obscured by the relatively poor mass resolution of this series.

Information on this point obtained from the more refined Series 2 data is hindered by the lower statistics, but there is supporting evidence for a minimum at N = 50 in the computer printout. These data were in good agreement with other measurements on U^{235} [2]. More positively Series 2 data indicate a higher value for the average emission in the mass region below symmetrical fission. This supports the view that the energy balance in the region of symmetric mass fission is explicable by a large increase in the

total neutron emission in going from most probable mass fission to symmetric mass fission.

A nuclear structure connection is apparently revealed in both series from an examination of the prompt emission as a function of the total kinetic energy. The effect for two separated total energy groups is shown in Fig. 3, and exemplifies the general observation that the slope for the light fragment group in particular increases as the total excitation energy is raised. The implication would seem to be that whereas closed shells are very rigid against deformation, nuclei are progressively more deformable as their nuclear content moves from closed-shell configuration. These experiments are considered to be further evidence for the existence of a deformable region of nuclei in the neighbourhood of 110 amu.

It is interesting to consider this situation in conjunction with movements of the total neutron emission, with energy, for a fragment pair. The conclusion drawn is that these movements are associated with the deformable light mass group of fragments in the region above 95 amu, and not with the complementary, heavy fragments that are strongly influenced by the N = 80 Z = 50 closed shells.

In conclusion it is observed that the measurements provide additionally an alternative means of studying nuclear structure and deformation in the deformable region. In relation to the systematics of nuclear fission they show a limitation to the concept of a universal neutron-emission curve for fission fragments [3]. Further work is being undertaken to obtain higher statistics and make quantitative assessments.

REFERENCES

[1] APALIN, V. F., DUBRYNIN, Yu. P., ZAKHAROVA, V. P., KUTIKOV, I.E. and MIKAELYAN, L. A., Atomnaja Energija 8 (1960) 1.

[2] APALIN, V. F., GRITSYUK, Yu. N., KUTIKOV, I. E., LEBEDEV, V. I. and MIKAELYAN, L. A., Ž. eksp. teor. Fiz. 46 (1964) 1192.

[3] TERRELL, J., Phys. Rev. 127 (1962) 880.

THE ENERGY BALANCE IN FISSION AND MONTE CARLO CALCULATIONS ON PROMPT-NEUTRON EMISSION *

G. E. GORDON AND N. K. ARAS**
DEPARTMENT OF CHEMISTRY AND LABORATORY FOR NUCLEAR SCIENCE,
MASSACHUSETTS INSTITUTE OF TECHNOLOGY,
CAMBRIDGE, MASS., UNITED STATES OF AMERICA

Abstract — Résumé — Аннотация — Resumen

THE ENERGY BALANCE IN FISSION AND MONTE CARLO CALCULATIONS ON PROMPT-NEUTRON EMISSION. The evaporation of neutrons from primary fission fragments has been treated by the Monte Carlo method. The total energy release E_T for fission of U^{236*} into a given pair of complementary, primary fragments is obtained from semi-empirical mass formulas. The average kinetic energy, $\bar{E}_K$, for a given mass ratio of division is obtained from the results of instrumental studies with the average sum of the fragment excitation energies, $\bar{E}_X$, being given by $E_T-\bar{E}_K$. The division of $\bar{E}_X$ between light and heavy complementary fragments is determined by a completely free parameter. The latter is adjusted to yield the experimental ratio of average number of prompt neutrons emitted by the light fragment, $\bar{\nu}_L$, to that of the heavy fragment, $\bar{\nu}_H$. Dispersion of the excitation energies is determined by dispersion in kinetic energies.

Primary mass yields are taken from instrumental fission studies. Charge distribution is assumed Gaussian (with $\sigma = 0.62$) about the most probable value, Z_p, for each mass. The latter are adjusted to give agreement with experimental results.

Nuclear level densities are assumed proportional to $\exp\{2\underline{a}^{1/2}(E-\delta)^{1/2}\}$, with $\underline{a} = A/13$; δ is a correction for odd-even effects. Monte Carlo iterations are performed by a computer for all primary fragments of appreciable yield.

Good agreement was obtained with several important experimental quantities: the dependence of $\bar{\nu}_A$ upon mass number, the neutron kinetic energy spectrum, and the average prompt gamma-ray energy release. In regions of large $\bar{\nu}_A$ the secondary charge-distribution curves are much broader than for the primary fragments, and sometimes asymmetric, with the low-Z side broader than the high-Z side. Dispersions in ν's are so large as to suggest that our assumption that $\bar{E}_K$ is the same for all charge divisions for a given mass division must be relaxed to obtain agreement with experimental data.

BILAN ÉNERGÉTIQUE DE LA FISSION ET CALCULS DE MONTE-CARLO RELATIFS A L'ÉMISSION DE NEUTRONS INSTANTANÉS. Pour étudier l'évaporation de neutrons dans les fragments de fission primaires, les auteurs ont eu recours à la méthode de Monte-Carlo. Ils ont déterminé l'énergie totale E_T libérée, lors de la fission du noyau composé $^{236}U^*$ en une paire de fragments primaires et complémentaires donnés par des formules de masse semi-empiriques. Pour un rapport de masses donné, l'énergie cinétique moyenne $\bar{E}_K$ a été obtenue à partir des résultats d'études expérimentales, la moyenne de la somme des énergies d'excitation des fragments $\bar{E}_X$ étant donnée par $E_T-\bar{E}_K$. La répartition de $\bar{E}_X$ entre les fragments complémentaires léger et lourd est déterminée par un paramètre entièrement libre. Ce dernier est ajusté pour donner le rapport expérimental du nombre moyen de neutrons instantanés émis par le fragment léger, $\bar{\nu}_L$, au nombre moyen de ces mêmes neutrons émis par le fragment lourd, $\bar{\nu}_H$. La dispersion des énergies d'excitation est déterminée par la dispersion des énergies cinétiques.

Les rendements en produits primaires selon la masse sont empruntés à des études expérimentales sur la fission. On admet que la distribution des charges est gaussienne (avec $\sigma = 0{,}62$), de part et d'autre de la valeur

---

* This work was in part supported by the United States Atomic Energy Commission under contract AT (30-1)905.

** Holder of a fellowship from the NATO Scientific Committee, Ankara, Turkey. Present address: Oak Ridge National Laboratory, Oak Ridge, Tenn., United States of America.

la plus probable, Z_p, pour chaque masse. Cette valeur est ajustée pour obtenir un bon accord avec les résultats expérimentaux.

On présume que les densités de niveau sont proportionnelles à $\exp[2\underline{a}^{1/2}(E-\delta)^{1/2}]$, avec $\underline{a} = A/13$; δ est une correction pour les effets impair-pair. Les itérations de Monte-Carlo sont effectuées par un ordinateur pour tous les fragments primaires pour lesquels le rendement est non négligeable.

Les résultats obtenus sont en bon accord avec plusieurs données expérimentales importantes: les variations de $\bar{\nu}_A$ en fonction du nombre de masse, le spectre de l'énergie cinétique des neutrons et la moyenne de l'énergie libérée des rayons gamma instantanés. Dans les régions où $\bar{\nu}_A$ est élevé, les courbes de distribution des charges secondaires sont beaucoup plus larges que celles des fragments primaires; elles sont quelquefois asymétriques, le côté où Z est faible étant plus large que le côté où Z est élevé. Les dispersions de ν sont si importantes que l'on ne peut s'en tenir strictement, semble-t-il, à l'hypothèse des auteurs selon laquelle $\bar{E}_K$ est la même pour toutes les répartitions de charges pour une répartition de masse donnée, pour obtenir un accord avec les données expérimentales.

ЭНЕРГЕТИЧЕСКИЙ БАЛАНС ПРИ ДЕЛЕНИИ И РАСЧЕТЫ ЭМИССИИ МГНОВЕННЫХ НЕЙТРОНОВ МЕТОДОМ МОНТЕ-КАРЛО. Расчет эмиссии нейтронов из первичных осколков деления мы производили методом Монте-Карло. Общее выделение энергии E_T для деления урана-236 на данную пару дополнительных первичных осколков было рассчитано с помощью полуэмпирических формул для массы. Средняя кинетическая энергия E_K для данного отношения масс деления получается по результатам приборных исследований средней суммы энергии возбуждения осколков E_x, получаемой как $E_T - E_K$. Распределение E_x между легкими и тяжелыми дополнительными осколками определяется полностью свободным параметром. Этот последний подгоняется для получения экспериментального отношения среднего числа мгновенных нейтронов, испущенных легким осколком, $\bar{U}_L$, к среднему числу тяжелых осколков $\bar{U}_H$. Распределение энергий возбуждения определяется по распределению кинетических энергий.

Первичные выходы масс получаются в результате приборного изучения деления. Предполагается, что распределение зарядов является гауссовским ($\sigma = 0{,}62$) около наиболее вероятных значений Z_p для каждой массы. Эти значения подгоняются таким образом, чтобы было согласие с экспериментальными результатами.

Плотности ядерных уровней предполагаются пропорциональными $\exp[2\underline{a}^{\frac{1}{2}}(E-\delta)^{\frac{1}{2}}]$, где $\underline{a} = A/13$; δ – является поправкой для нечетно-четных эффектов. Расчеты по методу Монте-Карло выполняются с помощью счетно-решающего устройства для всех первичных осколков, имеющих поддающийся оценке выход.

Получено хорошее согласие с несколькими важными экспериментальными величинами: зависимость $\bar{\nu}_A$ от массового числа, спектр кинетической энергии нейтронов и среднее выделение энергии мгновенных γ-лучей. В областях больших значений $\bar{\nu}_A$ кривые распределения вторичных зарядов являются более широкими, чем для первичных осколков и иногда асимметричными, в части с низким Z они шире, чем в части с высоким Z. Дисперсии в (ν) являются достаточно большими, чтобы сделать вывод, что наше предположение о том, что $\bar{E}_K$ является одинаковым для всех распределений зарядов для данных масс, должно быть изменено, чтобы достичь согласия с результатами эксперимента.

BALANCE ENERGETICO DE LA FISION Y CALCULO, BASADO EN EL METODO DE MONTE CARLO, DE LA EMISION DE NEUTRONES INMEDIATOS. Los autores han estudiado la «evaporación» de neutrones por los fragmentos primarios de fisión aplicando el método de Monte Carlo. La energía total liberada, E_T, por fisión del $^{236*}U$ a raíz de la formación de un par dado de fragmentos primarios de carácter complementario se obtiene a partir de fórmulas semiempíricas de la masa. La energía cinética media, $\bar{E}_K$, correspondiente a una razón másica dada, se deduce de los resultados experimentales, y la suma media de las energías de excitación de los fragmentos, $\bar{E}_X$, viene dada por $E_T - \bar{E}_K$. La distribución de $\bar{E}_X$ entre fragmentos complementarios ligeros y pesados se determina mediante un parámetro completamente libre. Este se ajusta de modo que exprese la razón, obtenida experimentalmente, del número medio de neutrones inmediatos emitidos por el fragmento ligero, $\bar{\nu}_L$, al número medio de los mismos emitidos por el fragmento pesado, $\bar{\nu}_H$. La dispersión de las energías de excitación viene determinada por la dispersión de las energías cinéticas.

Los rendimientos másicos primarios se determinan por estudio experimental de la fisión. Se supone que para cada masa, la distribución de la carga es gaussiana (con $\sigma = 0{,}62$), en torno al valor más probable, Z_p. Esta distribución se ajusta de modo que concuerde con los resultados experimentales.

Se supone que la densidad de los niveles nucleares es proporcional a $\exp[2\underline{a}^{1/2}(E-\delta)^{1/2}]$, siendo $\underline{a} = A/13$; δ es un factor de corrección para tener en cuenta los efectos de los núcleos impar-par. Se practican iteraciones de Monte Carlo con una calculadora electrónica para todos los fragmentos primarios de rendimiento apreciable.

Se ha obtenido una concordancia satisfactoria con varias magnitudes experimentales importantes: variación de $\bar{\nu}_A$ en función del número másico, espectro de la energía cinética de los neutrones y energía media liberada en forma de rayos gamma inmediatos. En regiones de $\bar{\nu}_A$ elevado, las curvas de distribución de carga secundaria son más aplanadas que las de los fragmentos primarios, y a veces asimétricas, con las correspondientes a los números atómicos bajos más aplanadas que las de los números atómicos elevados. La dispersión de los valores de ν es tan apreciable que no se puede aceptar estrictamente la hipótesis de los autores, según la cual $\bar{E}_K$ es la misma para todas las distribuciones de carga para una distribución de masa determinada, para que concuerde con los datos experimentales.

INTRODUCTION

The initial aim of these calculations was to investigate the effect of prompt-neutron emission upon the shape of the charge-distribution curve, i.e. independent fractional chain yield (designated fcy) as a function of nuclear charge Z for a given mass number A. The charge distributions of the primary fragments (i.e. prior to prompt-neutron emission) are of interest for comparison with theoretical predictions, but at present there are no measurements of primary distributions. A considerable body of data on the charge distributions of secondary fragments has been amassed, principally by radiochemical measurements of the independent yields of shielded and quasi-shielded nuclides [1, 2]. Unfortunately it would not be possible, even if the neutron multiplicities of each of the primary-fragment nuclides were known, to infer directly the primary charge distributions from those of the secondary fragments. Thus we have taken the approach of assuming reasonable primary distributions, performing Monte Carlo neutron-evaporation calculations to estimate neutron multiplicities for each primary nuclide, and computing the resulting secondary mass and charge distributions for comparison with experimental data. We were interested in the magnitude of difference between most-probable charge, Z_p, for the primary and secondary fragments of a given A. Also we wanted to learn whether or not the primary-to-secondary transformation introduces distortions into the charge-distribution curve (e.g. broadening, skewing, etc.).

During the work we have found that the calculations are useful for a detailed accounting of the energy released in the fission process. Also it appears that with the calculations it may be possible to determine the correct choices (or, at least, discard some incorrect ones) among sets of a priori equally reasonable assumptions about features of the fission process that are not amenable to direct experimental study. For example, it may be possible to find out if there is positive, negative or no correlation between the excitation energies of complementary fragments of a given event.

Some of the calculations reported here have been used previously in the interpretation of experiments on isomer-yield ratios [3] and ranges of fission fragments [4].

DESCRIPTION OF THE CALCULATIONS

In constructing a model for the calculations, one finds a number of points about which one can make any one of several a priori equally reasonable

assumptions. Often there are no direct experimental data upon which to base a choice among the set of reasonable assumptions. We have chosen a set of reasonable assumptions and compared the results of the calculations with a wide variety of experimental data, finding generally good agreement with most. In some cases we have also performed the calculations with alternate choices of assumptions and we discuss below the results of such variations. In later works we shall investigate the implications of additional variations of the assumptions. It is necessary to investigate these other assumptions to determine if a given set that gives reasonably good agreement with most experimental data is unique or merely one out of several sets that give agreement.

Organization of the calculations

In the calculations we treat a region of primary fragments up to 18 mass units long and 10 charge units wide. For each mass chain we first calculate the primary fractional chain yield, fcy, of each isobar according to

$$\mathrm{fcy} = \frac{1}{\sqrt{\pi C}} \exp\left[-(Z - Z_p)^2/C\right], \tag{1}$$

where C is the charge-dispersion parameter. All isobars having fcy below some given limit, generally 10^{-6}, are rejected as giving negligible contribution to total neutron emission, etc., and the fcy's of remaining isobars are renormalized to a sum of unity. The independent yield of each isobar is computed as $\mathrm{fcy} \cdot Y(A)$, the primary yield of mass chain A as obtained from instrumental fission studies.

A given number of iterations is performed for each of the isobars that has not been rejected. The first step of each iteration involves selection of an excitation energy of the primary fragment, via the Monte Carlo rejection technique [5], from the distribution obtained as discussed in the next section. The evaporation of neutrons is followed to completion as described in another section. After each neutron is emitted and at the end of each iteration, various quantities, e.g. neutron kinetic energies, γ-ray energy release, number of neutrons emitted, are weighted by the independent yield of the primary fragment and stored in appropriate histograms for later treatment and inclusion in the output data. When primary fragment (Z, A) emits n neutrons in an iteration, the secondary yield of species $(Z, A-n)$ is increased by $\mathrm{fcy}(Z) \cdot Y(A)$. At the end of each mass chain the spectrum of neutron kinetic energies is transformed to the laboratory system (assuming isotropic emission from a fragment of mass A having a uniform velocity corresponding to the average kinetic energy release for that chain), weighted by $Y(A)$, and added to the over-all laboratory-system neutron kinetic energy spectrum.

After all mass chains in the region have been treated, the various stored results are appropriately grouped and renormalized, average values and dispersions are computed, and the results printed. It requires about 1.2 min to treat an 18 mass unit region for 50 iterations per primary nuclide on an IBM-7094 computer.

Excitation-energy distributions

We assume that the average sum of the excitation energies, E_x, of complementary light (A_L, Z_L) and heavy (A_H, Z_H) fragments from fission of U^{236*} is given by

$$E_x = E_T - E_K(A_H/A_L), \tag{2}$$

where the total energy release, E_T, is given by

$$E_T = \Delta M(U^{236*}) - (\Delta M_L + \Delta M_H). \tag{3}$$

The mass excesses, ΔM, are obtained from mass equations and the average total kinetic energy release as a function of mass ratio, $\overline{E}_K(A_H/A_L)$, is taken from time-of-flight, semiconductor-detector or range measurements of fragment kinetic energies. Here we have had to make a choice among reasonable assumptions in the absence of direct experimental observations. From mass equations one finds that E_T for a given A_H/A_L has approximately parabolic dependence on Z_L (or Z_H) with the maximum value generally occurring at a Z_L value near Z_{p_L} as shown for mass ratio 139/97 in the lower part of Fig. 1. The assumption of Eq. (2) implies that $\overline{E}_K$ is the same for all charge division, Z_H/Z_L, for a given mass division. Changes in E_T with changing Z_H/Z_L thus require corresponding changes in $\overline{E}_x$, as illustrated in Fig. 1. We could have made the extreme opposite assumption, namely that $\overline{E}_K$ changes with Z_H/Z_L and $\overline{E}_x$ remains approximately constant.

The assumption of Eq. (2) requires the shape of the E_x distributions to be those of the E_K distributions for each mass division. As the latter appear to be approximately Gaussian [8], we assume that the E_x distributions are Gaussian with dispersions given by

$$\sigma_{E_x} = \sigma_{E_K} . \tag{4}$$

Assuming no correlation between the excitation energies, E_L and E_H, of the light and heavy fragments respectively, in each event we have

$$\sigma^2_{E_L} + \sigma^2_{E_H} = \sigma^2_{E_x} . \tag{5}$$

On general statistical grounds we assume that

$$\frac{\sigma^2_{E_H}}{\sigma^2_{E_L}} = \frac{\overline{E}_H}{\overline{E}_L} \equiv F(A_H/A_L). \tag{6}$$

Again, in the case of Eq. (5), we have no direct experimental check on the assumption. If there is a negative correlation between E_L and E_H, the σ_{E_L} and σ_{E_H} values could be much larger than indicated by Eq. (5). On the other hand, violations of the assumption of Eq. (2) as discussed above would cause

the σ_{E_L} and σ_{E_H} values to be smaller than those obtained from Eqs. (4) and (5). In principle, the excitation-energy-splitting parameter, $F(A_H/A_L)$, should be obtained from a complete theory of the fission process. However, in the absence of any completely satisfactory theory, we have left $F(A_H/A_L)$ as a free parameter to be varied until approximate agreement is obtained with the experimental value [9] of $\bar{\nu}_H/\bar{\nu}_L$, the ratio of average number of prompt neutrons emitted by the heavy fragments to that of the complementary light fragments as a function of mass ratio, A_H/A_L.

Treatment of neutron evaporation

After the excitation energy of a given primary fragment has been picked, de-excitation by the emission of neutrons and γ-rays is treated by the Monte Carlo method described by DOSTROVSKY, FRAENKEL and FRIEDLANDER [10], except that we ignore charged-particle emission. According to this treatment, level-densities of the residual nuclei as a function of excitation energy, E, are assumed to be given by

$$\omega(E) = \text{const} \quad \exp\left[2\sqrt{\underline{a}(E-\delta)}\right], \tag{7}$$

in which δ is the "characteristic level" or pairing-energy correction to account for reduced level density when the number of protons and/or neutrons in the residual nucleus is even. In most of the calculations we have assumed $\underline{a}$ to be given by A/γ, where γ is a parameter that is generally found to be in the range 8 to 13 MeV in other types of experiments.

This treatment assumes that a neutron is emitted whenever possible except that no neutron emissions may leave the residual nucleus with an excitation energy less than δ if δ is non-zero. Thus, the "effective" neutron-separation energy for nuclide Z, A is $S_n(Z,A)+\delta(Z,A-1)$. Any excitation energy remaining after all possible neutrons have been emitted is assumed to be given off as prompt γ-rays.

RESULTS OF CALCULATIONS

Choice of input parameters

The parameters for most of the calculations whose results are given below are as follows:

(1) Kinetic energy release and dispersion. Values for $\bar{E}_K$ and σ_{E_K} over most of the fission-product region were taken from the time-of-flight data of MILTON and FRASER [8] and the semiconductor-detector measurements by GIBSON et al. [7] respectively. In the low-yield, symmetric region, where instrumental studies are most subject to error, we have used kinetic energies based on ranges of specific fission products in aluminium [4]. Note, however, the special problem of kinetic energies discussed below in the next section.

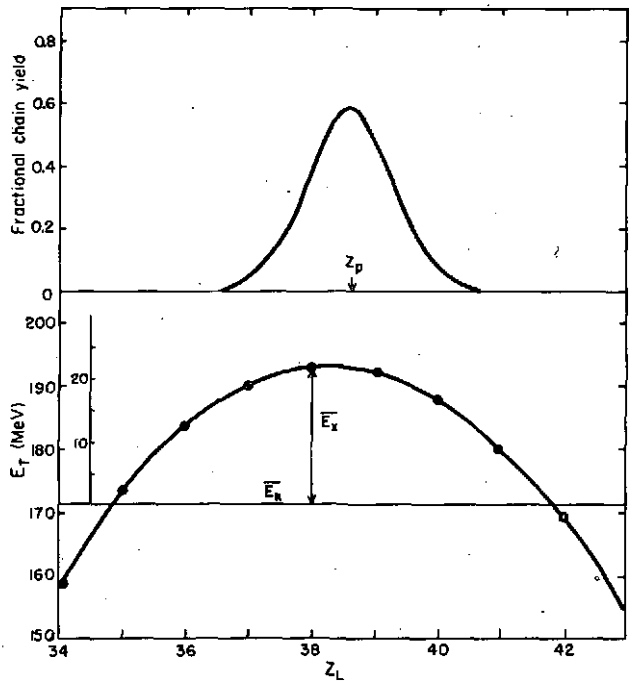

Fig. 1

Primary yield and E_T as a function of Z_L for mass division 139/97.
Upper: Primary fcy calculated according to Eq. (1) with Z_{p97}= 38.63 and C = 0.94.
Lower: E_T obtained from Seeger's mass formula [6],
$\overline{E}_K$ for 139/97 divisions is 171.5 MeV, the input value that gives an implied E_K approximately equal to the experimental values, 166.4 [7] or 167.8 [8].

(2) Primary yield-mass curve. Over most of the fission-product region primary-mass yields were taken from the work of MILTON and FRASER [8]. In the low-yield regions, where we were unable to read the yields from Milton and Fraser's linear plot, values were taken from preliminary results (not corrected for mass-dependent pulse-height defect) of semiconductor-detector experiments by GIBSON [11]. The latter were used for mass chains 75 to 79, 112 to 124 and 157 to 161. The values used are shown below in Fig. 10.

(3) Primary charge-distribution curves. We have assumed that fcy as a function of Z for primary fragments of mass A is given by Eq. (1), with C a constant for all masses, equal to 0.94 for most calculations, and equal to 0.4 for one calculation. As starting values we used the primary Z_p values suggested by WAHL et al. [2]. Later we made slight adjustments of the primary Z_p values to improve the agreement between calculated and experimental Z_p values for the secondary fragments. The final values used are shown below in Fig. 7.

(4) Mass excesses and pairing-energy corrections. All mass-excess values were taken from SEEGER's semi-empirical mass formula [6]. The

level-density pairing correction, δ of Eq. (7), was taken as 0 for odd-odd, δ_Z for even-Z, odd-N, δ_N for odd Z, even N, and $\delta_Z + \delta_N$ for even-even nuclides. The values of δ_Z and δ_N were assumed to be a smooth function of A and were taken from the evaluation of pairing effects on masses by SEEGER [6].

(5) Level-density parameter. The level-density parameters, a of Eq. (7), was assumed equal to A/γ. Initially a value of $\gamma = 8$ MeV was used, but slightly better agreement between calculated and experimental neutron kinetic energy spectra was obtained with $\gamma = 13$ MeV, which was used for all calculations reported here.

Excitation-energy cutoff; effect on kinetic energies

It is necessary to cut off the $E_{L,H}$ distributions at some energies above and below the most-probable E_L (or E_H) at which the probability becomes very small. We have applied the cutoff at $\bar{E}_{L,H} \pm 3\sigma_{L,H}$, at which the probability is about 1% of the peak value. However, the cutoff on the low-energy side often falls in the region of negative excitation energies as shown for the example of A = 97 in Fig. 2. Since we reject all negative excitation energies, the histogram of "acceptable" excitation energies may be quite asymmetric.

The zero-cutoff causes no difficulty in the evaporation calculations, but implies an E_K distribution different from that assumed for the input data. As excitation energy is cut off on the low-energy side, the implied E_K distribution is cut off on the high-energy side. Both the $\bar{E}_K$ and σ_{E_K} of the implied distributions are smaller than the input values as shown at the right of Fig. 2. We have exaggerated the sharpness of the E_K cutoff in Fig. 2 by assuming E_H always has the value $\bar{E}_H$. In the actual calculations E_L and E_H are assumed to be uncorrelated; thus, the E_K cutoff will be rounded off as shown below in Fig. 4. Fortunately, the cutoff problem is made less serious by the fact that, in general, the most-probable charge division is the one having the highest E_T and, thus, the least serious cutoff. This may be seen by considering the fcy curve for mass 97 in Fig. 1 and the E_L distributions of Fig. 2.

The programme was modified to allow it to store and print-out information on the implied E_K distributions. As expected, the resulting E_K and σ_{E_K} values were generally lower than the input values, in the worst cases by as much as 3 and 2 MeV respectively. In order to cause the implied E_K distributions to agree with our choice of experimental values we have raised the input values of $\bar{E}_K$ and σ_{E_K} as shown in Fig. 3. The implied $\bar{E}_K$ and σ_{E_K} values agree well with the experimental values in most mass regions, but we have allowed the σ_{E_K} values in the symmetric region to remain below the curve obtained by GIBSON et al. [7], as most kinds of experimental errors in this region would tend to increase the observed values.

In Fig. 4 we show histograms of the implied E_K distributions for three different mass splits. For mass 97, we compare the calculated curve with the experimental data obtained by MILTON and FRASER [8]. The histogram for A = 104 illustrates the case of a large difference between the input

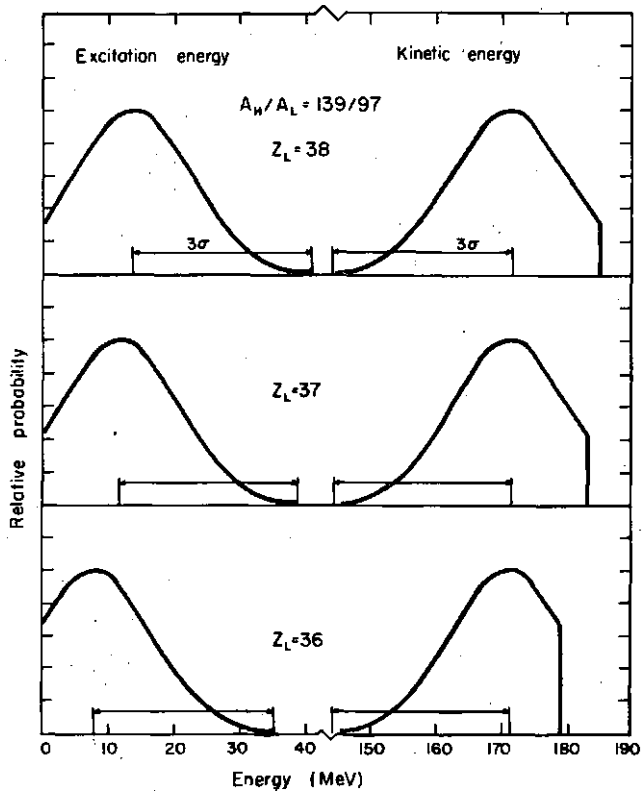

Fig. 2

E_{97} and implied E_K (139/97) distributions for various Z_{97} values, calculated from the data shown in Fig. 1, with σ_{E97} = 9.2 MeV (input value), and the assumption that the mass-139 fragment always has its average excitation energy, E_{139} = 8.3 MeV

and experimental $\bar{E}_K$ values and that for A = 119 shows a typical result in a region of high σ_{E_K}. The histogram for mass 97 is in good agreement with the experimental data. Many of the calculated histograms show asymmetries of the type present in that for mass 104. We are unable to determine whether or not this asymmetry is in disagreement with experimental results as, apart from the mass-97 data shown, there are no recent data on kinetic energies presented in this form. In older work on spontaneous fission of Cf^{252} [12], some of the E_K distributions for various ranges of mass ratio of division show asymmetries of this type.

Gamma-ray energy release

In Fig. 5 we plot the average γ-ray energy release, $\bar{E}_{\gamma L,H}$, per fragment as a function of A and the sum, $\bar{E}_{\gamma sum}$, of $\bar{E}_{\gamma L}$ and $E_{\gamma H}$ for complementary mass numbers as a function of A_L. There have been no studies of $\bar{E}_{\gamma sum}$ as

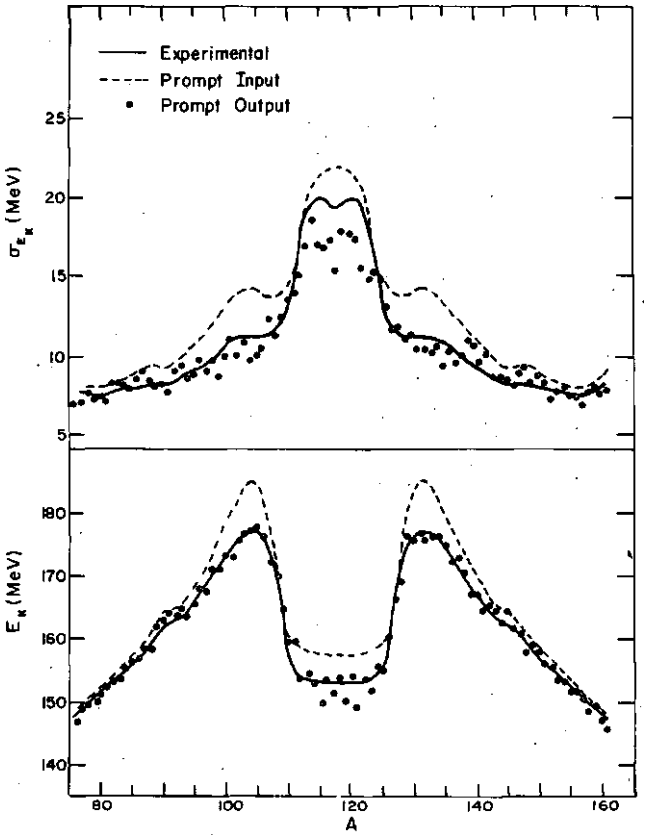

Fig. 3

Input and output values of $\bar{E}_K$ and σ_{E_K} from the (prompt) calculation compared with the experimental values

a function of A_H/A_L for fission of U^{236*}. In the case of Cf^{252} spontaneous fission, there does not appear to be any strong dependence of $\bar{E}_{\gamma sum}$ on mass number [12]. In regions where the number of γ-rays is small, the γ-ray energies are high. Our over-all weighted value of $\bar{E}_{\gamma sum}$ is 7.66 MeV, in excellent agreement with the experimental value of 7.2 ± 0.8 MeV [13]. The calculated value of 7.66 MeV includes the energy of long-lived isomeric states having half-lives so long that their decay energies are not included in the 7.2-MeV experimental value.

Previous calculations on the dissipation of fragment excitation energies have predicted $\bar{E}_{\gamma sum}$ values of 3.8 MeV [14] and 4.9 MeV [15], considerably smaller than the experimental value. The main reason for the larger $\bar{E}_{\gamma sum}$ values obtained in our work is the use of the pairing-energy correction for level densities. The excitation energy required for neutron emission is $S_n + \delta$ rather than merely S_n. Thus, with the use of δ's, more of the excitation energy appears as γ-rays and less as neutron evaporation, improving the calculated fit to $\bar{E}_{\gamma sum}$ and $\bar{\nu}_A$. In one calculation in which all δ values were set equal to zero, the over-all average $\bar{E}_{\gamma sum}$ value was 5.03 MeV.

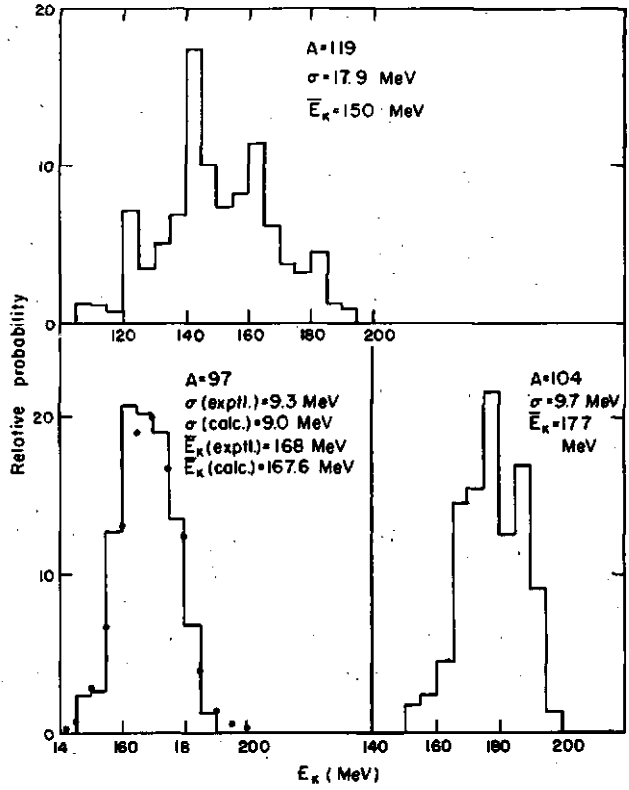

Fig. 4

Histograms of implied E_K distributions for several mass divisions, obtained from the input data shown in Fig. 3.
For A = 97, the points are experimental results of MILTON and FRASER [8], as are the experimental values of σ and $\bar{E}_K$ given.

The use of δ's, although not intended for that purpose, has in part the same effect on $\bar{E}_{\gamma sum}$ as a correction for angular momentum of the fragments. Prompt γ-ray angular distributions [16] and isomer-yield ratios [3] indicate high average spins (5 to 8 ħ) of primary fragments, even in thermal-neutron fission. High angular momentum tends to favour γ-ray emission relative to neutron evaporation at excitation energies not far above S_n [17]. If we use the simple assumption that the angular momentum is present as collective rotation, "unavailable" for neutron evaporation, and emitted after evaporation as γ-rays, the increase in $\bar{E}_\gamma$ per fragment would be about 0.4 to 1.2 MeV for assumed fragment moments of inertia of the rigid-body value (J_{rig}) or 0.3 J_{rig} respectively. Thus, the rotational effects could be large enough to give agreement with the experimental value of $\bar{E}_{\gamma sum}$ but they would not have the odd-even properties of the δ values that seem to be required to give smooth charge-distribution curves for even-mass secondary fragments as discussed below.

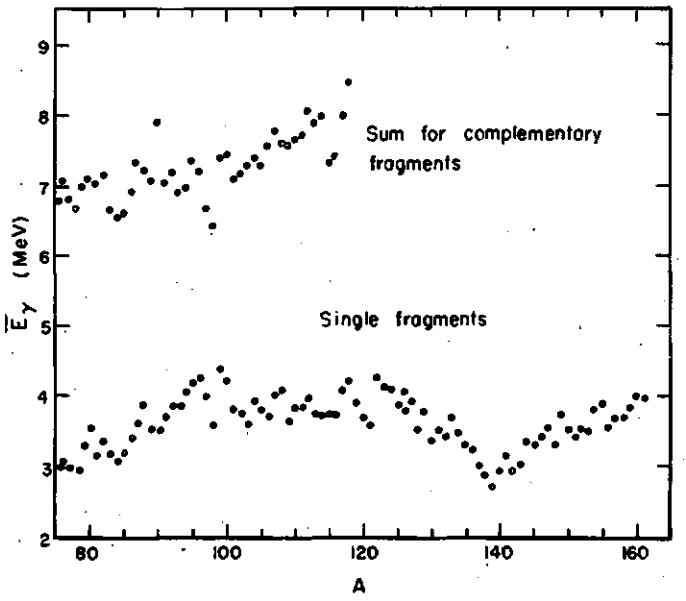

Fig. 5

Calculated average γ-ray energy release per fragment and sum of average γ-ray energy release for complementary fragments as a function of A

Neutron kinetic energy spectrum

In Fig. 6 we compare the calculated and experimental [18] laboratory-system kinetic energy spectra. The agreement is generally good, although in the high-energy, linear portion, the calculated spectrum drops off slightly faster with energy than the experimental one. The curve of Fig. 6, obtained with $\gamma = 13$ MeV, is in better agreement with the experimental data than that calculated with $\gamma = 8$ MeV for which the downward slope at high energies was greater. Better agreement with the experimental curve could probably be obtained by use of a γ-value greater than 13 MeV, but we felt constrained to keep to the range $8 \leq \gamma \leq 13$ MeV indicated by most analyses of the spacings of neutron-capture resonances. The value of $\gamma = 13$ MeV is in reasonable agreement with TERRELL's analysis of the gross fission neutron spectrum that yielded the result $a = 12 \pm 2$ MeV^{-1} corresponding to $\gamma = 10.5 \pm 1.5$ MeV [15].

Neutron multiplicities and charge-distribution curves

In the lower part of Fig. 7 we show the calculated points for $\overline{\nu}_A$ as a function of A compared with the experimental values [9]. The agreement is quite good except that the calculated points are slightly low in the region $100 \leq A \leq 106$ and generally high by about 0.15 ħ for $A \leq 138$. Improvements could perhaps be obtained by adjustment of $F(A_H/A_L)$ values, but we felt the fit was good enough for our purposes. Fluctuation of $\overline{\nu}_A$ values and related quantities is mainly due to statistical fluctuations in the Monte Carlo calcu-

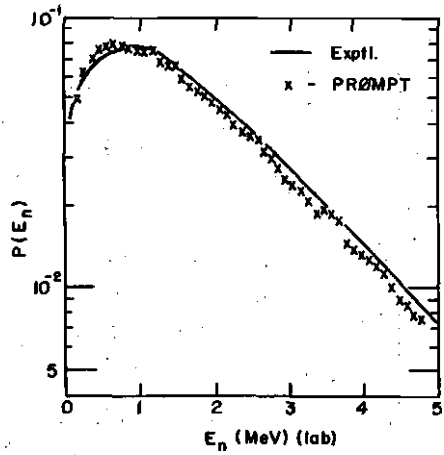

Fig. 6

Calculated (prompt) and experimental laboratory-system neutron kinetic energy spectra

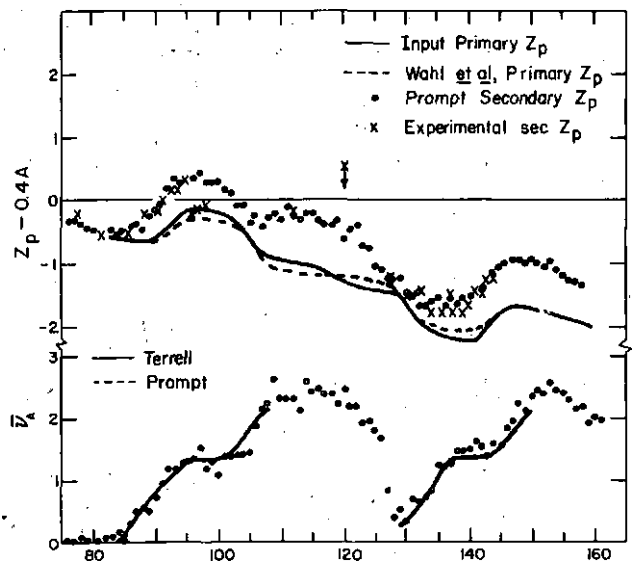

Fig. 7

Calculated (prompt) and experimental Z_p secondary and $\bar{\nu}_A$ (TERRELL [9]) as a function of A. Also shown are input Z_p primary values and those suggested by WAHL et al. [2].

lations. For most calculations, we ran only 50 iterations per primary nuclide.

Between A = 108 and 129 there are no experimental values of $\bar{\nu}_A$ for U^{236*} fission. MILTON and FRASER [8] assumed a $\bar{\nu}_A$ curve in that region based largely on Cf^{252} data. Their assumed curve, which rises to ~3.7 at A = 120, was in thermodynamic agreement with their E_K data and E_T from mass equa-

tions. In previous work [4], we found the E_K deficit at symmetric fission to be only 21 MeV instead of 36 MeV as determined by Milton and Fraser. Thus, the $\bar{\nu}_A$ values thermodynamically consistent with our measurements of E_K are considerably lower than those used by Milton and Fraser.

In Fig. 7 we show the primary and secondary Z_p values from the calculations and all known experimental secondary Z_p values. As shown, we have adjusted slightly the primary Z_p values suggested by WAHL et al. [2] to obtain better fits to the experimental secondary values. The calculated secondary Z_p values are actually weighted average charges, $\bar{Z}$, for each chain. As no serious asymmetries have been found in the secondary charge-distribution curves, we did not feel it necessary to do curve fitting at each mass number to obtain true Z_p values. Experimental secondary Z_p values were taken from the paper by WAHL et al. [2], with additional values for A = 112 [19], 127 [20] and an upper limit for A = 121 [21]. The agreement between calculated and experimental values is very good except for A = 96, 97 and 98. The experimental points may be in error because of isomerism in Nb^{96} and Nb^{97}, and the large uncertainty for Tc^{98} (see Ref. [2]).

Secondary fcy values for three mass chains are shown in Fig. 8. For comparison we have drawn curves calculated according to Eq. (1) with

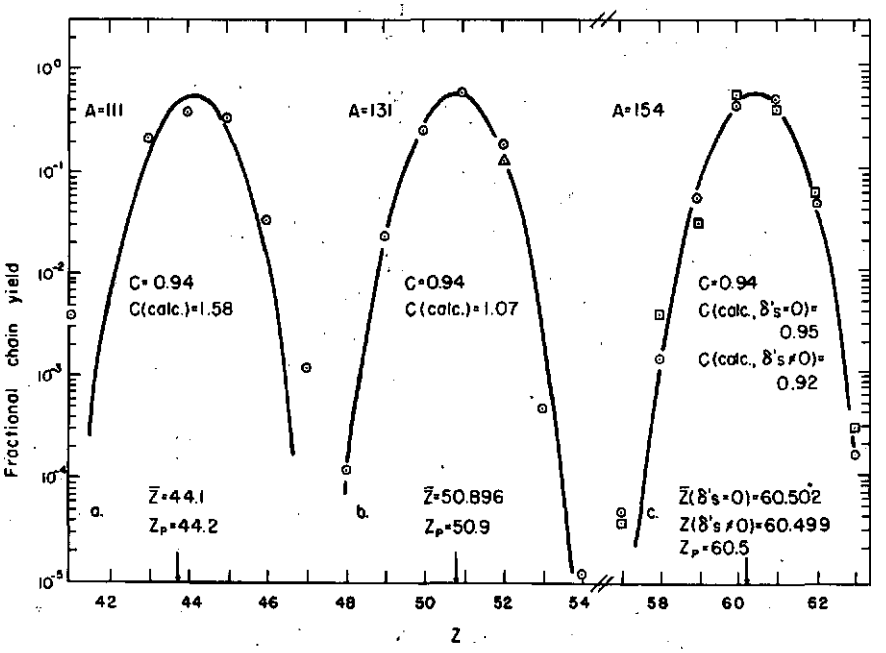

Fig. 8

Calculated secondary fcy values (shown as points) as a function of Z for three mass chains. The curves drawn in were calculated from Eq. (1) with C = 0.94 and Z_p that best fit the secondary fcy points.

⊙ Calculated using pairing-energy corrections (δ's)
⊡ Calculated with all δ's = 0
△ Experimental point [3]

C = 0.94 and Z_p values that best fitted the points. With the possible exception of mass 111, the points fall on approximately symmetric curves having $Z_p \approx Z$, indicating that our use of Z instead of Z_p in Fig. 7 is not in serious error.

The fcy points for A = 131 are typical of regions of small $\overline{\nu}_A$ (here about 0.6). The secondary fcy values fall on a nearly symmetric curve having C = 1.07, only slightly greater than that of the primary fragments, 0.94. The point for Te^{131} is in reasonable agreement with the experimental value of 0.124 ± 0.014 [3]. The points for A = 111 are typical of regions of large $\overline{\nu}_A$, in this case about 2.3. The calculated C, 1.58, is much greater than that of the primary fragments, and the points fall on a somewhat asymmetric curve that is broader on the low-Z side. This type of asymmetry would probably escape experimental detection as most independent-yield measurements are of species on the high-Z side.

The fcy values for A = 154 show the effect on an even-A chain of setting all δ values equal to zero. The points obtained using the pairing-energy corrections fall on a smooth curve that is unusually narrow for this region (see Fig. 9). Points obtained with all δ's = 0 show strong odd-even effects: fcy's of e-e nuclides are generally greater and those for o-o species lower than those obtained with pairing corrections. There is no experimental evidence for any such odd-even variation. In an extensive investigation of this point, HERRINGTON was unable to remove odd-even fluctuations without the use of pairing corrections [22]. Therefore, if our assumptions of smooth primary yield-mass and charge-distribution curves are correct, it is apparently necessary to include pairing corrections in the level-density expression to avoid odd-even fluctuations in the secondary fcy curves.

THOMAS and VANDENBOSCH suggested that, because of pairing effects on E_T, the primary yield of e-e species may be greater than for neighbouring odd-A species, which may in turn be greater than for o-o species [23]. Possibly an adjustment of primary yields as suggested would yield smooth fcy curves for secondary fragments without the use of pairing corrections. In the present formulation, no apparent odd-even fluctuations are introduced into the secondary fcy distributions for odd-A, as each member of the chains has about the same value of δ.

Setting δ's equal to zero also raises the ν_A values generally to about 0.3 n above the experimental values and lowers the average γ-ray energy release per fission from 7.66 to 5.03 MeV.

In Fig. 9 are shown the calculated C values of the secondary fragments. The scatter of points results from the strong dependence of C on the secondary yields of species far from Z_p, whose yields are very sensitive to fluctuations of the Monte Carlo process. Clearly, however, there are observable trends of C with changing A.

The C values obtained in the calculation are probably generally too large. Independent-yield data analysed by WAHL et al. [2] give $C = 0.94 \pm 0.15$ based mainly on mass chains 139 to 143, where we find $C \approx 1.15$. Part of the increase of our C values results from dispersion in ν_A larger than consistent with experimental data as discussed below. Also, the input C of the primary fragments, 0.94, may be too large. An input C of 0.4 gave a secondary C dependence on A having approximately the same features as those of Fig. 9, but generally displaced ~0.5 charge unit lower.

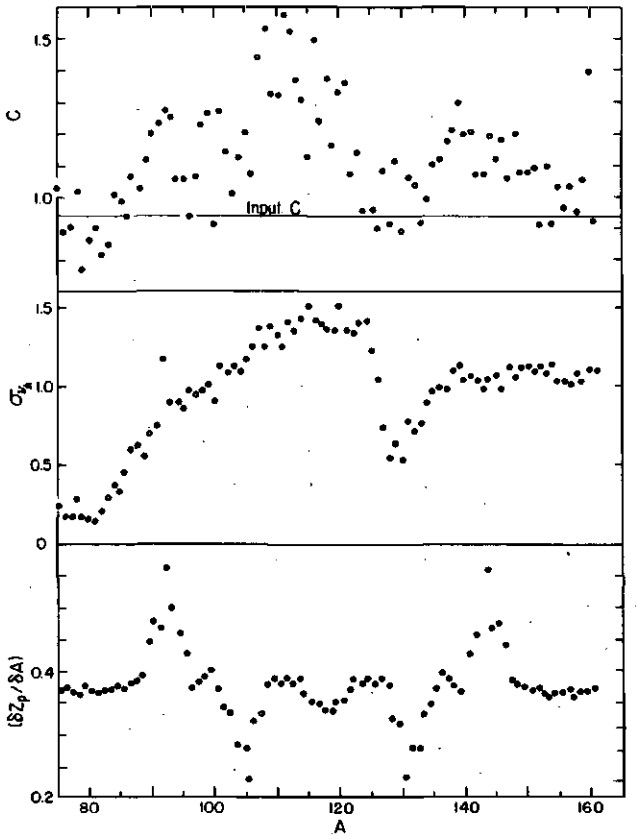

Fig. 9

Upper: Calculated C of the secondary fragments
Middle: Standard deviation σ_{ν_A}
Lower: Derivative $(\delta Z_p/\delta A)$ of the primary fragments.

There are only six mass chains for which independent yields are known for more than one isobar [2]. The five from A = 139 to 143 give C = 0.94 ± 0.15; the sixth, at A = 91, gives C = 1.48 ± 0.87. From our results in Fig. 9 it seems likely that there are large variations in C with A unless there are variations in C of the primary fragments in the opposite sense and of about the same magnitude as those shown for the secondary fragments in Fig. 9.

The value of C of the secondary fragments is a complicated function of C of the primary fragments, the $(\delta Z_p/\delta A)$ of the primary fragments, $\bar{\nu}_A$ and its derivatives with respect to A and with respect to Z_H/Z_L for constant A_H/A_L, the dispersion σ_{ν_A}, and, in regions of rapid change, the slope of the primary yield-mass curve. With C of the primary fragments kept constant with A, the next most important effects on secondary C values are probably σ_{ν_A} and $(\delta Z_p/\delta A)$. In Fig. 9 we see that the general trend of C parallels that of σ_{ν_A}, with perturbations caused by sudden large changes of $(\delta Z_p/\delta A)$. As noted below, the calculated σ_{ν_A} values are too large. If they can be reduced, the secondary C values will likewise be reduced.

The average number of prompt neutrons per U^{236*} fission (with 80-keV neutrons) is $\bar{\nu} = 2.47 \pm 0.03$, with $\sigma_\nu = 1.072 \pm 0.021$ [24]. In Fig. 9 we see that σ_{ν_A} for many mass chains is greater than the experimental value of σ_ν. We have calculated the neutron multiplicities of all pairs of complementary fragments assuming no correlation between ν_L and ν_H (as assumed by Eq. (5)), weighted each distribution by the primary yield and fcy for the division, and obtained the over-all neutron number distribution. This distribution has $\bar{\nu} = 2.59$ and $\sigma_2 = 1.39$; thus, $\bar{\nu}$ is slightly too high, but σ_2 is more seriously in error. The latter problem cannot be avoided by assuming a negative correlation between ν_L and ν_H. This would imply a negative correlation between E_L and E_H, giving σ_{E_x} values too small for agreement with experimental σ_{E_K} values. A positive correlation between E_L and E_H would give $\sigma_{L,H}$ values smaller than those obtained from Eqs. (5) and (6), but when the ν_L and ν_H values were combined assuming positive correlations, σ_ν would again be too large.

The most obvious method of reducing σ_ν is by relaxing the assumption implied by Eq. (2). If we were to allow $\bar{E}_K$ to vary with Z_H/Z_L for a given A_H/A_L, this could account for much of the observed dispersion in E_K rather than requiring a large σ_{E_x} as in our present treatment. In the limit, the change of E_T with Z_H/Z_L could be absorbed entirely by changing E_K and allowing $\bar{E}_x$ to remain constant and the distributions of E_x to be considerably narrower than in the present formulation. Thus, deviations from Eq. (2)

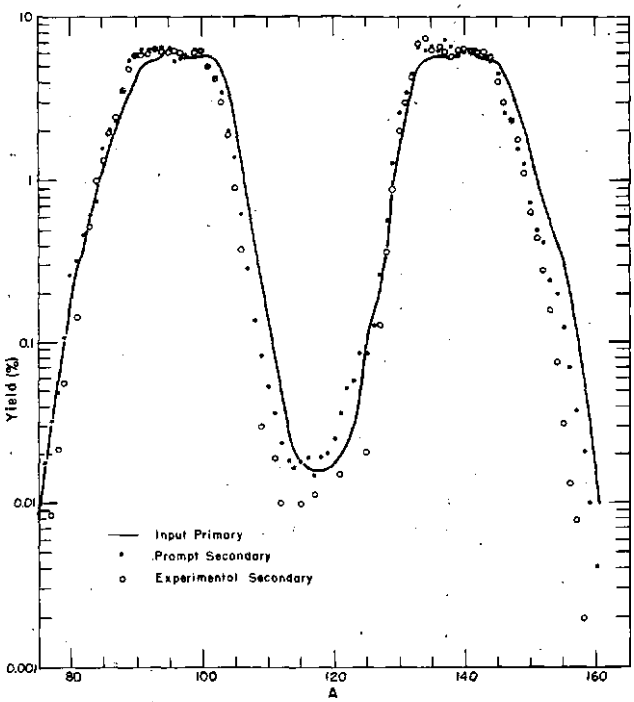

Fig. 10

Calculated (prompt) and experimental [18] secondary yield-mass points and curve of input primary yield-mass curve [8, 11].

cannot be directly determined from experiments, but seem inescapable in view of the inconsistency of our calculated σ_ν with experimental data. In future work we hope to examine the results obtained by relaxing the assumption of Eq.(2).

In Fig. 10 we compare calculated and experimental [18] secondary mass yields. The general features are reproduced, but in low-yield regions, near symmetric fission and on the wings of the peaks the calculated yields are too high. This is probably the result of errors in the primary yield-mass curve used. The calculated points do not reproduce some of the fine structure of the radiochemical curve, e.g. the "spike" at mass 134. This may be because of fine structure that was missed in the primary curve, but is more likely the result of improper treatment of neutron evaporation near shell edges.

CONCLUSIONS

The most important result is that the calculated σ_ν is larger than the experimental value. This result suggests strongly that there is not a fixed E_K distribution for all charge divisions for a given A_H/A_L, but that $\bar{E}_K$ varies with Z_H/Z_L, absorbing part or all of the variation of E_T.

The total energy release, E_T, obtained from SEEGER's mass formula [6] is well accounted for by $\bar{E}_K$ and $\bar{E}_{\gamma sum}$ values, and neutron kinetic energies in agreement with experimental data, and $\bar{\nu}$ higher than the experimental value by only 0.12 n, corresponding to an error in energy of ~0.8 MeV. The over-all accounting for E_T is thus much better than one would expect from errors in the mass equation alone.

The charge-dispersion parameter, C, of the secondary fragments is generally greater than that of the primary fragments, but we do not know by what amount as our results are based on $\sigma_{\nu A}$ values that are too large. The value of C of the secondary fragments probably varies appreciably with A. Any asymmetric distortions of the charge-distribution curve caused by neutron evaporation are not very serious. It is necessary to use pairing-energy corrections in the level-density expression to avoid odd-even fluctuations in the secondary charge-distribution curves for even-A fragments.

ACKNOWLEDGEMENTS

We wish to thank Miss Louise Wilson for her considerable help with the computer calculations. We acknowledge the assistance in the early phases of the work from Professor Demetrios G. Sarantites, Professor Richard D. Fink, and Dr. Arthur C. Herrington. We are grateful to Dr. Walter M. Gibson and Professor T. Darrah Thomas for the use of their data before publication. We thank Dr. James Terrell and Professor Charles D. Coryell for their helpful comments on this work. Calculations were performed on computers at the Massachusetts Institute of Technology Laboratory for Nuclear Science, the Massachusetts Institute of Technology Computation Center, and at the Oak Ridge National Laboratory.

REFERENCES

[1] CORYELL, C. D., KAPLAN, M. and FINK, R. D., Canad. J. Chem. 39 (1961) 646.
[2] WAHL, A. C., FERGUSON, R. L., NETHAWAY, D. R., TROUTNER, D. E. and WOLFSBERG, K., Phys. Rev. 126 (1962) 1112.
[3] SARANTITES, D. G., GORDON, G. E. and CORYELL, C. D., Phys. Rev. (to be published).
[4] ARAS, N. K., MENON, M. P. and GORDON, G. E., Nucl. Phys. (to be published).
[5] KAHN, H., Rpt. AECU-3259 (1954) (unpublished).
[6] SEEGER, P. A., Nucl. Phys. 25 (1961) 1.
[7] THOMAS, T. D., GIBSON, W. M. and SAFFORD, G., "Thermal-neutron-induced fission of U^{235}, U^{233} and Pu^{239}", these Proceedings II.
[8] MILTON, J. C. D. and FRASER, J. S., Canad. J. Phys. 40 (1962) 1626.
[9] TERRELL, J., Phys. Rev. 127 (1962) 880.
[10] DOSTROVSKY, I., FRAENKEL, Z. and FRIEDLANDER, G., Phys. Rev. 116 (1959) 683.
[11] GIBSON, W. M., private communication (1962).
[12] MILTON, J. C. D. and FRASER, J. S., Proc. 2nd UN Int. Conf. PUAE 15 (1958) 216.
[13] MAIENSCHEIN, F. C., PEELE, R. W., ZOBEL, W. and LOVE, T. A., Proc. 2nd UN Int. Conf. PUAE 15 (1958) 366.
[14] LEACHMAN, R. B., Phys. Rev. 101 (1956) 1005.
[15] TERRELL, J., Phys. Rev. 113 (1959) 527.
[16] HOFFMAN, M. M., Phys. Rev. 133 (1964) B714.
[17] GROVER, J. R., Phys. Rev. 123 (1961) 267.
[18] HYDE, E. K., The Nuclear Properties of the Heavy Elements III, Fission Phenomena, Prentice-Hall, Englewood Cliffs, N. J. (1964); contains most experimental data on fission with references to the original papers.
[19] KIMURA, K. and CORYELL, C. D., M. I. T. Laboratory for Nuclear Science Progress Report, M. I. T. - 2098-No. 64 (1964) 34 (unpublished).
[20] TROUTNER, D. E., WAHL, A. C. and FERGUSON, R. L., Phys. Rev. 134 (1964) B1027.
[21] WAHL, A. C. and NETHAWAY, D. R., Phys. Rev. 131 (1963) 830.
[22] HERRINGTON, A. C., Thesis, Dept. of Chem. Eng., Massachusetts Institute of Technology (1955) (unpublished).
[23] THOMAS, T. D. and VANDENBOSCH, R., Phys. Rev. 133 (1964) B976.
[24] DIVEN, B. C., MARTIN, H. C., TASCHEK, R. F. and TERRELL, J., Phys. Rev. 101 (1956) 1012.

DISCUSSION

V.I. LEBEDEV: With regard to Dr. Gordon's request that those doing experiments should make available data on kinetic energy distributions for a specific mass ratio, I should like to point out that care must be taken in comparing experimental and theoretical distributions since the former are subject to errors associated with the fragment-mass resolution and have so-called instrument resolution "tails". The latter have a considerable effect on the magnitude of the dispersion, particularly in the symmetric region. Bearing this in mind, it is nevertheless possible to see that the magnitude of kinetic energy dispersion, as shown in a paper presented earlier[1] decreases as the fragment-mass ratio increases. Our data are in very good agreement with the results on dispersion presented by Dr. Gordon.

[1] АПАЛИН В.Ф., ГРИЦЮК Ю.Н., КУТИКОВ И.Е., ЛЕБЕДЕВ В.И. и МИКАЭЛЯН Л.А., "Нейтроны и кинетическая энергия осколков при делении тяжелых ядер", these Proceedings I.

T. D. THOMAS: With regard to the excitation energy for a given mass division as a function of charge division, I have done some calculations similar to those of Vandenbosch. These indicate that the excitation energy changes by several MeV for a change of one unit in the charge and that the kinetic energy changes slowly. This would seem to indicate that the first assumption mentioned by Dr. Gordon is better than the second.

FISSION-NEUTRON SPECTRA OF U^{235}, Pu^{239} AND Cf^{252}

H. CONDÉ AND G. DURING
RESEARCH INSTITUTE OF NATIONAL DEFENCE, STOCKHOLM, SWEDEN

Abstract — Résumé — Аннотация — Resumen

FISSION-NEUTRON SPECTRA OF U^{235}, Pu^{239} AND Cf^{252}. Measurements of the fission neutron spectra from the neutron-induced fission of U^{235} and Pu^{239}, and the spontaneous fission of Cf^{252}, have been made. The spectra were measured with a time-of-flight technique using a plastic scintillator as the fission-neutron detector. The low energy part of the Cf^{252} fission-neutron spectrum (below 0.3 MeV) was also measured with a Li^6-glass detector replacing the plastic scintillator. The fissile materials were mounted in xenon-gas scintillation chambers. The primary neutrons were produced by a 2.5-MeV Van de Graaff accelerator with top terminal pulsing. The resolving time of the time-of-flight equipment was better than 3 ns. Results fitted to Maxwellian distributions, $\sqrt{E}e^{-E/T}$, are presented for neutron-induced fissions of U^{235} at 40 keV and 1.5 MeV of incident neutron energy and for Pu^{239} at 40 keV. Results are also given for the fission-neutron energy spectrum of Cf^{252}.

SPECTRES DES NEUTRONS DE FISSION DE ^{235}U, ^{239}Pu et ^{252}Cf. Les auteurs ont mesuré les spectres des neutrons émis dans la fission de ^{235}U et ^{239}Pu par des neutrons et dans la fission spontanée de ^{252}Cf. Ils ont mesuré les spectres par la méthode du temps de vol en utilisant un scintillateur en matière plastique comme détecteur des neutrons de fission. La partie à basse énergie du spectre des neutrons de fission de ^{252}Cf (en dessous de 0,3 MeV) a également été mesurée à l'aide d'un détecteur en verre au ^6Li, qui remplaçait le scintillateur en matière plastique. Les produits fissiles étaient placés dans des chambres à scintillations contenant du xénon. Les neutrons primaires ont été produits par un accélérateur Van de Graaff de 2,5 MeV avec impulsions terminales dans la partie supérieure. Le temps de résolution de l'appareillage à temps de vol était supérieur à 3 ns. Les auteurs présentent un ajustement des résultats aux relations maxwelliennes $\sqrt{E}e^{-E/T}$ pour les fissions de ^{235}U par des neutrons d'une énergie de 40 keV et 1,5 MeV, et pour la fission de ^{239}Pu par des neutrons d'une énergie de 40 keV. Ils donnent également les résultats ayant trait au spectre d'énergie des neutrons de fission de ^{252}Cf.

СПЕКТРЫ НЕЙТРОНОВ ДЕЛЕНИЯ УРАНА-235, ПЛУТОНИЯ-239 И КАЛИФОРНИЯ-252. Были произведены измерения нейтронных спектров деления урана-235 и плутония-239, вызванного нейтронами, и при спонтанном делении калифорния-252. Спектры были измерены методом времени пролета с помощью пластического сцинтиллятора в качестве детектора нейтронов деления. Для измерения низкоэнергетической части спектра нейтронов деления калифорния-252 (ниже 0,3 Мэв) вместо пластического сцинтиллятора использовался также Li^6-стеклянный детектор. Делящиеся материалы были вмонтированы в сцинтилляционные камеры с газообразным ксеноном. Первичные нейтроны были получены с помощью ускорителя Ван де Граафа энергией 2,5 Мэв с пульсирующим напряжением на кондукторе. Разрешающее время оборудования для измерений по времени пролета было лучше 3 наносекунд. Результаты, подогнанные под максвелловское распределение $\sqrt{E}\,e^{-E/T}$, приводятся для вызванных нейтронами делений урана-235 при энергии бомбардирующих нейтронов 40 кэв и 1,5 Мэв и для плутония-239 при 40 кэв. Приводятся также результаты для энергетического спектра нейтронов деления калифорния-252.

ESPECTROS DE LOS NEUTRONES DE FISIÓN DEL ^{235}U, ^{239}Pu y ^{252}Cf. Los autores midieron los espectros de los neutrones emitidos en la fisión del ^{235}U y del ^{239}Pu inducida por neutrones y en la fisión espontánea del ^{252}Cf. Efectuaron las determinaciones por el procedimiento del tiempo de vuelo, empleando un centelleador de material plástico como detector de los neutrones de fisión. También midieron la zona de bajas energías (inferiores a 0,3 MeV) del espectro correspondiente a los neutrones de fisión del ^{252}Cf, reemplazando para ello el centelleador de material plástico por un detector de vidrio con ^6Li incorporado. Los materiales fisionables se colocaron en cámaras de centelleo de xenón. Los neutrones primarios se produjeron mediante un acelerador de Van de Graaff de 2,5 MeV, con impulsión en el terminal superior. El tiempo de resolución del equipo utilizado para la determinación de los tiempos de vuelo fue inferior a 3 ns. Los autores presentan resultados ajustados a las distribuciones maxwellianas, $\sqrt{E}e^{-E/T}$, para fisiones del ^{235}U inducidas por neutrones

de 40 keV y 1,5 MeV de energía, y para el ^{239}Pu a 40 keV. Asimismo, exponen resultados correspondientes al espectro energético de los neutrones emitidos en la fisión del ^{252}Cf.

INTRODUCTION

The energy spectrum of the neutrons emitted in the fission process is of interest in fission theory and in reactor calculations. Several measurements have been made to study the neutron energy spectrum that results from spontaneous and thermal-neutron-induced fission. At higher incident neutron energies the experimental difficulties are greater and few measurements have been made. Most of these measurements were made at 4 and 14 MeV. A compilation of data up to 1963 was made by NILSSON [1]. Recently BARNARD et al. [2] have made measurements of the energy spectra from the fission of U^{238} induced by 2- and 5-MeV neutrons and also of the spectra from the thermal fissions of U^{235} and Pu^{239}.

TERRELL [3] calculated the fission-neutron spectra assuming that the neutrons were evaporated from the fragments in a time (10^{-20} to 10^{-14} s) during which the fragments have constant velocities. The calculations predict an essentially Maxwellian distribution of fission-neutron energies ($N(E) \sim \sqrt{E} e^{-E/T}$) in the laboratory system, which was found to be in good agreement with the experimental data available at that time. A similar distribution given by WATT [4] ($N(E) \sim e^{-aE} \sinh[b\sqrt{E}]$) was also discussed by Terrell and fitted to the same experimental data. Terrell also derived a relation between the average energy of fission neutrons, $\bar{E}$, and the average number of neutrons emitted per fission $\bar{\nu}$. After a recalculation [5] using experimental data up to 1962 the result was

$$\bar{E} = 0.74 + 0.653\ (\bar{\nu} + 1)^{\frac{1}{2}}\ (\text{MeV}).$$

At higher neutron energies, around 6 and 14 MeV, it is energetically possible that the fission occurs after the evaporation of one and two neutrons respectively. The fission-neutron energy spectra measured for incident neutron energies above 6 MeV will therefore have a low energy contribution caused by inelastically scattered neutrons [6].

The time-of-flight equipment described in Ref. [21] has been used in the present investigation. The results of the spectra from fission of U^{235} induced by 40-keV and 1.5-MeV neutrons, and Pu^{239} induced by 40-keV neutrons are given together with a Cf^{252} spontaneous fission spectrum.

EXPERIMENTAL ARRANGEMENTS

Two different experimental arrangements have been used in the present investigation.

The experimental arrangement and a block diagram of the electronic circuits used at the measurements of 40 keV of incident neutron energy are shown in Figs. 1 and 2. The measurements were made at the 2.5-MeV Van de Graaff accelerator of the Research Institute of National Defence, Stock-

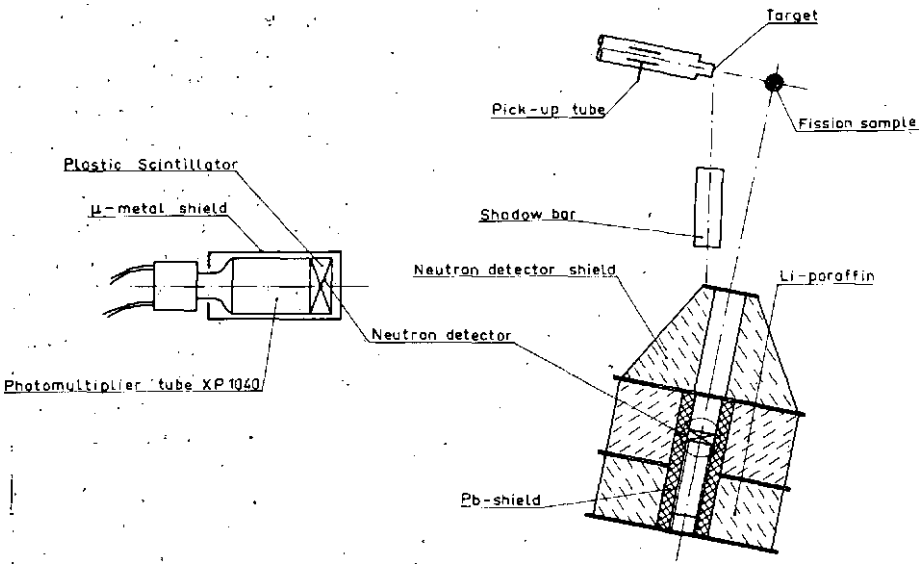

Fig. 1

Experimental arrangement of the time-of-flight equipment

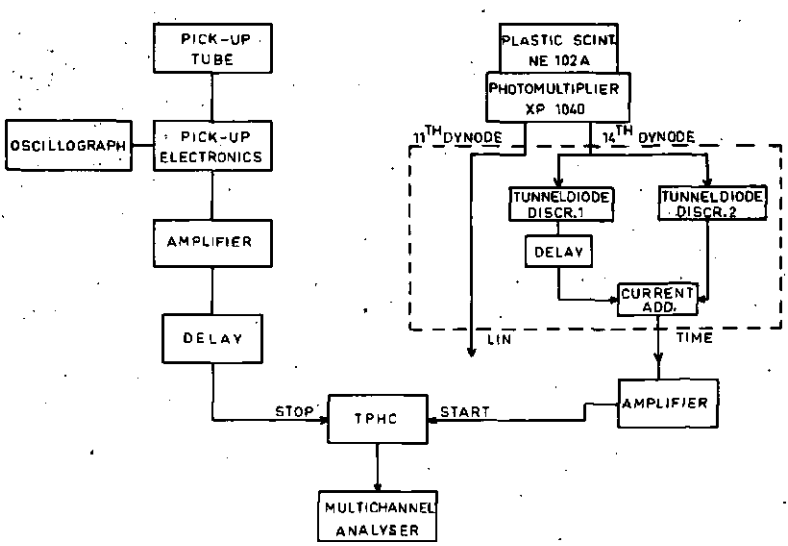

Fig. 2

Block diagram of the electronic circuits

holm, which is supplied with a beam bunching system giving pulses of about 1 ns with a frequency of 2 MHz. The pulsed neutrons were produced by the Li^7 (p, n) reaction in a thin lithium metal target with a thickness of about 4 keV for 2-MeV protons. The fission samples of U^{235} and Pu^{239} were in the

form of spheres with diameters of 2 cm. The samples were mounted close to the target. The neutron detector, a 5-in diam. × 2-in plastic scintillator described in Ref. [21], was placed at 70° to the direction of the ion beam and at a distance of 1 m from the fission sample. A lithium glass-detector 1 3/4-in diam. × 3/8 in placed 25 cm from the target was used to measure the incident neutron time-of-flight spectrum.

In the measurements of the neutron-induced fission of U^{235} at 1.5 MeV and of the spontaneous fission of Cf^{252} the fission samples were mounted in xenon-gas scintillation chambers. The pulse from the fission chamber started the time-to-pulse-height converter that was stopped by the pulse from the plastic scintillator neutron detector. A continuous beam from the Van de Graaff accelerator produced 1.5-MeV neutrons in a thin adsorbed tritium target by the T(p, n) reaction. The fission chamber surrounded by 1 mm of cadmium was placed 10 cm from the target, and the neutron detector was mounted at 90° to the direction of the ion beam at a distance of 1 m from the fission chamber.

The neutron energy spectrum from the spontaneous fission of Cf^{252} was measured with two different neutron detectors to cover a wide energy range. In the energy region from 70 to 500 keV use was made of a Li-glass detector (1 3/4-in diam. × 3/8 in) placed at 25 cm from the spontaneous fission source. Between 300 keV and 7 MeV the 5-in diam. × 2-in plastic scintillator described above was used placed at a distance of 1 m from the source.

Fission detectors

The fission detectors were constructed to give pulses contributing less than 1 ns to the resolution of the time-of-flight measurement. The fissile materials were painted on platinum foils and mounted in xenon-gas scintillation chambers. A wavelength shifter of quaterphenyl was deposited on the windows and the metal walls were coated with MgO.

After evacuation to less than 10^{-6} mm Hg, the chambers were filled with xenon-gas to a pressure of 0.5 atm. At this pressure the α-particles from the fissile material have longer ranges than the mean distance of 5 mm between the platinum foils. In this way the α-pulses were reduced in amplitude compared with the pulses caused by the fission fragments. The fast part of the pulses from the scintillation chambers had a rise time of less than 5 ns.

EXPERIMENTAL PROCEDURE

A typical time-of-flight spectrum obtained in the measurement of U^{235} at 1.5 MeV is shown in Fig. 3. The fission-neutron counting-rate was in this measurement about 1/min at a signal-to-background ratio of 1 : 1. In addition to the measurements of the fission-neutron time-of-flight spectra, the bias settings of the fission-neutron detector and the fission chamber were checked. The bias for the neutron detector corresponded to about 1/15 of the full energy peak, obtained by multiple Compton scattering of the γ-rays from an Am^{241} source. The bias of the fission chamber was set just above

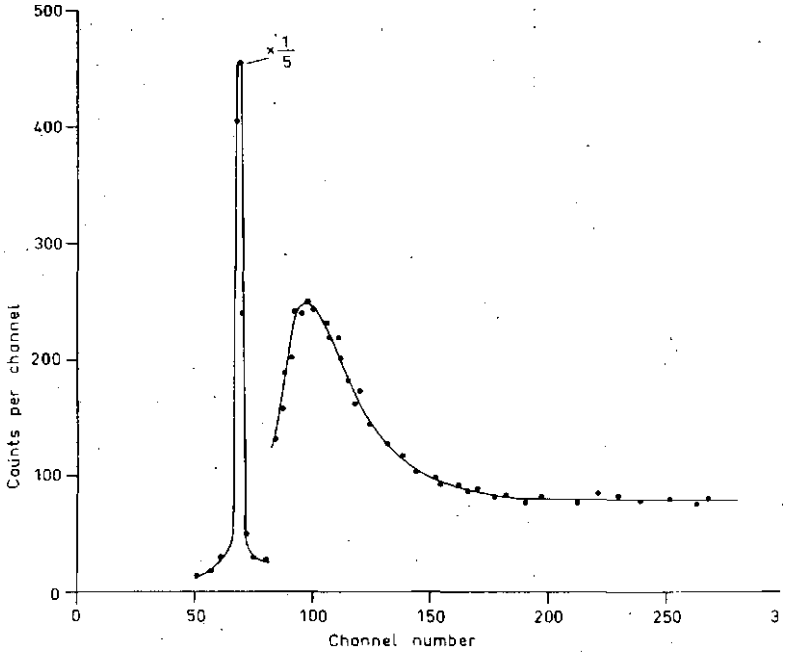

Fig. 3

Fission-neutron time-of-flight spectrum obtained in the measurement at 1.5 MeV of incident neutron energy

the peak of the pulse spectrum caused by the α-particles from the fissile material.

The number of nanoseconds per channel of the analyser was measured separately. In this measurement the same pulse was fed directly to the "start" input and via a delay-line to the "stop" input of the time-to-pulse-height converter. The delay-times of the lines were calibrated against a high precision frequency meter.

In the 40-keV measurements, made with a pulsed ion beam, the incident neutron time spectra were measured with a lithium glass detector. The background was measured with a lead sphere at the same position and of the same size as the fission sample to take account of the background caused by elastically scattered neutrons.

At 1.5 MeV the fission rate was measured with and without the Cd-shield around the fission chamber. The number of fissions induced by thermal neutrons were estimated to be less than 1% of the number of fissions induced by fast neutrons.

CORRECTIONS

Several corrections had to be applied to the observed fission-neutron time-of-flight spectra.

The background in the measurements at 40 keV of incident neutron energy was estimated from a separate run with a lead scatterer as discussed above. In the other measurements time-of-flight spectra were obtained that had a flat background distribution. However, in the high energy region of the spectra (above 6 MeV) the fission gamma peak had to be subtracted, which introduced an uncertainty in the high energy values.

The efficiencies of the neutron detectors, the plastic scintillator [21] and the lithium glass [7] vary with neutron energy, and the observed spectra were corrected for this effect.

Within the samples the fission neutrons induced secondary fissions and were scattered elastically and inelastically. The correction for these secondary reactions was negligible except for the measurements of U^{235} and Pu^{239} at 40 keV, where a large amount of fissile material was used. With the cross-section data from Ref. [8] and assuming that all the primary fission events were induced in the centres of the spheres, the correction in T was calculated using the data from Refs. [5] and [9] on the dependences of T on $\bar{\nu}$ and $\bar{\nu}$ on E_n respectively. The correction to the T-values was 0.5%.

To get a high fission rate and a good energy resolution the amount of fissile material must be large and the volume of the fission chamber must be small. To fulfil these requirements very thick fissile foils have to be used. However, with thick foils two corrections will be important. The fission fragments of high kinetic energies will be preferred and fragments emitted nearly parallel to the foil will be undetected. To ensure that these corrections would be small the fission foil thickness of U^{235} was not larger than 0.5 mg/cm^2.

RESULTS AND DISCUSSION

The experimental results of the present investigation are fitted to Maxwellian energy distributions, $N(E) \sim \sqrt{E} e^{-E/T}$. The spectra are shown in Fig.4 and the T-values are given by the slopes of the straight lines through the experimental points. In Table I are listed the different T-values of the present investigation. As predicted by the evaporation theory [3] the Maxwellian distribution gives a good fit to the fission-neutron energy spectrum. The deviation in the low-energy part of the U^{235} and Pu^{239} spectra at 40 keV may be caused by inelastic scattering of the fission neutrons within the source, as discussed above.

Table II is a compilation of the results from neutron-energy spectrum measurements of the neutron-induced fissions for U^{235} and Pu^{239}, and the spontaneous fissions for Pu^{240} and Cf^{252}. The average numbers of neutrons per fission ($\bar{\nu}$), taken from Refs. [9-11], are also given. The T-values from Table II, together with the result of the present investigation, are plotted in Fig. 5 against the corresponding $\bar{\nu}$-values. The curve represents the relation between the average energy of fission neutrons and the $\bar{\nu}$-values calculated by TERRELL [5] on the basis of the evaporation theory. In the calculations no allowance was made for variations in the excitation energy change per emitted neutron or in the fission channel spectrum, both of which vary with Z and A. The experimental points indicate a more rapid change in T

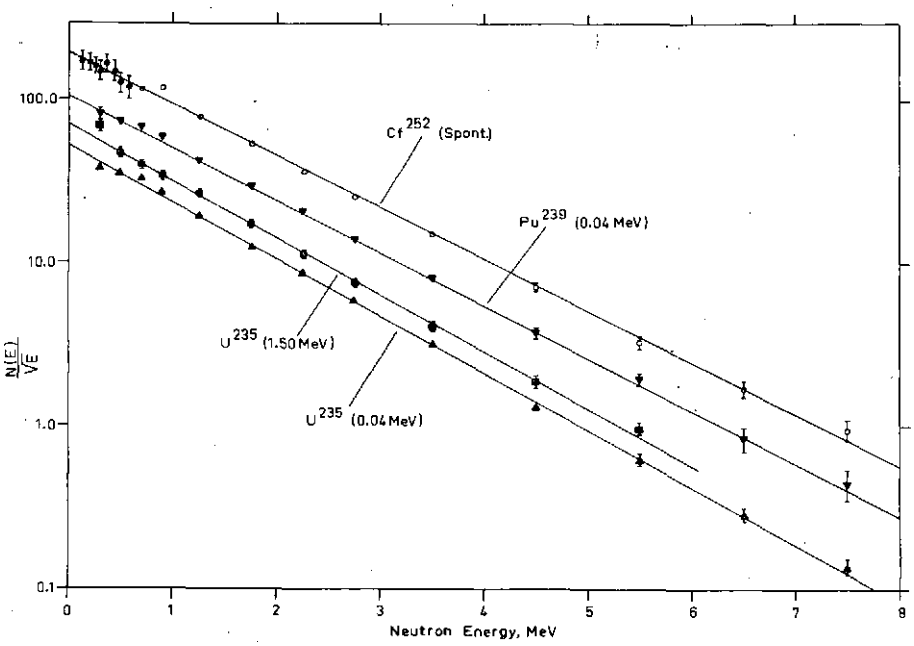

Fig. 4

Experimental results of the fission-neutron energy spectra of U^{235}, Pu^{239} and Cf^{252}. The experimental points are fitted to Maxwellian energy distributions $N(E) \sim \sqrt{E}e^{-E/T}$. The "temperatures" T are given in Table I.

TABLE I

RESULTS OF THE FISSION-NEUTRON ENERGY SPECTRA IN THE PRESENT INVESTIGATION

Isotope	Incident neutron energy (MeV)	Maxwellian temperature (MeV)
U^{235}	0.04	1.24 ± 0.04
U^{235}	1.50	1.25 ± 0.04
Pu^{239}	0.04	1.34 ± 0.04
Cf^{252}	Spont.	1.39 ± 0.04

TABLE II

RESULTS AND METHODS OF NEUTRON-ENERGY SPECTRUM MEASUREMENTS FOR THE NEUTRON-INDUCED FISSION OF U^{235} AND Pu^{239} AND FOR THE SPONTANEOUS FISSIONS OF Pu^{240} AND Cf^{252}

Fissile nuclide	Incident neutron energy (MeV)	Method	Maxwellian temperature T (MeV)	Average number of neutrons per fission ($\bar{\nu}$)	Reference
U^{235}	Thermal	Photoplate	1.37 ± 0.03	2.41	12
	Thermal	Photoplate	1.31 ± 0.01	2.41	13
	Thermal	Photoplate	1.27 ± 0.03	2.41	14
	Thermal	Prop. counter	1.24 ± 0.01	2.41	4
	Thermal	"Bramblett" counter	1.33 ± 0.03	2.41	15
	Thermal	Time-of-flight	1.28 ± 0.04	2.41	13
	Thermal	Time-of-flight	1.30 ± 0.03	2.41	2
	3.9	Threshold det.	1.38 ± 0.04	2.94	16
	14.1	Time-of-flight	1.37 ± 0.04	4.56	6
Pu^{240}	Spont.	"Bramblett" counter	1.19 ± 0.03	2.19	15
Pu^{239}	Thermal	Photoplate	1.51 ± 0.03	2.83	17
	Thermal	Photoplate	1.25 ± 0.04	2.83	14
	Thermal	"Bramblett" counter	1.39 ± 0.03	2.83	15
	Thermal	Time-of-flight	1.41 ± 0.03	2.83	2
	3.9	Time-of-flight	1.42 ± 0.03	3.45	18
	14.0	Photoplate	1.58 ± 0.08	5.07	19
Cf^{252}	Spont.	Photoplate	1.57 ± 0.05	3.77	20
	Spont.	"Bramblett" counter	1.37 ± 0.03	3.77	15
	Spont.	Time-of-flight	1.42 ± 0.05	3.77	20

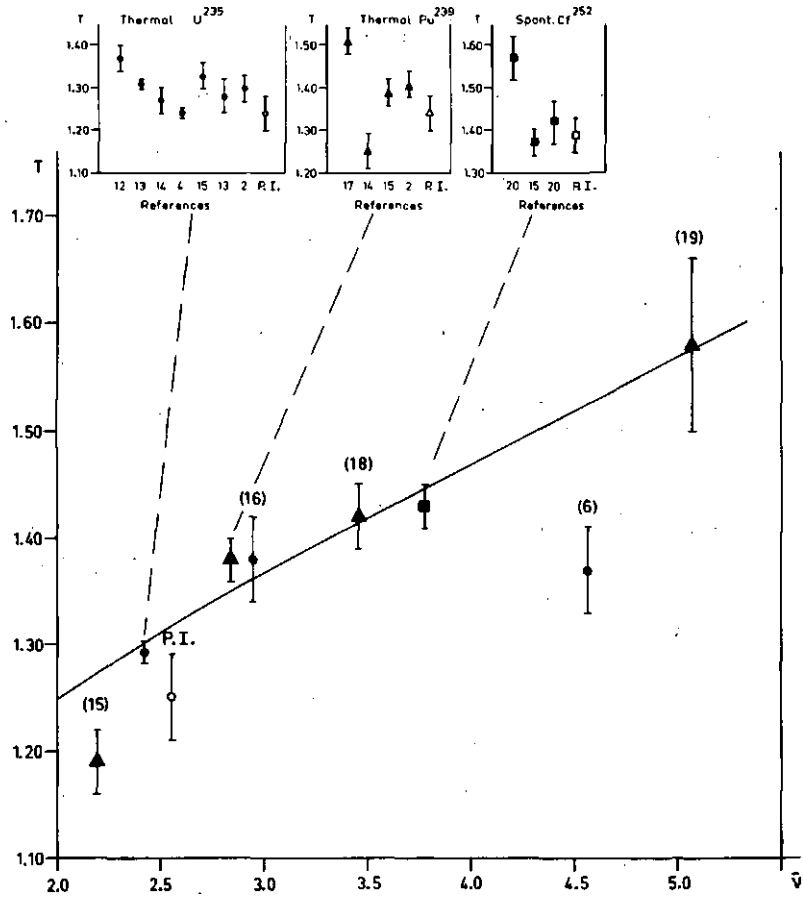

Fig. 5

The Maxwellian temperature T as a function of $\bar{\nu}$ for the data in Table II (filled signs) and for the present investigation (P.I.) (open signs). The circles, triangles and squares give the data of the uranium, plutonium and californium isotopes respectively. The curve represents the theoretical relation between T and $\bar{\nu}$ calculated by TERRELL [5].

with $\bar{\nu}$ in the region up to $\bar{\nu} \sim 3$, and above this $\bar{\nu}$-value a more flat curve than predicted by the simple evaporation theory.

However, more experimental information for one single isotope is needed to estimate the structure in the dependence of the Maxwellian temperature T on $\bar{\nu}$.

ACKNOWLEDGEMENTS

The authors thank Dr. N. Starfelt for his continuous interest in the work and Dr. A.T.G. Ferguson for many fruitful discussions on fast-neutron detectors. They also thank the Van de Graaff group at the Research Institute of National Defence for help in the production of neutrons.

REFERENCES

[1] NILSSON, I., Rpt. FOA 4 A 4237-44 (1962).
[2] BARNARD, E., FERGUSON, A.T.G., McMURRAY, W.R. and VAN HEERDEN, I.J., private communication.
[3] TERRELL, J., Phys. Rev. 113 (1959) 527.
[4] WATT, B.E., Phys. Rev. 87 (1962) 1037.
[5] TERRELL, J., Phys. Rev. 127 (1962) 880.
[6] VASILEV, Yu.A., ZAMYATNIN, Yu.S., ILIN, Yu.I., SIROTININ, E.I., TOROPOV, P.V. and FOMUSHKIN, E.F., Soviet Phys.-JETP 11 (1960) 483.
[7] SCHWARZ, S. and STRÖMBERG, L.G., to be published in Nucl. Phys.
[8] HUGHES, D.J. and SCHWARZ, R.B., Neutron Cross Sections, BNL-325, 2nd Ed., Brookhaven National Laboratory (1958).
[9] HOPKINS, J.C. and DIVEN, B.C., Nucl. Phys. 48 (1963) 433.
[10] MATHER, D.G., FIELDHOUSE, P. and MOAT, A., Phys. Rev. 133 (1964) B 1403.
[11] ASPLUND-NILSSON, I., CONDÉ, H. and STARFELT, N., Nucl. Sci. Engng 20 (1964) 527.
[12] NERESON, N., Phys. Rev. 85 (1952) 600.
[13] CRANBERG, L., FRYE, G., NERESON, N. and ROSEN, L., Phys. Rev. 103 (1956) 662.
[14] MUKHIN, K.N., BARKOV, L.M. and GERASIMOVA, reported by EROZOLIMSKII, B.G., Atomnaja Energija, Suppl. No.1 (1957) 74.
[15] BONNER, T.W., Nucl. Phys. 23 (1961) 116.
[16] BONDARENKO, I.I., KUZMINOV, B.D., KUTSAYEVA, L.S., PROKHOROVA, L.I. and SMIRENKIN, G.N., Proc. 2nd UN Int. Conf. PUAE 15 (1958) 353.
[17] NERESON, N., Phys. Rev. 88 (1953) 823.
[18] SMIRENKIN, G.N., Ž. eksp. teor. Fiz. 37 (1959) 1822.
[19] ZAMYATNIN, Y.S., SAFINA, I.N., GUTNIKOVA, E.K. and IVANOVA, N.I., Atomnaja Energija 4 (1958) 337.
[20] SMITH, A.B., FIELDS, P.R. and ROBERTS, J.H., Phys. Rev. 108 (1957) 411.
[21] CONDÉ, H., DURING, G. and HANSÉN, J., to be published.

DISCUSSION

A.T.G. FERGUSON: Dr. Terrell[1] pointed out the importance of the low-energy end of the fission neutron spectrum in distinguishing neutrons emitted from moving fragments from those emitted before scission. Adams, Barnard, van Heerden and myself have measured the fission neutron spectra from U^{235}, Pu^{239} and U^{238}. The fission neutron spectra, down to below 100 keV, were consistent with a form $E^{1/2}e^{-E/T}$. This agrees with the result found for Cf^{252} mentioned by Dr. During. In the case of U^{238}, fission spectra induced by neutrons of 2.1 MeV and 5.5 MeV showed a significant hardening of the spectrum at the higher energy, the average neutron energies being consistent with the expression $\overline{E} \approx 0.75 + 0.65\sqrt{\overline{\nu}+1}$ (MeV) given by Terrell.

[1] TERRELL, J., "Prompt neutrons from fission", these Proceedings II.

A LIQUID SCINTILLATOR EXPERIMENT FOR MEASURING $\bar{\nu}$ FOR Pu^{241}

J. W. BOLDEMAN
AUSTRALIAN ATOMIC ENERGY COMMISSION RESEARCH ESTABLISHMENT,
LUCAS HEIGHTS, N. S. W., AUSTRALIA

Abstract — Résumé — Аннотация — Resumen

A LIQUID SCINTILLATOR EXPERIMENT FOR MEASURING $\bar{\nu}$ FOR Pu^{241}. A 1-m-diam. tank of gadolinium-loaded liquid scintillator is being used for measurements of the number of prompt neutrons per neutron fission event for various target materials including Pu^{241}. Incident neutrons range in energy from thermal to 6 MeV. The thermal-neutron measurements use a collimated beam from the 10-kW reactor, MOATA. Neutrons of higher energy are produced with a 3-MeV Van de Graaff accelerator. The target material is incorporated in a methane proportional counter mounted at the centre of the liquid scintillator and within an evacuated flight path. Coincident pulses between this fission counter and the liquid scintillator indicate a fission event. Following each such event, pulses resulting from the detection of prompt neutrons in the liquid scintillator are counted for 40 μs. The number of pulses per fission event is converted to a pulse amplitude for recording in a pulse-height analyser.

The Van de Graaff accelerator is operated with externally triggered pulsing of such a kind that, during the 40-μs counting time, the DC proton or deuteron beam is interrupted, easing background problems especially in the case of Pu^{241} where only small amounts of material are available. At the same time there is essentially no loss in duty cycle. The efficiency of the liquid scintillator tank will be determined, using the accepted $\bar{\nu}$ value for the spontaneous fission of Cf^{252}. After making the usual corrections, a relative accuracy of 1% is expected for the $\bar{\nu}$ measurement.

MESURE DE $\bar{\nu}$ POUR ^{241}Pu, AU MOYEN D'UN SCINTILLATEUR LIQUIDE. L'auteur a utilisé une cuve de 1 mètre de diamètre contenant un scintillateur liquide chargé de gadolinium pour mesurer le nombre de neutrons instantanés par fission pour différents produits-cibles, notamment ^{241}Pu. L'énergie des neutrons incidents est comprise entre l'énergie thermique et 6 MeV. Les neutrons thermiques sont fournis sous forme d'un faisceau collimaté émis par le réacteur de 10 kW MOATA. Les neutrons de plus haute énergie sont produits par un accélérateur Van de Graaff, de 3 MeV. Le produit-cible est incorporé à un compteur proportionnel à gaz méthane monté au centre du scintillateur liquide et placé dans un canal pour trajectoire de vol où l'on a fait le vide. Chaque fois qu'il y a coïncidence entre impulsions enregistrées par le détecteur à fission et par le scintillateur liquide on sait qu'il y a eu fission. A la suite de chacune de ces fissions, les impulsions résultant de la détection des neutrons instantanés dans le scintillateur liquide sont comptées pendant 40 μs. Le nombre d'impulsions par fission est transformé en une amplitude d'impulsions qui est enregistrée dans un analyseur d'amplitude.

Le fonctionnement de l'accélérateur Van de Graaff est réglé de telle sorte que pendant le temps de comptage de 40 μs, le faisceau de protons ou de deutérons est interrompu, ce qui limite les difficultés dues au mouvement propre, particulièrement dans le cas de ^{241}Pu, où l'on ne dispose que de petites quantités de produit. En outre, il n'y a pratiquement pas de réduction du coefficient d'utilisation. Le rendement du scintillateur liquide est déterminé d'après la valeur de $\bar{\nu}$ admise pour la fission spontanée de ^{252}Cf. Après avoir procédé aux corrections habituelles, on peut s'attendre à une précision relative de 1% dans la mesure de $\bar{\nu}$.

ЭКСПЕРИМЕНТ С ЖИДКИМ СЦИНТИЛЛЯТОРОМ ДЛЯ ИЗМЕРЕНИЯ $\bar{\nu}$ ДЛЯ ПЛУТОНИЯ-241. Бак с жидким сцинтиллятором из газолиния диаметром 1 м используется для измерения числа мгновенных нейтронов на акт нейтронного деления в отношении различных материалов мишени, включая плутоний-241. Бомбардирующие нейтроны находятся в диапазоне энергий от тепловых до 6 Мэв. Для измерений тепловых нейтронов используется коллимированный пучок, получаемый на реакторе МОАТА мощностью 10 квт. Нейтроны более высоких энергий получаются с помощью ускорителя Ван де Граафа с энергией 3 Мэв. Материал мишени помещается в метановый пропорциональный счетчик, смонтированный в центре жидкого сцинтиллятора и в пределах удаленной траектории полета. Совпадающие импульсы между

этим счетчиком делений и жидким сцинтиллятором указывают акт деления. Вслед за каждым таким актом производится подсчет импульсов, получаемых в результате обнаружения мгновенных нейтронов в течение 40 микросекунд. Число импульсов на каждое деление переводится в амплитуду импульса для регистрации на анализаторе амплитуды импульсов.

Ускоритель Ван де Граафа работает с внешним импульсным пусковым устройством таким образом, чтобы за 40 микросекунд счетного времени ток в пучке протонов или дейтронов прерывался, облегчая проблемы фона, особенно в случае с плутонием-241, где имеются лишь небольшие количества материала. В то же время по существу нет потерь в полезно используемой доле времени цикла. Эффективность бака с жидким сцинтиллятором будет определяться при использовании принятой величины $\bar{\nu}$ для спонтанного деления калифорния-252. После обычных поправок ожидается получить относительную точность 1% для изменения величины $\bar{\nu}$.

MEDICION DEL $\bar{\nu}$ CORRESPONDIENTE AL ^{241}Pu CON UN CENTELLEADOR LIQUIDO. Se utiliza un tanque de 1 m de diámetro, que contiene un centelleador líquido activado por gadolinio, para medir el número de neutrones inmediatos por cada suceso de fisión inducida por neutrones en varias sustancias utilizadas como blanco, entre las que figura el ^{241}Pu. La energía de los neutrones incidentes oscila entre la región térmica y 6 MeV. Para las mediciones con neutrones térmicos, se utiliza un haz colimado procedente del reactor MOATA, de 10 kW. Los neutrones de energía superior se producen con un acelerador Van de Graaff de 3 MeV. La sustancia empleada como blanco se coloca en un contador proporcional de metano montado en el centro del centelleador líquido, en un conducto para trayectoria de vuelo de los neutrones en el que se ha practicado el vacío. Los impulsos coincidentes de este contador de fisión y del centelleador líquido indican un suceso de fisión. Inmediatamente después de cada uno de estos sucesos, se cuentan durante 40 μs los impulsos resultantes de la detección de neutrones inmediatos en el centelleador líquido. El número de impulsos por fisión se convierte en amplitudes, que se registran en un analizador de amplitud de impulsos.

El acelerador Van de Graaff funciona con impulsos accionados desde el exterior de forma que, durante el tiempo de recuento de 40 μs, se interrumpe el haz de protones o de deuterones portador de corriente continua, lo que simplifica los problemas planteados por la actividad de fondo, sobre todo en el caso del ^{241}Pu, sustancia sólo disponible en pequeñas cantidades. Al mismo tiempo, el ciclo de trabajo no sufre prácticamente interrupciones. Se determinará el rendimiento de recuento del tanque de centelleador líquido, utilizando el valor aceptado de $\bar{\nu}$ para la fisión espontánea del ^{252}Cf. Luego de introducir las correcciones habituales, se espera poder medir el coeficiente $\bar{\nu}$ una precisión relativa del 1%.

INTRODUCTION

The research programme at the Australian Atomic Energy Commission Research Establishment is concerned with the investigation of a high-temperature gas-cooled reactor system using beryllium oxide as moderator, commercial plutonium oxide as fuel, and thorium oxide as a fertile material. In addition to the Pu^{241} component of commercial plutonium, considerable quantities of this isotope will be produced during the fuel lifetime, since high fuel burnup is one of the prime requirements for the final reactor system. It has been estimated that the Pu^{241} may control up to 30% of the reactivity at certain stages of the fuel cycle; consequently accurate nuclear data are needed to predict the behaviour of such a reactor system. Furthermore, since the reactor system under study has a strong and time variant epithermal component in its neutron energy spectrum, the nuclear data in this region must be more accurate than is generally required.

The number of neutrons per fission ($\bar{\nu}$) for Pu^{241} has been measured on several occasions for thermal incident neutrons (Table I).

The available literature shows that the data for Pu^{241} are inferior to that for, e.g. U^{235}, and this may be attributed to experimental difficulties inherent in the use of the small samples and their lack of isotopic purity.

TABLE I

MEASURED $\bar{\nu}$ FOR THERMAL-NEUTRON FISSION OF Pu^{241}

Value	Reference
3.17 ± 0.12	[1]
2.91 ± 0.10	[2]
3.14 ± 0.06	[3]
3.023 ± 0.035	[4]
2.96 ± 0.08	[5]
2.93 ± 0.027	[6]
2.99 ± 0.16	[7]

No measurements have been made at any other neutron energy. There is a need, therefore, for additional thermal-neutron measurements, accurate to 1% if possible, and for measurements of $\bar{\nu}$ over a considerable range of neutron energies. An experimental programme with this aim is being undertaken using neutrons from the UTR type reactor, MOATA, and from suitable reactions using charged particle beams from a 3-MeV Van de Graaff accelerator.

EXPERIMENTAL METHOD

The experiment uses a large liquid scintillator (manufactured by Nuclear Enterprises (G.B.) Ltd.) of the type described by MOAT et al. [8] to detect the prompt neutrons from a fission event in a Pu^{241} sample. A 76-cm-diam. tank containing approximately 240 l of 0.5% gadolinium-loaded liquid scintillator is fitted with 12 5-in photomultiplier tubes (Fig. 1). Three banks of four photomultipliers operated in coincidence detect the liberation of gamma rays following the absorption of a neutron in the gadolinium loading. The average time for moderation and capture of fast neutrons is 10 μs.

A gas-flow fission counter is placed centrally in a 3-in diam. tube that runs axially through the scintillator tank. The target material is plated on to the anode of the fission chamber and exposed to a neutron beam passing through the axial tube. Ten milligrams of 77.2% Pu^{241}, obtained from the Atomic Energy Research Establishment, Harwell, is used and an additional counter containing Cf^{252} allows calibration of the neutron efficiency of the scintillator assuming the value of $\bar{\nu} = 3.785$ for the spontaneous fission of Cf^{252} given by HOPKINS and DIVEN (1963) [9].

A fission event is indicated by a coincidence between a fission counter pulse and a pulse from the scintillator caused by prompt fission gamma rays. Following the coincidence, pulses from the scintillator are counted for a 40-μs gating period. A block diagram of the electronics is shown in Fig. 2. The number of pulses received during the 40-μs gating period determines

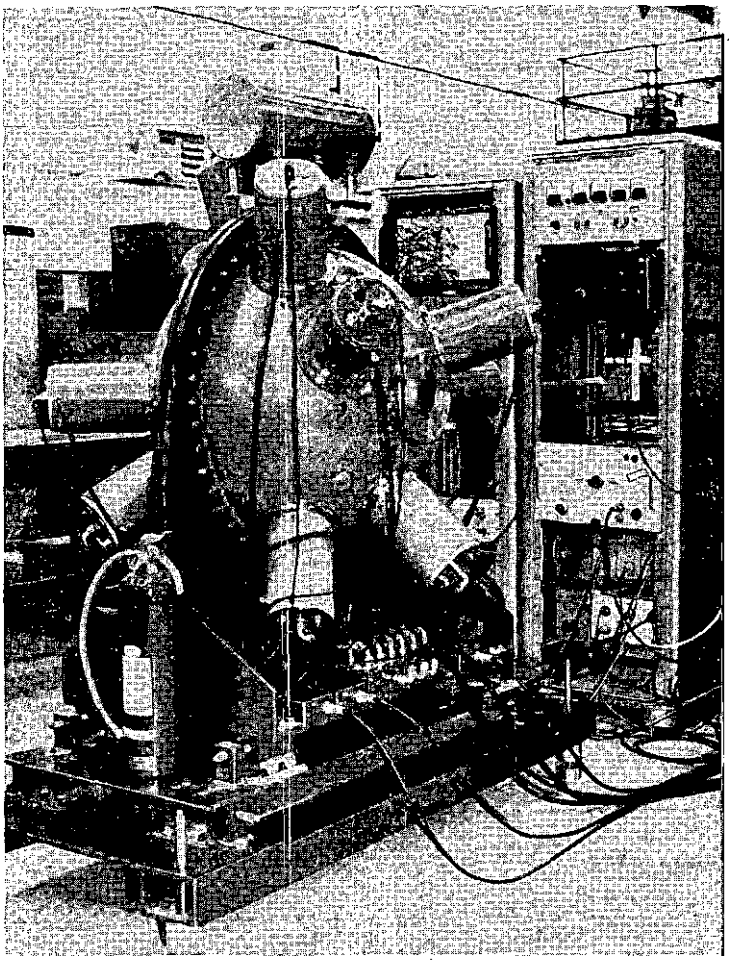

Fig. 1

The liquid scintillator tank

an address in the storage facility and a unit count is added at that address. Thus the probability of emission of one, two or three neutrons, etc., per fission is recorded, each in a separate channel. For each fission count, a background count for 40 μs is made 100 μs after the completion of the fission count by externally opening the scintillator gate and switching off the accelerator beam. The background counts are recorded directly into one channel of the temporary store. At the end of the counting cycle the information in the temporary store is transferred to the multiple unit counter and background counter, provided that a second fission event has not occurred during the 140-μs waiting period. If the latter does occur, all information for that particular counting cycle is discarded.

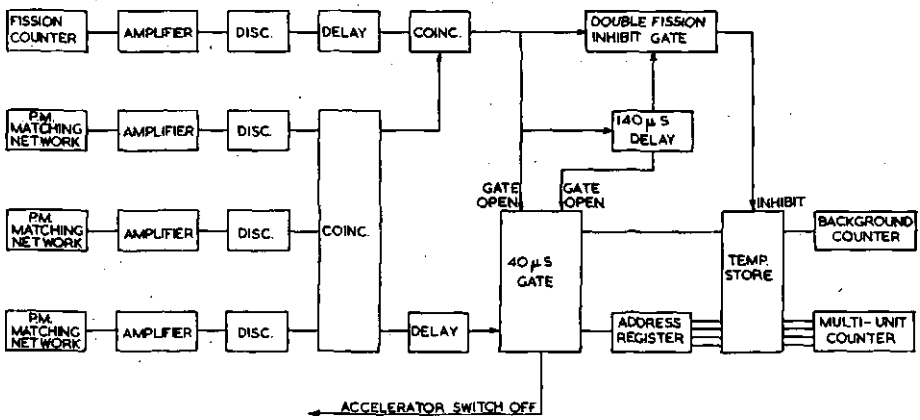

Fig. 2

Block diagram of electronics

THERMAL MEASUREMENTS

A collimated beam of thermal neutrons from MOATA passes through the central hole of the tank in an evacuated flight path. Collimation is achieved using first lead, then graphite and finally borated paraffin tubes. The tank is adequately shielded from the neutron beam and the major source of background comes from detection of environmental γ-rays. Background is reduced by surrounding the scintillator tank with walls of heavy concrete 3-ft thick. In addition to the Pu^{241} measurements, similar data will be obtained for Pu^{239} and Pu^{240}, firstly to verify the technique and secondly to facilitate corrections for these impurities in the Pu^{241} sample.

ACCELERATOR MEASUREMENTS

Neutrons in the energy range from 10 keV to 14 MeV are produced with a 3-MeV Van de Graaff accelerator using the $Li^7(p,n)Be^7$, $D(d,n)He^4$ and $D(T,n)He^4$ reactions. The direct shielding for the tank consists of 20 cm of iron, 45 cm of borated paraffin and finally 8 cm of lead (Fig. 3). The tapered neutron collimator itself consists of a polythene tube impregnated with boron. A concrete shield 3-ft thick surrounds the tank to reduce environmental background.

For measurements at these neutron energies, background caused by scattered neutrons presents a problem since the scattering cross-section of the counter materials and the fission cross-section for Pu^{241} are of the same order. Furthermore, with the small quantity of fissile material used it is necessary to use a continuous beam to achieve a sufficient fission rate. However, by cutting off the neutron beam immediately a fission event is recorded and keeping it off for the 40-μs period during which fission neutrons are counted, the background from scattered neutrons can be reduced by a factor of four. The accelerator has a deflection chamber following the ion

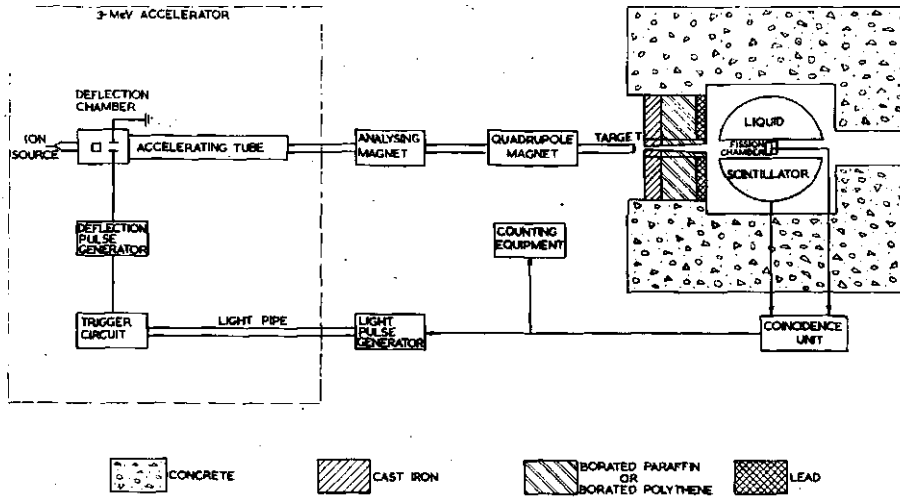

Fig. 3

Experimental arrangement of accelerator measurements

source. The application of a 600-V pulse to one of the deflection plates interrupts the beam for the period required for neutron counting. Light pulses, generated at the grounded end of the accelerator, produce a trigger pulse at the high-voltage terminal and this operates the deflection pulse circuit. The time between the fission counter pulse and the actual decay of the neutron beam at the target is less than 5 μs.

REFERENCES

[1] De SAUSSURE, G. and SILVER, E. G., Rpt. ORNL-2081 (1956).
[2] JAFFEY, A. H., HIBDON, C. T. and SJOBLOM, R., Rpt. ANL-5396 (1955).
[3] De SAUSSURE, G. and SILVER, E. G., Nucl. Sci. Engng 5 (1959) 49.
[4] KALASHNIKOVA, V. I., LEBEDEV, V. I., MIKAELYAN, L. A., SPIVAK, P. E. and ZAKHAROVA, V. P., Conf. Acad. Sci. USSR on the Peaceful Uses of Atomic Energy, Moscow. Session Div. Phys. Math. Sci. (1956) 123.
[5] JAFFEY, A. H., HIBDON, C. T. and SJOBLOM, R., J. nucl. Energy A, 11 (1959) 21.
[6] FERGUSON, A. T. G. and PATTENDEN, N., Rpt. ANL-6792 (1963) (work of Colvin, D. W. and Sowerby, M. W.).
[7] SANDERS, J. E., J. nucl. Energy 2 (1956) 247.
[8] MOAT, A., MATHER, D. S. and FIELDHOUSE, P., in Physics of Fast and Intermediate Reactors I IAEA, Vienna (1962) 139.
[9] HOPKINS, J. C. and DIVEN, B. C., Nucl. Phys. 48 (1963) 433.

GENERAL DISCUSSION

J.S. FRASER: I will, if I may, offer a comment relating to some of the recent work carried out on neutron yields from individual fragments, using several experimental techniques described at this Symposium and previously, for the purpose of measuring fragment energies and velocities. Now it is well known that the angular dispersion arising from prompt neutron recoil can cause a loss of coincidence counting-rate if equal solid angles are used on both sides of the apparatus. This applies to double velocity and double energy experiments whether solid-state or gas-ionization chambers are used in the latter. The point of my remark is that there is not only a loss of efficiency but that a bias is introduced into the results. This is so not only because the total number of neutrons is not constant for all mass ratios but because the average energy of the neutrons is not constant either. In the paper by Apalin et al. presented by Dr. Lebedev[1] and in the paper by Dr. Milton and myself[2] we have seen that the largest deviations occur near symmetric fission. As a consequence of these phenomena it is essential that experiments be designed with dissimilar solid angles for the two detectors, the ratio being made large enough to accommodate the recoil dispersion for the neutron-rich symmetric modes.

A. MOSSOP: As a user of data I wish to make a general comment on errors. We have heard during this Symposium of sets of results that differ from each other by amounts greater than would be expected from the quoted errors. For example, a -2% difference has been reported by Sowerby for recent boron pile measurements of $\bar{\nu}$ for Cf^{252} and Pu^{241} with quoted errors of 0.4% and 1.11% respectively[3]. This situation may be regarded as a typical between-within-group variation in which the total error is considerably larger than the within-group error. However, the errors that are being assigned to nuclear data appear to be the within-group errors and hence are merely estimates of the repeatability of the particular measurement. As a consequence they tend to be low since they do not allow for systematic variations. I appreciate that systematic errors are not easy to estimate; in fact, if they could be determined precisely, they could be allowed for, but I think a serious attempt ought to be made by experimenters to estimate such systematic effects, so that the quoted errors would be the true absolute values that the user requires.

---

[1] АПАЛИН В.Ф., ГРИЦЮК Ю.Н., КУТИКОВ И.Е. ЛЕБЕДЕВ В.И. и МИКАЭЛЯН Л.А., "Нейтроны и кинетическая энергия осколков при делении тяжелых ядер", these Proceedings I.

[2] MILTON, J.C.D. and FRASER, J.S., "The energies, angular distribution and yields of the prompt neutrons from individual fragments in the thermal-neutron fission of U^{233} and U^{235}", these Proceedings II.

[3] COLVIN, D.W. and SOWERBY, M.G., "Boron-pile $\bar{\nu}$ measurements", these Proceedings II.

PROMPT AND DELAYED GAMMA-RAYS, DELAYED NEUTRONS, BETA-ACTIVITY

(Sessions VII and VIII)

Review Paper

PROMPT AND DELAYED GAMMA-RAYS FROM FISSION

H. MAIER-LEIBNITZ, P. ARMBRUSTER AND H.J. SPECHT
TECHNISCHE HOCHSCHULE MÜNCHEN AND
KERNFORSCHUNGSANLAGE JÜLICH,
FEDERAL REPUBLIC OF GERMANY

Abstract — Résumé — Аннотация — Resumen

PROMPT AND DELAYED GAMMA-RAYS FROM FISSION. The following data about gamma-rays from fission are reported and discussed:

Total prompt gamma-ray spectrum, and average number and energy of gamma-rays; X-rays in prompt fission, and excitation of X-rays in matter; gamma-ray spectra as a function of the mass ratio in fission, gamma-lines in those spectra, and Doppler effect; anisotropy in gamma-emission relative to the direction of fragments; average gamma-energy and gamma-spectra as a function of mass of the fission products; delayed gamma-rays; delayed gamma-rays as a function of fission product mass.

RAYONS GAMMA INSTANTANÉS ET RETARDÉS PROVENANT DE LA FISSION. Le mémoire présente et discute les données suivantes sur les rayons gamma:

Spectre total des rayons gamma instantanés, nombre moyen et énergie moyenne des rayons gamma; rayons X dans la fission instantanée et excitation des rayons X dans la matière; spectres des rayons gamma en fonction du rapport des masses dans la fission, raies gamma présentes dans ces spectres et effet Doppler; anisotropie dans l'émission gamma par rapport à la direction des fragments; énergie gamma moyenne et spectres gamma en fonction de la masse des produits de fission; rayons gamma retardés; rayons gamma retardés en fonction de la masse des produits de fission.

МГНОВЕННЫЕ И ЗАПАЗДЫВАЮЩИЕ ГАММА-ЛУЧИ ПРИ ДЕЛЕНИИ. Приводятся и рассматриваются следующие данные относительно бета-лучей ядерного деления: общий спектр мгновенных гамма-лучей, среднее число и энергия гамма-лучей; рентгеновские лучи при делении мгновенными нейтронами, возбуждение рентгеновских лучей в веществе; спектры гамма-лучей как функция отношения масс при делении, гамма-линии в этих спектрах, доплеровский эффект; анизотропия при гамма-эмиссии в отношении направления осколков; средняя гамма-энергия и гамма-спектры как функция масс продуктов деления; запаздывающие гамма-лучи; запаздывающие гамма-лучи как функция масс продуктов деления.

RAYOS GAMMA DE FISION INMEDIATOS Y RETARDADOS. Se exponen y examinan los siguientes datos sobre los rayos gamma de fisión:

Espectro total de los rayos gamma inmediatos, número y energía medios de los rayos gamma; los rayos X en la fisión inmediata, excitación de rayos X en la materia; espectros de rayos gamma en función de la razón másica en la fisión, líneas gamma de dichos espectros, efecto Doppler; anisotropía en la emisión gamma con respecto a la dirección de los fragmentos; energía y espectros gamma medios en función de la masa de los productos de fisión; rayos gamma retardados; rayos gamma retardados en función de la masa de los productos de fisión.

The emission of gamma rays is the last stage in the fission process. Most or all of it occurs after the break-up of the fissioning nucleus and after the emission of the prompt neutrons. Thus one might expect that the gamma emission is determined mainly by something like the temperature of the nuclei after the neutron emission, and cannot be used to indicate special features of the fission process itself. Moreover, in view of the large number

of nuclides produced in fission and the complexity of their level schemes, one might not expect more than some averaged spectra without recognizable structure. However, the experiments have shown that all these simple predictions were wrong. The spectra show a large abundance of low-energy radiation which is an indication of high spin values resulting from the fission process; the angular correlation between the direction of the fission products and gamma rays indicates unusually high spin values; delayed gamma transitions occur in surprisingly large numbers; and the spectra, if analysed according to the mass ratio in fission, show a surprising number of resolved or near-resolved lines.

Thus the effort of the experimentalists in devising ingenious and difficult experiments has been well rewarded, and this may continue for some time. In this paper we shall briefly review the main results and indicate their possible meaning for the fission process and for nuclear structure. Experimental results on the γ-spectrum of the total of all fission fragments will be reviewed first. Then experiments on the mass dependence of the γ-spectra will be compiled. An interpretation of the experimental results will be given in the last part of the paper.

THE TOTAL OF ALL γ-QUANTA EMITTED

The spectrum

The energy dependence of the γ-spectrum has been investigated for several fissioning nuclei [1-4]. The γ-spectra obtained for different nuclei are the same within the accuracy of the measurements. An investigation of the dependence of the spectrum on the energy of the fission-inducing neutrons showed no dependence of the spectrum for neutron energies up to 14 MeV [5]. Only few of the measured spectra give values over the total range of the spectrum from 0.1 to 7 MeV, and these have been corrected for the response function of detectors. A comparison of spectra obtained in different experiments is difficult as the importance of this correction, and in some cases the influence of neutrons through capture and inelastic scattering in NaI, has been underestimated in many of the older experiments.

Our knowledge of averaged values for the prompt gammas is not very satisfactory. For the average gamma energy per fission, values of 7.2 and 8 MeV are given for U^{235} and of 8.2 and 9 MeV for Cf^{252}. The number of quanta emitted amounts to (9 ± 2) per fission. The values given for the number of quanta taken from the various experiments vary between 7 and 10 quanta per fission. The values given for Cf^{252} seem to be higher than the values given for U^{235}. The total number of quanta is known less accurately than the total energy. The average energy of the γ-quanta emitted promptly in low-energy fission is 1.0 ± 0.2 MeV. Accurate measurements of both average energy and number of prompt quanta per fission would seem desirable.

Figure 1 gives the γ-spectrum of U^{235} from the work of MAIENSCHEIN [1]. A Compton and a pair spectrometer were used in this measurement. Only 2% of the total energy appears in quanta with an energy higher than 2 MeV.

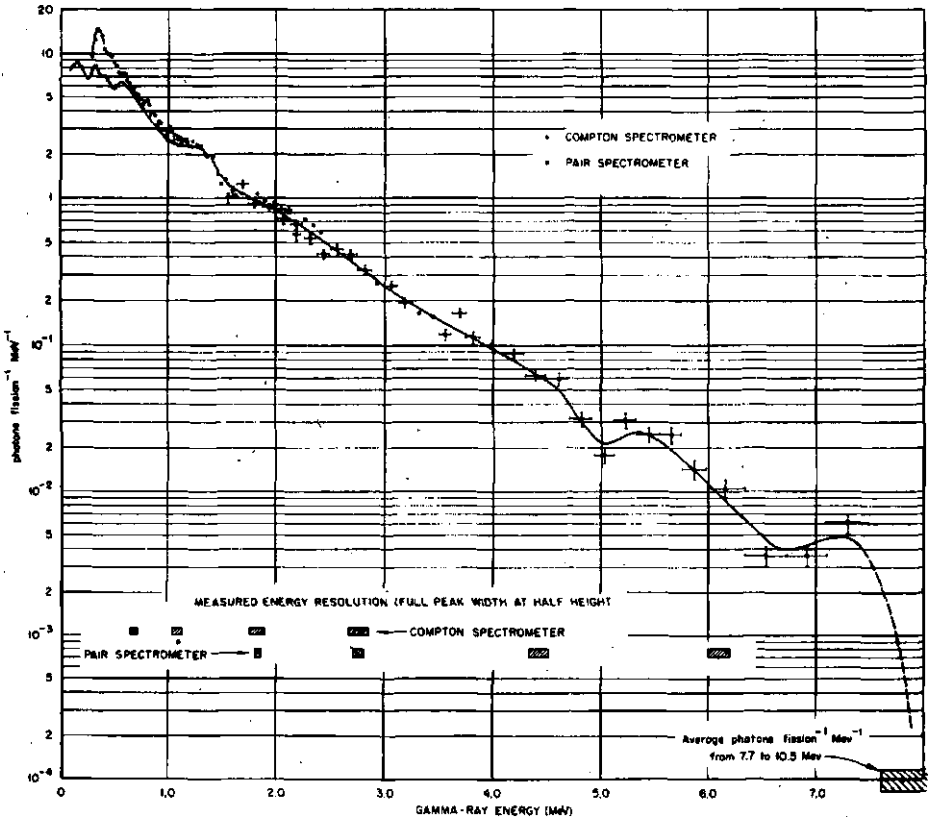

Fig. 1

The energy spectrum of prompt gamma rays from the thermal-neutron fission of U^{235} as measured by MAIENSCHEIN et al. [1] and RAU [4] (low-energy part)

The bulk of the quanta has energies between 0.3 and 1 MeV. The low-energy part of the spectrum shows a definite structure, as has been found by VOITOVETSKII et al. [6] and since confirmed by several other authors [4, 7]. Groups of lines with energies in the range of 100 to 500 keV have been reported. The low-energy part of the spectrum from the work of RAU [4] is included in Fig. 1.

Time-dependence of the spectrum

All measurements of the prompt γ-spectrum use coincidence techniques between γ-quanta and fission products with time resolutions between 10^{-9} s and 10^{-6} s. The limit of the delayed coincidence technique would seem to be in the range 10^{-9} to 10^{-10} s for the gamma energies considered. MAIENSCHEIN et al. [1] found that 5.7 % of the γ-quanta from U^{235} are emitted later than 1.2×10^{-7} s after fission. A similar result was obtained by JOHANSSON [8], who found about 6.5% of the total γ-quanta of Cf^{252} emitted in times greater than 10^{-8} s after fission. DESI et al. [9] investigated the

low-energy component of the spectrum between 25 and 100 keV. Half-lives between 10^{-9} and 10^{-10} s, decreasing with increasing energy of the quanta, have been found. Most of the prompt fission quanta are emitted in times shorter than 10^{-9} s, and the delayed coincidence technique can yield no information about them. Shorter times may be reached in view of the fact that fission fragments travel in vacuum with a speed of $\sim 10^9$ cm/s. The γ-quanta are emitted from fission fragments in flight. The determination of the emission time of a quantum may be reduced to a measurement of the distance between the starting point of the fragment and its position at the time of γ-emission. If this distance is measured with an accuracy of 10^{-2} cm, time measurements of 10^{-11} s seem feasible. The technique has been applied first by SKLIAREVSKII et al. [10] and has been much refined by JOHANSSON [11]. Skliarevskii et al. found a half-life of the radiation below 250 keV between 0.5×10^{-9} and 2.5×10^{-9} s. Johansson states that 55–65% of the γ-quanta are emitted with a half-life of 10^{-11} s, 15% with a half-life between 10^{-9} and 10^{-10} s, and only 15 to 25% are emitted with half-lives shorter than 10^{-11} s. Figure 2 gives a histrogram of the time distribution.

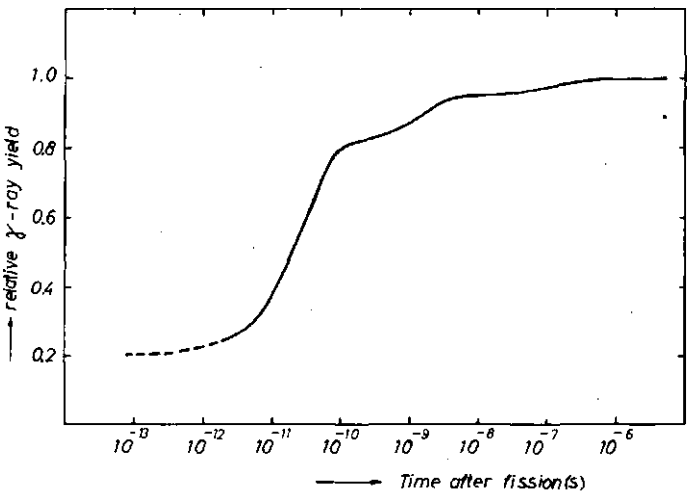

Fig. 2

Relative number of gamma quanta released at time t after fission (estimated with data from MAIENSCHEIN et al. [1] and JOHANSSON [8, 11]

Anisotropy of γ-emission

The angular correlation between the fission fragments and the γ-quanta has been studied by various authors [12–16]. An anisotropy has been found for several fissioning nuclides; emission in the direction of the fragments is more probable by 12 to 15% than at 90°. Within the accuracy of the measurements, no differences between the various nuclides have been detected. Figure 3 gives the angular distribution found by HOFFMANN [12]. The measurements are extremely sensitive to admixtures of prompt neutrons as these show a strong anisotropy of emission in the laboratory system.

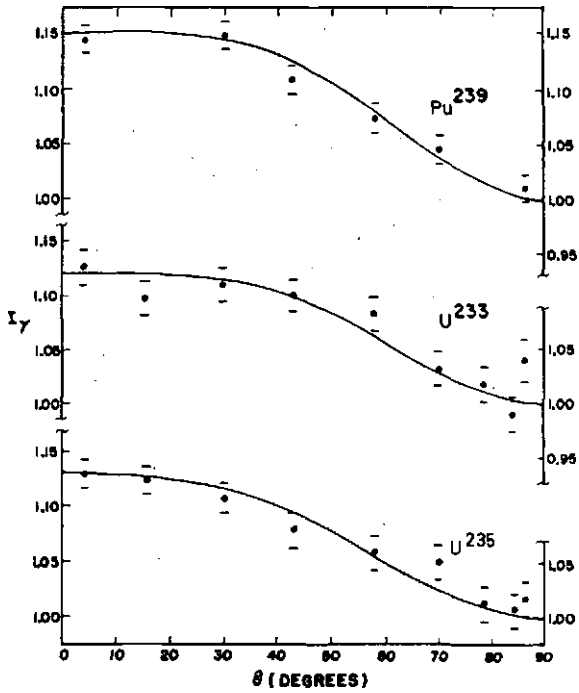

Fig. 3

Measured relative number of gamma rays having energy greater than 250 keV as a function of the angle to the fragment direction (from HOFFMAN [12])

Fast coincidences (10^{-9} s) combined with time-of-flight discrimination between neutrons and γ-quanta or effective neutron shields are necessary to establish the anisotropy of the emission of γ-quanta.

THE DE-EXCITATION OF FRAGMENT PAIRS AND SINGLE FRAGMENTS

MILTON and FRASER [17], using double time-of-flight techniques, measured the γ-spectrum of Cf^{252} in the energy range 0.3–1.4 MeV as a function of the mass ratio of the fragments. Similar measurements for U^{235}, using double ionization chambers, have been reported by RAU [4] and COOPERMAN [18]. All these early measurements suffer from fairly poor mass resolution. Only values in the high mass yield region are significant. The number of quanta and the total energy released vary only slowly within the region of high mass yields. A minimum near the mass split $128/A_1$ and a slight increase for increasing mass ratios is indicated in Ref. [17].

Measurements in the low-yield symmetric region have become possible recently [19]. A pair of solid-state detectors gives a mass resolution comparable to that given by the double time-of-flight method, with a total detection probability for fission products of a few per cent compared to 10^{-4} obtained by the double time-of-flight method. The total energy of γ-quanta

for U^{235} and its dependence on the mass ratio is given in Fig. 6a of Ref. [19]. Symmetric fission events have a higher γ-yield and energy release than asymmetric fission events. Fig. 6b of Ref. [19] gives the average quantum energy for U^{235} as a function of the mass ratio.

Measurements of the time dependence and angular correlation as a function of mass ratio have not been published until now.

Two methods have been applied to decide from which of the two fragments a certain γ-quantum is emitted. Both use the fact that the quanta are emitted from fragments in flight.

If a quantum is emitted in flight, its energy will be Doppler-shifted, and the angular correlation between the fragment and the γ-quantum will show a forward-backward anisotropy. The $0°/180°$-anisotropy and the energy-shift of the quantum energy have been used to correlate γ-quanta to certain fission fragments. RAMANNA et al. [14] first applied the method to decide between γ-quanta from light and heavy fission products. BOWMAN et al. [7, 20] observed the Doppler-shift in energy directly for certain γ-lines. MAIER-LEIBNITZ et al. [19] determined the total energy of γ-quanta and their mass dependence for U^{235} (Fig. 9 of Ref. [19]).

When the γ-quanta are emitted the fragments have moved from the point of fission. In times of 10^{-11} s they are separated by 10^{-2} cm. JOHANSSON [11] showed that most of the quanta are emitted after this time, and the separation is wide enough to assign the gamma rays to the fission fragments. Gamma spectra for single-fragment masses have been measured for the fast component of the spectrum (10^{-11}s) and for the delayed component (5×10^{-8} s). Figure 4 gives the result of the measurement for the fast component of the spectrum of Cf^{252}.

The saw-tooth mass dependence, well known from the number of neutrons, has been found independently by two completely different methods for the total number of prompt γ-quanta. The mass dependence [8] of the delayed component is given in Fig. 5.

CONVERSION ELECTRON AND K-X-RAY SPECTRA

Prompt K-X-rays are emitted by the fission fragments [21-23]. For U^{235} numbers of 0.1 to 0.2 quanta per fission have been measured [21, 23]; for Cf^{252} a number of 0.5 quanta per fission is reported [24]. HOHMANN [23] and GLENDENIN [24] state that most or all of the K-X-rays are produced by internal conversion. The number of X-rays fits with the number of γ-quanta if the plausible value of 2 is assumed for the multipolarity [24]. By counting electron tracks starting from the track of a fission fragment, BELOVITSKY et al. [25] directly proved that nearly all electrons with energies greater than 20 keV are emitted in times greater than 2.5×10^{-13} s. Thus, few if any of the electrons and X-rays are produced during the re-formation of the electron clouds. The detection of conversion electrons and their energy spectra has been reported during this Symposium [20, 24]. Lifetime measurements using the delayed coincidence technique for X-rays have been reported in Refs. [23] and [24].

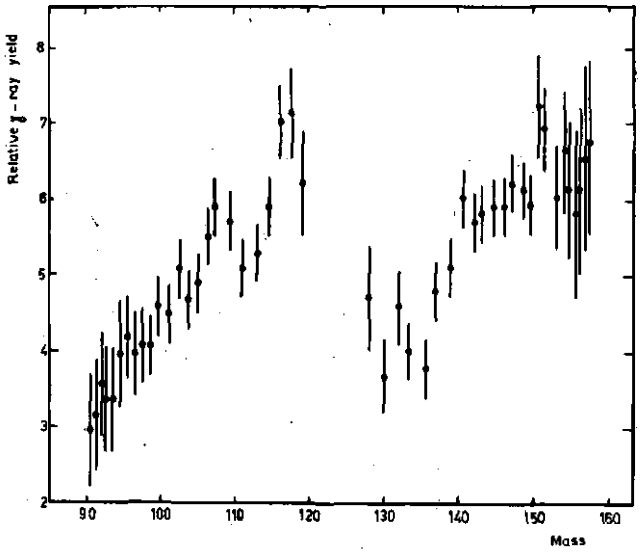

Fig. 4

Relative yield of prompt gamma rays from the spontaneous fission of Cf^{252} as a function of fragment mass (from JOHANSSON [11])

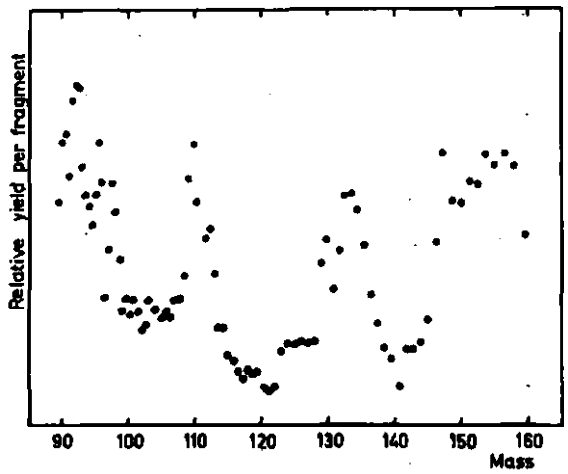

Fig. 5

Relative yield of delayed gamma rays from the spontaneous fission of Cf^{252} as a function of fragment mass (from JOHANSSON [8])

INTERPRETATION OF THE EXPERIMENTAL RESULTS

The spectrum

About 4–5 γ-quanta with an average energy of about 1 MeV are emitted from each of the fragments [1–4]. The observed spectrum peaks at about 0.3 MeV. Compared to the de-excitation after neutron capture, the fission spectrum is characterized by a higher number of quanta and an appreciably smaller average quantum energy. The fission fragments de-excite in several small energy steps compared to a nucleus after neutron capture, which de-excites in a few large steps.

Simple calculations have been made [26, 27] assuming the γ-emission takes place only if neutron emission is impossible energetically. Using the dependence of the level density on the excitation energy of the nucleus given by the statistical theory an energy slightly higher than half-a neutron binding energy for each fragment has been obtained. The calculated total γ-energy is 5 MeV. It is much smaller than the observed value. From this it must be concluded that the simple energy criterion used in the calculations is not satisfactory.

Each transition of the excited nucleus is characterized not only by a change in energy, but also by a change in spin. For a comparable change in excitation energy neutrons carry off much smaller spin than γ-quanta [11]. Assume the excited nucleus starts with a high initial spin. Prompt neutron emission reduces the spin by only a few units. Therefore, if the initial spin is high, the emission of the last neutron will leave the nucleus in a state with still rather high spin. Such a state will in general have rather high excitation energy because it arises from breaking up nucleon pairs or from high collective excitations. Thus the difference between observed and calculated γ-energy, about 1.5 MeV per fragment, may be understood. An excitation energy of 1.5 MeV may mean the breaking-up of two nucleon pairs, or excitation of something like the third vibrational state. In both cases, initial spin values of the nucleus after fission of the order of 10 would appear plausible.

High spin values for the nuclei before γ-emission are also supported by the high multiplicity of the γ-radiation (4 to 5 per fragment). If the spin difference between initial and final states were low, direct transitions would be highly probable. The observed number of transitions is plausible if one assumes mainly quadrupole transitions from initial states with spin about 8. The observed small average energy of the quanta further supports the assumption that a cascade of phonons contributes to the de-excitation of the fission fragments.

Lifetime

JOHANSSON [11] found the bulk of γ-quanta to be emitted within 10^{-11} s after fission. The average energy of the quanta emitted with a half-life of 10^{-11} s amounts to 0.7 MeV. The lifetime for 0.7-MeV single-particle transitions is of the order of 10^{-9} s. Only vibrational states of the quadrupole type have lifetimes as short as observed. The lifetime measurements com-

bined with the average energy unambiguously rules out single-particle transitions as contributing considerably to the de-excitation. A cascade of collective E2-transitions de-excites the fragments after neutron emission. The number of quanta per fragment directly determines the approximate value of the initial spin. Its value is about $I \approx 10$, a result which has been obtained indirectly from the high total energy emitted by γ-quanta.

The angular correlation

The experiments show that the direction of emission of the fission fragments is favoured for γ-emission.

An angular correlation between the direction of γ-emission and the direction of flight of the fragments can be only caused by a preferential orientation of the fragment spins relative to the deformation axis of the fissioning nucleus. STRUTINSKII [28] explained the observed anisotropy by quadrupole emission of nuclei with spins oriented perpendicular to the direction of flight of the fragments. HOFFMAN [12], using a different method of weighting the various possibilities of orientation of the emission direction to the initial spin, obtained essentially the same results as Strutinskii. The initial spins are oriented preferentially perpendicular to the deformation axis of the fissioning nucleus. The observed anisotropy can be explained assuming that the initial spin is of about $I \approx 8$ and the multipolarity of the emitted radiation is 2.

The mass ratio dependence

Average energy and number of γ-quanta are nearly constant within the region of high mass yields [17-19]. In the mass region of closed shells ($A \approx 128 - 134$), the total number of quanta is smaller than the average, and the energy of the quanta is higher than the average. The phonon energies for closed shell nuclei are appreciably higher than in the region between closed shells. This might be an explanation of the observed dependence.

In the region of symmetric fission, the energy released by γ-quanta seems to be higher by about 50% compared to that in the region of asymmetric fission [19]. This additional energy partly explains the energy deficit between the dip in kinetic energy [29] and the dip in the directly measured energy carried off by neutrons [30].

The average energy of the γ-quanta for symmetric fission events is smaller than for asymmetric fission [19]. The nuclei in the symmetric fission region are soft to deformation. Their phonon energies are expected to be low.

The mass dependence

The saw-tooth mass dependence of the number of prompt γ-quanta has been found by two independent methods [11, 19].

No mass dependence of the energy released by γ-emission should be observed if the competition between neutron- and γ-emission is determined only by energy considerations, as has been assumed by LEACHMAN and

KAZEK [26]. Only for total excitation energies smaller than the neutron binding energy should the energy released by γ-emission depend on the total excitation energy. Excitation energies smaller than the neutron binding energy will be observed in narrow mass regions around the closed shells [30]. This cannot explain the observed variation over the whole range of masses.

Gamma-emission compared to neutron-emission is increased for high initials spins of the fragments. The saw-tooth structure thus seems to reflect the mass dependence of the initial spin of the fragments [11]. The soft fragments between closed shells have large excitation energies and large initial spins, the more rigid closed shell nuclei have small excitation energies and small initial spins. The initial spin is correlated to the number of nucleons outside closed shells.

JOHANSSON [8] measured the mass dependence and energy spectrum of the delayed component ($10^{-8}-10^{-7}$ s). Gamma-quanta are observed only in certain mass regions (Fig. 5). A similar structure of the spectra in the mass regions A = 110 and A = 152 gives experimental evidence to the assumption that nuclei of stable deformation are not only found for masses A > 150, but also in the mass region of A = 110. Both energy spectra show rotational structure. The high yields of delayed γ-quanta in the mass regions of closed shells have been explained by transitions between high spin states of the vibrational spectrum of closed shell nuclei, which are to be separated only by ~ 0.1 MeV. These transitions are slow. As Johansson points out the low-lying vibrational states, the energy of which is about 1.5 MeV, should be found in the delayed spectrum. A high energy peak in mass region A$\sim$132 actually has been detected.

Two complementary fragments, which emit different γ-energies, will have different initial spins. The conservation of angular momentum demands for these mass splits an additional orbital angular momentum between the fragments. The existence of high spins in the excited fission fragments is an important feature of the fission process concerning the transition from the saddle point to scission. STRUTINSKII [28] and HOFFMAN [12] explain the high spins by assuming a non-axial breaking point in scission. This leads to angular momenta normal to the direction of the fission fragments. They show that the assumption of spins around 10 and quadrupole radiation explains the observed anisotropy.

The assumption of non-axial breaking points is not forcing in the case of equal and opposite spins of the fragments where the process could be regarded as the separation of two spinning tops. However, when the spin of the two fragments is much different, as the experiments show in the regions near closed shells, the spins must be compensated by orbital momenta between the two fragments which can be produced only by non-axial forces. The production of such momenta requires kinetic energies of the fragments at scission of about 2 MeV or more if we assume that the eccentric forces act at a distance not more than half the nuclear radius from the axis.

High spins may be produced either by breaking up nucleon pairs or by collective excitations. Both processes will be connected mainly with those nuclei containing a large number of nucleons outside closed shells, and will therefore lead to the observed saw-tooth structure. From Johansson's work

one can conclude that vibrations and rotations are an important part of the excitation after fission.

REFERENCES

[1] MAIENSCHEIN, F.C., PEELE, R.W., ZOBEL, W. and LOVE, T.A., Proc. 2nd UN Int. Conf. PUAE 15 (1958) 366.

[2] SMITH, A.B., FIELDS, P.R. and FRIEDMAN, A.M., Phys. Rev. 104 (1956) 699.

[3] BOWMAN, H.R. and THOMPSON, S.G., Proc. 2nd UN Int. Conf. PUAE 15 (1958) 212.

[4] RAU, F.E.W., Ann. Phys., Paris 10 (1963) 252.

[5] PROTOPOPOV, A.N. and SIRJAGER, B.M., Soviet Phys.-JETP 7 (1958) 231.

[6] VOITOVETSKII, V.K., LEVIN, B.A. and MARCHENKO, E.V., Soviet Phys.-JETP 5 (1957) 184.

[7] BOWMAN, H.R., THOMPSON, S.G. and RASMUSSEN, J.O., Phys. Rev. Lett. 12 (1964) 195.

[8] JOHANSSON, S.A.E., Nucl. Phys. (in press).

[9] DESI, S., LAJTAI, A. and NAGY, L., Acta Phys. Acad. Sci. hung. 15 (1962) 185.

[10] SKLIAREVSKII, V.V., FOMENKO, D.E. and STEPANOV, E.P., Soviet Phys.-JETP 5 (1957) 220.

[11] JOHANSSON, S.A.E., Nucl. Phys. 60 (1964) 378.

[12] HOFFMAN, M.M., Phys. Rev. 133 B (1964) 714.

[13] DESI, S., GRAFF, G., LAJTAI, A. and NAGY, L., Phys. Lett. 3 (1963) 343.

[14] KAPOOR, S.S. and RAMANNA, R., Phys. Rev. 133 B (1964) 598.

[15] BLINOV, M.V., KAZARINOV, N.M., PROTOPOPOV, A.N. and SHIRYAEV, B.M., Soviet Phys.-JETP 16 (1963) 1159.

[16] SKARSVAG, K. and SINGSTAD, J., Nucl. Phys. 62 (1965) 103.

[17] MILTON, J.C.D. and FRASER, J.S., Phys. Rev. 111 (1958) 877.

[18] COOPERMAN, L. and ROY, R.R. Phys. Rev. 132 (1963) 371.

[19] MAIER-LEIBNITZ, H., SCHMITT, H., ARMBRUSTER, P., "Average number and energy of gamma-rays emitted as a function of fragment mass in U^{235} thermal-neutron-induced fission", these Proceedings II.

[20] BOWMAN, H.R., THOMPSON, S.G., WATSON, R.L., KAPOOR, S.S. and RASMUSSEN, J.O., "The prompt gamma-ray, prompt electron and prompt X-ray spectra associated with fission fragments of specific mass", these Proceedings II.

[21] SKLIAREVSKII, V.V., STEPANOV, E.P. and MEDVEDEV, B.A., Soviet Phys.-JETP 9 (1959) 225.

[22] LEACHMAN, R.B., Proc. 2nd UN Int. Conf. PUAE 15 (1958) 331.

[23] HOHMANN, H., Z. Phys. 172 (1963) 143.

[24] GLENDENIN, L., UNIK, J.P. and GRIFFIN, H.C., "Determination of primary nuclear charge of fission fragments from their characteristic K-X-ray emission in spontaneous fission of Cf^{252}", these Proceedings I.

[25] BELOVITSKIJ and LEBEDEV, Proceedings Conf. on Nuclear Structure, Paris (1964).

[26] LEACHMAN, R.B. and KAZEK, C.S., Phys. Rev. 105 (1957) 1511.

[27] TERRELL, J., Phys. Rev. 113 (1959) 527.

[28] STRUTINSKII, V.M., Soviet Phys.-JETP 10 (1960) 613.

[29] MILTON, J.C.D., and FRASER, J.S., Canad. J. Phys. 40 (1962) 1626.

[30] APALIN, V.F., GRITSYUK, N., KUTIKOV, I., LEBEDEV, V. and MIKAELYAN, L., Nucl. Phys. 55 (1964) 249.

THE PROMPT GAMMA-RAY, PROMPT ELECTRON AND PROMPT X-RAY SPECTRA ASSOCIATED WITH FISSION FRAGMENTS OF SPECIFIC MASS

H.R. BOWMAN, S.G. THOMPSON, R.L. WATSON,
S.S. KAPOOR* AND J.O. RASMUSSEN
LAWRENCE RADIATION LABORATORY, UNIVERSITY OF CALIFORNIA,
BERKELEY, CALIF., UNITED STATES OF AMERICA

Abstract — Résumé — Аннотация — Resumen

THE PROMPT GAMMA-RAY, PROMPT ELECTRON AND PROMPT X-RAY SPECTRA ASSOCIATED WITH FISSION FRAGMENTS OF SPECIFIC MASS. Well-defined prompt gamma-rays, prompt-conversion electrons and prompt K-X-rays have been observed in coincidence with moving fission fragments of Cf^{252}. In a few cases, the masses and charges of the nuclei emitting the gamma-rays and conversion electrons have been identified.

The gamma-ray, prompt-electron and prompt X-ray energies as well as the two fission fragments' energies were measured with high-resolution solid-state detectors. The masses of the fragments were deduced from their energies, and the nuclear charges were determined by measuring the K-X-ray energies associated with different masses. The magnitude and sign of the Doppler shift in gamma-ray energy allowed assignment of the gamma-ray lines to single members of fragment pairs. The Doppler shift also provides an independent measure of the fragment velocity and hence the fragment mass after neutron emission.

The results of the X-ray measurements are consistent with the view that the majority of the prompt X-rays emitted during the spontaneous fission of Cf^{252} are the result of internal conversion during the de-excitation of low-energy collective states of the primary fission fragments.

Apart from the specific results discussed above, the most important consequence of these experiments has been the demonstration that it is possible to study the properties of individual fission fragments, as identified by their characteristic radiations, rather than studying the properties of an average fission fragment with an average mass and charge. The consequences of this advance in the technique of studying fission fragments are being explored.

SPECTRES DE RAYONS GAMMA INSTANTANÉS, D'ÉLECTRONS INSTANTANÉS ET DE RAYONS X INSTANTANÉS ASSOCIÉS À DES FRAGMENTS DE FISSION DE MASSE DONNÉE. Des rayons gamma instantanés, des électrons de conversions instantanés et des rayons X K instantanés bien définis ont été observés en coïncidences avec des fragments de fission de ^{252}Cf en mouvement. Dans un petit nombre de cas, les masses et charges des noyaux émettant les rayons gamma et les électrons de conversion ont été identifiées.

Les énergies des rayons gamma, des électrons instantanés et des rayons X instantanés ainsi que les énergies des deux fragments de fission ont été mesurées au moyen de détecteurs à semi-conducteurs à fort pouvoir de résolution. Les masses des fragments ont été obtenues à partir de leurs énergies, et les charges des noyaux ont été calculées par mesure des énergies des rayons X K associées à différentes masses.

La grandeur et le signe du déplacement Doppler dans l'énergie des rayons gamma ont permis d'attribuer les raies gamma à des membres isolés de paires de fragments. Le déplacement Doppler permet aussi de déterminer indépendamment la vitesse du fragment et, partant, la masse du fragment après l'émission de neutrons.

Les résultats des mesures des rayons X confirment l'impression que la majorité des rayons X instantanés émis au cours de la fission spontanée de ^{252}Cf sont dus à une conversion interne pendant la désexcitation d'états collectifs de faible énergie des fragments de fission primaires.

En dehors des résultats particuliers décrits ci-dessus, les auteurs estiment que la conséquence la plus importante de leurs recherches a été de démontrer la possibilité d'étudier les propriétés des différents fragments de fission, identifiés par leur rayonnement propre — au lieu d'étudier les propriétés d'un fragment de fission moyen, de masse et de charge moyennes. Les auteurs étudient les conséquences de ce perfectionnement de la méthode utilisée pour étudier les fragments de fission.

---

* On leave of absence from the Atomic Energy Establishment Trombay, Bombay, India.

МГНОВЕННЫЕ ГАММА-КВАНТЫ И СПЕКТРЫ МГНОВЕННЫХ ЭЛЕКТРОНОВ И МГНОВЕННЫХ РЕНТГЕНОВСКИХ ЛУЧЕЙ, СВЯЗАННЫЕ С ОСКОЛКАМИ ДЕЛЕНИЯ УДЕЛЬНОЙ МАССЫ. Наблюдались хорошо определенные мгновенные гамма-кванты, мгновенные конверсионные электроны и рентгеновское К-излучение в совпадении с движущимися осколками деления калифорния-252. В нескольких случаях были установлены массы и заряды ядер, испускающих гамма-кванты и конверсионные электроны.

Энергии гамма-квантов, мгновенных электронов и мгновенных рентгеновских лучей, а также энергии двух осколков деления были измерены с помощью твердого счетчика с высокой разрешающей способностью. Массы осколков были выведены на основе их энергий, а ядерные заряды были определены путем измерения энергий рентгеновского К-излучения, связанных с различными массами. Величина и отметка Допплеровского смещения в энергии гамма-кванта позволили причислить линии гамма-квантов к отдельным членам осколочных пар. Допплеровское смещение обеспечивает также независимое измерение скорости осколка и, следовательно, массы осколка после испускания нейтронов.

Результаты измерений рентгеновских лучей согласуются с мнением, что большинство мгновенных рентгеновских лучей, излучаемых во время спонтанного деления калифорния-252, является результатом внутренней конверсии в ходе высвечивания совокупных состояний низкой энергии первичных осколков деления.

Авторы полагают, что помимо обсужденных выше конкретных результатов наиболее важным следствием их экспериментов явилась демонстрация того, что имеется возможность изучения свойств отдельных осколков деления, установленных характеристиками из излучений (вместо того, чтобы изучать свойства среднего осколка деления с помощью средней массы и заряда). Раскрываются преимущества этого усовершенствования в методе изучения осколков деления.

ESPECTROS DE RAYOS GAMMA, ELECTRONES Y RAYOS X INMEDIATOS, VINCULADOS A FRAGMENTOS DE FISION DE MASA DETERMINADA. En coincidencia con fragmentos en movimiento provenientes de la fisión del ^{252}Cf, los autores observaron rayos gamma, electrones de conversión y rayos X K inmediatos. En algunos casos, pudieron identificar las masas y las cargas de los núcleos que emiten los rayos gamma y los electrones de conversión.

Las energías de los rayos gamma, de los electrones y de los rayos X inmediatos, así como también las energías de los dos fragmentos de fisión, se midieron con detectores de semiconductores, de elevado poder de resolución. Las masas de los fragmentos se dedujeron de sus respectivas energías y las cargas nucleares se determinaron midiendo las energías de los rayos X K vinculadas a las distintas masas. La magnitud y el signo del desplazamiento de Doppler permitió asignar les líneas espectrales de los rayos gamma, a cada uno de los componentes de cada par de fragmentos. El desplazamiento de Doppler permite también medir independientemente la velocidad de los fragmentos y, por consiguiente, la masa de éstos después de la emisión de un neutrón.

Los resultados de las mediciones realizadas sobre los rayos X concuerdan con la hipótesis de que la mayoría de los rayos X inmediatos emitidos durante la fisión espontánea del ^{252}Cf, son resultado de la conversión interna en los fragmentos de la fisión primaria, durante la desexcitación de estados colectivos de baja energía.

Además de los resultados concretos examinados en la memoria, la consecuencia más importante de los experimentos descritos es la demostración de que es posible estudiar por separado las propiedades de cada fragmento de fisión, identificado por sus radiaciones características (en lugar de estudiar las propiedades de un fragmento de fisión medio, con masa y carga también medias). Se estudian actualmente las consecuencias de este adelanto logrado en la técnica de estudio de los fragmentos de fisión.

INTRODUCTION

This paper presents results from a detailed experimental study of the prompt gamma rays, prompt electrons and prompt X-rays emitted in the spontaneous fission of Cf^{252}, in particular from the investigations of the energy distributions of these radiations as a function of the mass of the fission fragments.

The aim of such an extensive study is to provide a body of experimental data from which a number of general features of the fission process may

be deduced, and against which proposed theories may be tested. The study of these prompt radiations, in addition, provides a potential means of investigating the final stages in the de-excitation mechanism of very neutron-rich nuclei. We would like to stress that our principal object here is to present experimental results in a reasonably complete manner, and that a theoretical interpretation has not been aimed at.

This work is a continuation of a more general study [1-3] covering all the prompt radiations associated with spontaneous fission, which has been in progress at this laboratory since the discovery of Cf^{252} [4].

In the first series of experiments, the energies of the prompt gamma rays in coincidence with the fission fragments were measured with a NaI gamma-ray detector. The sorting of these spectra with respect to the fragment mass ratios revealed a large number of discrete gamma-ray energies. These measurements were further extended by using a high resolution lithium-drifted germanium gamma-ray detector. The dependence of these gamma-ray energies on the velocity and direction of motion of the fragments showed that many of these gamma rays were emitted from moving fragments. These Doppler shifts in the gamma-ray energies provided an effective means of identifying the emitting fragment of a fragment pair.

The second series of experiments was carried out to measure the electron spectra in coincidence with fission. The sorting of the electron data according to the fragment masses also revealed a number of peaks predominantly concentrated in the low-energy region. The structure in the conversion electron spectra was found to be clearly associated with the previously measured gamma-ray lines.

The third series of experiments involved the measurements of the energies of K-X-rays with a lithium-drifted silicon detector in coincidence with fission fragments. The data have been analysed to obtain the most probable charge (Z_p) of the individual fragments, the number of the X-rays emitted per fragment, and the average time of the X-ray emission from different fragments. A by-product of the X-ray measurements has been the independent and direct measurement of the nuclear charge of californium.

EXPERIMENTAL APPARATUS

Figure 1 shows the experimental arrangement used in these experiments. A weightless Cf^{252} fission source, prepared by self-transfer on to a thin nickel foil, was placed between two solid-state fission detectors. The first series of experiments was done using a NaI counter for gamma-ray detection mounted in line with the two fission detectors along the axis of fission (Fig. 1). The high resolution gamma-ray measurements were made by replacing the NaI detector with a lithium-drifted germanium detector operated at liquid nitrogen temperature. For the electron spectra and the X-ray measurements, a lithium-drifted silicon detector operated at dry ice temperature was used. In each of the experiments, pulses from the three detectors were fed to standard transistor amplifiers and then to a triple coincidence unit of the zero cross-over type having a time resolution of 50 ns. The chance coincidence rate in all the measurements was less than 1% of the true coincidence rate. If the pulses from the three detectors were in co-

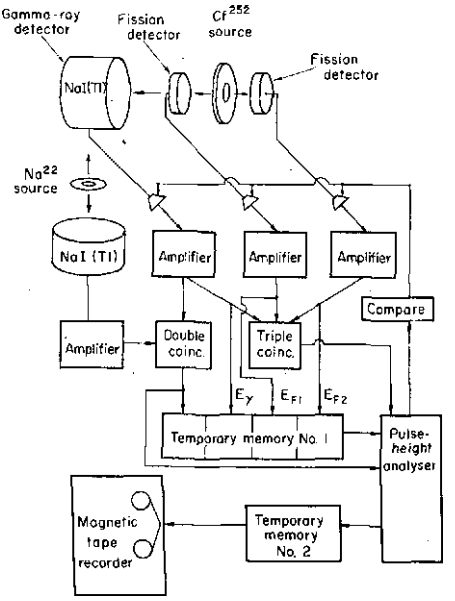

Fig. 1

Schematic diagram of the experimental arrangement used in these experiments. The NaI detector was used in the early gamma-ray measurements and was later replaced with a lithium-drifted germanium detector for high resolution gamma-ray measurements and a lithium-drifted silicon detector for measuring the electron and the X-ray spectra.

incidence, then the amplifier outputs were stored in temporary memory # 1. The three detector pulse heights were then analysed serially by the pulse-height analyser. The digital outputs of the pulse-height analyser were in turn stored in correlated form in memory # 2. The output of memory # 2 was written on magnetic tape each time memory # 2 became full. The magnetic tape could be read back at the end of each run, and the data could be observed just as they came in during the experiment.

To eliminate electronic drift during the runs, digital stabilizers of the type described by NAKAMURA and LA PIERRE [5] were used. For the pulse-height stabilization during the gamma-ray work, a Na^{22} source of positron annihilation radiation was placed between the fission gamma-ray detector and a second NaI detector, as shown in Fig. 1. Whenever a double coincidence between the two 511-keV gamma radiations was observed, the temporary memory and the pulse-height analyser were informed that the radiation detected by the fission gamma-ray detector was not a fission-fragment gamma ray, but a 511-keV annihilation photon. The digital output of the pulse-height analyser was then compared with a predetermined channel number to check the gain of the system. If the gain had changed, then a DC signal was sent to the appropriate variable gain preamplifier to stabilize the gain of the system. The pulse-height dispersion introduced by the system was always less than 0.1%. A number of different sources were used for stabilization during the many different experiments, depending on the radiation detected

and the energy range involved: The fission-fragment detectors were stabilized in a very similar way.

DATA HANDLING

The triple coincidence pulse-height data recorded on magnetic tape for each of these experiments were processed on the IBM 7094 computer. The fission-fragment energies were obtained by normalizing the first moments of the light- and heavy-fragment pulse-height distributions to the first moments of the respective energy distributions obtained previously by time-of-flight measurements [6]. The fission-fragment masses were first calculated using momentum conservation and the relation between energy and mass. By using the relationships between the average number of neutrons as a function of fragment mass and total kinetic energy (obtained from earlier measurements [2, 3]), an iterative type of calculation was carried out to obtain the fragment masses before and after neutron emission. The triple coincidence data in each case were sorted on the computer according to the masses of the fragments after neutron emission and, in some cases, according to the total kinetic energy of the fragments.

PROMPT GAMMA RAYS

When the NaI gamma-ray energy spectra were sorted according to fission-fragment mass ratio, a number of definite peaks appeared in the energy range from 150 to 600 keV. The spectra changed markedly for different mass ratios, as shown in Fig. 2b, which explains why the discrete structure is nearly obscure in a total prompt gamma-ray spectrum such as that given in Fig. 2a, where no sorting according to mass ratio or direction is made. The spectra shown in Fig. 2b were subject to a further restriction such that only gamma rays emitted from fission events in which heavy fragments were travelling towards the gamma detector were counted. The dependence of the energy of the gamma rays on the direction of motion of the fragments can be seen by comparing the two spectra shown in Fig. 2c. The dashed and solid lines represent the gamma-ray spectra for the two cases: when the heavy fragments ($M = 140 \pm 2$) were moving towards the gamma-ray detector, and away from the detector. From the measured sign and the magnitude of the Doppler shift it is therefore possible to identify the emitting fragment of the fragment pair.

Measurements with lithium-drifted germanium gamma-ray detectors have resulted in a great improvement in the gamma-ray energy resolution. Spectra for the energy range of 300 to 600 keV are shown in Figs. 3a and 3b (for the mass intervals 109 to 111 and 137 to 139) for the two cases: light fragments travelling towards the gamma-ray detector, and heavy fragments travelling towards the gamma-ray detector. Individual gamma-ray peaks are well-resolved, and by comparing Figs. 3a and 3b, the energies can be corrected for Doppler shift and the peaks identified with heavy or light fragments. Inspection of Fig. 3 shows 3 peaks identified with light fragments

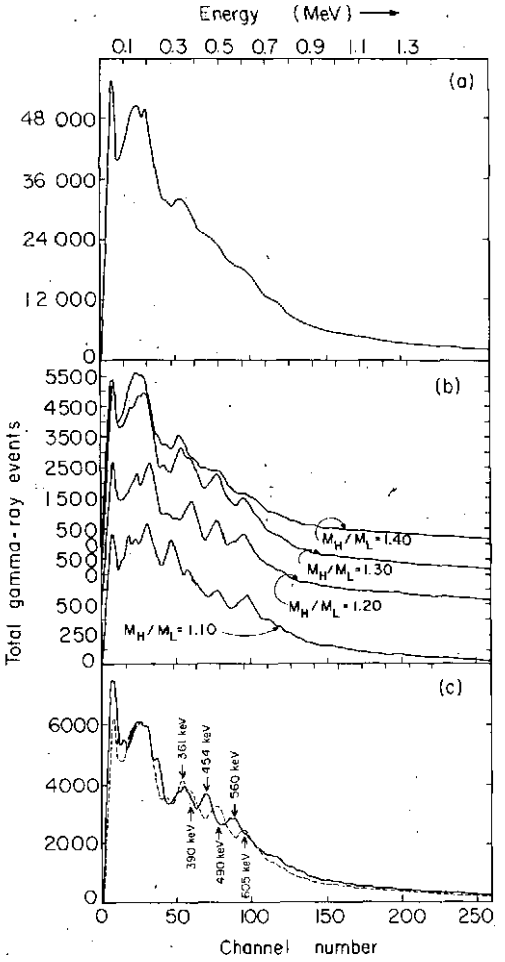

Fig. 2

(a) Total prompt gamma-ray energy distribution from the spontaneous fission of Cf^{252} (using a NaI detector)

(b) Spectra of prompt gamma-rays associated with various values of mass ratio (M_H/M_L)

(c) The dependence of prompt gamma-ray energy on the velocity and direction of motion of the fragments. The dashed and solid lines represent the gamma-ray spectra for the two cases: (1) when the heavy fragments ($M = 140 \pm 2$) were moving towards the gamma-ray detector and (2) away from the detector.

(E, I, L) and 12 identified (and labelled alphabetically) with heavy fragments. These lines will be discussed later in the analysis of the electron data.

Figure 4 is a three-dimensional model of the gamma-ray spectra in the energy range below 300 keV for each mass group ranging from 90 to 165. These spectra are more complex than those in the high-energy region, and only about a dozen of the lines in Fig. 4 have been assigned to definite fragments.

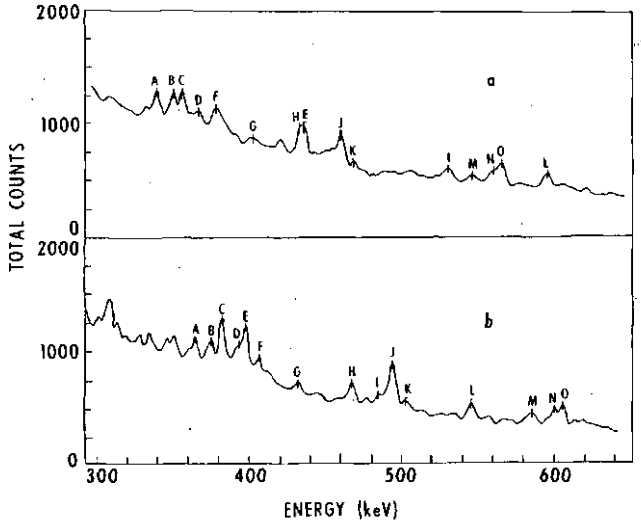

Fig. 3

The prompt gamma-ray spectra measured with a lithium-drifted germanium detector for the fragment mass ranges of 109-111 (137-139):
(a) light fragments moving towards the gamma-ray detector and
(b) heavy fragments moving towards the gamma-ray detector

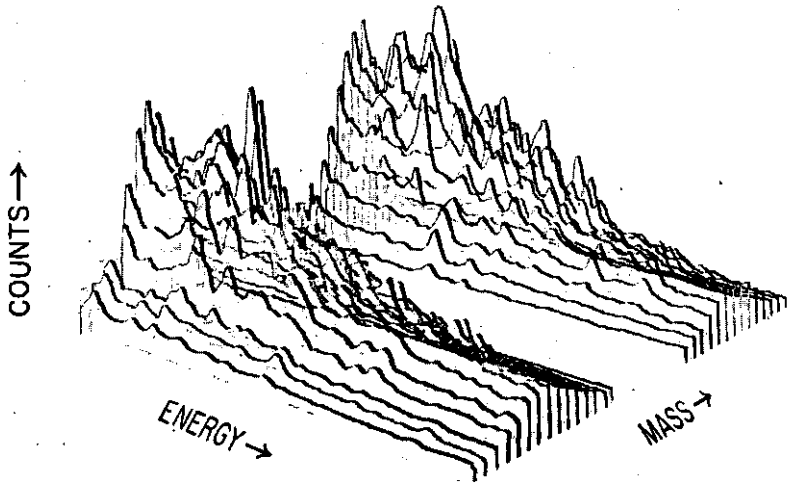

Fig. 4

The observed prompt gamma-ray energy spectra below 300 keV for selected intervals of fragment mass

In Figs. 5a, b, c, and d, the effect of sorting the low-energy gamma-ray data according to total kinetic energy for a single mass interval is shown. This means of selection can be used to demonstrate that a particular line cannot be associated with neutron capture (n, γ) in or about the gamma-ray

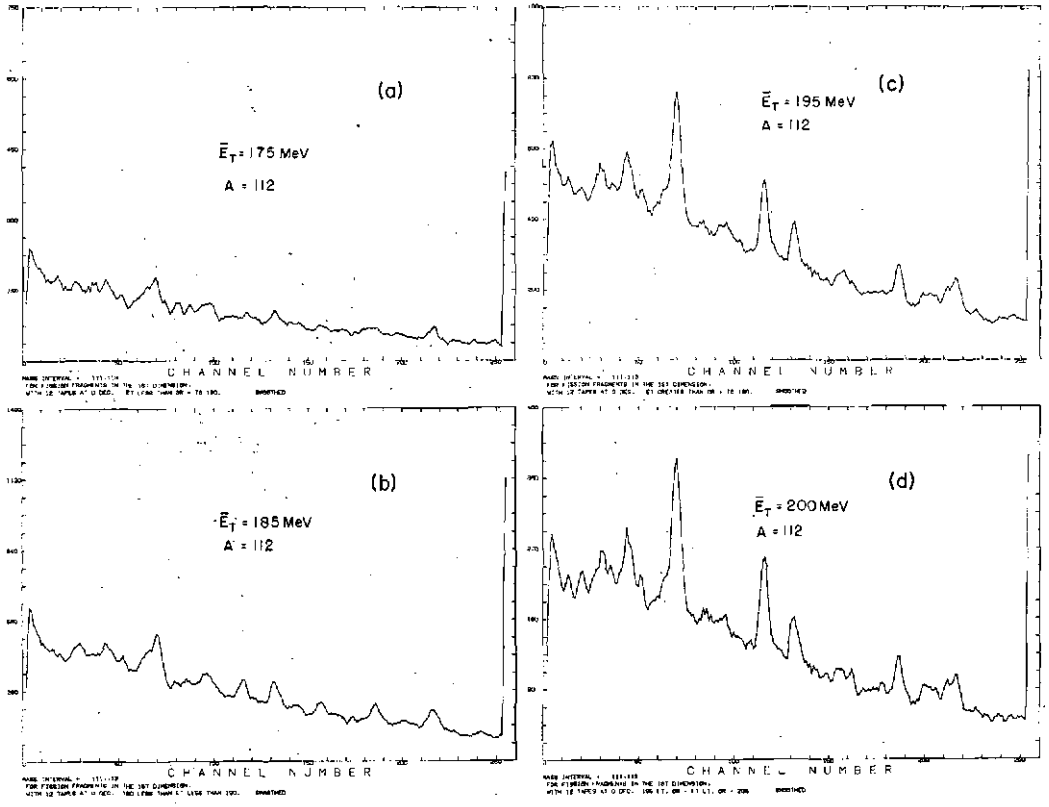

Fig. 5

The prompt gamma-ray energy spectra (below 300 keV) sorted according to total kinetic energy (E_T) for a single interval of fragment mass

crystal. If these lines were indeed coming from neutron capture, the intensities should decrease with increasing total kinetic energy. In Fig. 5, as can be seen, the reverse of this occurs.

PROMPT ELECTRON SPECTRA

The prompt electron energies were measured in coincidence with fission fragments by means of a lithium-drifted silicon electron detector. A large (~ 5 000 gauss) inhomogeneous magnetic field of the configuration proposed by MALMFORS [7] was used to steer the electrons round a block of lead, which shielded the electron detector from the fission fragments and gamma rays. Electrons having a wide range of energies precess in a trochoidal orbit in the fringing field of a large electromagnet. The electron detector was mounted inside a vacuum chamber 90° around the magnet from the fission source. The electron spectra in the energy range 300 to 600 keV are shown in Fig. 6 for the mass intervals 107-111 and 137-141.

The geometry of the system was such that only electrons emitted near 90° with respect to the fragment flight path were accepted into the electron spectrometer; however, the finite size of the fragment detector and the rather large acceptance angle of the magnetic field introduced an amount of angular dispersion from the strictly 90° configurations. This effect resulted in a considerable broadening of the electron energy peaks and is the predominant contribution to the experimental resolution.

Figure 7 shows a three-dimensional model of the electron spectra below 300 keV. These low-energy electron data have been analysed along with the low-energy gamma-ray data, and about a dozen lines have been found that correspond to both sets of data.

X-RAY EXPERIMENT

The energy distributions of the K-X-rays were measured with a lithium-drifted silicon detector operated at dry ice temperatures to obtain the best energy resolution (full width at half maximum (FWHM) = 3.5 keV). The X-ray detector was mounted close to one of the fragment detectors to obtain a high solid angle for the detection of the X-rays emitted from fragments stopped in the fission detector. Figure 8 shows a three-dimensional plot of the observed X-ray energy distributions as a function of the mass of the fragments moving towards the X-ray detector. Figure 9 shows the energy spectra of the X-rays from mass 140 moving (a) towards and (b) away from the detector.

It can be seen from Fig. 9 that the fraction of the fragment X-rays detected is much larger when that particular fragment is moving towards the X-ray detector. This difference in intensity is largely because the X-rays are emitted all along the fragment path. From the observed ratio of intensities of X-rays it has therefore been possible to determine the relative solid angle of detection and the average time of X-ray emission from different fragment masses. Figure 10 shows the average time of emission for K-X-rays from different fragment masses as obtained from the above analysis.

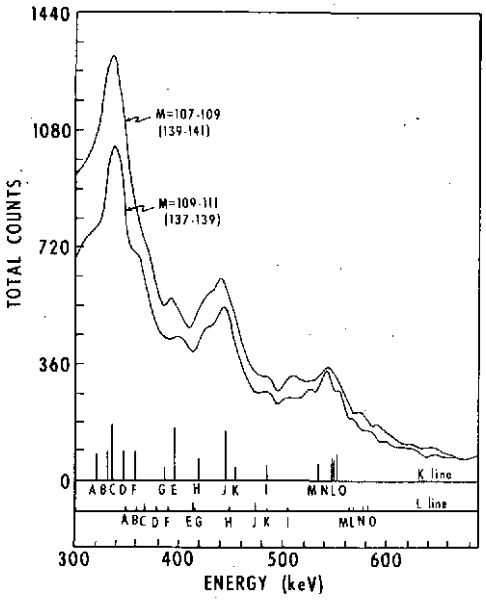

Fig. 6

The prompt electron energy spectra associated with fission fragment mass (a) 107-109(139-141) and (b) 109-111 (137-139). The vertical lines at the bottom are the calculated locations of K- and L-electron lines using gamma-ray data from Fig. 3. As a rough guide, the line lengths are taken from the intensities of the gamma-rays.

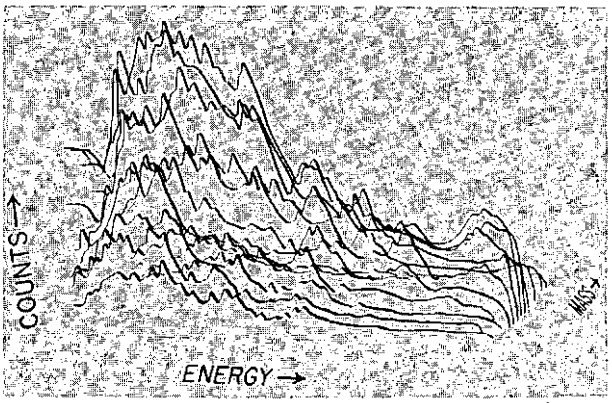

Fig. 7

The prompt electron energy spectra (below 300 keV) for selected intervals of light fragment mass. Electron spectra measured at 90° to the direction of motion of the fragments are identical for light and heavy fragment pairs.

The observed number of K-X-rays per fission, corrected for detector geometry, X-ray attenuation and detection efficiency, are shown as a function of the final mass (M_f) in Fig. 11.

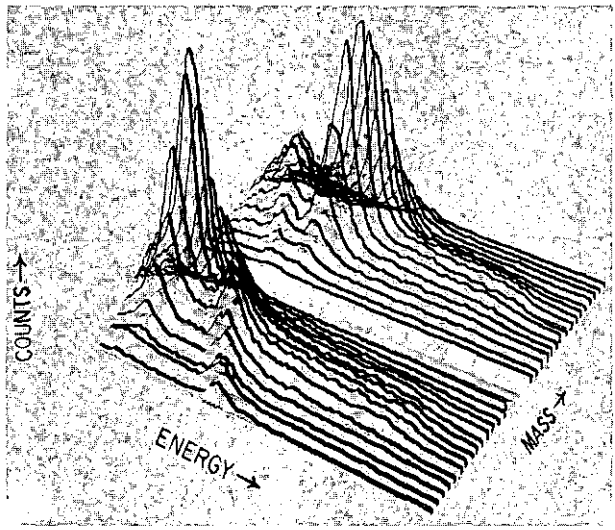

Fig. 8

The observed energy spectra of prompt K-X-rays for 36 intervals of the fragment masses moving towards the detector

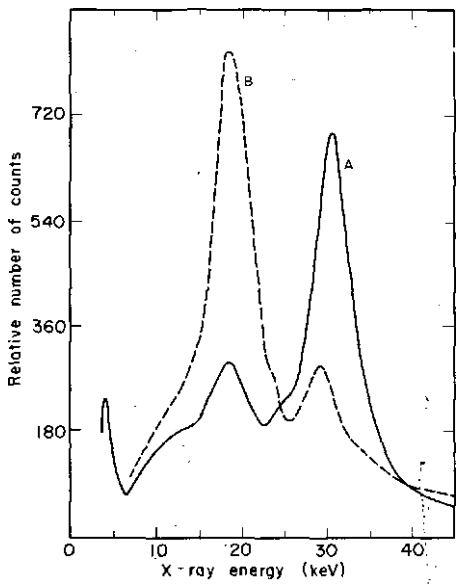

Fig. 9

The measured prompt K-X-ray energy spectra in coincidence with mass 140 moving (a) towards and (b) away from the X-ray detector

The most probable charge, (Z_p), for each mass interval was obtained in the following way. For each value of Z, the expected K-X-ray energy

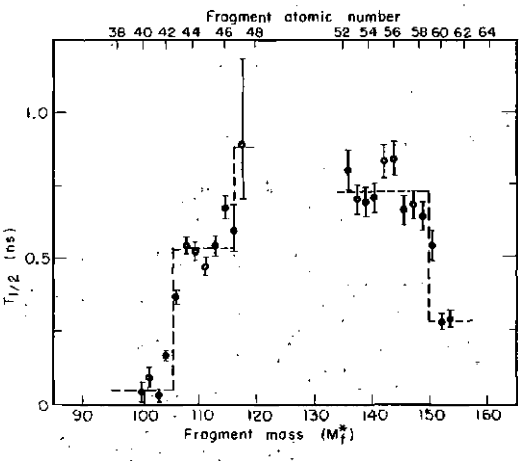

Fig. 10

The measured half-life for K-X-ray emission as a function of the final masses (M_f^*) and atomic numbers of the fission fragments (corrected for mass dispersion)

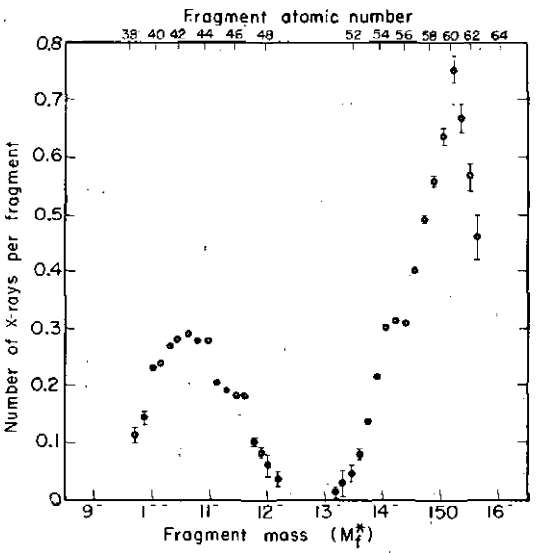

Fig. 11

The observed yield per fragment of K-X-rays as a function of final masses (M_f^*) and atomic numbers of the fission fragments (corrected for mass dispersion)

distribution curve was computed by the addition of four Gaussian distributions corresponding to the K_{α_1}, K_{α_2}, K_{β_1} and K_{β_2}, each having a FWHM corresponding to the observed energy resolution and having average energies and intensity ratios as given by WAPSTRA et al. [8]. The calculated distributions were compared with the observed X-ray energy distributions to obtain the most probable values.

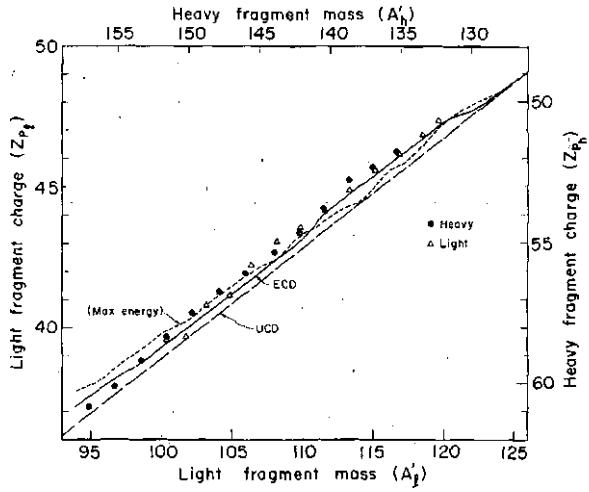

Fig. 12

The most probable charge (Z_p) versus the initial mass of the fragments (A_i) (corrected for mass dispersion) as determined from the X-ray measurements. The curves calculated on the hypothesis of maximum energy released, equal charge displacement (ECD) and unchanged charge distribution (UCD), are also shown in the figure.

The plot of measured Z_p versus initial mass of the fragments, A_i, is shown in Fig. 12. (These data have been corrected for mass dispersion effects.)

DISCUSSION OF RESULTS

Prompt gamma-ray and prompt electron spectra

The results of a preliminary analysis of the gamma-ray and electron data are given in Table I, where a few of the observed gamma-ray lines are listed by their energies (E_γ), along with tentative assignment of mass, A, and proton number, Z. The masses were arrived at by comparing the gamma-ray peak intensities as a function of mass with various spectra obtained at 0°, 90° and 180° with respect to the direction of motion of the fragments. The errors (± 1 mass unit) are estimates based on a study of the mass dispersion, associated with these lines, as a function of total kinetic energy.

The atomic numbers were obtained from the K-X-ray measurements. The errors (± 1 unit of charge) are estimates based on the over-all charge dispersion in the X-ray measurements. The last column in Table I, labelled "K-electron located", denotes whether a line could be found in the electron data corresponding to a line in the gamma-ray spectra. Selection of the electron and gamma-ray data according to fragment total kinetic energy as well as mass was used as a means of identifying lines associated with both spectra. An example of how this was carried out can be seen by comparing

TABLE I

TENTATIVE ASSIGNMENT OF PROMPT GAMMA-RAY LINES

Z±1	A±1	E_γ(keV)	$T_{\frac{1}{2}}(10^{-9}$ s)	K-electron located
43	106	170	> 0.5	Yes
44	108	123	< 0.5	Yes
44	109	419	< 0.5	Yes
44	110	572	< 0.5	Yes
		508	< 0.5	Yes
		239	< 0.5	Yes
		149	> 0.5	Yes
		98	0.8 ± 0.2	No
		76	> 0.5	No
44	112	210	< 0.5	Yes
		158	< 0.5	Yes
		103	0.5 ± 0.2	No
46	116	125	< 0.5	No
47	116	145	< 0.5	No
54	138	420	< 0.5	Yes
54	139	586	< 0.5	Yes
		582	< 0.5	Yes
		568	< 0.5	Yes
		382	< 0.5	Yes
54	140	479	< 0.5	Yes
		453	< 0.5	Yes
54	142	488	< 0.5	Yes
55	139	394	< 0.5	Yes
55	140	371	< 0.5	Yes
		365	< 0.5	Yes
56	144	354	< 0.5	Yes
		111	0.6 ± 0.2	No
60	150	261	< 0.5	No
		134	—	Yes
59	150	245	< 0.5	No
		120	< 0.5	Yes

the electron spectra of Fig. 6 with the gamma-ray spectra for the same mass interval in Fig. 2c. There is a general similarity in the gamma-ray structure for the energy range of 300 to 600 keV, shown in Fig. 2c, obtained with a NaI detector, and in the electron spectra shown in Fig. 6. The three gamma-ray peaks in Fig. 2c (376, 472 and 583 keV) have been found to be associated with the three broad peaks in the electron spectra. Using the higher resolution gamma-ray data from Fig. 3a and 3b with the peaks labelled alphabetically, we have calculated the expected locations of the associated K- and L-conversion lines and have plotted them below the electron spectra as shown in Fig. 6.

The limits on the half-lives for gamma-ray emission in Table I were estimated from the measured Doppler shifts in gamma-ray energy. The three measured lifetimes were obtained by varying the length of the flight path of the fragments and observing the Doppler shift. The geometry of the electron detection system was such that electrons emitted after 10^{-9} s would not have been detected and may account for the few cases where electron lines could not be located. Low yield in conversion electrons could also be the result of E1-type gamma-ray transitions.

It is interesting to note that the measured gamma-ray energies associated with masses greater than 144 seem to suggest the existence of rotational transitions ($4^+ \rightarrow 2^+$, $2^+ \rightarrow 0^+$) indicating the onset of large stable nuclear deformations at about 88 to 90 n. This onset of deformation is consistent with the results of Coulomb excitation studies of stable nuclei in the region of Nd^{150}. Some yield of Nd^{150} can be expected from fission of Cf^{252} and the measured gamma-ray energies for mass 150 do indeed agree with the known 260- and 132-keV energies [9] of the first two excited states of Nd^{150}.

Emission of X-rays

The measured half-lives for the K-X-ray emission (0.1-0.9 ns) are consistent with the view that most of these X-rays are emitted as a result of the process of internal conversion during the de-excitation of the low-energy collective states of the primary fission fragments. If any vacancy in the K-shell were created because of the fission act itself, the time of emission of the subsequent X-rays is expected to be much smaller ($\sim 10^{-14}$ s).

The observed number of K-X-rays per fission from the light and the heavy fragment groups are found to be (0.24 ± 0.02) and (0.32 ± 0.02) respectively. The X-ray yield curve shown in Fig. 11 is the result of a combination of complex effects caused by variations in the average gamma-ray yield, energy, conversion co-efficient and fluorescent yield, and their dependence on fragment mass and charge. The abrupt increase in the X-ray yield for fragment masses greater than 144 is consistent with the expected onset of large nuclear deformation in the neighbourhood of 88 n and is consistent with the measured gamma-ray energies.

The results of our measurements of Z_p versus the initial mass of the fission fragments are shown plotted in Fig. 12. For comparison, we also show the results of the predictions of several well-known empirical relationships. Therefore, in the figure we show the values of Z_p versus A_i calculated by MILTON [10] for the maximum energy release on the basis of

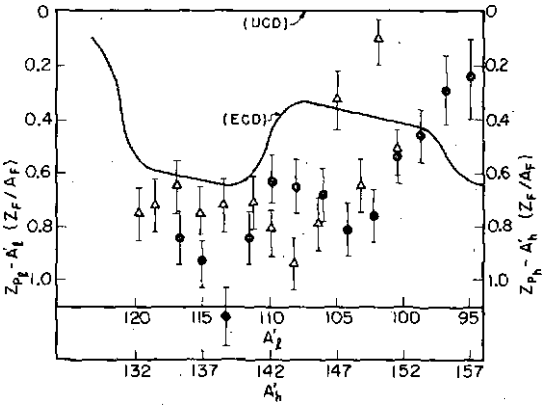

Fig. 13

The deviation of the measured charges from the unchanged specific charge, plotted on a complementary scale for the light and heavy fragments

Seeger's mass formula. The two other curves shown in Fig. 12 are calculated on the hypothesis of equal charge displacement (ECD) [11] applied to the instant of scission and unchanged charge distribution (UCD). Though none of the above hypotheses fits the data well, the experimental values are found to be in better agreement with the calculated curve based on equal charge displacement (ECD). GLENDENIN and UNIK [12] have also recently determined Z_p versus mass from the X-ray measurements with NaI(Tl) detector, and also found that the hypothesis of ECD fits their data better. A detailed plot of the measured charges in our experiments is shown in Fig. 13, where the deviations of the measured charge from the unchanged specific charge (UCD) are plotted for both the light and the heavy fragments on a complementary scale. That the data points corresponding to the light and the heavy fragments describe the same curve indicates that the sum of the measured charges of the complementary fragments do indeed add up to 98 within the experimental uncertainty of 0.2 units. The sum of the charges of the complementary fragments, averaged over all the events, was actually found to be (97.9 ± 0.2).

It can be seen from Fig. 13 that, in general, the fragments in the light group have a higher specific charge than those in the heavy group. However, this does not appear to be true within each group itself. The trend of variation of charge density with the fragment mass as observed in the present work is quite similar to that obtained in the radiochemical work for the thermal fission of U^{235}. The observed increase in the charge density with the fragment mass in the region of mass 90-106 is not understood on the basis of any proposed hypothesis.

REFERENCES

[1] BOWMAN, H.R. and THOMPSON, S.G., Proc. 2nd UN Int. Conf. PUAE 15 (1958) 212.

[2] BOWMAN, H.R., THOMPSON, S.G., MILTON, J.C.D. and SWIATECKI, W.J., Phys. Rev. 126 (1962) 2120.

[3] BOWMAN, H.R., TOMPSON, S.G., MILTON, J.C.D. and SWIATECKI, W.J., Phys. Rev. 129 (1963) 2133.
[4] THOMPSON, S.G., STREET, K., GHIORSO, A. and SEABORG, G.T., Phys. Rev. 80 (1950) 790.
[5] NAKAMURA, M. and LA PIERRE, R., Lawrence Radiation Lab. Rpt. UCRL-11494 (1964).
[6] FRASER, J.S., MILTON, J.C.D., BOWMAN, H.R. and THOMPSON, S.G., Canad. J. Phys. 41 (1963) 2080.
[7] MALMFORS, K.G., Ark. Fys. 13, 21 (1957).
[8] WAPSTRA, A.H., NIJGH, G.J., VAN LIESHOUT, R., Nuclear Spectroscopy Tables, North-Holland Publishing Co., Amsterdam (1959).
[9] ANDREEV, D.S., GRINBERG, A.P., GUSINSKII, G.M., EROKHINA, E.I. and LEMBERG, I.Kh., Izv. Akad. Nauk SSSR, Ser. fiz. 24 (1960) 1474.
[10] MILTON, J.C.D., Lawrence Radiation Lab. Rpt. UCRL-9883 Rev. (1962).
[11] PAPPAS, A.C., Proc. UN Int. Conf. PUAE 7 (1956) 19.
[12] GLENDENIN, L.E., GRIFFIN, H.C. and UNIK, J.P., private communication.

AVERAGE NUMBER AND ENERGY OF GAMMA-RAYS EMITTED AS A FUNCTION OF FRAGMENT MASS IN U^{235} THERMAL-NEUTRON-INDUCED FISSION*

H. MAIER-LEIBNITZ†, H.W. SCHMITT AND P. ARMBRUSTER‡
OAK RIDGE NATIONAL LABORATORY, OAK RIDGE, TENN., UNITED STATES OF AMERICA

Abstract — Résumé — Аннотация — Resumen

AVERAGE NUMBER AND ENERGY OF GAMMA-RAYS EMITTED AS A FUNCTION OF FRAGMENT MASS IN U^{235} THERMAL-NEUTRON-INDUCED FISSION. The average number and energy of gamma-rays emitted as a function of fragment mass in U^{235} thermal-neutron-induced fission have been measured. A three-parameter correlation experiment was performed in which two silicon surface barrier detectors were used to measure the fission product energies, and a 5-in-diam., 4-in-thick NaI(Tl) scintillation crystal was used to measure the gamma-ray energies. Extreme care was taken in the experimental arrangement to avoid counting direct fission neutrons, scattered gamma-rays and neutrons, and other false events. Data were recorded event-by-event in a system similar to that used in previous energy correlation experiments at Oak Ridge, and were analysed according to a "weighting method" proposed by Maier-Leibnitz. The total number and energy of the gamma-rays for both fragments as a function of mass ratio were obtained directly. The number and energy of gamma-rays for individual fragment masses were determined by making use of the variation in laboratory angular distribution and energy of the gamma-rays emitted from moving fragments. In particular, the 0° to 180° ratio of the number of gamma-rays from a moving source emitting isotropically in its centre-of-mass system is proportional to $1 + 2 \times 2v/c$; similarly the 0° to 180° ratio in total gamma energy is proportional to $1 + 2 \times 3v/c$. Thus by comparing appropriate ratios in the analysis for light and heavy fragments moving towards or away from the gamma-ray detector, one obtains these quantities as a function of individual fragment mass.

Results of preliminary analyses show interesting similarities in behaviour to those for neutrons. Both the total energy and average quantum energy of gamma-rays are essentially constant over most of the range of mass ratios; however a broad minimum is observed for the total energy in the region where $M_H \sim 130$, i.e. where $Z_H \sim 50$ or $N_H \sim 82$. An increase is observed in the total energy as the mass ratio approaches unity. The number and energy of gamma-rays emitted from individual fragments is observed to increase in both fragment groups and shows similar mass dependence, as has been observed for prompt neutrons. The average quantum energy in the mass range of closed shells seems to be higher.

NOMBRE MOYEN ET ÉNERGIE MOYENNE DES RAYONS GAMMA ÉMIS, EN FONCTION DE LA MASSE DES FRAGMENTS DE LA FISSION DE ^{235}U PAR DES NEUTRONS THERMIQUES. Les auteurs ont procédé à une expérience comportant trois paramètres afin d'établir une corrélation entre le nombre moyen et l'énergie moyenne des rayons gamma émis lors de la fission de ^{235}U par des neutrons thermiques, d'une part, et la masse des fragments de fission d'autre part. Dans cette expérience, l'énergie des produits de fission a été mesurée au moyen de deux détecteurs au silicium à barrière de surface, et l'énergie des rayons gamma, à l'aide d'un cristal de NaI(Tl) de 10,16 cm d'épaisseur et de 12,70 cm de diamètre. De grandes précautions ont été prises dans la préparation de l'expérience afin d'éviter le comptage des neutrons provenant directement de la fission, des rayons gamma et neutrons diffusés, ainsi que de tous autres événements parasites. Les données relatives à chaque événement ont été enregistrées séparément au moyen d'un appareillage analogue à celui qui avait été utilisé à Oak Ridge lors d'expériences antérieures de corrélation masse-énergie et ont été analysées d'après une méthode «de pondération» mise au point par Maier-Leibnitz.

---

* Research sponsored by the United States Atomic Energy Commission under contract with the Union Carbide Corporation.

† Physik-Department der Technischen Hochschule München, Munich, Federal Republic of Germany. Visitor to Oak Ridge National Laboratory, October 1963-April 1964.

‡ Institut fur Neutronenphysik, Kernforschungsanlage Jülich, Jülich, Federal Republic of Germany. Visitor to Oak Ridge National Laboratory, April-July 1964.

Le nombre total et l'énergie totale des rayons gamma pour les deux fragments de fission, exprimés en fonction du rapport des masses, ont été mesurés directement. Le nombre et l'énergie des rayons gamma pour les différentes masses ont été déterminés au moyen de la variation de la distribution angulaire et de l'énergie des rayons gamma émis par des fragments en mouvement. En particulier, le rapport 0°/180° des nombres de rayons gamma provenant d'une source en mouvement dont l'émission est isotrope dans son système de centre de masse est proportionnel à $1+2\times3\ v/c$; de même, le rapport 0°/180° de l'énergie totale des rayons gamma est proportionnel à $1+2\times3\ v/c$. En comparant des rapports appropriés pour des fragments légers et lourds se rapprochant ou s'éloignant du détecteur à rayons gamma, on obtient donc ces quantités en fonction des différentes masses de fragments.

D'après les résultats d'analyses préliminaires, on observe une analogie intéressante entre le comportement des rayons gamma et celui des neutrons. L'énergie totale et l'énergie quantique moyenne des rayons gamma sont l'une et l'autre essentiellement constantes dans presque tout l'intervalle des rapports de masse, mais on observe un minimum peu accusé de l'énergie totale dans la région où $M_H \sim 130$, c'est-à-dire où $Z_H \sim 50$ ou $N_H \sim 82$. On observe une augmentation de l'énergie totale à mesure que le rapport des masses tend vers l'unité. On constate que le nombre et l'énergie des rayons gamma émis par les différents fragments augmentent pour les deux groupes de fragments et présentent, par rapport à la masse, une dépendance semblable à celle qui a été observée pour les neutrons instantanés. L'énergie quantique moyenne dans l'intervalle des masses correspondant aux couches saturées paraît plus élevée.

СРЕДНЕЕ ЧИСЛО И ЭНЕРГИЯ ИСПУСКАЕМЫХ ГАММА-КВАНТОВ КАК ФУНКЦИЯ МАССЫ ОСКОЛКА ПРИ ДЕЛЕНИИ УРАНА-235, ВЫЗВАННОМ ТЕПЛОВЫМИ НЕЙТРОНАМИ. Измерены среднее число и энергия испускаемых гамма-квантов как функция массы осколка при делении урана-235, вызванном тепловыми нейтронами. Проведен эксперимент по корреляции трех параметров, в котором использовались два барьерных детектора с кремниевыми поверхностями для измерения энергий продуктов деления, а для измерения энергий гамма-квантов использовался сцинтилляционный кристалл NaJ(Tl) диаметром 12,5 и толщиной 10 см. Чрезвычайно большое внимание уделено экспериментальному расположению, чтобы избежать отсчета непосредственных нейтронов деления, рассеянных гамма-квантов и нейтронов, а также других ошибочных явлений. Данные последовательно записывались по системе, аналогичной той, которая использовалась в предыдущих экспериментах в Окридже по корреляции энергии и анализировались в соответствии со "взвешивающим методом", предложенным Майером-Лейбнитцем.

Общее число и энергия гамма-квантов для обоих осколков были непосредственно получены как функция отношения масс. Число и энергия гамма-квантов для масс индивидуальных осколков были определены путем использования вариаций лабораторного углового распределения и энергии гамма-квантов в соответствии со скоростью гамма-испускающего осколка. В частности, отношение числа гамма-квантов 0–180° от движущегося источника, излучающего изотропно в своей системе центра-массы, является пропорциональным $1+2{,}2\ v/c$; аналогично отношение 0–180° в общей гамма-энергии является пропорциональным $1+2{,}3\ v/c$. Таким образом, сравнивая соответствующие отношения при анализе для легких и тяжелых осколков, движущихся по направлению к или от гамма-квантового детектора, можно получить такие количества, как функцию массы индивидуального осколка.

Результаты предварительного анализа показывают интересные сходные черты поведения гамма-лучей с поведением нейтронов. Как общее число, так и общая энергия гамма-квантов в основном остаются постоянными для большинства интервалов отношения масс. Однако наблюдался широкий минимум для общей энергии в области, где $M_H \sim 130$, т.е. где $Z_H \sim 50$ или $N_H \sim 82$. Наблюдалось увеличение в общей энергии по мере того, как отношение масс приближалось к единице. Число и энергия гамма-квантов, испускаемых из отдельных осколков, указало на увеличение в обеих группах осколков и обнаружило аналогичную зависимость от масс, как это наблюдалось для мгновенных нейтронов. Средняя энергия кванта в интервале масс закрытых оболочек, по-видимому, будет более высокой.

NÚMERO Y ENERGÍA MEDIOS DE LOS RAYOS GAMMA EMITIDOS EN FUNCION DE LA MASA DE LOS FRAGMENTOS EN LA FISION DEL ^{235}U INDUCIDA POR NEUTRONES TÉRMICOS. Se han medido el número y la energía medios de los rayos gamma emitidos en función de la masa de los fragmentos en la fisión del ^{235}U inducida por neutrones térmicos. Se ha realizado un experimento de correlación con tres parámetros, en el que se utilizaron dos detectores de barrera superficial (silicio) para medir la energía de los productos de fisión, y un centelleador de NaI(Tl), de 12,5 cm de diámetro y 10 cm de espesor, para medir la energía de los rayos gamma. En la preparación del experimento se procedió con sumo cuidado para evitar el recuento

de los neutrones que proceden directamente de la fisión, así como de los rayos gamma y neutrones dispersos y de otros sucesos parásitos. Se registraron los datos relativos a cada suceso, con arreglo a un sistema análogo al seguido en experimentos de correlación de energía previamente realizados en Oak Ridge, datos que se analizaron conforme a un «método de ponderación» ideado por Maier-Leibnitz.

Se determinó directamente el número y energía totales de los rayos gamma correspondientes a los dos fragmentos en función de la razón másica. Por otra parte, el número y energía de los rayos gamma correspondientes a la masa de cada fragmento se evaluó a partir de la variación medida en laboratorio de la distribución angular y de la energía de los rayos gamma emitidos por fragmentos móviles. En particular, la razón 0°/180° del número de rayos gamma provenientes de una fuente en movimiento que emite isotrópicamente en su sistema de centro de masa, es proporcional a $1 + 2 \times 2\ v/c$; análogamente, la razón 0°/180° de la energía total de los rayos gamma es proporcional a $1 + 2 \times 3\ v/c$. Así pues, comparando las razones apropiadas en el análisis de los fragmentos ligeros y pesados que se mueven hacia el detector de rayos gamma o se alejan del mismo, se obtienen esas magnitudes en función de la masa de cada fragmento.

Los resultados de los análisis iniciales muestran interesantes analogías con los correspondientes a los neutrones. Tanto el número total como la energía cuántica media de los rayos gamma permanecen prácticamente constantes en casi todo el intervalo de razones másicas, aunque se observa un mínimo poco marcado en la región en que $M_H \sim 130$, es decir, en que $Z_H \sim 50$ ó $N_H \sim 82$. A medida que la razón másica se aproxima a la unidad, se registra un aumento de la energía total. El número y la energía de los rayos gamma emitidos por cada fragmento aumentan en ambos grupos de fragmentos y presentan una variación en función de la masa, análoga a la observada para neutrones inmediatos. El valor medio de la energía cuántica en el intervalo de masa correspondiente a las capas saturadas, parece ser más elevado.

INTRODUCTION

The gamma spectrum emitted by each of the primary fission fragments may be described by two quantities, which characterize in first approximation the spectrum, the total gamma energy E_γ and the total number of promptly emitted quanta N_γ [1–4]. A method to determine these quantities from the response function of a gamma detector and a measured pulse-height spectrum is given first. A coincident detection of the two fragments and the gamma quanta gives the mass ratio dependence of E_γ and N_γ [4–6]. Most of the gamma quanta are emitted within times of 10^{-13}–10^{-9} s after fission. If the fragments travel in vacuum, they are still at full speed at the emission time of the gamma quanta. The gamma energy will be Doppler-shifted, and the solid angle between the fragments and the gamma detector will be changed relativistically. A forward-backward anisotropy of gamma emission in the direction of flight of the fragments results. This has been used to distinguish between quanta emitted from the light and from the heavy fragment [7]. The method has been refined and is described. Preliminary results for the thermal fission of U^{235} are given.

METHOD

Weighting method over a spectrum

The following weighting procedure has been used to obtain from the pulse-height spectrum S(q) produced in the detector, the total number n and the total energy e of the quanta emitted by the source.

The response function of the detector $W(q, \nu)$ may be defined as the probability that a quantum of energy $h\nu$ incident on the detector gives rise to

an energy release hq in the detector. The desired total number of quanta and their total energy are defined by

$$n = \int_0^{\nu_{max}} n(\nu)\, d\nu$$

$$e = \int_0^{\nu_{max}} n(\nu)\, h\nu\, d\nu\,. \tag{1}$$

Weighting factors g(q) are introduced, which correlate the measured spectrum S(q) to the quantities n and e

$$n = \int_0^{q=\nu} S(q)\, g_n(q)\, dq$$

$$e = \int_0^{q=\nu} S(q)\, g_e(q)\, dq\,. \tag{2}$$

The measured spectrum S(q) on the other hand is related to the response function $W(q, \nu)$ and the energy-dependent probability $p(\nu)$ that a quantum emitted by the source will reach the detector.

$$p(\nu) = \Omega\, a(\nu) \tag{3}$$

$$S(q) = \int_0^{\nu_{max}} n(\nu)\, p(\nu)\, W(q, \nu)\, d\nu \tag{4}$$

where Ω = solid angle between source and detector;

$a(\nu)$ = non-absorption probability between source and detector.

Eqs. (2) and (3) give a representation of n and e, from which by comparison with Eq. (1) integral equations for the weighting factors are obtained

$$p(\nu) \int_0^{\nu} W(q, \nu)\, g_n(q)\, dq = 1$$

$$p(\nu) \int_0^{\nu} W(q,\nu)\, g_e(q)\, dq = h\nu\,. \tag{5}$$

The response function will be represented by a matrix. This representation

is better suited to handle a pulse-height spectrum in a limited number of channels.

Eq. (5) can be written

$$\sum_k W_{ki}\ g_k^n = \frac{1}{p_i}$$

$$\sum_k W_{ki}\ g_k^e = \frac{h\nu_i}{p_i}. \tag{6}$$

A solution of Eq. (6) demands a knowledge of the response function W_{ki} and of the probability p_i. Both these quantities are fixed properties of the experimental set-up and have to be determined only once. The solution of a system of k linear equations gives the weighting factors g_k. Each registered count of energy q has to be weighted according to Eq. (2). The sum over all weighted counts gives the desired total number of gamma quanta, and also the total energy

$$n = \sum_k S_k\ g_k^n$$

$$e = \sum_k S_k\ g_k^e \tag{2a}$$

The anisotropy of gamma emission from moving fragments

Let the anisotropy be defined as

$$\alpha = \frac{\omega(\theta_1) - \omega(\theta_2)}{\omega(\theta_1) + \omega(\theta_2)} \tag{7}$$

where ω are emission probabilities in the directions θ_1 and θ_2. Anisotropies in a non-moving system will be indexed by 0, indices n and e refer to number of quanta and total energy respectively.

$\alpha_0 = 0$ for $\theta_2 = \theta_1$ and $\theta_2 = \theta_1 + 180$
$\alpha_0 \neq 0$ for all other values of $\theta_2 \neq \theta$

Only measurements in directions with $\alpha_0 = 0$ are independent of possible preferential orientations between the fragment spins and the direction of flight of the fragments, which might give rise to unknown anisotropies $\alpha_0 \neq 0$.

$$\omega_0(\theta_1) = \omega_0(\theta_1 + 180°) \tag{8}$$

Emission from moving systems shows an anisotropy for $\theta_2 = \theta_1 + 180°$.

$$\alpha_n = 2\beta \cos\theta + f(\beta^2) \tag{9a}$$

with

$\beta = \frac{v}{c}$, and $f(\beta^2)$ negligible for small values of β.

The energy of a quantum emitted from a moving system is Doppler-shifted. The total energy emitted into two opposite directions shows an anisotropy

$$\alpha_e = 3\beta \cos\theta + f(\beta^2). \tag{9b}$$

The anisotropies α_n and α_e may be calculated for gamma emission from fission fragments, if the velocities of the fragments are assumed to be known. The anisotropy is largest for $\theta = 0$, that is in forward-backward direction, and it is independent from possible anisotropies in the non-moving system.

Determination of single fragment gamma data from 0°/180° anisotropy

The calculable 0°/180° anisotropies of fission-fragment gamma emission may be used to determine the number of gamma quanta and the total energy emitted from single fragments. Let B stand for the number of quanta, and let E represent the total energy E emitted from a pair of fission fragments of mass split M/(A − M), and let B_M and B_{A-M} stand for the same quantities referred to single fragments of mass M, and (A − M) respectively. The number of quanta incident on the detector during the time of measurement are called b, which is given by Eq. (10) with p defined by Eq. (3), and with $n_F(M)$ given as the number of fissions of mass split M/(A − M) during the time of measurement.

$$b = p\, B\, n_F(M) \tag{10}$$

The quantity b will be measured for two cases, with the fragments of mass M moving in the direction of the gamma detector and with the fragments of the same mass moving in the opposite direction. For the two cases the following equations between the measured quantities b and the desired quantities B_M and B_{A-M} hold

$$\begin{aligned} \frac{b_1}{p\, n_F} &= B_M(1+\alpha_M) + B_{A-M}(1-\alpha_{A-M}) \\ \frac{b_2}{p\, n_F} &= B_M(1-\alpha_M) + B_{A-M}(1+\alpha_{A-M}). \end{aligned} \tag{11}$$

With $(b_1 - b_2)/(b_1 + b_2) = \Delta$ and making use of momentum conservation between the fragments, Eq. (11) can be written

$$\frac{B_M}{B} = \frac{M}{A}\left(1 + \frac{\Delta}{\alpha_{A-M}}\right)$$

$$B = \frac{b_1 + b_2}{2\ p\ n_F\ (M)} \quad . \tag{12}$$

b/p equals by definition the weighted quantities n and e. Introducing n and e from Eq. (2a) and α_n and α_e from Eq. (9) into Eq. (12) gives

$$\frac{N_M}{N} = \frac{M}{A}\left(1 + \frac{\Delta_n}{2\beta_{A-M}\cos\theta}\right) \text{ with } N = \frac{n_1 + n_2}{2\ n_F(M)}$$

$$\frac{E_M}{E} = \frac{M}{A}\left(1 + \frac{\Delta_e}{3\beta_{A-M}\cos\theta}\right) \text{ with } E = \frac{e_1 + e_2}{2\ n_F(M)} \quad . \tag{12a}$$

Determination of fragment mass

A coincident measurement of the ionizations produced by complementary fission fragments in two fission-fragment detectors has been widely used to determine the masses of the fragment pair. From the total ionization measured in the detectors the kinetic energy of the fission fragments after prompt neutron emission may be calculated, assuming that a correct calibration procedure exists. Momentum conservation holds rigorously between complementary fragments before neutron emission. These pre-neutron emission masses M are to be determined from the double post-neutron energy measurement. In the analysis a pseudo-mass m^x is introduced and momentum conservation is formally assumed between these masses and the measured energies.

$$m^x = A\ \frac{E_{A-m^x}}{E_{m^x} + E_{A-m^x}} \tag{13}$$

The pre-neutron masses can be calculated from the pseudo-masses, if the mass dependence of the number of prompt neutrons is known, and if isotropic neutron emission in the centre of mass system is assumed.

$$M = m^x + \Delta m^x \text{ with } \Delta m^x = \frac{m^x}{A}\nu_{A-m^x} - \left(\frac{A - m^x}{A}\right)\nu_{m^x} \tag{14}$$

where ν_{m^x} = number of neutrons emitted from fragments of mass m^x;

ν_{A-m^x} = number of neutrons emitted from complementary fragments.

The mass corrections Δ_{m^x} for a pair of complementary fragments are equal in amount, but of opposite sign. The accuracy of mass determination by the double energy measurement is comparable to the double time-of-flight measurement, if the above neutron emission correction is made.

Besides, the mass distribution determined by the double energy measurement has to be corrected for prompt neutron emission. The number of events N(M) in the mass region ΔM is calculated from the measured distribution $N(m^x)$

$$N(M) = N(m^x)\,\frac{dm^x}{dM} = N(m^x)\left[1 - \frac{\nu_{m^x} + \nu_{A-m^x}}{A}\right]. \tag{15}$$

For two complementary fragments the corrections are equal. Ratio of yields, as the quantity Δ of Eq. (12a), are not affected by the correction. The corrections of the absolute values of N and E are smaller than 1%.

EXPERIMENTAL ARRANGEMENT

Figure 1 gives a schematic view of the experimental set-up. The experiment has been carried out at the beam HN-1 of the ORR-Reactor. A 80 $\mu g/cm^2$ evaporated deposit of U^{235} on a 30 $\mu g/cm^2$ self-supporting carbon foil in a thermal neutron flux of 10^8 $n/cm^2.s$ has been used as a fission source. The source has been mounted between a pair of surface barrier detectors in an evacuated chamber. The detection probability of the two detectors for fragment pairs is 2.6%. A number of 135 pairs of complementary fragments has been registered per second. The detectors have been calibrated by a technique described by SCHMITT et al. [8].

Coincident gamma quanta have been detected by 5-in-diam, 4-in-thick NaI crystals. Coincidences between pulse-height spectra from 50 to 110 MeV fission fragments and gamma quanta in the energy range of 0.1 to 6.0 MeV have been registered by a fast-slow coincidence circuit with a time resolution of $2\tau = 10^{-7}$ s. This rather large time resolution has become necessary, as all gamma quanta in the whole energy range had to be registered without losses in the coincidence circuits. A time-of-flight discrimination between gamma quanta and prompt fast neutrons is not possible for such a large time resolution. A 7.5-in-thick block of Li^6H between the fission source and the NaI crystal has been used as a neutron shield. It reduces the ratio of the numbers of prompt neutrons and gamma quanta incident on the gamma detector by a factor of 130 without producing any gamma radiation. The distance between the fission source and the gamma detector is 43 cm. Triple coincidence rates of about 110/min have been observed. A second gamma detector, 98 cm from the source, in connection with a coincidence resolving time of 25 ns, has been used to achieve a time-of-flight discrimination between neutrons and gamma quanta. A reduction of the ratio of neutrons and gamma quanta by a factor of 8 is possible, whereas the number of triple coincidences is reduced to 15/min, and about 30% of the events are lost in the coincidence circuits. The efficiency of the Li^6H shield of the first gamma detector has been checked by the second detector with time discrimination.

A TMC-three-parameter analyser directly transferred the addresses of the three correlated pulses event-by-event to paper punch. 430, 117 triple

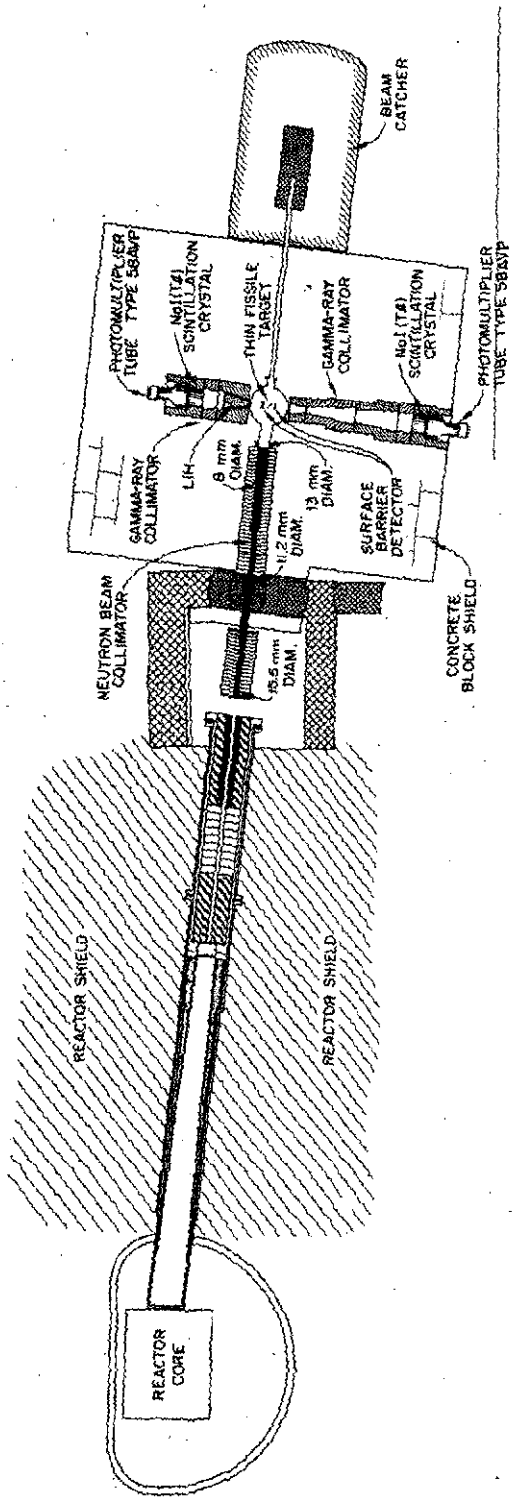

Fig. 1

Schematic view of the setup used in the three-parameter gamma-correlation experiment

coincidences, 3,201,972 binary coincidences and 15,560 background triple coincidences have been collected in a first run during a total time of measurement of about 140 hours. A preliminary and incomplete analysis of the data obtained will be given.

DATA ANALYSIS

The response function W_{ik} of a 5-in × 4-in NaI crystal has been determined by RAU [9] and BERGQUIST [10]. A combination of the matrices given by these authors has been used for the calculation of the g-factors. As the fission gamma spectrum peaks at energies smaller than 1 MeV and the g-factors are very sensitive to changes in the low-energy matrix elements these elements have been taken from the matrix given by Rau. The latter matrix is divided in energy intervals of 0.2 MeV compared with the matrix given by Bergquist, which is divided in 0.4-MeV intervals. The factor p of Eq.(4) has been calculated with $\Omega = 5.0 \times 10^{-3}$ from the attenuation factor $a(\nu)$ in the Li^6H shield. The g-factors are obtained by solving the system of linear equations defined by Eq.(6). Figure 2 gives the weighting factors for the number of gamma quanta n and the total energy e. The increase of g_n for small energies is caused by the strong absorption of soft quanta in the Li^6H shield. For increasing energies the decreasing absorption in the neutron shield and the NaI crystal partly compensate. The weighting factors g_e increase with increasing energy.

The weighting method reduces the three-parameter experiment in the first step of the analysis to a two-parameter experiment. According to Eq. (2a) all fission-fragment pulses are weighted by the weighting factor g given by the pulse height of the coincident gamma pulse. The weighted fragment pulses constitute a matrix, the elements of which are characterized by the two pulse heights in the surface barrier detectors. This matrix is transferred into an energy-versus-energy matrix. The already mentioned calibration procedure uses a linear dependence between pulse height and energy

$$E = (a + b\,M)I + (c + d\,M). \tag{16}$$

The determination of the calibration constants a, b, c, and d is described in Ref. [8].

Events with the fragments of mass M moving in the direction of the gamma detector, indexed in Eq.(12a) by 1, and events indexed by 2, appear in the matrix on different sides of the diagonal defined by $E_1 = E_2$. Eq.(13) correlates the energies of a fragment pair with its pseudo-masses m^x. Summation of all events with constant mass for the two halves of the matrix gives the weighted total numbers n_1 and n_2, and the weighted total energies e_1 and e_2 of Eq.(12a).

The total energy E and the total number N emitted by a fragment pair may be calculated from the values n and e, if $n_F(M) = n_F\,\eta(M)$ is introduced into Eq.(12a). The total number of binary fissions in the time of measurement of the triple coincidence experiment n_F has been determined from the total time, the live time of the analyser, and the rate of binary events.

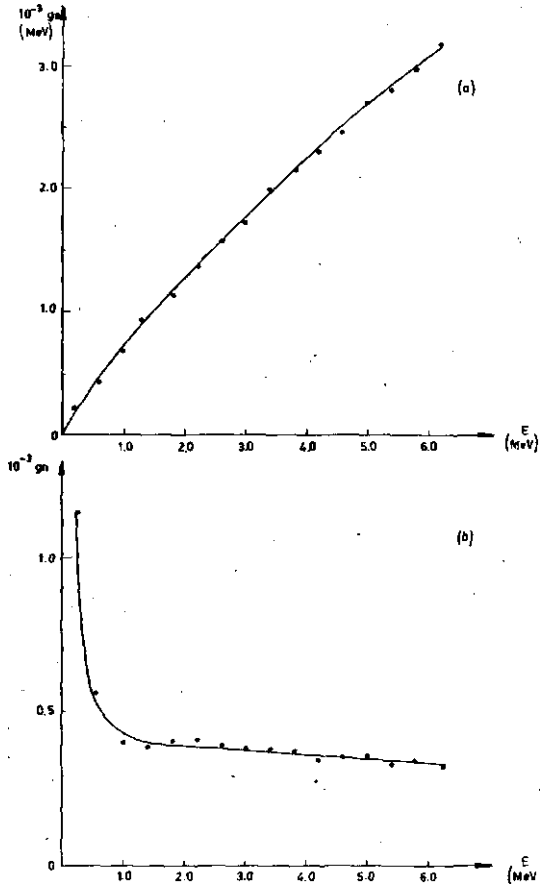

Fig. 2

(a) The weighting factor g_e for determining the total energy E versus the energy released by the quantum in the gamma detector

(b) The weighting factor g_n for determining the total number of quanta N

The yields $\eta(m^x)$ are taken from the binary coincidence experiment. The mass distribution is normalized to 200%. The yields of $\eta(m^x)$ and $\eta(A - m^x)$ have to be equal, as the prompt neutron correction of Eq. (15) does not change the ratio of yields of two complementary fragments, and the yields $\eta(M)$ and $\eta(A - M)$ are equal by definition. In the cases where complementary masses had no equal yields in the measured binary mass distribution the average value of the two yields has been calculated. The ratio of this average yield and the yield actually obtained from the analysis increases with increasing mass ratio from 1.00 for A = 118 to 1.2 for A = 80. Unequal yields of complementary fragments in a double-energy-experiment are caused by the calibration of the detectors. As the calibration of the detectors and the analysis of data for the binary and triple experiment are the same, the above-mentioned ratio of yields has been used as a correction factor for the yield distributions of the triple coincidence experiment.

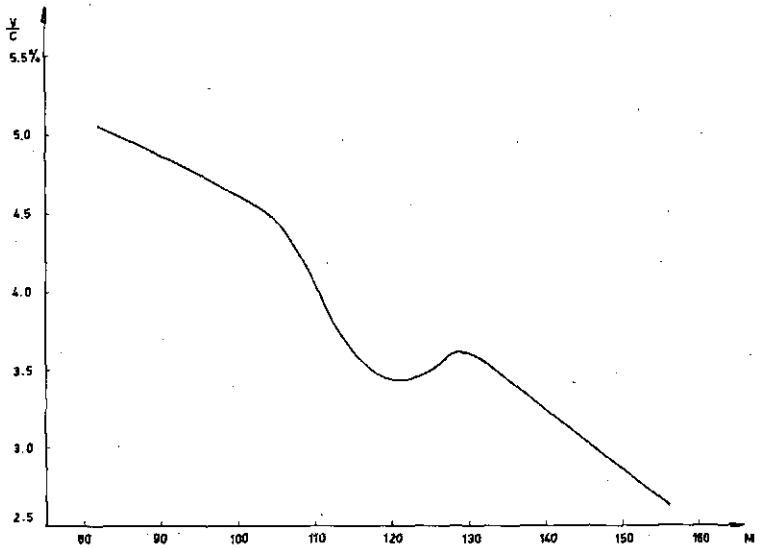

Fig. 3

The average value of the ratio $\beta = v/c$ as a function of fragment mass for U^{235}

Figure 3 gives $\beta = v/c$ as a function of fragment mass for U^{235} determined from the average velocities quoted in Ref. [11]. The quantity Δ of Eq. (12) is calculated from the corrected values of n and e.

An average value of cos θ has to be introduced into Eq. (12a) in order to calculate the single fragment gamma yields. This value is 0.96 ± 0.005 for the given geometry of source and detectors.

Anisotropies caused by neutrons leaking through the neutron shield may be estimated from Eq. (17), as long as the contribution of neutrons to Δ, compared to gamma quanta, is small.

$$\Delta = \Delta_\gamma + \Delta_n \quad \text{with } \Delta_n = \frac{\epsilon}{2} \frac{p_n \omega_n}{p_\gamma \omega_\gamma} \frac{\nu_M - \nu_{A-M}}{\nu} \frac{\nu}{N} \tag{17}$$

ϵ = anisotropy factor of n-emission, $\epsilon = 4.7$

p_γ and p_n attenuation factors in neutron shield,
$p_\gamma = 0.4$, $p_n = 3 \times 10^{-3}$

ω_γ and ω_n average total detection probabilities in NaI-crystal,
$\omega_\gamma = 0.90$, $\omega_n = 0.19$

$\frac{\nu_M - \nu_{A-M}}{\nu}$ = relative difference of the numbers of neutrons emitted by complementary fragments;

$-1 < \frac{\nu_M - \nu_{A-M}}{\nu} < 1$

ν = total number of neutrons/fission
N = total number of quanta/fission

$\frac{\overline{\nu}}{N} = 0.35$

The values of Δ_n are about 10^{-3}. The measured values of Δ may be corrected for neutron leakage, as the mass dependence of all quantities of Eq. (17) is known. The neutron leakage correction affects the accuracy in the number and energy of quanta emitted by single fragments by less than 2%. The statistical errors in the triple coincidence experiment are greater or equal 4%, thus the neutron leakage correction is within the statistical errors.

Random coincidences give rise to a background in the triple coincidence experiment. 4.5 background coincidences/min compared to 110 real coincidences/min make a 4% background correction for the absolute values of n and e. A background run has been analysed completely, and the triple coincidence run has been corrected for random coincidences.

RESULTS

Figure 4 gives raw fragment pulse-height distributions in the two surface barrier detectors for a binary and triple coincidence experiment. The two spectra are shifted in the pulse-height scale by about 4 channels, as

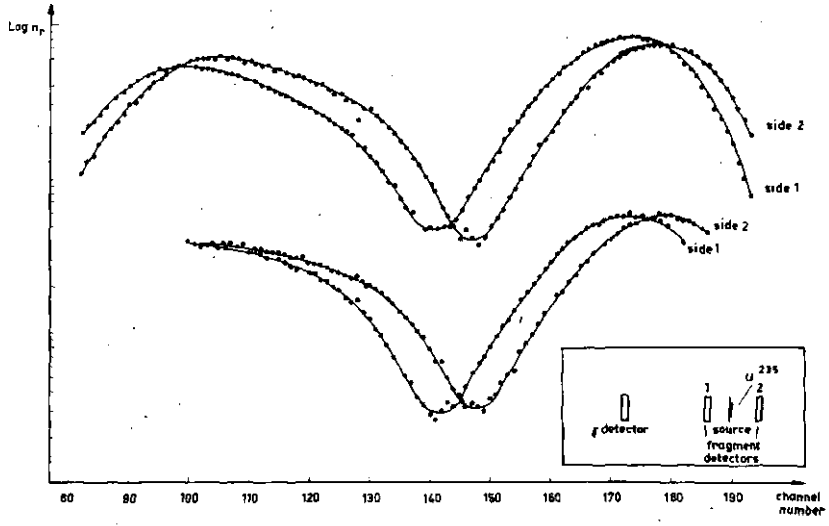

Fig. 4

Pulse-height spectra from U^{235} fission fragments. Numbers of events are plotted in a log-scale versus the channel number. The two lower curves are spectra from the binary experiment. The two upper curves have been obtained from the triple experiment. The spectra are correlated to the fission-fragment detectors as demonstrated by the inset.

fragments reaching detector 1 have been slowed down in the carbon backing of the fission source by a few MeV. The number of events for comparable pulse heights are equal for both detectors in the binary experiment. The triple experiment gives higher numbers of events if the light fragments are approaching the gamma detector, and correspondingly smaller numbers of events if they are moving from the gamma detector. Without any analysis

Fig. 4 clearly demonstrates that the 0°/180° anisotropy of gamma emission from light fragments is larger than from heavy fragments.

Figure 5 gives mass distributions from a binary experiment and a triple experiment. The distributions are uncorrected for anisotropies caused by leakage neutrons or by inequalities of $\eta(m^x)$ and $\eta(A - m^x)$ in the binary distribution.

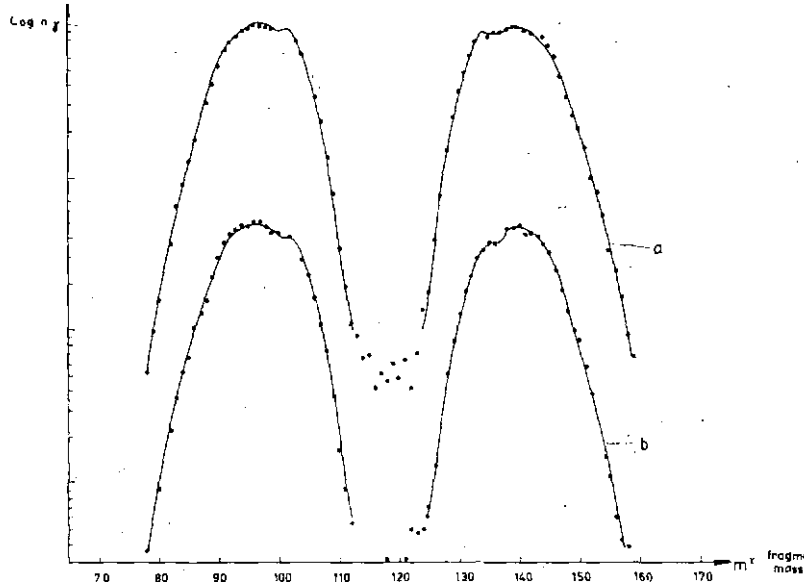

Fig. 5

Mass distributions for U^{235} from (a) a binary and (b) a weighted triple gamma-correlation experiment. The yields are plotted in a log-scale versus a pseudo-fragment mass scale.

No absolute values of E_γ and N_γ will be given in the preliminary analysis. The analysis showed a very high number of pulses in the lowest channels. A higher number of these pulses is produced in the NaI-crystal than assumed in the response function used in the calculation of the g-factors. An investigation of the production of low-energy quanta in the gamma detector is necessary before absolute values can be given. The relative mass and mass ratio dependences are not very sensitive to the values of the g-factors for the lowest channels.

Figure 6 gives the mass ratio dependence of the total energy and the average quantum energy. The energy scale for the total energy might be changed in a final analysis by ± 20%. The average energy is plotted versus a relative scale. The total energy is constant within ±5% for the mass region of high mass yields. A broad minimum in the region of $M \sim 130$ has been found. An increase of the total energy in the region of symmetric fission seems to be indicated. The average quantum energy decreases with increasing mass ratio in the region of high mass yields. In the region near $M \sim 130$ the average quantum energy is increased by about 20%.

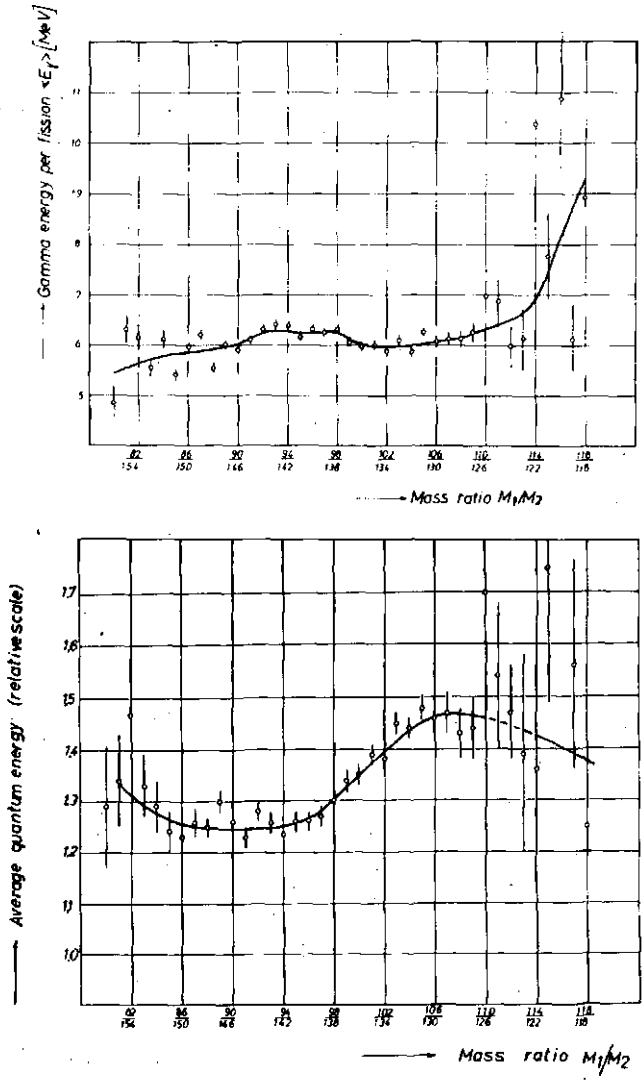

Fig. 6

(a) Total gamma energy released in U^{235} fission versus the mass ratio. The absolute values are uncertain within ± 20%.

(b) Quantum energy versus the mass ratio

The total energy is plotted versus the fragment mass in Fig. 7. In both the fragment groups the gamma energy increases with increasing mass. A saw-tooth dependence of the gamma energy has been obtained. Near closed shells, that is near $M \sim 84$ and $M \sim 130$, the gamma energy has its smallest values. A difference in the total energy of about 3–4 MeV between closed shell nuclei and nuclei far from shells has been found in both the fragment groups.

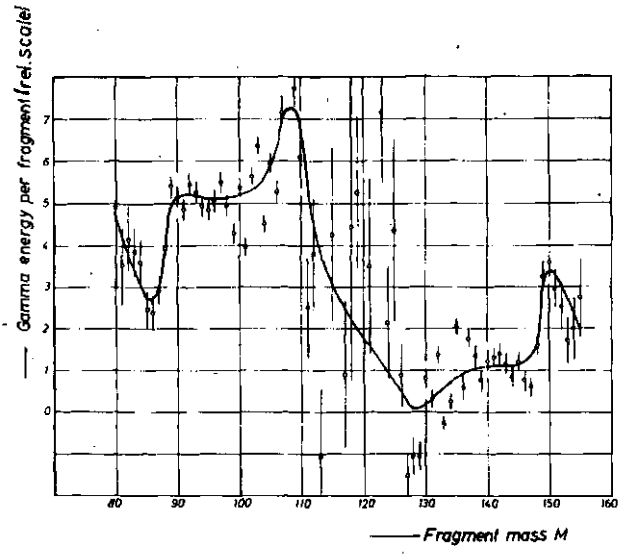

Fig. 7

Total gamma energy released in U^{235} fission as a function of fragment mass

The small average total gamma energy that is emitted from heavy fragments, as compared with that from light fragments, should not be taken as a final result. A shift of either the whole light or heavy fragment group versus the mass region of symmetric fission could cause this large difference of the average total energies.

For both the fragment groups, the average number, and average total energy are calculated. The average values serve as reference points. The mass dependence in the two groups referred to these reference points has been plotted in Figs. 8 and 9. The relative scales have been adjusted in order to make the reference points for the two groups equal, i.e. the average number of quanta and the average quantum energy for the two groups are assumed to be equal.

The average energy per quantum seems to show no strong mass dependence (Fig. 8). The average energy in the closed shell region near A=130 is higher than in regions far from closed shells. The saw-tooth dependence of the total energy results from such a dependence of the number of gamma quanta. This is demonstrated in Fig. 9.

DISCUSSION

The preliminary results obtained show the principal ideas represented in the first part of the paper to be experimentally practicable.

The experimental method needs further refinement. Unknown errors, probably originating from the calculation of the weighted mass distribution from the fission fragment energy data, seem to be present. The statistical errors given in Fig. 7 are much smaller than the fluctuations actually ob-

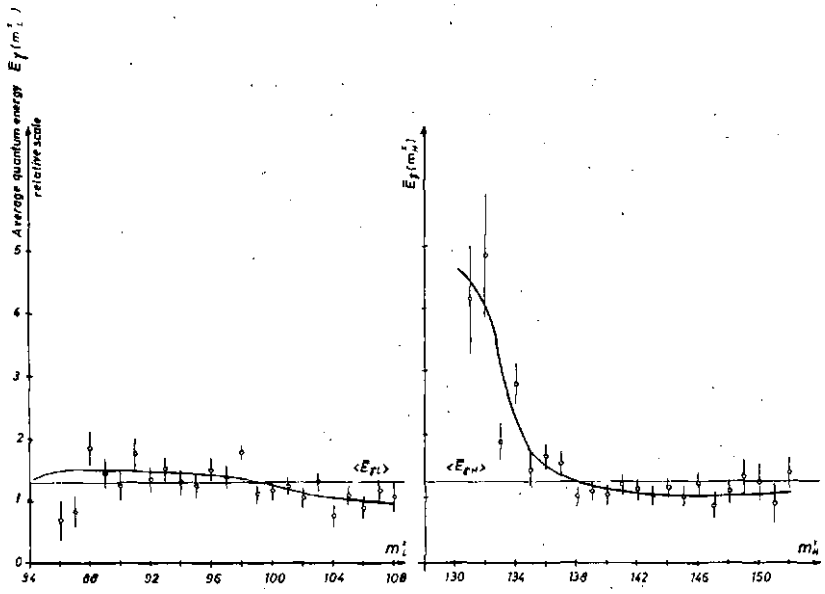

Fig. 8

Quantum energy of U^{235} prompt gamma quanta plotted versus the fragment mass for the two groups of fission fragments. In this representation the average energies in both groups are assumed to be equal.

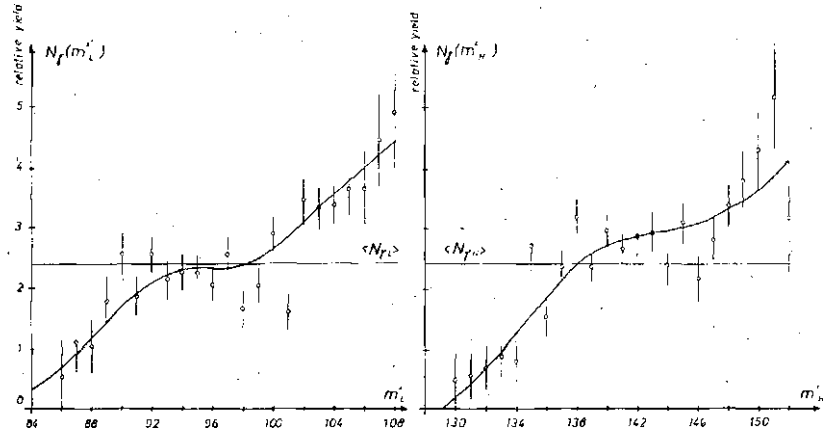

Fig. 9

The mass dependence of the number of quanta emitted from U^{235} fission fragments is plotted for the two fragment groups. The average numbers of gamma quanta in the two groups are assumed to be equal.

served. The errors of Figs. 8 and 9 are estimated from a least-squares fit. They are larger by a factor of three compared to the statistical errors.

Whether a difference in the average numbers of quanta between the two fragment groups exists or not, has not yet been established. RAMANNA

et al. [7] found a small difference, which would give rise to minor changes in Fig. 9.

The determination of absolute numbers and energies depends on further straightforward studies of the response function of the gamma detector.

A detailed discussion of all possible errors and corrections will be given in a later publication. The data will be further analysed by corresponding weighting factors to give the dependence from certain intervals of gamma energy.

The following conclusions, which are independent of further analyses, are stated:

(1) Most of the gamma quanta are emitted from moving fragments.

(2) In the region of high mass yields of U^{235}, neither the total number nor the total energy emitted by gamma quanta essentially depends on the mass ratio of the fragments [4-6].

(3) For symmetric fission of U^{235} the total gamma energy is higher than for asymmetric fission.

(4) In the region of $M_L/M_H = 106/130$ the average quantum energy has a maximum [5].

(5) The mass dependence of the number of quanta emitted shows a saw-tooth structure [12]. Nuclei in the region of closed shells emit a small number of high energy quanta.

(6) The average quantum energy shows no essential mass-dependence. The quantum energy near $M = 130$, however, is appreciably higher than for other mass numbers.

An interpretation of these results in connection with further experiments in the fields is given in the review paper[1] by two of the authors, and the reader is referred to the discussion of results in that paper.

ACKNOWLEDGEMENTS

Two of us (H. Maier-Leibnitz and P. Armbruster) are greatly indebted to the Physics Division of the Oak Ridge National Laboratory for the friendly hospitality and the support of the experiment during their visit to the Laboratory. The technical assistance of D.G. Peach in all stages of the experiment is gratefully acknowledged.

REFERENCES

[1] MAIENSCHEIN, F.C., PEELE, R.W., ZOBEL, W. and LOVE, T.A., Proc. 2nd UN Int. Conf. PUAE 15 (1958) 366.

[2] SMITH, A.B., FIELDS, P.R. and FRIDMAN, A.M., Phys. Rev. 104 (1956) 699.

[3] BOWMAN, H.R. and THOMPSON, S.G., Proc. 2nd UN Int. Conf. PUAE 15 (1958) 212.

[4] RAU, F.E.W., Ann. Phys., Paris 10 (1963) 252.

[5] MILTON, J.C.D. and FRASER, J.S., Phys. Rev. 111 (1958) 877.

[1] MAIER-LEIBNITZ, H., ARMBRUSTER, P. and SPECHT, H.J., "Prompt and delayed gamma-rays from fission", these Proceedings II.

[6] COOPERMAN, L. and ROY, R.R., Phys. Rev. 132 (1963) 371.
[7] KAPOOR, S.S. and RAMANNA, R., Phys. Rev. 133 B (1964) 598.
[8] SCHMITT, H.W., KIKER, W.E. and WILLIAMS, C.W., Phys. Rev. 137 B (1965) 837.
[9] RAU, F., Nuckleonik 5 (1963) 191.
[10] BERGQUIST, private communication.
[11] MILTON, J.C.D. and FRASER, J.S., Canad. J. Phys. 40 (1962) 1626.
[12] JOHANSSON, S.A.E., Nucl. Phys. 60 (1964) 378.

THE ANGULAR DISTRIBUTION OF GAMMA-RAYS FROM THE FISSION OF U^{235}

G. GRAFF, A. LAJTAI AND L. NAGY
CENTRAL RESEARCH INSTITUTE OF PHYSICS,
BUDAPEST, HUNGARY

Abstract — Résumé — Аннотация — Resumen

THE ANGULAR DISTRIBUTION OF GAMMA-RAYS FROM THE FISSION OF U^{235}. The angular distribution of gamma-rays from thermal-neutron-induced fission has been measured with respect to the axis of fission. The gamma radiation intensities were found to be higher in the direction of fission-fragment motion than in that normal to it. The anisotropy proved to be nearly the same for photon threshold energies of 120 keV and 600 keV.

DISTRIBUTION ANGULAIRE DES RAYONS GAMMA RÉSULTANT DE LA FISSION DE ^{235}U. Les auteurs ont mesuré la distribution angulaire des rayons gamma résultant de la fission par des neutrons thermiques, par rapport à l'axe de la fission. Ils ont observé que les intensités des rayons gamma étaient plus élevées dans la direction du mouvement des fragments de fission que dans le plan normal à cette direction. L'anisotropie s'est avérée être pratiquement la même pour les seuils d'énergie des photons de 120 keV et 600 keV.

УГЛОВОЕ РАСПРЕДЕЛЕНИЕ ГАММА-КВАНТОВ ПРИ ДЕЛЕНИИ УРАНА-235. Проведены измерения углового распределения гамма-квантов в отношении оси деления, вызванного делением тепловых нейтронов. Напряженность гамма-излучения оказалась более высокой в направлении перемещения осколка деления, чем в направлении, перпендикулярном движению. Анизотропия оказалась почти той же для пороговых энергий фотона порядка 120 и 600 кэв.

DISTRIBUCION ANGULAR DE LOS RAYOS GAMMA Y DE LOS NEUTRONES EN LA FISION DEL ^{235}U. Los autores midieron la distribución angular de los rayos gamma provenientes de la fisión inducida por neutrones, respecto al eje de fisión. Las intensidades de la radiación gamma en la dirección del movimiento de los fragmentos de la fisión, fueron mayores que en la dirección normal a aquélla. La anisotropía es aproximadamente igual para fotones de energía umbral de 120 y 600 keV.

INTRODUCTION

Study of fission-fragment behaviour, i.e. processes involved in the de-excitation of the highly excited fragments, is of great interest as it may enable an insight into the physical mechanism of nuclear fission to be obtained. The angular distribution of the prompt gamma-rays from the fission fragments measured relative to the fission axis is expected to yield information about the angular momenta of fission fragments. In the measurements performed to date [1-5], the angular distribution was found to be anisotropic. STRUTINSKI [6] assumes this to be caused by the rather high angular momenta imparted to the fission fragments by non-colinear scission. The nature of the anisotropy allows both the magnitude of fragment angular momentum and the multipolarity of the photons emitted to be inferred.

The measuring method employed in the experiments made it possible to evaluate, in addition to the angular distribution of gamma-rays, the energy distribution of the fission neutrons at various angles to the flight di-

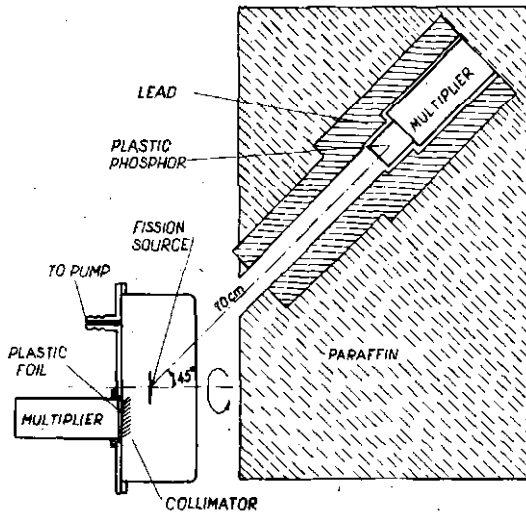

Fig. 1

Schematic diagram of the experimental arrangement

rection of fission fragments. An experiment is reported here that enabled the angular distribution of the photons emitted in thermal-neutron fission of U^{235} to be determined to a higher accuracy compared with the results of an earlier measurement [3].

EXPERIMENTAL ARRANGEMENT

The schematic diagram of the experimental setup, comprising fission as well as gamma detectors and uranium target, is given in Fig. 1. The neutron beam emerges from the reactor channel through a 4-mm wide and 45-mm high slit in a direction parallel to the plane of the fission target placed inside an aluminium vessel. The fission source enriched to about 90% in U^{235} was 50 mm in diameter and of 1 mg/cm^2 thickness. Three thin wires kept the aluminium source backing in a central position on the axis of the vessel. To reach the detector the fission fragments had to pass through a collimator consisting of thin-walled nickel tubes, 1.8 mm in diameter and 9 mm long. The distance from target to detector was selected so that the neutrons and gamma-rays from the reactor could not reach the detector directly. As this distance was about 6.5 cm, the aluminium vessel was kept at a pressure of 0.01 mm Hg. The angle between the detected fission fragments and the direction of the gamma-rays was varied by angular displacement of the vessel.

The gamma detector was placed at 70 cm from the fission source and provided with a lead and paraffin shield. As the gamma detector is in a fixed position, the gamma-rays always cross the same thickness of absorbent before reaching the detector; this method of varying the angle seems to be

preferable to turning the gamma detector. Incidentally, absorption was minimized by selecting a 0.5-mm thick wall for the vessel, which had such a large diameter that the gamma-rays caused by wall activation had to pass the lead shield to reach the detector.

Both multipliers were of 56 AVP type; the plastic phosphors mounted on the multipliers were 17 μm thick for the fission and 50 mm × 50 mm for the other detector.

The pulses from the multiplier plates were taken to a 100-ns time-to-pulse height converter, essentially similar to the device developed by GARG [7] containing, in addition, a unit for preventing the formation of double background [8]. The pulses from the converter were passed to a multichannel pulse-height analyser, the gate of which was controlled by the coincidence pulses from the dynodes. The energy response at either side could be varied by means of discriminators coupled to the dynodes. The discriminator bias for the gamma response was determined by making use of the gamma radiations from Co^{57} and Cs^{137} corresponding to about 120 keV and 600 keV threshold energies respectively. On the fission side the discriminator was biased so that on replacing the fission source with bare aluminium backing, the discriminator delivered but a negligible number of pulses compared with the fission counts. Simultaneously, the uranium alpha counts could be suppressed.

RESULTS

The intensity of gamma rays was measured at 90°, 112.5°, 135°, 157.5° and 180° to the fragment direction. At each angle up to 10^6 fission counts were taken and several runs were made to average over the errors due to various fluctuations. As an example, in Fig. 2 the pulse distributions as measured at 180° and 90° are shown. The sharp peak represents the contribution of fission gammas, and the time distribution of the neutrons appears on the left of the peak and the background is contributed by the counts falling into the channels on the right. The full width at the half maximum of the gamma peak is 4.5 ns. This width is attributable mainly to the appreciable difference in fission-fragment flight times resulting partly from energy loss in the uranium target.

The numbers of gammas, per 10^6 fission, found in the experiment at different angles, with threshold energies set to 120 keV or 600 keV, were:

	120 keV	600 keV
at 90°	448 ± 2	112 ± 1.5
at 112.5°	457 ± 2	
at 135°	470 ± 2	117 ± 1.5
at 157.5°	482 ± 2	
at 180°	478 ± 2	119 ± 1.5

A least-squares fit of these data, using for the angular distribution of the gamma rays the expression $n(\nu) \sim 1 + B \sin^2 \nu$, gives B = - 0.071 ± 0.005 at 120 keV, and B = - 0.060 ± 0.015 at 600 keV. From these the estimated values

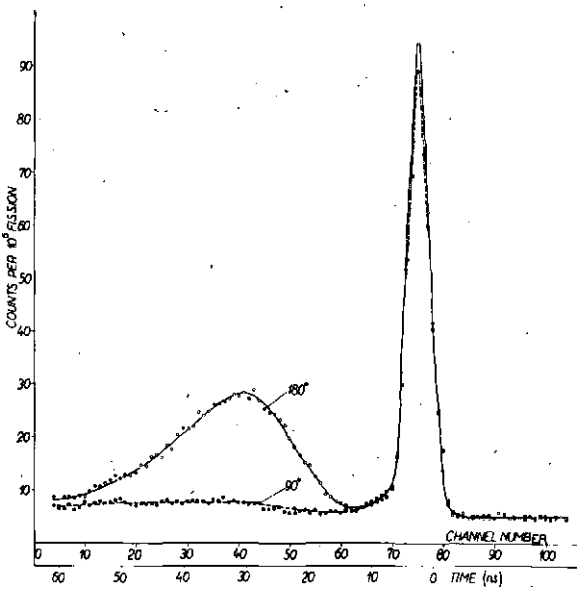

Fig. 2

Time-of-flight distribution of gamma-rays and neutrons measured at 90° and 180° to the direction of fission-fragment motion

of the anisotropy, defined by $a = [n(180°) - n(90°)] / n(90°)$, are 7.6% and 6.4% at 120 keV and 600 keV respectively.

Using the expression for the angular distribution of gamma-rays suggested by STRUTINSKI [6], $B = k_L(\hbar^2 j/IT)^2$, where I and T are the moment of inertia and fragment temperature respectively, and $k_L = 1/8$, $-3/8$ for $L = 1$/dipole/and $L = 2$ / quadrupole/. The sign of B thus obtained suggests quadrupole emission. With T = 0.4 MeV [4], and assuming fragments with average mass 120 and rigid body moment of inertia, the angular momentum j was estimated to be about 7 units.

It should be noted that in an earlier measurement [3] performed by authors, the relative intensities were found to be different from present results. The reason for this is partly that with the flight path of 50 cm chosen for the previous experiment there must have been an appreciable contribution from fission neutrons to the gamma peak, the value of which varied from angle to angle. Another source of error was the variation in multiplier gain on the fission side caused by the magnetic field upon change in multiplier position. Because of the overload on the fission side in the earlier experiment the variation in count-rate due to the variation in multiplier gain did not remain proportional in the slow and fast system. In present set of measurements various arrangements were made to prevent the fission detector from overloading. Pulse widths were reduced, very small pulses were cut off at the multiplier output and the number of gammas and fast neutrons from the reactor was decreased. Even part of these measures proved sufficient to overcome the effects of overloading.

As a final result the character of the anisotropy found in the measurement is similar to that obtained by other authors but its extent was found to be less. It was found to be almost the same at either of the threshold energies used.

REFERENCES

[1] LEACHMAN, R.B., Proc. 2nd UN Int. Conf. PUAE 15 (1958) 331.

[2] BLINOV, M.V., KAZARINOV, N.M., PROTOPOPOV, A.N. and SHIRYAYEV, B.M., Ž. eksp. teor. Fiz. 43 (1962) 1644.

[3] DÉSI, S., GRAFF, G., LAJTAI, A. and NAGY, L., Phys. Lett. 3 (1963) 343.

[4] KAPOOR, S.S. and RAMANNA, R., Phys. Rev. 133 (1964) B598.

[5] HOFFMAN, M.M., Phys Rev. 133 (1964) B714.

[6] STRUTINSKI, V.M., Ž.eksp. teor. Fiz. 37 (1959) 861.

[7] GARG, J.B., Nucl. Instrum. Meth. 6 (1960) 72.

[8] DÉSI, S., LAJTAI, A. and NAGY, L., Acta phys. Acad. Sci. hung. 15 (1962) 185.

DISCUSSION

(on the foregoing four papers)

W. GIBSON: In the paper we presented[1], attention is drawn to the decrease in the conversion electron yield per fragment that appears at high fragment masses. I should be interested to hear whether Dr. Bowman has seen a similar decrease in the conversion electron yield.

H. R. BOWMAN: We have not completed any calculations on the intensity of electrons per fragment. We do have the efficiencies and this will be something we shall be studying.

T. D. THOMAS: It has been pointed out by both Armbruster and Maier-Leibnitz that angular distribution intensities have to be corrected for the motion of the fragments. Since the anisotropy reported by Dr. Nagy is approximately the same as this effect, I should like to know whether this correction has been made in his data.

L. NAGY: No, the correction has not been made. By applying the correction, the anisotopy will be increased.

M. S. MOORE: Would anyone care to comment on what one might expect the orbital angular momentum between the fragments to be?

H. MAIER-LEIBNITZ: Something like 10, since the saw-tooth curve seems to indicate that one fragment may have much more spin than the other.

W. SWIATECKI: There are estimates of the angular momentum of fission fragments in the literature. Estimates have been made by several authors, including Hoffman and, recently, Nix, who has calculated the average angular momentum and the distribution around the average. Nix used a simplified version of the liquid drop model.

L. E. GLENDENIN: I should like to comment on the emission of K-X-rays by fission fragments in the region of deformed nuclei. It has been suggested by Vandenbosch that the decrease in K-X-ray yield found experimentally for $Z > 60$ and $A > 156$ is caused by the drop in the $K/_{L+M}$ conversion ratio for the low-energy (~ 70 keV) transition from the first excited rotational level to the ground level typical of this region. Calculations of the K-X-ray yield for this transition in the primary-fission products of Cf^{252} are indeed in qualitative agreement with the experimental yield curve (see Fig. 5 of my paper[2]) but the values are too low by a factor of about 3. This may indicate the existence of other low-energy transitions of this type at higher levels of the excited fission fragment. We still have no explanation, however, for Thomas' observations that the yield of higher-energy conversion electrons (>100 keV) as a function of fragment mass is similar to that of the K-X-rays.

T. D. THOMAS: In order to get quantitative agreement between the calculated number of K-X-rays and the measured number, Glendenin assumes contributions from higher members of the rotational bands. The internal

---

[1] THOMAS, T. D., ATNEOSEN, R. A., GIBSON, W. M. and PERLMAN, M. L., "X-rays emitted in coincidence with the fission of Cf^{252}", these Proceedings I.

[2] GLENDENIN, L. E., UNIK, J. P. and GRIFFIN, H. C., "Determination of the primary nuclear charge of fission fragments from their characteristic K-X-ray emission in spontaneous fission of Cf^{252}", these Proceedings I.

conversion of these transitions could provide the high-energy electrons seen in our experiments.

L. E. GLENDENIN: There is not enough K-conversion in the higher-energy transitions among the higher rotational levels to account for the observed K-X-ray yields.

S. S. KAPOOR: I think that the energies of the first 2^+ state have to be accurately known in order to interpret the X-ray-yield variations with mass. The values obtained by extrapolation to these neutron-rich nuclei are only rough estimates.

P. ARMBRUSTER: If the L-conversion probability is large compared with γ-emission ($\alpha_L > 1$) and if K-conversion does not contribute to the decay of a low-lying state, you should find a drop in the K-X-ray intensity but not in the electron intensity. Has the contribution of L-conversion been taken into account in your new calculation?

L. E. GLENDENIN: The electrons from L-conversion of the transition from the lowest rotational level are too low in energy ($\lesssim$ 60 keV) to be observed in the conversion electron experiments.

Review Paper

DELAYED NEUTRONS AND PHOTONEUTRONS FROM FISSION PRODUCTS

S. AMIEL
SOREQ NUCLEAR RESEARCH CENTRE,
ATOMIC ENERGY COMMISSION, YAVNE, ISRAEL

Abstract — Résumé — Аннотация — Resumen

DELAYED NEUTRONS AND PHOTONEUTRONS FROM FISSION PRODUCTS. Delayed neutrons: Most studies of the delayed neutrons from fission have involved analysis of the kinetic behaviour of fission chain-reacting systems, analysis of the gross neutron decay (resolved into six groups with approximate half-lives of 0.2, 0.5, 2, 6, 22 and 55 s) and some measurements of the neutron spectra (the energies extend from 0.1 to 1.2 MeV, peaking in the range 0.2 to 0.5 MeV). Rapid separations of fission-produced halogens have indicated seven isotopes ($Br^{87,88,89,90}$ and $I^{137,138,139}$), and rare gas analysis has indicated 1.5-s Kr and 6-s Rb as definite delayed neutron precursors. These identified precursors account for some 80% of the total delayed neutron yields.

Theoretical predictions of possible precursors point to a few tens of such nuclides to be found mainly in regions just above closed neutron shells. Total neutron yields are observed to increase with mass number and decrease with atomic number of the fissioning nuclide. Yields are nearly independent of the energy of the incident fissioning neutron at energies up to several MeV. In this range observed group yields, especially of the long-lived precursors, are in fairly good agreement with fission mass and charge distributions, and calculated neutron emission probabilities.

Further detailed studies of delayed neutron precursors (particularly in the difficult short half-life region) require development of ultra-fast radiochemical separation procedures (or on-line isotope separation) and fast neutron spectroscopy of high resolution and efficiency.

Photoneutrons: A knowledge of the intensities and gamma-ray spectra of fission products is of practical importance in reactor technology, particularly with respect to gamma heating, shielding and radiation effects. Gamma-rays of energies greater than 2.23 and 1.67 MeV cause emission of photoneutrons from deuterium and beryllium respectively, and are important in the kinetics of heavy water and beryllium-moderated reactors.

The rate of photoneutron emission after fission represents the composite decay of the corresponding gamma-ray-emitting nuclides in the mixture of fission product chains. The gross photoneutron decay curves from both D_2O and beryllium have been resolved into nine groups with half-lives ranging from a few seconds to ~13 d. Each of these groups represents a complex composite of nuclides. Detailed information on the constituents of these groups is important for reactors in which fission products fractionation may take place and affect relative group abundances. Such information exists only for the longer-lived fission products whose properties and yields are well known, and where experimental results are in agreement with calculated values based on fission mass and charge distributions and decay schemes. The characterization of individual nuclides in the more complex short-lived groups is indeed a formidable task, but this information is of considerable practical and theoretical importance, and warrants further extensive study.

NEUTRONS RETARDÉS ET PHOTONEUTRONS ÉMIS PAR DES PRODUITS DE FISSION. Neutrons retardés: La plupart des études sur les neutrons retardés émis par des produits de fission impliquent l'analyse du comportement cinétique des systèmes qui subissent une réaction de fission en chaîne, l'analyse de la désintégration totale des neutrons (se résolvant en six groupes avec des périodes d'environ 0,2, 0,5, 2, 6, 22 et 55 s) et certaines mesures des spectres de neutrons — ayant une énergie comprise entre 0,1 et 1,2 MeV, avec des pics dans la gamme de 0,2 à 0,5 MeV. Des séparations rapides des halogènes produits par fission ont mis en évidence la présence de sept isotopes ($^{87,88,89,90}Br$ et $^{137,138,139}I$), et le dosage des gaz rares a permis d'identifier Kr (1,5 s) et Rb (6 s) comme précurseurs de neutrons retardés. Environ 80% des rendements totaux en neutrons retardés doivent être attribués aux précurseurs ainsi identifiés.

A la suite de recherches théoriques, quelques dizaines de ces nucléides ont été identifiés comme précurseurs possibles; ils se trouvent situés pour la plupart immédiatement au-dessus des couches neutroniques saturées. On constate que les rendements totaux en neutrons augmentent avec le nombre de masse du nucléide

qui subit la fission et décroissent avec son numéro atomique. Les rendements sont presque indépendants de l'énergie du neutron incident provoquant la fission, jusqu'à une énergie de plusieurs MeV. Dans cette gamme d'énergie, les rendements par groupes observés, en particulier ceux des précurseurs à période longue, sont en assez bon accord avec les distributions selon la masse et selon la charge et avec les probabilités calculées d'émission de neutrons.

Pour étudier de manière plus détaillée les précurseurs de neutrons retardés – en particulier dans la région difficile des périodes courtes – il faudrait mettre au point des méthodes ultra-rapides de séparation radiochimique – ou de séparation des isotopes suivie de détection immédiate – et une technique de spectroscopie des neutrons rapides à fort pouvoir de résolution et rendement élevé.

Photoneutrons: Il est particulièrement important de connaître les intensités et les spectres des rayons gamma des produits de fission dans la technologie des réacteurs, en particulier pour ce qui est de l'échauffement dû aux rayons gamma, des protections et des effets des rayonnements. Les rayons gamma ayant une énergie supérieure à 2,23 et 1,67 MeV provoquent l'émission de photoneutrons par le deutérium et le béryllium, respectivement, et jouent un rôle important dans la cinétique des réacteurs ralentis à l'eau lourde et au béryllium.

L'émission de photoneutrons consécutive à la fission est due à la décroissance de tous les nucléides émetteurs gamma présents dans le mélange des séries radioactives issues des produits de fission. Les courbes totales de décroissance des photoneutrons émis par D_2O et Be se résolvent en neuf groupes et les périodes s'échelonnent entre quelques secondes et 13 j environ. Chacun de ces groupes correspond à un ensemble complexe de nucléides. Il est important de disposer de données détaillées sur les constituants de ces groupes pour les réacteurs dans lesquels il peut se produire un fractionnement de la fission qui peut modifier les abondances relatives des groupes. Ces données n'existent que pour les produits de fission à longue période dont les propriétés et les rendements sont bien connus; les résultats expérimentaux concordent avec les valeurs obtenues à partir des distributions selon la masse et la charge et des schémas de désintégration. L'identification des différents nucléides appartenant aux groupes à courte période, plus complexes, présente des difficultés considérables, mais étant donné l'importance de ces données du point de vue tant pratique que théorique, il serait justifié de poursuivre des études approfondies à ce sujet.

ЗАПАЗДЫВАЮЩИЕ НЕЙТРОНЫ И ФОТОНЕЙТРОНЫ ПРОДУКТОВ ДЕЛЕНИЯ. Запаздывающие нейтроны. Большая часть работ по запаздывающим нейтронам деления связана с проведением анализа кинетического поведения систем цепной реакции деления, с анализом общего распада нейтронов (распадающихся на 6 групп с приблизительными периодами полураспада 0,2; 0,5; 2; 6; 22 и 55 сек) и с некоторыми измерениями нейтронных спектров (энергии в пределах от 0,1 до 1,2 Мэв с максимумом в диапазонах 0,2–0,5 Мэв). Быстрое отделение галогенов, образовавшихся в результате деления, указывает на наличие 7 изотопов (бром-87, 88, 89, 90 и йод-137, 138, 139), а анализ инертного газа указывает на наличие криптона (1,5 сек) и рубидия (6 сек) как определенных предшественников запаздывающих нейтронов. Эти предшественники и объясняют наличие около 80% общего выхода запаздывающих нейтронов.

Теоретические предсказания возможных предшественников указывают на несколько десятков подобных нуклидов, которые должны находиться главным образом в областях, находящихся как раз над закрытыми оболочками нейтронов. Обнаружено, что общий выход нейтронов увеличивается вместе с массовым числом и уменьшается вместе с атомным числом делящихся нуклидов. Эти выходы почти независимы от энергии бомбардирующих делящихся нейтронов при энергиях до нескольких Мэв. В этом диапазоне выходы наблюдаемой группы, особенно группы долгоживущих предшественников, достаточно хорошо согласуются с массой деления и распределениями заряда, а также с расчетной вероятностью испускания нейтронов.

Дальнейшее детальное исследование предшественников запаздывающих нейтронов (в частности, в трудной области короткого периода полураспада) требует усовершенствования методов сверхбыстрого радиохимического отделения предшественников (или изотопного разделения на линии), а также быстрой нейтронной спектроскопии с высокой разрешающей способностью и эффективностью.

Фотонейтроны. Знание интенсивности и спектров гамма-лучей продуктов деления имеет большое практическое значение в реакторной технике, в частности, что касается эффектов нагревания гамма-лучами, экранирования и радиации. Гамма-лучи с энергией, большей чем 2,23 и 1,67 Мэв, являются причиной эмиссии фотонейтронов из дейтерия и бериллия соответственно и очень важны для изучения кинетики тяжеловодных реакторов с замедлителем из бериллия.

Интенсивность испускания фотонейтронов после деления представляет собой сложный распад соответствующих нуклидов, испускающих гамма-лучи в смеси из цепочки продуктов деления. Общие кривые распада фотонейтронов из D_2O и Be были разделены на 9 групп с периодом полураспада в диапазоне от нескольких секунд до приблизительно 13 дней. Каждая из этих групп представляет собой сложный состав нуклидов. Детальная информация относительно компонентов этих групп очень важна для тех реакторов, в которых может иметь место фракционированное деление, влияющее на относительную групповую распространенность. Подобная информация существует только в отношении долгоживущих продуктов деления, характеристики и выход которых хорошо известны, и результаты экспериментов согласуются с расчетными значениями, основанными на распределении массы и заряда деления и схемах распада. Характеристика отдельных нуклидов в более сложных короткоживущих группах является действительно большой задачей, но эти данные имеют большое практическое и теоретическое значение и заслуживают дальнейшего широкого изучения.

NEUTRONES RETARDADOS Y FOTONEUTRONES DE LOS PRODUCTOS DE FISION. Neutrones retardados: La mayoría de los estudios realizados sobre los neutrones retardados emitidos en el proceso de fisión han entrañado el análisis del comportamiento cinético de los sistemas de fisiones en cadena, el análisis de la desintegración neutrónica total (resuelta en 6 grupos con períodos del orden de 0,2, 0,5, 2, 6, 22 y 55 s), y algunas mediciones de los espectros neutrónicos (extendiéndose la gama de energías de 0,1 a 1,2 MeV, con el valor máximo en el intervalo de 0,2-0,5 MeV). La separación rápida de los halógenos producidos por fisión ha señalado a 7 isótopos ($^{87, 88, 89}$ y ^{90}Br, y $^{137, 138}$ y ^{139}I) como precursores de neutrones retardados, y el análisis de los gases nobles ha permitido determinar otros dos, a saber, el Kr con período de 1,5 s, y el Rb de 6 s. A estos precursores identificados, corresponde el 80% aproximadamente de los rendimientos totales de neutrones retardados.

Las predicciones teóricas de los posibles precursores señalan que en las regiones que siguen inmediatamente a las capas neutrónicas completas han de encontrarse unas cuantas decenas de tales núclidos. Se ha observado que los rendimientos neutrónicos totales aumentan con el número másico y disminuyen con el número atómico del núclido que sufre la fisión. Estos rendimientos son prácticamente independientes de la energía del neutrón incidente para energías de hasta varios MeV. En este intervalo de energías, los rendimientos de grupo observados, en particular en el caso de precursores de período largo, concuerdan bastante satisfactoriamente con las distribuciones másicas y de cargas de la fisión y con las probabilidades de emisión neutrónica calculadas.

Para poder realizar estudios más detallados de los precursores de neutrones retardados (en particular en la difícil región de los de período corto) se han de perfeccionar métodos de separación radioquímica ultrarrápida (o de separación con recuento simultáneo), y de espectroscopia de neutrones rápidos de poder de resolución y rendimiento elevados.

Fotoneutrones: El conocimiento de los espectros gamma y de los productos de fisión reviste importancia de orden práctico, en tecnología de los reactores, particularmente en lo que respecta al calentamiento gamma, el blindaje y los efectos de las radiaciones. Los rayos gamma de energías superiores a 2,23 MeV y a 1,67 MeV provocan la emisión de fotoneutrones por el deuterio y el berilio, respectivamente, y se han de tener muy en cuenta en los cálculos de cinética de los reactores moderados por agua pesada y por berilio.

El índice de emisión de los fotoneutrones después de la fisión representa la desintegración combinada de los correspondientes núclidos emisores de rayos gamma en la mezcla de cadenas de productos de fisión. Las curvas globales de desintegración fotoneutrónica tanto del D_2O como del Be se han resuelto en 9 grupos con períodos que abarcan de unos pocos segundos a 13 d, aproximadamente. Cada uno de estos grupos representa un conjunto complejo de núclidos. La información detallada sobre los elementos constitutivos de estos grupos tiene importancia en el caso de reactores en los que puede tener lugar un fraccionamiento de la fisión, e influye en la abundancia relativa de los grupos. De esa información se dispone sólo respecto de los productos de fisión de período más largo, cuyas propiedades y rendimientos son bien conocidos; los resultados experimentales concuerdan con los valores calculados partiendo de las distribuciones másicas y de las cargas y de los esquemas de desintegración. La caracterización de los diversos núclidos pertenecientes a los grupos más complejos, de período corto, constituye realmente una labor formidable, pero se estima que esta información posee considerable importancia tanto práctica como teórica, y que merece ser estudiada de una manera más completa.

DELAYED NEUTRONS

Introduction

A number of radioactive nuclides formed in fission are known to emit neutrons in the course of their decay. The neutron emission is a small fraction of the total fission product decay and the half-lives of the corresponding emitters are short, ranging from a fraction of 1 s to just under 1 min. These nuclides, known as delayed neutron precursors, are neutron-rich nuclides, having a few neutrons in excess of a closed-shell configuration; if they decay by beta-ray emission to an excited state of the daughter with an energy in excess of the binding energy of a neutron, de-excitation by neutron emission is energetically possible. Neutron emission from the excited daughter nucleus (the neutron emitter) is then an instantaneous process, and its rate is determined by the decay of the precursor. A schematic representation of the delayed-neutron emission process is given in Fig. 1.

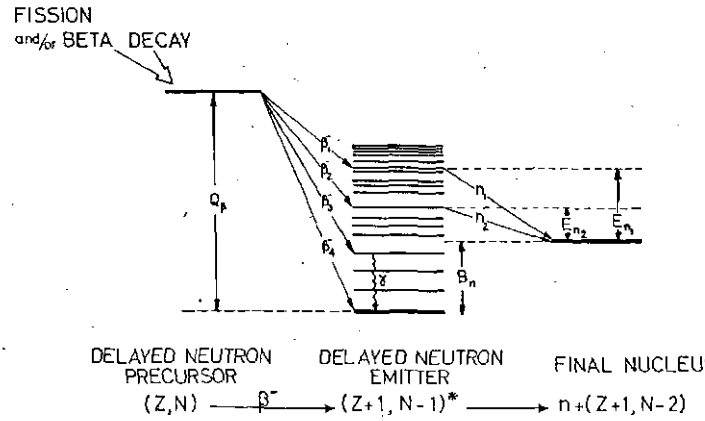

Fig. 1

Schematic representation of delayed-neutron emission

The phenomenon of delayed-neutron emission was first observed by ROBERTS et al. in 1939 and was interpreted immediately by Bohr and Wheeler. Numerous subsequent investigations were directed towards the measurement of the gross properties of delayed-neutron emission in fission products, viz. the half-lives, yields and energies as a function of the fissioning nuclide and type and energy of fission. In parallel and somewhat later, radiochemical investigations were aimed at identifying and characterizing individual delayed-neutron precursors. A major part of the interest in these investigations lies in the great importance of delayed neutrons in the kinetic behaviour and control of fission chain reactors. From another angle it is of fundamental importance to determine the formation and the nuclear properties of the neutron-rich nuclides produced in fission, especially above closed shells, where neutron emission is a possible mode of decay.

In recent years, several reviews were published on delayed neutrons in fission, notably those of KEEPIN [1, 2], and just recently KEEPIN has pre-

pared a thorough compilation of the information available on the subject until 1964 [3].

Gross decay measurements

Gross measurements of the composite decay, i.e. decay rates and group abundances, have been made by irradiation of the fissionable nuclide with particles of appropriate energy, followed by rapid transfer of the sample and measurement of the neutron emission with a flat response neutron detector (usually an array of BF_3 counters in paraffin). Measurements have been made on various fissionable nuclides, ranging from Th^{232} to Cf^{252}, using either spontaneous fission sources or irradiating fluxes of thermal neutrons, fission spectrum neutrons, neutrons at different energies obtained from accelerators, or energetic gamma rays.

The most comprehensive and detailed measurements of gross decay rates, group half-lives and group abundances of delayed neutrons were carried out at Los Alamos by KEEPIN et al. [4] for thermal and fast fission of thorium, uranium and plutonium isotopes. By using short neutron bursts as well as long irradiations to saturation, these authors were able to resolve the multi-component neutron decay by iterative least-squares analysis with a computer. Six exponential components were found to yield the best results. Despite a striking similarity between the delayed-neutron group half-lives of the various fissionable nuclides at various energies, the respective values are yet distinctly different. On the other hand, group abundances vary considerably from nuclide to nuclide. Table I shows some of these results. Figure 2 presents measured values of total delayed-neutron yields (i.e. the total number of delayed neutrons emitted per fission, in percentages) for different fissionable nuclides, as observed in spontaneous fission and neutron- and gamma-induced fission. A regularity is observed: the yield increases with mass number within an isotopic series and diminishes with increasing atomic number of the fissioning nuclide. The effect of varying the energy of the fission-inducing neutrons on the total and individual group yields was studied by MAKSIUTENKO [5] and others and is demonstrated in Fig. 3. The yields are nearly independent of the energy of the incident fissioning neutron up to energies of several MeV (measured up to ~3.5 MeV), but they are considerably higher at 14-15 MeV.

Inspecting the individual group yields from various fissionable nuclides at two incident neutron energy ranges (Fig. 4) one observes that the relative group abundances within each energy range are in general similar for the two ranges, with a systematic increase of yield at the higher energy. Figure 5 shows the individual group yields for isotopes of uranium and plutonium. A sharp increase of all the individual yields with mass number is seen for group numbers 2 and above, while the yield of the first group is constant for uranium and drops somewhat for plutonium.

The information on delayed neutrons in photofission is only fragmentary, and the data rather poor because of low accelerator bremsstrahlung intensities and low fission yields. Total delayed-neutron yields in the photofission of Th^{232} and U^{238} are constant in the range of E_γ = 12 to 20 MeV [6] and the composite decay follows the six-group classification, the corresponding-

TABLE I

DELAYED-NEUTRON HALF-LIVES AND YIELDS*

	Fast fission			Thermal fission		
Group No.	Half-life (s)	Relative abundance	Total yield (n/F)	Half-life (s)	Relative abundance	Total yield (n/F)
U^{235}						
1	54.51 ± 0.94	0.038 ± 0.003		55.72 ± 1.28	0.033 ± 0.003	
2	21.84 ± 0.54	0.213 ± 0.005		22.72 ± 0.71	0.219 ± 0.009	
3	6.00 ± 0.17	0.188 ± 0.016	0.0165	6.22 ± 0.23	0.196 ± 0.022	0.0158
4	2.23 ± 0.06	0.407 ± 0.007	± 0.0005	2.30 ± 0.09	0.395 ± 0.011	± 0.0005
5	0.496 ± 0.029	0.128 ± 0.008		0.610 ± 0.083	0.115 ± 0.009	
6	0.179 ± 0.017	0.026 ± 0.003		0.230 ± 0.025	0.042 ± 0.008	
U^{238}						
1	52.38 ± 1.29	0.013 ± 0.001				
2	21.58 ± 0.39	0.137 ± 0.002				
3	5.00 ± 0.19	0.162 ± 0.020	0.0412			
4	1.93 ± 0.07	0.388 ± 0.012	± 0.0017			
5	0.490 ± 0.023	0.225 ± 0.013				
6	0.172 ± 0.009	0.075 ± 0.005				

TABLE I (cont.)

	Fast fission			Thermal fission		
Group No.	Half-life (s)	Relative abundance	Total yield (n/F)	Half-life (s)	Relative abundance	Total yield (n/F)
Pu^{239}						
1	53.75 ± 0.95	0.038 ± 0.003		54.28 ± 2.34	0.035 ± 0.009	
2	22.29 ± 0.36	0.280 ± 0.004		23.04 ± 1.67	0.298 ± 0.035	
3	5.19 ± 0.12	0.216 ± 0.018	0.0063	5.60 ± 0.40	0.211 ± 0.048	0.0061
4	2.09 ± 0.08	0.328 ± 0.010	± 0.0003	2.13 ± 0.24	0.326 ± 0.033	± 0.0003
5	0.549 ± 0.049	0.103 ± 0.009		0.618 ± 0.213	0.086 ± 0.029	
6	0.216 ± 0.017	0.035 ± 0.005		0.257 ± 0.045	0.044 ± 0.016	
Pu^{240}						
1	53.56 ± 1.21	0.028 ± 0.003				
2	22.14 ± 0.38	0.273 ± 0.004				
3	5.14 ± 0.42	0.192 ± 0.053	0.0088			
4	2.08 ± 0.19	0.350 ± 0.020	± 0.0006			
5	0.511 ± 0.077	0.128 ± 0.018				
6	0.172 ± 0.033	0.029 ± 0.006				

* from KEEPIN et al., Phys. Rev. 107 (1957) 1044

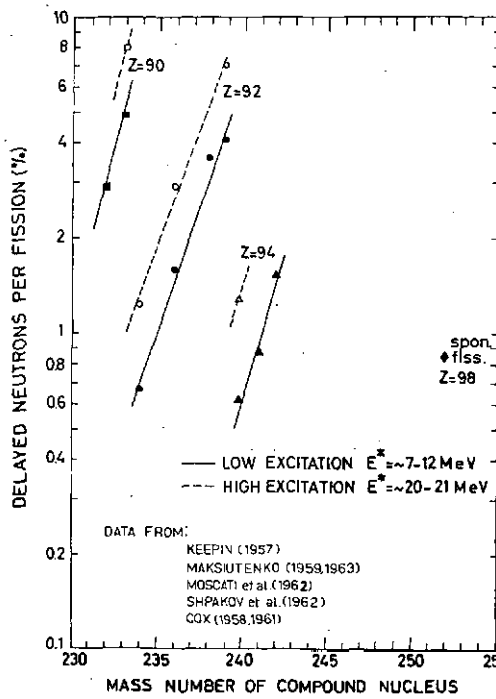

Fig. 2

Absolute total delayed-neutron yields for fission of different nuclides

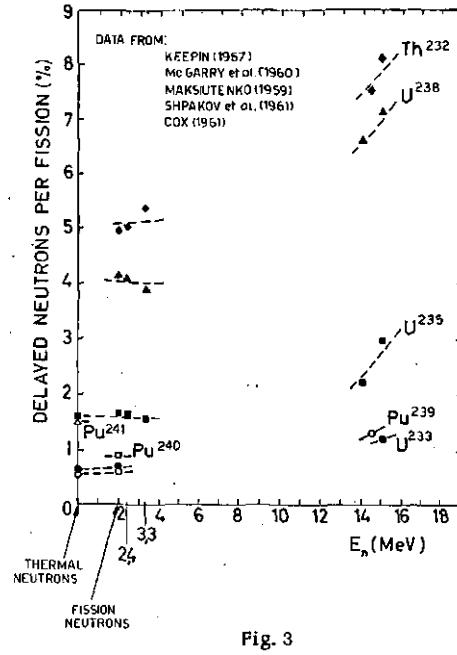

Fig. 3

Variation of total delayed-neutron yields with energy of fissioning neutrons

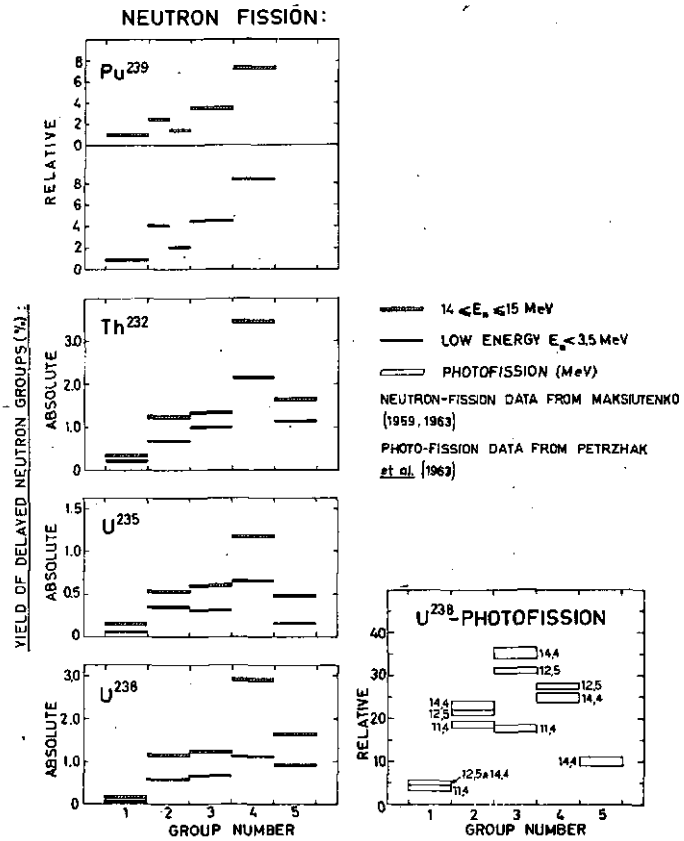

Fig. 4

Individual delayed-neutron group yields from various fissionable nuclides

half-lives and relative abundances being generally similar to those observed in neutron-induced fission (see Fig. 4) [7].

Delayed-neutron precursors from the spontaneous fission of Cf^{252}, collected by recoil on to a pneumatically operated catcher, were found to consist of only three groups, with half-lives of 20, 2.0 and 0.5 s and neutron yields in the range 0.22 to 0.35% [8].

A search for delayed-neutron precursors among the products of the fission of elements of $Z < 90$ in high energy (> 300 MeV) interactions has yielded negative results; only light element delayed-neutron precursors (Li^9, C^{16} and N^{17}) produced by spallations were observed [9]. Positive results were obtained, however, from fission of nuclides of $Z \geq 90$, irradiated with high energy protons. The absence of fission-produced delayed-neutron precursors in the first case is probably because in these elements the high-energy symmetrical fission, which takes place after the prompt cascade and evaporation stages, yields products on the neutron deficient side or near the stability line of nuclides, where delayed-neutron emission is not possible, as will be discussed later. In the second case, the low fission barrier of

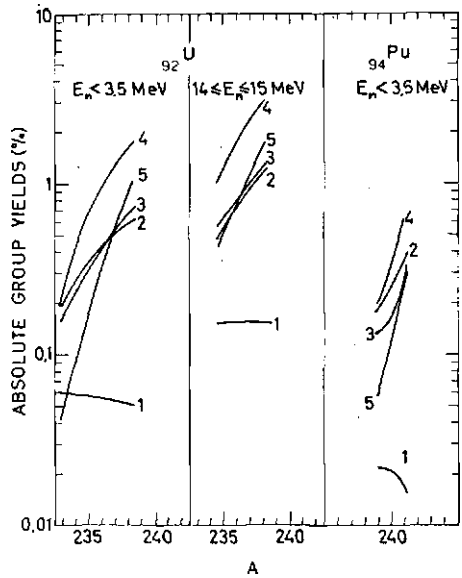

DATA FROM: KEEPIN(1957), COX(1961), MAKSIUTENKO(1959,1963).

Fig. 5

Absolute individual delayed-neutron group yields for isotopes of uranium and plutonium

the commonly known fissionable elements allows de-excitation by asymmetric fission from low residual excitation energies after the prompt processes have taken place; and this permits the formation of the expected delayed-neutron precursor.

Energies of delayed neutrons

For practical reasons most neutron energy measurements so far have been aimed at obtaining mean energy values. Experiments to obtain spectra were subject to poor resolution and yielded only coarse distribution patterns. Measurements of delayed neutrons from thermal fission of U^{235} were made with a He^3 spectrometer by BATCHELOR and HYDER [10], who used various irradiation and decay times to emphasize individual groups while suppressing the others. The results were processed by iterative subtraction, using the six group classification, and gave the spectra shown in Fig.6. Cloud chamber measurements of the fourth group were in general agreement with He^3 spectrometer measurements [11]. In both cases resolutions were ~10% or worse, and therefore did not disclose any fine structure or distinct peaks in the spectra. However, in addition to mean energies, the results give an idea of the high-energy tail (e.g. the results of BONNER et al. [11] suggest an end point at ~3.5 MeV for the fourth group neutrons).

KEEPIN [3] suggests a correlation between the average energies of the neutrons and the average fission chain length, since longer chains consisting mainly of nuclides farther from the stability line, have larger β-decay energies and greater energy excess, $Q_\beta - B_n$, available to the delayed neutrons.

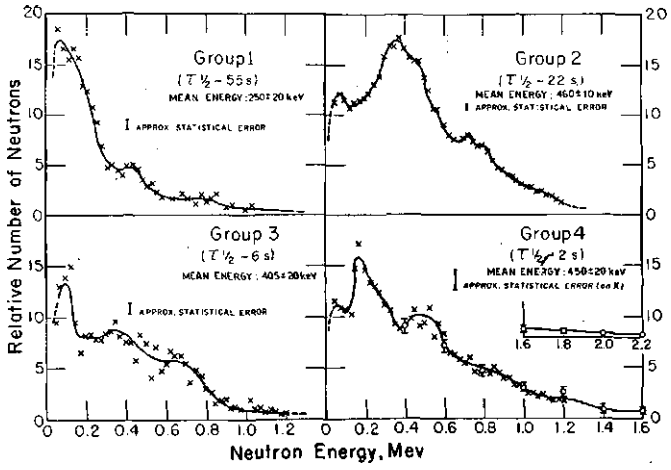

(x) He^3 spectrometer data of BATCHELOR and HYDER (1956)
(o) Cloud chamber data of BONNER et al. (1956)

Fig. 6

Measured delayed-neutron group spectra (from thermal fission of U^{235})

The observed neutron spectra, being of a continuous form, have led several investigators to suggest that there is a continuum of levels above the energy B_n in the excited intermediate. On the basis of this assumption neutron emission probabilities have been calculated. However, with the present lack of sufficiently precise data and good resolution, these conclusions may be premature. Improved energy measurements of the individual groups and of separated precursors is a prerequisite for clarifying the decay characteristics of both the delayed-neutron precursors and the emitters. Such measurements must further be complemented by a study of the other de-excitation modes to obtain detailed decay schemes, etc.

Identification of delayed-neutron precursors

Radiochemical separation and identification of the precursors requires very rapid techniques, a problem which becomes greatly intensified as the half-lives of the nuclides involved become shorter than ~1/2 min and separation may be possible only with volatile elements where the specificity of separation and transport are exceptionally good.

Heavy bromine and iodine isotopes were identified in early experiments as delayed-neutron precursors, using rapid chemical separations and recoil range techniques (Snell, Sugarman and others, 1947-53). The most detailed investigation of the halogens was that performed by PERLOW and STEHNEY [12] who used gas-flow techniques to separate bromine and iodine individually from the thermal fission of U^{235}. Their results are given in Table II, and show that at least three of the reported groups are composites. These authors also determined the presence of delayed neutrons in separated fission-produced rare gases [13]. On the basis of reported half-lives they assigned a ~1.5-s activity to Kr^{92-94} and a 6-s activity (growing in from a 2-s krypton parent) to Rb^{92-93}. The yields of these nuclides in the thermal

TABLE II

IDENTIFIED HALOGEN DELAYED-NEUTRON PRECURSORS
(from PERLOW and STEHNEY (1959))

Element	$T_{\frac{1}{2}}$ (s)	Isotope	Relative neutron yield (at saturation)
Bromine	54.5	Br^{87}	0.37 ± 0.08
	16.3 ± 0.8	Br^{88}	1.00
	4.4 ± 0.5	Br^{89}	1.9 ± 0.4
	1.6 ± 0.6	Br^{90}	1.5 ± 0.6
Iodine	24.4 ± 0.4	I^{137}	1.00
	6.3 ± 0.7	I^{138}	0.47 ± 0.05
	2.0 ± 0.5	I^{139}	0.38 ± 0.05

fission of U^{235} were $\sim 7 \times 10^{-3}$% and $\sim 1 \times 10^{-3}$% respectively, which together amounts to ~ 0.5% of the total delayed neutrons.

Diffusion experiments (COWAN and ORTH [14]) indicated that ~ 80% or more of the delayed-neutron activity of uranium arises from bromine and iodine (a conclusion based on the observed diffusion rates). Gas trapping experiments performed on the samples after diffusion also excluded significant contributions from rare gas precursors and daughter products of rare gases.

Attempts to detect delayed-neutron emission from fission product antimony were made by several investigators, but so far results have been negative (e.g. [15]). Preliminary positive results reported from our laboratory indicated ~10-s low abundance delayed-neutron activity from a rapidly separated halogen-free fission product mixture, but no assignment was made [16].

The nuclear properties of the individual delayed-neutron precursors are quite obscure, and very little has been reported. Of great importance are P(n) values, the neutron branching ratios. ARON et al. [17] measured these values directly (by counting the neutrons and betas) for halogens separated from 14-MeV neutron fission of U^{238} and Th^{232}. The experimental results are included in Table III. Previous investigations were interfered with, especially when measuring B^{87}, by the Br^{86}, which has the same $T_{1/2}$, and only recently was Br^{86} identified, characterized and ruled out as a delayed-neutron precursor [18].

Practical aspects of delayed-neutron emission

The major practical importance of delayed neutrons is in reactor control, since the prompt neutron generation time is too short for safe regulation of a controlled chain reaction. Detailed reactor kinetic calculations require accurate values of the delayed-neutron fractions and periods as well as a

knowledge of the relative effectiveness of the delayed neutrons in causing fission [19]. A problem of particular importance concerns the possible loss of delayed-neutron reactivity in advanced design reactors that are meant to operate at temperatures greater than 2000°C [14].

A practical application of delayed-neutron emission is its use for analysis of fissionable nuclides; thus the isotopic composition of uranium, thorium, plutonium, etc. can be determined rapidly and non-destructively with high sensitivity and precision [20].

Basic considerations and predictions of delayed-neutron phenomena

Figure 1 illustrates the process of delayed-neutron emission; neutron emission is possible only when $Q_\beta - E_{\beta i} = E_i \geq B_n$ for the β-transition from the precursor (Z, N) to the emitter (Z+1, N−1). Because of the effect of closed-neutron shells in lowering the binding energy of extra neutrons, it was generally assumed that delayed-neutron emission is a phenomenon associated with nuclides having a few neutrons in excess of N = 50 and 82, which are the closed shells present at the peaks of the mass distribution in fission.

A more fundamental treatment for the probability of delayed-neutron emission, P(n), (= the ratio of delayed-neutron yield to the cumulative fission yield of the precursor) was given by PAPPAS [21, 22] and KEEPIN [23], using β-decay theory. P(n) is given by

$$P(n) = \int_{B_n}^{Q_\beta} f(Z+1, Q_\beta - E)\omega(E)\frac{\Gamma_n}{\Gamma_n + \Gamma_\gamma}\, dE \Big/ \int_{B_n}^{Q_\beta} f(Z+1, Q_\beta - E)\omega(E)dE$$

where: $f(Z+1, Q_\beta - E)$ is the Fermi function, giving the Z and E dependence of the transition; $\omega(E)$ is the density of levels in the intermediate nuclide excited to an energy E; $\Gamma_n \Gamma_\gamma$ are the partial widths for neutron and gamma-ray emission; P(n) is a value expected to be constant and characteristic for each precursor independent of the latter's origin.

Using the above formula, and introducing certain assumptions[1], Keepin and Pappas calculated neutron emission probabilities, from which they predicted a systematics of possible delayed-neutron precursors among fission products. These predictions were sorted out by additional criteria of suitable half-lives and fission yields to interpret experimental observations[2]. Figure 7 shows KEEPIN's predictions [23] together with the already identified precursors. One can see that the process most likely to produce

[1] These were: (i) Averaging the values of the matrix elements for the β transition; (ii) using an approximate level density formula based on the statistical model, although the regions concerned are below the applicability of this model and shell effects are pronounced; (iii) assuming $\Gamma_n/(\Gamma_n+\Gamma_\gamma)=1$ for $E_n \geq 50$ keV for neutrons of orbital angular momentum of $\ell = 0, 1$; (iv) averaging angular momentum and parity effects; (v) using predicted nuclear masses.

[2] Pappas introduced a term, $Z_N - Z$, for the distance from stability (where Z_N is the most stable Z for the neutron number N). P(n) increases with $(Z_N - Z)$, and the minimum value of this term for a nuclide to show delayed-neutron characteristics is 5 - 6 for odd Z and 7 - 8 for even Z nuclides of N ≥ 52 and ≥ 84.

TABLE III

COMPARISON BETWEEN CALCULATED AND EXPERIMENTAL DELAYED-NEUTRON YIELDS USING EXPERIMENTAL P_n VALUES

Group No.	Delayed-neutron precursors	Absolute chain yield (%)	Z_p	Fractional cumulative yield of precursors	Absolute yield of precursors (%)	Experimental delayed-neutron emission probability: P_n Aron et al. (1964)	Absolute yield of delayed-neutron precursors: Calculated [b] individual	Calculated [b] total	Experimental: Keepin (1957) 6 periods	Experimental: Keepin (1964) 9 periods analysis	Experimental: Maksiutenko (1958, 1963)	Ratio *
U^{235} thermal fission												
1	55 s $_{35}Br^{87}$	2.5	34.52	0.95	2.37	0.031	0.073	0.073	0.052	0.058	0.062	0.80
2	16 s $_{35}Br^{88}$	3.55	34.91	0.84	2.98	0.06	0.179	0.299	0.346	0.382	0.387	1.28
	24 s $_{53}I^{137}$	6.15	53.26	0.65	3.99	0.03	0.120					
3	4.5 s $_{35}Br^{89}$	4.70	35.42	0.56	2.63	0.07	0.184	0.254	0.310	0.390	0.326	1.54
	6.3 s $_{53}I^{138}$	6.65	53.45	0.53	3.52	0.02	0.070					
4	1.6 s $_{35}Br^{90}$	5.75	35.84	0.31	1.78	≤0.1 [a]	≤0.178	≤0.378	0.624	0.511	0.660	1.35
	2.0 s $_{53}I^{139}$	6.40	53.82	0.31	1.98	≤0.1 [a]	≤0.198					
							Total:	1.00	1.33	1.34	1.43	
							Ratio of calculated to experimental:					0.70 - 0.75

TABLE III (cont.)

U^{238} fast fission													
1	55 s	$_{35}Br^{87}$	0.8	34.5	0.95	0.76	0.031	0.024	0.024	0.054		0.049	2.14
2	16 s	$_{35}Br^{88}$	1.4	34.9	0.84	1.18	0.06	0.071	0.195	0.564		0.620	3.03
	24 s	$_{53}I^{137}$	6.0	53.2 [a]	0.69	4.14	0.03	0.124					
3	4.5 s	$_{35}Br^{89}$	2.5	35.2	0.69	1.73	0.07	0.121	0.197	0.667		0.718	3.00
	6.3 s	$_{53}I^{138}$	6.0	53.3	0.63	3.78	0.02	0.076					
4	1.6 s	$_{35}Br^{90}$	3.4	35.6	0.43	1.46	≤0.1	≤0.146	≤0.368	1.599		1.795	2.03
	2.0 s	$_{53}I^{139}$	6.0	53.7	0.37	2.22	≤0.1	≤0.222					
								Total:	0.784	2.88		3.18	
								Ratio of calculated to experimental:					0.24 - 0.27
U^{238} fission with 14-15-MeV neutrons													
1	55 s	$_{35}Br^{87}$	1.9	34.9	0.84	1.60	0.031	0.050	0.050			0.156	3.12
2	16 s	$_{35}Br^{88}$	2.3	35.3	0.63	1.45	0.06	0.087	0.183			1.187	6.50
	24 s	$_{53}I^{137}$	5.1	53.3 [a]	0.63	3.21	0.03	0.096					
3	4.5 s	$_{35}Br^{89}$	2.7	35.6	0.43	1.16	0.07	0.081	0.137			1.216	8.88
	6.3 s	$_{53}I^{138}$	5.0	53.4 [A]	0.56	2.80	0.02	0.056					
4	1.6 s	$_{35}Br^{90}$	3.1	36.0	0.20	0.62	≤0.1	≤0.062	≤0.139			2.929	21.1
	2.0 s	$_{53}I^{139}$	4.8	54.1 [A]	0.16	0.77	≤0.1	≤0.077					
								Total:	0.509			5.49	
								Ratio of calculated to experimental:					0.09

* Ratio for U^{235} taken between Keepin's nine period values and calculated ones; for fast fission of U^{238} between average experimental values and calculated ones.

Z_p Values from: WAHL et al. [34]; MILTON [38]; McHUGH [39].

A APOLLONOVA et al. [36,37].

a Estimated.

b Estimated errors: ±25%

Data from: KEEPIN et al. [4]; MAKSIUTENKO [5,25,31,32].

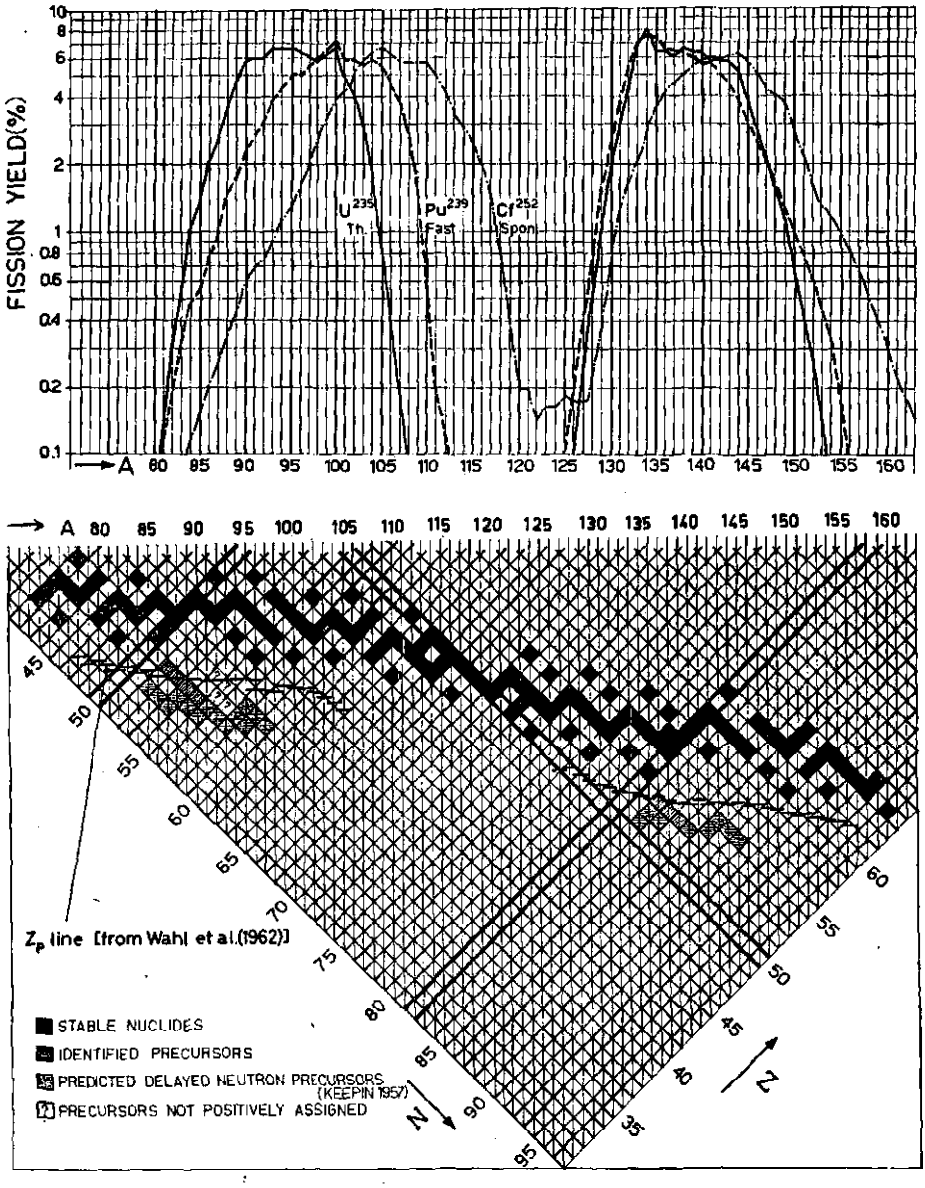

Fig. 7

Delayed-neutron precursors among fission products

(a) Distribution of mass in fission

(b) Predicted delayed-neutron precursors, and most probable charge in fission, Z_p

delayed-neutron precursors is fission that results in neutron-rich nuclides far from the stability line. The majority of the predicted precursors are odd Z nuclides and there are more of them at the light mass peak of the fis-

sion mass curve. Pappas' prediction points to ~50 possible precursors. Keepin narrows down the predicted precursors according to experimental criteria (to fit the six periods and appreciable fission yields) and indicates ~29 precursors, dividing them into main precursors and contributors.

In an attempt to work out a general systematics of delayed-neutron precursors PAPPAS and RUDSTAM [24] have suggested that such precursors might frequently be present outside closed-shell regions, although this does not appear to be borne out by the delayed-neutron yield data available at present.

Analysis and evaluation of experimental data

The analysis of the delayed-neutron periods into six groups seems to be very precise and affords an extremely accurate description of reactor dynamic behaviour, as has been demonstrated in a wide variety of kinetic experiments in different laboratories. U^{235} and Pu^{239} values have been corroborated in detail by independent period-versus-reactivity measurements on bare metal critical assemblies at Los Alamos [3]. The excellent agreement obtained between experiment and calculations ("inhour equation" of reactor kinetics) in the region of prompt critical reactivity provides a sensitive check on the accuracy of short-period delayed-neutron data, and good evidence against the existence of a seventh shorter period of appreciable abundance.

However, the nuclear chemist and physicist are interested in the detailed specifications and data for individual precursors, and here we come up against some dilemmas.

PERLOW and STEHNEY's identification [12] of nine delayed-neutron precursors of different half-lives belonging to only four groups demonstrated the complex composition of each of these groups as obtained in gross decay analysis. This situation probably becomes more complicated for the shorter-period groups. It is clear that the resolution of the gross decay curve into six exponentials is a mathematical result that, despite its great utility in reactor kinetics, certainly cannot be expected to provide full detailed information about the individual delayed-neutron precursors.

Attempts to relate total delayed-neutron yields to known fission systematics were made by KEEPIN [23], who suggested (basing his argument on thermal- and fast- (i.e. fission spectrum) fission data) that longer average chain lengths should lead to higher neutron yields. The solid lines of Fig. 2 support this assumption. The dotted lines, for the yield at 14 MeV, look similar but introduce a problem, better demonstrated in Fig. 3; the data at 14 MeV indicate an appreciable increase of the yield where one expects shorter chains, suggesting either that the yield-versus-chain length correlation becomes invalid at higher energies, or that the 14-MeV yield data are erroneous. Figure 8 shows the shift of the nuclear charge distribution curve towards stability upon increasing the energy from thermal to 14-MeV neutrons (a shift of ~0.7 units). As already noted, this implies lower yields of the known and predicted precursors (see Fig. 7). This problem becomes more complicated in the light of the data of Fig.4, where we see a systematic increase in the yields of all groups at higher energies of the incident neutron.

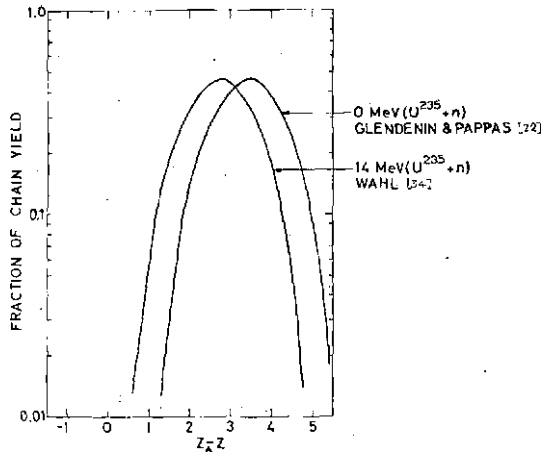

Fig. 8

Charge distribution curves for thermal- and 14-MeV-neutron fission of U^{235}

Table IV emphasizes this phenomenon. The most serious dilemma is the increase in the yield of the first group, which is believed to consist largely of Br^{87} [26].

COX et al. [8] stated, with reference to their study of Cf^{252} separated halogen fission products, that "it must be emphasized that the analysis does not give unique results and that many other combinations of delayed-neutron periods and yields can be hypothesized". In the Cf^{252} results, in order to fit the data into the accepted six-group classification, the absence of the 6-s I^{138} that is abundant in U^{235} fission was explained [8] by imposing a comparatively larger yield on its group partner, Br^{89}, a requirement hard to accept in the face of the other experimental data. The value of 20 s obtained instead of 24.4 s for I^{137} poses another problem, although this may be caused partly by the poor statistical accuracy of the Cf^{252} decay curve. Also, the neglect of growth-decay effects in the decay analysis can affect somewhat the reported half-lives and yields. The entire discussion of Cf^{252} results was based on the assumption that the light peak of Cf^{252} fission products does not contain delayed-neutron precursors. Although supported by the predictions (and if not correct the matter would be further complicated), this assumption nevertheless requires experimental verification.

Attempts to calculate the abundances of delayed-neutron precursors and compare these with experimental data seem dubious also. Again, in a limited treatment one obtains acceptable results, but a further check using additional parameters upsets the agreement. Tables IV and V may serve as examples. In the first table we calculated absolute yields of individual precursors (of i = 1, 2, 3, and 4), using well-established absolute chain yields, most probable nuclear charge (Z_p) distribution [34, 38, 39] and experimentally determined neutron branching ratios. The results were compared with experiment. For the first two groups in thermal fission of U^{235} the agreement is fair (viz. within ~25%). Since it has been experimentally shown that the first delay group in U^{235} is essentially all Br^{87} [26] one would expect that its relative con-

TABLE IV

ABSOLUTE DELAYED-NEUTRON INDIVIDUAL GROUP YIELDS AND YIELD RATIOS FOR FISSION AT DIFFERENT ENERGIES

Group No.	Approx. $T_{\frac{1}{2}}$ (s)	Th^{232}			U^{233}			U^{235}			U^{238}			Pu^{239}		
		Y_L [a] (%)	Y_H [b] (%)	Y_H/Y_L	Y_L (%)	Y_H (%)	Y_H/Y_L	Y_L (%)	Y_H (%)	Y_H/Y_L	Y_L (%)	Y_H (%)	Y_H/Y_L	Y_L (%)	Y_H (%)	Y_H/Y_L
1	55	0.195	0.355	1.82	-	-		0.063	0.153	2.43	0.051	0.156	3.06	-	-	
2	22	0.685	1.243	1.81	-	-		0.363	0.535	1.47	0.606	1.187	1.96	-	-	
3	6	1.001	1.365	1.36	-	-		0.335	0.600	1.79	0.686	1.216	1.78	-	-	
4	2.3	2.158	3.456	1.60	-	-		0.665	1.170	1.76	1.716	2.929	1.71	-	-	
5	0.5	1.158	1.655	1.43	-	-		0.163	0.482	2.96	0.916	1.621	1.77	-	-	
Total yield		5.20	8.07	1.55			1.6	1.59	2.94	1.85	3.98	7.11	1.79	0.62 K	1.3 S	2.1

[a] Y_L Yield from fission with $E_n \leq 3.8$ MeV
[b] Y_H Yield from fission with $14 \leq E_n \leq 15$ MeV

All data from Maksiutenko (1959, 1963) except those marked by K (from Keepin (1957)) and S (from Shpakov (1961))

TABLE V

COMPARISON BETWEEN CALCULATED AND EXPERIMENTAL DELAYED-NEUTRON YIELDS USING CALCULATED P_n VALUES

Group No.	Delayed-neutron precursors	Absolute chain yield (%)	Z_p	Fractional cumulative yield of precursor	Absolute yield of precursor (%)	Calculated delayed-neutron emission probability: P_n	Absolute yield of delayed-neutron precursors					Ratio*
							Calculated[b]		Experimental			
									Keepin		Maksiutenko	
							individual	total	(1957) 6 periods	(1964) 9 periods analysis	(1958, 1963)	
U^{235} thermal fission												
1	55 s $_{35}Br^{87}$	2.5	34.52	0.95	2.37	0.025	0.058	0.058	0.052	0.058	0.062	1.00
2	16 s $_{35}Br^{88}$	3.55	34.91	0.84	2.98	0.053	0.157	0.474	0.346	0.382	0.387	0.81
	24 s $_{53}I^{137}$	6.15	53.26	0.65	3.99	0.079	0.317					
3	4.5 s $_{35}Br^{89}$	4.70	35.42	0.56	2.63	0.113	0.298	0.447	0.310	0.390	0.326	0.87
	6.3 s $_{53}I^{138}$	6.65	53.45	0.53	3.52	0.042	0.149					
4	1.6 s $_{35}Br^{90}$	5.75	35.84	0.31	1.78	0.133	0.236	0.356	0.624	0.511	0.660	1.43
	2.0 s $_{53}I^{139}$	6.40	53.82	0.31	1.98	0.061	0.120					
							Total:	1.34	1.33	1.34	1.43	

TABLE V (*cont.*)

U^{238} fast fission													
1	55 s	$_{35}Br^{87}$	0.8	34.5	0.95	0.76	0.025	0.019	0.019	0.054		0.049	2.71
2	16 s	$_{35}Br^{88}$	1.4	34.9	0.84	1.18	0.053	0.063	0.394	0.564		0.620	1.50
	24 s	$_{53}I^{137}$	6.0	53.2[a]	0.69	4.14	0.080	0.331					
3	4.5 s	$_{35}Br^{89}$	2.5	35.2	0.69	1.73	0.113	0.195	0.354	0.667		0.718	1.96
	6.3 s	$_{53}I^{138}$	6.0	53.3	0.63	3.78	0.042	0.159					
4	1.6 s	$_{35}Br^{90}$	3.4	35.6	0.43	1.46	0.133	0.194	0.330	1.599		1.796	5.15
	2.0 s	$_{53}I^{139}$	6.0	53.7	0.37	2.22	0.061	0.136					
								Total:	1.09	2.88		3.18	
								Ratio of calculated to experimental:					0.34 - 0.38
U^{238} fission with 14-15-MeV neutrons													
1	55 s	$_{35}Br^{87}$	1.9	34.9	0.84	1.60	0.025	0.040	0.040			0.156	3.90
2	16 s	$_{35}Br^{88}$	2.3	35.3	0.63	1.45	0.053	0.077	0.334			1.187	3.56
	24 s	$_{53}I^{137}$	5.1	53.3[a]	0.63	3.21	0.080	0.257					
3	4.5 s	$_{35}Br^{89}$	2.7	35.6	0.43	1.16	0.113	0.131	0.249			1.216	4.89
	6.3 s	$_{53}I^{138}$	5.0	53.4[A]	0.56	2.80	0.042	0.118					
4	1.6 s	$_{35}Br^{90}$	3.1	36.0	0.20	0.62	0.133	0.082	0.129			2.929	22.7
	2.0 s	$_{53}I^{139}$	4.8	54.1[A]	0.16	0.77	0.061	0.047					
								Total:	0.752			5.49	
								Ratio of calculated to experimental:					0.14

* Ratio for U^{235} taken between Keepin's *nine period* values and calculated ones; for fast fission of U^{238} between average experimental values and calculated ones.

Z_p Values from: WAHL et al. [34]; MILTON [38]; McHUGH [39].

A APOLLONOVA et al. [36,37].

a Estimated.

b Estimated errors: ±25%

Data from: KEEPIN et al. [4]; MAKSIUTENKO [5,25,31,32].

tribution to the first group of other fissionable nuclides at various energies will be the same, but the results of calculations in the table do not support this assumption.

Another attempt, in Table V, is based on the assumption that the first group is entirely caused by Br^{87} and that the 20-s group of Cf^{252} is entirely caused by I^{137}, taking into account PERLOW and STEHNEY's [12] experimental values for the relative abundances of barium and iodine isotopes. The calculated results are compared with KEEPIN's [3] recent nine-period least-squares analysis of U^{235} gross decay data. The comparison looks good for thermal fission of U^{235} (although it implies disagreement with measured P(n) values of ARON et al. [17]). For fission of U^{238} with fast neutrons (for which the increase of total delayed-neutron yield compared with thermal energies is insignificant) and for U^{238} fission with 14-MeV neutrons, the agreement deteriorates.

FIEDLER and HERMANN [27] reported in a short note that they obtained good agreement between delayed-neutron group yields, cumulative fission yields and P(n) values for the first four groups in U^{235} thermal fission. However, they found that these calculations were invalid for 14-MeV fission, where the experimental delayed-neutron yield was twice the calculated value. Their conclusion was either that the measured yields at 14 MeV are wrong, or that there are other precursors present in the fission mass yield valley; the available experimental evidence does not support the latter conjecture. BEMIS [15] calculated the contributions of the known precursors to the corresponding groups in U^{235} thermal fission, using KEEPIN's data [4] and PERLOW and STEHNEY's [12] relative halogen abundances. The calculations are self-consistent, but disagree markedly with both experimental P(n) values and with the well-established delayed-neutron group yield data. Furthermore, the agreement worsens when one applies these calculations to the delayed-neutron yields from the same precursors and groups in U^{238} fission.

Another attempt, by KRISYUK [28], to evaluate the contribution of bromine and iodine isotopes to the total neutron emission, contained several unjustified assumptions (he assumed the halogen ratios obtained in thermal fission of U^{235} to be the same as in 15-MeV neutron fission of U^{238}, and the predicted upper values of P(n) and relative group abundances in 15-MeV fission to be the same as in 3.3 MeV fission).

The above inconsistencies lead one to speculate that either the experimental results are incomplete and some are wrong, or some basic assumptions that have been made may not be valid. One such assumption is the constancy of P(n). Several investigators have stated that P(n) should be a constant unless the delayed-neutron precursor is formed in an excited state that β-decays to the delayed-neutron emitter, a very unlikely case, since isomerism is not expected to occur in the regions beyond closed shells [23]. Discussing their reported increase in the total delayed-neutron yield with the energy of the inducing neutrons, SHPAKOV, PETRZHAK et al. [29] indicate that the increase in yield "is presumably due to the increased probability of emission of a neutron from the given nucleus depending on certain characteristics of the fission process".

Whatever interpretation or mechanism is suggested, it is evident that further understanding of detailed delayed-neutron emission characteristics

in fission requires precise and rigorous investigation of production parameters, and the decay characteristics of individual precursors, including those as yet unidentified. It is also evident from the above discussion that continued investigations of delayed-neutron emission in fission will have a strong bearing on the understanding of the fission process itself, and therefore can be used as a probe in the study of both fission and the neutron-rich products of fission.

PHOTONEUTRONS

A knowledge of the gamma-ray spectra and intensities of fission products is of practical importance in reactor technology, mainly from the points of view of heating, shielding and radiation effects. In a class by themselves are gamma rays of energies greater than 2.23 and 1.67 MeV, which cause emission of photoneutrons from deuterium and beryllium respectively in heavy water and beryllium moderated reactors. The photoneutrons are important in reactor kinetics and are the predominant source of neutrons after reactor shutdown. Except for beryllium and deuterium the only nuclides that have neutron binding energies lower than some gamma rays emitted from radioactive nuclides are O^{17} and C^{13}, with neutron binding energies of 4.14 and 4.9 MeV respectively; however, the abundance of these nuclides in reactor materials is low and the corresponding effective gamma rays are rather rare.

The experimental work so far reported on the photoneutron emission caused by fission-product gamma rays on beryllium and D_2O has dealt with the resolution of the decay of the gross photoneutron activity (several groups with half-lives ranging from 2.5 s to about two weeks were found) and with the determination of the relative yields of these groups. Since these studies were performed to obtain the minimum number of practical and simple equations suitable for engineering use, no attempt was made to interpret all the possible decay components.

The decay of photoneutron activity has been fitted by computer least-squares analysis to nine decay groups for both D_2O and, more recently, beryllium photoneutrons [2]. The group half-lives and abundances are generally quite different for beryllium photoneutrons than for D_2O photoneutrons; these data are summarized in Table VI. The yield values for beryllium were obtained by multiplying Keepin's β_j values (delay fractions) by $\nu(U^{235}) = 2.43$. Each of these groups in D_2O and in beryllium photoneutron decay represents a complex composite of nuclides. Detailed information on the constituents of the groups is important for reactors in which fission-product fractionation may take place and affect relative group abundances. Such information exists for the longer-lived fission products whose properties and yields are well-known, and experimental results are in agreement with calculated values based on fission mass and charge distribution and decay schemes. The information is incomplete for many shorter-lived groups and for some long-lived fission products of low fission yield where decay schemes are not clear enough. The latter, however, contribute negligibly to the gross photoneutron activity.

TABLE VI

PHOTONEUTRON GROUPS FROM U^{235} THERMAL FISSION PRODUCT GAMMAS *

In D_2O				In beryllium		
Group index	Half-life	Photoneutrons/fission	Group index	Assumed emitter	Group half-life	Photoneutrons/fission
1	12.8 d	0.12×10^{-5}	1	Ba^{140}	12.8 d	0.139×10^{-5}
2	53 h	0.25×10^{-5}	2	Te^{132}	77.7 h	0.092×10^{-5}
3	4.4 h	0.78×10^{-5}	3	Te^{131} + others	12.1 h	0.632×10^{-5}
4	1.65 h	5.65×10^{-5}	4	I^{135}, La^{142}, Kr^{87}, Kr^{88}	3.11 h	0.78×10^{-5}
5	27 min	5.01×10^{-5}	5	Te^{134}, I^{134}, Br^{84}, Cs^{138}	43.2 min	0.88×10^{-5}
6	7.7 min	8.14×10^{-5}	6	Xe^{138}, Rb^{89}, Mo^{101}	15.5 min	8.94×10^{-5}
7	2.4 min	17.0×10^{-5}	7	Sb^{133}, Kr^{89}, Rb^{90}	3.2 min	4.50×10^{-5}
8	41 s	49.5×10^{-5}	8	I^{136}, Br^{87}	1.3 min	8.90×10^{-5}
9	2.5 s	158.0×10^{-5}	9	Kr^{90}, Se^{87}	0.51 min	4.95×10^{-5}

* from Keepin (1962)

An analysis performed recently by our group [30] to resolve the constituents of the gross photoneutron activity produced by U^{235} fission products in D_2O was in excellent agreement (within ± 5%) with the activities calculated for times ≥1 h after the end of an irradiation. The computer calculations were based on known data for fission mass and charge distributions, gamma-ray energies and abundances, the excitation function for deuterium photodisintegration, counting efficiencies, etc. For shorter periods, nuclear data (mainly decay scheme details) are incomplete and the discrepancies between the calculated and experimental values are considerable.

In the case of beryllium, photoneutrons can be produced by many more fission product gamma rays than in D_2O, and therefore the resolution of this activity into a sum of exponentials is more complex. The main difficulty lies in the great number of parent-daughter decay chains requiring calculations of both decay and growth.

KEEPIN [2, 3] has summarized the available data on photoneutrons from the reactor physicist's point of view. This approach emphasizes mainly a mathematical treatment suitable for reactor calculations, and to this end the individual photoneutron activities are bracketed together in groups. It is of little concern how many individual photoneutron activities are present, although it is desirable to reduce the number of effective photoneutron groups, provided the accuracy is not impaired, since this simplifies calculations. An illustration of this approach is the group half-lives quoted in Table VI which are mostly composites and have no nuclear physical significance.

Photoneutrons can also serve as a means for nuclear structure studies, although their potentialities have so far not been exploited in full. For example, de-excitation by the emission of energetic photons may be detected in difficult cases by photoneutron counting; a case where this technique can be used is the study of low-abundance cross-over transitions masked by pile-up of the predominant low-energy gamma rays. This information may also be used to measure nuclide distributions from different fissionable species under various conditions, and therefore for further clarification of the fission process.

It is thus of great importance for both practical and fundamental purposes to study in detail the origin of photoneutron emission, by detailed characterization of the individual nuclides, especially the short-lived ones, responsible for this phenomenon.

ACKNOWLEDGEMENTS

I would like to thank Amos Notea for his invaluable help, especially in sorting out the delayed-neutron data and preparing Tables IV and V. It is a pleasure to thank also Dr. Keepin for making available the galleys of Chapters 4 and 5 of his book "Physics of Nuclear Kinetics", and other reports of his work. I would also like to thank Ziggy Frenkel for his skilful preparation of drawings.

REFERENCES

[1] KEEPIN, G.R., in Progress in Nuclear Energy 1, Pergamon Press, London (1956).
[2] KEEPIN, G.R., Nucleonics 20 (1962) No. 8, 150.
[3] KEEPIN, G.R., in Physics of Nuclear Kinetics, Addison Wesley Co. (1965) ch. 4 and 5.
[4] KEEPIN, G.R., WIMETT, T.F. and ZEIGLER, R.K., Phys. Rev. 107 (1957) 1044; J. nucl. Energy 6 (1957) 1.
[5] MAKSIUTENKO, B.P., Ž. eksp. teor. Fiz. 35 (1958) 815.
[6] MOSCATI, G. and GOLDEMBERG, J., Phys. Rev. 126 (1962) 1098.
[7] PETRZHAK, K.A., KONDRATKO, M.Ya., NIKOTIN, O.P. and TEPLIKH, V.F., Atomnaja Energija 15 (1963) 157.
[8] COX, S., FIELDS, P., FRIEDMAN, A., SJOBLOM, R. and SMITH, A., Phys. Rev. 112 (1958) 960.
[9] DOSTROVSKY, I., DAVIS, R., POSKANZER, A. and REEDER, P., Brookhaven National Laboratory, private communication (1964).
[10] BATCHELOR, R. and HYDER McK, H.R., J. nucl. Energy 3 (1956) 7.
[11] BONNER, T.W., BAME, S.J. and EVANS, J.E., Phys. Rev. 101 (1956) 1514.
[12] PERLOW, G.J. and STEHNEY, A.F., Phys. Rev. 113 (1959) 1269.
[13] STEHNEY, A.F. and PERLOW, G.J., Bull. Amer. phys. Soc. II, 6 (1961) 62.
[14] COWAN, G.A. and ORTH, C.J., Proc. 2nd UN Int. Conf. PUAE 7 (1958) 328.
[15] BEMIS, C.E., Ph. D. Thesis, Massachusetts Institute of Technology (1964).
[16] YELLIN, E., SONNINO, T. and AMIEL, S., unpublished results (1964-5).
[17] ARON, P.M., KOSTOCHKIN, O.I., PETRZHAK, K.A. and SHPAKOV, V.I., Atomnaja Energija 16 (1964) 368.
[18] STEINBERG, E.P. and SCHWARTZ, L.L., Phys. Rev. 130 (1963) 1472.
[19] KEEPIN, G.R., Proc. Conf. on Reactor Kinetics and Control, Tucson, Ariz. (1963).
[20] AMIEL, S., Analyt. Chem. 34 (1962) 1683.
[21] PAPPAS, A.C., United States AEC Rpt AECU-2806 (1953).
[22] PAPPAS, A.C., Proc. 2nd UN Int. Conf. PUAE (1958).
[23] KEEPIN, G.R., J. nucl. Energy 7 (1958) 13.
[24] PAPPAS, A.C. and RUDSTAM, G., Nucl. Phys. 21 (1960) 353.
[25] MAKSIUTENKO, B.P., Atomnaja Energija 15 (1963) 157.
[26] CORYELL, C.D. and WILLIAMS, E.T., Massachusetts Institute of Technology, private communication (1964).
[27] FIEDLER, J. and HERMANN, G., Angew. Chem. 75 (1963) (No. 22) 1131.
[28] KRISYUK, I.T., Atomnaja Energija 16 (1964) 146.
[29] SHPAKOV, V.I., PETRZHAK, K.A., BAK, M.A., KOVALENKO, S.S. and KOSTOCHKIN, O.I., Atomnaja Energija 11 (1961) 539.
[30] JULIANO, J.O. and AMIEL, S., unpublished results (1964).
[31] MAKSIUTENKO, B.P., Atomnaja Energija 7 (1959) 474.
[32] MAKSIUTENKO, B.P., Atomnaja Energija 15 (1963) 321.
[33] McGARRY, W.I., OMOHUNDRO, R.J. and HOLLOWAY, G.E., Bull. Amer. phys. Soc. II, 5 (1960) (No. 5, part 1) 33.
[34] WAHL, A.C., FERGUSON, R.L., NETHAWAY, D.R., TRAUTNER, D.E. and WOLFSBERG, K., Phys. Rev. 126 (1962) 1112.
[35] COX, S.A., Phys. Rev. 123 (1961) 1735.
[36] APOLLONOVA, A.N., KRISYUK, I.T. and USHATSKII, V.N., Radiohimija 4 (1962) 587.
[37] APOLLONOVA, A.N., KRISYUK, I.T. and USHATSKII, V.N., Radiohimija 4 (1962) 711.
[38] MILTON, D., Rpt. UCRL-9883 (1962).
[39] McHUGH, J.A., Rpt. UCRL-10673 (1963).

COMPARISON OF OBSERVED DELAYED-NEUTRON ABUNDANCES WITH CALCULATED FISSION YIELDS OF NEUTRON PRECURSORS

G. HERMANN, J. FIEDLER*, G. BENEDICT, W. ECKHARDT, G. LUTHARDT, P. PATZELT AND H. D. SCHÜSSLER
INSTITUT FÜR ANORGANISCHE CHEMIE UND KERNCHEMIE DER UNIVERSITÄT MAINZ, FEDERAL REPUBLIC OF GERMANY

Abstract — Résumé — Аннотация — Resumen

COMPARISON OF OBSERVED DELAYED-NEUTRON ABUNDANCES WITH CALCULATED FISSION YIELDS OF NEUTRON PRECURSORS. Cumulative fission yields of known and predicted delayed-neutron precursors were calculated using recent mass- and charge-distribution data. These yields were then compared with abundances of the 55-, 22-, 6-and 2-s neutron periods in various low-energy fission reactions, i.e. neutron emission probabilities were calculated by minimizing the deviations between observed and calculated abundances. The number and kind of precursors involved in each period have been varied as well as the assumptions made on most probable primary charge and its dispersion.

The abundances reported in low-energy fission can be explained satisfactorily by the known precursors. Some of the predicted precursors may be present but their calculated contributions are comparatively small. Some other predicted precursors lead to bad agreement with abundance data and to unlikely emission probabilities. Several questionable mass-assignments of precursor nuclides are corroborated.

Emission probabilities were used for estimating delayed-neutron abundances in 14-MeV neutron fission. The values obtained are much smaller than reported abundances. This discrepancy cannot be accounted for by unknown precursors, at least for fission of Th^{232} and U^{238} by 14-MeV neutrons, since only a relatively small fraction of the delayed-neutron activity remains after a rapid halogen separation. Therefore, the absolute abundances for both reactions are remeasured by a new method that involves no absolute counting. Preliminary abundances obtained are much lower than the reported values, and are in good agreement with the expected values.

COMPARAISON ENTRE LES ABONDANCES OBSERVÉES DE NEUTRONS RETARDÉS ET LES RENDEMENTS DE FISSION CALCULÉS POUR LES PRÉCURSEURS DE NEUTRONS. Les auteurs ont calculé, au moyen de données récentes sur la distribution selon la masse et la charge, les rendements cumulatifs de fission en produits dont on sait ou dont on suppose qu'ils sont des précurseurs de neutrons retardés. Ces rendements ont été alors comparés aux abondances pour les périodes de neutrons de 55, 22, 6 et 2 s, lors de différentes réactions de fission à basse énergie, c'est-à-dire que les probabilités d'émission de neutrons ont été calculées en réduisant au minimum les écarts entre les abondances observées et les abondances calculées. On a fait varier le nombre et l'espèce des précurseurs mis en jeu dans chaque période ainsi que les hypothèses admises quant à la charge primaire la plus probable et à sa dispersion.

Le rôle des précurseurs connus peut expliquer de manière satisfaisante les abondances enregistrées dans la fission à basse énergie. Il est possible que certains des précurseurs supposés interviennent dans la réaction, mais d'après les calculs, leurs contributions aux abondances sont relativement faibles. A partir des hypothèses concernant d'autres précurseurs supposés, on obtient des résultats qui sont loin de concorder avec les données relatives à l'abondance des neutrons et on aboutit à des probabilités d'émission qui ne semblent pas devoir se vérifier. Dans plusieurs cas, les masses attribuées de manière hypothétique à des nucléides précurseurs reçoivent confirmation.

Ces probabilités d'émission ont été utilisées pour évaluer les abondances de neutrons retardés dans la fission par neutrons de 14 MeV. Les valeurs obtenues sont bien inférieures aux données qui ont été publiées. Cet écart ne peut pas être expliqué par l'existence des précurseurs inconnus — au moins en ce qui concerne la fission de ^{232}Th et de ^{238}U par neutrons de 14 MeV — car seule une partie relativement peu importante

*Now at MacMaster University, Hamilton, Ont. Canda.

de l'activité donnant des neutrons retardés persiste après une séparation rapide par les halogènes. C'est pourquoi, pour les deux réactions, les abondances absolues sont mesurées à l'aide d'une nouvelle méthode qui ne comporte pas de comptage absolu. Les abondances obtenues provisoirement sont très inférieures aux valeurs qui ont été publiées et sont en bon accord avec les valeurs attendues.

СРАВНЕНИЕ НАБЛЮДАЕМОЙ РАСПРОСТРАНЕННОСТИ ЗАПАЗДЫВАЮЩИХ НЕЙТРОНОВ С РАСЧЕТНЫМИ ВЫХОДАМИ ПРЕДШЕСТВЕННИКОВ НЕЙТРОНОВ ПРИ ДЕЛЕНИИ. Суммарные выходы известных и предсказанных предшественников запаздывающих нейтронов при делении были рассчитаны при использовании последних данных о распределении масс и зарядов. Эти выходы затем были сравнены с распространенностью нейтронов за периоды в 55, 22, 6 и 2 секунды в различных реакциях деления низкой энергии, т.е. вероятность испускания нейтронов подсчитывалась путем сведения к минимуму отклонений между наблюдаемой и расчетной распространенностью. Количество и вид предшественников, связанных с каждым периодом, изменялись, как и сами предположения о наиболее вероятном первичном заряде и его дисперсии.

Распространенность, относящаяся к делению при низких энергиях, может быть удовлетворительно объяснена. Некоторые из предсказанных предшественников могут присутствовать, однако их расчетные вклады сравнительно малы. Некоторые другие предсказанные предшественники плохо согласуются с данными о распространенности и приводят к малой вероятности испускания. Подтверждается несколько сомнительных определений массовых чисел изотопов предшественников.

Эти вероятности испускания использовались для вычисления распространенности запаздывающих нейтронов при нейтронном делении с энергией 14 Мэв. Полученные величины значительно меньше, чем размеры распространенности, о которой докладывается. Такое расхождение нельзя объяснить наличием неизвестных предшественников — по крайней мере при делении тория-232 и урана-238 нейтронами с энергией 14 Мэв —, поскольку только сравнительно небольшая часть активности запаздывающих нейтронов сохраняется после быстрого разделения галогенов. Поэтому абсолютная распространенность в случае обоих реакций измеряется новым методом, который не связан с проведением абсолютного счета. Предварительные размеры распространенности значительно меньше, чем значения, о которых докладывается, и они хорошо согласуются с предполагаемыми величинами.

COMPARACION DE LAS ABUNDANCIAS OBSERVADAS DE NEUTRONES RETARDADOS CON LOS RENDIMIENTOS DE FISION CALCULADOS PARA LOS PRECURSORES NEUTRONICOS. Se han calculado los rendimientos acumulativos de fisión de precursores conocidos y presuntos de neutrones retardados, utilizando datos recientes, relativos a la distribución de masas y cargas. Estos rendimientos se han comparado con las abundancias de los neutrones de período 55, 22, 6 y 2 s en varias reacciones de fisión de baja energía, esto es, las probabilidades de emisión neutrónica se han calculado reduciendo al mínimo las discrepancias entre las abundancias observadas y las calculadas. Se ha hecho variar el número y la especie de los precursores considerados en cada período, así como las hipótesis admitidas acerca de la carga primaria más probable y de su dispersión.

Los resultados ya publicados sobre abundancias en la fisión de baja energía pueden explicarse satisfactoriamente por los precursores conocidos. Es posible que intervengan algunos de los precursores presuntos, pero sus contribuciones calculadas son más bien secundarias. Los resultados relativos a otros precursores presuntos distan mucho de concordar con los datos referentes a la abundancia y suponen probabilidades de emisión sumamente remotas. Se confirman varias masas dudosas asignadas a núclidos precursores. Estas probabilidades de emisión se han utilizado para determinar la abundancia de neutrones retardados en la fisión inducida por neutrones de 14 MeV. Esta discrepancia no puede atribuirse a precursores desconocidos (al menos en el caso de la fisión del ^{232}Th y del ^{238}U por neutrones de 14 MeV), puesto que después de separar rápidamente los halógenos sólo queda una fracción relativamente pequeña de la actividad neutrónica retardada. Por ello, las abundancias absolutas correspondientes a ambas reacciones se vuelven a medir por un nuevo método que no exige recuentos absolutos. Las abundancias inicialmente obtenidas son mucho menores que las indicadas en la memoria y concuerdan satisfactoriamente con los valores previstos.

The absolute abundance, Y_n, of a delayed-neutron period in a fission reaction depends on the cumulative fission yields, Y_c, and the neutron emission probabilities, P_n, of all precursors A, B, C... contributing to that period:

$$Y_n = P_n^{(A)} Y_c^{(A)} + P_n^{(B)} Y_c^{(B)} + P_n^{(C)} Y_c^{(C)} + \ldots \quad (1)$$

P_n is a constant for each precursor nuclide. Y_n-values have been measured for various fission reactions. The corresponding Y_c-values, however, have not yet been reported. They must be estimated by multiplying mass yields by those fractional cumulative yields that are expected according to charge-distribution systematics. Y_n- and Y_c-values can then be compared by solving an appropriate set of Eq. (1) with regard to the P_n-values, minimizing the deviations between observed and calculated abundances. The aptness of fit is indicated by the standard deviations of P_n and Y_n. Such a comparison should show whether the observed abundances can be reasonably explained by known precursors or whether it has to be assumed that unknown precursors contribute strongly. Also, some conclusions on charge distribution may be drawn by varying the assumptions made in deriving fractional cumulative yields; assumptions leading to good agreement with abundance data appear more likely than others.

PAPPAS [1, 2] and KEEPIN [3] first compared delayed-neutron abundances with precursor yields. Since then new precursors have been discovered [4-6] and the knowledge of charge-distribution in low-energy fission has been extended [7, 8]. It therefore appeared worthwhile to repeat this comparison with all the data now available. Only the 55-, 22-, 6- and 2-s periods were considered. Results are given in Section 1. Similar, but, we believe, cruder comparisons were recently carried out by SCHINDEWOLF [9] and by KRISYUK [10]. Our data suggested experiments on the contribution of non-halogen precursors and on abundances in 14-MeV-neutron fission described in Sections 2 and 3.

1. COMPARISON OF DELAYED-NEUTRON ABUNDANCES WITH PRECURSOR YIELDS

First we tried to correlate delayed-neutron abundances for fission of U^{233}, U^{235} and Pu^{239} by thermal neutrons and of Th^{232} and U^{238} by fission neutrons with cumulative yields of known precursors. These are [5]: in the 55-s period Br^{87}, 22-s period Br^{88} and I^{137}, 6-s period Br^{89} and I^{138}, 2-s period Br^{90} and I^{139}. The mass assignments of bromine precursors in the 6- and 2-s periods are somewhat doubtful [5]. However, any other assignment leads to unrealistic results.

Delayed-neutron abundances were taken from KEEPIN et al. [11], and mass yields from a recent compilation [12]. Fractional cumulative yields, Y_c^f, were estimated with various sets of values of the parameters Z_p and c of the Gaussian charge distribution [7]:

$$P_n = (c\pi)^{-1/2} \exp[-(Z - Z_p)^2/2], \quad (2)$$

$Y_c^f = \sum_0^Z P_n$. Briefly, the following variations were tried:

(i) "Emp.I". Although experimental data support c = 0.95 [7], we also used narrower dispersions with c = 0.80 and 0.65. With these c-values,

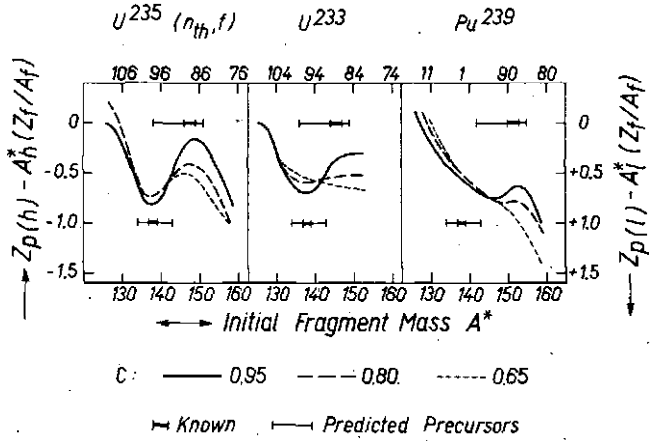

Fig. 1

Empirical Z_p-functions for thermal-neutron fission of U^{235}, U^{233} and Pu^{239} derived with Gaussian charge distributions of various widths, characterized by c. Subscripts f, h and l refer to the fissioning nucleus, heavy and light fragments respectively, A* denotes the mass number before neutron emission. The regions of known or prospective delayed-neutron precursors are indicated by bars.

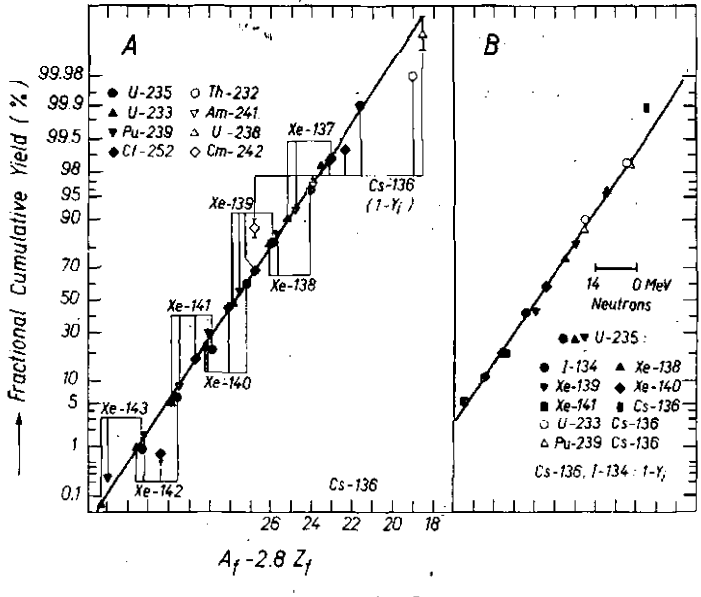

Fig. 2

(A) Correlation of fractional cumulative yields for various low-energy fission reactions by a probability-scale plot against A_f-2.8 Z_f. Some fractional independent yields are included, plotted as $1-Y_f^{(i)}$. (B) Similar correlation for yields in slow-neutron fission with those in 14-MeV neutron fission by plotting them against an arbitrarily chosen distance.

empirical Z_p-functions for U^{233}, U^{235} and Pu^{239} fission respectively were constructed from available fractional yields [7, 8, 12]. Figure 1 shows some

examples, plotted as $\Delta_Z = Z_p - A^*(Z_f/A_f)$ versus A^*, Δ_Z is the deviation from the unchanged specific charge. Initial fragment masses A^* were estimated from the neutron emission curves of TERRELL [13] and of APALIN et al. [14]. Whenever their respective values disagree, separate Z_p-functions were constructed. The use of c = 0.80 reduces the scattering of experimental Δ_Z-values in some regions.

For Th^{232} and U^{238} fission the available data are too scarce for this treatment. Fractional cumulative yields for these reactions were estimated as demonstrated in Fig. 2A. Experimental Y_c^i-values for various fission reactions can be correlated in a probability scale plot versus $(A_f - 2.8\ Z_f)$, resulting in a straight line[1]. Fractional independent yields, Y_i^f, give the same relation, if plotted as $(1-Y_i^f)$. Y_c^f- values for Th^{232} and U^{238} fission were extrapolated from calculated Y_c^i-values for U^{233}, U^{235} and Pu^{239} fission, using a "universal" slope ("u") for all nuclides and also an individual slope ("i") for each nuclide.

(ii) "Emp. II". In an earlier treatment [16] we assumed the Z_p-function for U^{235} to be valid for all fission reactions. Data for heavy fragments were read at A_h^*, those for light fragments at $(A_f - A_l^*)$.

(iii) "ECD". In addition, Z_p-values were calculated according to the equal-charge displacement rule [17], using recent Z_A-values [18]. We have found [19] that this combination predicts the Z_p-values for $U^{235}(n_{th}, f)$ quite well.

Table I shows some results in form of standard deviations, σ_n, between observed and calculated abundances. These and other results can be summarized as follows.

The empirical treatment based on recent data (Emp. I) is superior to that based on older data (Emp. II) and to the ECD rule. On the average, the relative σ_n-values are 1 : 1.4 : 3 in the order Emp. I-Emp. II-ECD.

The numerous variations tested with recent data (Emp. I) show: TERRELL's [13] neutron emission curves lead to about 30% lower σ_n-values than APALIN's curves [14]. All the values given in Table I were obtained with TERRELL's data. The standard deviations for the 55-s period diminish by nearly one order of magnitude, if U^{233} data are not included and if Y_n-values for U^{235} and Pu^{239} fission by fission neutrons (instead of thermal neutrons) are used; in the 22-s period, rejection of U^{233} data result in a slight improvement. The values for the 55- and 22-s periods shown in the table refer to these favourable conditions.

For the c-values we find: For both the 22-s and the 6-s period, c = 0.80 gives the best fits. For the 2-s period, however, c = 0.95 is superior, if yields for Th^{232} and U^{238} fission are extrapolated with the "universal" slope (left column); if individual slopes are used, c = 0.80 is at least equivalent (right column). It should be mentioned that in the 22-s and the 6-s periods only the yields for U^{233} and Pu^{239} fission depend strongly on the c-value. Thus,

[1] The choice of $(A_f - 2.8\ Z_f)$ was suggested by the correlation of log Y_n with $(A_f - 3\ Z_f)$ found by KEEPIN [15]. The plot used means that $(Z-Z_p)$ is proportional to $(A_f - 2.8\ Z_f)$. A proportionality between $(Z-Z_p)$ and $(A_f - 2.4\ Z_f)$ can be derived from the equal-charge displacement rule.

TABLE I

STANDARD DEVIATIONS OF DELAYED-NEUTRON ABUNDANCES CALCULATED WITH KNOWN PRECURSORS

Z_p-function		Standard deviation (n/100 fissions)				
Method	c	55 s	22 s	6 s	2 s	
Emp. I	0.95	0.0012	0.057	0.042	0.036	0.087
	0.80	0.0021	0.046	0.031	0.066	0.053
	0.65	0.0020	0.050	0.041	0.11	
Emp. II	0.95	0.011	0.079	0.071	0.30	
	0.65	0.011	0.049	0.030	0.10	
ECD	0.95	0.024	0.094	0.12	0.29	
	0.65	0.012	0.10	0.11	0.19	

$c \approx 0.80$ seems to be more appropriate for these reactions than $c = 0.95$ that was measured for $U^{235}(n_{th}, f)$ by WAHL [7] [2].

The neutron emission probabilities obtained do not depend strongly on the conditions used. This is shown for bromine precursors in Table II and for iodine precursors in Table III. Mean values given include values not shown. They are compared with experimentally obtained neutron emission probabilities as measured by ARON et al. [20], and also with values deduced from the relative initial activities in $U^{235}(n_{th}, f)$ reported by PERLOW and STEHNEY [5]. Also, some early theoretical estimates by KEEPIN [3] (based on data available in 1957) are given. For bromine precursors, our P_n-values agree quite well with experimental data, except Br^{89}. For iodine precursors, however, our P_n-values are much higher than those obtained from experimental results, but are closer to theoretical estimates.

In spite of these discrepancies, our values may be used as "apparent" P_n-values of known precursors to predict neutron abundances of its first four delayed-neutron groups. This is demonstrated in Fig. 3 where observed abundances and our estimates are compared for the fission reactions so far discussed. Only the U^{233} data of the 55-s period deviate strongly. Similar comparisons for some other reactions are given in Table IV. The abundances for $Cf^{252}(sp, f)$ are taken from COX et al. [21], those for $Pu^{240}(n_f, f)$ from KEEPIN et al. [11] and those for $Pu^{241}(n_{th}, f)$ from COX [22]. Precursor yields were estimated from the probability-scale plot as described previously. Again, observed and calculated values are in reasonable agreement, except for the spontaneous fission of Cf^{252}, in which roughly equal abundances of the 22-, the 6- and the 2-s periods are predicted but only the 22- and the 2-s periods have been observed [21]. Using experimental P_n-values,

[2] More recent data for $U^{235}(n_{th}, f)$ support $c = 0.86 \pm 0.04$, see WAHL, A. C., "Mass and charge distribution in low-energy fission", these Proceedings I.

TABLE II

NEUTRON EMISSION PROBABILITIES OF KNOWN BROMINE PRECURSORS

c	Neutron emission probability (%) [e]			
	Br^{87}	Br^{88}	Br^{89}	Br^{90}
0.80 u	2.64 (1.1)	5.9 (24)	4.6 (22)	26 (12)
0.80 i			4.3 (23)	26 (9)
0.95 u	2.63 (0.8)	6.0 (27)	3.8 (34)	21 (7)
0.95 i				20 (18)
Mean value [a]	2.64 ± 0.03	6.1 ± 1.6	4.3 ± 1.3	24 ± 3
Experiment [b]	3.1 ± 0.6	6.0 ± 1.6	7 ± 2	
Experiment [c]	2.6 ± 0.5	5.8 ± 1.6	12 ± 3	15 ± 4
Theory [d]	2	2	14	22

[a] Weighted prop. $1/\sigma$.
[b] ARON et al. (1964).
[c] Relative values of PERLOW and STEHNEY (1959), normalized at Br^{87}.
[d] KEEPIN (1958).
[e] In parentheses relative standard deviation in percentages.

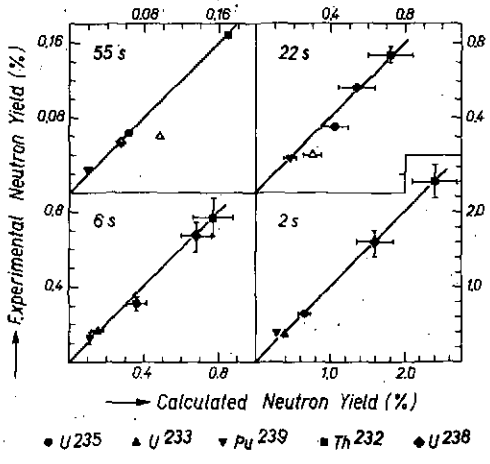

Fig. 3

Comparison of observed delayed-neutron yields of the 55-, 22-, 6- and 2-s periods with yields calculated from neutron-emission probabilities derived from this work. The data are for thermal-neutron fission of U^{233}, U^{235} and Pu^{239}, and for fission-neutron fission of Th^{232} and U^{238}. Experimental data from KEEPIN et al. [11].

TABLE III

NEUTRON EMISSION PROBABILITIES OF KNOWN IODINE PRECURSORS

c	Neutron emission probability (%)[e]		
	I^{137}	I^{138}	I^{139}
0.80 u	5.4 (18)	8.2 (10)	19 (17)
0.80 i		8.8 (10)	22 (14)
0.95 u	5.2 (23)	8.4 (13)	19 (7)
0.95 i			29 (19)
Mean value[a]	5.2 ± 1.1	8.2 ± 1.0	19 ± 3
Experiment[b]	3.0 ± 0.5	2.0 ± 0.5	
Experiment[c]	3.0 ± 0.6	2.2 ± 0.5	4.5 ± 1.5
Theory[d]	9	18	43

[a] Weighted prop. $1/\sigma$.
[b] ARON et al. (1964).
[c] Values normalized at I^{137}.
[d] KEEPIN (1958).
[e] In parentheses relative standard deviation in percentages.

the calculations lead to considerably lower abundances in all three cases. For the 22-, 6- and 2-s periods, the abundances are reduced by factors of about 0.7, 0.4 and 0.3.

To calculate abundances for fission reactions induced by 14-MeV neutrons, fractional cumulative yields were estimated from the corresponding yields in slow-neutron fission as follows. It was assumed that the yields for both reactions lie on a straight line in a probability-scale plot against an arbitrarily chosen distance. The appropriate slope was obtained by plotting known yields [7, 8, 12] scattered over the entire range. As shown in Fig. 2B, this treatment results in a constant slope[3]. The curve for the light fragments gives a slope not as steep as the one shown for the heavy fragments. Calculated abundances are presented in Table V together with observed values obtained from relative period abundances [24-26] and absolute total yields of delayed neutrons [26-29]. The calculated abundances are much lower than the observed ones, for example by a factor of about 3 for Th^{232} and U^{238} fission. These discrepancies persist even if cumulative yields for slow-neutron fission are used that are necessarily an upper limit of the cumulative yields in fast neutron fission.

[3] This implies that the c-values for slow and fast neutron fission are similar and that the Z_p-values are shifted for nearly the same distance in the Z-scale for all fission decay chains considered.

TABLE IV

CALCULATED AND OBSERVED DELAYED-NEUTRON ABUNDANCES FOR SOME LOW-ENERGY FISSION REACTIONS

Reaction	Abundances (n/100 fissions)					Ref.
		55 s	22 s	6 s	2 s	
$Cf^{252}(sp, f)$	calc.	0.004	0.15	0.13	0.12	
	obs.[a]	-	0.22 (1)	-	0.29 (4)	b
$Pu^{240}(n_f, f)$	calc.	0.030	0.28	0.20	0.23	
	obs.[a]	0.025 (3)	0.24 (2)	0.17 (5)	0.31 (3)	c
$Pu^{241}(n_t, f)$	calc.	0.018	0.33	0.33	0.43	
	obs.[a]	0.015 (2)	0.36 (4)	0.27 (5)	0.61 (10)	d

[a] Absolute errors in parentheses.
[b] COX et al. (1958).
[c] KEEPIN et al. (1957).
[d] COX (1961).

Finally we tried to draw some conclusions on contributions of prospective precursors by inserting them, in addition to known precursors, into the least-squares procedure. Of course, only main contributors can be indicated by this approach. The procedure was checked with some nuclides known to have low neutron emission probabilities. These are the 6-s rubidium and the 1.5-krypton precursor with mass numbers 92 or 93 found by STEHNEY and PERLOW [6], and the 1.9-s Sb^{135} for which BEMIS [30] has set an upper limit of P_n.[4] According to Table VI, these nuclides are not predicted as main precursors, in agreement with experience. Rb^{92} and Rb^{93} fit into the 6-s period but with low P_n-values. Kr^{92}, Kr^{93} and Sb^{135} lead to negative P_n-values or large standard deviations of Y_n- or P_n-values.

Next we inserted the possible precursors listed by PAPPAS [2], one by one. Unknown half-lives were estimated by extrapolating known half-lives in a plot of log $T_{1/2}$ versus mass number. In doubtful cases, precursors were assigned to two periods. Several prospective precursors gave negative P_n-values or (and) large standard deviations, namely: in the 22-s period Cs^{141}, in the 6-s period Se^{87}, Sn^{135}, Te^{136}, in the 2-s period Se^{88}, Te^{137}, Te^{138}. The remaining nuclides are shown in Table VII. Besides P_n-values and standard deviations of Y_n, the table contains in the last column expected contributions to period abundances in $U^{235}(n_{th}, f)$. To the 22-s period Te^{136} may contribute appreciably. This would reduce the P_n-value for I^{137} from 5.2% (Table III) to 3.2%, which is close to the observed value

[4] See also DEL MARMOL, P., NÈVE DE MEVERGNIES, M. and SPEECKE, A., "Search for delayed-neutron precursors in antimony and arsenic fission products", these Proceedings II; TOMLINSON, L., "Short-lived antimony and arsenic isotopes formed in fission", these Proceedings II.

TABLE V

CALCULATED AND OBSERVED DELAYED-NEUTRON ABUNDANCES FOR SOME FISSION REACTIONS BY 14-MeV NEUTRONS

Target		Abundances (n/100 fissions)				References	
		55 s	22 s	6 s	2 s	rel.	abs. Y_n
Th^{232}	calc.	0.12	0.53	0.42	0.98		
	obs.	0.36	1.24	1.36	3.4	a	b,c
U^{233}	calc.	0.056	0.10	0.027	0.024		
	obs.	0.098	0.26	0.12	0.80	d	d
U^{235}	calc.	0.069	0.23	0.11	0.15		
	obs.	0.15	0.54	0.61	1.16	a	b,f
U^{238}	calc.	0.059	0.35	0.33	0.70		
	obs.	0.16	1.20	1.22	2.9	a	b,f
Pu^{239}	calc.	0.019	0.051	0.018	0.020		
	obs.	0.069	0.27	0.24	0.51	e	c

[a] MAKSYUTENKO (1958)
[b] MAKSYUTENKO (1959)
[c] SHPAKOV (1962)
[d] MAKSYUTENKO (1963 b)
[e] MAKSYUTENKO (1963 a)
[f] McGARRY (1960)

of 3.0%. Whereas Te^{137} and As^{85} [5] do not improve the fits in the 6-s and the 2-s periods respectively, Rb^{94}, $Sr^{97,98}$ and $Cs^{142,143}$ lead to considerable improvement for the 2-s period. Certainly, the validity of these results should not be over-estimated because several unknown precursors could simultaneously occur. Furthermore, some of the nuclides mentioned above would have to have rather high neutron emission probabilities that appear energetically unlikely. Nevertheless, a search for precursors among those elements is suggested.

2. CONTRIBUTION OF NON-HALOGEN PRECURSORS TO DELAYED-NEUTRON ACTIVITY

The strong discrepancies between observed and calculated abundances in the 14-MeV fission of Th^{232} and U^{238} (Table V) appeared to indicate that about 70% of the delayed-neutron activity in these reactions arise from non-

[5] See also DEL MARMOL, P., NÈVE DE MEVERGNIES, M. and SPEECKE, A., "Search for delayed-neutron precursors in antimony and arsenic fission products", these Proceedings II; TOMLINSON, L., "Short-lived antimony and arsenic isotopes formed in fission", these Proceedings II.

TABLE VI

NEUTRON EMISSION PROBABILITIES, P_n, OF KNOWN NON-HALOGEN PRECURSORS

Period	Precursors	P_n (%)		Rel. standard dev.[a]			c
		obs.	calc.	Y_n	P_n^{Br}	P_n^{I}	
6 s	Rb^{92}	0.02[b]	0.4 ± 0.9	1.2	1.4	1.1	0.8 i
	Rb^{93}	0.03[b]	-0.3 ± 2.2	1.2	0.7	1.3	0.8 i
2 s	Kr^{92}	0.4[b]	12 ± 9	0.9	3	1.5	0.8 i
			20 ± 30	1.1	14	6	0.9 i
	Kr^{93}	1.3[b]	-45 ± 40	1.0			0.8 i
			-35 ± 20	0.8			0.8 u
			35 ± 20	0.8	2.4	6	0.9 i
			7 ± 20	2.1	1.7	5	0.9 u
	Sb^{135}	<1[c]	-45 ± 20	0.7			0.8 i
			- 6 ± 35	1.2	6	11	0.8 u
			-30 ± 10	0.5			0.9 i
			- 7 ± 11	2.0	2.2	3	0.9 u

[a] Relative to the standard deviations without third precursor.
[b] Estimated from data of STEHNEY and PERLOW (1961).
[c] BEMIS (1964).

halogen precursors. Firstly we tried to support this supposition by measuring which fraction of delayed-neutron activity remains in a sample after a rapid halogen separation. To check our experimental procedure, similar experiments for $U^{235}(n_{th}, f)$ were carried out that allow a comparison with the results obtained by SNELL et al. [31] and by COWAN and ORTH [32] who found that less than 20% of the activity arose from non-halogen precursors. Recently, WILLIAMS and CORYELL [33] observed 0.5 ± 0.5% contribution of non-bromine precursors to the 55-s period.

Two different separation procedures were employed:

(i) Bromide and iodide were simultaneously extracted using tri-phenyltinhydroxide (ϕ_3SnOH), introduced by BOCK et al. [34], and the aqueous phase was counted. About 98 to 99% of Br^- and I^- are extracted even from concentrated solutions of uranyl and thorium nitrate. To reduce IO_3^- and BrO_3^-, SO_2 was added. At pH~ 1, the extraction is selective, as is demonstrated in Fig. 4. The upper γ-spectrum was obtained from a halogenide extract. Then, the sample was treated with NaOH, which removes all the activity from the organic phase, and finally the halogens were removed from this aqueous phase by extracting Br_2 and I_2 into CCl_4. The lower spectrum shows no more prominent γ-lines indicating the absence of other fission

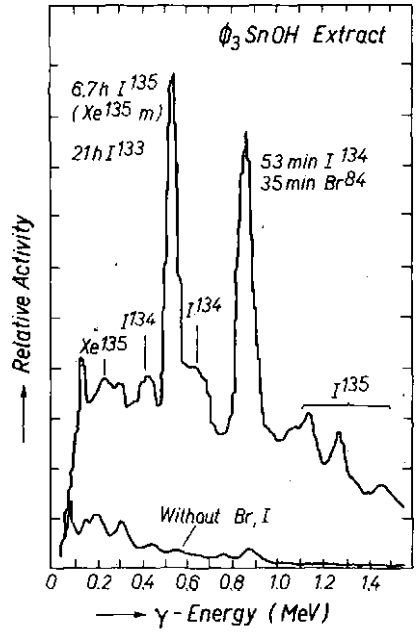

Fig. 4

Solvent extraction of halogen activities from a fission-product mixture using tri-phenyl-tinhydroxide. The upper γ-spectrum shows all the components in the organic phase, the lower spectrum shows results after bromine and iodine have been removed from the ϕ_3SnOH-fraction.

products in the original ϕ_3SnOH-phase. In some runs, exchange with solid ϕ_3SnOH was used.

(ii) Alternatively, halogens were separated by heterogeneous exchange with pre-formed silver chloride [35]. This method is less selective, because at least part of tellurium is lost on the precipitate.

Some decay curves obtained with a BF_3-counter are shown in Fig. 5, averaged from several runs. Symbols and thick lines refer to the halogen-free samples. For comparison, decay-curves of unseparated standard samples are shown as thin lines, shifted to the late part of the curves for halogen-free samples by multiplying them with the factors indicated. These factors correspond to the fraction of the 55-s period remaining. In the majority of the curves the halogen-free samples show an increased contribution of shorter lived precursors.

Initial activities of both halogen-free and unseparated samples were calculated by computer-analysis using, as a first approximation, periods found for unseparated delayed-neutron activities by KEEPIN et al. [11] and by MAKSYUTENKO [24] respectively. Table VIII gives results for $U^{235}(n_{th},f)$. Except for some runs when the fastest possible extraction was used, the various methods gave quite consistent results: about 2, 8 and 20% of the 55-, 22- and 6-s periods respectively remain after the halogen separation. It is interesting that a similar fraction of the delayed-neutron activity is exchanged with cadmium sulphide on cellulose, introduced by ZIEGLER [36].

TABLE VII

CALCULATED NEUTRON EMISSION PROBABILITIES OF SOME POSSIBLE PRECURSORS

Period	Precursors	Neutron emission probability (%) [a]			Standard deviation of Y_n [b]	Contrib. U^{235} th [c]
		3rd Prec.	Br	I		
22 s	Sn^{134}	12 ± 13	6.1 ± 1.5	4.1 ± 1.8	1.2	1 ± 1
	Te^{136}	3.0 ± 2.2	5.9 ± 1.3	3.2 ± 2.0	1.0	15 ± 10
6 s	Te^{137}	0.4 ± 3.4	4.4 ± 1.6	8.5 ± 3.4	1.2	1 ± 7
2 s	As^{85}	19 ± 7	6.6 ± 5.2	35 ± 4	0.6	18 ± 6
	Rb^{94}	4.6 ± 2.2	24 ± 2	20 ± 2	0.7	15 ± 8
	Sr^{97}	8 ± 3	26 ± 2	17 ± 2	0.5	12 ± 5
	Sr^{98}	31 ± 8	28 ± 1	15 ± 1	0.4	11 ± 3
	Cs^{142}	2.9 ± 0.7	23 ± 2	21 ± 1	0.4	15 ± 5
	Cs^{143}	10 ± 3	18 ± 3	20 ± 2	0.5	30 ± 10

[a] Calculated with c = 0.80, i, except As^{85} (c = 0.95, i).
[b] Relative to the standard deviation without the third precursor.
[c] Contribution (in percentages to period abundance in $U^{235}(n_{th}, f)$.

TABLE VIII

FRACTION OF DELAYED-NEUTRON ACTIVITY REMAINING AFTER RAPID SEPARATION OF HALOGENS: DATA FOR $U^{235}(n_{th}, f)$

Method	Runs	1st counting (s) [b]	Fraction remaining (%) [a]		
			55 s	22 s	6 s
Extraction ϕ_3SnOH (1×)	5	29	1.9	6	13
Extraction ϕ_3SnOH (1×)	2	16	6	12	18
Extraction ϕ_3SnOH (2×)	6	50	2.5	8	
Exchange AgCl	2	17	2.0	6	25
Extr. + exchange	2	27	2.0	11	10
Exchange CdS	4	17	2.2	8	6

[a] Estimated errors about 20%.
[b] Start of counting.

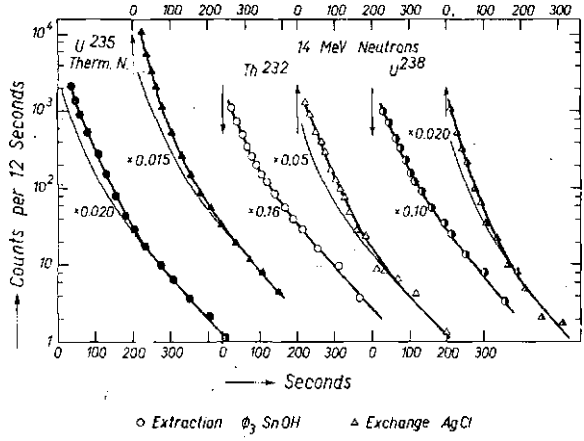

Fig. 5

Decrease of delayed-neutron activity measured after bromine and iodine were removed from the sample by extraction with triphenyl-tinhydroxide or by exchange with silver chloride. Curves for thermal-neutron fission of U^{235} and for 14-MeV-neutron fission of Th^{232} and U^{238} are shown. The corresponding curves for unseparated samples (thin lines) are shifted to the late part of the curves for halogen-free samples by multiplying with the factors given.

For 14-MeV fission, the remaining fractions of the 55- and 22-s periods are higher and depend on the separation procedure, exchange with AgCl giving the lower values (Table IX). But the fractions are far below the values of about 70% expected from the discrepancies of calculated and observed abundances. Thus, unknown precursors cannot account for the high observed abundances in fission of Th^{232} and U^{238} by 14-MeV neutrons.

3. ABSOLUTE DELAYED-NEUTRON ABUNDANCES IN FISSION OF Th^{232} AND U^{238} BY 14-MeV NEUTRONS

The results given in Section 2 lead to some doubts on the high abundances of delayed-neutron emitters reported for the fission of Th^{232} and U^{238} by 14-MeV neutrons [24, 27–29]. Unfortunately, none of these experiments has been published in detail. We are re-measuring these values, using a method similar to the "R-value" method for fission-yield determinations. The essential point is that it does not involve any absolute counting.

A few grams of U^{238} (0.3% U^{235}) or Th^{232} metal are irradiated with 14-MeV neutrons and the decay of the delayed-neutron activity is followed. Irradiation and counting are repeated several times and corresponding counting-rates are summed. From these samples, Mo^{99} is isolated as fission monitor and β-counted. To calibrate both the neutron- and β-counter, the same kind of experiment is carried out with well-investigated fission reactions, i.e. $U^{235}(n_{th}, f)$ and also $Th^{232}(n_2, f)$. Abundance data for these reference systems are taken from KEEPIN et al. [11].

Preliminary results are shown in Table X. Both calibrations give consistent results. It should be mentioned that the data obtained with $Th^{232}(n_2, f)$ as reference reaction were measured in independent runs with counters

TABLE IX

FRACTION OF DELAYED-NEUTRON ACTIVITY REMAINING AFTER RAPID SEPARATION OF HALOGENS: DATA FOR FISSION Th^{232} AND U^{238} BY 14-MeV NEUTRONS

Target	Method	Runs	1st counting (s) [b]	Fraction remaining (%) [a]		
				55 s	22 s	6 s
Th^{232}	Extraction ϕ_3SnOH (1×)	6	20	14	19	17
	Extraction ϕ_3SnOH (1×) [c]	2	45	6	20	
	Extraction ϕ_3SnOH (2×)	1	53	14	20	
	Exchange ϕ_3 SnOH [c]	2	45	6	23	
	Exchange AgCl	2	19	5	12	16
U^{238}	Extraction ϕ_3 SnOH (1×)	5	34	8	16	
	Exchange AgCl	2	13	2	6	17

[a] Estimated error about 20%.
[b] Start of counting.
[c] 50 g thorium nitrate irradiated in solution.

TABLE X

ABSOLUTE ABUNDANCES OF DELAYED-NEUTRON PERIODS FOR FISSION OF Th^{232} AND U^{238} BY 14-MeV NEUTRONS

Period	Absolute abundance (n/100 fissions)			
	Th^{232}		U^{238}	
	observed	calc. [a]	observed	calc. [a]
55 s	0.13 ± 0.02 [b]	0.12	0.050 ± 0.004 [b]	0.059
	0.13 ± 0.02 [c]			
22 s	0.37 ± 0.04 [b]	0.53	0.37 ± 0.04 [b]	0.35
	0.40 ± 0.07 [c]			
6 s	0.33 ± 0.05 [b]	0.42	0.42 ± 0.07 [b]	0.33
	0.51 ± 0.11 [c]			
2 s	~0.9	0.98	~0.6	0.70

[a] MAKSYUTENKO (1958).
[b] By comparison with $U^{235}(n_{th}, f)$.
[c] By comparison with $Th^{232}(n_2, f)$.

different to those for which $U^{235}(n_{th}, f)$ was used as reference. The abundances obtained are much lower than the reported values (Table V) but agree quite well with values calculated from the neutron emission probabilities and cumulative precursor yields derived in Section 1.

ACKNOWLEDGEMENTS

We wish to thank Professor F. Strassmann for his continued interest and the facilities he provided, and the Bundesministerium für Wissenschaftliche Forschung for financial support.

It came to the attention of the authors after writing this paper that an excellent review of delayed neutrons, as well as other fission physics data, is included in G. R. Keepin's new book, "Physics of Nuclear Kinetics" (Addison Wesley, 1965), which we cite here in view of its special pertinence to the subject of our paper.

REFERENCES

[1] PAPPAS, A. C., AECU Rpt. 2086 (1953).
[2] PAPPAS, A. C., Proc. 2nd UN Int. Conf. PUAE 15 (1958) 373.
[3] KEEPIN, G. R., J. nucl. Energy 7 (1958) 13.
[4] PERLOW, G. J. and STEHNEY, A. F., Phys. Rev. 107 (1957) 776.
[5] PERLOW, G. J. and STEHNEY, A. F., Phys. Rev. 113 (1959) 1269.
[6] STEHNEY, A. F. and PERLOW, G. J., Bull. Amer. phys. Soc. 6 (1961) 62; and private communication (1961).
[7] WAHL, A. C., FERGUSON, R. L., NETHAWAY, D. R. TROUTNER, D. E. and WOLFSBERG, K., Phys. Rev. 126 (1962) 1112.
[8] WOLFSBERG, K., Phys. Rev. (in press).
[9] SCHINDEWOLF, U., Nuclear Chemistry meeting, Geneva (Sep. 1961); and private communication (1963).
[10] KRISYUK, I. T., Atomnaja Energija 16 (1964) 146.
[11] KEEPIN, G. R., WIMETT, T. F. and ZEIGLER, R. K., Phys. Rev. 107 (1957) 1044.
[12] HERRMANN, G., Habilitationsschrift Mainz (June 1961); rev. ed. Radiochim. Acta (in press).
[13] TERRELL, J., Phys. Rev. 127 (1962) 880.
[14] APALIN, V. F., GRITSYUK, Yu. N., KUTIKOV, I. E., LEBEDEV, V. I. and MIKAELYAN, L. A., Nucl. Phys. 55 (1964) 249, IAE-Rpt. 710 (1964).
[15] KEEPIN, G. R., Nucleonics 20 8 (1962) 150.
[16] FIEDLER, J., Dissertation, Mainz (1963).
[17] GLENDENIN, L. E., CORYELL, C. D. and EDWARDS, R. R., In Radiochemical Studies: The Fission Products (CORYELL, C. D. and SUGARMAN, N., Eds.) McGraw-Hill, New York (1951) 489.
[18] KUMMEL, H., MATTAUCH, J. H. E., THIELE, W. and WAPSTRA, A. H., Bull. Amer. phys. Soc. 8 (1963) 366; and private communication (1963).
[19] FIEDLER, J. and HERRMANN, G., Z. Naturf. 18a (1963) 553.
[20] ARON, I. M., KOSTOCHKIN, O. I., PETRZHAK, K. A. and SHPAKOV, V. I., Atomnaja Energija 16 (1964) 368.
[21] COX, S., FIELDS, P., FRIEDMAN, A., SJOBLOM, R. and SMITH, A., Phys. Rev. 112 (1960) 960.
[22] COX, S. A., Phys. Rev. 123 (1961) 1735.
[24] MAKSYUTENKO, B. P., Ž. eksp. teor. Fiz. 35 (1958) 815; English translation: Soviet Phys. - JETP 35 (1958) 565.
[25] MAKSYUTENKO, B. P., Atomnaja Energija 15 (1963) 157; English translation: Soviet J. atomic Energy 15 (1964) 848.

[26] MAKSYUTENKO, B.P., Atomnaja Energija 15 (1963) 321; English translation: Soviet J. atomic Energy 15 (1964) 1042.

[27] MAKSYUTENKO, B.P., Atomnaja Energija 7 (1959) 474; German translation: Kernenergie 3 (1960) 590.

[28] McGARRY, W.I., OMOHUNDRO, R.J. and HOLLOWAY, G.E., Bull. Amer. phys. Soc. 5 (1960) 33.

[29] SHPAKOV, V.I., PETRZHAK, K.A., BAK, M.A., KOVALENKO, S.S. and KOSTOCHKIN, O.I., Atomnaja Energija 11 (1961) 539; English translation: Soviet J. atomic Energy 11 (1962) 1190.

[30] BEMIS, C.E., Ph. D. Thesis, Massachusetts Institute of Technology (1964).

[31] SNELL, A.H., LEVINGER, J.S., MEINERS, E.P., SAMPSON, M.P. and WILKINSON, R.G., Phys. Rev. 72 (1947) 545.

[32] COWAN, G.A. and ORTH, C.J., Proc. 2nd UN Int. Conf. PUAE 7 (1958) 328.

[33] WILLIAMS, E.T. and CORYELL, C.D., NYO Rpt. 10063 (1963) 34.

[34] BOCK, R., NIEDERAUER, H.T. and BEHRENDS, K., Z. analyt. Chem. 190 (1962) 33.

[35] FIEDLER, J., GROSSMANN, D., HERRMANN, G., KIEFER, W., MUNDSCHENK, H. and SCHMIDT, D., Angew. Chem. 75 (1963) 1130.

[36] ZIEGLER, M. and GIESELER, M., Z. analyt. Chem. 191 (1962) 122.

ИЗМЕНЕНИЕ ОТНОСИТЕЛЬНЫХ ВЫХОДОВ ЗАПАЗДЫВАЮЩИХ НЕЙТРОНОВ

МАКСЮТЕНКО Б.П.*
ФИЗИКО-ЭНЕРГЕТИЧЕСКИЙ ИНСТИТУТ, ОБНИНСК
СССР

Abstract — Résumé — Аннотация — Resumen

VARIATION OF RELATIVE YIELDS OF DELAYED NEUTRONS. The relative yields of delayed neutrons from uranium-238 on fission by neutrons with average energies of 1.5, 2.3, 3.8, 5.75, 6.5 and 15 MeV were measured.

The decay curves were processed on a computer by the least-squares method for set half-life values. This method makes it possible to assess, independently of accuracy of identification, the deformation of the decay curve of the delayed neutrons, and consequently to judge the changes in yield of the different groups. The rounded-off values of the half-lives used in the calculations were 55, 24, 15.5, 5.2 and 2.2 s. In a number of experiments the shorter-lived groups could not be separated because of the length of time (5.5 s) needed to switch off the ion current on the Van de Graaff accelerator.

The results are given in the form of the ratio between the yield of each group and the first (with a half-life of 55 s).

The ratio between the yields of the groups changes unevenly. Where fission is induced by neutrons in the 2.3-6-MeV energy region (the region between the "steps" in the fission cross-section), this ratio either does not change (for the groups with half-lives of 5.2 and 0.5 s) or decreases smoothly with increase in energy by from 10 to 40% (for the groups with half-lives of 24, 15.5 and 2.2 s). At an energy of 6.5 MeV (where the n, nf reaction already occurs) the ratio of the yields is sharply increased as compared to that at $E_n = 5.75$ MeV, except for the group with a half-life of 15.5 s, in which the opposite tendency is observed. There is also a sharp change in the ratio of the yields in the region of the first "step" in the fission cross-section, i.e. close to the fission threshold of uranium-238 at $E_n = 1.5$ MeV. At a neutron energy of 15 MeV a decrease in the ratio of the yields is again apparent, but we do not yet have a detailed picture for the range 7-15 MeV.

The ratio of the yields for uranium-235 and plutonium-239 in the range 0.025 eV-6 MeV follows the pattern observed for uranium-238 over the corresponding range.

VARIATION DES TAUX DE NEUTRONS RETARDES. L'auteur a mesuré les taux de neutrons retardés dans la fission de l'uranium-238 par des neutrons ayant une énergie moyenne de 1,5, 2,3, 3,8, 5,75, 6,5 et 15 MeV.

Les courbes de désintégration ont été traitées à l'aide d'ordinateurs électroniques par la méthode des moindres carrés pour les périodes prises en considération. Ce procédé permet, quelle que soit l'exactitude de l'identification, d'évaluer la déformation de la courbe de désintégration des neutrons retardés et, partant, la modification du taux des différents groupes. Lors des calculs, on a utilisé pour les périodes les valeurs arrondies suivantes: 55, 24, 15,5, 5,2 et 2,2 s. Dans plusieurs expériences, il n'a pas été possible de séparer les groupes à périodes plus courtes, en raison du délai (5,5 s) nécessaire pour interrompre de courant d'ions dans l'accélérateur Van de Graaff.

Les résultats sont indiqués sous la forme d'un rapport entre le taux de chaque groupe et celui du premier groupe (ayant une période de 55 s).

Le rapport entre les taux des groupes accuse des variations de caractère différent. Lorsque les neutrons qui provoquent la fission ont une énergie de 2,3 à 6 MeV (région située entre les «degrés» de la section efficace de fission), ce rapport reste invariable (pour les groupes à période de 5,2 et 0,5 s) ou bien il décroît régulièrement, avec l'augmentation de l'énergie, de 10 à 40% (pour les groupes à période de 24, 15,5 et 2,2 s). Pour une énergie de 6,5 MeV (là où la réaction n, nf est déjà en cours), le rapport des taux subit une brusque augmentation si on le compare à celui obtenu pour $E_n = 5,75$ MeV, sauf pour le groupe d'une période de 15,5 s

* Доклад представил Б.Д. Кузьминов

dans lequel on observe la tendance opposée. On constate également une modification brusque du rapport entre les taux dans la région du premier «degré» de la section efficace de fission, c'est-à-dire au voisinage du seuil de fission de l'uranium-238 pour $E_n = 1,5$ MeV. Pour une énergie de neutrons de 15 MeV, la diminution du rapport entre les taux devient de nouveau apparente, mais l'auteur de dispose pas encore d'une courbe détaillée pour l'intervalle de 7 à 15 MeV.

Le rapport des taux pour l'uranium-235 et le plutonium-239 dans la gamme d'énergie comprise entre 0,025 eV et 6 MeV évolue conformément à la courbe établie pour l'uranium-238 dans le domaine correspondant.

ИЗМЕНЕНИЕ ОТНОСИТЕЛЬНЫХ ВЫХОДОВ ЗАПАЗДЫВАЮЩИХ НЕЙТРОНОВ С ЭНЕРГИЕЙ. Измерены относительные выходы запаздывающих нейтронов от урана-238 при делении его нейтронами со средней энергией 1,5; 2,3; 3,8; 5,75; 6,5 и 15 Мэв.

Кривые распада обрабатывались на электронно-счетной машине методом наименьших квадратов при заданных значениях периодов полураспада. Такой метод дает возможность независимо от правильности идентификации судить о деформации кривой распада запаздывающих нейтронов, и, следовательно, судить об изменении выходов отдельных групп. Округленные значения периодов полураспада, использовавшихся в расчетах: 55; 24; 15,5; 5,2 и 2,2 сек. Более короткие группы в ряде экспериментов не могли быть выделены из-за большой (5,5 сек) длительности времени выключения ионного тока на ускорителе типа Ван де Граафа.

Результаты будут приведены в виде отношения выходов каждой из групп к первой (имеющей период полураспада 55 секунд).

Характер изменения отношения выходов групп разный. В интервале энергий нейтронов, вызывающих деление, от 2,3 до 6 Мэв (область между "ступеньками" в сечении деления) это отношение либо не меняется (для групп с периодами полураспада 5,2 и 0,5 сек), либо плавно уменьшается с ростом энергии на величину от 10 до 40% (для групп с периодами полураспада 24; 15,5 и 2,2 сек). При энергии 6,5 Мэв (там, где уже идет реакция n, nf) отношение выходов резко возрастает по сравнению с тем же при энергии нейтронов 5,75 Мэв, за исключением группы с периодом полураспада 15,5 сек, у которой наблюдается противоположная тенденция. Резкое изменение отношения выходов наблюдается и в районе первой "ступеньки" в сечении деления, т.е. вблизи порога деления урана-238 при $E_n = 1,5$ Мэв. При энергии нейтронов 15 Мэв снова заметно уменьшение отношения выходов, однако, мы еще не имеем детального хода в интервале 7—15 Мэв.

Отношение выходов для урана-235 и плутония-239 в интервале 0,025 эв—6 Мэв следует закономерности, установленной для урана-238 в соответствующей области.

MEDICION DE LOS RENDIMIENTOS RELATIVOS DE NEUTRONES RETARDADOS. El autor midió los rendimientos relativos de neutrones retardados en la fisión del uranio-238 por neutrones de las siguientes energías medias: 1,5, 2,3, 3,8, 5,75, 6,5 y 15 MeV.

Las curvas correspondientes al rendimiento se trataron en una calculadora electrónica por el método de los cuadrados mínimos para determinar valores de los períodos. Este método permite, independientemente de la precisión con que se hace la identificación, evaluar la deformación de la curva de decrecimiento de los neutrones retardados y, por ende, las variaciones en el rendimiento de los diversos grupos. Los valores redondeados correspondientes a los períodos utilizados en los cálculos fueron: 55, 24, 15,5, 5,2 y 2,2 s. En toda una serie de experimentos, los grupos de período más corto no se pudieron separar por ser mayor el tiempo (5,5 s) necesario para interrumpir la corriente iónica del acelerador Van de Graaff.

Los resultados se expresan sobre la base del rendimiento correspondiente a cada uno de los grupos y dividido por el rendimiento del primero (con un período de 55 s).

La diferencia entre las razones de rendimiento al pasar de un grupo a otro no es constante. En la región energética de los neutrones causantes de la fisión, de 2,3 hasta 6 MeV (región situada entre «los escalones» de las secciones eficaces de fisión) esta razón no cambia (para los grupos con período de 5,2 y 0,5 s), o disminuye paulatinamente al aumentar la energía, desde un 10 hasta un 40% (para los grupos con período de 24, 15,5 y 2,2 s). Para energías de 6,5 MeV (en las que también tiene lugar la reacción n, nf) la razón de los rendimientos aumenta de manera brusca en comparación con la observada cuando $E_n = 5,75$ MeV, a excepción del grupo con un período de 15,5 s, en el que se ha observado la tendencia opuesta. El cambio brusco en la razón de los rendimientos se produce también en la región del primer «escalón» de la sección eficaz de fisión, es decir, junto al umbral de fisión para el uranio-238, cuando $E_n = 1,5$ MeV. Para neutrones de 15 MeV de energía la razón de los rendimientos disminuye de manera notable; sin embargo, no se conocen los detalles para el intervalo comprendido entre 7 y 15 MeV.

La razón de los rendimientos para el uranio-235 y el plutonio-239 en el intervalo de 0,025 eV a 6 MeV sigue las tendencias observadas en el caso del uranio-238 en la región correspondiente.

Кривая распределения масс осколков при изменении энергии нейтронов, вызывающих деление, деформируется. Было бы странным полагать, что это обстоятельство не скажется на выходах осколков-родоначальников запаздывающих нейтронов и тем самым на отношениях выходов групп.

До настоящего времени были известны относительные выходы запаздывающих нейтронов при делении ряда элементов нейтронами в диапазоне энергий 0–4 Мэв и при $E_n = 15$ Мэв [1,2]. Данные первой области указывали на независимость от энергии отношения выходов групп, а при $E_n = 15$ Мэв наблюдалось их изменение в 1,5–2 раза по сравнению с низкоэнергетической областью.

Расширение диапазона энергий и повышение точности разложения кривых распада при обработке данных на электронно-счетной машине (по сравнению с ручной) позволили выявить некоторые закономерности отношения выходов групп с изменением энергии нейтронов вызывающих деление.

Рассмотрим это на примере урана-238. Нами изучены относительные выходы для этого элемента у порога деления, далее – с интервалом 2 Мэв – между первой и второй "ступеньками" в сечении деления, в середине второй "ступеньки" и при энергии 15 Мэв. Часть опытов была проведена на каскадном генераторе на толстой мишени из тяжелого льда (реакция $\mathcal{D}(d,n)He^3$, E_n 2,3 и 3,8 Мэв) и на толстой тритиевой мишени (реакция $\mathcal{T}(d,n)He^4$, E_n 15 Мэв). Другая часть – на генераторе Ван-де-Граафа: реакция $\mathcal{T}(p,n)He^3$, толстая мишень, $E_n \sim 1,6$ Мэв и реакция $\mathcal{D}(d,n)He^3$ $E_n = 5,75$ и 6,5 Мэв. Как видно, мишени были достаточно толстыми, чтобы получить приемлемую статистическую точность, и достаточно тонкими, чтобы выявить соответствующий эффект. Бо́льшие массы образцов (50–80 г) и большое пролетное расстояние от точки облучения до центра счетного блока не позволили сделать время движения образца менее 0,2 сек, поэтому группа с периодом полураспада 0,2 сек не выделялась. При работе на генераторе Ван-де-Граафа фон после выключения наблюдался в течение 5 сек, что делало бессмысленным выделение группы с периодом 0,5 сек. Все полученные кривые распада имели хорошую статистическую точность (интегральный счет 10^6 импульсов). Разложение на составляющие производилось на электронно-счетной машине при заданных периодах полураспада. Для выяснения точности такого приближения расчет одной из кривых проводился также другим методом, где одновременно определялись и относительные выходы и постоянные распада. Разница между первым и вторым вариантом расчета для постоянных распада лежала в некоторых случаях в 7-м знаке и никогда не отличалась более чем на 0,8%. Разница в относительных выходах была в пределах от 0,1% до 4%. Это показывает, что для наилучшего описания кривой уже достаточно 6–7 параметров разложения, а разложение при заданных периодах полураспада является достаточно аккуратным. Отметим еще, что везде производилось разложение "22-сек группы" на две с периодами полураспада 24 и 15,5 сек. Имеющаяся статистическая точность для этого оказывается достаточной.

Результаты для урана-238 приведены в таблице и для наглядности показаны на рисунке. Выход "55-сек группы" везде принят за единицу.

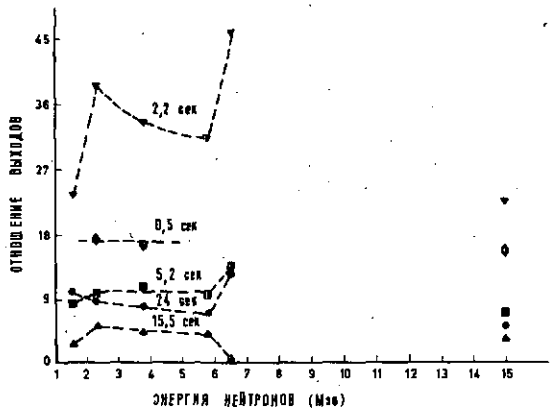

Рис.1

Изменение относительных выходов запаздывающих нейтронов.

ВЫХОДЫ ЗАПАЗДЫВАЮЩИХ НЕЙТРОНОВ ОТ УРАНА-238

T, сек	Относительные выходы	
	1,6 Мэв	2,3 Мэв
55	1	1
24	9,07 ±0,13	8,68±0,45
15,2	2,692±0,011	5,24±0,27
5,2	8,42 ±0,17	9,46±0,58
2,2	23,3 ±1,0	38,6 ±2,0
0,5		17,2 ±2,7
	3,8 Мэв	5,75 Мэв
55	1	1
24	7,82 ±0,42	6,93±0,31
15,2	4,24 ±0,23	3,81±0,15
5,2	10,46 ±0,67	9,18±0,66
2,2	33,2 ±1,8	30,69±0,78
0,5	16,3 ±2,6	
	6,5 Мэв	15 Мэв
55	1	1
24	12,31 ±0,37	4,95±0,15
15,2	0,59 ±0,23	3,37±0,14
5,2	13,3 ±0,6	7,00±0,32
2,2	45,7 ±3,4	22,2 ±1,3
0,5		15,2 ±1,5

Для большинства групп характерным является резкое изменение отношения выходов в окрестностях первой и второй "ступеньки" в сечении деления и плавное изменение – между ними. Независимо от правильности идентификации этот результат свидетельствует о деформации кривой распада и, следовательно, об изменении отношения выходов групп. Результаты измерений на других элементах – уране-235, плутонии-239 (3), – также показывают плавное изменение отношения выходов с энергией в диапазоне от 0 до 6 Мэв аналогично их поведению для урана-238 между "ступеньками".

Итак, изменение отношения выходов различных групп запаздывающих нейтронов есть факт, появление которого следовало ожидать. Теория не в состоянии в настоящее время ни рассчитать, ни предсказать хотя бы качественно направление этих изменений. Экспериментальный материал, очевидно, следует дополнить измерениями на других ядрах, особенно на тории-232, и более аккуратными измерениями абсолютных выходов. Такая работа в настоящее время продолжается и ряд новых материалов находится в обработке. Ясно, что изменение отношения выходов групп запаздывающих нейтронов связано с изменением выходов масс и зарядов осколков. Информация, полученная при изучении выходов запаздывающих нейтронов, по-видимому, будет полезной в этом отношении.

ЛИТЕРАТУРА

[1] КИПИН Г.Р. "Атомная энергия", 4 (1958)250.
[2] МАКСЮТЕНКО Б.П. ЖЭТФ, 35, 3(9)(1958).
[3] МАКСЮТЕНКО Б.П. Бюллетень информационного центра по ядерным данным (Госкомитет по использованию атомной энергии СССР) Вып.1, стр.266(1964).

DISCUSSION

(on the foregoing three papers)

P. del MARMOL: I would have thought that the increase in yields of delayed-neutron groups with bombarding energy could be explained in terms of an increasing contribution of delayed-neutron emitters from the wings and the valley of the mass distribution.

S. AMIEL: I think this is unlikely. The problem is the nearly constant group half-lives that one observes and that are almost independent of energy. It is difficult to assume that the new precursors have the same half-life values. I would personally discourage any speculation until we have more reliable data at our disposal.

C. BEMIS: I should like to emphasize a point mentioned in Dr. Amiel's survey paper. When one uses gross delayed-neutron decay data (as for example that of Keepin et al.) to predict the contributions of individual precursors to a particular half-life group, growth-decay relationships may become extremely important depending upon the periods and yields involved. In all gross decay analyses made thus far, there has been no provision for the contribution to precursors of a particular half-life group caused by growth from the parent nuclei of the precursors. In this respect, existing gross delayed-neutron decay analyses in general are not unique solutions but represent the most convenient and tractable representation of delayed-neutron characteristics for use in reactor kinetics calculations.

In effect, all analyses in which growth-decay effects are neglected (whether these be analyses of gross decay, of radiochemically separated activities, or whatever) are extrapolations of the decay portion of a growth-decay curve, and the initial activity obtained by such a process has no physical meaning, unless an appropriate correction is applied: i.e. a factor of the type $[-\lambda_2/\lambda_2-\lambda_1 A_p^0]$, where λ_1 and λ_2 are decay constants for the parent and precursor respectively and A_p^0 is the initial saturated activity of the parent, must be subtracted from the extrapolated initial activity value obtained when growth-decay effects are neglected. Of course, the cumulative fission yield of the precursor in question must be used in the final calculation.

Corrections for growth-decay effects of this sort are, however, difficult (or impossible) to make because in most cases the parent nuclei have not yet been identified and hence their yields and decay constants are unknown.

S. AMIEL: Dr. Hermann, I note that your results are completely at variance with all the published data on 14-MeV fission. You claim a decrease in yield by a factor of > 2, while the published results are ~2 larger, i.e. there is a difference of a factor of >4. You find agreement between the calculations and your experimental results. We used your P(n) values to check our calculations, as you will see in Tables IV and V of my paper. As I mentioned in the paper, the fit is fairly good for thermal fission but the disagreement with the fast fission data for U^{238} was considerable, although experimental results and fission yield data are well known and are not disputed. How do you account for this?

G. HERRMANN: As can be seen from Tables V and X of our paper, our abundances for the 14-MeV-neutron fission of U^{238} are on average smal-

ler by a factor of 3 than the values reported hitherto. Compared to the abundances for the fission of U^{238} by fission neutrons, our abundances of the 55-, 22-, 6- and 2-s periods are smaller by factors of 0.9, 0.7, 0.4 and 0.2 respectively.

The discrepancy you mention for the fission of U^{238} by fission neutrons is caused by the fact that you used much smaller chain yields and fractional yields than we did, in particular for the bromine precursors. Our calculated Y_n values are therefore much higher than yours. To give you an example, we use chain yields of 2.1 and 2.6% and fractional yields of 1.00 and 0.98 for Br^{87} and Br^{88}.

G. R. KEEPIN: I should just like to point out here that, quite independently of any theoretical considerations of fission systematics, the available radiochemical separation data and the corresponding delayed-neutron gross decay data do appear to be in general agreement, viz. the gross decay data for U^{235} fission have been fitted[1] by least-squares analysis (neglecting growth-decay effects, which are not expected to be large[2]) to the seven major periods of radiochemically separated bromine and iodine activities, plus the two shorter periods of 0.5 s and 0.2 s (5th and 6th delay groups). The resulting total fitted yields for each of the first four delayed-neutron groups agree within indicated uncertainties with the corresponding radiochemical yields (determined from least-squares analysis, again neglecting growth-decay effects). Thus gross decay data analysis and the existing chemical separation data for U^{235} provide a fairly consistent picture of delayed-neutron precursor periods and yields in U^{235} fission, the only case for which radiochemical group yield data exist.

---

[1] KEEPIN, G. R., Physics of Nuclear Kinetics, Addison Wesley (1965).

[2] The total delayed-neutron activity following an irradiation time T can be written as a sum of terms of the form

$$A_d^0(1-e^{-\lambda_d T})e^{-\lambda_d t} + A_p^0\left[\frac{\lambda_p}{\lambda_p-\lambda_d}(1-e^{-\lambda_d T})e^{-\lambda_d t} - \frac{\lambda_d}{\lambda_p-\lambda_d}(1-e^{-\lambda_p T})e^{-\lambda_p t}\right]$$

where A_d^0 and λ_d are the saturation activity and decay constant of a given delayed-neutron precursor, and A_p^0 and λ_p are the saturation activity and decay constant of the parent of that precursor.

In general $\lambda_p > \lambda_d$. For the case $\lambda_p \gg \lambda_d$ the above expression reduces to

$$(A_d^0 + A_p^0)(1-e^{-\lambda_d T})e^{-\lambda_d t}.$$

In the absence of detailed information on the yields and periods of parents of precursors, this case is normally assumed in the analysis of delayed-neutron decay data. Furthermore in the Z, A region of large delayed-neutron abundances there is generally a strong decrease in fission nuclide yield with increasing Z along a fission chain, so that the parent of a given precursor tends to be much less abundant than the precursor nuclide. This effect, and the above-mentioned period effect both tend to diminish the magnitude and importance of growth-decay corrections. (Subsequent quantitative estimates of growth-decay effects by G. Herrmann of Mainz (private communication, May 1965) based on yield and period estimates for parents of precursors in U^{235} fission confirm that growth-decay effects can indeed be neglected; at least in U^{235} fission.) In any case, a knowledge of the yields and periods of parents of precursors is clearly required before detailed growth-decay corrections can be accurately applied to the analysis of delayed-neutron decay data.

In addition we have seen again here today reasonably good agreement between experimental and calculated delayed-neutron yields in low-energy fission[3]. On the other hand, the well-known serious discrepancies between theory and experiment persist at higher neutron energies, a notable example being the case of 14-MeV-neutron-induced fission where theory and systematics predict only ~1/3 of the reported yield. Here we have a very well defined problem that should be quite amenable to direct experimental check; all experimental data thus far have indicated a strong increase (roughly a doubling) in delayed-neutron yield as one passes from low-energy fission to 14-MeV fission[4]. On the other hand, our understanding of the delayed-neutron process, as determined from fission charge and mass distributions and neutron emission probabilities, predicts a decrease in delayed-neutron yield at 14 MeV. This is due mainly to the shift in the charge-distribution curve towards stability with increasing energy of the neutron-inducing fission, which results in decreased yields of the neutron-rich fission products.

At this Symposium, measured yields in U^{238} and Th^{232} fission at 14 MeV have for the first time been reported[3] to be in agreement with theoretical predictions. This question of whether delayed-neutron yield increases or decreases at higher energies can be readily resolved by direct experimental measurements of absolute delayed-neutron yield at 14 MeV. It is suggested, and even urged, that this comparatively easy measurement be carried out independently in a few different laboratories in order to resolve this question in the near future.

[3] HERMANN, G., FIEDLER, J., BENEDICT, G., ECKHARDT, W., LUTHARDT, G., PATZELT, P. and SCHÜSSLER, H.D., "Comparison of observed delayed-neutron abundances with calculated fission yields of neutron precursors", these Proceedings II.

[4] See summary of data in AMIEL, S., "Delayed neutrons and photoneutrons from fission products", these Proceedings II.

SEARCH FOR DELAYED-NEUTRON PRECURSORS IN ANTIMONY AND ARSENIC FISSION PRODUCTS

P. del MARMOL, M. NÈVE de MEVERGNIES AND A. SPEECKE*
CEN - SCK, MOL, BELGIUM

Abstract — Résumé — Аннотация — Resumen

SEARCH FOR DELAYED-NEUTRON PRECURSORS IN ANTIMONY AND ARSENIC FISSION PRODUCTS. Antimony and arsenic fission products are isolated by a fast radiochemical procedure and their activity measured by neutron counting. Irradiations are performed at the BR2 reactor in an external beam of 1.5×10^9 n/cm^2·s and fission products of arsenic and antimony can be isolated from 2 g U^{235} with a chemical yield of about 40% in two seconds. The whole process is performed automatically.

A 2-s half-life is observed that cannot be attributed to halogen or rare gas delayed-neutron precursors and thus must be produced by arsenic or antimony. Work is in progress for finding which of these elements is responsible for the 2-s half-life.

RECHERCHE DES PRÉCURSEURS DE NEUTRONS RETARDÉS DANS L'ANTIMOINE ET L'ARSENIC PRODUITS PAR LA FISSION. L'antimoine et l'arsenic produits par la fission de ^{235}U sont isolés par une méthode de séparation radiochimique rapide et leur activité est mesurée par comptage des neutrons.

L'irradiation est effectuée dans le réacteur BR2 au moyen d'un faisceau externe de $1,5 \cdot 10^9$ n/cm^2·s, et on peut isoler en deux secondes As et Sb produits par la fission dans deux grammes de ^{235}U, avec un rendement chimique d'environ 40%. Toute l'opération est automatique.

On observe une période de 2 s, qui ne peut être attribuée à des précurseurs de neutrons retardés qui seraient des halogènes ou des gaz rares, et doit donc être produite par As ou Sb. Des expériences sont en cours afin de déterminer auxquels de ces éléments doit être attribuée cette période de 2 s.

ПОИСКИ ПРЕДШЕСТВЕННИКОВ ЗАПАЗДЫВАЮЩИХ НЕЙТРОНОВ В ПРОДУКТАХ ДЕЛЕНИЯ СУРЬМЫ И МЫШЬЯКА. Продукты деления сурьмы и мышьяка изолируются в результате быстрого химического процесса, а их активность измеряется методом счета нейтронов. Облучение проводилось на выведенном пучке реактора BR2, с потоком $1,5 \cdot 10^9$ н/см^2/сек, и продукты деления сурьмы и мышьяка можно выделить из двух граммов урана-235 с химическим выходом порядка 40% через 2 сек. Весь процесс происходит автоматически.

Наблюдается период полураспада, равный 2 сек, который нельзя отнести к предшественникам запаздывающих нейтронов, являющимся галогенами или благородными газами, и который, следовательно, должен быть произведен сурьмой и мышьяком. В настоящее время ведется работа для выяснения того, какой из этих элементов обуславливает период полураспада, равный 2 сек.

BUSQUEDA DE PRECURSORES DE NEUTRONES RETARDADOS EN LOS PRODUCTOS DE FISION DEL ANTIMONIO Y DEL ARSENICO. Los productos de fisión del antimonio y del arsénico se separan por un procedimiento radioquímico rápido y su actividad se mide por recuento neutrónico. Las irradiaciones se efectúan mediante el reactor BR2, en un haz externo cuyo flujo es de $1,5 \times 10^9$ n/cm^2·s; los productos de fisión del As y del Sb pueden separarse de 2 g de ^{235}U con un rendimiento químico del 40%, aproximadamente, en 2 s, aplicando un proceso totalmente automático.

Se ha observado un período de 2 s que no puede atribuirse a halógenos o gases nobles precursores de neutrones retardados y que, por tanto, debe corresponder al As o al Sb. Prosiguen los trabajos para averiguar cuál de estos elementos origina dicho período.

---

* Present address: Laboratory of Analytical Chemistry, Rijksuniversiteit, Gent, Belgium.

INTRODUCTION

The six groups of delayed neutron emitters found in thermal-neutron fission of U^{235}, and grouped according to their half-lives, were shown by a detailed study of their iodine and bromine components [1] to contain usually more than one delayed-neutron precursor per group (with the probable exception of 55.6 s Br^{87}, which seems to fulfil a unique group by itself).

Semi-quantitative considerations [2-5] based on neutron-binding energies, β-decay systematics and comparisons with yields of the delayed-neutron groups in other types of fission have led to the conclusion that only a fraction of the delayed-neutron precursors (d.n.p.) were known. However SUGIHARA [6], using spin considerations, concluded there were limitations to the possibility of some isotopes fulfilling the other favourable conditions of being d.n.p.

Nevertheless, if one uses the yields of halogen d.n.p. measured by PERLOW and STEHNEY [1] and if one supposes that only Br^{87} is responsible for the 55 s groups and that Br^{88} and I^{137} share the 22-s group, and any other isotope is excluded, one can easily see that more than 30% of the delayed neutron activities remain unaccounted for.

The 1.5-s Kr and 6-s Rb d.n.p. discovered in noble gases [7] have too low a yield to be the major components of the unknown activities.

Neutron-binding energies, as extrapolated by semi-empirical mass formula, and thermal-neutron fission mass yields show [2-5] that d.n.p. should be searched for with the highest likelihood of success among nuclides having a few neutrons above magic numbers (i.e. above 50 or 82 neutrons). Among the preferred elements are arsenic and antimony.

An excellent experimental tool has been provided by GREENDALE and LOVE [8] who improved the Marsh apparatus for isolating arsenic and antimony as arsine and stibine from other elements. Heating the zinc on which the acid decomposes to give nascent hydrogen resulted in fast radiochemical separations with high yields.

The present work of investigating possible d.n.p. of arsenic and antimony was based on this method.

EXPERIMENTAL PROCEDURES

The apparatus shown in Fig. 1 was mounted at the BR2 reactor at Mol to detect the short-lived arsenic and antimony fission isotopes. The part surrounded by dotted lines was enclosed in an aluminium box facing the T7-channel of the reactor so that the thermal-neutron beam, after a fast-neutron shutter was opened, could irradiate the quartz cell B. The box was surrounded by a suitable shielding.

D is an extensible rubber balloon and H a glass flask, both containing nitrogen. Flasks E and F, the latter containing drierite, can stop any splash from the solution; the drierite purified the gases from most of the iodine (carried as SbI_3). The operations proceeded as follows.

The solution to be irradiated, consisting of U^{235} (usually 1 g) and Sb^{+5} or As^{+5} carriers in solution in about 25 cm^3 of 30% H_2SO_4, was introduced in A with the electromagnetic valves V_1, V_3 and V_5 closed and valves V_2 and V_4 open; stopcocks R_1, R_2 and R_5 were open, and R_3 and R_4 were closed.

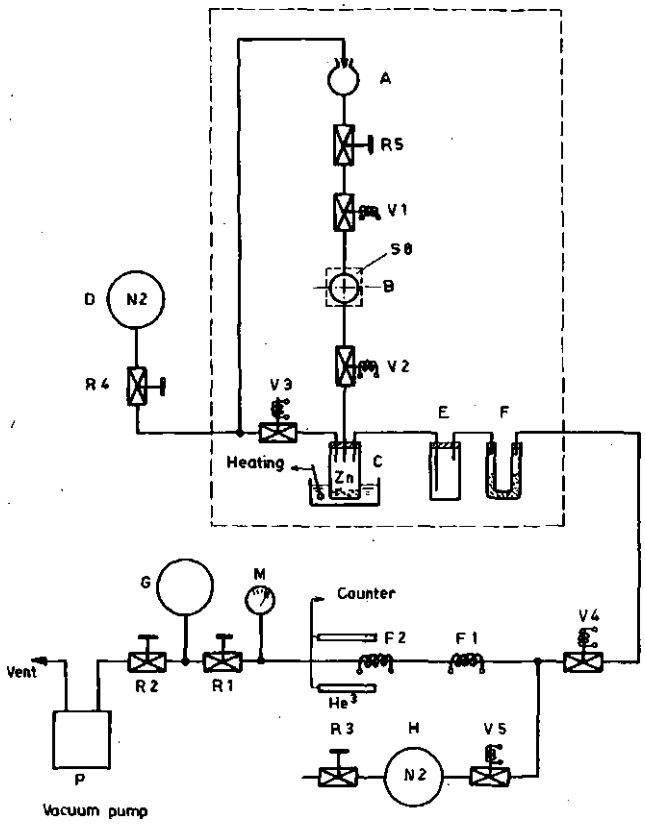

Fig. 1

Irradiation circuit

The whole apparatus was then evacuated by the vacuum pump P. When V_2 was closed and V_1 and R_4 opened the solution was pushed by the nitrogen of D into the irradiation cell B.

All further operations proceeded automatically by the preset timers. The shutter was opened and the cell B irradiated in a flux of about 1.6×10^9 n/cm^2 · s. At the end of the irradiation, the shutter was closed, V_2 opened, and the solution fell on zinc preheated by an oil bath at 100°C. AsH_3 and SbH_3 gases were sucked by the vacuum through E and F, and were partially decomposed and stopped after passing through quartz furnaces F_1 and F_2, which were heated at preset temperatures.

The gas burst was then stopped by closing V_4, and V_5 was opened for a short time (about 0.5 s) to release N_2, which rinsed residual gases from the furnaces. The activity was then counted by means of an array of 5 He_3 counters connected to a T.M.C. 400-channel multiscaler. The time intervals chosen were 0.1 s for the first 20 s and 1 s for later times.

The over-all efficiency of the counters as measured with a source of 56-s Br^{87} delayed neutrons was about 7%.

The gases were evacuated into a 5-l glass vessel G after closing R_2.

Quartz wool plugs, through which were bored 2-mm diam. holes, were placed in the middle and just behind the furnaces, the first one to permit more thorough heating of the gases and the second one to permit collection of metallic arsenic or antimony. The second furnace was surrounded by the neutron counters protected from heat by a water-cooled copper tube. The furnaces could be heated from room temperature up to 1000°C. Figure 2

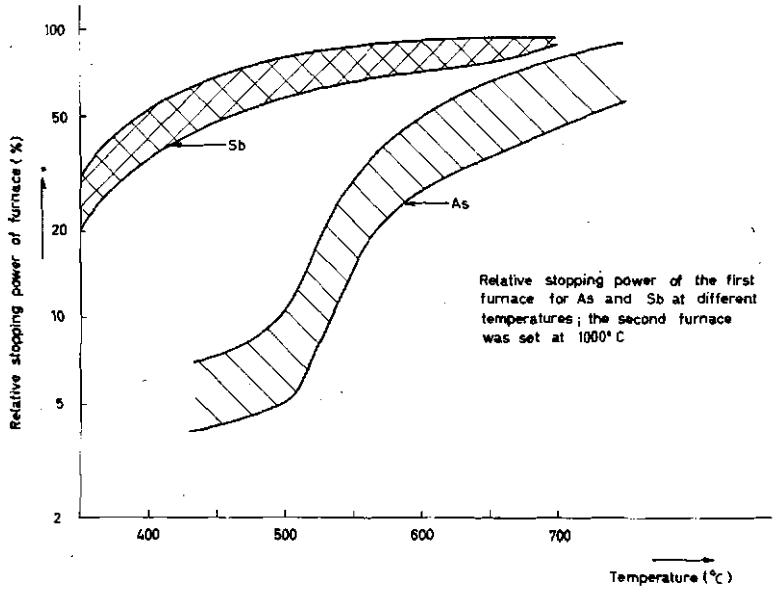

Fig. 2

Relative stopping power of the first furnace for arsenic and antimony at different temperatures; the second furnace was set at 1000°C

shows the relative stopping power of the first furnace for arsenic and antimony at various temperatures when the second furnace was set at 1000°C (i.e. yield of arsenic or antimony ceased after the first furnace with respect to the amount stopped in both furnaces). These yields were measured in the laboratory by arsenic or antimony tracers, and the spreads were caused by variations in the speed of the gas burst. In practice the fast bursts used in the reactor experiments tended to push both curves towards higher temperatures.

It can be seen that although it is difficult to separate one element from the other there are means to discriminate between the two. For instance, if the temperature of F_1 is set at 500°C and that of F_2 (surrounded by the counters) is set at 1000° C, most of the antimony should be stopped by F_1 and arsenic will be stopped after F_2. On the other hand, if F_1 is at room temperature and F_2 set at 500°C, most of the antimony will be stopped and counted while arsenic passes through.

To measure reaction yields of antimony, either a tracer of 60-d Sb^{124} was added to the carrier, or I^{132} and I^{133} coming from Sb^{132} and Sb^{133} were measured by absolute γ-counting. With arsenic it was not possible to use tracers of 26.6-h As^{76} as half-lives and γ-ray energies interfered with I^{133}

activities; it was found easier to activate the arsenic carrier stopped in the furnace after the runs.

For both elements the furnace was rinsed with boiling aqua regia, and the quartz wool plugs were added to the solution to be counted or activated.

Typical irradiation times ranged from 5 to 60 s. This was followed by a gas collection time of 2 to 5 s, and a 0.5-nitrogen rinsing. Average arsenic and antimony yields varied from 1 to 20% according to the temperature or the speed of the gas burst.

RESULTS AND DISCUSSION

Irrespective of the furnace temperatures a half-life of 2.2 ± 0.2 s was observed. Activities extrapolated to the end of irradiation were usually a few thousand counts per second. Half-lives in the 20-s range were also seen but were of too low intensity to be studied; they were possibly caused by contaminants. However, important contaminations by iodine or bromine d.n.p. as 2.7-s I^{137} were ruled out by the following arguments.

Decontamination factors for iodine are better than 10^4 and long irradiation times did not show a noticeable amount of 22-s I^{137}. For instance (Fig.3) in a run of 40-s irradiation time the observed activity extrapolated to the end of irradiation for the short half-life was 1050 counts/s. In this case no drierite was used in order to observe the activity of halogen contaminants. The initial activity of the longer component that could have a 22-s half-life was about 20 counts/s. If one uses the yields measured by PERLOW and STEHNEY [1], and if one supposes that the 1050 counts are caused by both 2.7-s I^{139} and 6-s I^{138} (Fig. 3 shows this to be very improbable) one should obtain for 22-s I^{137} an initial activity of about 900 counts. Therefore I^{139} contaminants seem to be excluded. Similar arguments can be used to reject bromine contaminants.

Table I shows the results of a few runs where antimony and arsenic yields were measured, the first by using an Sb^{124} tracer, the latter by activation.

The element responsible for the 2.2-s half-life should show a constant ratio of initial neutron activity versus yield, taking into account that experimental errors on these ratios are large (about 30%) and caused mainly by the difficulty of measuring the γ-rays of Sb^{124} and As^{76} in the presence of the I^{131}, I^{132} and I^{133} grand-daughter activities.

With antimony it can be clearly seen that this ratio increases with temperature. Thus antimony (if it is a d.n.p.) cannot solely be responsible for the 2.2-s half-life. In the case of arsenic this ratio appears to be independent of temperature and the spreads are smaller than with antimony.

As antimony is known to form hydrides, Sn^{113} (tracer and carrier) was added in an experiment. No large change in initial neutron activity was observed and the decontamination factor was better than 10^4.

If one assumes that part of the 2.2-s activity is produced by an antimony d.n.p., the ratio "initial neutron activity versus arsenic yield" tends to worsen, thus antimony seems to take no part or only to be a minor component of the 2.2-s activity. The closest half-life of a known antimony isotope would

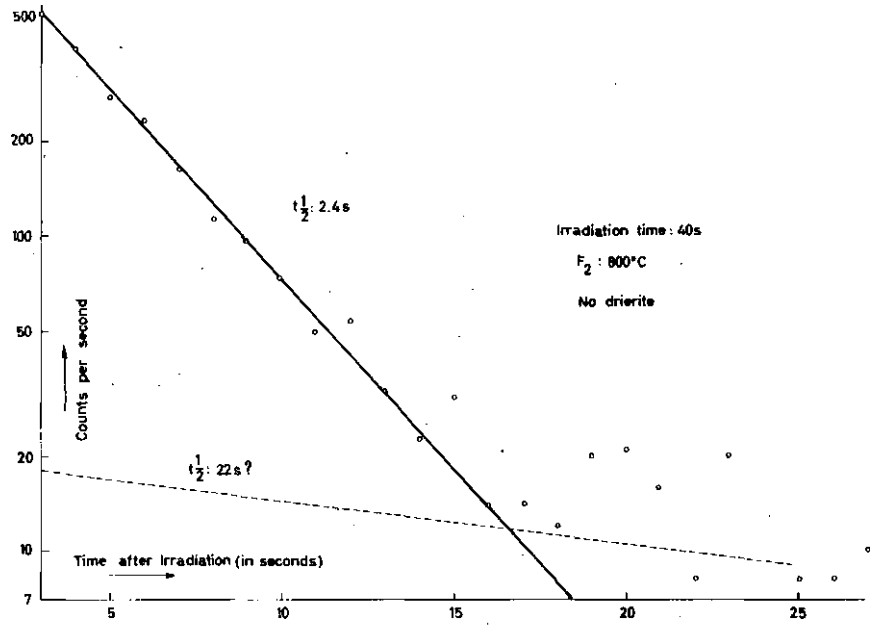

Fig. 3

Decay of the neutron activity counted after the second furnace.
No drierite was used to observe possible halogen contaminants.

be the recently discovered [9] 1.9-s Sb^{135}. The upper limit we can set at its contribution (or at the contribution of an Sb^{136} or Sb^{137} isotope of similar half-life) would be 0.3% of the total d.n.p. A neutron-branching ratio for Sb^{135} would have an upper limit of 1%.

This half-life therefore seems to be associated with arsenic of mass 85 or higher, and contributes to about 1.25% of known delayed-neutron emitters or, using KEEPIN's [2] values, to 3% of the 2.3-s group.

These yields were measured by comparison with the well-known 55-s neutron activity of a U^{235} source irradiated and counted under the same conditions.

ACKNOWLEDGEMENTS

We wish to thank Miss M. Vreys for many tests to check the stopping power of the furnaces; Mr. Vansteelandt, who was responsible of the building of the mechanical part of the apparatus and of the irradiation facilities; Mr. E. Mies, who designed and assembled the electronical part; and Mr. J. Colard for counting the tracers and iodine decay products.

One of us (P.d.M.) is grateful to Dr. A.F. Stehney, of the Argonne National Laboratory, for valuable advice on the experimental procedure.

TABLE I

RATIOS OF NEUTRON ACTIVITIES TO ANTIMONY AND ARSENIC YIELDS AT DIFFERENT FURNACE TEMPERATURES [a]

Temperature[b] (°C)	Neutron activity[c] / Yield antimony	Neutron activity[c] / Yield arsenic
400	4.3	11.8
450	5.0	9.5
450	3.2	16.3
475	6.2	7.7
550	12.9	11.6
600	9.8	13.4
1000 (F_1 at 600)	6.7	-
1000 (F_1 at 700)	12.5	12.8
1000 (F_1 at 700)	10.3	11.5

(a) In each case 1.025 g of 90%-enriched U^{235} was used.
(b) F_1 was at room temperature if not stated otherwise.
(c) Initial neutron activities are corrected to saturation and given in units of 10^2 counts/s. Yields are given in percentages.

REFERENCES

[1] PERLOW, G.J. and STEHNEY, A.F., Phys. Rev. 113 (1959) 1269.
[2] KEEPIN, G.R., J. nucl. Energy 7 (1958) 13.
[3] PAPPAS, A.C., Proc. 2nd UN Int. Conf. PUAE 15 (1959) 373.
[4] PAPPAS, A.C. and RUDSTAM, G., Nucl. Phys. 21 (1960) 353.
[5] KRISIUK, I.J., Atomnaja Energija 15 (1964) 1042.
[6] SUGIHARA, T.T., Clark University Annual Progress Rpt (1962) 49 (unpublished).
[7] STEHNEY, A.F. and PERLOW, G.J., Bull. Amer. phys. Soc. II 6 (1961) 62.
[8] GREENDALE, A.E. and LOVE, D.L., Analyt. Chem. 35 (1963) 632.
[9] BEMIS, C.E., GORDON, G.E. and CORYELL, C.D., J. inorg. nucl. Chem. 26 (1964) 213.

SHORT-LIVED ANTIMONY AND ARSENIC ISOTOPES FORMED IN FISSION

L. TOMLINSON
ATOMIC ENERGY RESEARCH ESTABLISHMENT, HARWELL, BERKS, UNITED KINGDOM

Abstract — Résumé — Аннотация — Resumen

SHORT-LIVED ANTIMONY AND ARSENIC ISOTOPES FORMED IN FISSION. The application of a new technique for the rapid separation of short-lived antimony and arsenic isotopes from fission products is described. The gamma spectra of Sb^{128}, Sb^{129} and Sb^{130} have been measured and previous observations confirmed. A new delayed-neutron activity of 2-s half-life has been detected. The experimental data indicate that this activity is due to two isotopes, one of antimony and the other of arsenic. These are tentatively assigned to Sb^{135} and one of the isotopes As^{85-87}.

RADIOANTIMOINE ET RADIOARSENIC A COURTE PÉRIODE PRODUITS PAR LA FISSION. L'auteur expose l'application d'une méthode nouvelle visant à séparer rapidement le radioantimoine et le radioarsenic à courte période des autres produits de fission. Il a mesuré les spectres gamma de ^{128}Sb, ^{129}Sb et ^{130}Sb et obtenu confirmation d'observations précédentes. L'auteur a décelé une nouvelle activité émettant des neutrons retardés et ayant une période de 2 s. Selon des données expérimentales cette activité est due à deux radioisotopes: un radioantimoine et un radioarsenic que l'auteur identifie provisoirement comme étant ^{135}Sb et l'un des radioisotopes $^{85-87}As$.

КОРОТКОЖИВУЩИЕ ИЗОТОПЫ СУРЬМЫ И МЫШЬЯКА, ОБРАЗОВАВШИЕСЯ ПРИ ДЕЛЕНИИ. Описывается применение нового метода быстрого отделения короткоживущих изотопов сурьмы и мышьяка от продуктов деления. Проведено измерение гамма-спектров сурьмы-128, 129 и 130, подтверждаются результаты предыдущих наблюдений. Отмечена активность новых запаздывающих нейтронов с периодом полураспада 2 сек. Экспериментальные данные свидетельствуют о том, что возникновение этой активности связано с двумя изотопами: изотопом сурьмы и изотопом мышьяка. В предварительном порядке предполагается, что один из них — сурьма-135, другой — один из изотопов мышьяка-85, 87.

ISOTOPOS DE PERIODO CORTO DEL ANTIMONIO Y DEL ARSENICO FORMADOS POR FISION. El autor describe la aplicación de una nueva técnica para separar rápidamente los isótopos de período corto del antimonio y del arsénico de los productos de fisión. Se han medido el espectro gamma del ^{128}Sb, ^{129}Sb y ^{130}Sb y se han confirmado las observaciones anteriores. Se ha detectado una nueva actividad neutrónica retardada cuyo período es de 2 s. Los resultados experimentales indican que esta actividad se debe a dos isótopos, uno del antimonio y otro del arsénico, que se suponen son el ^{135}Sb, y uno de los isótopos $^{85-87}As$, respectivamente.

INTRODUCTION

Information about the short-lived antimony isotopes with mass numbers greater than 129 and of the short-lived arsenic isotopes with mass numbers greater than 81 is very limited. Calculations show that antimony isotopes up to mass 137 and arsenic isotopes in the mass region 82-87 should have cumulative fission yields greater than 0.25%. To obtain nuclear data concerning these isotopes, whose half-lives range down to 1 s or less, a very rapid method of separation from fission products is necessary. In the present paper a suitable method, based on the formation of gaseous antimony

and arsenic hydrides, is described. Data on the emission of gamma rays, and neutrons from antimony and arsenic isotopes, are also presented.

EXPERIMENTAL

Apparatus

When an acid solution containing antimony and arsenic ions is electrolyzed, the gaseous hydrides of these metals are produced at the cathode. If the acid solution also contains dissolved U^{235}, and the whole system is irradiated with neutrons, then the isotopes of antimony and arsenic formed in fission should be converted into the hydride form and thus separated. An electrolytic cell that gives a high yield of these hydrides and can be operated in a nuclear reactor, as described previously [1], is shown in Fig. 1. It is

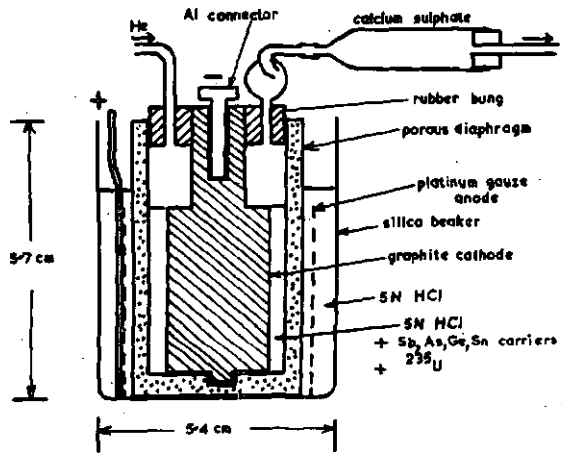

Fig. 1

Electrolytic cell operated in a reactor

now reported that both tin and germanium hydrides are also formed in this cell in appreciable yields.

The electrolytic cell was placed in a beam hole in the LIDO swimming pool reactor where a thermal-neutron flux of about 1.4×10^{11} n/cm^2 · s was available. The gaseous hydrides of antimony, arsenic, tin and germanium formed when a current of 40–50 A was passed through the cell, were swept out of the reactor along a narrow pipe with a flow of helium gas. Outside the reactor, the gases passed through a heated silica tube where the hydrides were decomposed and the metals deposited as a film. A suitable counter was placed adjacent to the deposited metals.

The same irradiation time was used in all experiments and was controlled by the starting of the reactor. The reactor core in a shut-down condition was moved into a reproducible position opposite the electrolytic cell. The reactor power was then raised at a constant rate (doubling time 22 s)

up to a maximum of 100 kW. On attaining 100 ± 1 kW, a fast shut-down occurred and the reactor power fell to below 10 kW in less than 1 s. Several minutes after shut-down, the reactor core was moved to a distant region of the pool.

Gamma spectra of antimony isotopes

A series of experiments were carried out in which gamma-spectra measurements were made on antimony separated at various times after irradiation. Using a low helium flow rate (350 ml/min), it was possible to absorb the tin hydride with a large calcium sulphate trap situated outside the reactor [1]. The silica decomposition tube was maintained at 480°C, so that only antimony hydride was decomposed, arsenic and germanium hydrides passing through unchanged. The separation time was 20 s including an electrolysis time of 10 s.

The separated antimony was counted with a 7.6-cm × 7.6-cm sodium iodide crystal covered with a 2.5-cm thick perspex beta absorber and with a methane gas flow proportional counter.

Neutron counting – experimental method

By using an electrolysis time of 4 s and a faster helium flow (1.32 l/min) the time required after the end of the irradiation to complete the separation was reduced to 6.5 s. Because of the high gas flow rate it was no longer possible to trap out tin hydride with calcium sulphate, thus a mixture of four hydrides reached the heated silica tube. Neutrons were counted with three boron trifluoride counters surrounded by paraffin moderator.

RESULTS

Gamma spectra of antimony isotopes

Sb^{129}

To test the experimental technique, Sb^{129} was separated and its gamma spectrum compared with the published spectrum [2]. Separation was delayed until 5 h after irradiation to allow the shorter-lived isotopes to decay. The first spectrum obtained indicated that Sb^{129} was the major constituent but a small amount of a shorter-lived isotope was also present. The latter had decayed when the second spectrum was measured 40 min later (Fig. 2). The published spectrum for Sb^{129} is plotted on the same energy scale for comparison. The half-life measured by beta counting was 4.7 h.

Sb^{128}

The spectrum of Sb^{128} was obtained by further analysis of the spectra obtained after a 5-h cooling period. By subtracting the second spectrum (Fig. 2) from the first, the spectrum of a short-lived component was obtained. It comprised two peaks at 0.315 and 0.75 MeV. These are assigned to Sb^{128}

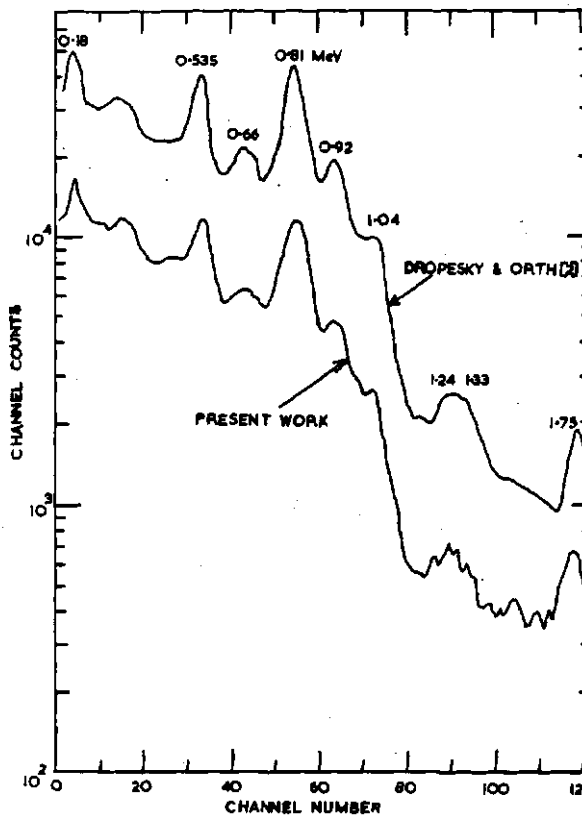

Fig. 2

Gamma spectrum of Sb^{129}

(10 min), which before separation would be in equilibrium with Sn^{128} (58 min), while all other short-lived antimony isotopes would have decayed.

Sb^{130}

Antimony isolated 2 h after irradiation consists of a mixture of Sb^{128} (10 min), Sb^{129} (4.6 h), Sb^{130} (37 min) and Sb^{131} (25 min). By allowing this mixture to decay for a sufficient period, only Sb^{129}–Te^{129} and Sb^{130} remained. As the shape of the Sb^{129}–Te^{129} spectrum was known from the previous experiment, the Sb^{130} spectrum was obtained by subtraction. It contained two major peaks at 0.20 and 0.33 MeV, in agreement with the only other published spectrum of this isotope [2]. By following the decay of these peaks and resolving the resulting decay curve the half-life was found to be 39 ± 3 min.

Delayed-neutron emission

The first experiments carried out using neutron counters resulted in initial count-rates of about 10^3/s. However, half-lives of 55, 24 and 4.5 s

obtained when the decay curves were analysed indicated that iodine and bromine isotopes were being counted. This result was surprising as the gamma-spectra studies and laboratory tests had shown no signs of halogen contamination. It was concluded that the halogens were only liberated from the cell when it was operated in a high gamma flux. Radiation-induced reactions in the aqueous hydrochloric acid would be expected to produce oxidizing agents (e.g. chlorine) and these would convert any bromide or iodide ions in solution into volatile bromine and iodine.

By adding potassium bromide and iodide as hold-back carriers together with a reducing agent (sodium thiosulphate), the formation of free halogens was suppressed and the shape of the neutron decay curve abruptly altered. The major activity (initially 350 counts/s) now had a half-life of 2 s and the minor component (initially 5 counts/s) had a half-life of about 16 s. The latter activity was so weak that no definite conclusions regarding its origin could be inferred from the data. It was assumed, however, that the 2-s activity was caused by one of the following: antimony, arsenic, germanium or tin.

To discover which of these elements was responsible, use was made of the differences in thermal stability of their hydrides. A series of experiments was carried out in which all conditions were kept constant except the temperature of the silica decomposition tube, which varied between 340 and 950°C. It was found that the half-life of the neutron activity remained constant, within the statistical errors, at 2.0±0.2 s throughout the whole temperature range. A plot of this 2-s activity versus temperature is shown in Fig. 3. These experiments were then repeated in the laboratory, but using

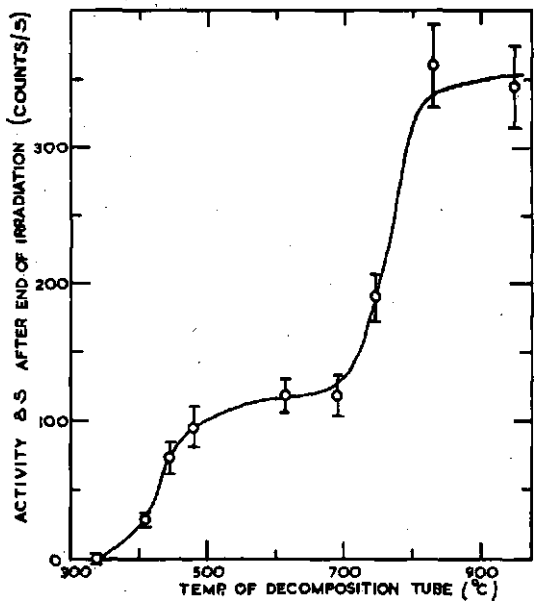

Fig. 3

Effect of the temperature of the decomposition tube on the neutron activity of the 2-s component

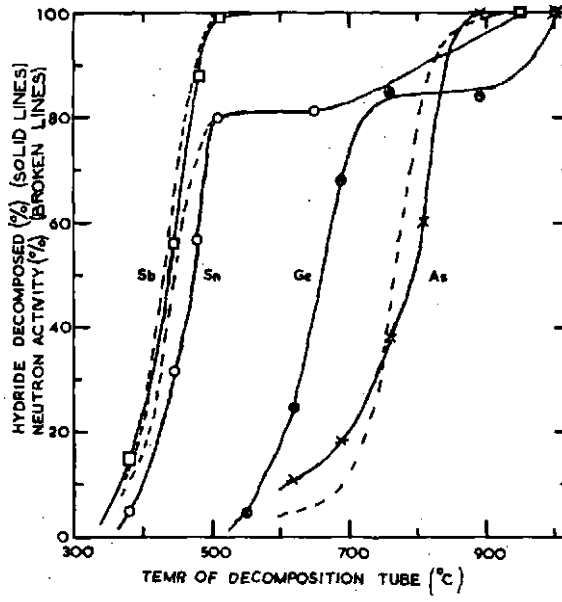

Fig. 4

Effect of temperature on the decomposition of antimony, tin and germanium hydrides (solid lines represent percentage decomposition of the hydrides; broken lines represent percentage neutron activity)

radioactive tracers of antimony, arsenic, germanium and tin so that the decomposition of their hydrides could be measured. The results are summarized in Fig. 4.

If Figs. 3 and 4 are compared it is apparent that the 2-s activity must be caused by two elements, the portion of the curve (Fig. 3) between 340 and 510°C being caused by a tin or antimony isotope, while the large increase in activity between 510 and 950°C can only be accounted for by neutrons from germanium or arsenic. The neutron activity between 340 and 510°C is plotted on a percentage basis as two broken lines in Fig. 4. One plot assumes that the neutron activity at 510°C is 100%, corresponding to cpmplete decomposition of antimony hydride, while the other takes the activity at 510°C as 80%, corresponding to 80% decomposition of the tin hydride. Unfortunately, the curves of per cent neutron activity could, within the experimental error, follow either the tin or antimony hydride decomposition curves. No positive decision can therefore be reached from these data as to which element is responsible for the neutron activity in this region.

After subtracting the portion of the curve in Fig. 3 below 510°C and plotting the remainder on a percentage basis, the neutron activity follows, with reasonable agreement, the arsenic hydride decomposition curve (Fig. 4). It is concluded, therefore, that this section of the curve is caused by an arsenic isotope.

DISCUSSION

The data obtained on the gamma spectra of antimony isotopes confirms that published previously, notably by DROPESKY and ORTH [2].

The delayed-neutron precursors, of which there appear to be at least two, both of 2-s half-life, have not previously been reported. Delayed-neutron precursors among the fission products occur at mass numbers just beyond the 50- and 82-n closed shells [3]. The nuclide must also have at least two neutrons in excess of the closed shell. The only arsenic isotopes that fit these requirements and have reasonable fission yields are As^{85}, As^{86} and As^{87}. It is concluded, therefore, that the 2-s arsenic precursor is one of these, but as none of their half-lives are known it is not possible to decide between them.

The other 2-s delayed-neutron precursor is tentatively assigned to Sb^{135} on the following evidence:

(i) The half-life of Sb^{135} has recently been measured and found to be 1.9 s [4].

(ii) Sb^{136} and Sb^{137}, the only other antimony isotopes that could be delayed-neutron precursors, have smaller calculated fission yields than Sb^{135} and will probably have shorter half-lives also.

(iii) From fission yield and nuclear considerations, Sn^{134} is the only tin isotope that could be a delayed-neutron precursor. Its half-life has been reported as 20 s [5].

Calculations have been made in an attempt to find the fractional contribution of these antimony and arsenic isotopes to the total delayed-neutron yield. Owing to errors associated with the energy dependence of the neutron counting assembly and with the thermal-neutron flux determination, the answers can only be considered as very approximate.

However, the absolute delayed neutron yields are calculated as:

$$Sb^{135} \sim 0.0002 \text{ n/fission}$$

$$As^{85\text{-}87} \sim 0.0005 \text{ n/fission.}$$

Taking the total delayed-neutron yield for the thermal-neutron fission of U^{235} as 0.0158 n/fission [6], the percentage contributions to the total delayed-neutron yield are

$$Sb^{135} \sim 1\%;\ As^{85\text{-}87} \sim 3\%.$$

Similarly, their contribution to the 2-s delayed-neutron period, again using the data of KEEPIN [6] as a basis of calculation, are

$$Sb^{135} \sim 3\%;\ As^{85\text{-}87} \sim 8\%.$$

ACKNOWLEDGEMENTS

The author is indebted to G.N. Walton for invaluable suggestions and discussions throughout this work. The assistance provided by R.G. Buckland

and J. T. McCammon during the early stages is gratefully acknowledged. Thanks are also due to G. Stroud and operators of the LIDO reactor, and members of the Electronics Division, without whose efforts this work would not have been possible.

REFERENCES

[1] TOMLINSON, L., Anal. chim. Acta. 31 (1964) 545; ibid. 32 (1965) 157.
[2] DROPESKY, B.J. and ORTH, C.J., J. inorg. nucl. Chem. 24 (1962) 1301.
[3] PAPPAS, A.C., Proc. 2nd UN Int. Conf. PUAE 15 (1958) 373; PAPPAS, A.C. and RUDSTAM, G., Nucl. Phys. 21 (1960) 353.
[4] BEMIS, C.E., GORDON, G.E. and CORYELL, C.D., J. inorg. nucl. Chem. 26 (1964) 213.
[5] GREENDALE, A.E. and LOVE, D.L., Analyt. Chem. 35 (1963) 1712.
[6] KEEPIN, G.R., Nucleonics 20 (1964) 150.

DISCUSSION

(on the foregoing two papers)

C. BEMIS: How do you eliminate halogen contamination in your experiments?

L. TOMLINSON: The decay curve is completely different from what one would expect if there were halogen contamination. Dr. del Marmol has also discussed this in his paper[1] and has arrived at the same conclusion.

C. BEMIS: Have you made tracer studies with halogen activities to check the contamination?

L. TOMLINSON: Yes, we have made tracer studies, using added bromide and iodide in the laboratory, but not in the reactor. The experiments showed very high decontamination factors for bromine and iodine, and these will be reported in a future publication.

[1] del MARMOL, P., NÈVE DE MEVERGNIES, M. and SPEECKE, A., "Search for delayed-neutron precursors in antimony and arsenic fission", these Proceedings II.

INDIRECT DETERMINATION OF HALF-LIVES OF SHORT-LIVED FISSION GASES USING A GAS FLOW METHOD

P. PATZELT AND G. HERRMANN
INSTITUT FÜR ANORGANISCHE CHEMIE UND KERNCHEMIE
DER UNIVERSITÄT MAINZ,
MAINZ, FEDERAL REPUBLIC OF GERMANY

Abstract — Résumé — Аннотация — Resumen

INDIRECT DETERMINATION OF HALF-LIVES OF SHORT-LIVED FISSION GASES USING A GAS FLOW METHOD. Since the investigation of charge distribution in nuclear fission requires the determination of primary yields of individual fission products, which in most cases are either short-lived themselves or grow from short-lived precursors, very rapid and effective separations of neighbouring members of a fission chain have to be carried out. Making use of the extremely high emanating power of certain uranium compounds, separations are performed most easily for the fission gases in more than a dozen fission-product chains. Yield calculations as well as the effective emanating power of thick target layers, however, may be influenced considerably by the half-life data of the gases. Therefore the half-lives of the krypton and xenon isotopes Kr^{89}-Kr^{93} and Xe^{137}-Xe^{143} have been determined with great precision by using a rate-of-flow method in connection with an improved charged-electrode technique.

Measurements were made via the active deposit of long-lived decay products on the electrodes. Flow-rate, irradiation time, cooling period and counting arrangements were chosen in such a way that measurements of individual daughter products became strongly favoured. In some cases, for reasons of selectivity, radiochemical separations proved to be indispensable.

Results obtained are: Kr^{89}, 3.11 ± 0.06 min; Kr^{90}, 32.1 ± 0.8 s; Kr^{91}, 8.36 ± 0.15 s; Kr^{92}, 1.92 ± 0.07 s; Kr^{93}, 1.17 ± 0.04 s; Xe^{137}, 3.87 ± 0.15 min; Xe^{138}, 14.5 ± 0.5 min; Xe^{139}, 40.4 ± 1.3 s; Xe^{140}, 13.33 ± 0.27 s; Xe^{141}, 1.70 ± 0.05 s; Xe^{142}, 1.15 ± 0.04 s; and Xe^{143}, 0.96 ± 0.02 s.

The half-lives were obtained by extrapolating the appropriate β-decay curves or decay curves of γ-peaks. The data listed are average values of a number of runs, resulting from a $w_i \sim 1/\sigma^2$ weighting procedure. All calculations were made at the computer centre of Mainz University.

DÉTERMINATION INDIRECTE DES COURTES PÉRIODES DE PRODUITS DE FISSION GAZEUX, PAR UNE MÉTHODE A COURANT GAZEUX. Etant donné que l'étude de la répartition des charges dans la fission nucléaire exige que l'on détermine les rendements primaires en produits de fission qui, dans la plupart des cas, sont eux-mêmes des produits à courte période ou proviennent de précurseurs à courte période, il faut procéder à des séparations très rapides et efficaces de membres voisins d'une série radioactive. Si l'on utilise le pouvoir d'émanation extrêmement élevé de certains composés de l'uranium, on sépare le plus facilement les produits de fission gazeux dans plus d'une douzaine de séries radioactives. Cependant, les calculs de rendement, de même que le pouvoir d'émanation effectif des cibles en couches épaisses, peuvent être sensiblement influencés par les données relatives à la période des gaz. C'est pourquoi on a déterminé avec une grande précision les périodes des isotopes du krypton et du xénon, de ^{89}Kr à ^{93}Kr et de ^{137}Xe à ^{143}Xe, par une méthode à courant gazeux et un procédé perfectionné avec électrode chargée.

Les auteurs ont effectué des mesures par l'intermédiaire des produits de désintégration à longue période déposés sur les électrodes. Le débit, le temps d'irradiation, le temps de refroidissement et les dispositions relatives au comptage on été choisis de manière que les mesures des divers produits de filiation soient grandement facilitées. Dans certains cas, des séparations radiochimiques se sont révélées indispensables pour des raisons de sélectivité.

Les résultats obtenus sont les suivants: ^{89}Kr, 3,11 ± 0,06 min; ^{90}Kr, 32,1 ± 0,8 s; ^{91}Kr, 8,36 ± 0,15 s; ^{92}Kr, 1,92 ± 0,07 s; ^{93}Kr, 1,17 ± 0,04 s; ^{137}Xe, 3,87 ± 0,15 min; ^{138}Xe, 14,5 ± 0,5 min; ^{139}Xe, 40,4 ± 1,3 s; ^{140}Xe, 13,33 ± 0,27 s; ^{141}Xe, 1,70 ± 0,05 s; ^{142}Xe, 1,15 ± 0,04 s; et ^{143}Xe, 0,96 ± 0,02 s.

Les auteurs ont obtenu les périodes en extrapolant les courbes de désintégration bêta ou de décroissance des pics gamma appropriées. Les chiffres indiqués représentent les valeurs moyennes d'un certain nombre

d'expériences et résultent d'un mode de pondération tel que $w_i \sim 1/\sigma^2$. Tous les calculs ont été effectués au centre d'ordinateurs de l'Université de Mayence.

КОСВЕННОЕ ОПРЕДЕЛЕНИЕ ПЕРИОДОВ ПОЛУРАСПАДА КОРОТКОЖИВУЩИХ ГАЗООБРАЗНЫХ ПРОДУКТОВ ДЕЛЕНИЯ С ИСПОЛЬЗОВАНИЕМ МЕТОДОВ ГАЗОВОГО ПОТОКА. Поскольку исследование распределения зарядов при ядерном делении требует определения первичных выходов отдельных продуктов деления, которые в большинстве случаев являются либо короткоживущими сами по себе, либо происходят из короткоживущих предшественников, то необходимо провести очень быстрое и эффективное разделение соседних членов цепочки продуктов деления. Используя чрезвычайно высокую эманационную способность некоторых урановых соединений, наиболее легко разделить газообразные продукты деления в более чем 12 цепочках продуктов деления. Расчеты выходов, а также эффективная эманационная способность толстых слоев мишени могут, однако, испытывать существенное влияние со стороны данных о периоде полураспада газов. Поэтому периоды полураспада изотопов криптона и ксенона ($Kr^{89}-Kr^{93}$ и $Xe^{137}-Xe^{143}$) были определены с большой точностью при использовании метода скорости потока совместно с улучшенным методом заряженного электрода.

Измерения производились посредством активного отложения долгоживущих продуктов распадах на электродах. Скорость потока, время облучения, период охлаждения и система счета избирались таким образом, чтобы измерения отдельных дочерних продуктов оказались наиболее благоприятными. В некоторых случаях в целях селективности оказались необходимыми радиохимические разделения.

Полученными результатами являются: Kr^{89} – 3,11 ± 0,06 мин; Kr^{90} – 32,1 ± 0,8 сек; Kr^{91} – 8,36 ± 0,15 сек; Kr^{92} – 1,92 ± 0,07 сек; Kr^{93} – 1,17 ± 0,04 сек; Xe^{137} – 3,87 ± 0,15 мин; Xe^{138} – 14,5 ± 0,5 мин; Xe^{139} – 40,4 ± 1,3 сек; Xe^{140} – 13,33 ± 0,27 сек; Xe^{141} – 1,70 ± 0,05 сек; Xe^{142} – 1,15 ± 0,04 сек; Xe^{143} – 0,96 ± 0,02 сек.

Периоды полураспада были получены посредством экстраполяции соответствующих кривых бета-распада или кривых распада гамма-пиков. Перечисленные данные являются средними величинами ряда опытов в результате процедуры взвешивания $w_i \sim 1/\sigma 2$. Все расчеты были произведены в вычислительном центре при университете в Майнце.

DETERMINACION INDIRECTA DEL $T_{\frac{1}{2}}$ DE LOS GASES DE FISION DE PERIODO CORTO POR UN METODO DE CIRCULACION. Dado que el estudio de la distribución de las cargas en la fisión nuclear requiere la determinación de los rendimientos primarios de los diferentes productos de fisión, que por lo general son de período corto o derivan de precursores de período corto, es preciso poder llevar a cabo separaciones muy rápidas y eficaces de los eslabones contiguos de una cadena de fisión. Aprovechando el poder de emanación sumamente elevado de ciertos compuestos de uranio, se pueden practicar con gran facilidad separaciones de los gases en más de una docena de cadenas de productos de fisión. Pero el cálculo de los rendimientos y del poder de emanación efectivo de blancos en forma de capas gruesas pueden resultar considerablemente afectados por los datos relativos al período de los gases. En consecuencia, los autores han determinado con gran precisión los períodos de los isótopos ^{89}Kr - ^{93}Kr y ^{137}Xe - ^{143}Xe aplicando un método basado en la velocidad de circulación de estos gases, junto con una técnica perfeccionada de carga de electrodos.

Efectuaron mediciones basadas en la cantidad de productos activos de desintegración de período largo depositada en los electrodos. La velocidad de circulación, el tiempo de irradiación y de enfriamiento, así como los aparatos de recuento se escogieron de forma que facilitaba grandemente la medición de cada uno de los productos descendientes. En algunos casos, fue indispensable, por razones de selectividad radioquímica, proceder a separaciones.

Los resultados obtenidos son: ^{89}Kr: 3,11 ± 0,06 min; ^{90}Kr: 32,1 ± 0,8 s; ^{91}Kr: 8,36 ± 0,15 s; ^{92}Kr: 1,92 ± 0,07 s; ^{93}Kr: 1,17 ± 0,04 s; ^{137}Xe: 3,87 ± 0,15 min; ^{138}Xe: 14,5 ± 0,5 min; ^{139}Xe: 40,4 ± 1,3 s; ^{140}Xe: 13,33 ± 0,27 s; ^{141}Xe: 1,70 ± 0,05 s; ^{142}Xe: 1,15 ± 0,04 s; ^{143}Xe: 0,96 ± 0,02 s.

Los períodos de semidesintegración se determinaron extrapolando las curvas correspondientes de desintegración beta o las curvas de atenuación de los picos gamma. Los datos enumerados representan los promedios resultantes de una serie de mediciones, a los que se ha aplicado un coeficiente de ponderación $w_i \sim 1/_{\sigma} 2$. Todos los cómputos se han realizado en el centro de cálculo electrónico de la Universidad de Maguncia.

INTRODUCTION

The investigation of charge distribution in nuclear fission has become a major subject in nuclear chemistry dealing with the fission process. This

investigation requires the determination of primary yields of individual fission products. Since in most cases these fission products are either short-lived themselves or grow from short-lived precursors by β-decay, very rapid and effective radiochemical separations of neighbouring members of a fission chain have to be carried out. Except for shielded or quasi-shielded nuclides, separations are most easily performed for the fission gases krypton and xenon in more than a dozen fission-product chains [1-3]. Making use of the extremely high emanating power of certain uranium compounds, separations may be done continuously throughout the irradiation [1-3]. Yield calculations as well as the effective emanating power of thick target layers, however, may be influenced considerably by the half-life data of the gases [2]. Therefore the half-lives of the krypton and xenon isotopes Kr^{89}-Kr^{93} and Xe^{137}-Xe^{143} have been determined with great precision by using a rate-of-flow method in connection with an improved charge-electrode technique.

In the rate-of-flow method the radioactive noble gases are swept through a tube by a suitable carrier gas of known constant flow rate. The daughter products of the decaying gases, which are being formed as positively charged recoil atoms, deposit on electrostatically charged electrodes (negative polarity). The daughter activities on the electrodes decrease exponentially with increasing distance from the uranium target so that from these activities A_i (the distance of the electrodes from the irradiated uranium sample) and the linear flow rate of the carrier gas the half-lives of the gaseous precursors may easily be calculated. Flow rate, irradiation time and cooling period after irradiation may be chosen in such a way as to emphasize relative contributions of individual daughter products, which are thereby strongly favoured. In addition, selective measurements are often achieved by counting the activity of a single gamma peak, or even following its decay.

If sufficient selectivity is not obtained the desired daughter product has to be separated radiochemically from interfering nuclides.

It should be noted that this indirect method of determining short half-lives has two main advantages over any direct procedure. Firstly, as a rule long-lived nuclides, the decay properties and mass assignment of which are very well known, are available for the measurements. Secondly, an unambiguous mass assignment for the short-lived fission gases is possible because of the genetic connection in a fission chain.

EXPERIMENTAL

A schematic diagram of the apparatus [4] used to determine the half-lives is shown in Fig. 1. The main part of it consists of a long tube into which the electrodes for collecting the recoil products are fitted at a distance of 10 cm from each other. These electrodes are stainless steel grids ($\sim$530 meshes/cm^2) to which normally a negative potential of 1 kV was applied. Under those conditions about 90% of the decay product atoms deposit on the electrodes.

Irradiations were made at a thermal flux of $\sim 2 \times 10^8$ n/cm^2.s, using a Cockcroft-Walton accelerator as a neutron source (N). About 500 mg of 90%-enriched U^{235} converted to uranyl stearate were irradiated (U).

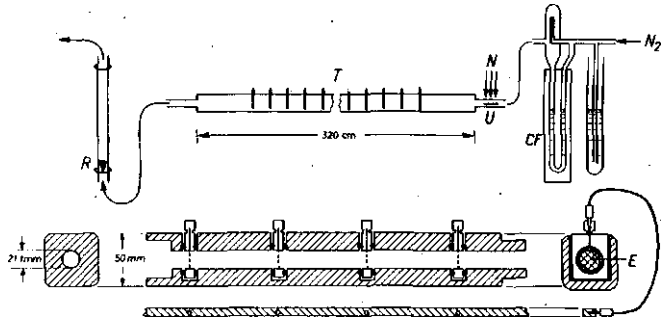

Fig. 1

Experimental setup with section through the tube

Nitrogen was used as a carrier gas for fission krypton and xenon escaping from the uranium sample. The gas velocity was measured with a capillary flow-meter before the gas entered the tube (CF and T), and with a rotameter (R) after leaving the tube, so that any loss of gas at the electrode fittings, for instance, could easily be detected[1].

Before the experiments began the flow-meters had to be calibrated very carefully. Three different calibrating procedures, which are described elsewhere [3], were used, showing that the maximum uncertainty for flow rates of about 0.5 - 15 cm/s is about 1.5%. Flow rates in this range proved to be most convenient for determining half-lives from 3 min down to 1 s.

EVALUATION

Half-lives of Kr^{89}, Xe^{137}, Xe^{138}, Xe^{140} and Xe^{141} (when measuring Ce^{141} daughter) have been obtained from the appropriate single-component decay curves by fitting a straight line to the ln A_j (method of the weighted ordinates). Since in the original counting data the activity appears as a function of the distance from the target, a transformation of distance into time equivalent must either be made before the analysis, or the half-life is even more easily calculated afterwards from the equation

$$T_{\frac{1}{2}}(s) = \frac{r^2 \pi X_{\frac{1}{2}}}{u},$$

where r is the radius of the tube, $X_{\frac{1}{2}}$ the distance at which the activity has decreased to its half-value, and u the flow rate in cm^3/s.

The half-lives of Kr^{90}, Kr^{91}, Kr^{92}, Kr^{93}, Xe^{141} (measuring La^{141} daughter), Xe^{142} and Xe^{143} had to be determined from complex decay curves of activity/electrode versus time. A least-squares method of interpolation by a sum of exponentials was used in calculating the initial intensities A_{ij}[2] and standard deviations σ_{ij}[2]. The standard deviations were in most cases

[1] A loss of gas would naturally give rise to erroneous half-lives.

[2] Denoting activity and standard deviation of the ith component and the jth electrode respectively.

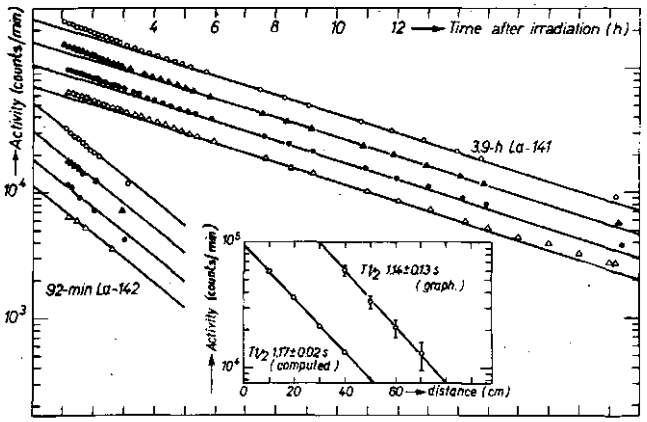

Fig. 2

Determination of half-life of Xe^{142} from lanthanum decay curves

of the order of $\leqslant 1\%$, differing by no more than a factor of 2 from each other for a given component. So the A_j could be treated as data points of equal statistical accuracy. Again a straight line was fitted to the ln A_j, thus giving the half-life of the gaseous precursor along with its standard deviation.

Figure 2 shows a graphical analysis of the system La^{141}/Ce^{141}-La^{142}. The resulting error for the half-life of Xe^{142}, however, is much smaller when using the least-squares method for computation of the half-life.

All calculations were made on the SIEMENS 2002 computer at Mainz University.

RESULTS

The results obtained are summarized in Tables I and II. The half-lives listed are always averaged values of a number of runs. They result from a $w_i \sim 1/\sigma^2$ weighting procedure, where σ is the standard deviation of a single determination. If not indicated otherwise the errors given are mean errors of the average value (Gauss) allowing for a 1.5% maximum uncertainty of gas-flow measurement by propagation of errors. In some cases the half-lives are in excellent agreement with data from literature. Differences compared with former half-life data are negligible, particularly for the relatively long-lived isotopes except for Xe^{138}, which until recently was considered to decay with a half-life of 17 min [15]. From the indirect measurement using the gas-flow method we find 14.8 ± 0.7 min. Because of the limitation of the indirect method at extremely low flow rates[3] necessary to determine half-lives longer than 10 min, the half-life of this nuclide was also measured directly by gamma-spectrometry. Xe^{138} has four prominent gamma-peaks [6]. For two of them, at 1.78 and 2.01 MeV, there are no serious interferences to be expected from the lines of 32.2-min Cs^{138} daughter.

[3] For a typical flow rate of ~0.15 cm/s the relative error is about ± 7%.

TABLE I

HALF-LIVES OF KRYPTON ISOTOPES

Mass number	Half-life	Descendant determined	Procedure[a]	Literature data[b]
89	3.11 ± 0.06 min	Sr^{89} (50.5 d)	β	3.18 min [9]
				2.6 min [10]
90	32.1 ± 0.8 s	(Sr^{90}) Y^{90} (64 h)	chem., β	33 s [9, 11, 12]
91	8.36 ± 0.15 s	Sr^{91} (9.7 h)	γ tot.	9.8 s [10]
	8.2 ± 0.3 s	Y^{91} (58 d)	chem., β	10 s [9]
92	1.92 ± 0.07 s	Sr^{92} (2.7 h)	chem., γ 1.37	3 s [10]
93	1.17 ± 0.04 s	Y^{93} (10 h)	chem., β	2 s [10]
			γ 0.26, 0.94	
94	⩽ 1 s	Y^{94} (20 min)	chem., β	1.4 s [10]

[a] Denoting: β: total β-rays counted; γ tot.: total γ-radiation counted; γ 1.37: selective counting of 1.37-MeV γ-rays; chem.: radiochemical separation of descendant before counting

[b] References in brackets

TABLE II

HALF-LIVES OF XENON ISOTOPES

Mass number	Half-life	Descendant determined	Procedure[a]	Literature data[b]
137	3.87 ± 0.15 min	Cs^{137} (30 a)	chem., γ 0.66	3.9 min [15,16]
138	14.8 ± 0.7 min[c]	Cs^{138} (32.2 min)	γ 1.44	17 min [5]
	14.5 ± 0.5 min[c]		direct counting of Xe^{138}, γ 1.78 and γ 2.01	14.0 min [7]
139	40.4 ± 1.3 s	Ba^{139} (85 min)	γ 0.15	41 s [10]
140	13.33 ± 0.27 s	Ba^{140} - La^{140} (12.8 d)	γ tot.	16 s [10]
141	1.69 ± 0.10 s	Ce^{141} (32.5 d)	chem., γ 0.145	1.7 s [11,12]
	1.71 ± 0.03 s	La^{141} (3.9 h)	chem., β	
142	1.18 ± 0.04 s	La^{142} (92 min)	chem., β	~1.5 s [13]
	1.15 ± 0.04 s		chem., γ 0.63	
143	0.96 ± 0.02 s	Ce^{143} (33 h)	chem., β	1 s [10]
	1.1 ± 0.3 s		chem., γ 0.036/0.145	

a Denoting: β: total β-rays counted; γ tot.: total γ-radiation counted; γ 1.37: selective counting of 1.37-MeV γ-rays; chem.: radiochemical separation of descendant before counting

b References in brackets

c Mean error of a single determination

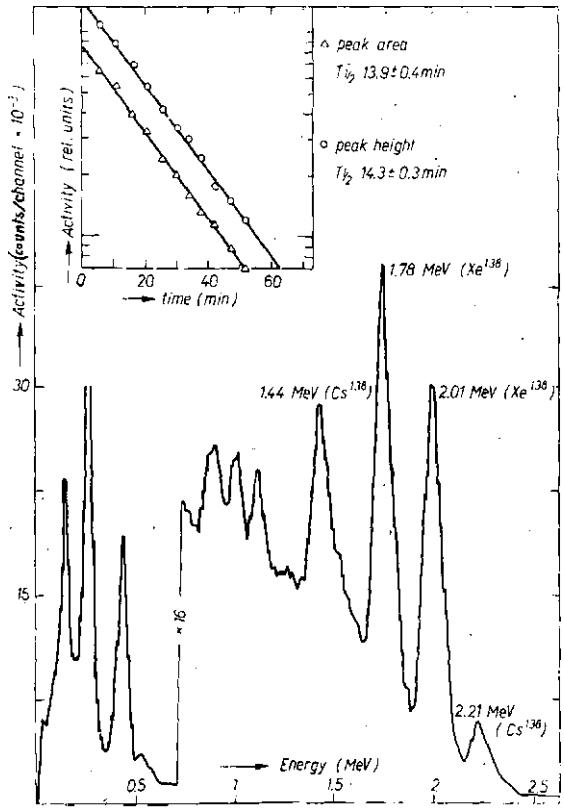

Fig. 3

Gamma spectrum of Xe^{138} and decay of 2.01-MeV peak

As is shown in Fig. 3 the 2.01-MeV peak decays with roughly a half-life of 14 min, thus confirming the value recently published by CLARKE and THODE [7]. A somewhat longer half-life (~ 15 min) was found for the decay of the 1.78-MeV peak, probably caused by a small background of Cs^{138}. In Table II a mean value is given for the decay of both peaks, although the half-life for that of the 2.01-MeV line seems to be more reliable.

Major deviations from literature data are encountered in the short-lived krypton isotopes particularly; e.g. Kr^{92} and Kr^{93}. Only an upper limit of Kr^{94} half-life may be given as yet. The very low cumulative yield of this nuclide [2] and consequently a very low intensity of 20-min Y^{94} daughter in the presence of bulk activity Y^{92}, Y^{93} and small amounts of Y^{91} makes the measurement of the half-life rather difficult. For similar reasons the half-lives of the isotopes Kr^{95} and Xe^{144}, or even of heavier nuclides, are still missing.

From decay systematics of neutron-rich krypton and xenon isotopes (Fig. 4) one expects these half-lives to be shorter than 1 s. Nevertheless, they should be accessible to determination using the apparatus described above. Experiments will be made as soon as the reactor at Mainz University, with its higher neutron flux, will have begun operation.

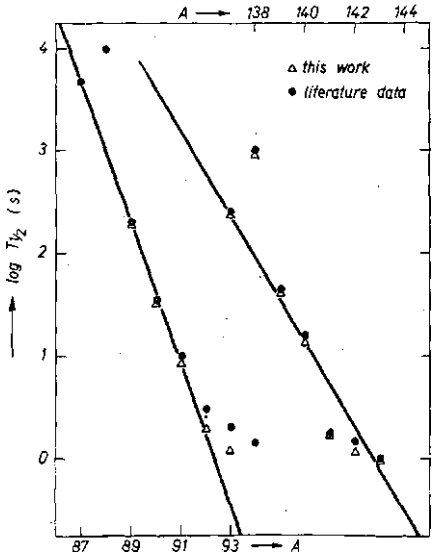

Fig. 4

Decay systematics of neutron-rich krypton and xenon isotopes - log $T_{\frac{1}{2}}$ = f (mass number)

DISCUSSION

From a more theoretical point of view it seems to be interesting that linear functions log $T_{\frac{1}{2}}$ versus mass number are obtained over a wide range of half-lives, and that obviously no distinction needs to be made between even and odd masses as, for example, in the ANDERSSON systematics [8].

From Fermi β-decay theory one would expect a linear relationship only for isotopes of constant ft-value. Therefore only β-emitters of the same type of transition would reveal the linear trend. There is, however, reason to suppose that allowed transitions may predominate. The fact that the linear trend does show up may be due to the very high disintegration energy [14] of all the isotopes involved here. Differences in the relative contributions of various β-decay branches of the isotopes compared will be "wiped out" to some extent if the decay energy is high in comparison with the spacing of the levels populated by the β-decay.

Two nuclides not obeying the rule of linearity are 50 + 2 n Kr^{88} and 82 + 2 n Xe^{138}, the true half-lives of which are 10 times longer than the expected values from the systematics. Maximum deviations from linearity of other half-lives do not exceed a factor of 3 for Kr^{93} and Xe^{141}. Except for Xe^{142}, the new half-lives fit the straight lines better than corresponding data taken from literature (see Fig. 4).

REFERENCES

[1] WAHL, A.C., J. inorg. nucl. Chem. 6 (1958) 263.

[2] WAHL, A.C., FERGUSON, R.L., NETHAWAY, D.R., TROUTNER, D.E. and WOLFSBERG, K., Phys. Rev. 126 (1962) 1112.

[3] PATZELT, P., Dissertation, University of Mainz, (to be submitted).
[4] RODENBUSCH, H. and HERRMANN, G., Z. Naturf. 16a (1961) 577.
[5] GLASOE, G.N. and STEIGMAN, J., Phys. Rev. 58 (1940) 1.
[6] THULIN, S., Ark. Fys. 9 (1955) 137.
[7] CLARKE, W.B. and THODE, H.G., Canad. J. Phys. 42 (1964) 213.
[8] ANDERSSON, G., Nucl. Phys. 24 (1961) 666.
[9] KOFOED-HANSEN, O. and NIELSSEN, K.O., Phys. Rev. 82 (1951) 96; and Kgl. Danske Vid. Selsk., Mat. Fys. Medd. 26, No. 7 (1951).
[10] DILLARD, C.R., ADAMS, R.M., FINSTON, H. and TURKEVICH, A., in Radiochemical Studies: The Fission Products (CORYELL, C.D. and SUGARMAN, N., Eds.) New York (1951) 624.
[11] OVERSTREET, R. and JACOBSON, L., in Radiochemical Studies: The Fission Products (CORYELL, C.D. and SUGARMAN, N., Eds.) New York (1951) 621.
[12] KATCOFF, S. and GOLDSTEIN, A., Rpt. LA-548 (1946).
[13] WOLFSBERG, K., NETHAWAY, D.R., MALAN, H.P. and WAHL, A.C., J. inorg. nucl. Chem. 12 (1960) 201.
[14] WAHLGREN, M.A. and MEINKE, W.W., J. inorg. nucl. Chem. 24 (1962) 1527.
[15] SUGARMAN, N., J. chem. Phys. 17 (1949) 11.
[16] HOLM, G.B., FÄGERQUIST, U. and BERGSTROM, I., Phys. Lett. 6 (1963) 324.

RECENT EXPERIMENTS ON THE BETA ACTIVITY OF FISSION PRODUCTS FROM THE THERMAL-NEUTRON FISSION OF U^{233}, U^{235} AND Pu^{239}

H. J. SPECHT AND H. SEYFARTH
PHYSIK-DEPARTMENT DER TECHNISCHEN HOCHSCHULE MÜNCHEN,
MUNICH, FEDERAL REPUBLIC OF GERMANY

Abstract — Résumé — Аннотация — Resumen

RECENT EXPERIMENTS ON THE BETA ACTIVITY OF FISSION PRODUCTS FROM THE THERMAL-NEUTRON FISSION OF U^{233}, U^{235} AND Pu^{239}. The build-up of beta-activity of fission products from the low-energy fission of U^{233} and U^{235} has been measured as a function of the time t after starting the irradiation of the fissionable material with thermal neutrons. By differentiating the beta-activity divided by the constant fission product rate one obtains the mean beta-decay rate $\beta(t)$ per fission as a function of the time t after fission. The uranium targets were mounted within a 4π proportional counter, coincident conversion electrons and γ-rays being thereby eliminated. The background of fast neutrons and γ-rays was strongly reduced by using a neutron beam tube with a liquid nitrogen-cooled bismuth single crystal filter. The fission product rate was measured with the same counter.

The measurements cover the time interval from 0.01 s to 10 h. The results are compared with other experimental data and existing theories. The total number of beta-decays per fission was found to be 5.25 ± 0.2 and 5.93 ± 0.2 for U^{233} and U^{235} respectively compared with theoretical values of 5.27 and 6.10 respectively.

RÉCENTES EXPÉRIENCES SUR L'ACTIVITÉ BÊTA DES PRODUITS DE LA FISSION DE ^{233}U, ^{235}U et ^{239}Pu PAR DES NEUTRONS THERMIQUES. Les auteurs ont mesuré l'activité bêta cumulative des produits de la fission de ^{233}U et ^{235}U à basse énergie, en fonction du temps t comptés à partir du début de l'exposition des matières fissiles aux neutrons thermiques. En différenciant et en divisant par la vitesse constante de formation des produits de fission on obtient la vitesse moyenne de désintégration $\beta(t)$ par fission en fonction du temps t après la fission. Les cibles d'uranium avaient été montées à l'intérieur d'un compteur proportionnel 4π, ce qui a permis d'éliminer les rayons gamma et les électrons de conversion coïncidents. Le bruit de fond des neutrons rapides et des rayons gamma a été considérablement réduit par l'utilisation d'un canal à faisceau de neutrons muni d'un filtre à monocristal de bismuth refroidi à l'azote liquide. La vitesse de formation des produits de fission a été mesurée à l'aide du même compteur.

Les mesures couvrent l'intervalle de temps compris entre 0,01 s et 10 h. Les auteurs comparent les résultats des mesures à d'autres données expérimentales et aux théories existantes. Ils ont constaté que le nombre total de désintégrations β par fission était égal à $5,25 \pm 0,2$ et $5,93 \pm 0,2$ pour ^{233}U et ^{235}U, respectivement, contre des valeurs théoriques de 5,27 et 6,10 respectivement.

НЕДАВНИЕ ЭКСПЕРИМЕНТЫ ОТНОСИТЕЛЬНО БЕТА-АКТИВНОСТИ ПРОДУКТОВ ДЕЛЕНИЯ ПРИ ДЕЛЕНИИ УРАНА-233, УРАНА-235 И ПЛУТОНИЯ-239 ПОД ДЕЙСТВИЕМ ТЕПЛОВЫХ НЕЙТРОНОВ. Создание бета-активности продуктов деления при делении урана-233 и урана-235 под действием малой энергии измерялось как функция времени t после начала облучения мишени делящегося материала с помощью тепловых нейтронов. Путем дифференцирования бета-активности, разделенной на постоянную скорость продуктов деления, можно получить основную скорость бета-распада $\beta(t)$ на деление как функцию времени t после деления. Урановая мишень была установлена внутри 4π пропорционального счетчика. Поэтому исключались совпадающие электроны преобразования и гамма-лучи. Фон быстрых нейтронов и гамма-лучей был существенно уменьшен путем использования трубки нейтронного пучка вместе с отдельным кристаллическим фильтром из висмута, охлаждаемого жидким азотом. Тем же самым счетчиком была замерена плотность продуктов деления.

Измерения охватывали промежутки во времени от 0,01 сек до 10 часов. Результаты измерений сравниваются с другими экспериментальными данными и существующими теориями.

Найдено общее количество бета-распадов на деление 5,25 ± 0,2 для урана-233 и 5,93 ± 0,2 для урана-235 по сравнению с теоретическими величинами в 5,27 и 6,10 соответственно.

EXPERIMENTOS RECIENTES SOBRE LA ACTIVIDAD BETA DE LOS PRODUCTOS DE LA FISION DEL ^{233}U, ^{235}U Y ^{239}Pu, INDUCIDA POR NEUTRONES TERMICOS. Los autores midieron la acumulación de actividad beta proveniente de los productos de la fisión de ^{233}U y ^{235}U a baja energía, en función del tiempo t transcurrido desde el comienzo de la irradiación del material fisionable con neutrones térmicos. Diferenciando la actividad beta dividida por el índice constante de formación de productos de fisión, se obtiene el índice medio de desintegraciones beta $\beta(t)$ por fisión, en función del tiempo t transcurrido desde la fisión. Los blancos de U se montaron en el interior de un contador proporcional 4π. Por consiguiente, se eliminaron los electrones de conversión coincidentes con rayos γ. La actividad de fondo debida a los neutrones rápidos y a los rayos γ se redujo acentuadamente utilizando un tubo de haz neutrónico con un filtro preparado con un monocristal de bismuto enfriado mediante hidrógeno líquido. El índice de formación de productos de fisión se midió con el mismo contador.

Las mediciones abarcan el intervalo de tiempo 0,01 s hasta 10 h. Los resultados se comparan con otros datos experimentales y con las teorías existentes. El número total de desintegraciones beta por fisión fue 5,25 ± 0,2 y 5,93 ± 0,2 para el ^{233}U y el ^{235}U, respectivamente, en tanto que los correspondientes valores teóricos son 5,27 y 6,10.

INTRODUCTION

The charge density of the fragments produced by nuclear fission is smaller than that of stable nuclei with equal mass. In a short time following fission, several neutrons are emitted from the highly excited fragments. The remaining neutron excess is removed by several beta decays. For U^{235} the mean beta decay rate per fission $\beta(t)$ as a function of the time t after fission has been calculated by various authors [1–7]. These calculations are most reliable for times of more than 1 h where the half-lives of the long-lived fission products are known. The results of the calculations differ widely for the first hour after fission. For such short times, assumptions have to be made about the primary charge distribution, the structure of the mass valley, the relation between half-life and beta-decay energy and the average γ-energy per decay [7]. Apart from one early experiment [8] there are only two measurements [9, 10] of the beta-decay rate of U^{235} fission products for times smaller than one hour. In view of the discrepancies between these data and the theoretical values it seemed necessary to repeat the measurements in a refined form, including the shortest possible half-lives of ~0.1 s, and to extend them to other fissionable isotopes for which new calculations exist [7]. Experiments on U^{233} and U^{235} are here reported covering the time interval from 10^{-2} s to 10 h. Experiments on Pu^{239} are being prepared.

METHOD

A direct measurement of the beta-decay rate $\beta(t)$ is possible using a pulsed reactor or fast rabbits in order to get irradiation times small compared to the shortest possible half-lives of the beta-emitters. The decay rate can be determined indirectly by measuring the built-up beta-activity of a source in which fission fragments are produced at a constant rate [9,

10]. At a time T, the mean beta-decay rate of a fragment generated at a time t' amounts to $\beta(T-t')$. Then at the time T, after starting the irradiation of the fissionable material with thermal neutrons, a total beta-activity b(T) will be measured given by the expression

$$b(T) = N \cdot \int_0^T \beta(T-t')dt' = N \cdot \int_0^T \beta(t)dt$$

where N denotes the constant fission rate. The beta-activity b(T) divided by the constant fission product rate N is equal to the number of beta-particles per fission that have been released at a time T after fission. By differentiating one obtains the mean decay rate $\beta(t)$ as a function of time after fission. The total number of beta-particles per fission is given by

$$\int_0^\infty \beta(t)dt = \int_0^T \beta(t)dt + \int_T^\infty \beta(t)dt.$$

The first term of the sum is measured while the second can be calculated exactly for $T > 1$ h from the known half-lives of the long-lived fission products.

EXPERIMENTAL ARRANGEMENT

Figure 1 shows the experimental setup. A methane-flow 4π proportional counter with two wires is used to measure the beta-activity built-up. In this way coincident γ-rays and conversion electrons are eliminated. The target, mounted in the centre of the counter, consists of two layers of uranium-acetate (0.5 mg/cm^2) enriched to about 98% and electrosprayed on to both sides of a 2.7 mg/cm^2 aluminium foil. The thermal-neutron beam traverses the counter through thin windows of 1 mg/cm^2 mica to avoid activation of the counter material. The constant fission rate can be measured without any background by discriminating against the high α-activity of the active material with a single channel analyser. To count β-particles at a correspondingly higher voltage the target is sandwiched between two 3.7 mg/cm^2 mica foils to absorb the fission products and α-particles, and to get a true 4π geometry for all β-particles. The background of fast neutrons and γ-rays in the β-plateau of the counter is strongly reduced by using a liquid-nitrogen-cooled bismuth single crystal filter in the neutron beam. At the end of the beam tube the thermal-neutron flux amounts to 4×10^6, the fast neutron flux to 10^3, and the γ-flux to less than 10^3 compared with values of 5×10^{12}, 6×10^{11} and 10^{13} near the reactor core (n/cm$^2 \cdot$ s). The total background of the counter was of the order of 1.5×10^3/s compared with a measured beta activity of the order of 3×10^4/s after 1 h irradiation.

The time-dependence of the beta-activity built-up is measured in the following way. A shutter of 0.5 mm Cd placed between the end of the beam tube and the proportional counter is operated by a magnet and can be opened within a time of approximately 0.01 s. At the beginning of a cycle the shutter is closed. If a full period of the measurement is taken as 100, then at the Time 0 a timer described elsewhere [11] triggers the time-to-pulse-height

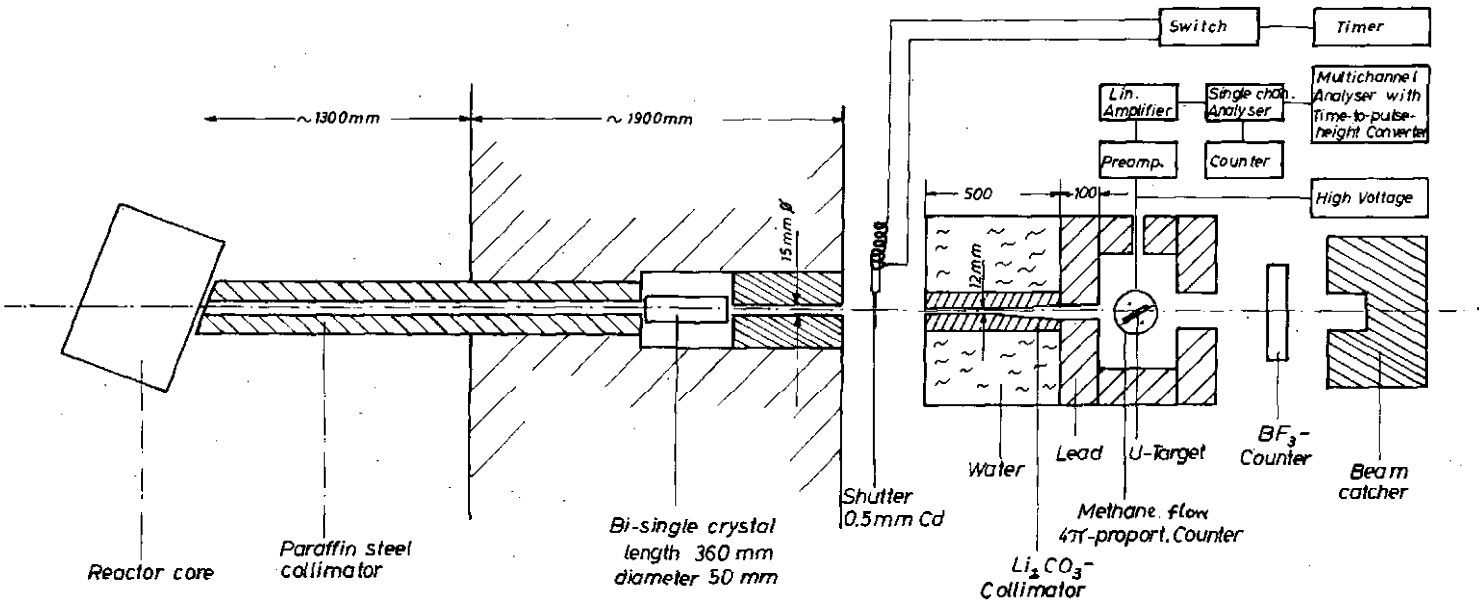

Fig. 1

Experimental arrangement

converter to a TMC 1000-channel-analyser and the background is measured. At Time 1 a second signal from the timer opens the shutter and the beta activity of the fission fragments produced is measured. At Time 11 a third signal closes the shutter. The activity then decreases towards background level and at Time 100 the period is automatically repeated. Period times of 1, 10 and 100 min corresponding to 0.01, 0.1 and 1 s/channel may be chosen. For longer irradiation times the activity is measured directly by a simple scaler. The constancy of the neutron flux can be controlled by a BF_3 proportional counter.

After opening the shutter the measured intensity of the background immediately increases more than two-fold. This jump is well defined and may be easily be distinguished from the time-dependent beta activity following the jump. The increased background is caused mainly by the prompt radiation connected with fission, i.e. neutrons, γ-rays, and conversion electrons.

RESULTS

The results of the measurements performed up to now are given in Figs. 2-4. Figure 2 shows the mean number of beta-particles $\int_0^T \beta(t)dt$ from the low-energy fission of U^{233} and U^{235} as a function of the irradiation time, i.e. the time T after fission. The dotted lines have slope 1 corresponding to a constant decay rate. The number of beta particles emitted within 10 h after fission is found to be 3.5 ± 0.2 and 4.2 ± 0.2 for U^{233} and U^{235} respectively. The average number of beta particles released at times greater than 10 h has

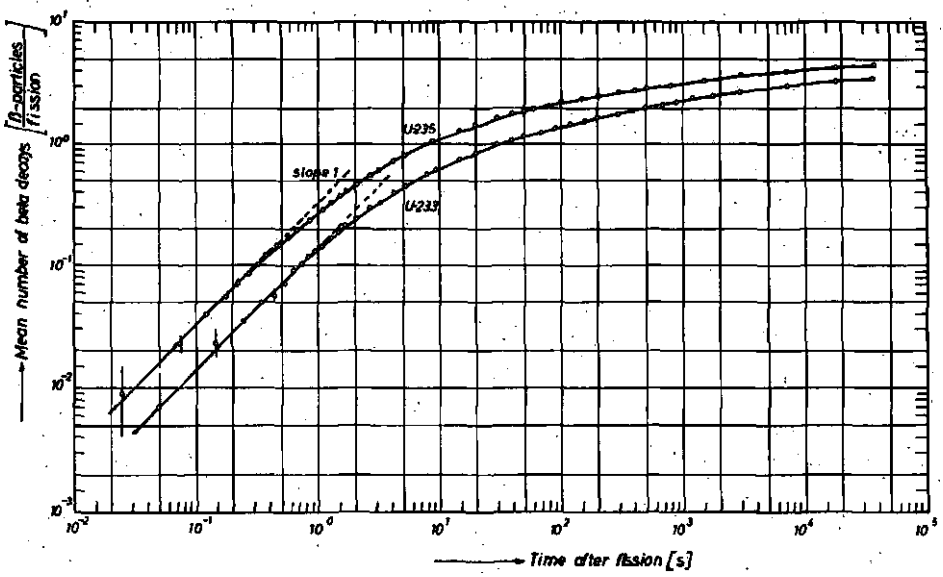

Fig. 2

Observed number of beta-particles per fission $\int_0^T \beta(t)dt$ from the thermal-neutron fission of U^{233} and U^{235} as a function of the time T after fission

been calculated from the radiochemical mass yields [12] and the known half-lives of the long-lived fission products. Since nearly all the fragments produced primarily have decayed at times smaller than 10 h, no special assumptions concerning the primary charge distribution enter into the calculations. The values obtained amount to 1.75 and 1.73 for U^{233} and U^{235} respectively. The total number of beta particles per fission add up to 5.25 ± 0.2 and 5.93 ± 0.2 for U^{233} and U^{235} respectively. The latter value may be compared with the data 6.6 ± 0.9 and 6.6 ± 0.2 given by ALZMANN [9] and ARMBRUSTER [16]. On the other hand the total number of beta particles per fission can be computed from the conservation of total charge, i.e. the radiochemical mass yields and the first stable charges of each chain. Values of 5.27 and 6.10 have been obtained for U^{233} and U^{235} respectively; the latter value agrees with data given elsewhere [1, 2, 5, 16]. Within the accuracy of the measurement there is good agreement between the experimental and the calculated number of beta decays per fission.

The mean beta-decay rate $\beta(t)$ as a function of the time t after fission is given in Figs. 3 and 4 for U^{233} and U^{235} respectively, together with other experimental and calculated data available. The curves have been obtained

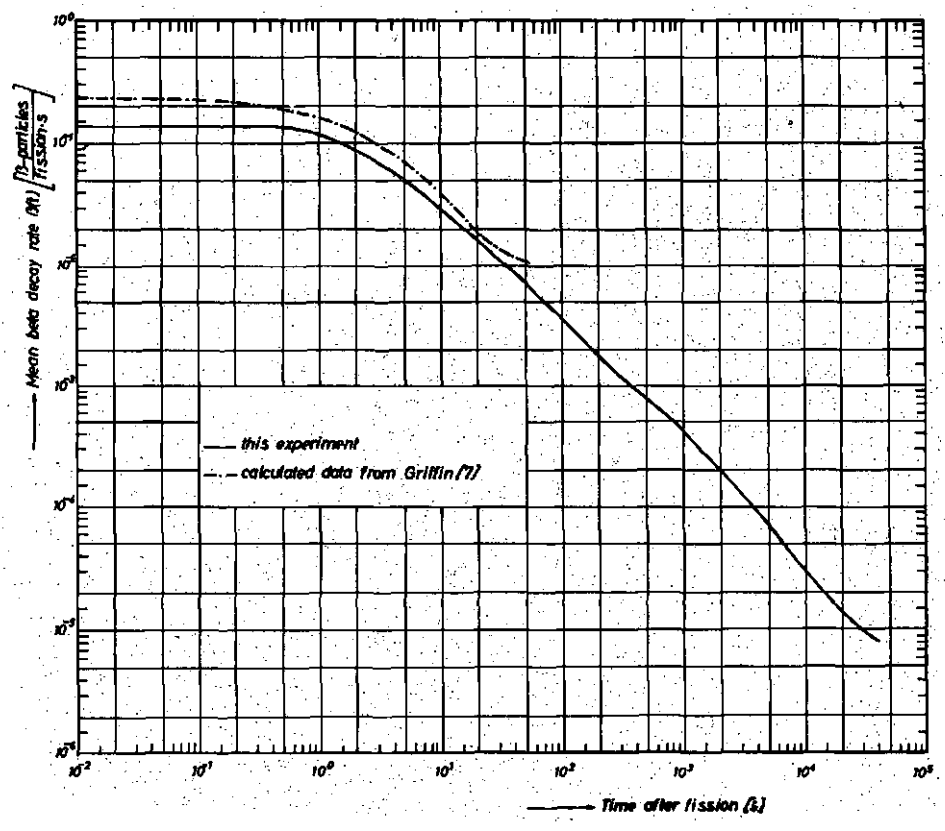

Fig. 3

Mean beta-decay rate $\beta(t)$ from the thermal-neutron fission of U^{233} as a function of the time t after fission

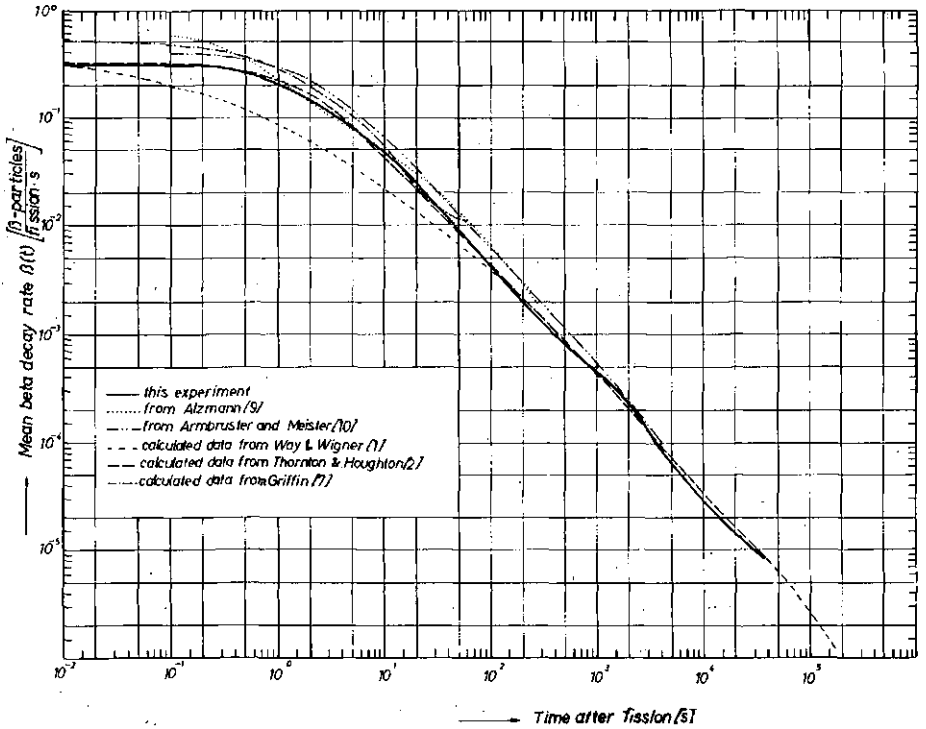

Fig. 4

Mean beta-decay rate β(t) from the thermal-neutron fission of U^{235} as a function of the time t after fission

by carefully differentiating the time-dependent number of beta particles shown in Fig. 2.

CORRECTIONS AND ACCURACY

Various corrections have been applied to the measured data. The overall dead-time losses of the proportional counter and the electronic circuit have been measured directly by counting the decreasing activity of a 2.58-h Mn^{56} beta source mounted inside the 4π counter. They are about <7%. The fission product rate has to be corrected for absorption of fragments in the active layers of the target. Using a mean range of 4.9 mg/cm^2 in uranium acetate estimated from the known ranges in metallic uranium [13] and the remaining components [14, 15], the absorption losses are calculated to be 4.1% and 5.7% for the U^{233} and U^{235} layers respectively. (The values are different because of different thicknesses.) The absorption of beta-particles in the target may be evaluated from the energy of those particles that are just absorbed on vertical emission (67 keV), and from the mean energy of the particles as a function of the time t after fission [3, 10]. Assuming allowed spectra and weighting with the decay rate, the absorption losses are

estimated to be 0.9% and 2.9% after irradiation times of 1 s and 10 h respectively. Conversion electrons coincident within the resolving time of the circuit are not measured. Conversion electrons emitted in isomeric transitions may be neglected up to 10 h after fission; the value of 0.07 given by Ref. [2] is entirely caused by transitions with much longer half-lives. Fluctuations of the neutron flux were observed only for irradiation times greater than 1 h. Values of <1.5% were found using the BF_3 counter; corrections may be easily made.

The absolute error of the measured number of beta particles plotted in Fig. 2 amounts to 6% and 4% for U^{233} and U^{235} respectively. The error resulting from all corrections is only about 1%. The predominant part of the error is caused by the fission product rate. The active layers are rather inhomogeneous and therefore lead to fission products having energies similar to α-particles. Because of the enormous α-activity of the active material the lower part of the fission product spectrum could not be measured with better accuracy. For U^{235} the slight discrepancy between the experimental and calculated number of beta decays (see previous section) is therefore likely to be caused by an incorrect fission rate. The rate is independent of time. To achieve the most correct set of data that is possible the U^{235} data given in Figs. 2 and 4 have therefore been multiplied by a constant factor of 1.04 that equalizes the measured and calculated number of beta particles 4.37, released at 10 h after fission. The relative error of all data plotted in Fig. 2 is estimated to be <2%. Because of differentiation the error of the mean beta-decay rate of U^{233} shown in Fig. 3 amounts to about 5% up to 10^3 s and to about 10% up to 10 h, the error of the decay rate of U^{235} shown in Fig. 4 to about 2% to 1 s and to about 5% for times $> 10^2$ s.

DISCUSSION OF RESULTS

Other experimental data and various calculations of the decay-rate $\beta(t)$ only exist for U^{235} as indicated in Fig. 4. For all times our measurement yields lower values compared with the former ones, mainly because of the correct total number of beta decays determined in the present experiment. Great discrepancies between our data and theoretical values are found for the most interesting time interval <10 s where the various assumptions entering into the calculations are most critical. WAY and WIGNER [1] neglect the fact that the beta decay of fission products is largely a chain process, the beta decay of one nucleus being the source of the succeeding nucleus. As pointed out by THORNTON and HOUGHTON [2] the chain process leads to a lower initial activity than the statistical method of Way and Wigner indicates, and tends to maintain that activity for a longer time. This effect is observed in our measurement. On the other hand GRIFFIN's approach [7] is essentially similar to that of Way and Wigner, but takes full account of the chain process. The calculated data are higher than our values by an average of about 60%. This seems to be partly because the parameters of the computation have been fitted to the older measurements. Since these differences are quite similar for the decay rate of U^{233} as indicated in Fig. 3, a refinement of the present parameterization of the model would be desirable.

A remarkably good agreement exists between our data and the older semi-empirical calculations of THORNTON and HOUGHTON [2]. This is somewhat surprising since only the total number of beta particles and data for times longer than 1 h after fission are needed for evaluating the important parameters.

When a comparison is made of the measured decay rate for U^{233} and U^{235}, the greater activity of the latter isotope for short times is easily understood. The larger total number of beta particles resulting from the higher mass leads to a primary charge distribution shifted away from the line of stability. A greater displacement leads to higher decay energies with correspondingly higher decay constants and hence greater activity. Figure 3 as well as Fig. 4 shows a constant decay rate up to nearly 0.4 and 0.2 s respectively, i.e. much shorter half-lives do not exist. On the other hand the measured decay rates are identical within the accuracy given for all times greater than about 10 min. By that time most of the primary fission products have decayed and the influence of the primary charge distribution may be neglected. There seems to be some structure in the decay rates not found in earlier experiments. A similar structure was found in the two sets of data.

ACKNOWLEDGEMENTS

The authors wish to thank Professor H. Maier-Leibnitz for his continuous interest in this work. They are also indebted to Dr. P. Armbruster for many valuable discussions.

REFERENCES

[1] WAY, K. and WIGNER, E. P., Phys. Rev. 73 (1948) 1318.
[2] THORNTON, J. K. and HOUGHTON, W. J., J. appl. Phys. 24 (1953) 1377.
[3] KNABE, W. E. and PUTMAN, G. E., Rpt. APEX-448 (1958).
[4] BOLLES, R. C. and BALLOU, N. E., Nucl. Sci. Engng. 5 (1958) 179.
[5] PERKINS, J. F. and KING, R. W., Nucl. Sci. Engng. 3 (1958) 6.
[6] BJÖNERSTEDT, R., Ark. Fys. 16 (1959) 293.
[7] GRIFFIN, J., Rpt. LA-2811 and Add. I, II, Los Alamos (1963); Phys. Rev. 134 (1964) B 817.
[8] HILL, D. and LANZL, L., Rpt. CP-1827 (1944).
[9] ALZMANN, G., Nukleonik 3 (1961) 295.
[10] ARMBRUSTER, P. and MEISTER, H., Z. Phys. 170 (1962) 274.
[11] WUNDERLICH, F., Diplomarbeit, Technische Hochschule München (1962).
[12] WALKER, W. H., Rpt. AECL 1054 (1960).
[13] NIDAY, J. B., Phys. Rev. 121 (1961) 1471.
[14] FULMER, C. B., Phys. Rev. 108 (1957) 1113.
[15] ALEXANDER, J. M. and GAZDIK, M. F., Phys. Rev. 120 (1960) 874.
[16] ARMBRUSTER, P., HOVESTADT, D., MEISTER, H. and SPECHT, H. J., Nucl. Phys. 54 (1964) 586.

DISCUSSION

L. YAFFE: You point out quite correctly that conversion electrons coincident within the resolving time of the circuit are not measured. Then you

say later in the paper that "Conversion electrons emitted in isomeric transitions may be neglected up to 10 h after fission". I do not understand this. Surely any isomeric transition following a beta-decay delayed by a time greater than a few microseconds would be measured by your counter.

H.J. SPECHT: All conversion electrons emitted in isomeric transitions would, of course, be measured by our counter. We made no corrections because we found that the estimated total number of conversion electrons, 0.07 (Ref. [2]), is essentially caused by transitions with much longer half-lives than 10 h. A comparison of the measured total number of beta-particles per fission with the calculated values would seem to indicate that the number of conversion electrons contributing to the beta-decay rate within 10 h after fission is very low indeed.

L. YAFFE: Yes, but it is surely cyclic thinking to assume that this must be true since your results agree with calculations. You are, of course, helped by the fact that your beta source (the target) is thick to conversion electrons. Surely some corrections would have to be made.

H.J. SPECHT: The cut-off energy was about 67 keV.

A. MOSSOP: I wish to comment on some work in progress at Windscale in which we are making direct estimates of the specific gamma activity following fission of U^{235} and Pu^{239}. We use a double fission chamber to measure absolute fission rate by a coincidence technique and then the chamber interior is dissolved chemically so that the fission product activity can be estimated by liquid counting of gammas. So far such measurements have been made for U^{235} and Pu^{239} for decay times from approximately 20 min to several hundred hours following an irradiation period of 24 h. The results show that the ratio of the Pu^{239} to U^{235} specific gamma activity has a value of about 0.85 for a decay of 20 min, rising to unity at approximately 20 h decay and further to about 1.1 at 100 h. While the absolute values will clearly depend on irradiation time, it is thought that those parts of any curve for decay times that are short compared with the particular irradiation time of that curve will be universal.

FISSION AT INTERMEDIATE AND HIGH EXCITATION ENERGIES

(Session VIII)

Review Paper

FISSION OF HEAVY ELEMENTS BY HIGH-ENERGY PROTONS *

G. FRIEDLANDER
CHEMISTRY DEPARTMENT, BROOKHAVEN NATIONAL LABORATORY,
UPTON, N.Y., UNITED STATES OF AMERICA

Abstract — Résumé — Аннотация — Resumen

FISSION OF HEAVY ELEMENTS BY HIGH-ENERGY PROTONS. A brief survey is given of the phenomenology of fission-like break-up processes induced in high-Z elements by protons of high energies, with principal emphasis on the GeV region. Charge dispersions are discussed in some detail. New charge dispersion data in various mass regions for products formed in lead and uranium interactions with 2.9-GeV and 28-GeV protons are reviewed. The pronounced differences between the lead and uranium results are discussed. The double-humped charge dispersion curves observed near A = 130 for uranium "fission" products are interpreted in terms of two different mechanisms, characterized by low and high deposition energies. This interpretation is confirmed by recoil experiments, particularly by data on angular distributions and range spectra for neutron-deficient and neutron-excess products of uranium "fission". From the charge dispersions, yield-versus-mass curves for the 2.9-GeV and 28-GeV interactions are constructed and these are compared with the yield-versus-mass distributions at lower energies. In the uranium interactions, a single broad maximum, centred at A ≈ 110, is found in the mass distribution, broader at 28 than at 2.9 GeV. With lead as the target, the mass distribution is flat in the region 40 < A < 140. Values of fission cross-sections derived from the yield-versus-mass curves are discussed in the light of fission cross-sections obtained by other methods and at other bombarding energies.

FISSION D'ÉLÉMENTS LOURDS PAR PROTONS DE HAUTE ÉNERGIE. L'auteur présente un bref aperçu de la phénoménologie des processus de rupture analogues à la fission qui sont provoqués dans des éléments à numéro atomique élevé par des protons de haute énergie, en insistant particulièrement sur la région des énergies de l'ordre des GeV. Il discute en détail la dispersion des charges et fait le point de nouvelles données relatives à la dispersion des charges dans plusieurs régions de la masse pour des produits formés au cours des interactions du plomb et de l'uranium avec des protons de 2,9 GeV et 28 GeV. Il examine les différences très nettes entre les résultats relatifs au plomb et les résultats relatifs à l'uranium. Il interprète les courbes de dispersion des charges à deux sommets, observées dans la région de A = 130 pour les produits de fission de l'uranium, en fonction de deux mécanismes différents qui seraient caractérisés par des énergies de dépôt faibles et élevées. Cette interprétation est confirmée par des expériences de recul, en particulier par des données sur les distributions angulaires et des spectres de parcours pour des produits de fission de l'uranium dont les uns ont un excédent et les autres un déficit de neutrons. A partir des dispersions des charges, l'auteur établit les courbes de distribution selon la masse pour des interactions avec des protons de 2,9 GeV et de 28 GeV et il les compare aux courbes de distribution selon la masse pour des énergies inférieures. Pour ce qui est des interactions de l'uranium, on distingue dans la distribution selon la masse un large sommet unique centré à A ≈ 110, plus large pour 28 GeV que pour 2,9 GeV. Lorsque la cible est constituée par du plomb, la distribution selon la masse est plane dans la région 40 < A < 140. L'auteur discute les valeurs des sections efficaces de fission déterminées à partir des courbes de distribution selon la masse à la lumière des sections efficaces de fission obtenues par d'autres méthodes et avec d'autres énergies de bombardement.

ДЕЛЕНИЕ ТЯЖЕЛЫХ ЭЛЕМЕНТОВ С ПОМОЩЬЮ ПРОТОНОВ ВЫСОКОЙ ЭНЕРГИИ. Дается краткий обзор феноменологии процессов расщепления, подобных делению, вызываемых в элементах с большим значением Z с помощью протонов высокой энергии, причем упор делается на район с энергией порядка биллионов электронвольт. Подробно обсуждаются рассеяния зарядов. Рассматриваются новые данные о рассеянии зарядов в различных районах масс для продуктов, формирующихся при взаимодействиях свинца и урана с протонами 2,9

* Work supported by the United States Atomic Energy Commission.

и 28 Бэв. Обсуждаются указанные различия между результатами для свинца и урана. Дается объяснение кривых рассеяния двугорбового заряда, наблюдавшихся вблизи A = 130 для продуктов "деления" урана с точки зрения двух различных механизмов, характеризующихся низким и высоким выделением энергий. Такое объяснение подтверждается экспериментами на отдачу, и особенно данными по угловому распределению и спектру пробега продуктов "деления" урана с недостатком нейтронов и избытком нейтронов. На основе дисперсии зарядов строятся кривые выхода по сравнению с массой для взаимодействий 2,9 и 28 Бэв. Эти кривые сравниваются с распределениями выход—масса при более низких энергиях. При взаимодействиях урана в распределении массы найден единичный широкий максимум, с центром в A ≈ 110, более широкий при 28, чем при 2,9 Бэв. В случае, когда свинец является мишенью, распределение массы является плоским в районе 40 < A < 140. Обсуждаются значения сечений деления, выведенные на основании кривых выход—масса в свете сечений деления, полученных с помощью других методов и при других энергиях бомбардировки.

FISION DE ELEMENTOS PESADOS MEDIANTE PROTONES DE ELEVADA ENERGIA. *El autor examina* sucintamente la fenomenología de los procesos de ruptura del tipo fisión inducidos en elementos de número atómico alto mediante protones de elevada energía y hace especial hincapié en las energías del orden de los GeV. Analiza luego con cierto detenimiento las dispersiones de carga. Presenta nuevos datos acerca de la dispersión de carga en diversas regiones de masa, para productos formados en interacciones del plomo y del uranio con protones de 2,9 GeV y 28 GeV. Analiza las acusadas diferencias entre los resultados logrados con el plomo y con el uranio. Las curvas de dispersión de cargas con dos máximos observadas para valores próximos a A = 130 en los productos de la «fisión» del uranio, se interpretan en términos de dos mecanismos distintos caracterizados por bajas y altas energías de depósito. Esta interpretación es confirmada por los resultados de los experimentos de retroceso, y en especial, por los datos sobre la distribución angular y los espectros de alcance para los productos de la fisión del uranio con exceso y con defecto de neutrones. Partiendo de las dispersiones de carga, se construyen curvas de rendimiento en función de la masa para las interacciones con protones de 2,9 GeV y 28 GeV; esas curvas se comparan luego con las distribuciones rendimiento en función de la masa a menores energías. En las interacciones del uranio, la distribución de masas — más ensanchada a 28 que a 2,9 GeV — presenta un solo máximo aplanado, con centro en A ≈ 110. Utilizando plomo como blanco, la distribución de masas es plana en la región 40 < A < 140. A la luz de las secciones eficaces de fisión obtenidas por otros métodos y a otras energías de bombardeo, el autor analiza los valores de las secciones eficaces de fisión deducidos de las curvas de rendimiento en función de la masa.

1. INTRODUCTION

Break-up of a nucleus into two or more fragments with comparable masses can be induced by many different types of projectiles having a wide range of kinetic energies. Fission defined in this somewhat loose sense is thus a rather general phenomenon: even nuclei of light elements such as copper and silver have been shown to undergo two-body break-up at sufficiently high bombarding energy. Thoughout most of this paper the term "fission" is used in this general sense of two-body (or three-body, etc.) break-up, without the implication that the mechanism is necessarily akin to that of low-energy fission.

This survey deals with fission of heavy elements ($Z \geq 82$) by high-energy (> 100 MeV) protons. Even in this limited field the literature is extensive, and no attempt has been made to cover it systematically or completely. Fortunately, comprehensive reviews of high-energy fission have appeared in recent books by HYDE [1] and by PERFILOV, LOZHKIN and OSTROUMOV [2]. We shall therefore concentrate on selected topics and emphasize the GeV-energy range.

The complexity of high-energy fission phenomena has so far defied detailed theoretical treatment, so that this paper is largely confined to phenomenological discussions. However, the general validity of the cascade-

evaporation model [1, 3] for the description of most high-energy reactions is implicitly assumed, and fission will be discussed in this framework as a process competing with particle evaporation in the second, slower stage of the reaction. It follows that, even in the bombardment of a given nuclide with a given energy of protons, a variety of fissioning nuclei is produced because the cascade can lead to different products, each with a spectrum of excitation energies [4], and because, in the de-excitation of these cascade products by evaporation, fission can presumably compete to varying degrees throughout the evaporation paths[1]. As we shall see, even this complex qualitative picture may not be adequate to account for all the observations. Some high-energy "fission" products appear to behave as if they could not at all be produced in a two-step reaction with energy equilibration in the intermediate excited nucleus.

Among the important characteristics of fission are the distributions of fission products according to A and Z. In discussions of low-energy fission it is customary to consider the mass distributions first. Since the primary products of low-energy fission are far on the neutron excess side of the β-stability valley, yield-versus-mass curves can be constructed from data on the cumulative yields of long-lived or stable end products of the β-decay chains, without detailed knowledge of the dispersion of primary yields along these chains [8]. In high-energy fission the situation is quite different: charge dispersion curves become very broad, extending to both sides of β-stability, and thus detailed knowledge of isobaric yield distributions in various mass regions is required for the construction of a yield-versus-mass curve. We therefore discuss charge dispersion first.

CHARGE DISPERSION AND CHARGE DISTRIBUTION

By charge dispersion we mean the distribution of independent fission yields among the isobars at a given mass number. The term charge distribution, sometimes used to denote the same concept, is more properly reserved for the manner in which the nuclear charge divides itself between the two fragments in the fission act. To deduce information on charge distribution from measured charge dispersions, the Z of the fissioning nucleus must be known.

Charge dispersion

There are few published studies explicitly designed to investigate the charge dispersion in high-energy fission. A number of authors [9-12] showed

[1] Attempts to derive the dependence of the fission width Γ_f on A, Z, and excitation energy E^* from experimental data on fission and spallation cross-sections of uranium and thorium by 340-MeV protons have led to contradictory results. LINDNER and TURKEVICH [5] found that the assumption of Γ_f/Γ_n independent of E^* up to ~100 MeV, but a strong function of Z^2/A, fitted the experiments best. SHAMOY [6], with cruder assumptions about the cascade stage, concluded that the same data could be fitted with the assumption that $\Gamma_f/\Gamma_n = 0$ for large E^* so that fission competes only in the final stages of evaporation. In the region of lead and bismuth, the variation of Γ_f/Γ_n with E^* may be very different from that in the uranium region [7]. For $E^* >> 100$ MeV, no attempts to arrive at the dependence of Γ_f/Γ_n on A, Z and E^* have been published.

that, in the region of a few hundred MeV proton energy, charge dispersion curves for uranium fission generally broaden with increasing energy as evidenced, e.g. by the appearance of neutron-deficient nuclides among the fission products, along with the well-known neutron-excess products of low-energy fission. Also, the peaks of the charge dispersion curves (often designated as Z_p) move closer to the line of beta stability [11-13]. If the charge dispersions are assumed to be Gaussian, their full widths at half maximum (FWHM) at a few hundred MeV are 3 to 4 Z-units, and the Z_p values lie 0 to 2 Z-units to the neutron-excess side of β-stability (Z_A). This is to be compared with the charge dispersion curves for thermal-neutron fission, which have FWHM $\approx$ 1.6 Z-units and $Z_A - Z_p$ between 3 and 4 [8].

These observations are in qualitative accord with the predictions of the cascade-evaporation model [11]. The amount of energy deposited in a nucleus is certainly expected to increase on the average with increasing bombarding energy [4], and this means that more evaporation must occur. Evaporation may happen either before or after fission, but in either case neutrons will be the most probable particles evaporated [14], and the decrease in neutron/proton ratios of the average fission products observed with increasing bombarding energy is thus readily explained. Similarly, a broadening of charge dispersion curves is expected from any spread around the average excitation energy of a fissioning species and especially from the existence of not one fissioning species, but a whole spectrum of fissioning nuclei (see Introduction).

The results of a study of independent and chain yields of caesium and barium isotopes in uranium fission by protons with energies between 100 MeV and 3 GeV were used by FRIEDLANDER et al. [15] to construct charge dispersion curves for the mass region 125 to 140. In going from 100-MeV to 380-MeV proton energy these authors found $Z_A - Z_p$ to decrease from 1.44 to 0.85 and the widths of the dispersion curves to increase from 3.3 to 5.2 Z-units. At still higher proton energies the charge dispersion curves showed structure, becoming definitely double-humped above 1 GeV, with a peak on the neutron-excess side centred on $Z_A - 1.9$, a valley in the neighbourhood of $Z_A - 0.5$, and a peak on the neutron-deficient side with its maximum at about $Z_A + 1.5$ and gradually broadening with increasing energy. Figure 1 shows the charge dispersion curves at 0.10, 0.38, 1.0 and 2.9 GeV taken from Ref. [15]. It should be pointed out that these are not strictly charge dispersion curves in the conventional sense since the abscissa is N/Z rather than Z. This representation was chosen because the data were obtained over a range of mass numbers rather than for a single mass chain, and a plot against Z (or rather $Z - Z_A$) would require a choice of Z_A for each A, whereas the N/Z plots are independent of Z_A values. The use of fission yield data over a range of mass numbers to deduce charge dispersion requires some knowledge of the variation of mass yield over this mass range. In Ref. [15], the yield per mass number was assumed to be constant for $125 < A < 140$, an assumption justified at 100 and 380 MeV [16] but not, as we shall see in the section below on Mass Distribution, at 2.9 GeV, and perhaps not at 1 GeV. The data defining the 2.9-GeV curve in Fig. 1 were therefore adjusted to correspond to A = 131, according to the shape of the mass yield curve deduced

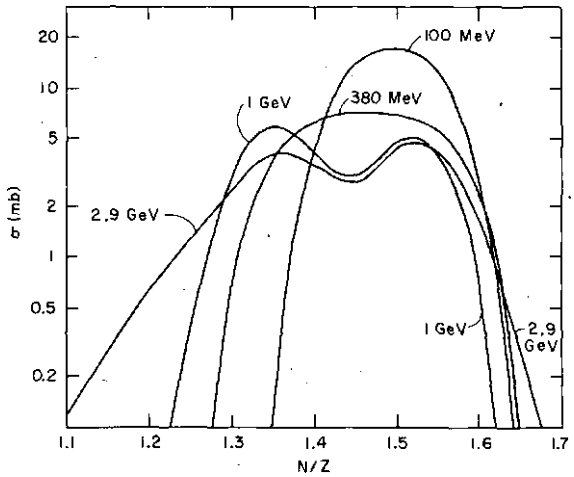

Fig. 1

Charge dispersion curves for products in the region of A = 131 formed in interactions of uranium with protons of various energies [15]. The 2.9-GeV curve has been corrected for the variation of yield per mass number over the range of A used in constructing the curve.

in the section on Mass Distribution (Fig. 6); the resulting change in the curve is relatively small, consisting merely in a slight raising of the right-hand (neutron-excess) branch and a slight lowering of the left-hand (neutron-deficient) branch.

In an effort to map the shapes of charge dispersion curves in several other product mass regions for the fission of uranium by 2.9-GeV protons, selected yield data were obtained in the following regions of A; 37-42 [17], 45-49 [18], 66-74 [19], 79-85 [17] and 100-115 [20]. The same authors also determined formation cross-sections for the same products in 28-GeV bombardments of uranium and in 2.9-GeV and 28-GeV bombardments of lead. In each mass regions, cross-sections for formation (some independent, some cumulative) of several members of one isobaric family were determined, e.g. Pd^{109}, Cd^{109}, In^{109}; Br^{83}, Rb^{83}, Sr^{83}, Y^{83}; Zn^{72}, Ga^{72}, As^{72}, Se^{72}; V^{47}, Sc^{47} and Ca^{47}; and the yields of products of nearby mass numbers were used as an additional aid in defining the charge dispersion. Where appropriate, small corrections for the slopes of the mass-yield curves (Fig. 6) were made as described above. Preliminary results of some of these largely unpublished charge dispersion studies are shown in Figs. 2-5. They are representative of the whole set. A number of interesting features are readily seen in these graphs:

(i) The differences in charge dispersion between 2.9-GeV and 28-GeV proton bombardments are rather slight. A small tendency towards broadening of the curves at the higher energy is discernible, particularly for the lead bombardments.

(ii) Charge dispersion curves for lead and uranium fission differ drastically, the yields of products with large N/Z ratios being substantially lower from lead than from uranium. This divergence be-

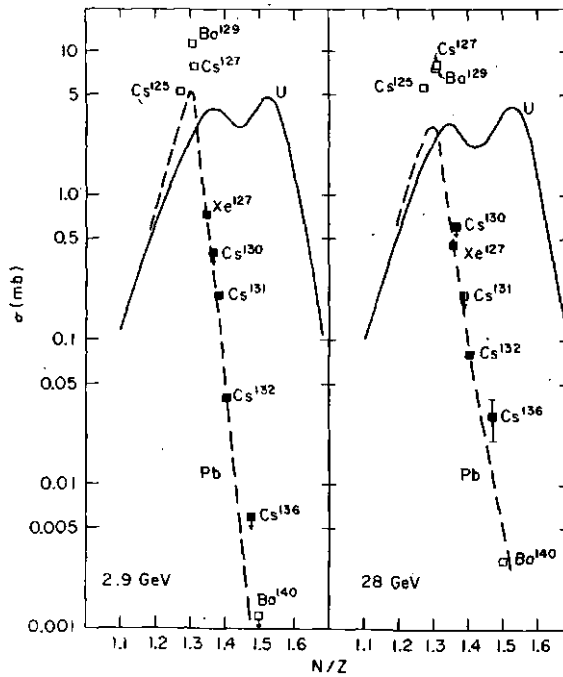

Fig. 2

Charge dispersion curves for A ≈ 131 from uranium and lead interactions with 2.9- and 28-GeV protons. The 2.9-GeV uranium curve is taken from [15], with correction for the slope of the yield-versus-mass curve; the 28-GeV uranium curve was constructed as described in [15] from unpublished data [52]. The experimental points [52] for the lead interactions are shown, filled squares indicating independent yields, open squares cumulative yields, and arrows signifying upper limits.

comes more pronounced with increasing product mass. On the far neutron-deficient side the curves for the two targets are similar, with a tendency for lead cross-sections to be actually slightly higher than the corresponding uranium cross-sections.

(iii) The doubly peaked charge dispersion curve found for the A ≈ 130 region in uranium fission is not observed at low A-values (Figs. 4 and 5). In the region of A ≈ 109, too few independent-yield data are available to define the neutron-excess side of the curve unambiguously. As indicated in Fig. 3, the cumulative yields of Pd^{109}, Cd^{115} and Pd^{112} can be fitted with a variety of dispersion curves, ranging from a flat-topped, asymmetric single hump to a pronounced double peak; the latter gives, however, the best fit to the data at both energies.

Further mapping of charge dispersion curves for the products of various high-energy fission processes is clearly desirable, particularly in mass regions not yet covered (A > 140) and at other proton energies. However, as pointed out by several authors, e.g. [15, 21, 22], the existing data appear

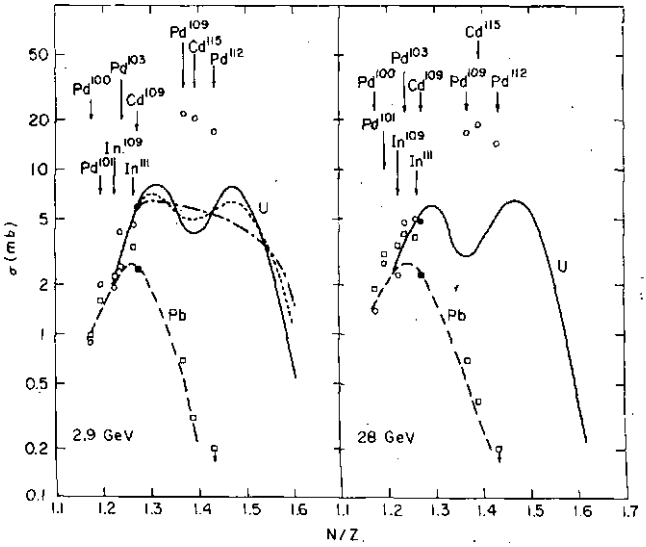

Fig. 3

Charge dispersion curves for the region 100<A<115 from uranium and lead interactions with 2.9- and 28-GeV protons.
Circles: uranium; squares: lead; filled points: independent yields; open points: cumulative yields. Data from [20].
The three uranium curves drawn in the 2.9-GeV graphs are shown to indicate that the data on the neutron-excess side are insufficient to define the charge dispersion; the same is true at 28 GeV.
However, at both energies the measured cumulative yields are best fitted by curves with pronounced double humps, such as the solid curves shown.

to indicate that, at GeV energies, what we have called fission products probably originate, in fact, in at least two different types of process. This is suggested most strongly by the double peak in the charge dispersion at $A \approx 131$, but also by the large differences between the lead and uranium curves in all mass regions (much larger than would be expected merely from the N/Z ratios of U^{238} and $Pb^{206-208}$) and, as we shall see in the section on Energetics, by the differences in the recoil behaviour of different products.

The neutron excess products observed in the uranium interactions, e.g. those in the right-hand peaks at A = 131 (Fig. 2), have been interpreted [15] as arising from low-deposition-energy fission processes[2]. In Ref. [15], each of the charge dispersion curves in the GeV region was analysed into two branches, under the assumption that the neutron-excess branch is symmetrical. The second, neutron-deficient branch obtained by difference turned out to be a rather broad peak, with its maximum near N/Z = 1.35 (which corresponds to $Z_A + 1.5$) and quite asymmetric. One might have expected the lead data to approximate this neutron-deficient branch of the uranium curve, but a glance at Fig. 2 shows that this is too naive a picture: the lead curve peaks

[2] The absence of a double peak at $A \leq 72$ is consistent with this interpretation, since low-deposition-energy fission does not give rise to such low-mass products in appreciable yield.

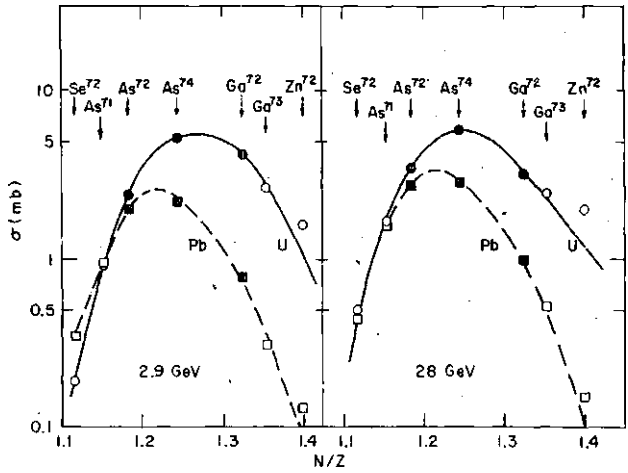

Fig. 4

Charge dispersion curves for A ≈ 72 from uranium and lead interactions. Meaning of symbols as in Fig. 3. Data from [19].

at N/Z ≈ 1.30 and is much narrower than the neutron-deficient peak of the uranium curve. Even the assumption of a broad, asymmetric neutron-excess peak for uranium would not bring the two neutron-deficient peaks into agreement. One is forced to the conclusion that the uranium interactions differ from the ones in lead not only in the low-deposition energy fission processes, but also in the details of the high-deposition-energy mechanism (or mechanisms) giving rise to the more neutron-deficient products. This is indicated also by the persistence of substantial lead-uranium yield differences at mass numbers as low as 47, 39 and 22.

Charge distributions

In the energy range up to a few hundred MeV, where the dispersion in Z of fissioning nuclei must still be quite small, attempts have been made to analyse yield data in terms of certain charge-distribution models. The hypothesis of unchanged charge distribution (preservation of N/Z in the fission act) was proposed by GOECKERMANN and PERLMAN [23] to account for the observed yield patterns in bismuth fission by 190-MeV deuterons. Whether this hypothesis is also applicable to uranium fission in the region of a few hundred MeV is less clear. PATE [24] concluded that the hypothesis of equal charge displacement, taken over from low-energy fission, was more appropriate for uranium and thorium fission up to a few hundred MeV. Yet other authors, e.g. [25] have successfully analysed their data with unchanged charge distribution. RUDSTAM and PAPPAS, in a rather detailed analysis of uranium fission by 170-MeV protons [26], found the experimental results to lie half-way between the predictions of the two hypotheses. In the GeV range, equal charge displacement is certainly no longer applicable, whereas no contradiction to unchanged charge distribution has appeared [15]. However,

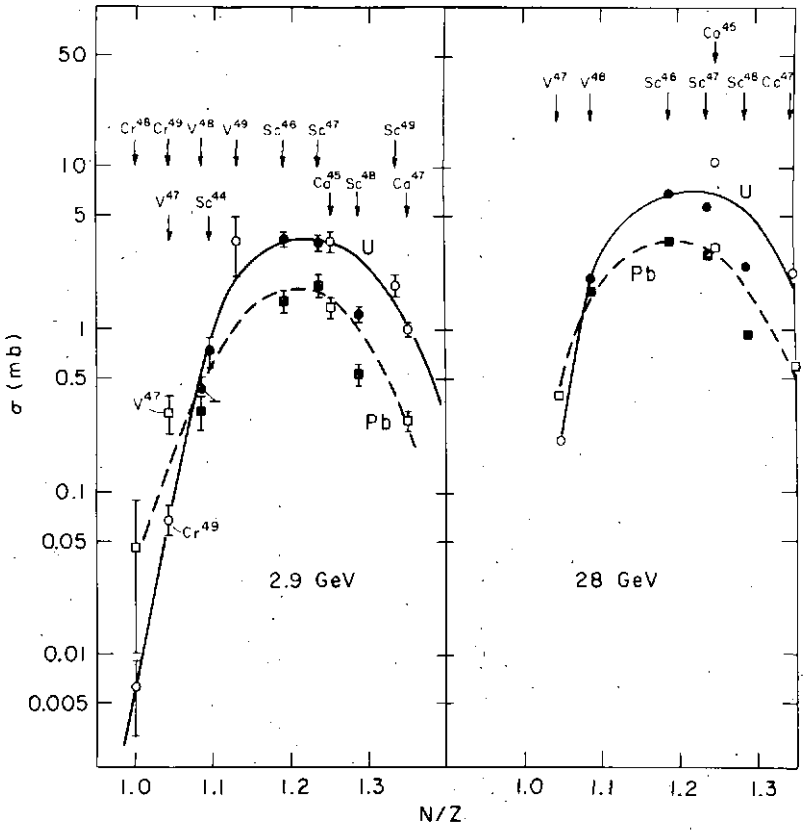

Fig. 5

Charge dispersion curves for A ≈ 47 from uranium and lead interactions. Meaning of symbols as in Fig. 3. Data from [18]. The yields of Sc^{48} appear to be anomalously low, an observation made in other yield studies also and possibly caused by decay scheme complications.

a detailed analysis of charge distribution at GeV energies cannot be attempted with data available at present.

MASS DISTRIBUTION

A number of authors have published yield-versus-mass curves for uranium fission by protons with energies between 100 and 480 MeV, and these are reviewed in Ref. [1]. At 100 MeV, the double-humped curve, so well-known in low-energy fission, is still barely visible (peak-to-valley ratio ~1.3); but at higher energies single-peaked curves are found, with rather flat maxima. With increasing bombarding energy the centre of this flat region moves slowly to lower A (reaching A ≈ 114 at E_p = 340 MeV [11]) and the curves broaden, particularly on the low-mass side (they become distinctly asymmetric [16]). In this energy region, the curves have been traced

for the mass range from $A \approx 60$ to $A \approx 165$, with cross-sections per mass number down to about 0.1 mb. The far wings have not been systematically investigated, although isolated product yields in the transition region between fission and spallation products ($A \approx 170$-200) have been reported both for 340-MeV [11] and for 680-MeV [27] fission of uranium. The valley in this region appears to be at least a factor of 2×10^3 lower than the peak of the fission distribution at 340 MeV, and very little is known about how rapidly it fills in with increasing proton energy.

The general broadening of the mass-yield curve with increasing bombarding energy has also been confirmed by measurement of the range ratios of the light and heavy fragments in experiments with uranium-loaded emulsions [1, 2].

The mass-yield curves for bismuth fission in the energy range 100 to 700 MeV appear to show qualitatively similar behaviour to those for uranium fission [2, 9, 28, 29, 30]. Single peaks are observed, with maxima (at about 10 mb) shifting from $A \approx 100$ to $A \approx 95$ and widths increasing with increasing proton energy. However, at any given proton energy the bismuth curve is less than half as wide as the uranium curve. The valley between spallation and fission products ($A \approx 130$-140) is shallower for bismuth than for uranium, about 1/100 and 1/20 of the fission peak at 480 and 660 MeV respectively [3, 29, 30].

In the GeV-energy region, no complete studies of yield-versus-mass curves have been published for uranium or bismuth fission. WOLFGANG et al. [31] concluded from their data on selected products formed in the interactions of lead with protons up to 3-GeV kinetic energy, that no fission peak could be discerned in the yield-versus-mass curve but that the spallation and fission regions blend into each other, with yields at all mass numbers in the range $15 < A < 209$ within one order of magnitude. Unpublished results by Shudde and Carnahan [1] on various products formed in uranium by 5.7-GeV protons indicated that here a fission product peak is still prominent, but the data were insufficient to define it in detail[3].

With the aid of the charge dispersion curves discussed earlier it is now possible to construct fairly reliable yield-versus-mass curves for 2.9- and 28-GeV interactions with both lead and uranium, at least up to $A \approx 140$. Total yields at mass numbers 20, 21, 22, 39, 47, 67, 72, 83, 109 and 131 were determined from the available charge dispersion curves and are plotted against A in Fig. 6. A fission product peak is clearly seen for uranium interactions at both energies, whereas the distributions for the lead interactions show, in agreement with earlier estimates [31], no structure in the region $40 < A < 140$. It is interesting that, even in going from 3- to 28-GeV proton energy, the uranium yield-versus-mass curve broadens markedly, even though few reactions of lower Z-targets have shown any important cross-section variations in this energy range. The peaks appear to be centred at $A \approx 110$ and $A \approx 107$ at 2.9 and 28 GeV respectively, but the exact positions of these maxima are, of course, not well determined. The 2.9-GeV and 28-GeV curves for uranium are compared in Fig. 7 with curves obtained at lower energies using the more familiar logarithmic cross-section scale.

[3] Some of the cross-sections reported by these authors [1], e.g. those for Ba^{140}, Cd^{115}, Pd^{112}, Pd^{109} and Ga^{73}, have been found [15, 19, 20] to be seriously in error.

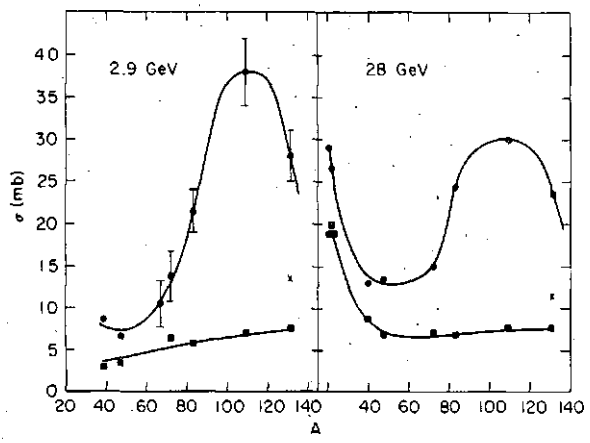

Fig. 6

Yield-versus-mass curves for uranium and lead interactions.
The experimental points (circles for uranium, squares for lead data) were obtained from the charge dispersion curves of Figs. 2-5 and from similar data for A = 20-22 [33], 37-42 [17], 66-67 [19] and 83 [17].
The crosses at A = 131 indicate the cross-sections under the neutron-excess peaks of the charge dispersions, under the assumption that these peaks are symmetric.

The upturn of both the lead and uranium curves at low A (Fig. 6) is not confined to the 28-GeV region; it is also present at 2.9 GeV as indicated by measured Na^{22} and Na^{24} yields [1, 32], but is not shown in the graph because the mass spectrometrically determined cumulative cross-sections for neon production [33] used to define the low end of the 28-GeV curves are not yet available at the lower energy. The formation of low-mass products ($A \lesssim 40$), with yields rapidly increasing as the proton energy is raised from ~ 0.5 to ~ 10 GeV, is usually ascribed to so-called fragmentation, presumably a rapid break-up process distinct from fission [31, 1, 2]. Little can be said at present about the yield-versus-mass curve for this process. As we shall discuss in the section on Energetics, there is evidence that the neutron-deficient products in the mass number range 100–130 also originate in a fast break-up process; they might, in fact, be partners of the light fragmentation products. In any case, the yield-versus-mass curves of Fig. 6 cannot be considered as entirely arising from "fission" in the narrower sense of a "slow" process, even though the peaks in the uranium curves at $A \approx 110$ can probably be safely ascribed to this mechanism.

FISSION CROSS-SECTIONS

Cross-sections for high-energy fission have been estimated by several methods, including ion-chamber measurements, nuclear-emulsion determinations, and integrations under yield-versus-mass curves for fission products. In the region from 100 MeV to 400 MeV the fission cross-sections for uranium and thorium are about 1.45 ± 0.15 b and 0.8 ± 0.1 b respectively, with no noticeable trend with energy [1, 2]. Thus, approximately 75 ± 10 and

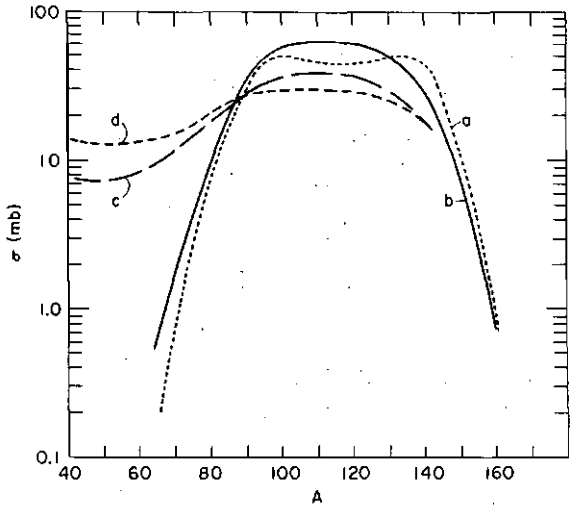

Fig. 7

Yield-versus-mass curves for uranium interactions with protons of various energies: (a) 100 MeV [16], (b) 170 MeV [26], (c) 2.9 GeV [this paper], (d) 28 GeV [this paper].

45 ± 10% of all inelastic interactions in uranium and thorium respectively, lead to fission in this energy range. No difference apart from experimental errors has been found between the fissionabilities of U^{238} and U^{235}. Some representative values of uranium fission cross-sections above 150 MeV are shown in Fig. 8.

Cross-sections for proton-induced fission of bismuth are also shown in Fig. 8. They show a definite increase with increasing proton energy, from ~0.1 b at 100 MeV to ~0.2 b at 400 MeV. It is interesting that the cross-section values obtained from summing of radiochemical data fall systematically below the ion-chamber data for bismuth fission, whereas the situation is exactly reversed for the uranium results.

Above 480-MeV bombarding energy, the only published values of fission cross-sections are those based on measurements with loaded nuclear emulsion. From their measurements at 600 MeV [34] and 20 GeV [35], de CARVALHO and co-workers conclude that the cross-sections for fission of uranium, thorium, and bismuth all decrease by a factor of about 4 over this energy interval.

With the help of the yield-versus-mass curves of Fig. 6, it is now possible to estimate fission cross-sections for uranium and lead at 2.9 and 28 GeV from the product yields. Assuming the uranium curves to be symmetrical about A = 110 and A = 107 respectively, and arbitrarily considering the entire yield in the mass ranges $50 < A < 170$ and $50 < A < 164$ respectively, as arising from binary fission, we obtain fission cross-sections of 1.28 and 1.21 b at 2.9 and 28 GeV respectively. These values, with ±15% error estimates, are shown as the filled squares in Fig. 8. As discussed at the end of the section on mass distribution, they are probably to be considered as upper limits to the binary fission cross-sections. On the other hand, something like a lower limit can be estimated by considering in each of the fission yield

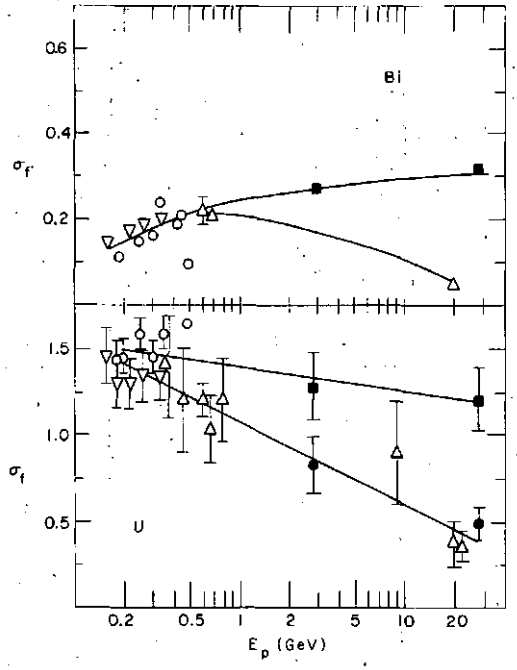

Fig. 8

Fission cross-sections of bismuth and uranium as a function of proton energy. Below 0.5 GeV only representative values are given. For a more complete summary see [1, 2, 35]. The symbols indicate the methods used: ∇ ionization chamber, △ nuclear emulsion, O product yield summation. The filled squares and filled circles are the upper and lower limits obtained from the yield-versus-mass curves discussed in the text. The lines are drawn for orientation only.

curves of Fig. 6 a constant background as being caused by processes other than fission, and taking this as equal to the yield at A = 50 (7.5 and 12.7 mb per mass number). The resulting values of 0.83 and 0.48 b for σ_f are shown in Fig. 8 as the filled circles. These latter values agree well with the trend of σ_f versus E_p found by de Carvalho et al. However, the following considerations of total inelastic cross-sections suggest that these values may be somewhat too low.

If the values of 0.83 and 0.48 b are accepted for σ_f at 2.9 and 28 GeV, then the remaining product yields in the region $50 < A < 170$ (0.90 b and 1.45 b respectively) must arise from processes other than binary fission (e.g. "fragmentation"). With these values and the spallation yields for $A > 170$ (measured for $A > 220$ [36, 37] and estimated from [38] for $170 < A < 220$) one then arrives at total inelastic cross-sections of ~2.3 and ~2.5 b at 2.9 and 28 GeV[4]. With the entire yields in the region $50 < A < 170$ ascribed to fission

[4] Yields for $A < 50$ have been ignored in this estimate, under the assumption that any product in this region is always accompanied by a heavier product. Ternary fission has not been taken into account, since PERFILOV et al. [39] found at 9 GeV a ratio of triple to double events of only 0.02.

($\sigma_f \approx 1.28$ and 1.21 b), a similar estimate leads to total inelastic cross-sections of ~1.9 b. The direct measurements of inelastic cross-sections for 24-GeV protons by ASHMORE et al. [40] extrapolate to 2.0 b for uranium.

At present, the two lines drawn in the uranium graph of Fig. 8 must be considered as indicating approximate upper and lower limits to σ_f in the GeV region. Perfilov's value of $\sigma_f = 0.9 \pm 0.3$ b at 9 GeV [39], obtained with a uranium-loaded emulsion, has too large an error to define the curve any more closely. Measurements of uranium and other fission cross-sections at 3 GeV are in progress [41] using the mica-track technique of PRICE and WALKER [42]; in this measurement only events in which two fragments with $A \lesssim 40$ are emitted are registered as fissions.

Unfortunately, the yield-versus mass curves for lead at GeV energies do not allow a very clear-cut interpretation in terms of fission cross-sections, since they show no peak in the region of expected fission products. Taking all the yields for $40 < A < 130$ as being due to binary fissions, one obtains σ_f values of 0.27 and 0.31 b at 2.9 and 28 GeV. These values are shown in Fig. 8 along with the bismuth data, and may be considered upper limits. It is likely that the true curve of σ_f versus E_p for bismuth (or lead) lies somewhere between the two curves sketched. In any case, it is clear that fission in bismuth or lead does not occur in more than ~20% of inelastic collisions at any energy.

It is interesting to note that fissionability, even at these high bombarding energies, is a very strong function of nuclear size. PERFILOV [43] has observed that experimental data on fission cross-sections of various elements at energies above a few hundred MeV can be represented by the equation $\sigma_f / \sigma_{inelastic} = \exp [0.682(Z^2/A - 36.25)]$.

ENERGETICS

Information on such matters as kinetic energies of specific fission fragments, the energy deposition during the cascades preceding particular fission modes, and the angular distributions and angular correlations of fission fragments has been deduced from observations in nuclear emulsions and from radiochemical experiments on the recoil properties of fission products [1, 2].

Among the important results of these studies is the finding that the kinetic energy of the incident proton does not contribute significantly to the kinetic energies of the products, but that these are determined essentially by Coulomb repulsion (see, e.g. [44]). In fact, the kinetic energy of a given product generally decreases with increasing bombarding energy, presumably because the charge and mass of the complementary fragment decreases as a result of increased pre-fission evaporation and cascade emission [45]. Results of Monte Carlo cascade calculations on the relation between momentum transfer and deposition energy [4, 46, 47] have been used to deduce, from measured recoil behaviour of specific products, the deposition energies for processes leading to these products [47, 21, 25].

In connection with the two-humped charge dispersion near A = 130 (see above), it is interesting that ALEXANDER et al. [21] in their study of iodine

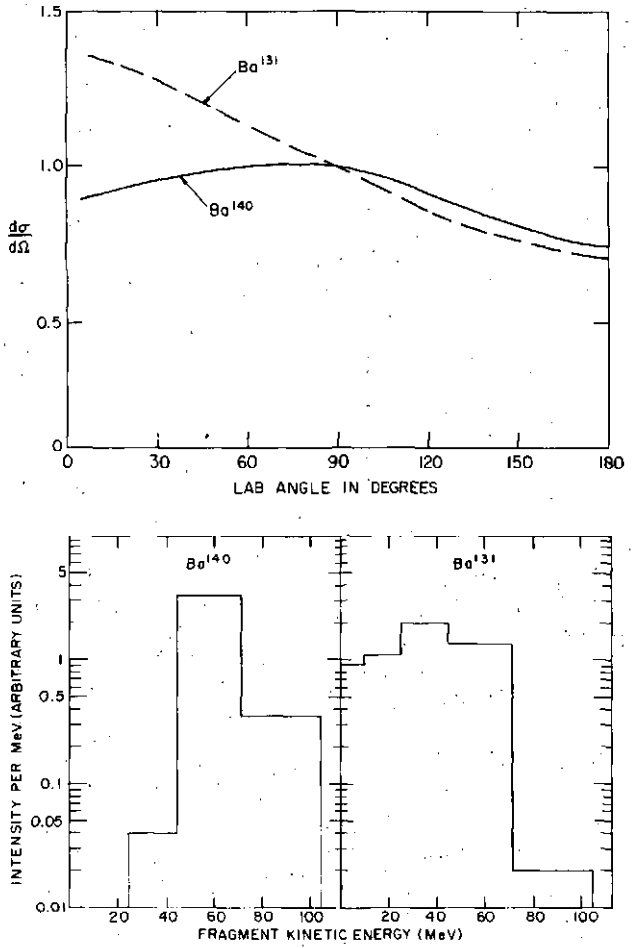

Fig. 9

Results of differential recoil experiments on Ba^{131} and Ba^{140} formed in the interaction of uranium with 2.2-GeV protons [48].
Top: Angular distribution in the laboratory system
Bottom: Kinetic energy spectra obtained from the differential range measurements 90° to the beam:

isotopes from 3- and 6.2-GeV bombardments of uranium, found the neutron excess isotopes $I^{130-135}$ to be associated with deposition energies of 60–90 MeV, whereas deposition energies for formation of neutron-deficient $I^{121-124}$ were 210–270 MeV. Also, the former had kinetic energies of ~65 MeV, compatible with Coulomb repulsion from reasonable fission partners, whereas the kinetic energies of the neutron-deficient iodines were only about 30–40 MeV. The authors concluded that, at GeV energies, the neutron-deficient iodines (as well as such light products as Cu^{64}) probably result from processes other than binary fission; this is in accord with the interpretation of the two-branched charge dispersion curves as arising from two different mechansims.

More decisive evidence on this point comes from differential recoil experiments in which the range spectra and angular distributions of Ba^{140}, Ba^{131}, Pd^{103} and Mo^{99} from 2.2-GeV proton interactions with thin uranium targets were determined [48]. The neutron-deficient products, Ba^{131} and Pd^{103}, have smaller mean energies and broader energy distributions than the neutron-excess species, Ba^{140} and Mo^{99}. Energy spectra for the barium isotopes, taken at 90° to the beam, are shown in Fig. 9. The angular distributions in the laboratory system, also shown in Fig. 9, are much more strongly forward peaked for Ba^{131}(and Pd^{103}) than for Ba^{140} (and Mo^{99}). When transformed into a system in which the intensities in the forward and backward hemispheres are equal, the Ba^{140} data are symmetric about and peaked at 90° (angular distribution of the form $1-0.2\cos^2\theta$). The data are entirely consistent with a low-deposition-energy two-step mechanism (fast cascade and slow evaporation-plus-fission) leading to Ba^{140} and Mo^{99}. The analysis of the Ba^{131} and Pd^{103} recoil data is not yet complete, but it is likely that they are incompatible with such a fast-slow process. Similar experiments on the production of Na^{24} from bismuth by 3-GeV protons led to the conclusion that this reaction could not result from a two-step mechanism involving an intermediate system with a lifetime $\gtrsim 10^{-20}$ s [49].

Measurements of fission fragments with solid-state detectors will probably give the greatest amount of detailed information about high-energy fission processes in the future. The first such study, using both singles and coincidence counting of fission fragments from 156-MeV proton interactions with uranium, bismuth and gold, was carried out by KOWALSKI [50]. He was able to deduce a wealth of information on differential fission cross-sections, angular correlations, momentum transfers to the fissioning nuclei, and spectra of total kinetic-energy release. A similar coincidence experiment with uranium irradiated by 2.2-GeV protons is being carried out at Brookhaven [51] and has already shown that the technique is applicable at GeV energies also.

STATUS AND PROSPECTS

Perhaps the most striking fact about high-energy fission which emerges from this survey is the primitive and incomplete state of our knowledge, even concerning empirical information. A great deal of radiochemical work is needed to complete the picture on charge dispersions and yield-versus-mass-distributions. For example, we do not know, even for normal uranium targets, over what region of product masses the double-peaked shape of charge-dispersion curves observed at $A \approx 130$ extends. Also, the yield-versus-mass distribution for $140 < A < 220$ is uncharted in the GeV region. Very little is known about differences between U^{235} and U^{238} as target materials at high energies. Data on thorium fission at hundreds of MeV are sparse; in the GeV region they are non-existent. Likewise, no measurements have been reported for targets with $Z > 92$. In view of the very striking differences between lead (or bismuth) and uranium, information on product distributions for high-energy interactions with other nuclei certainly seems desirable.

The energy dependence of fission cross-sections in the GeV region is still somewhat uncertain, partly because different operational definitions

of what constitutes fissions may be implicit in the interpretations of different types of measurements. More complete yield-versus-mass data for fission products, together with new physical measurements, e.g. with emulsions and mica detectors, should help to clarify this situation.

For information about high-energy fission sufficiently detailed to make tests of theoretical models possible, in-beam experiments with counter detection of fragments appear most promising. Coincidence measurements with energy-sensitive detectors, and possibly with other methods of discrimination such as dE/dx counters or time-of-flight measurements, are needed to sort out the complex processes indicated by the data available at present. Only when we can establish the major partners in a given break-up process, can we even give a sound operational definition of high-energy fission and distinguish it from other processes. Beyond that, it is reasonable to expect that direct counter experiments, so successful in recent years in revealing details of low-energy fission processes, will similarly clarify the more complex phenomena of high-energy fission reactions and eventually even facilitate their theoretical interpretation.

REFERENCES

[1] HYDE, E.K., The Nuclear Properties of the Heavy Elements III, Fission Phenomena, Prentice Hall Inc., Englewood Cliffs, N.J. (1964) 401.

[2] PERFILOV, N.A., LOZHKIN, O.V. and OSTROUMOV, V.I., Nuclear Reactions Induced by High Energy Particles, Moscow (1962). English transl.: Unpublished Rpt UCRL-Trans. 949 (1964).

[3] MILLER, J.M. and HUDIS, J., Annu. Rev. nucl. Sci. 9 (1959) 159.

[4] METROPOLIS, N., BIVINS, R., STORM, M., MILLER, J.M., FRIEDLANDER, G. and TURKEVICH, A., Phys. Rev. 110 (1958) 204.

[5] LINDNER, M. and TURKEVICH, A., Phys. Rev. 119 (1960) 1632.

[6] SHAMOV, V.P., Soviet Phys.-JETP 6 (1958) 268.

[7] HUIZENGA, J.R. and VANDENBOSCH, R., in Nuclear Reactions 2 (ENDT, P.M. and SMITH, P.B., Eds.) North-Holland Publishing Co., Amsterdam (1962).

[8] WAHL, A.C., "Mass and charge distribution in low-energy fission", these Proceedings I.

[9] VINOGRADOV, A.P., ALIMARIN, I.P., BARANOV, V.I., LAVRUKHINA, A.K., BARANOVA, T.V., PAVLOTSKAYA, F.I., BRAGINA, A.A. and YAKOVLEV, Yu.V., Proc. Conf. Acad. Sci. USSR on the Peaceful Uses of Atomic Energy (Akademija nauk SSSR, Moscow, 1955). English trans.: AEC Rpt. TR-2435 (1956) part 2, 65.

[10] LINDNER, M. and OSBORNE, R.N., Phys. Rev. 94 (1954) 1323.

[11] FOLGER, R.L., STEVENSON, P.C., and SEABORG, G.T., Phys. Rev. 98 (1955) 107.

[12] PATE, B.D., FOSTER, J.S. and YAFFE, L., Canad. J. Chem. 36 (1958) 1691.

[13] LAVRUKHINA, A.K. and KRASAVINA, L.D., J. nucl. Energy 5 (1957) 236.

[14] DOSTROVSKY, I., RABINOWITZ, P. and BIVINS, R., Phys. Rev. 111 (1958) 1659.

[15] FRIEDLANDER, G., FRIEDMANN, L., GORDON, B. and YAFFE, L., Phys. Rev. 129 (1963) 1809.

[16] STEVENSON, P.C., HICKS, H.G., NERVIK, W.E. and NETHAWAY, D.R., Phys. Rev. 111 (1958) 886.

[17] DOSTROVSKY, I. and STOENNER, R.W., private communication (1964).

[18] CHU, Y.Y., private communication (1964).

[19] KAUFMAN, S., Phys. Rev. 129 (1963) 1866, and private communication (1964).

[20] PORILE, N.T., private communication (1964).

[21] ALEXANDER, J., BALTZINGER, C. and GAZDIK, M.F., Phys. Rev. 129 (1963) 1826.

[22] RUDSTAM, G., "Fission yields in the iodine region" these Proceedings II.

[23] GOECKERMANN, R.H. and PERLMAN, I., Phys. Rev. 76 (1949) 628.

[24] PATE, B.D., Canad. J. Chem. 36 (1958) 1707.

[25] NOSHKIN, V.E., Jr. and SUGIHARA, T.T., J. inorg. nucl. Chem. (in press).

[26] RUDSTAM, G. and PAPPAS, A.C., Nucl. Phys. 22 (1961) 468.

[27] PAVLOTSKAYA, F. I. and LAVRUKHINA, A. K., J. nucl. Energy 5 (1957) 149.
[28] BILLER, W. F., Ph. D., Thesis, University of California, Rpt. UCRL-2067 (1952).
[29] MURIN, A. N., PREOBRAZHENSKY, B. K., YUTLANDOV, I. A. and YAKIMOV, M. A., Proc. Conf. Acad. Sci. USSR on the Peaceful Uses of Atomic Energy (Akademija nauk SSSR, Moscow, 1955). English transl.: AEC Rpt. TR-2435 (1956), part 2, 101.
[30] KALIAMIN, A. V., MURIN, A. N., PREOBRAZHENSKY, B. K. and TITOV, N. E., Soviet J. Atomic Energy (English Transl.) 4 (1958) 196.
[31] WOLFGANG, R., BAKER, E. W., CARETTO, A. A., CUMMING, J. B., FRIEDLANDER, G. and HUDIS, J., Phys. Rev. 103 (1956) 394.
[32] HUDIS, J. and TANAKA, S., private communication.
[33] HUDIS, J. and SCHAEFFER, O. A., private communication.
[34] de CARVALHO, H. G., POTENZA, G., RINZIVILLO, R., SASSI, E. and VANDERHAEGHE, G., Nuovo Cim. 25 (1962) 880.
[35] de CARVALHO, H. G., CORTINI, G., MUCHNIK, M., POTENZA, G., RINZIVILLO, R. and LOCK, W. O., Nuovo Cim. 27 (1963) 468.
[36] PATE, B. D. and POSKANZER, A. M., Phys. Rev. 123 (1961) 647.
[37] POSKANZER, A. M., private communication (1964).
[38] SHUDDE, R. H., Ph. D., Thesis, University of California, Rpt UCRL-3419 (1956).
[39] PERFILOV, N. A., DAROVSKIKH, V. F., DENISENKO, G. F. and OBUKHOV, A. I., Soviet Phys.-JETP 11 (1960) 517.
[40] ASHMORE, A., COCCONI, G., DIDDENS, A. N. and WETHERELL, A. M., Phys. Rev. Lett. 5 (1960) 576.
[41] HUDIS, J. and KATCOFF, S., private communication.
[42] PRICE, P. B. and WALKER, R. M., Phys. Lett. 3 (1962) 113.
[43] PERFILOV, N. A., Soviet Phys.-JETP 14 (1962) 623.
[44] DOUTHETT, E. M., and TEMPLETON, D. H., Phys. Rev. 94 (1954) 128.
[45] SUGARMAN, N., CAMPOS, M. and WIELGOZ, K., Phys. Rev. 101 (1956) 388.
[46] PORILE, N. T., Phys. Rev. 120 (1960) 572.
[47] PORILE, N. T. and SUGARMAN, N., Phys. Rev. 107 (1957) 1410; ibid. 111 (1958) 1746.
[48] CRESPO, V. P., CUMMING, J. B. and POSKANZER, A. M., private communication.
[49] CUMMING, J. B., CROSS, R. J., HUDIS, J. and POSKANZER, A. M., Phys. Rev. 134B (1964) 167.
[50] KOWALSKI, L., Ann. Phys., Paris 9 (1964) 211.
[51] CUMMING, J. B., PERLMAN, M. L. and REMSBERG, L. P., private communication.
[52] FRANZ, E. M. and FRIEDLANDER, G., unpublished results.

О ДЕЛЕНИИ ЯДЕР ПРИ СРЕДНИХ И ВЫСОКИХ ЭНЕРГИЯХ ВОЗБУЖДЕНИЯ

Н.А. ПЕРФИЛОВ
РАДИОИНСТИТУТ АН СССР, ЛЕНИНГРАД
СССР

Abstract — Résumé — Аннотация — Resumen

NUCLEAR FISSION AT HIGH AND MEDIUM ENERGY OF EXCITATION. A review of experimental research on nuclear fission at high and medium energy of excitation. Certain aspects of nuclear fission theory in this range of energy are also considered.

FISSION NUCLÉAIRE À HAUTE ET MOYENNE ÉNERGIE D'EXCITATION. Revue générale des travaux expérimentaux de recherche sur la fission nucléaire à haute et moyenne énergie d'excitation. Certains aspects de la théorie de la fission nucléaire dans ce domaine d'énergie sont également examinés.

О ДЕЛЕНИИ ЯДЕР ПРИ СРЕДНИХ И ВЫСОКИХ ЭНЕРГИЯХ ВОЗБУЖДЕНИЯ. В работе дается обзор экспериментальных исследований по делению ядер при средних и высоких энергиях возбуждения. Рассматриваются также отдельные положения в теории деления ядер в этой области энергий.

FISION NUCLEAR A ENERGIAS DE EXCITACION ELEVADA E INTERMEDIA. Se analizan los trabajos de investigación experimental sobre la fisión nuclear a energías de excitación elevada e intermedia. Se examinan además ciertos aspectos de la teoría de la fisión nuclear en este intervalo de energías.

К настоящему времени, кроме обзоров [1—4], относительно давних, по делению ядер при средних и высоких энергиях возбуждения, вышла в свет превосходная книга доктора Хайда [5] "Деление ядер", в которой с достаточной полнотой представлены как ранние, так и современные результаты исследований в данной области.

Данная работа ставит целью напомнить некоторые из основных экспериментальных фактов, относящихся к теме. Ссылки на литературные источники весьма ограничены из-за краткости текста. Более подробные сведения по проблеме деления при средних и высоких энергиях в историческом аспекте можно найти в вышеупомянутых обзорах [1—4].

1. ЭНЕРГИЯ ВОЗБУЖДЕНИЯ ДЕЛЯЩИХСЯ ЯДЕР

При облучении ядер протонами с кинетической энергией до 40—50 Мэв реакция, во многих случаях, идет через образование составного ядра, возбужденного до энергии, равной сумме кинетической энергии частицы и ее энергии связи в составном ядре. Когда ядра бомбардируются частицами, например протонами с $E_p \cong 100$ Мэв, то имеет место прямое взаимодействие частицы с нуклонами. В результате появляются каскадные частицы (или частицы выбивания) и ядра-остатки. Каскад развивается преимущественно

в направлении потока бомбардирующих частиц, разветвляясь на большие углы при увеличении энергии частиц, и состоит преимущественно из нейтронов, протонов и в какой-то мере из альфа-частиц. Со значительно меньшей вероятностью в каскаде, возможно, могут находиться частицы с бо́льшим зарядом и массой (литий, бериллий, бор и более тяжелые). В процессе взаимодействия протона или нейтрона высокой энергии с нуклонами ядра могут рождаться мезоны, а также другие частицы, не входящие в структуру ядра. Однако появление этих частиц, которые могут сопровождать деление, не связано с делением ядра, а лишь с первичной реакцией взаимодействия и развитием каскада. Ядро, оставшееся после прохождения каскада, оказывается в возбужденном состоянии. Энергия возбуждения зависит от степени развития каскада в каждом индивидуальном случае и варьируется от небольших значений до величины энергии бомбардирующей частицы. Среднее значение энергии возбуждения возрастает с ростом энергии действующих частиц и с ростом массового числа ядра – мишени.

Если энергия возбуждения определяется только для совокупности делящихся ядер, то зависимость от массового числа меняется на обратную; наблюдается возрастание энергии возбуждения с уменьшением массового числа от урана до висмута, вследствие исключения из общей статистики ядер с малым возбуждением, для которых деление не может осуществиться.

На рис.1 показана зависимость начальной энергии возбуждения от энергии протонов для делящихся ядер: U, Bi, Au, Ta, вычисленная с применением метода случайных испытаний [11], в сравнении с экспериментальными значениями [6–10]. На том же рисунке для сравнения дана зависимость

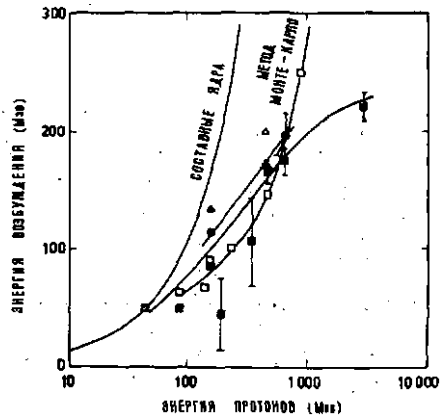

Рис.1

Начальная энергия возбуждения делящихся ядер при облучении урана протонами с энергией 45, 82, 155, 156, 192, 340, 460 и 660 Мэв и 3 Бэв, висмута протонами с энергией 156, 450 и 660 Мэв, золота протонами с энергией 156 Мэв, тантала протонами с энергией 450 Мэв. Энергия возбуждения вычислена из расчетной связи продольная составляющая импульса – энергия возбуждения [6]. Продольные, составляющие импульса делящихся ядер определены в работах [7–10]. Там же приведены значения энергии возбуждения ядер в случае образования составного ядра и полученные в расчете каскадной стадии взаимодействия по методу Монте-Карло [11]:

■ уран-238; ● висмут-209
▲ золото-197; Δ тантал-181.

энергии возбуждения от энергии протонов в предположении образования составного ядра.

Заряд и масса ядра-остатка после прохождения каскада, очевидно, определяется как разности $Z - \Sigma Z_K$ и $M - \Sigma M_K$, где Z_K и M_K – заряды и массы каскадных частиц. Число частиц в каскаде увеличивается вместе с ростом энергии бомбардирующих протонов. Например, для мишени из урана при возрастании энергии протона от 450 до 940 Мэв число каскадных заряженных частиц возрастает от 3 до 9 [11]. Число каскадных нейтронов определится по числу протонов с превышением в $[(A - Z)/Z](\sigma_{pn}/\sigma_{pp})$ раз. Здесь σ_{pn} и σ_{pp} – сечения рассеяния протон-нейтрон и протон-протон внутри ядра.

Однако данные, приведенные выше, не определяют заряд и массу ядра, а также и его энергию возбуждения в момент деления. При энергии возбуждения, много большей порога для деления и энергии связи нуклона в ядре, делению может предшествовать процесс испарения нейтронов и заряженных частиц. Масса и заряд ядра перед делением, а также и энергия возбуждения, определяется соотношением между делительной и частичной ширинами, различными при заданной энергии возбуждения для разных элементов периодической таблицы. Соотношения между ширинами, делительной Γ_f и нейтронной Γ_n, являются одним из основных вопросов, выяснение которого существенно для понимания механизма деления.

2. СЕЧЕНИЯ ДЛЯ ДЕЛЕНИЯ. ОТНОШЕНИЯ ШИРИН Γ_f/Γ_n

1. Средние энергии

На рис.2 отражена зависимость σ_f от энергии нейтронов для ядер $Z \geq 90$ и для области энергий, где отдельные энергетические уровни составного ядра уже не влияют на ход сечения. Ступенчатый рост сечения при $E_n \cong 6$ Мэв объясняется возможностью реакции (n, nf)[1]. Подробные ступенчатые изменения в ходе сечения с энергией нейтронов наблюдаются и при более высоких энергиях, когда могут иметь место реакции (n, xnf) при $x > 1$.

Поперечное сечение для деления компаунд-ядра равно:

$$\sigma_f = \sigma_c \cdot \Gamma_f/\Gamma ,$$

где σ_c – сечение образования компаунд-ядра. Для средних энергий нейтронов можно положить $\Gamma = \Gamma_f + \Gamma_n$. Ванденбош и Хьюзенга [14] вычислили отношение ширин Γ_n/Γ_f для ряда элементов и их изотопов (рис.3) не только для деления нейтронами, но и из опытов по делению ядер гамма-квантами, а также из анализа функций возбуждения реакций (α, xn) на ядрах с высоким сечением деления. На графиках отражена зависимость Γ_n/Γ_f от Z и A. От энергии возбуждения отношения ширин или совсем не зависят, или эта зависимость слабая.

Для ядер с $Z < 90$ зависимость сечения деления от энергии существенно иная. Эта зависимость характеризуется быстрым возрастанием с увеличе-

[1] *Недавно* [13] *ступенчатый ход зависимости* $\sigma(E)$ *наблюден также при делении ядер* Ra^{226} *ионами гелия.*

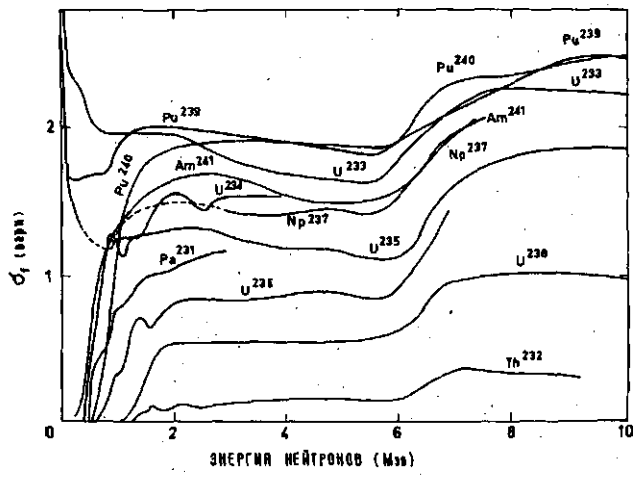

Рис.2

Зависимость поперечного сечения деления ядер от энергии нейтронов (компиляция данных и ссылки на первоисточники приведены в статье Хенкеля [12]).

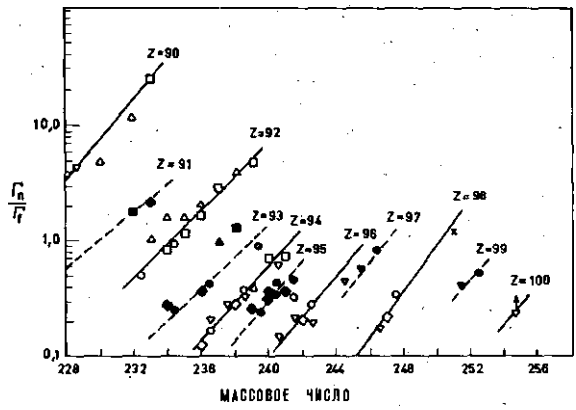

Рис.3

Значения Γ_n/Γ_f как функция массового числа делящегося ядра [14] (квадраты относятся к данным, полученным из значений сечений деления ядер при облучении нейтронами с энергией 3 Мэв, и соответствуют энергии возбуждения 8–10 Мэв. Треугольники относятся к данным, полученным из фотоделения, и соответствуют энергии возбуждения 8–12 Мэв. Кружки, ромбы и перевернутые треугольники относятся к средним значениям Γ_n/Γ_f, полученным из исследования функции возбуждения продуктов реакции расщепления, и соответствуют средней энергии возбуждения примерно 13, 18 и 23 Мэв. Крестик соответствует энергии возбуждения около 44 Мэв.

нием энергии возбуждения (см. например, рис.4), откуда делается вывод, что в большинстве случаев (свыше 90%) деление предшествует испусканию первого нейтрона в испарительной цепочке. Вычисленные из результатов измерений σ_f и σ_T отношения ширин Γ_f/Γ_n (считая $\sigma_T = \sigma_f + \sigma_n \simeq \sigma_n$) для ядер Bi, Pb, Tl, Au являются также быстро возрастающими функциями энергии возбуждения (рис.4).

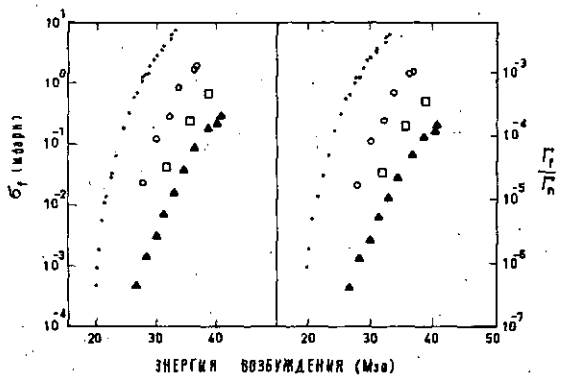

Рис.4

Зависимость сечения деления ядер и Γ_f/Γ_n (см. уравнение (1)) от энергии возбуждения при облучении висмута, свинца, таллия и золота ионами He^4 [15]:

● – висмут; ○ – свинец;
□ – таллий; ▲ – золото.

В работе Хьюзенги и Ванденбоша [4] выражение для Γ_f/Γ_n в зависимости от энергии возбуждения бралось в виде:

$$\frac{\Gamma_f}{\Gamma_n} = \frac{K_0 a_n [2a_f^{\frac{1}{2}}(E^* - E_f)^{\frac{1}{2}} - 1]}{4A^{\frac{2}{3}} a_f (E^* - B_n)} \times \exp\left[2a_f^{\frac{1}{2}}(E^* - E_f)^{\frac{1}{2}} - 2a_n^{\frac{1}{2}}(E^* - B_n)^{\frac{1}{2}}\right], \quad (1)$$

здесь: $K_0 = \hbar^2/gmr_0^2$, B_n и E_f соответственно энергия связи нейтрона в составном ядре и барьер деления, a_n и a_f – константы в зависимости плотности уровней от энергии возбуждения E^*, $\rho(E^*) \sim \exp[2(aE^*)^{\frac{1}{2}}]$ исходного ядра и ядра в седловой точке. Оказывается, что экспериментальную кривую Γ_f/Γ_n (рис.4) с помощью выше написанного выражения можно воспроизвести лишь при условии, что $a_f > a_n$. Так, для Au^{197} наилучшее согласие получается при $E_f = 15{,}81$ Мэв; $a_n = 21{,}4$; $a_f = 26{,}62$ Мэв$^{-1}$.

2. *Высокие энергии*

Ранее нами [16] были рассмотрены экспериментальные данные по зависимости σ_f от энергии протонов и параметра Z^2/A. Результат следующий: отношение σ_f/σ_T где σ_T – сечение неупругого взаимодействия, плавно возрастает с увеличением энергии протонов, достигает своего максимального значения и затем или остается величиной постоянной, не зависящей от дальнейшего увеличения энергии, или, если изменяется, то очень медленно (несколько уменьшается [17]). Для области насыщения зависимости σ_f/σ_T от Z^2/A хорошо определяется в полулогарифмическом масштабе прямой линией для области ядер от урана до тантала. Соответствующая экспонента записывается в виде:

$$\sigma_f/\sigma_T = \exp\{0{,}682\,[Z^2/A - 36{,}25]\}. \quad (2)$$

По измерениям Де Карвальо и соавторов [19] эта зависимость удовлетворяется и при делении ядер, в том же интервале Z, гамма-квантами с энергиями до 1000 Мэв (рис.5).

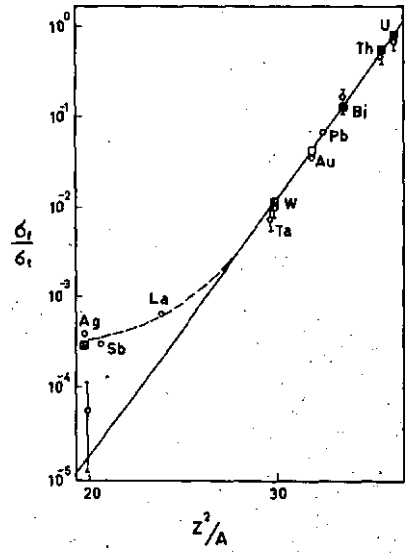

Рис.5

Зависимость делимости ядер в области насыщения сечения деления от Z^2/A при облучении протонами высокой энергии и γ-квантами [18–19]:

○ – p (Перфилов); ■ – γ (Де Кавальо); □ – γ (Юнгерман, Штейнер).

Экспериментальные сечения в области лантана и более легких ядер не удовлетворяют выше написанной экспоненте. В особенности велико было наблюдено расхождение для серебра, для которого Беккер и Катков [20] при $E_\gamma = 3$ Бэв дали значение $\sigma_f \simeq 100$ мб, вместо долей миллибарна, которые следуют из зависимости (2).

Для выяснения причин, приводящих к разногласиям, в нашей лаборатории было предпринято обстоятельное изучение [21] короткопробежных продуктов ядерных расщеплений, вызываемых протонами с энергиями 2–9 Бэв в фотослое (AgBr+желатина). Анализировались ядерные расщепления Ag, Br, сопровождаемые образованием двух короткопробежных частиц, разлетающихся, в основном, в двух противоположных направлениях. Из анализа угловых и пробеговых характеристик был сделан вывод, что большинство расщеплений Ag, Br такого типа следует отнести не к делениям ядер Ag или Br, а к расщеплениям, в которых образуется один короткопробежный фрагмент и ядро отдачи. Для деления ядер Ag или Br при энергии протонов 2–9 Бэв получена верхняя граница сечения около 1 мбн.

Полученный результат дает нам основание считать, что, по-видимому, истиное значение σ_f/σ_T и в области лантан-серебро близко следует экспоненте (2), а несоответствие, как и ранее нами считалось [16], обязано наложению на процесс деления процесса фрагментации, приводящего к появлению фрагмента и ядра отдачи.

В настоящее время сотрудником нашей лаборатории Быченковым В.С. ведутся исследования деления ядер вольфрама протонами при энергии 660 Мэв. Из анализа энергетических спектров заряженных частиц, сопровождающих деление, следует, что, в среднем, около 40% α-частиц и 20% про-

тонов, сопровождающих деления, излучаются ядром до его разделения. Остальные излучаются осколками при снятии возбуждения.

Подобный вывод сделан на основании сравнения спектров α-частиц и протонов, сопровождающих деление, со спектрами тех же частиц, наблюдающихся при реакциях отщепления от вольфрама и серебра и брома фотоэмульсии (Усредненное ядро AgBr можно рассматривать, как продукт симметричного деления вольфрама).

На рис.6 слева можно видеть три спектра α-частиц, нормированные к единице (спектр от AgBr пересчитан от системы координат, связанной

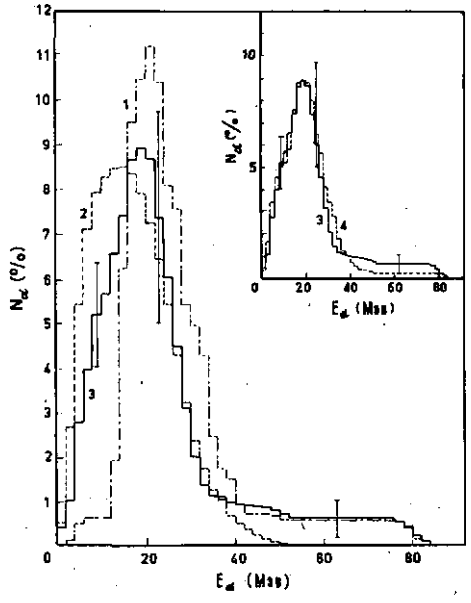

Рис.6

Энергетические спектры α-частиц, сопровождающих деление W, расщепления W и Ag протонами 660 Мэв:

1 – α от распада W;
2 – α от распада AgBr (с поправкой на движение продуктов деления);
3 – α при делении W;
4 – сумма 1-го (ст.вес 0,4) и 2-го (ст.вес 0,6) спектров.

с движущимся осколком, к лабораторной системе).

В правой части показано, что для получения формы спектра α-частиц, сопровождающих наблюденные в опыте случаи деления, необходимо взять 40% спектра отщепления от W и 60% спектра отщепления AgBr.

3. *Многозарядные ионы*

Изучение процесса деления ядер при облучении многозарядными ионами интересно по ряду причин: при полном слиянии ядра мишени и многозарядного иона (70–80% от всех случаев взаимодействия) новое ядро будет обладать большим угловым моментом; энергией возбуждения, значительно бо́льшей, чем можно получить для компаунд-ядра при бомбардировке легкими

частицами (протонами, нейтронами, He^4-ионами); недостатком нейтронов по сравнению с обычными изотопами того же элемента. Отмеченные особенности компаунд-ядра, образующегося при бомбардировке тяжелыми ионами, позволяют исследовать влияние перечисленных факторов на процесс деления. Особенно существенно получение экспериментальных данных по делению многозарядными ионами ядер из области где $Z^2/A \leq 0{,}67$ из-за возможности сопоставления с выводами теории на основе развития жидкокапельной модели в применении к делению [25–29].

Зависимость сечения деления от энергии при облучении нескольких ядер ионами углерода дана на рис.7. Для изотопов урана оно близко к пол-

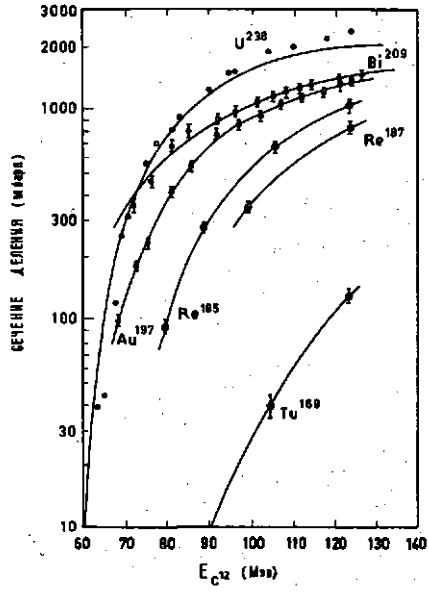

Рис.7

Сечение деления ядер при облучении U^{238} [22], Bi^{209}, Au^{197} [23], Re^{185}, Re^{187}, Tu^{169} [24] ионами C^{12}. Сплошная кривая в случае урана соответствует расчетному значению сечения образования составного ядра. Сплошные кривые в других случаях проведены через экспериментальные значения сечений деления.

ному сечению в результате того, что компаунд-ядро делится как от полного слияния, так и от частичного. Для легких ядер сечение составляет долю от полного, тем меньшую, чем легче ядро.

При облучении ионами типа O^{16} и C^{12} таких ядер, как висмут, золото и более легких, из-за высокого барьера делятся, в основном, лишь ядра, получившиеся в результате полного слияния.

Приведем некоторые результаты по делению ядер от Cs до W многозарядными ионами C^{12}, O^{16}, в основном, по сравнительно недавно опубликованной работе Сиккеланда [30].

Зависимость сечения деления (как части от полного сечения) от энергии возбуждения представлена на рис.8 для ядер от Cs^{133} до W^{182} при облучении ионами O^{16}.

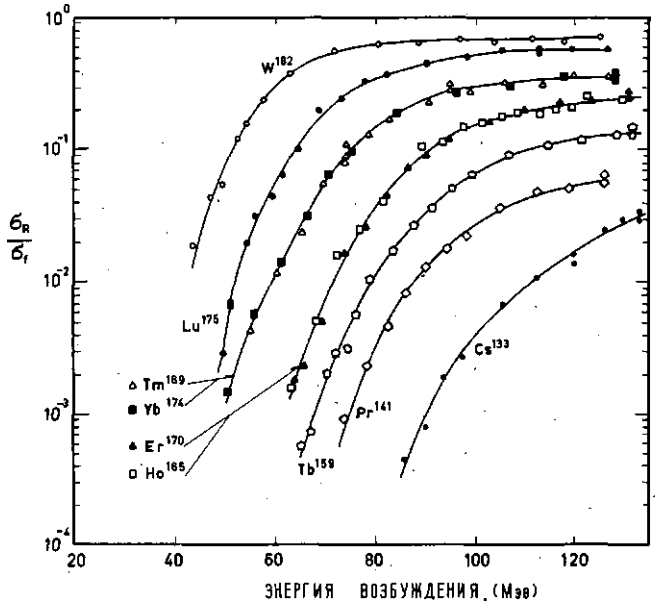

Рис.8

Зависимость сечения деления от энергии возбуждения для ядер от Cs^{133} до W^{182} при облучении ионами O^{16}.

На рис.9 отражена зависимость сечения деления как от энергии возбуждения, так и от величины углового момента для компаунд-ядер: а) таллия-197, полученного [24] облучением танталла ионами кислорода, и рения — ионами углерода; b) рения-181 от облучения [30] туллия, хольмия, тербия ионами углерода, кислорода и неона соответственно. Различие в сечениях при одинаковой энергии возбуждения обязано влиянию углового момента на величину барьера для деления.

На рис.10 представлена зависимость отношения σ_f/σ_t от Z^2/A по результатам опытов Сиккеланда [30] в сравнении с подобной зависимостью, полученной нами ранее для деления ядер протонами [16]. Если значения для σ_f/σ_t брать при выходе на плато, то $\ln\sigma_f/\sigma_t$ от Z^2/A (Z^2/A берется для компаунд-ядра) представится прямой

$$\ln\sigma_f/\sigma_t = 0{,}455(Z^2/A - 34{,}43)\,.$$

Из сопоставления с подобной зависимостью, полученной при делении протонами следует: а) для всего выбранного интервала значений Z^2/A делимость при действии ионами больше делимостей при действии протонами, б) с уменьшением Z^2/A разница в делимостях при действии ионов и протонов — возрастает. Так, для Ag эта разница, как следует из экстраполяции, около двух порядков.

Большие значения отношения σ_f/σ_t при действии ионов можно связать или с влиянием недостатка нейтронов в компаунд — ядре при делении ионами, или с понижением барьера деления в результате передачи делящемуся ядру

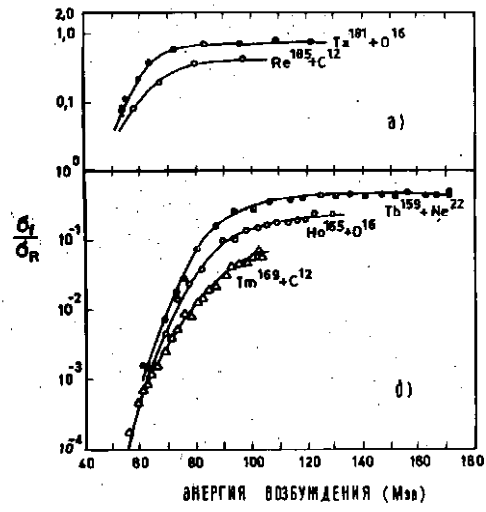

Рис.9

Экспериментальные значения отношения σ_f/σ_t как функция энергии возбуждения при облучении ряда ядер ионами O^{16}. Вероятность деления как функция энергии возбуждения и углового момента ядер для составного ядра:

а – Tl^{197} [30]; б – Re^{181} [31].

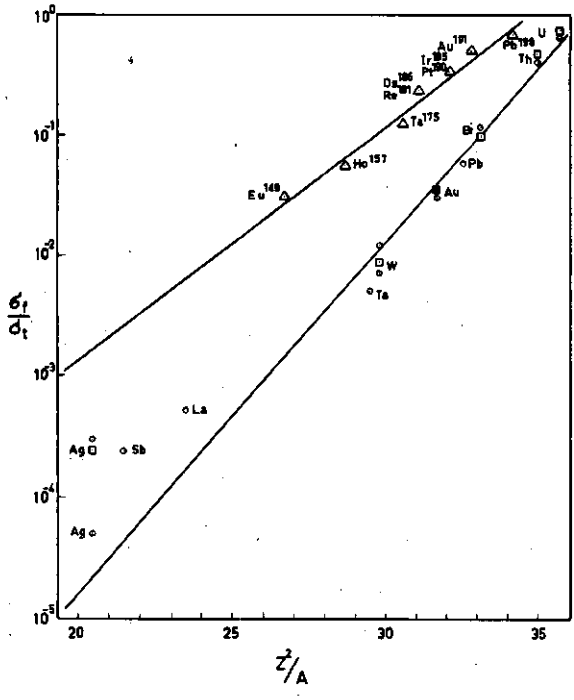

Рис.10

Зависимость σ_f/σ_t при насыщении от Z^2/A при облучении ядер ионами O^{16}:

○ – p (Перфилов); ■ – γ (Юнгерманн, Штейнер);
□ – γ (Де Кавальо); △ – O^{16} (Результаты Сиккеланда).

большего углового момента. Последний фактор, возможно, имеет главное значение.

В связи с выше сказанным, было бы интересно продолжить опыты по делению тяжелыми ионами для таких легких ядер как Ag, для которых полученные сечения деления протонами очень ненадежны.

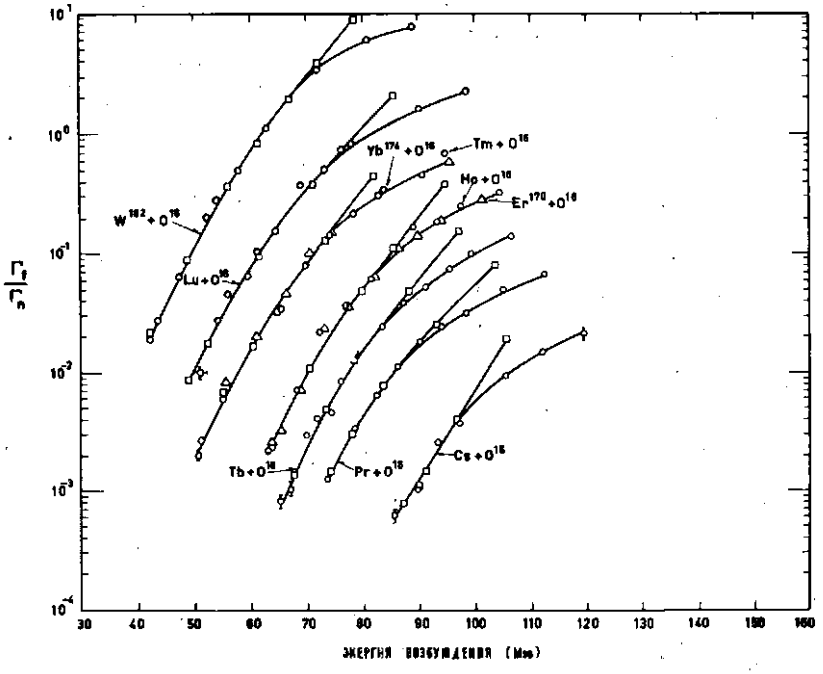

Рис.11

Экспериментальные и расчетные значения Γ_f/Γ_n ядер, образованных при облучении ряда мишеней ионами O^{16} [30]:

●, ▲ – экспериментальные значения; ■ – расчетные.

На следующем рисунке 11 даны значения экспериментально определенного отношения Γ_f/Γ_n в сопоставлении с вычисленными значениями для отношения ширин. При вычислении Γ_f/Γ_n использовалось выражение (1) с учетом энергии вращения (и, следовательно, углового момента) для состояния – основного и соответствующего седловой точке.

$$\frac{\Gamma_f}{\Gamma_n} = \frac{K_0 a_n [2af^{1/2}(E^* - Ef - R_s^0)^{1/2} - 1]}{4A^{2/3}\, af\,(E^* - B_n - R_e^0)} \times$$

$$\times \exp[2af^{1/2}(E^* - E_f - R_s^0)^{1/2} - 2a_n^{1/2}(E^* - B_n - R_e^0)^{1/2}] \qquad (3)$$

$R_e^0 = \hbar I^2/2\mathcal{J}_e^0, \quad R_s^0 = \hbar I^2/2\mathcal{J}_s^0,$

где $\mathcal{J}_e^0$ и $\mathcal{J}_s^0$ эффективные моменты инерции для сферического ядра и ядра в седловой точке.

Как видим, при высоких энергиях наблюдается заметное расхождение вычисленных и экспериментальных значений. Чтобы получить согласие, по-видимому, для некоторых параметров, входящих в выражение (3), надо ввести зависимость от энергии возбуждения. Сиккеланд отмечает, что расхождение можно устранить, предположив, что с возрастанием энергии возбуждения: а) или $\Gamma_{зч}$ увеличивается[1]; б) или $\sigma_{пс}/\sigma_т$ уменьшается ($\sigma_{пс}$ – сечение полного слияния иона и ядра); в) или $\mathcal{J}_e^0/\mathcal{J}_s^0$ увеличивается; г) или a_f/a_n уменьшается. Как видим, имеем слишком много параметров, которые могут меняться с энергией возбуждения. Необходимо дальнейшее изучение особенностей деления ядер многозарядными ионами.

3. РАСПРЕДЕЛЕНИЕ ПРОДУКТОВ ДЕЛЕНИЯ ПО МАССАМ, КИНЕТИЧЕСКИМ ЭНЕРГИЯМ И УГЛАМ

1. Распределение по массам

Эволюция массового распределения осколков в зависимости от энергии возбуждения и места ядра в таблице элементов видна из рис.12. На рис.12 имеем распределение по массам продуктов деления урана-235 тепловыми

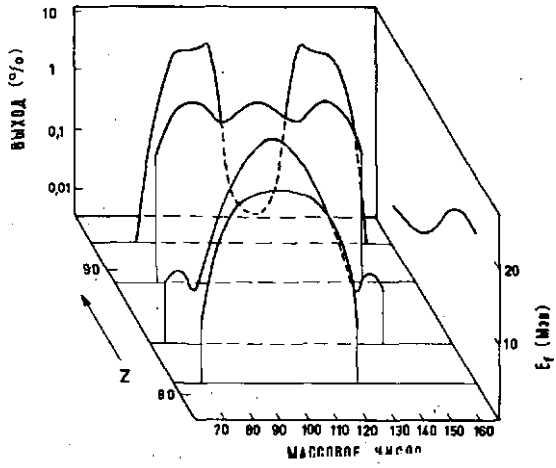

Рис.12

Массовое распределение осколков деления ядер при облучении U^{235} тепловыми нейтронами [31], Ra^{226} протонами с энергией 11 Мэв [32], Bi^{209} протонами с энергией 36 Мэв [33] и Au^{197} ионами He^4 с энергией 45 Мэв [34]. Приведены также значения барьеров деления ядер.

нейтронами [31], радия протонами 11 Мэв [32], висмута протонами с энергией 36 Мэв [33] и золота альфа-частицами 45 Мэв [34]. Для урана массовое распределение осколков преимущественно асимметрично. Для радия вклады симметричного и асимметричного деления соизмеримы. У висмута симметричное деление преобладает, но еще заметны два максимума от асимметричных по массам делений при энергиях, близких к пороговым. У

[1] Γ^{37} – ширина для испарения заряженных частиц.

продуктов деления золота альфа-частицами распределение имеет один максимум. Изменение вида массового распределения осколков с ростом энергии возбуждения хорошо представлено распределением по массам продуктов деления урана и висмута при существенно различных энергиях возбуждения (см. рис.13 и 14). Кривая 4 на рис.14 относится к продуктам деления зо-

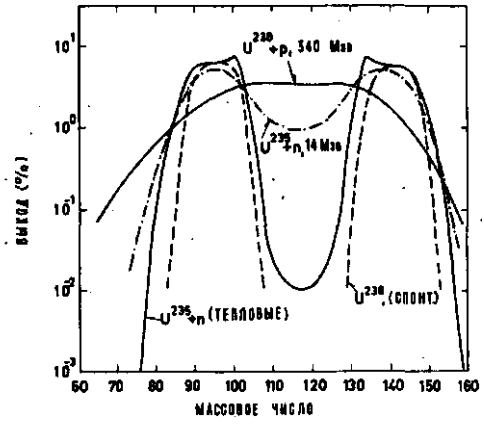

Рис. 13

Распределение осколков деления по массам при спонтанном делении U^{238} [35], при облучении U^{235} тепловыми нейтронами [32], нейтронами с энергией 14 Мэв [36] и при облучении U^{238} протонами с энергией 340 Мэв [37].

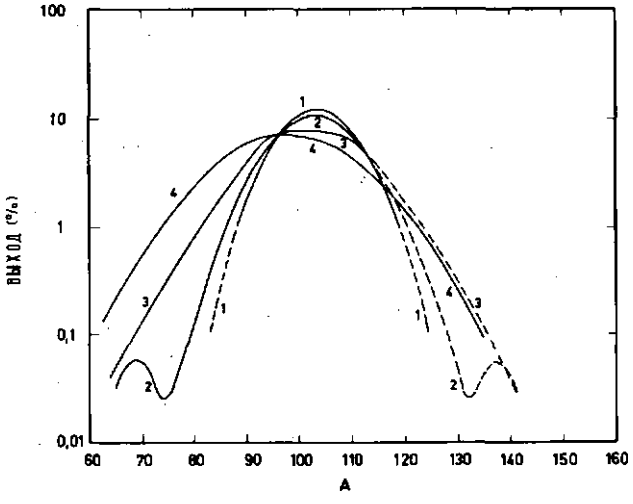

Рис. 14

Распределение осколков деления ядер по массам при облучении висмута дейтонами с энергией 22 Мэв (кривая 1) [39], протонами с энергией 36 (кривая 2) и 58 Мэв (кривая 3) [34], золота ионами C^{12} с энергией 112 Мэв (кривая 4) [40].

лота ионами C^{12} с энергией 112 Мэв. При возрастании энергии бомбардирующих частиц кривые массового распределения уширяются за счет по-

явления и возрастания числа более асимметричных случаев деления и некоторой убыли делений симметричных.

Массовое распределение осколков с двумя максимумами принято объяснять влиянием на процесс деления заполненных нуклонных оболочек [40, 41] или кластерной структурой ядра [42], а распределение с одним максимумом-делением ядерного вещества с высокой энергией возбуждения, допускающим, при теоретическом анализе, применение жидко-капельной модели. Трехгорбое массовое распределение продуктов деления радия послужило основной причиной для гипотезы, выдвинутой рядом исследователей [45, 46] о наличии двух различных механизмов деления.

Преимущественно асимметричный характер деления тяжелых ядер при низких энергиях возбуждения обусловлен, по-видимому, влиянием на процесс деления замкнутых оболочек из 82 нейтронов и 50 протонов в тяжелом осколке. Об этом свидетельствует, в частности, устойчивое положение правого пика массовых кривых, соответствующего тяжелым продуктам асимметричного деления, в широком диапазоне делящихся ядер (рис.12). С ростом энергии возбуждения ядра, как можно ожидать, влияние оболочечных эффектов ослабляется, вклад преимущественно асимметричного деления уменьшается, а, соответственно, вклад преимущественно симметричного деления, при котором, как можно предположить, оболочки не проявляются, – увеличивается. Быстрый рост выходов продуктов симметричного деления тяжелых ядер с ростом энергии возбуждения отражает некоторым образом скорость исчезновения оболочечных эффектов и прекращается, когда оболочки полностью разрушаются, и деление ядер становится преимущественно симметричным. При дальнейшем возрастании энергии возбуждения, как и в случае висмута, массовое распределение осколков деления тяжелых ядер просто расширяется.

При переходе от тяжелых ядер к более легким увеличивается барьер деления (рис.12), увеличивается необходимая для деления энергия возбуждения ядер, что приводит к уменьшению влияния оболочек на процесс деления. Другой причиной изменения характера массового распределения осколков при переходе от тяжелых к более легким ядрам может являться различная степень деформации этих ядер в седловой точке. Для тяжелых ядер, у которых форма ядра в седловой точке не сильно отличается от исходной формы, может проявляться влияние структуры исходного ядра. Для более легких ядер, которые претерпевают сильное изменение формы до седловой точки, следовало бы ожидать значительного уменьшения влияния структуры исходного ядра на процесс деления. Быть может, этим, отчасти, можно объяснить экспериментально установленный факт, что при примерно одинаковой энергии возбуждения исходного ядра, 20–30 Мэв, деление тяжелых ядер урана, тория еще преимущественно асимметрично [36, 25, 47], у радия соизмерим вклад асимметричной и симметричной форм деления [32], а асимметричная форма деления ядер висмута составляет доли процента [33].

Уширение массового распределения можно связать с возрастанием энергии возбуждения ядра. Так, Обуховым [48] для отношения вкладов симметричного к асимметричному делению дается выражение:

$$Y_1/Y_2 \simeq \exp[-\Delta E/T], \qquad (4)$$

где T – температура ядра, ΔE – разница в потенциальной энергии при кри-

тических деформациях, определяющих вид деления Y_1 и Y_2. Так как в модели жидкой капли асимметричной формы ядра в седловой точке соответствует большая величина потенциальной энергии деформации в сравнении с симметричной формой, то выше написанное простое выражение (4) качественно объясняет наблюдаемое уменьшение выходов осколков с увеличением отношения их масс. С ростом энергии возбуждения, соответственно, температуры ядра, разница в величине потенциальной энергии критической деформации ΔE, играет все меньшую роль в относительном выходе двух продуктов деления, что приводит к наблюдаемому расширению распределения осколков по массам.

Струтинский [49] и Никс [27] в рамках модели жидкой капли, исходя из представления о статистическом равновесии в седловой точке, получили выражение типа 4 для вероятности конкуренции деления с тем или иным отношением масс осколков, которое может быть представлено как

$$P(U) = \frac{1}{(2\pi T/K_m)^{1/2}} \exp[-(U-1/2)^2/(2T/K_m)], \qquad (5)$$

где $U = m_1/(m_1+m_2)$,

K_m – константа жесткости по отношению к изменению формы ядра.

Выражение для Y_1/Y_2 можно получить, как отмечено Обуховым, также непосредственно из теории Бора и Уиллера [50]. Действительно по Бору и Уиллеру, при зависимости плотности уровней от энергии возбуждения $\rho \sim \exp[2(aE^*)^{1/2}]$, вероятность деления пропорциональна:

$$W \sim \{[2a^{1/2}(E^*-E_f)^{1/2} - 1]\exp[2a^{1/2}(E^*-E_f)^{1/2}]\} + 1$$

и конкуренцию двух делений с различающейся формой ядра при прохождении через вершину потенциального барьера, с соответствующим барьером деления E_f^1 и E_f^2 можно представить отношение:

$$\frac{Y_1}{Y_2} = \frac{\{[2a^{1/2}(E^*-E_f^{(1)})^{1/2} - 1]\exp[2a^{1/2}(E^*-E_f^{(1)})^{1/2}]\} + 1}{\{[2a^{1/2}(E^*-E_f^{(2)})^{1/2} - 1]\exp[2a^{1/2}(E^*-E_f^{(2)})^{1/2}]\} + 1}. \qquad (6)$$

Из экспериментально определенного массового распределения осколков деления, зная величину барьера E_f для симметричного деления с помощью равенства (5) можно определить разницу ΔE_f барьеров деления ядра на неравные части. На рис.15 приведены зависимости полуширин массового распределения осколков $W_{1/2}$ от энергии возбуждения для деления компаунд-ядра из области около висмута. Кривая "а" по формуле (6), крестики – значения по формуле (4), кривая "в" – расчетная зависимость [27] и прямая – согласно зависимости: $W_{1/2} = E_c^* + 7$, полученной из эксперимента Нойзилем и Файрхоллом [36] для деления ядер свинца вблизи порога.

2. *Кинетическая энергия осколков*

Полагая, что кинетическая энергия осколков определяется исключительно их кулоновским расталкиванием и что $Z_1/Z_2 = A_1/A_2$, получим для осколков сферической формы:

$$\overline{E}_K = \frac{Z_1 \cdot Z_2 e^2}{r_1 + r_2} = \frac{Z_0^2 e^2}{r_0 A_0^{1/3}} \left\{ \frac{A_т / A_л}{\left(1 + \frac{A_т}{A_л}\right)^{1/3} \left[1 + \left(\frac{A_т}{A_л}\right)^{1/3}\right]} \right\} = \frac{Z_0^2}{A_0^{1/3}} f(A_т / A_л). \quad (7)$$

Здесь Z_0 и A_0 – зарядовое и массовое числа делящихся ядер.

Из выражения (7) следует, что $\overline{E}_K$ имеет максимум при делении на осколки равных масс. Эксперимент дает, как известно, для среднего значения

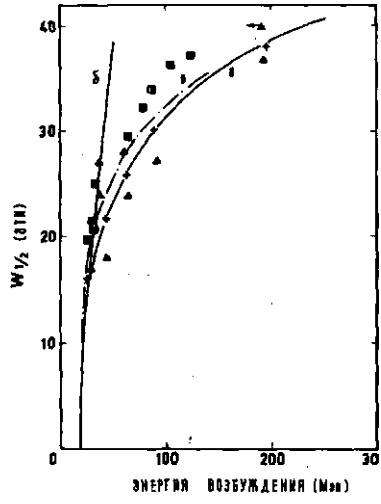

Рис.15

Расчетная и экспериментальная зависимость ширины при полумаксимуме массового распределения осколков деления. Экспериментальные значения ширины массового распределения осколков деления ядер, близких к Po^{210}, взяты из работ [33, 34, 38, 39, 27, 43, 44]:

а – кривая по формуле (6);
б – прямая согласно зависимости $W_{1/2} = E^*_{зр} + 7$;
в – расчетная зависимости по формуле (5);
▲▲▲ – радиохимический метод;
■■■ – твердый детектор;
××× – значения по формуле (4).

E_K при делении урана тепловыми и медленными нейтронами, кривую с минимумом в области симметричного деления (рис.16). Одним из объяснений наличия минимума в области симметричного деления ядер урана является предположение о большой деформации осколков при их разделении, ослабляющей влияние замкнутых оболочек. При увеличении энергии возбуждения влияние оболочек ослаблено, и деление на осколки равных масс может происходить из состояний с меньшей деформацией и, следовательно, минимум в кинетической энергии будет с возрастанием энергии возбуждения постепенно исчезать (рис.16).

Интересно отметить, что подобно связи в уменьшении провала в области симметричного деления в кривой масс и кинетической энергии при делении тяжелых ядер с ростом энергии частиц (рис.13), при переходе от тяжелых ядер к более легким уменьшение провала в области симметричного деления в массовых кривых (рис.12) сопровождается уменьшением провала в кине-

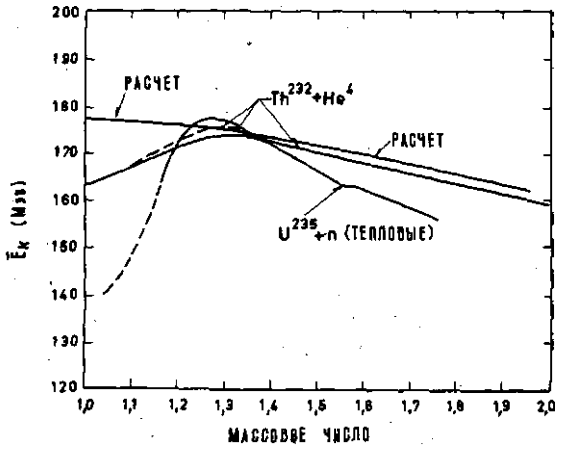

Рис.16

Зависимость средней кинетической энергии пары осколков деления от отношения их масс в случае деления ядер при облучении U^{235} тепловыми нейтронами [51], Th^{232} ионами He^4 с энергией 22 Мэв (пунктир), 29,5 Мэв [52]. Приведена также расчетная [51] зависимость для делящегося ядра U^{236}.

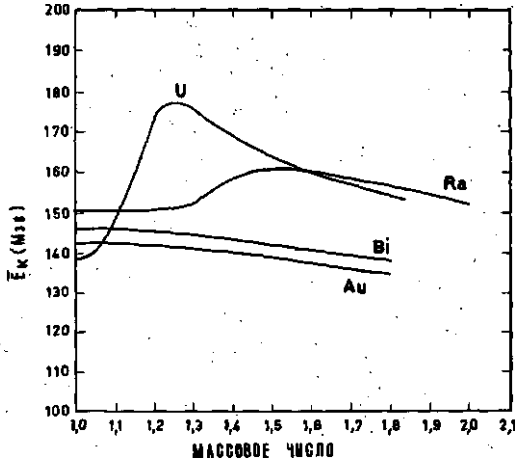

Рис.17

Зависимость средней кинетической энергии пары осколков деления от отношения их масс в случае деления ядер при облучении U^{235} тепловыми нейтронами [51], Ra^{226} дейтонами с энергией 14 Мэв [46], Bi^{209} и Au^{197} ионами He^3 с энергией 25,5 Мэв [46].

$$\bar{E}_K = \frac{Z^2 e^2}{r_0 A^{1/3}} \left\{ \frac{A_т/A_л}{\left(1+\frac{A_т}{A_л}\right)^{5/3}\left[1+\left(\frac{A_т}{A_л}\right)^{1/3}\right]} \right\}$$

тической энергии осколков симметричного деления (рис.17). В случае золота как выход, так и кинетическая энергия осколков имеют максимальное значение при делении на осколки равной массы.

Как было показано Террелом [55], для ядер от тория до формия зависимость (7) хорошо удовлетворяется при $f(A_т/A_л)$ = константе = 0,121. Для

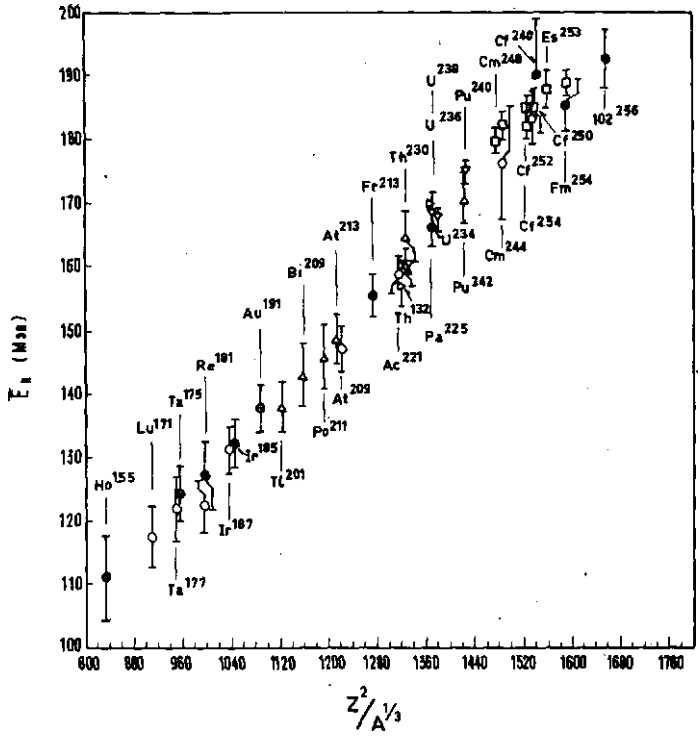

Рис.18

Зависимость средней кинетической энергии осколков деления от $Z^2/A^{1/3}$ делящегося ядра [51, 53, 54]:

○ – углерод-12; ● – кислород-16; △ – гелий-4; ▽ – нейтроны тепловые; ▷ – гамма; ⊏ – спонтанные.

$$\bar{E}_K = 17{,}5 + 0{,}109\,\frac{Z^2}{A^{2/3}}$$

более широкого интервала значений Z (рис.18) среднее значение кинетической энергии лучше описывается выражением:

$$\bar{E}_K = 17{,}5 + 0{,}109\,Z^2/A^{1/3}\,. \qquad (8)$$

Экспериментальная зависимость кинетической энергии осколков типа (8) указывает на то, что форма осколков в момент разделения отлична от сферической. Если представить ядро в момент разделения в форме двух касающихся, равномерно заряженных эллипсоидов, то, чтобы энергия их электростатического взаимодействия [26] удовлетворяла равенству (8), необходимо допустить, чтобы отношение полуосей эллипсоида C/A изменялось от 1,92 до 2,25 в исследуемом интервале делящихся ядер.

Угловое распределение осколков. Определяется величиной вектора орбитального момента L, вносимого в ядро частицей. Если вектор L, направление которого перпендикулярно пучку, преобладает по величине над значениями собственных спинов ядра и частиц, то угловое распределение будет анизотропным с максимумами в направлениях вперед и назад по

отношению к пучку. Теоретический анализ явления [55, 56] показывает, что если ввести в рассмотрение вектор K – проекцию результирующего вектора момента I на направление линии разлета осколков, то угловая анизотропия определится параметром $p = \left(\frac{I_m}{2\overline{K}}\right)$, где : I_m – максимальное значение I, $\overline{K}$ – среднее значение K,

$$\overline{K}^2 = \frac{1}{\hbar^2}\,\frac{\mathcal{J}_\perp \cdot \mathcal{J}_\parallel}{\mathcal{J}_\perp - \mathcal{J}_\parallel}\cdot T = \mathcal{J}_{\text{эфф}}\ T/\hbar^2\,, \tag{9}$$

$\mathcal{J}_\parallel$ и $\mathcal{J}_\perp$ – моменты инерции, параллельный и перпендикулярный оси симметрии ядра соответственно,

T – ядерная температура.

Для значений параметра P порядка единицы

$$\frac{\sigma(0°)}{\sigma(90°)} \simeq 1 + \frac{P}{2} = 1 + \frac{I_m^2}{8\overline{K}^2}\,, \tag{10}$$

а при больших "p" распределение имеет вид $1/\sin\theta$.

Экспериментальные данные по делению ядер частицами разных энергий и разной природы подтверждают основные выводы теории: 1) что при делении многозарядными ионами анизотропия возрастает как с ростом энергии частиц (I_m растет быстрее, чем K), так и с увеличением массы делящего иона [23]; 2) Величина угловой анизотропии уменьшается с ростом параметра Z^2/A (рис.19). Это обстоятельство связывается с предположением, что с ростом Z^2/A деление может происходить с более высокого уровня возбуждения. Здесь при сопоставлении величины анизотропии для ядер из области уран-плутоний и золото-висмут следует учитывать величину барьера для деления. У последних барьер для деления относительно большой из-за уменьшения Z^2/A и температура ядра в седловой точке, следовательно, понижается при одинаковой вносимой в ядро энергии; 3) Несколькими авторами [7, 57] было подмечено, что асимметричное деление тяжелых ядер более анизотропно, чем симметричное. Наблюдаемая зависимость анизотропии деления тяжелых ядер от отношения масс осколков объясняется [56] наложением делений после испускания нейтрона и до испускания. После испускания нейтрона будет преобладающим деление асимметричное, с меньшим K в результате понижения T, что и приводит к наблюдаемому эффекту.

Для ядер из области золото-висмут, у которых деление при средних энергиях возбуждения происходит преимущественно до испарения нейтрона, можно ожидать корреляций величины анизотропии с отношением масс осколков, если полагать, что с ростом отношения масс растет и барьер для деления. К настоящему моменту опубликованных опытных данных, относящихся к обнаружению этого эффекта, мало. Имеется одно исследование [58], в котором получено, что для отношения масс 1,53, при облучении висмута альфа-частицами с энергией – 42 Мэв, анизотропия уменьшилась, а не возросла, как следовало ожидать из-за возрастания барьера. Выход для отношения 1,53 определялся по брому. Авторы (Флинн и др. [58]) полагают, что увеличение K^2 в этом случае может быть связано не только

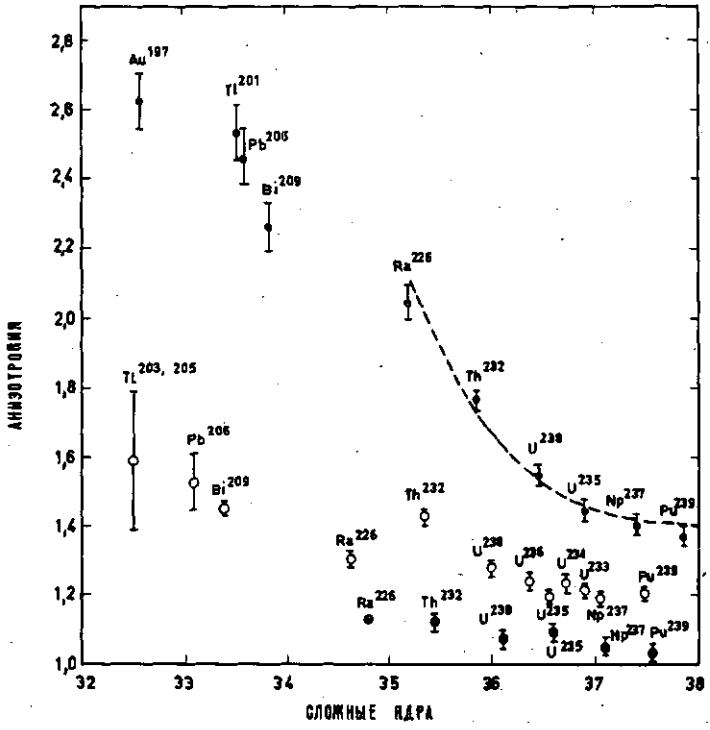

Рис.19

Зависимость анизотропии углового распределения осколков деления от Z^2/A составного ядра при облучении ряда ядер протонами, дейтонами и ионами He^4 [59—61].

• – 43 Мэв – He^4; о – 21 Мэв – H^2; ● – 11 Мэв – P

$$\frac{\sigma(0°)}{\sigma(90°)} \approx 1 + \frac{P}{2} \approx 1 + \frac{I_m^2}{8\bar{K}^2}; \qquad \bar{K}^2 = \frac{1}{\hbar^2}\frac{\mathcal{J}_\perp \cdot \mathcal{J}_\parallel}{\mathcal{J}_\perp - \mathcal{J}_\parallel} \cdot T = \frac{\mathcal{J}_{эфф} T}{\hbar^2}$$

с увеличением $\mathcal{J}_{эфф}$, обязанному форме ядра в седловой точке, но, возможно, и с большей температурой для седловой конфигурации, приводящей к Br^{83} в качестве легкого осколка.

При облучении ядер протонами высоких энергий (сотни Мэв) нет вполне убедительных указаний (с большим превышением над экспериментальными ошибками) на анизотропию в угловом распределении. По-видимому, развитие каскада, предшествующее делению, дезориентирует ядра по направлению момента I.

В заключение нашего сообщения напомню некоторые данные о делении ядер π-, μ-мезонами.

Медленные π^--мезоны. При облучении тяжелых ядер медленными π^--мезонами наблюдается деление ядер [62, 63]. Вероятность деления ядер урана-238 медленными π^--мезонами, т.е. отношение числа делений к числу мезонов, поглощенных ядрами урана, к числу составляет значение около 0,4—0,5. Для висмута и вольфрама около 0,02; 0,002 соответственно.

Примерно в 10% от всех делительных событий деление сопровождается излучением протонов с энергиями 10—60 Мэв, имеющих изотропное распределение по углам.

Распределение осколков по пробегам имеет вид кривой с одним максимумом при среднем значении пробега около 12 Мэв (рис.20).

Отмеченные экспериментальные факты указывают на следующий механизм взаимодействия медленных π^--мезонов с ядрами: π^--мезон захватывается на боровскую орбиту атома урана, образуя мезоатом урана. Затем π^--мезон с вероятностью, большей, чем вероятность распада, на μ^--мезон

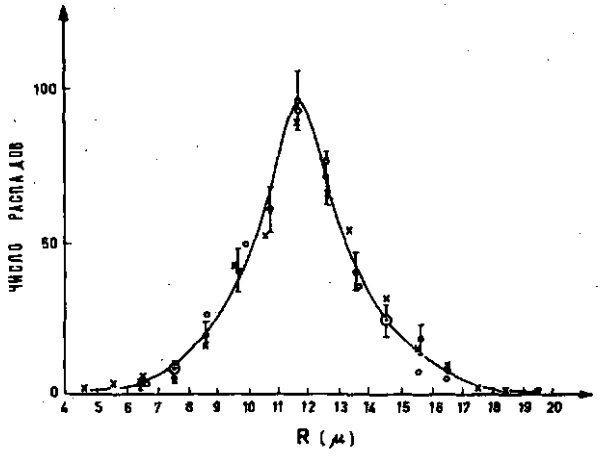

Рис.20

Распределение по пробегам одиночных осколков деления ядер при облучении урана π^+-мезонами с энергией 280 Мэв [64]:

• – π^+, E = 280 Мэв; × – π^-, медл.; o – P, E = 350 Мэв.

и нейтрино, захватывается преимущественно парой нуклонов (n, p). Масса покоя π^--мезона, ~140 Мэв, реализуется в кинетическую энергию двух нуклонов, разлетающихся под углом 180° один относительно другого.

$$\pi^- + \left\{\begin{matrix} n+p \to n+n \\ p+p \to n+p \end{matrix}\right\} + 140 \text{ Мэв}.$$

По-видимому, с бо́льшей вероятностью взаимодействие происходит с нуклонами поверхности ядра, поэтому один из них часто выходит за пределы ядра с полной кинетической энергией, а кинетическая энергия второго нуклона реализуется (частично или полностью) в энергию возбуждения ядра ($50 < E^* < 80$ Мэв).

Возбужденное ядро при переходе в основное состояние, в зависимости от отношения Γ_f/Γ, делится на какой-то стадии возбуждения или растрачивает свою энергию на испарение частиц (преимущественно нейтронов) и излучение гамма-квантов.

Видим, следовательно, что деление ядер при захвате медленного π^--мезона сводится к делению под действием быстрых нуклонов.

π- мезоны высоких энергий. Приведу экспериментальные факты по делению ядер урана π^+-мезонами с энергией 280 Мэв (данные Ивановой Н.С. [64]). 1) В большинстве случаев (~80%) взаимодействий π^+-мезонов с ядрами урана, сопровождающихся делением ядер, имеет место

поглощение π^+-мезона. 2) Поглощение π^+-мезона осуществляется так же, как и для медленных π^--мезонов, с большей вероятностью на паре нуклонов, преимущественно на паре протон-нейтрон. 3) Таким образом, деление ядер под действием мезонов высоких энергий вызывается прохождением через ядро быстрых нуклонов, возникающих в результате процессов рассеяния и поглощения быстрых мезонов. Наличие случаев деления, зарегистрированных в эмульсии, наряду с выходящим рассеянным мезоном, позволяет отнести около 20% наблюденных делений за счет возбуждения ядра нуклоном отдачи.

Деление медленными μ^--мезонами. Возможны два пути: а) при захвате μ^--мезона ядром по реакции:

$$p+\mu^- \to n+\gamma+105 \text{ Мэв},$$

средняя энергия возбуждения 12–20 Мэв. Следовательно, деление μ^--мезонами сводится к делению нейтронами с энергиями около 18 Мэв; б) деление возможно также при прямой передаче энергии ядру при переходе 2p – 1s в мезоатоме. Энергия перехода равна 6,3 Мэв. С большей вероятностью (0,07–0,25) идет деление с захватом μ^--мезона ядром [65, 66]. Безрадиационный переход с делением осуществляется с меньшей примерно на порядок вероятностью.

ЛИТЕРАТУРА

[1] HALPERN I., Annual Rev. Nucl. Sci. 9 (1959) 245.
[2] KRAUT A., Nukleonik 2 (1960) 105, 149.
[3] ПЕРФИЛОВ Н.А., ЛОЖКИН О.В., ШАМОВ В.П., УФН 70, 3 (1960).
[4] HUIZENGA J.R. and VANDENBOSCH R., Nuclear Reactions 2 (Eds. ENDT P.M. and SMITH P.B.) Amsterdam (1962) 42.
[5] HYDE E.K., Fission Phenomena, Prentice-Hall, Inc., New Jersey (1964).
[6] PORILE N.T., Phys. Rev. 120 (1960) 572.
[7] MEADOWS J.W., Phys. Rev. 110 (1958) 1109.
[8] KOWALSKI L., STEPHAN C., LANGEVIN-JOLIOT H. and RADVANYI, P., Phys. Lett. 2 (1962) 356.
[9] STEINER H. and JUNGERMANN J.A., Phys. Rev. 101 (1956) 807.
[10] PORILE N.T. and SUGARMAN N., Phys. Rev. 107 (1957) 1410.
[11] METROPOLIS N., BIVINS R., STORM M., TURKEVICH A., MILLER J.M. and FRIEDLANDER G., Phys. Rev. 110 (1958) 185, 204.
[12] HENKEL R.L., Fast Neutron Physics 4 (Eds. MARION J.B. and FOWLER J.L.) (1963) 2001.
[13] GINDLER J.E., BATE G.L. and HUIZENGA J.R., Phys. Rev. 136 (1964) B, 1333.
[14] VANDENBOSCH R. and HUIZENGA J.R., Proc. 2nd UN Int. Conf. PUAE 15 (1958) 284.
[15] HUIZENGA J.R., CHAUDHRY R. and VANDENBOSCH R., Phys. Rev. 126 (1962) 210.
[16] ПЕРФИЛОВ Н.А., ЖЭТФ 41 (1961) 871.
[17] de CARVALHO H.G., CORTINI G., MUCHNIK M., POTENZA G., RINZIVILLO R., and LOCK W.O., Nuovo Cim. 27 (1963) 468.
[18] JUNGERMAN J.A. and STEINER H.M., Phys. Rev. 106 (1957) 585.
[19] CARVALHO H.G., CORTINI G., MUCHNIK M., RINZIVILLO R. and SASSI E., Nucl. Phys. 53 (1964) 345.
[20] BAKER E.W. and KATCOFF S., Phys. Rev. 126 (1962) 729.
[21] ГОРИЧЕВ П.А. ЛОЖКИН О.В., ПЕРФИЛОВ Н.А.; ЖЭТФ 45 (1963) 1784.
[22] VIOLA V.E. and SIKKELAND T., Phys. Rev. 128 (1962) 767.
[23] BRITT H.C. and QUINTON A.R., Phys. Rev. 120 (1960) 1768.
[24] GILMORE J., THOMPSON S.G. and PERLMAN I., Phys. Rev. 128 (1962) 2276.

[25] BURNETT D.S., Lawrence Radiation Laboratory Report (Thesis) Univ. of California rep. UCRL - 11006 (1963).
[26] COHEN S. and SWIATECKI W.J., Ann. Phys. 19 (1962) 67.
[27] NIX J.R., Lawrence Radiation Laboratory Report Univ. of California rep. UCRL - 11338 (1964).
[28] PLASIL F., Lawrence Radiation Laboratory Report Univ. of California rep. UCRL - 11193 (1963).
[29] СТРУТИНСКИЙ В.М., ЛЯШЕНКО Н.Я., ПОПОВ Н.А., ЖЭТФ 43 (1962) 584.
[30] SIKKELAND T., Phys. Rev. 135 (1964) B 669.
[31] KATCOFF S., Nucleonics 18 No.11 (1960) 201.
[32] JENSEN R.C. and FAIRHALL A.W., Phys. Rev. 109 (1958) 942.
[33] SUGIHARA T.T., ROESMER J. and MEADOWS J.W., Phys. Rev. 121 (1961) 1179.
[34] NEUZIL E.F. and FAIRHALL A.W., Phys. Rev. 129 (1963) 2705.
[35] RAO N.M., Radiochemische Untersuchungen über die Spontane Spaltung des U^{238}-Kernes, (Dissertation), Köln (1962).
[36] ПРОТОПОПОВ А.Н., ТОЛМАЧЕВ Г.М., УШАТСКИЙ В.Н., ВЕНЕДИКТОВ Р.В., КРИСЮК И.Т., РОДИОНОВ А.П., ЯКОВЛЕВА Г.В., "Атомная энергия", 5 (1958) 130.
[37] STEVENSON P.C., HICKS H.G. NERVIC W.E. and NETHAWAY D.R., Phys. Rev. 111 (1958) 886.
[38] FAIRHALL A.W., Phys. Rev. 102 (1956) 1335.
[39] BLANN H.M., Phys. Rev. 123 (1961) 1356.
[40] MAYER M.G., Phys. Rev. 74 (1948) 235.
[41] MEITNER L., Nature 165 (1950) 561.
[42] FAISSNER H. and WILDERMUTH K., Nucl. Phys. 58 (1964) 177.
[43] GOECKERMANN R.H. and PERLMAN I., Phys. Rev. 76 (1949) 628.
[44] МУРИН А.Н., ПРЕОБРАЖЕНСКИЙ Б.К., ТИТОВ Н.Е., Изв. АН СССР 4 (1955) 577.
[45] TURKEVICH A., and NIDAY J.B., Phys. Rev. 84 (1951) 52.
FAIRHALL A.W., JENSEN R.C. and NEUZIL E.F., Proc. 2nd UN Int. Conf. PUAE 15 (1958) 452.
[46] BRITT H.C., WEGNER H.E. and GURSKY J., Phys. Rev. 129 (1963) 2239.
[47] UNIK J.P. and HUIZENGA J.R., Phys Rev. 134 (1964) B 90.
[48] ОБУХОВ А.И., ЖЭТФ 38 (1960) 271.
[49] СТРУТИНСКИЙ В.М., ЖЭТФ 45 (1963) 1891, 1900.
[50] BOHR N. and WHEELER J., Phys. Rev. 56 (1939) 426.
[51] MILTON J.C.D. and FRASER J.S., Canad. J. Phys. 40 (1962) 1626.
[52] BRITT H.C. and WHETSTONE S.L., Phys. Rev. 133 (1964) B 603.
[53] BRANDT R., THOMPSON S.G. GATTI R.G. and PHILLIPS L., Phys. Rev. 131 (1963) 2617.
[54] БОЧАГОВ Б.А., КОМАР А.П., СОЛЯКИН Г.Е., ФАДЕЕВ В.И., Атомная энергия 11 (1961) 540.
[55] СТРУТИНСКИЙ В.М., ЖЭТФ 30 (1956) 606. Атомная энергия 2 (1958) 508.
GRIFFIN J.J., Phys. Rev. 116 (1959) 107.
[56] HALPERN I. and STRUTINSKI V.M., Proc., 2-nd UN Int. Conf. PUAE 15 (1958) 408.
[57] COHEN B.L., FERRELLE-BRYAN B.L., COOMBE D.J. and HULLINGS M.K., Phus. Rev. 98 (1955) 685.
ПРОТОПОПОВ А.Н., ЭЙСМОНТ В.П., Атомная энергия 5 (1959) 644.
WINHOLD B.J. and HALPERN I., Phys Rev. 103 (1956) 990.
[58] FLYNN K.F., GLENDENIN L.E. and HUIZENGA J.R., Nucl. Phys. 58 (1964) 321.
[59] COFFIN G.T. and HALPERN I., Phys. Rev. 112 (1958) 536.
[60] CHAUDHRY R., VANDENBOSCH R. and HUIZENGA J.R., Phys. Rev. 126 (1962) 220.
[61] BATE C.L., CHAUDRY H. and HUIZENGA J.R., Phys. Rev. 131 (1963) 722.
[62] ПЕРФИЛОВ Н.А., ИВАНОВА Н.С., ЖЭТФ 28 (1955) 732; 29 (1955) 551.
[63] ПЕРФИЛОВ Н.А., ЛОЖКИН О.В., ШАМОВ В.П., ЖЭТФ 28 (1955) 655.
[64] ИВАНОВА Н.С., ЖЭТФ 34 (1958) 1381.
[65] JOHN W. and FRY W.F., Phys. Rev. 91 (1953) 1234.
[66] БЕЛОВИЦКИЙ Г.Е., КАШУКЕЕВ Н.Т., МИХУЛ А., ПЕТРАШКУ М.Г., РОМАНОВА Т.А. ТИХОМИРОВ В.А., ЖЭТФ 38 (1960) 404.

Дополнительная литература

1. FRASER J.S., MILTON J.C.D., BOWMAN H.R. and THOMPSON S.G., Com. J. Phys. 41 (1963) 2080.
2. TERRELL J., Phys. Rev. 113 (1959) 527.
3. VANDENBOSCH R. and HUIZENGA J.R., Phys. Rev. 127 (1962) 212.
4. VIOLA V.E. and SIKKELAND T., Phys. Rev. 130 (1963) 2044.
5. БОЛЬШОВ В.И., ПРОХОРОВА Л.И., ОКОЛОВИЧ В.Н., СМИРЕНКИН Г.Н., "Атомная энергия" 17 (1964) 28.
6. БОЧАГОВ Б.А., КОМАР А.П., СОЛЯКИН Г.Е., ЖЭТФ 38 (1960) 1374.

MESURES DE SECTIONS EFFICACES ABSOLUES DE FISSION INDUITE PAR DES PROTONS DE 156 MeV, UTILISANT LE MICA COMME DÉTECTEUR DE FRAGMENTS DE FISSION

M. MAURETTE ET C. STEPHAN
FACULTÉ DES SCIENCES, ORSAY, FRANCE

Abstract — Résumé — Аннотация — Resumen

MEASUREMENT OF ABSOLUTE CROSS-SECTIONS OF FISSION INDUCED BY 156-MeV PROTONS, USING *MICA AS A FISSION FRAGMENT DETECTOR.* The fission of elements of medium Z induced by 156-MeV protons is difficult to demonstrate, owing to the particularly small cross-section of the reaction. The detection of fission fragments by means of sheets of mica seemed to be a technique well suited to this type of experiment. In the sheets of synthetic mica that we used it was only the fission fragments that left microscopically identifiable traces. Moreover, these samples contain very few impurities likely to undergo fission, so practically no parasitic traces are observed. The targets consisted of metals of not less than 99.999% purity.

We determined the absolute cross-sections of fission induced by 156-MeV protons in the case of lanthanum (5 μb) and praseodymium (6 μb), and estimated those of cadmium, indium, tin and antimony (≤ 0.1 μb).

The sheets of mica were placed on each side of the metal sheet. The kinetics of the reaction explain why more traces were found on the mica sheets placed on the front face. As thick targets were used to take account of self-absorption, we determined (in the case of uranium and gold) the ratio of yields between a thin target and a thick target, and then extrapolated our results to the other elements.

We made checks by comparing the absolute cross-sections for fission (induced by 156-MeV protons) in uranium, bismuth, gold and tantalum, as obtained by this method, with those obtained by counters at this energy. The observed agreement was very good.

MESURES DE SECTIONS EFFICACES ABSOLUES DE FISSION INDUITE PAR DES PROTONS DE 156 MeV UTILISANT LE MICA COMME DÉTECTEUR DE FRAGMENTS DE FISSION. La fission d'éléments de Z moyen induite par des protons de 156 MeV est difficile à mettre en évidence en raison de la section efficace particulièrement faible de la réaction. Les auteurs ont pensé que la détection des fragments de fission à l'aide de micas était une technique bien adaptée à ce type d'expérience. En effet, dans les feuilles de mica synthétique qu'ils ont utilisées, seuls les fragments de fission laissent des traces identifiables au microscope. De plus ces échantillons contiennent très peu d'impuretés susceptibles de fissionner. On n'observe donc pratiquement pas de traces parasites. Les cibles étaient constituées par des métaux de pureté égale à 99,999% au moins.

Les auteurs ont déterminé les sections efficaces absolues de fission, induite par des protons de 156 MeV pour le lanthane (5 μb) et le praséodyme (6 μb) et évalué celles du cadmium, de l'indium, de l'étain et de l'antimoine (≤ 0,1 μb).

Les micas étaient placés de chaque côté de la feuille de métal — la cinétique de la réaction explique qu'on ait trouvé davantage de traces sur les micas placés sur la face avant. Les cibles étant épaisses, pour tenir compte de l'auto-absorption, les auteurs ont déterminé pour l'uranium et l'or le rapport des rendements entre cible mince et cible épaisse et extrapolé leurs résultats aux autres éléments.

Ils ont effectué des contrôles en comparant les sections efficaces absolues de fission induite par des protons de 156 MeV sur l'uranium, le bismuth, l'or et le tantale obtenues par cette méthode, avec celles qu'ils ont obtenues à cette énergie avec des compteurs. L'accord observé est très bon.

ИЗМЕРЕНИЯ АБСОЛЮТНЫХ ЭФФЕКТИВНЫХ СЕЧЕНИЙ ДЕЛЕНИЯ, ВЫЗВАННОГО ПРОТОНАМИ С ЭНЕРГИЕЙ 156 Мэв, С ИСПОЛЬЗОВАНИЕМ СЛЮДЫ В КАЧЕСТВЕ ДЕТЕКТОРА ОСКОЛКОВ ДЕЛЕНИЯ. Деление элементов группы среднего Z, вызванное протонами с энергией 156 Мэв, трудно поддается обнаружению в связи с исключительно слабым эффективным сечением реакции. Полагали, что обнаружение осколков деления с помощью слюды является методом, хорошо применимым к данному типу эксперимента. Действительно, в

слоях синтетической слюды, которая нами была использована, только осколки деления оставляют следы, обнаруживаемые под микроскопом. Более того, в этих образцах содержится очень небольшое количество примесей, способных делиться. Поэтому следы вредных примесей практически не наблюдаются. Мишенями были металлы с чистотой по меньшей мере 99,999%.

В отношении лантана (5 мкб) и празеодима (6 мкб) были установлены абсолютные эффективные сечения деления, вызванного протонами с энергией 156 Мэв. То же было проделано в отношении кадмия, индия, олова и сурьмы ($\lesssim$ 0,1 мкб).

Слюда помещалась с обеих сторон металлического листа. Кинематика реакции показывает, что большее количество следов было обнаружено на слюде, находящейся на передней лицевой стороне. Мишени были плотные с тем, чтобы учесть самопоглощение. Для урана и золота нами установлено соотношение выходов между тонкой и толстой мишенями. Затем эти результаты были экстраполированы на другие элементы.

Нами были проведены контрольные измерения путем сравнения полученных по этому методу абсолютных эффективных сечений деления, вызванного протонами в 156 Мэв на уране, висмуте, золоте и тантале, с сечениями, полученными при этой энергии с помощью счетчиков. Наблюдаемое соответствие весьма удовлетворительное.

MEDICION DE SECCIONES EFICACES ABSOLUTAS DE FISION INDUCIDA POR PROTONES DE 156 MeV UTILIZANDO MICA COMO DETECTOR DE FRAGMENTOS DE FISION. Es difícil poner de manifiesto la fisión de elementos de número atómico medio inducida por protones de 156 MeV, en razón de la sección eficaz particularmente reducida que corresponde a la reacción. Los autores estiman que la detección de fragmentos de fisión con ayuda de mica constituye una técnica apropiada para este tipo de experimento. En efecto, en las hojas de mica sintética que han utilizado, sólo los fragmentos de fisión dejan trazas que se pueden identificar bajo el microscopio. Además, este material contiene muy pocas impurezas fisionables. Por tanto, no se observan prácticamente trazas parásitas. Los blancos consistieron en metales de una pureza de 99,999% como mínimo.

Los autores han determinado las secciones eficaces absolutas de fisión, inducidas por protones de 156 MeV, correspondientes al lantano (5 μb) y al praseodimio (6 μb), y calculado las del cadmio, indio, estaño y antimonio ($\leq$ 0,1 μb).

Las hojas de mica se colocaron de ambos lados de la lámina metálica. La cinemática de la reacción explica que se haya encontrado un mayor número de trazas en las hojas de mica colocadas en la cara anterior. Como los blancos eran gruesos, los autores han determinado en el caso del uranio y del oro la razón de los rendimientos entre blanco delgado y blanco grueso para tener en cuenta la autoabsorción y han extrapolado los resultados a los otros elementos.

Como medida de control, han comparado las secciones eficaces absolutas de fisión inducida por protones de 156 MeV en el uranio, el bismuto, el oro y el tántalo, obtenidas por este método, con las determinadas mediante contadores para la misma energía. La concordancia observada es muy satisfactoria.

INTRODUCTION

Depuis la découverte de la fission, on a cherché à mettre ce phénomène en évidence pour des éléments de plus en plus légers. COHEN et SWIATECKI [1] ont prévu à partir du modèle de la goutte liquide que la fission ne pourrait pas être observée pour des éléments dont le paramètre de fissibilité x serait inférieur à 0, 39. Nous avons essayé de démontrer l'existence du phénomène de fission pour des éléments placés un peu au-dessus de cette limite: pour Pr et La, x $\sim$ 0,52 et pour Sb, Sn, In et Cd x $\sim$ 0,45. Nous avons déterminé pour ces métaux la section efficace absolue de fission induite par des protons de 156 MeV. Ces mesures sont intéressantes car elles peuvent apporter des renseignements sur la hauteur de la barrière de fission.

TECHNIQUE EXPÉRIMENTALE

Nous avons mesuré les sections efficaces absolues de fission en détectant les fragments de fission par les traces qu'ils laissent dans les micas. On rend ces traces visibles au microscope optique en plongeant, pendant quelques minutes, les échantillons irradiés dans de l'acide fluorhydrique [2]. Les micas étaient placés, immédiatement après avoir été clivés, de chaque côté de la feuille du métal fissile de $\sim 0,5$ mm d'épaisseur. Nos échantillons mesuraient 5×10 mm^2 et étaient traversés dans l'air par un faisceau de protons uniforme sur toute leur surface. Les sections efficaces étaient obtenues en comptant les traces observées dans les deux micas.

Le flux de protons était déterminé à partir du nombre de traces de fragments de fission comptées dans des micas placés contre des couches minces d'uranium ou d'or déposées sur de l'aluminium très pur. Nous avons utilisé les sections efficaces absolues de fission obtenues avec des semi-conducteurs à jonction [3]. L'épaisseur des couches minces a été déterminée pour l'uranium par comptage des particules α émises, pour l'or en comparant la quantité d'or-198 formé par activation aux neutrons de pile à la quantité formée dans une feuille mince d'or de poids connu exposée au même flux de neutrons.

Nous avons utilisé au cours de nos expériences des métaux de pureté très élevée. Elle était estimée à 99,999% pour l'antimoine, l'étain et le cadmium, et à 99,9999% pour l'indium. Pour augmenter le nombre de traces, nous avons utilisé des échantillons de métal de $\sim 0,5$ mm d'épaisseur, infiniment épais pour les fragments de fission. Cette façon de procéder avait en plus l'avantage d'éviter des manipulations supplémentaires susceptibles d'introduire des impuretés. Nous avons donc dû déterminer le nombre d'atomes qui peuvent interagir pour donner des traces. Nous avons comparé pour l'or et l'uranium le nombre de traces obtenues après irradiation de micas placés, d'une part, derrière des échantillons épais, d'autre part, derrière des couches minces d'épaisseur connue déposées sur de l'aluminium très pur. Le nombre d'atomes susceptible de donner des traces trouvé ainsi est $6,4 \cdot 10^{18}$ atomes/cm^2 pour l'uranium. Ce nombre est inférieur à celui obtenu précédemment [2] mais le résultat tient compte du critère d'identification qui était vraisemblablement plus sévère.

Après l'essai de différents types de micas, nous avons choisi d'utiliser du mica synthétique car les traces parasites dues à la fission d'impuretés incluses y étaient particulièrement rares: $3 \cdot 10^3$ traces/cm^2 pour un flux de $2,4 \cdot 10^{16}$ protons/cm^2. Ces détecteurs ont la propriété de n'enregistrer une particule lourde chargée que si sa perte d'énergie par unité de longueur est supérieure à une valeur critique [4]. $(dE/dx)_{critique} \sim 15$ MeV/(mg/cm^2) pour du mica synthétique. Cette propriété permet dans notre expérience de n'enregistrer pratiquement que les fragments de fission. En particulier, les noyaux de recul ne peuvent pas être vus. Par contre il est probable que nous avons compté tous les fragments de fission. Dans le cas très défavorable d'un fragment $^{38}_{20}$Ca obtenu lors d'une fission dissymétrique improbable du cadmium, les courbes calculées à partir des relations parcours-énergie théoriques de LINDHARD et al. [5] prévoient qu'un tel fragment donnera une trace visible si son énergie cinétique est supérieure à environ 17 MeV (fig. 1). Or l'énergie prévue pour ce fragment de fission est au moins de 35 MeV en considérant deux sphéroïdes en contact.

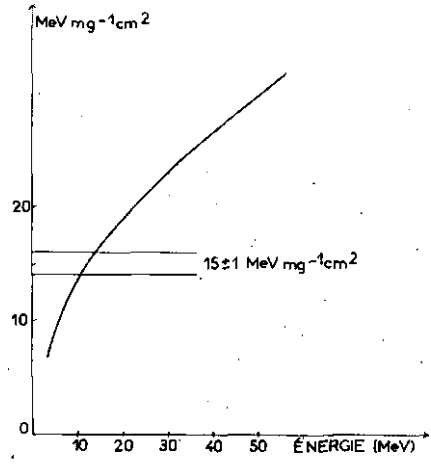

Figure 1

Perte d'énergie en MeV par mg/cm² pour un ion $^{35}_{24}Ca$ en fonction de son énergie.

RÉSULTATS ET DISCUSSION

L'ensemble des résultats obtenus est représenté sur le tableau I. Nous avons effectué des corrections suivant les éléments pour tenir compte des différences d'épaisseur effectives et du pourcentage de traces trop courtes pour être identifiées. Les sections efficaces absolues de fission du bismuth, de l'or et du tantale ont été mesurées par cette méthode pour établir une comparaison avec les valeurs obtenues par ailleurs avec des semi-conducteurs à jonction [3, 6]. L'accord est très satisfaisant. Les sections efficaces absolues de fission trouvées pour le praséodyme et le lanthane sont du même ordre de grandeur. Ce résultat est prévu par la théorie car les paramètres de fissibilité $x = (Z^2/A)/(Z^2/A)_{critique}$ de ces éléments sont très voisins. Il en est de même pour les quatre métaux Sb(Z = 51), Sn(Z = 50), In(Z = 49), Cd(Z = 48). Les impuretés devant être de nature et de proportion variables suivant les éléments, la cohérence des résultats semble montrer qu'elles n'interviennent pas de façon primordiale dans les sections efficaces obtenues.

La cinématique de la réaction nous a permis d'expliquer partiellement qu'on ait trouvé davantage de traces sur les micas placés sur la face avant. En effet les fragments émis dans la demi-sphère avant sont plus nombreux. De plus l'énergie plus grande de ces fragments se traduit par des traces plus longues, comme on le voit sur l'histogramme relatif à l'or mince de la figure 2. L'épaisseur effective sera donc plus grande de ce côté. Cela ne suffit cependant pas à expliquer les rapports obtenus pour les cinq derniers éléments du tableau. On pourrait les expliquer en supposant une émission préférentielle des fragments à 90° par rapport à la direction des protons incidents dans le système du centre de masse. Mais on peut également penser que pour les éléments légers Sb, Sn, In, Cd certains fragments de fission émis vers l'arrière ont une énergie trop faible pour donner des traces visibles. Nous en avons tenu compte dans l'évaluation de l'erreur sur la

TABLEAU I

RÉSULTATS EXPÉRIMENTAUX

Elément	Moniteur	Sections efficaces de fission		Rapport Avant-Arrière	
		Micas	Semi-conducteurs	Observé	Calculé
Bi	U mince	125 mb ± 16 mb	126 mb ± 20 mb	1,5	1,4
Au	"	24 mb ± 4 mb	24 mb ± 4 mb	1,5	1,5
Ta	Au mince	1,6 mb ± 0,6 mb	2,0 mb ± 0,3 mb	1,5	1,5
Pr	"	5,5 µb ± 2 µb		1,7	1,8
La	"	3,0 µb ± 1,5 µb		2,9	1,9
Sb	"	0,35 µb ± 0,2 µb		3,9	2,1
Sn	"	0,24 µb ± 0,13 µb		2,6	2,1
In	"	0,28 µb ± 0,14 µb		3,1	2,1
Cd	"	0,30 µb ± 0,16 µb		4,4	2,1

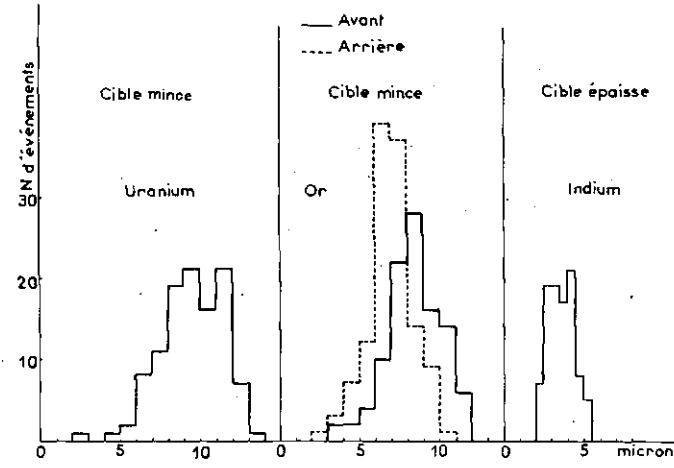

Figure 2

Histogrammes des longueurs de traces observées dans les micas pour des fragments de fission de l'uranium, de l'or et de l'indium.

TABLEAU II

BARRIÈRES DE FISSION

Elément	Fujimoto Yamaguchi	Goutte liquide
Pr + proton	56 MeV	40,6 MeV
La + proton	60 MeV	46 MeV
Sb + proton	70 MeV	49 MeV
Sn + proton	71 MeV	49,5 MeV
In + proton	72 MeV	49 MeV
Cd + proton	73 MeV	49 MeV

section efficace. Quant au lanthane la formation rapide d'oxyde sur la feuille métallique servant de cible peut expliquer ce résultat.

La figure 2 représente des histogrammes de longueurs de traces pour quelques éléments. Les longueurs trouvées sont compatibles avec les résultats obtenus à partir des relations parcours-énergie [5]. Pour les quatre éléments les plus légers on peut en déduire une énergie des fragments de fission individuels de l'ordre de 40 MeV en accord avec l'énergie prévue à partir du modèle de la goutte liquide. Ces histogrammes nous permettent également de conclure que les traces observées dans les micas placés devant ces quatre métaux ne sont pas dues à la fission d'impuretés constituées par des éléments lourds.

Nous avons comparé les résultats expérimentaux à ceux obtenus par la méthode de calcul utilisée précédemment [7]. Cette méthode consiste à utiliser les formules de Fujimoto et Yamaguchi pour évaluer les largeurs d'émission d'un neutron et les largeurs de fission. On constate que les noyaux qui fissionnent de façon notable sont ceux résultant d'une cascade p, n laissant le noyau résiduel très excité, et ceux où le proton incident est resté dans le noyau cible. On constate également que les probabilités de fission sont à peu près identiques après évaporation de 0, 1, 2 neutrons. Pour retrouver les résultats expérimentaux nous avons été amenés à prendre les valeurs de barrière de fission indiquées pour le tableau II. La différence est importante entre ces valeurs et celles que l'on obtient en utilisant les formules de COHEN et SWIATECKI [1] où le paramètre de fissibilité est $x = (Z^2/A)/48,4$ [8]. Ceci peut s'expliquer par le fait que dans la zone de masses considérée, les effets de couches sont importants. Des calculs préliminaires par la méthode de HUIZENGA et al. [9] semble donner des résultats comparables.

CONCLUSION

La technique de détection des traces de fragments de fission par les micas nous a permis d'obtenir avec une précision relativement bonne les sections efficaces absolues de fission induite par les protons de 156 MeV sur des éléments de Z moyen. En outre, le fait que les valeurs obtenues pour le bismuth et l'or concordent avec celles obtenues précédemment permet de conclure que l'efficacité de détection ne varie pas quand les micas sont soumis à un flux très élevé de particules. Les calculs effectués montrent que d'autres mesures à des énergies de protons plus faibles seraient nécessaires pour obtenir une détermination précise des barrières de fission.

REMERCIEMENTS

Nous tenons à remercier tout particulièrement M. J. Walker qui nous a beaucoup aidé au début de ce travail, et qui nous a procuré les métaux très purs. Nous remercions également M. Perlman pour son aide dans la préparation des échantillons à irradier, ainsi que L. Kowalski pour sa collaboration au début de ces expériences.

RÉFÉRENCES

[1] COHEN, S. et SWIATECKI, W. S., Ann. Phys. 22 (1963) 406-37.
[2] DEBEAUVAIS, M., MAURETTE, M., MORY, J. et WALKER, R., Int. J. appl. Rad. Isotopes 15 (1964) 289-99.
[3] KOWALSKI, L. et STEPHAN, C., J. Phys. Radium 24 (1963) 901-3.
[4] FLEICHER, R. L., PRICE, P. B. and WALKER, R. M., Phys. Rev. 133 (1964) 1443-9.
[5] LINDHARD, J., SCHARFF, M. et SCHIØTT, H. E., Mat. Fys. Medd. Dan. Vid. Selsk. 33 14 (1963)
[6] PERLMAN, M. and STEPHAN, C., Phys. Rev. (à paraître).
[7] KOWALSKI, L., Thèse 1962.
[8] BURNETT, D., GATTI, R., PLASIL, F., PRICE, P., SWIATECKI, W. and THOMPSON, S. G., UCRL 11079 (1963).
[9] HUIZENGA, J. R., CHAUDHRY, R. and VANDENBOSCH, R., Phys. Rev., 126 (1962) 210-9.

DISCUSSION

(on the foregoing three papers)

J.R. NIX: I have a comment regarding Dr. Perfilov's experimental plots of σ_f/σ_t versus Z^2/A. For cases in which the excitation energy is not so high, so that a compound nucleus is usually formed, it appears to me that a theoretical calculation of σ_f/σ_c versus Z^2/A should be carried out. Neglecting processes other than fission and neutron emission, one could use the theoretical expressions for Γ_n and Γ_f to calculate at each step i of the de-excitation chain the relative probability for neutron emission, $P_n^{(i)} = \Gamma_n^{(i)}/(\Gamma_n^{(i)} + \Gamma_f^{(i)})$; the ratio σ_f/σ_c would then be given by $1 - \prod_i P_n^{(i)}$. The calculated quantity σ_f/σ_c (which should approximately equal σ_f/σ_t) would depend sensitively upon the difference between the fission barrier and the neutron binding energy. Since for $(Z^2/A)/(Z^2/A)_{crit} \lesssim 0.67$ the calculated liquid drop fission barriers should vary as $[constant - (Z^2/A)]\, A^{2/3}$, whereas for $(Z^2/A)/(Z^2/A)_{crit} \gtrsim 0.67$ they are essentially proportional to $[(Z^2/A)_{crit} - (Z^2/A)]^3\, A^{2/3}$, the dependence of σ_f/σ_c upon Z^2/A would not necessarily be expected to be linear.

H. de CARVALHO: With regard to the identification of fission fragments by means of nuclear emulsion, when the fission has been induced by high-energy protons, I want to draw attention to the following aspects of our measurements. First, we used a strong discriminatory photographic development procedure so as to allow only particles with high charges, $Z \geq 10$, to be recorded. This reduced the background by a very large factor, leaving only the fission and the high-energy fragmentation tracks to be dealt with. Secondly, the fissions of a very heavy nucleus, induced by high-energy protons, do look very like the ones obtained by protons of less energy. In the case of bismuth, however, the ratio of fission tracks to the background of fragmentation tracks is no longer favourable, and this may cause difficulties. However, the fission tracks from one particular nucleus, e.g. uranium, have well-defined range distribution and one may identify them by plotting the range spectrum.

This was the case with uranium fission at 20-GeV proton energy. For elements of less mass than bismuth, the situation is less favourable and it is necessary to fix criteria regarding the asymmetry of the fragments plus range measurements. In the case of silver it is necessary to fix such criteria very accurately since, otherwise, the results may be quite unreliable.

G. FRIEDLANDER: What were, in fact, the criteria for considering events as fissions? As a specific example, would an event, in which one fragment has charge 15, be considered a fission event?

H. de CARVALHO: Events with charge 15 do not seem to be very common. In fact, I think Dr. Swiatecki would be better able to answer this question, as he has been studying the fission of heavy and light nuclei.

N.A. PERFILOV (Chairman): The criteria which we used were, first, total path of less than 15 μm and, secondly, our subjective assessment of the appearance of the tracks. A fragment with charge 15 is a rare event and thus it is difficult to describe the outward appearance of the track of such a fragment in photo-emulsion.

G. CORTINI: I wish to comment on the point raised by Dr. Friedlander regarding the emulsion work. Our results are based on certain standard criteria used in determining which events should be regarded as fissions. Such criteria were based essentially on the known properties of low-energy fission products. For uranium these criteria seem to be well justified by the striking difference that we have observed between the total number of events, as well as their general appearance, in uranium-loaded versus unloaded emulsions.

W. SWIATECKI: May I comment on the distinction between fission and what might be called fragmentation. On the basis of the simplest considerations of the deformation energy of a nucleus one does expect, theoretically, such a distinction to be present. From an analysis of the balance between surface and electrostatic energies it appears that for elements heavier than, say, silver (with a fissionability parameter $X \gtrsim 0.4$) one can make a distinction between fission and fragmentation, but this distinction disappears for lighter elements. I cannot go into details, but would just like to point out that the interpretation of experiments should be attempted with these theoretical considerations in mind.

M. DEBEAUVAIS: May I ask Dr. Stéphan whether he has taken into account the fact that only fission fragments penetrating at an angle of more than 6° can be recorded in mica?

C. STEPHAN: By comparing thick-target and thin-target measurements for uranium and gold elements, in which case we know the absolute fission cross-section, we were able to make the necessary correction automatically. Having regard to the poor statistical accuracy of our measurements, it could be considered that the results were the same for all the elements studied.

M. DEBEAUVAIS: Do you not think that more sensitive solid-state detectors, made of plastic material for example, would be more useful?

C. STEPHAN: We did consider using plastic detectors, but the background was too high. The material would need to be very pure.

M. DEBAUVAIS: What material did you use?

C. STEPHAN: We used Macrophol.

M. SOWINSKI: I should like to make two technical comments on behalf of a joint working group in laboratories at CERN, at Naples and in Warsaw. This joint group developed, independently of several other groups (e.g. Hudis and Katcoff, as mentioned in Dr. Friedlander's paper, and the Rio de Janeiro-Zürich group, whose paper[1] is to be presented), a sandwich technique in which a very thin fissioning layer is sandwiched between two mica sheets, held together in a fixed relative position. After irradiation and processing, correlated pairs of tracks are looked for.

Now, the first point I should like to stress is that single mica sheets can be safely used as absolute fission detectors only if the bombarding particles have low energy; as the incoming energy is increased, an increasing background of other tracks, originating for instance from spallation recoils, will appear, so that quite appreciable corrections will be required. This point is made quite clear by our results: in a slow-neutron-U^{235} sandwich all tracks were correlated, with less than 1% exceptions, while in a uranium

[1] de CARVALHO, H.G., da SILVA, A.G., ALVES, R.N., BÖSCH, R. and WÖLFLI, W., "Angular distributions of U^{238} fission fragments produced by mono-energetic gamma rays", these Proceedings II.

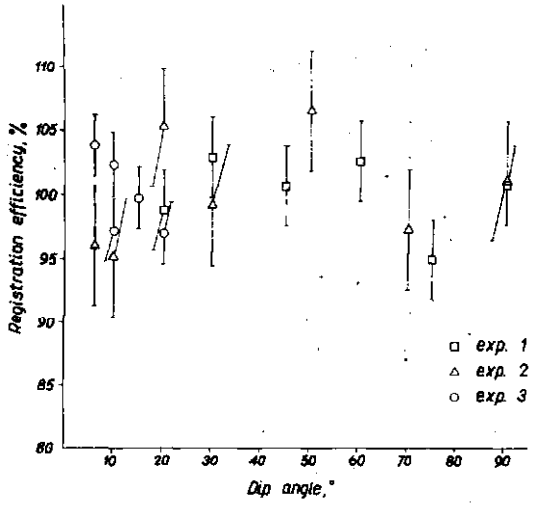

Fig. A

Detection efficiency considered as a function of dip angle

sandwich exposed to 18-GeV protons many uncorrelated tracks were found in preliminary exposures.

The second point I want to mention is the detection efficiency, considered as a function of the dip angle. Here we had considerable difficulty, first, because tracks with small ($\lesssim 30°$) and large ($> 80°$) dip angle were partly lost, and, secondly, because working conditions appeared to be extremely sensitive with respect to the results of dip-angle measurements. In order to clarify these points we made several measurements. Mica sheets were irradiated in vacuum chambers using small fissioning sources, under controlled angle and flux conditions, so that the efficiency could be directly measured as a function of the dip angle. In this way better processing and working conditions were achieved and a full efficiency between 20° and 90° was rather easily obtained in the different laboratories. The very last result, obtained a few days ago in Warsaw, is still better: we got full efficiency in the range from 6° to 90°. This is shown in Fig. A; it should be noted that all the experimental points fall within the interval 0.95–1.05. The efficiency for sandwiches amounts to $(96 \pm 4)\%$.

M. PETRASCU: I want briefly to present the results mentioned in Dr. Perfilov's paper. We studied Pu^{239} fission induced by negative μm mesons, using the scintillation-chamber method. The chamber, constructed for this purpose, is shown in Fig. B1. At the left-hand side is the compartment for plutonium and on the right-hand side the compartment for uranium. Both compartments were viewed by a photomultiplier of the AVP-58 type. Fig. B2 shows the experimental arrangement and the general layout of the experiment. The work was performed with the synchrocyclotron at Dubna. The μm meson beam came from a new exit channel of increased intensity, and it first had to pass the first scintillation counters in coincidence and then the scintillation chamber. The pulses of the scintillation counters were fed into a gate that was opened for 0.5 ms and the pulses of the chamber were analysed by a

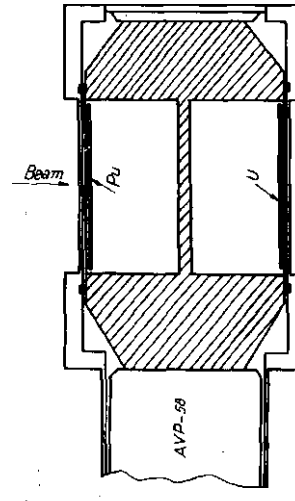

Fig. B1

Outline of the scintillation chamber

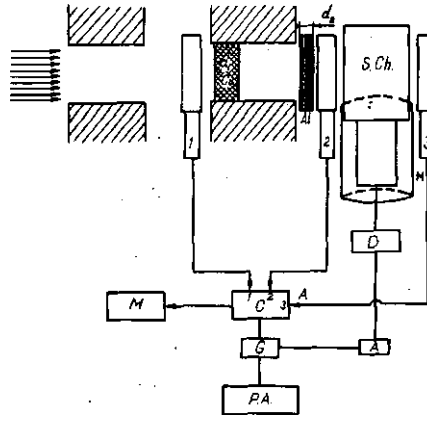

Fig. B2

Block diagram of the experiment; 1, 2, 3: plastic scintillation counters; S.Ch.; gaseous scintillation chamber; M: magnetic shield; D: fast discriminator; A: amplifier; C: coincidence scheme; M: monitor; G: 0.5 μs gate; PA: 400-channel analyser

400-channel analyser. Fig. B3 shows the background and Fig. B4 shows the effect of the plutonium target. Next, Fig. B5 shows the combined effects of both the uranium and plutonium targets. The chamber was operated in the following manner. First, a mixture of nitrogen and argon was introduced into the compartment containing plutonium and then the compartment was evacuated and the background measured. The gas mixture was then introduced into both chambers.

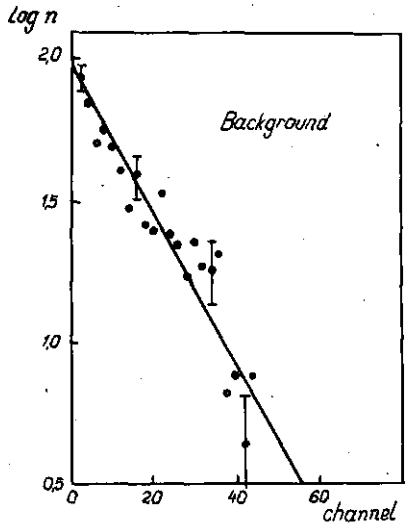

Fig. B3

The background taken with the two compartments evacuated at a pressure of about 10^{-2} torr

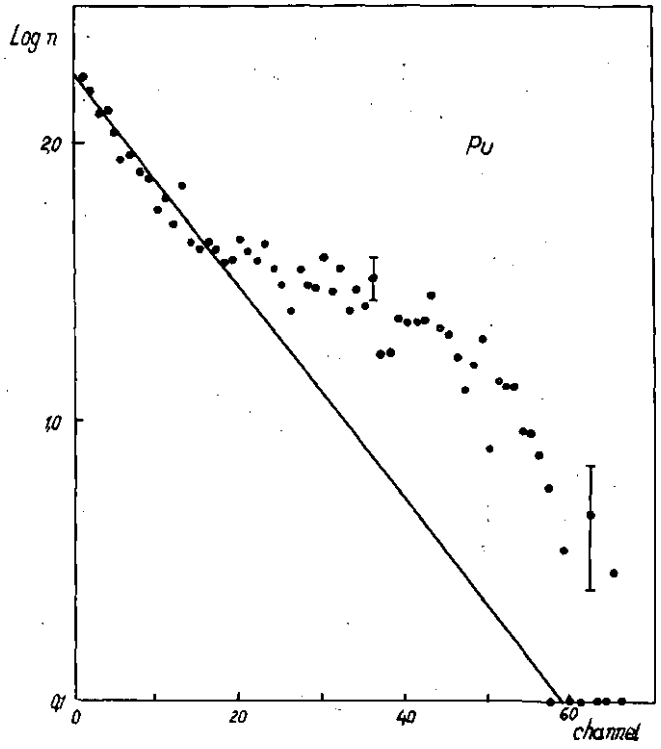

Fig. B4

The pulse-height distribution of the counts obtained with scintillation gas in the plutonium compartment

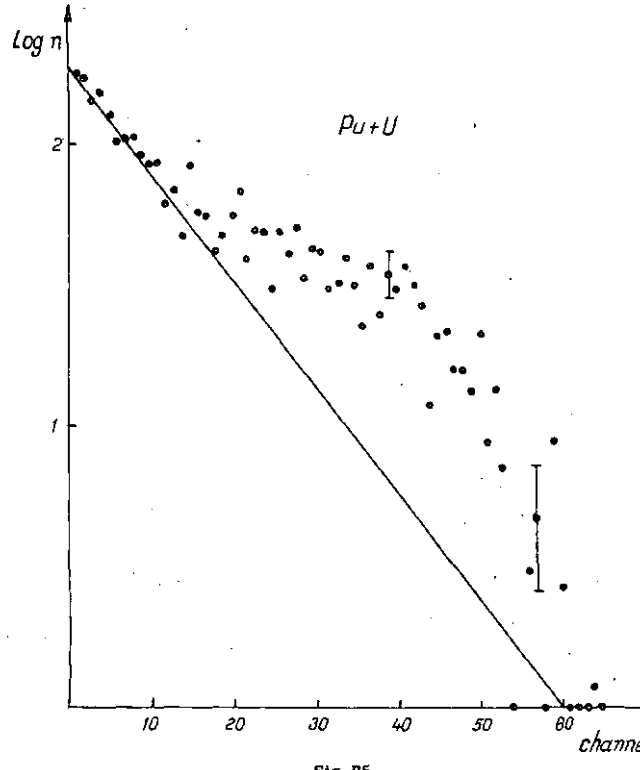

Fig. B5

The pulse-height distribution of the counts obtained with scintillation gas in both compartments of the chamber

It follows from the experimental results that the ratio between the fission probability for plutonium and uranium is about 10, which may indicate an important contribution of the radiationless mechanism. However, the lower limit of the ratio Pu/U $\geqslant 4$ (taking into account standard errors) agrees with the mechanism based on the nuclear capture of the μm meson. Indeed, by applying the empirical formula given by Huizenga[2]

$$\frac{P^{Z\,A}}{P^{U}} = 1.3\left(\frac{Z^2}{A} - 34.7\right)$$

one obtains the ratio

$$\frac{Pu^{239}\,(\mu m^- + p)}{U^{238}\,(\mu m^- + p)} \cong 6\,.$$

[2] HUIZENGA, J.R., GINDLER, J.E. and DUFFIELD, R.B., "Relative Photofission Yields of Several Fissionable Materials", Phys. Rev. 95 (1954) 1009.

Further experiments are now in progress to investigate the time distribution of the fission fragments and also to look for the possible re-emission of the meson from the fission fragment.

FISSION YIELDS IN THE IODINE REGION

G. RUDSTAM
CERN, GENEVA, SWITZERLAND

Abstract — Résumé — Аннотация — Resumen

FISSION YIELDS IN THE IODINE REGION. Independent yields of all iodine isotopes from I^{118} to I^{134} except I^{122} (short-lived), I^{127} (stable) and I^{129} (long-lived) resulting from irradiating natural uranium with 590-MeV and 19-GeV protons have been measured. In addition, cross-sections (mostly cumulative) of many xenon and tellurium isotopes have been obtained. In the experiments extensive use has been made of an electromagnetic isotope separator, constructed at CERN for nuclear reaction studies, by which the iodine (or tellurium) isotopes were separated from samples chemically isolated from the irradiated targets. In the study of xenon isotopes the uranium target was heated in a small oven connected to the separator via a cold trap to stop unwanted activities. After the separation, the activity of the samples was measured by counting methods. In certain cases (I^{118}, I^{119}, I^{120}, I^{121}, Xe^{118}, Xe^{119}, Xe^{120}, Xe^{121}) spectroscopic investigations were performed to provide information for the conversion of the counting data to absolute counting-rates needed for the determination of the fission yields.

The experiments show a significant shift in the isotopic cross-section distribution when the 19-GeV results are compared with those obtained at the lower irradiation energy. The yields far out at the neutron-deficient wing increase considerably whereas the other part of the distribution is depressed. A comparison with spallation data indicates that the neutron-deficient part of the distribution might result from the spallation of uranium. Spallation gives negligible yields in the iodine region at 590 MeV, but at 19 GeV these cross-sections are expected to be much larger. The competition with spallation decreases the probability for fission, and consequently the yields of the fission products will decrease.

RENDEMENTS DE FISSION DANS LA RÉGION DE L'IODE. L'auteur a mesuré les rendements indépendants de la fission de l'uranium naturel par des protons de 590 MeV et de 19 GeV, en isotopes de l'iode allant de ^{118}I à ^{134}I, à l'exception de ^{122}I (à courte période), ^{127}I (stable) et ^{129}I (à longue période). Il a obtenu en outre les sections efficaces (pour la plupart, cumulatives) de formation pour un grand nombre d'isotopes du xénon et du tellure. Dans les expériences, il a beaucoup utilisé un séparateur électromagnétique d'isotopes, qui avait été construit au CERN pour des études de réactions nucléaires, et qui lui a permis de séparer les isotopes de l'iode (ou du tellure) des échantillons chimiquement isolés des cibles irradiées. Lors de l'étude sur les isotopes du xénon, la cible d'uranium a été chauffée dans un petit four, qui était relié au séparateur par un piège froid destiné à arrêter les activités indésirables. Après la séparation, l'auteur a mesuré l'activité des échantillons par des méthodes de comptage. Dans certains cas (^{118}I, ^{119}I, ^{120}I, ^{121}I, ^{118}Xe, ^{119}Xe, ^{120}Xe, ^{121}Xe), il a procédé à des études spectroscopiques pour obtenir les renseignements permettant de convertir les données de comptage en taux de comptage absolus nécessaires à la détermination des rendements de fission.

Les expériences indiquent qu'un déplacement important intervient dans la distribution isotopique des sections efficaces lorsqu'on compare les résultats obtenus avec les protons de 19 GeV et ceux qui ont été obtenus avec les protons de 590 MeV. A l'extrémité, dans la partie où il y a un déficit de neutrons, les rendements augmentent considérablement, tandis que dans l'autre partie de la distribution il y a une dépression. Une comparaison avec les données relatives à la spallation montre que la partie de la distribution où il y a un déficit de neutrons pourrait être le résultat de la spallation de l'uranium. Pour 590 MeV, la spallation donne des rendements négligeables dans la région de l'iode, mais pour 19 GeV ces sections efficaces seront probablement beaucoup plus grandes. Par suite de la concurrence de la spallation, la probabilité de fission diminue et les rendements en produits de fission aussi.

ВЫХОДЫ ПРОДУКТОВ ДЕЛЕНИЯ В ОБЛАСТИ ИЗОТОПОВ ЙОДА. Измерены независимые выходы продуктов деления всех изотопов йода, начиная с йода-118 и кончая йодом-134, за исключением йода-122 (короткоживущий), йода-127 (стабильный) и йода-129 (долгоживущий), которые были получены в результате облучения природного урана протонами с энергией 590 Мэв и 19 Бэв. Кроме того, получены сечения (главным образом кумулятивные) многих изотопов ксенона и теллурия. При проведении экспериментов широко использовался

электромагнитный сепаратор изотопов, построенный в ЦЕРН для исследования ядерных реакций, с помощью которого изотопы йода (или теллурия) выделялись из образцов, химически изолированных от облученных мишеней. При изучении изотопов ксенона урановая мишень нагревалась в небольшой печи, соединенной с сепаратором посредством охлаждаемой ловушки, для прекращения нежелаемых активностей. После разделения активность образцов была измерена методами счета. В некоторых случаях (йод-118, йод-119, йод-120, йод-121, ксенон-118, ксенон-119, ксенон-120, ксенон-121) были проведены спектроскопические исследования с целью получения информации для перевода данных счета в абсолютные скорости счета, необходимые для определения выходов продуктов деления.

Эксперименты показывают значительное смещение в распределении изотопных сечений при сравнении результатов с энергией 19 Бэв с результатами, полученными при меньшей энергии облучения. Выходы на крайней части кривой, соответствующей ядру с недостатком нейтронов, значительно увеличиваются, в то время как другая часть распределения убывает. Сравнение с данными о расщеплении показывает, что часть распределения, соответствующая ядрам, с недостатком нейтронов может быть результатом расщепления урана. Расщепление дает незначительные выходы в области изотопов йода при энергии 590 Мэв, однако при 19 Бэв эти сечения, как предполагается, должны быть значительно большими. Конкуренция с расщеплением уменьшает вероятность деления, и поэтому выходы продуктов деления уменьшатся.

RENDIMIENTOS DE FISION EN LA REGION DEL YODO. El autor ha medido, por separado, los rendimientos de todos los isótopos del yodo, desde el ^{118}I al ^{134}I, salvo el ^{122}I (de período corto), el ^{127}I (estable) y el ^{129}I (de período largo), resultantes de la irradiación de uranio natural con protones de 590 MeV y 19 GeV. Además, ha determinado las secciones eficaces (acumulativas en la mayoría de los casos) de muchos isótopos del xenón y del teluro. En estos experimentos el separador electromagnético de isótopos construido en el CERN para efectuar estudios sobre las reacciones nucleares se ha utilizado reiteradamente para separar isótopos del yodo (o del teluro) de muestras químicamente aisladas de los blancos irradiados. En el estudio de los isótopos del xenón, el blanco de uranio se calentó en un pequeño horno conectado con el separador por medio de una trampa fría, a fin de detener las actividades inconvenientes. Después de la separación, la actividad de las muestras se determinó por recuento. En algunos casos (^{118}I, ^{119}I, ^{120}I, ^{121}I, ^{118}Xe, ^{119}Xe ^{120}Xe y ^{121}Xe) se efectuaron investigaciones espectroscópicas para obtener información a fin de convertir los resultados de los recuentos en índices absolutos de recuento, necesarios para determinar los rendimientos de fisión.

Los experimentos han puesto de manifiesto un importante desplazamiento de la distribución isotópica de la sección eficaz cuando se comparan los resultados obtenidos con protones de 19 GeV y los conseguidos a energías de irradiación más bajas. Los rendimientos correspondientes al extremo de la rama deficiente en neutrones aumentan considerablemente, en tanto que la parte restante de la distribución acusa una depresión. Una comparación efectuada con los datos correspondientes a la espalación indica que la rama deficiente en neutrones puede atribuirse a la espalación del uranio; el rendimiento de ésta resulta despreciable en la región del yodo al efectuar la irradiación a 590 MeV, pero se espera que con neutrones de 19 GeV estas secciones eficaces sean mucho más elevadas. La competencia con la espalación reduce la probabilidad de fisión y, por consiguiente, se traduce en una disminución del rendimiento de productos de fisión.

INTRODUCTION

Independent yields of iodine isotopes, formed by irradiating natural uranium with 590-MeV and 18-GeV protons, have been measured. Iodine was chosen for study because of its many measurable isotopes. Thus independent cross-sections have been obtained for all isotopes from I^{118} to I^{134} with the exception of I^{127}(stable) and I^{129}(long-lived). Xenon and tellurium isotopes were also studied to provide information on the parent effect in the measured cross-section. Cumulative yields were determined for numerous xenon and tellurium isotopes and, in addition, for the iodine isotope I^{135}.

EXPERIMENTAL

In high-energy reactions a sample, after chemical separation, might still contain a large number of radioactive components. The difficulty of resolving the resulting complex decay curve was avoided by including isotope separation in the experimental procedure. For this, the electromagnetic isotope separator at CERN [1], especially designed for nuclear reaction studies, was used. The samples obtained from this separator are well suited for activity measurements, and accurate cross-section determinations can be carried out [2].

The chemical separation procedures preceding the isotope separation were simple. After a few purification steps, iodine was converted to silver iodide and tellurium to tellurium tetrabromide, and these compounds were fed to the ion sources of the separator. In the case of xenon, the uranium target was heated to 950°C in a small oven, and the gas mixture leaving the target was introduced into the ion source after having passed a cold trap (-70°C) and a special iodine trap consisting of silver nitrate at 195°C.

The activity of the separated samples was measured with calibrated beta counters, gamma- and X-ray spectrometers and a coincidence counter detecting annihilation radiation from positrons.

By using an isotope dilution technique, and adding a measured amount of I^{131} to the target solution, the yield of chemistry and isotope separation could be determined. In this way, the cross-sections of the iodine isotopes were related to the cross-section of Na^{24}, formed in aluminium monitor foils included in the target stack, and thereby converted to absolute cross-sections. From parent-daughter relationships the yields of xenon and tellurium isotopes could be tied to those of iodine isotopes, and thus also converted to the absolute scale.

For a determination of cross-sections from counting data, some knowledge about the disintegration schemes is required. Therefore, spectroscopic studies of previously little known or unknown xenon and iodine isotopes were also carried out [3]. Three new xenon activities, Xe^{118}, Xe^{119} and Xe^{120}, were found.

RESULTS AND DISCUSSION

The yield distributions of iodine isotopes at 590 MeV and 18 GeV are given in Figs. 1 and 2 respectively. In Fig. 1 are included, for comparison, some iodine cross-sections interpolated from data obtained by ALEXANDER, BALTZINGER and GAZDIK [4]. Cumulative yields of iodine, xenon and tellurium isotopes have been plotted in Fig. 3 (590 MeV) and Fig. 4 (18 GeV).

The cross-sections at 590 MeV vary in a smooth manner (cf. Fig. 1). The only surprising result is the high cross-section of I^{132}. At 18 GeV (Fig. 2) the peak around mass 132 is still more pronounced. Furthermore, the yields of very light iodine isotopes (mass less than 123) have increased at the expense of the others, which are lower than at 590 MeV by a factor of about two. It seems probable that the light-mass part of the isotopic distribution is caused by a reaction other than fission. Support for this is given by BRANDT's investigations [5] where it is shown that the range of these light iodine iso-

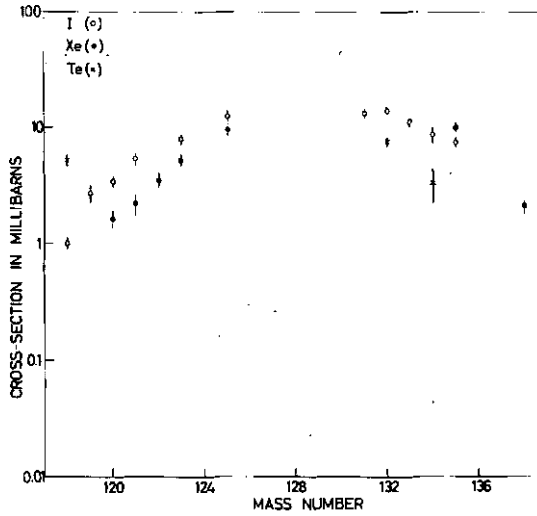

Fig. 1

Distribution of iodine isotopes from the irradiation of uranium with 590-MeV protons (open circles). The closed circles are cross-sections obtained by interpolation from the results given in Ref. [4].

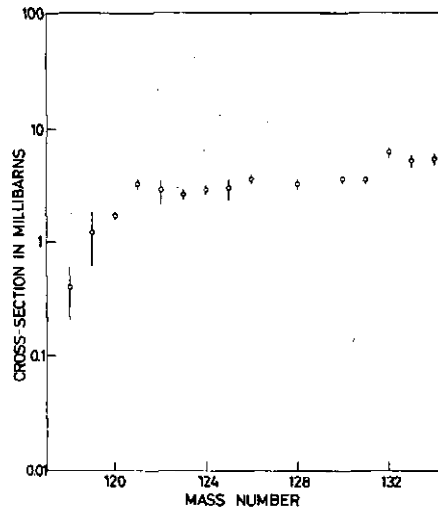

Fig. 2

Distribution of iodine isotopes from the irradiation of uranium with 18-GeV protons

topes is considerably shorter than the range of the heavy isotopes of the same element. The range-versus-mass curve has a step-wise appearance with a break at mass number 124, the heavier isotopes having about double the range of the lighter ones. A comparison with data from the spallation of tantalum and gold with 18-GeV protons [6] suggests that the light iodine isotopes might be formed by the spallation of uranium. The isotopic distribution

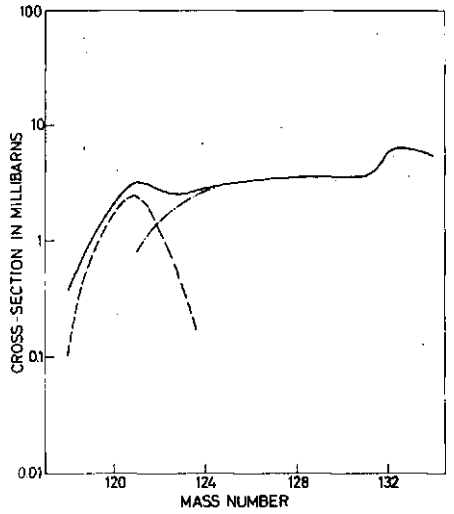

Fig. 3

Cumulative yields of iodine (open circles), xenon (closed circles) and tellurium isotopes (crosses) from the irradiation of uranium with 590-MeV protons

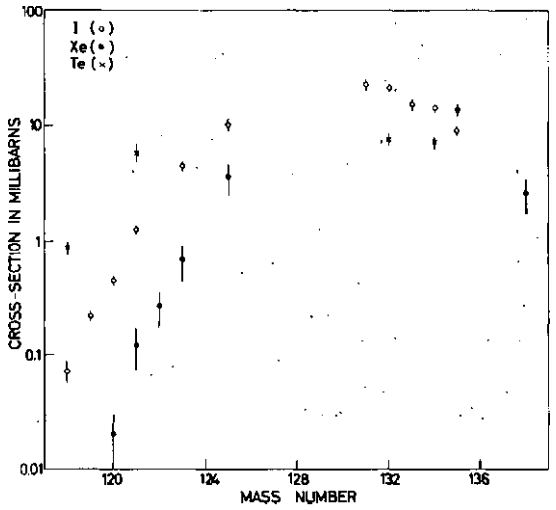

Fig. 4

Cumulative yields of iodine (open circles), xenon (closed circles) and tellurium isotopes (crosses) from the irradiation of uranium with 18-GeV protons

obtained in this spallation investigation has its peak at mass number 121, and its left wing is similar to the left wing of the distribution shown in Fig. 2. An analysis of the uranium results at 18 GeV in terms of a spallation part, identical to that obtained from gold, and a fission part is indicated in Fig. 5.

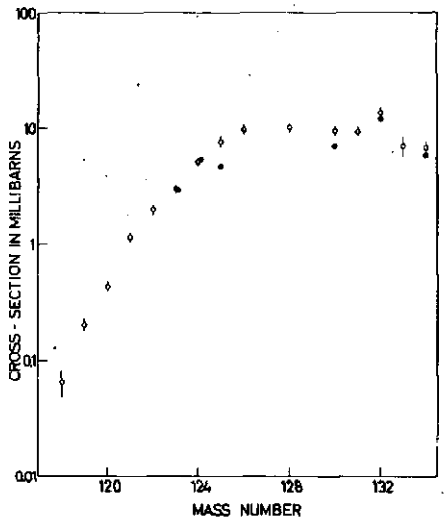

Fig. 5

Decomposition of the iodine distribution at 18 GeV (solid curve) in terms of a spallation part (dashed curve) and a fission part (dot-and-dash curve)

In the 590-MeV results, the spallation part is missing because the yields are too low. At 18 GeV, however, the spallation yields have grown considerably, and judging from the magnitude of the fission part (mass number 124 and heavier), spallation is about as probable as fission at this energy. This is in reasonable accord with the finding of DE CARVALHO et al. [7] that the fissionability of uranium at 20 GeV is about one-third of what it is at 600 MeV.

REFERENCES

[1] ANDERSSON, G., HEDIN, B. and RUDSTAM, G., Nucl. Instrum. Meth. 28 (1964) 245; RUDSTAM, G., SUNDELL, S. and ANDERSSON, G., ibid 255.

[2] ANDERSSON, G. and RUDSTAM, G., Nucl. Instrum. Meth. 29 (1964) 93.

[3] ANDERSSON, G., RUDSTAM, G. and SÖRENSEN, G., Ark. Fys. (in press).

[4] ALEXANDER, J.M., BALTZINGER, C. and GAZDIK, M.F., Phys. Rev. 129 (1963) 1826.

[5] BRANDT, R., "Ranges of iodine and bromine isotopes produced in the interaction of high-energy protons with uranium", these Proceedings II.

[6] RUDSTAM, G. and SÖRENSEN, G., to be published.

[7] DE CARVALHO, H.G., CORTINI, G., MUCHNIK, M., POTENZA, G., RINZIVILLO, R. and LOCK, W.O., Nuovo Cim. 27 (1963) 468.

RANGES OF IODINE AND BROMINE ISOTOPES PRODUCED IN THE INTERACTION OF HIGH-ENERGY PROTONS WITH URANIUM

R. BRANDT
CERN, GENEVA, SWITZERLAND
AND
MAX PLANCK INSTITUT FÜR KERNPHYSIK,
HEIDELBERG, FEDERAL REPUBLIC OF GERMANY

Abstract — Résumé — Аннотация — Resumen

RANGES OF IODINE AND BROMINE ISOTOPES PRODUCED IN THE INTERACTION OF HIGH-ENERGY PROTONS WITH URANIUM. Conventional range experiments using a thick uranium foil together with aluminium catchers and monitors are carried out at the two CERN accelerators with 0.55-GeV and 18.2-GeV protons. Iodine (or bromine) is chemically isolated and separated in the CERN radioisotope separator. This gives carrier-free samples containing essentially only one pure radioactive istope. The chemical yield is determined also. The analysis of the data gives directly the range for each istope in uranium.

All iodine istopes have the same range at 0.55-GeV proton energy, i.e. they are all produced in a fission process. It was known previously that neutron-rich iodine isotopes have about the same range whether the proton energy is above or below 1 GeV, and that neutron-deficient iodine isotopes show a drastic decrease of about one half when the proton energy increases above 1 GeV. It is shown that this decrease in range occurs rather suddenly, giving a step-function in the range - versus - iodine isotopic mass curve. The neutron-deficient isotopes having a decreased range above 1-GeV proton energy are the same as those for which a strong increase in their excitation function above 1 GeV has been observed. Bromine istopes show essentially the same range behaviour. The strong increase in the production of neutron-deficient isotopes is again observed at high bombarding energies.

The discussion will concentrate on these neutron-deficient isotopes. They are produced essentially only above 1 GeV and have at the higher combarding energy only about one half the range of normal fission products, indicating that they are produced by a process other than fission. These findings will be discussed in the light of "spallation" and "fragmentation" models, both terms being redefined.

ISOTOPES DE L'IODE ET DU BROME PRODUITS PAR L'INTERACTION DE PROTONS DE HAUTE ENERGIE AVEC L'URANIUM. Des expériences classiques sur des feuilles d'uranium épaisses avec des pièges en aluminium et des détecteurs sont faites dans les deux accélérateurs du CERN au moyen de protons de 0,55 GeV et de 18,2 GeV. L'iode (ou le brome) est chimiquement isolé et séparé dans le séparateur de radioisotopes du CERN. Cette opération permet d'obtenir des échantillons sans entraîneur qui ne contiennent essentiellement qu'un seul radioisotope pur. Le rendement chimique est également déterminé. L'analyse des données indique directement le parcours de chaque isotope dans l'uranium.

Pour une énergie des protons de 0,55 GeV, le parcours de tous les istopes de l'iode est le même, c'est-à-dire qu'ils sont tous produits par un processus de fission. On savait précédemment que ceux des isotopes de l'iode qui sont riches en neutrons ont à peu près le même parcours que l'énergie des protons, qu'elle soit supérieure ou inférieure à 1 GeV, et que les isotopes de l'iode pauvres en neutrons accusent une diminution nette du parcours de la moitié environ lorsque l'énergie des protons augmente au-delà de 1 GeV. L'auteur montre que cette diminution de parcours se produit assez brusquement en donnant une fonction échelonnée de la courbe du parcours en fonction de la masse isotopique de l'iode. Les isotopes pauvres en neutrons qui ont un parcours moindre au-dessus d'une énergie de 1 GeV sont les mêmes que ceux pour lesquels on a observé une forte augmentation de leur fonction d'excitation au-dessus de 1 GeV. Les isotopes du brome accusent essentiellement le même comportement en ce qui concerne le parcours. La courbe de rendement isotopique en brome à partir de l'uranium présente les mêmes caractéristiques principales que la courbe correspondante pour l'iode. La forte augmentation de la formation des isotopes pauvres en neutrons s'observe à nouveau aux énergies de bombardement élevées.

La discussion porte principalement sur ces isotopes pauvres en neutrons. Ils ne sont produits essentiellement qu'au-dessus de 1 GeV; aux énergies de bombardement élevées, leur parcours n'est qu'environ la moitié de celui des produits de fission normaux, ce qui indique qu'ils sont formés par un processus autre que la fission. L'auteur examine ces résultats compte tenu des modèles de « spallation » et de « fragmentation » et donne de nouvelles définitions de ces deux termes.

ПРОБЕГИ ИЗОТОПОВ ЙОДА И БРОМА, ПОЛУЧЕННЫХ ПРИ ВЗАИМОДЕЙСТВИИ ПРОТОНОВ БОЛЬШОЙ ЭНЕРГИИ С УРАНОМ. Обычные эксперименты по пробегам с использованием толстой урановой фольги вместе с алюминиевыми ловушками и дозиметрами проводятся на двух ускорителях ЦЕРН с протонами, имеющими энергии 0,55 Бэв и 18,2 Бэв. Иод (или бром) выделяется химическим путем и разделяется в сепараторе радиоизотопов в ЦЕРН. В результате получают образцы без носителя, содержащие по существу только один чистый радиоактивный изотоп. Определяется также выход химических продуктов. Анализ данных позволяет получить непосредственно пробег для каждого изотопа в уране.

Все изотопы йода имеют один и тот же пробег при энергии протонов 0,55 Бэв, т.е. они все образуются в процессе деления. Ранее было известно, что изотопы йода с избытком нейтронов имеют приблизительно один и тот же пробег, независимо от того, превышает ли энергия протонов 1 Бэв или она ниже этого уровня, а также, что изотопы йода с недостатком нейтронов дают резкое сокращение, приблизительно на половину, при увеличении энергии протонов свыше 1 Бэв. Показывается, что это сокращение пробега происходит довольно внезапно, приводя к скачку на кривой зависимости пробега от массы изотопа йода. Изотопы с недостатком нейтронов, имея сокращенный пробег при энергии протонов свыше 1 Бэв, являются теми же самыми изотопами, в отношении которых наблюдалось сильное увеличение функции возбуждения свыше 1 Бэв. Изотопы брома по существу имеют ту же самую зависимость пробегов. Кривая выхода изотопов брома из урана имеет те же самые основные особенности, что и соответствующая кривая для йода. Сильное увеличение производства изотопов с недостатком нейтронов снова наблюдается при больших энергиях бомбардирующих частиц.

Обсуждение касается главным образом этих изотопов с недостатком нейтронов. Они получаются по существу только при энергии свыше 1 Бэв, и их пробег при более высокой энергии бомбардирующих частиц составляет только приблизительно половину пробега обычных продуктов деления, что говорит о том, что они получаются не в результате деления, а другим путем. Эти выводы обсуждаются в свете моделей "расщепления" и "фрагментации", причем дается новое определение этим терминам.

ALCANCE DE LOS ISOTOPOS DEL YODO Y DEL BROMO PRODUCIDOS EN LA INTERACCION DE PROTONES DE ALTA ENERGIA CON EL URANIO. En los dos aceleradores del CERN se llevan a cabo experimentos de tipo tradicional sobre determinación del alcance de protones de 0,55 GeV y de 18,2 GeV, utilizando una gruesa lámina de uranio juntamente con captadores de aluminio y contadores. En el separador de radioisótopos del mismo centro se procede a la separación, previo aislamiento por procedimientos químicos, del yodo (o del bromo). Esta operación proporciona muestras libres de portador que en esencia se componen de un solo radioisótopo puro. También se determina el rendimiento químico. El análisis de los datos proporciona directamente el alcance de cada isótopo en el uranio.

Para una energía protónica de 0,55 GeV, todos los isótopos del yodo tienen el mismo alcance, es decir, que todos ellos se producen en un proceso de fisión. Se sabía ya que los isótopos del yodo ricos en neutrones tienen aproximadamente el mismo alcance - tanto si la energía de los protones es superior a 1 GeV o inferior a este valor - y que el alcance de los isótopos de ese mismo elemento deficientes en neutrones disminuye a la mitad aproximadamente, cuando la energía de los protones supera 1 GeV. El autor pone de manifiesto que esta disminución del alcance se produce de una manera bastante brusca, proporcionando una función escalonada para la curva del alcance en función de la masa isotópica del yodo. Los isótopos deficientes en neutrones cuyo alcance disminuye para una energía de los protones superior a 1 GeV son los mismos para los que se ha observado un fuerte aumento de su función de excitación por encima de 1 GeV. De forma análoga, se comportan, en cuanto al alcance, los isótopos del bromo. La curva de rendimiento isotópico del bromo procedente del uranio presenta las mismas características principales que la curva correspondiente al yodo. El fuerte aumento en la producción de isótopos deficientes en neutrones vuelve a observarse empleando altas energías de bombardeo.

El autor centra su estudio en esos isótopos deficientes en neutrones, que prácticamente se producen sólo a niveles superiores a 1 GeV; a energías de bombardeo más elevadas, su alcance está limitado aproximada-

mente a la mitad del alcance de los productos de fisión normales, lo que indica que se forman en virtud de un proceso distinto del de fisión. El autor examina estas conclusiones teniendo en cuenta modelos de « espalación » y de « fragmentación », definiendo de nuevo estos dos términos.

INTRODUCTION

In comparing the interactions of high-energy protons ($E_p > 1$ GeV) in uranium to those of lower energy ($E_p < 1$ GeV), one finds in the mass region with $\sim 70 < A < \sim 150$ three interesting features [1, 2]:

(i) A strong increase in the production of neutron-deficient isotopes.

(ii) These neutron-deficient isotopes show a strong decrease in their range when the proton bombarding energy exceeds 1 GeV.

(iii) A decrease in the formation cross-section of neutron-excess isotopes that are considered to be fission products.

The two accelerators at CERN provide irradiation possibilities at 500 MeV and 18 GeV. At these energies a great variety of isotopes is produced for each element given. The CERN Radioisotope Separator [3]) is well-suited for radio-chemical studies and yields samples that contain essentially only one isotope. This enables a fairly accurate study to be made of the isotopic yield distributions of one element. RUDSTAM [5] has carried out such an isotopic yield distribution study for iodine produced from uranium. It seemed interesting to study now the ranges of different iodine isotopes in uranium using the isotope separator, together with Rudstam's values for the production cross-sections of these isotopes. In addition, it seemed interesting to extend the studies to a "light" fission fragment. Here the element bromine was chosen since its isotopes can be easily separated in the isotope separator. Preliminary results for the ranges and cross-sections of bromine in uranium will be presented.

EXPERIMENTS CONCERNING THE BOMBARDING PROCEDURES

The targets used for the internal irradiations at 550 MeV [6] and 18 GeV [7] have been described elsewhere. Since an essential part of the experiments consists in the determination of Na^{24} produced in an aluminium monitor foil, and since Na^{24} in aluminium can also be produced by secondary particles [6], it seemed interesting to study at 18 GeV which part of an internal target is "useful" for investigations, and how much Na^{24} in the monitor foil is produced via secondary reactions in the "useful" region.

The experiment was started by comparing the production of Tb^{149} in a thin gold foil to the production of F^{18} in a thin aluminium foil, mounted together in a uranium target sandwich (30μm Al + 10μm Al + 30μm Al + 0.002-in uranium + 30μm Al + 12μm Au + 30μm Al). The production of Tb^{149} in gold has a threshold at ~600 MeV [8], and it is safe to assume that at these total target thicknesses it is not produced by secondary particles. F^{18} in aluminium has a production threshold at ~50 MeV [6]. In the top part of Fig. 1 one sees the ratio of the production of these two isotopes as a function of the distance from the leading edge of the target. The ratio remains constant

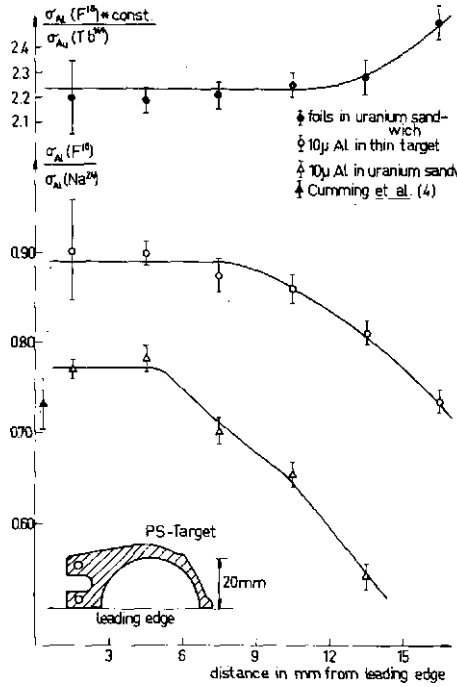

Fig. 1

Results of the study of secondary effects of 18 GeV. At the top is the ratio $\sigma_{Al}(F^{18}) : \sigma_{Au}(Tb^{149})$ in a normal uranium sandwich as a function of the distance from the leading edge of the target. Below this is given $\sigma_{Al}(F^{18}) : \sigma_{Al}(Na^{24})$ as a function of the distance from the leading edge for several targets. The exact composition of the targets is described in the text. Only the statistical uncertainties in the ratios are shown. The value given by CUMMING et al. [4] for $\sigma_{Al}(F^{18}) : \sigma_{Al}(Na^{24})$ is included for comparison. The shape of the target is shown at the bottom left.

within 5% (only the point at 15-mm distance shows a relative increase in the F^{18} production). Since, in the same target, the $\sigma_{Al}(F^{18}) : \sigma_{Al}(Na^{24})$[1] ratio changes by 40% over the same distance (see below), it is concluded that the production of F^{18} in aluminium is a good measure of the primary flux up to 15-mm distance from the leading edge.

The next step consists in measuring the ratio

$$S = \sigma_{Al}(F^{18}) : \sigma_{Al}(Na^{24}) \tag{1}$$

in a target as thin as possible. A 10μm aluminium foil was sandwiched between two 15μm aluminium foils (to compensate for recoil effects). The ratio of the cross-sections is again measured as a function of the distance from the leading edge (10-mm × 3-mm strips were counted). Figure 1 shows that this ratio is rather high at the leading edge and decreases slowly. This decrease is considered to be caused by an increased production of Na^{24} via secondary particles. The value for $S = 0.89 \pm 0.04$ is measured near the lead-

[1] The symbol $\sigma_{Al}(F^{18})$ is the cross-section for F^{18} in aluminium.

ing edge and is considered to be the "true" value uninfluenced by secondary particles.

Finally, a typical CERN uranium target sandwich (30μm Al + 10μm Al + 30μm Al + 0.002-in uranium + 30μm Al + 10μm Al + 30μm Al) was irradiated. The 10μm aluminium monitor foils were cut into 10-mm × 3-mm strips and S was again determined as a function from the leading edge. The results are shown in Fig. 1. At the leading edge S is (12 ± 3)% lower than for the very thin target, and this ratio decreases with increasing distance from the edge. From this one can conclude:

(i) Only the first ~6 mm of the target should be used for radiochemical studies that are sensitive to low-energy secondary particles (certainly fission studies belong in this category).

(ii) In the determination of absolute cross-sections one has to correct for the fact that the amount of Na^{24} produced in the aluminium monitor foil is (12 ± 3)% too high.

(iii) In the range studies, as described later, one does not need to take this effect into account, provided the same target area is always used. (In range studies only the ratio of the activity in the catcher foils and uranium foil is important.) The uncertainties shown in Fig. 1 do not include the uncertainties in the ratio of counting efficiencies for F^{18} and Na^{24} in aluminium, since one wants to know only the difference in S for different target thicknesses. This should be kept in mind when the values are compared with those measured by CUMMING et al. [4] whose target thickness of 70 mg/cm² was between the uranium sandwich (133 mg/cm²) and the very thin target (10.8 mg/cm²). Further details of this work will be published elsewhere [9].

The interesting question on how the shape of the isotopic distribution of bromine produced in uranium at 18 GeV varies with target thickness (in particular targets of ~100 μg/cm² uranium between two 40μm aluminium foils compared to standard CERN uranium targets) will have to be followed up in the future. This question is irrelevant for the range measurements since it is known that the range of neutron excess fission products is independent of the bombarding energy within uncertainties quoted later.

FURTHER EXPERIMENTAL PROCEDURES

The typical CERN uranium sandwiches (see above) were irradiated. Conventional range experiments require the determination of the amount of activity produced in the forward foil (F), in the backward foil (B) and uranium (U). From these three measurements the so-called range R can be calculated [1]:

$$R = 2 \times W \times \frac{(F + B)}{U} \qquad (2)$$

where W is the thickness of the uranium foil. Another quantity of interest is the F/B-ratio.

The amount of activity of one isotope in a given foil is determined in the manner described by RUDSTAM [5]. The independent and cumulative yields in the iodine experiments were determined by the use of different chemical separation times for the daughter from the parent. Tellurium and xenon determinations were not carried out in the catcher foils. A simplified version of the chemical procedure described by STEHNEY and SUGARMAN [10] was used in the bromine experiments. It is found that iodine and xenon isotopes do not leave the uranium target during irradiation [5]. For bromine this question cannot yet be answered conclusively. Only one determination of the absolute cross-section of Br^{80} at 18 GeV was carried out. The isotope dilution technique using Br^{82} was employed [5]. The result is given later and is in agreement with what one would expect as a cross-section. Also two determinations of the absolute value for the range of Br^{80} were carried out, giving again reasonable answers. (Hagebø [11] also found that bromine can be extracted easily from irradiated uranium compounds simply by heating, but that one needs considerably higher temperatures to extract bromine from uranium metal by heating.)

RESULTS

The results of the iodine experiments at 18 GeV are shown in Fig. 2 and Table I. (The production of iodine in the uranium foil was determined by RUDSTAM [5].) When the values are compared with those measured

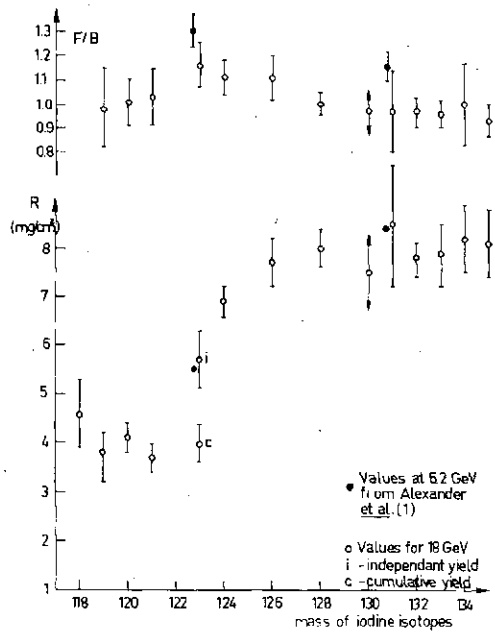

Fig. 2

Ranges R and F/B-ratios in uranium for iodine isotopes produced at 18 GeV. The systematic uncertainty is shown for I^{130}. For all other isotopes only the relative errors, compared with I^{130} are given (compare with Table I).

TABLE I

RANGES R AND F/B-RATIOS FOR IODINE ISOTOPES FROM URANIUM AT 18 GeV

Isotope	Number of determinations in forward	backward	Mode[a]	R^b mg/cm²	F/B^b
118	1	2	c	4.6 ± 0.7 ←	
119	3	3	c	3.7 ± 0.5 ←	0.98 ± 0.17 ←
120	7	4	c	3.8 ± 0.5	0.92 ± 0.19
			i	4.3 ± 0.6	1.00 ± 0.20
			p	4.1 ± 0.3 ←	1.01 ± 0.10 ←
121	8	4	c	3.9 ± 0.4	0.98 ± 0.18
			i	3.1 ± 0.6	1.02 ± 0.20
			p	3.7 ± 0.3 ←	1.03 ± 0.12 ←
123	11	7	c	4.0 ± 0.4 ←	1.17 ± 0.12
			i	5.7 ± 0.6 ←	0.88 ± 0.15
			p	4.0 ± 0.3	1.16 ± 0.09 ←
124	8	6	i	6.9 ± 0.3 ←	1.11 ± 0.07 ←
126	7	6	i	7.7 ± 0.5 ←	1.11 ± 0.09 ←
128	3	3	i	8.0 ± 0.4 ←	1.00 ± 0.05 ←
130	4	4		7.5 ± 0.8 ←	0.97 ± 0.10 ←
131	4	2	p	8.5 ± 1.3 ←	0.97 ± 0.17 ←
132	9	7	c	7.9 ± 0.8	0.97 ± 0.14
			i	7.8 ± 0.4 ←	0.97 ± 0.07 ←
133	9	6	c	7.9 ± 0.6 ←	0.96 ± 0.06 ←
			i	9.0 ± 1.2	1.45 ± 0.25
134	4	5	c	9.1 ± 1.6	1.20 ± 0.15
			i	8.2 ± 0.7 ←	1.00 ± 0.17 ←
135	7	6	c	8.1 ± 0.7 ←	0.93 ± 0.07 ←

[a] The radiochemical mode "i" indicates independent, "c" cumulative and "p" partially cumulative yields. The last term is explained in the text.

[b] The systematic uncertainty is shown for I^{130}. For all other isotopes only the relative errors compared to I^{130} are given. The values indicated with arrows are used for Fig. 2.

previously by ALEXANDER et al. [1] one finds general agreement.[2] The values measured by them have considerably smaller uncertainties. In this paper a much larger number of ranges for individual isotopes are reported.

The range-versus-isotopic-mass curve is rather flat in the mass interval of $126 \leq A \leq 135$. Around the mass 124 this range drops rather drastically to about one-half of the fission-fragment range, thus giving a step function

[2] Ref. [1] also contains more ranges for unseparated groups of iodine isotopes.

in the curve. The independent and cumulative yields agree always within the limits of errors, as shown in Table I. The exception is I^{123}, which can be readily explained. In the cumulative yield of I^{123} the parent isotope Xe^{123} decays in, which is for the element xenon already on the low-range side, since Xe^{123} is relatively more neutron deficient than I^{123}.

RUDSTAM [5] has shown that the cumulative yield for I^{123} is considerably higher than its independent yield. The independent range for I^{123} is just in the transition between the high and low values, the cumulative range for I^{123} is already as low as the range of all other neutron-deficient isotopes. Table I shows, not only independent and cumulative yields, but also partially cumulative yields. This has been done for certain isotopes where the uncertainty in the results could be reduced by using, in all foils, the results of the same parent-daughter separation times. Figures 1 and 2 also show the F/B-ratios. These ratios increase at 6.2 GeV by $(15 \pm 4)\%$ when one compares neutron-excess and neutron-deficient isotopes [1]. All the results found in this work have uncertainties of $\sim 10\%$, and are compatible with this slight increase.

The results of the iodine experiment at 550 MeV are shown in Fig. 3 and Table II. The range curve is rather flat. The absolute value of the range equals the range of the neutron-excess isotopes at 18 GeV within the limits of error. However, one observes here again a slight decrease in range of $\sim 20\%$ for the neutron-deficient isotopes.

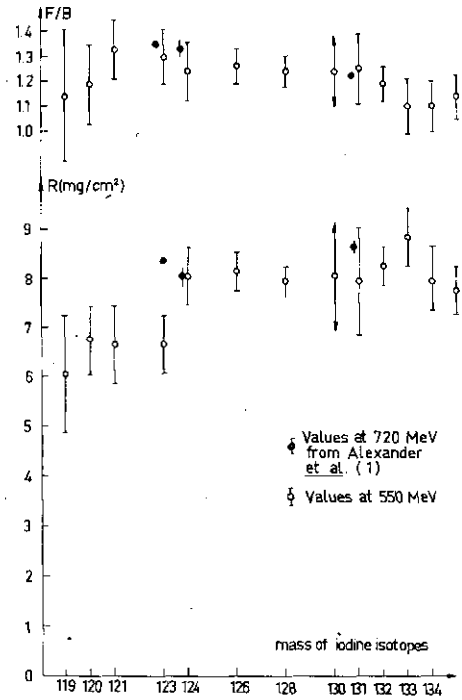

Fig. 3

Ranges R and F/B-ratios in uranium for iodine produced at 550 MeV. The systematic uncertainty is shown for I^{130}. For all other isotopes only the relative errors compared with I^{130} are given (compare with Table II).

TABLE II

RANGES R AND F/B-RATIOS FOR IODINE ISOTOPES FROM URANIUM AT 550 MeV

Isotope	Number of determinations in forward	Number of determinations in backward	Mode[a]	R^b mg/cm²	F/B^b
119	2	1	c	6.0 ± 1.2	1.13 ± 0.27
120	4	4	c	6.7 ± 0.7	1.18 ± 0.16
121	4	4	c	6.6 ± 0.8	1.32 ± 0.12
123	5	4	i	6.6 ± 0.6	1.29 ± 0.11
124	6	3	i	8.0 ± 0.6	1.23 ± 0.12
126	6	3	i	8.1 ± 0.4	1.25 ± 0.07
128	3	3	i	7.9 ± 0.3	1.23 ± 0.06
130	3	1	i	8.0 ± 1.1	1.23 ± 0.14
131	2	2	p	7.9 ± 1.1	1.24 ± 0.14
132	5	4	i	8.2 ± 0.4	1.18 ± 0.07
133	3	4	c	8.8 ± 0.6	1.09 ± 0.11
134	4	3	c	7.9 ± 0.7	1.09 ± 0.10
135	6	3	c	7.7 ± 0.5	1.13 ± 0.09

[a] The radiochemical mode "i" indicates independent, "c" cumulative and "p" partially cumulative yields. The last term is explained in the text.

[b] The systematic uncertainty is shown for I^{130}. For all other isotopes only the relative errors compared to I^{130} are given.

This decrease can be physically real or it can be because the uranium-foil values needed for Eq. (2) are taken from RUDSTAM's work at 590 MeV [5]). One preliminary experiment on a uranium foil at 550 MeV seems to indicate that the range curve is in reality rather flat, and that the cross-sections for neutron-deficient iodine isotopes vary rapidly in this energy range. (The reason for studying ranges at 550 MeV and not at 590 MeV is that the intensity of the machine is higher at the lower energy and for these experiments rather high proton fluxes are needed.)

Figure 4 and Table III show the preliminary results for the bromine ranges in uranium. The ranges relative to Br^{82} are given for 550 MeV, and the range curve is rather flat. At 18 GeV it is again observed that the neutron-deficient isotopes Br^{75} and Br^{76} have approximately one-half the range of neutron-excess isotopes. But the uncertainties in the values are too large to allow us to conclude that the ranges have again a step-like behaviour. Finally, it should be pointed out that no corrections for scattering effects, etc., on the ranges have been made since these corrections are much smaller than the uncertainties reported here [12].

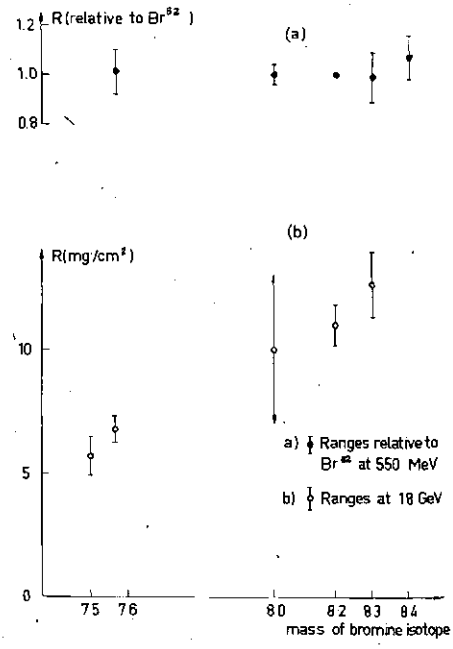

Fig. 4

Preliminary ranges of bromine isotopes in uranium (compare with Table III).

(a) Ranges relative to Br^{82} at 550 MeV.
(b) Ranges at 18 GeV. The systematic uncertainty is given for Br^{80}. For all other isotopes only the relative errors compared with Br^{80} are given.

In range studies one does not need to know the details of the disintegration scheme of one isotope since the interest is concentrated on relative amounts of isotopes in the three different foils. However, it is possible to estimate roughly the absolute counting efficiencies for all the bromine isotopes and this yields absolute cross-sections. Preliminary results for the bromine isotope production cross-section are shown in Fig. 5. At 550 MeV only cross-sections relative to Br^{82} are shown. At 18 GeV one determination for the absolute cross-section of Br^{80} has been made. The essential result here is that the relative amount of neutron-deficient bromine isotopes increases strongly when one goes from 550 MeV to 18 GeV, thus repeating the behaviour of the iodine region. (The cross-sections have not been corrected for the effect of secondary particles producing Na^{24} in the monitor foils, as described in a preceding section.)

DISCUSSION

The discussion will concentrate on the main result of this paper: the step-function in the range-versus-iodine-isotopic-mass curve at 18 GeV. It now seems useful to summarize results of different experiments investi-

TABLE III

A. PRELIMINARY RESULTS FOR BROMINE RANGES AND CROSS-SECTIONS RELATIVE TO Br^{82} AT 550 MeV

Isotope	Number of determinations			Relative R	Relative F/B	Relative σ	Mode[a]
	Uranium	F	B				
74	1	0	0			0.002 ± 0.001	p
75	2	0	0			0.0015 ± 0.0003	c
76	3	3	2	1.01 ± 0.09	1.02 ± 0.08	0.0052 ± 0.0003	p
78	2	0	0			0.20 ± 0.04	i
80	5	3	4	1.00 ± 0.04	1.04 ± 0.04	0.53 ± 0.02	i
82	-	-	-	1.0	1.0	1.0	
						1.29 ± 0.13	i
83	5	3	4	0.99 ± 0.10	1.06 ± 0.09	2.32 ± 0.23	c
84	3	1	1	1.07 ± 0.9	0.84 ± 0.10	1.08 ± 0.05	c

B. PRELIMINARY RESULTS FOR BROMINE RANGES AND CROSS-SECTIONS AT 18 GeV

Isotopes	Number of determinations			R(mg/cm²)[b]	(F/B)[b]	σ(mb)	Mode[a]
	Uranium	F	B				
74	1	0	0			0.07 ± 0.01	p
75	3	1	2	5.7 ± 0.8	1.5 ± 0.2	0.94 ± 0.08	c
76	4	2	2	6.8 ± 0.5	1.26 ± 0.13	1.50 ± 0.05	p
80	3	2	3	10.0 ± 3.0	1.4 ± 0.2	8.6 ± 1.6	i
82	1	2	2	11.0 ± 0.8	1.35 ± 0.08	7.1 ± 0.2	i
83	3	2	3	12.6 ± 1.3	1.6 ± 0.2	11.8 ± 0.7	c
84	1	0	0			4.2 ± 0.8	c

[a] The radiochemical mode "i" indicates independent, "c" cumulative and "p" partially cumulative yields. The last term is explained in the text.

[b] The systematic uncertainty is shown for Br^{80}. For all other isotopes only the relative errors compared to Br^{80} are given.

gating nuclides in the iodine region produced by high-energy protons from uranium:

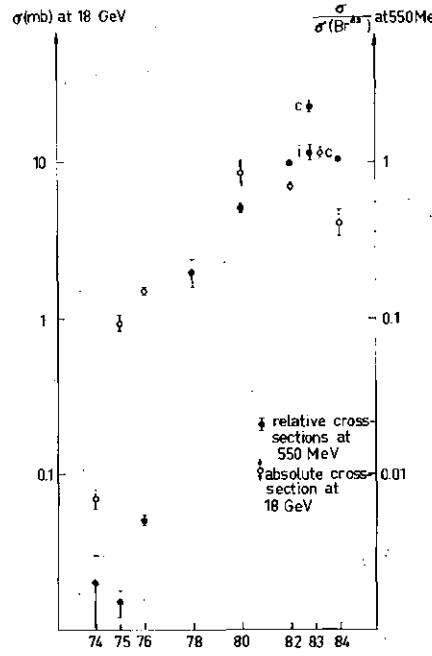

Fig. 5

Preliminary cross-sections of bromine isotopes. The cross-sections relative to Br^{82} are given at 550 MeV. The absolute cross-sections at 18 GeV are shown. The systematic uncertainty is shown for Br^{80}. For all other isotopes only the relative errors compared with Br^{80} are given (compare with Table III).

(i) The cross-section measurements [1, 2, 5] indicate that below ~1 GeV only fission products are formed and that those fission products are predominantly neutron-excess isotopes. Above ~1 GeV the very neutron-deficient isotopes show a strong increase in their production cross-section, and these neutron-deficient isotopes are also typical spallation products when produced from targets like lanthanum.

(ii) The thick-target range measurements make it highly probable that all isotopes produced below ~1 GeV are fission products since they have all about the same range. At energies above 1 GeV precisely those neutron-deficient isotopes that show a decrease of one-half in their range show a strong increase in their production cross-section. The above-mentioned step-function indicates that the transition occurs rather suddenly.

(iii) The differential range studies on one neutron-excess and one neutron-deficient barium isotope show that the neutron-excess isotope has a sharply peaked differential range distribution, just as one expects for a typical fission product. The neutron-deficient barium isotope has a quite different, much broader, differential range distribution (CUMMING [13]).

From these experimental findings one can conclude:

(i) Neutron-excess isotopes are produced in a fission process. There seems to be no drastic difference in the fission process itself whether a low-energy or high-energy proton initiates such a process in a uranium nucleus. (One could go one step further and speculate that the fission pro-

cess is connected with low-momentum transfer reactions of the high-energy proton to the uranium nucleus, i.e. where the total excitation energy of the nucleus after the so-called fast cascade is much smaller than the total binding energy of the nucleus.)

(ii) The neutron-deficient isotopes mentioned above are produced not in a fission process, but by some other process.

Before one turns to the last question, i.e. what kind of process might yield these neutron-deficient isotopes, it seems useful to re-define some terms:

(i) A fission product is formed in a process similar to the slow neutron-induced fission process for which this kind of reaction was observed first. An essential part is statistical equilibrium in the nucleus (compound nucleus) before it starts to separate into its two roughly equal parts.

(ii) A spallation product is formed in a high-energy reaction where the fast cascade process is clearly separated in time from the slow de-excitation of the residual nucleus (SERBER model [14]). For historical and practical purposes a fission product is not considered a spallation product.

(iii) A fragmentation product is formed in a high-energy reaction of such a kind that the fast cascade process and the following nuclear de-excitation cannot be separated in time. This definition was originally proposed by WOLFGANG et al. [15]. It obviously suffers from not being connected with a clear theoretical model to explain this process. However, recent experiments [Na^{24} from Bi^{16}] have proved unambiguously the existence of fragmentation products in the sense defined above.

Using the given set of definitions, it is obvious that these neutron-deficient isotopes must be either spallation or fragmentation products. The only way to decide this question is to investigate whether they are formed in a two-step process or not. Results of experiments of this kind have not been published, so that it is impossible to decide this problem now. However, it might be interesting to note that experiments of this kind are in progress elsewhere, and that preliminary results seem to indicate that these neutron-deficient isotopes might be fragmentation products (CUMMING [13]).

Finally, however, it should be noted that it is premature to put too much emphasis on definitions since we do not yet know sufficient experimental facts.

ACKNOWLEDGEMENTS

Experiments of the kind reported here can only be carried out with the help of many people. It is a pleasure to acknowledge the help of Dr. G. Rudstam, who supplied the data for iodine in uranium, all computer programmes for data analysis, and initiated many stimulating discussions. S. Sundell, G. Droz and Mrs. R. Mohr helped in the experiments. Dr. J.B. Cumming kindly allowed his data to be used before publication. The co-operation of and discussions with all other members of the Nuclear Chemistry Group are also acknowledged.

REFERENCES

[1] ALEXANDER, J.M., BALTZINGER, C. and GAZDIK, M.F., Phys. Rev. 129 (1963) 1826.

[2] FRIEDLANDER, G., FRIEDMAN, L., GORDON, B. and YAFFE, L., Phys. Rev. 129 (1963) 1809.

[3] ANDERSON, G., HEDIN, B. and RUDSTAM, G., Nucl. Instrum. Meth. 28 (1964) 245; RUDSTAM, G., SUNDELL, S. and ANDERSON, G., ibid. 255; ANDERSON, G. and RUDSTAM, G., ibid. 29 (1964) 93.

[4] CUMMING, J.B., HUDIS, J., POSKANZER, A.M. and KAUFMANN, S., Phys.Rev. 128 (1962) 2392.

[5] RUDSTAM, G., "Fission yields in the iodine region", these Proceedings II.

[6] GOEBEL, K., SCHULTES, H. and ZÄHRINGER, Z., CERN Rpt. 64-12 (1964).

[7] BRANDT, R., GFELLER, Ch., ZAKRZEWSKI, J., CERN Rpt. 64-49 (1964).

[8] CUMMING, J.B., Ann.Rev. nucl. Sci. 13 (1963) 282.

[9] GFELLER, Ch. et al., to be published.

[10] STEHNEY, A.F. and SUGARMAN, N., J.chem.Phys. 20 (1952) 629.

[11] HAGEBØ, E., CERN, private communication.
HAGEBØ E., PAPPAS, A.C. and AAGARD, P., J.inorg.nucl.Chem. 26 (1964) 1639.

[12] PANONTIN, J.A. and SUGARMAN, N., J.inorg.nucl.Chem. 25 (1963) 1321.

[13] CUMMING, J.B., Brookhaven National Laboratory, private communication.

[14] SERBER, R., Phys.Rev. 72 (1947) 1114.

[15] WOLFGANG, R., BAKER, E.M., CARETTE, A.A., CUMMING, J.B., FRIEDLANDER, G. and HUDIS, J., Phys.Rev. 103 (1956) 394.

[16] CUMMING, J.B., CROSS, R.J., Jr., HUDIS, J. and POSKANZER, A.M., Phys.Rev. 134 (1964) B167.

ANGULAR DISTRIBUTIONS OF U^{238} FISSION FRAGMENTS PRODUCED BY MONO-ENERGETIC GAMMA RAYS

H. G. DE CARVALHO
CENTRO BRASILEIRO DE PESQUISAS FÍSICAS,
RIO DE JANEIRO, BRAZIL
A. G. DA SILVA AND R. N. ALVES
INSTITUTO DE ENGENHARIA NUCLEAR,
RIO DE JANEIRO, BRAZIL
R. BÖSCH AND W. WÖLFLI,
LABORATORIUM FÜR KERNPHYSIK,
EIDG. TECH. HOCHSCHULE, ZÜRICH, SWITZERLAND

Abstract — Résumé — Аннотация — Resumen

ANGULAR DISTRIBUTIONS OF U^{238} FISSION FRAGMENTS PRODUCED BY MONO-ENERGETIC GAMMA RAYS. The angular distribution of U^{238} fission fragments has been measured using mica plates as detectors. The fission process was induced by mono-energetic gamma rays of the following discrete energies: 6.07, 6.75, 6.80, 7.38, 7.64, 7.73 and 9.00 MeV.

The sources of mono-energetic gamma-rays were (n, γ) reactions on seven different target elements in the SAPHIR reactor of the E.T.H. in Zurich. The gamma-ray line absolute intensities were of the order of 10^6 photons/cm² s. The neutron and gamma-ray backgrounds were estimated with a bismuth target.

DISTRIBUTION ANGULAIRE DES FRAGMENTS DE LA FISSION DE ^{238}U PAR RAYONS GAMMA MONO-ÉNERGÉTIQUES. Les auteurs ont mesuré la distribution des fragments de la fission de ^{238}U en utilisant des feuilles de mica comme détecteurs. Le processus de fission était provoqué par des rayons gamma monoénergétiques ayant les énergies discrètes suivantes: 6,07, 6,75, 6,80, 7,38, 7,64, 7,73 et 9,00 MeV.

Les sources de rayons gamma monoénergétiques étaient constituées par des réactions (n, γ) sur sept matériaux cibles différents placés à l'intérieur du réacteur SAPHIR de l'Ecole polytechnique fédérale à Zurich. Les intensités absolues des raies gamma étaient de l'ordre de 10^6 photons/cm² s. Le bruit de fond dû aux neutrons et aux rayons gamma a été évalué au moyen d'une cible de bismuth.

УГЛОВОЕ РАСПРЕДЕЛЕНИЕ ОСКОЛКОВ ДЕЛЕНИЯ УРАНА-238 ПОД ДЕЙСТВИЕМ МОНОЭНЕРГЕТИЧЕСКИХ ГАММА-ЛУЧЕЙ. Измерялось угловое распределение осколков деления урана-238 с использованием пластинок слюды в качестве детекторов. Процесс деления вызывался моноэнергетическими гамма-лучами следующих дискретных энергий: 6,07; 6,75; 6,80; 7,38; 7,64; 7,73 и 9,00 Мэв.

Источником моноэнергетических гамма-лучей были реакции (n, γ) на семи различных элементах мишени в реакторе "Сапфир" Высшего технического института в Цюрихе. Абсолютные интенсивности линии гамма-лучей составляли величину порядка 10^6 фотонов/см² в сек. Фон нейтронов и гамма-лучей оценивался с помощью висмутовой мишени.

DISTRIBUCION ANGULAR DE LOS FRAGMENTOS DE LA FISION DEL ^{238}U INDUCIDA POR RAYOS GAMMA MONOENERGETICOS. Se ha medido la distribución angular de los fragmentos de fisión del ^{238}U utilizando placas de mica como detectores. El proceso de fisión se indujo con rayos gamma monoenergéticos de las siguientes energías discretas: 6,07, 6,75, 6,80, 7,38, 7,64, 7,73, y 9,00 MeV.

Los rayos gamma monoenergéticos provenían de las reacciones (n, γ) en siete elementos diferentes utilizados como blanco en el reactor Saphir de la Escuela Politécnica Federal de Zurich. Las intensidades absolutas de las líneas gamma fueron del orden de 10^6 fotones/cm².s. La actividad de fondo (neutrones y rayos gamma) se midió con un blanco de Bi.

The angular distributions of fission fragments from the photofission of uranium by mono-energetic gamma rays were measured at three different energies.

The present experiment was made possible by using two recently developed techniques, i.e. the use of a nuclear reactor as a source of nearly mono-energetic gamma rays and the development by PRICE and WALKER [1], of a method that uses mica as a specific fission fragment detector.

The source of highly collimated mono-energetic gamma rays was obtained, through (n, γ) reaction, by placing suitable target elements in a transversal channel of the 1-MW SAPHIR reactor in Würenlingen, Switzerland. Details of the experimental arrangement have been published elsewhere [2, 3]. The gamma-ray line absolute intensities were of about 10^6 photons/cm^2 · s and the total integrated dose was of the order of 2×10^{10} photons/cm^2. The neutron and gamma-ray background was estimated by a bismuth target, used as a blank, to produce less than 10% of the total number of tracks in the case of the aluminium target. For yttrium and nickel targets the contribution of background was smaller than 5% and 1% respectively. Targets of yttrium, aluminium and nickel produced gamma-ray lines of energies 6.07, 7.73 and 9.00 MeV respectively, which are known to an accuracy of ± 10 keV.

Mica can be used as a specific fission-fragment detector with great advantage over nuclear emulsion since mica does not record low Z-particles ($Z < 20$). Furthermore it is free from distortions and can be exposed to a very high dose of gamma radiation without any ill effects.

Some preliminary experiments were performed to check the reliability of the measurements of angular distribution using plates in which the fission-fragment tracks were known to have an isotropic angular distribution. The measured distribution of tracks as a function of the projected angle was found to be isotropic within statistical errors. However, the distribution of tracks per unit solid angle as a function of the angle of dip was found to show a curious result as indicated in Fig. 1. As can be seen from this figure, the combination of scanner visual acuity and recording and/or "fading" properties of mica, distorts the distribution that should have been isotropic. For this reason only tracks with dip angles between 15° and 45° were used in the present measurements. It is worthwhile to point out that this effect was observed for all the scanners and may cause systematic errors.

The anisotropy parameters b/a in the equation

$$w(\theta) = 1 + \frac{b}{a} \sin^2 \theta$$

were calculated from the track distribution of the projected angle.

The experimental data for Y are shown in Fig. 2. The curve through the points represents a function that was fitted to the data by the least-squares method.

Values of the anisotropy parameter for mono-energetic gamma rays, calculated by the least-squares method, are shown in Table I.

Figure 3 shows the values of b/a obtained with mono-energetic gamma rays by DE CARVALHO et al. [3] and by FORKMAN and JOHANSON [4], together with the average values of b/a for 0.5-MeV intervals calculated

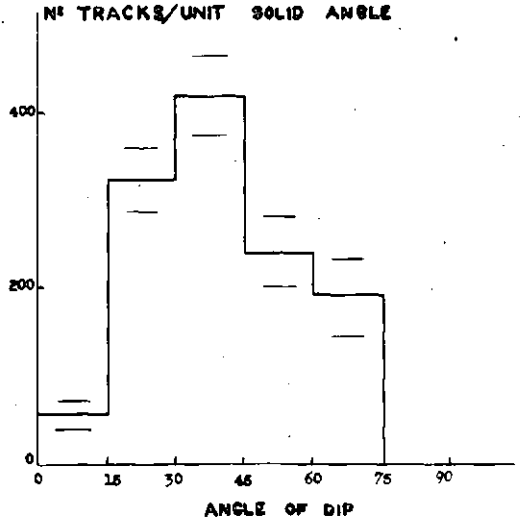

Fig. 1

Frequency distribution of fragment tracks from thermal-neutron fission of U^{235} as a function of the dip angle (beta)

TABLE I

VALUES OF THE ANISOTROPY PARAMETER FOR MONO-ENERGETIC GAMMA RAYS

Target	Energy (MeV)	b/a
Y	6.07	12±9
Al	7.72	0.7±0.4
Ni	9.00	0.7±0.2

from the bremsstrahlung data of BAERG [5] using the photon difference method [6] and the preliminary results of the present work.

These results indicate that near the fission threshold the anisotropy parameter decreases very rapidly with increasing energy and above 7.7 MeV the anisotropy becomes negligible in accordance with the theory of A. Bohr.

It would be interesting to investigate the angular distributions at energies below and in the neighbourhood of 6 MeV where the anisotropy may be smaller than at 6.07.

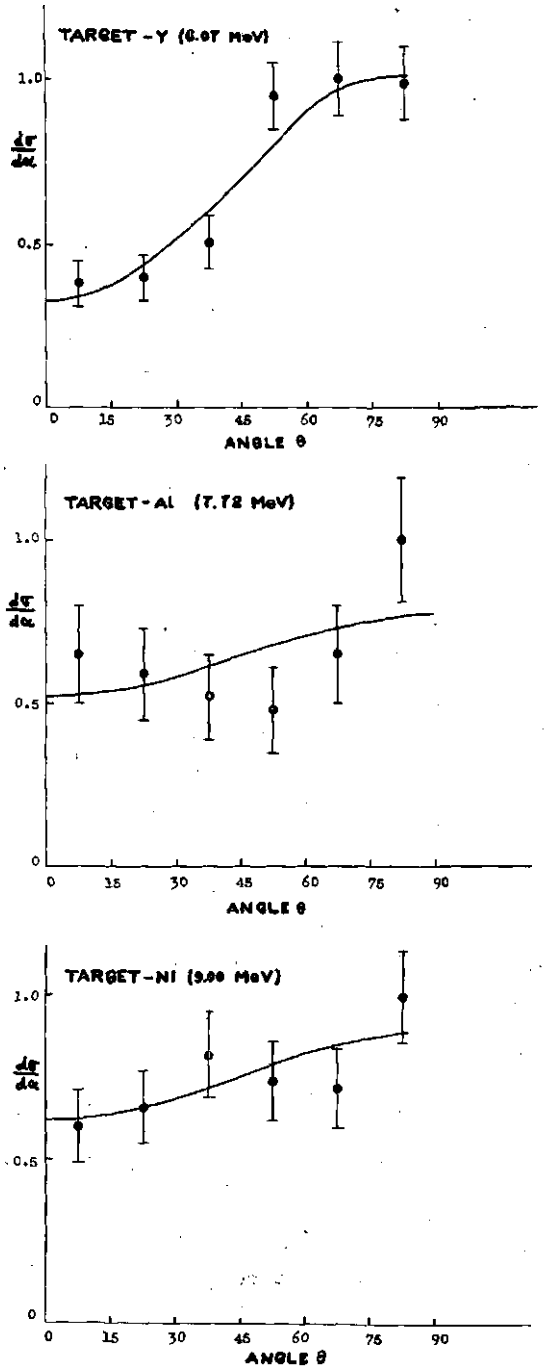

Fig. 2

Angular distributions w(θ, 15 < dip angles < 45) of photofission fragments from U^{238} for mono-energetic gamma-ray energies of 6.07, 7.72 and 9.00 MeV

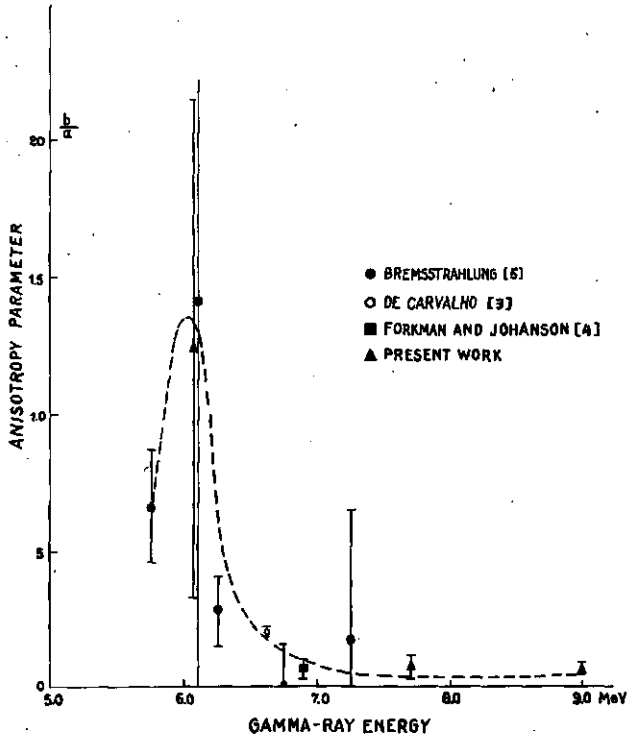

Fig. 3

Anisotropy parameter (b/a) as a function of the gamma-ray energy

ACKNOWLEDGEMENTS

We are grateful to L. T. Auler, M. Grinberg and Miss E. J. Schumacher for help in the preparation of this paper. We are indebted to the staff of the SAPHIR reactor for helping with the exposure and to the staff of the Instituto de Energia Atômica for exposures to slow neutrons. Thanks are also due to the Conselho Nacional de Pesquisas and the Comissão Nacional de Energie Nuclear for providing funds.

REFERENCES

[1] PRICE, P. B. and WALKER, R. M., Phys. Lett. 3 (1962) 113.

[2] JARCZIK, J., KNÖPFELL, H., LANG, J., MÜLLER, R. and WÖLFLI, W., Nucl. Instrum. Meth. 13 (1961) 287.

[3] DE CARVALHO, H. G., MANFREDINI, A., MUCHNIK, M., SEVERI, M., BÖSCH, R. and WÖLFLI, W., Nuovo Cim. 29 (1963) 463.

[4] FORKMAN, B. and JOHANSON, S. A. E., Nucl. Phys. 20 (1960) 136.

[5] BAERG, A. P., BARTHOLOMEW, R. M., BROWN, F., KATZ, L. and KOWALSKI, S. B., Canad. J. Phys. 37 (1959) 1418.

[6] KATZ, L. and CAMERON, A. G., Canad. J. Phys. 29 (1951) 518.

[7] GOLDEMBERG, J., private communication.

APPENDIX

VALUES OF THE AVERAGE PHOTOFISSION CROSS-SECTIONS FOR THE ENERGY INTERVALS SHOWN

E (MeV)	$\bar{\sigma}$ [a]	(b/a) [b]
5.5 - 6.0	3.0	6.6 ± 2.0
6.0 - 6.5	5.0	4.4 ± 1.0
6.5 - 7.0	6.0	2.05 ± 0.24
7.0 - 7.5	7.0	1.72 ± 0.17

[a] $\bar{\sigma}$ average photofission cross-section in millibarns

[b] b/a obtained with bremsstrahlung

THE BREMSSTRAHLUNG SPECTRUM P(E, E_0) [7] FOR 0.5-MeV INTERVALS

E_0	E_0 - 0.25				
	5.75	6.25	6.75	7.25	7.75
5.75	6.80	13.90	17.90	20.40	22.11
6.25		5.70	11.95	15.45	17.70
6.75			4.80	10.30	13.35
7.25				4.10	9.10
7.75					3.50

СЕЧЕНИЯ ДЕЛЕНИЯ Ta^{181}, Re, Pt, Au^{197}, Pb, Bi^{209}, Th^{232}, U^{235} И U^{238} ПРОТОНАМИ С ЭНЕРГИЕЙ 150–660 Мэв*

В.А. КОНЬШИН, Е.С. МАТУСЕВИЧ и В.И. РЕГУШЕВСКИЙ
ФИЗИКО-ЭНЕРГЕТИЧЕСКИЙ ИНСТИТУТ, ОБНИНСК
СССР

Abstract — Résumé — Аннотация — Resumen

FISSION CROSS-SECTIONS OF Ta^{181}, Re, Pt, Au^{197}, Pb, Bi, Th, U^{235} AND U^{238} FOR PROTONS WITH AN ENERGY OF 150-660 MeV. The measurements were carried out on the synchrocyclotron of the Joint Institute for Nuclear Research, with a maximum proton energy of 660 MeV. The fission events were recorded by visual observation of the fission-fragment tracks left on glass after treating. The absolute recording efficiency was determined by the number of U^{235} and Pu^{239} fissions in a known thermal-neutron flux, and the number of U^{235} fissions in a neutron flux from a Ra-α-Be standard source. The proton flux was determined by measuring the absolute number of β-disintegrations of Na^{24} occurring in the Al^{27} (p, 3pn) Na^{24} reaction (whose cross-section is known with an accuracy of ± 5%), using a scintillation gamma-spectrometer. Samples were irradiated both in an external proton beam and within the chamber of the synchrocyclotron. The fission cross-sections were measured in the proton energy range 150-660 MeV. The corrections applied are discussed. The results of the measurements are compared with earlier figures, and the dependence of fissility of the nuclei investigated on the parameter Z^2/A is determined.

SECTIONS EFFICACES DE FISSION DE ^{181}Ta, Re, Pt, ^{197}Au, Pb, Bi, Th, ^{235}U et ^{238}U PAR DES PROTONS DE 150 A 660 MeV. Les mesures ont été faites sur le synchrocyclotron de l'Institut unifié de recherches nucléaires, à l'aide de protons d'une énergie maximale de 660 MeV. Pour enregistrer les événements de fission, on a examiné visuellement les traces des fragments de fission apparaissant sur le verre après traitement. L'efficacité absolue de l'enregistrement était déterminée par le nombre de fissions de ^{235}U et ^{239}Pu dans un flux de neutrons thermiques connu et de ^{238}U dans un flux de neutrons provenant d'une source étalonnée Ra-Be. Quant au flux de protons, on l'a établi en mesurant, à l'aide d'un spectromètre gamma à scintillation, le nombre absolu des désintégrations bêta de ^{24}Na qui se produisent au cours de la réaction ^{27}Al(p, 3pn) ^{24}Na (dont la section efficace est connue avec une précision de ± 5%). L'irradiation des échantillons se faisait au moyen d'un faisceau de protons aussi bien à l'extérieur qu'à l'intérieur de la chambre du synchrocyclotron. Les sections efficaces de fission ont été mesurées pour une énergie des protons allant de 150 à 660 MeV. Les corrections apportées font l'objet d'une discussion. Les auteurs comparent les résultats des mesures aux valeurs obtenues antérieurement; ils établissent la relation de dépendance entre la fissibilité des noyaux étudiés et le paramètre Z^2/A.

СЕЧЕНИЯ ДЕЛЕНИЯ Ta^{181}, Re, Pt, Au^{197}, Pb, Bi^{209}, Th^{232}, U^{235} и U^{238} ПРОТОНАМИ С ЭНЕРГИЕЙ 150–660 Мэв. Измерения проводились на синхроциклотроне ОИЯИ с максимальной энергией протонов 660 Мэв. Регистрация актов деления осуществлялась с помощью визуального просмотра следов осколков деления, возникающих в стеклах после протравливания. Абсолютная эффективность регистрации осколков определялась по числу делений U^{235} и Pu^{239} в известном тепловом потоке нейтронов и U^{238} в потоке нейтронов от эталонного источника Ra-α-Be. Поток протонов определялся измерением абсолютного числа β-распадов Na^{24}, возникающего в реакции Al^{27} (p,3 pn) Na^{24} (сечение которой известно с точностью ±5%), с помощью сцинтилляционного гамма-спектрометра. Облучение образцов проводилось как на выведенном пучке протонов, так и внутри камеры синхроциклотрона. Сечения деления измерены в интервале энергией протонов 150–660 Мэв. В работе обсуждаются введенные поправки. Результаты измерений сравниваются с более ранними измерениями; получена зависимость делимости исследованных ядер от параметра Z^2/A.

SECCIONES EFICACES DEL ^{181}Ta, Re, Pt, ^{197}Au, Pb, Bi, Th, ^{235}U y ^{238}U, POR PROTONES DE 150 A 660 MeV. Las mediciones se efectuaron en un sincrociclotrón, con protones de $E_{máx}$ = 660 MeV. Los sucesos de fisión se registraron por observación visual de las trazas de los fragmentos de fisión que aparecían en las placas

* На симпозиуме зачитано только название доклада.

después de su tratamiento. La eficacia absoluta de registro de los fragmentos se determinó según el número de fisiones del ^{235}U y ^{239}Pu en un flujo conocido de neutrones térmicos, y según el número de fisiones del ^{238}U en el flujo neutrónico emitido por una fuente patrón de Ra-α-Be. El flujo protónico se determinó por medición del número absoluto de desintegraciones β en el ^{24}Na formado en virtud de la reacción $^{27}Al(p, 3pn)^{24}Na$ (cuya sección eficaz se conoce con una precisión de ± 5%) con ayuda de un espectrómetro gamma de centelleo. Las muestras se irradiaron en un flujo protónico exterior y dentro de la cámara del sincrociclotrón. Las secciones eficaces de fisión se midieron en el intervalo de energía de los protones comprendido entre 150 y 660 MeV. En la memoria se examinan las correcciones introducidas. Los resultados de las mediciones se comparan con los de otras efectuadas anteriormente y se determina la variación de la capacidad de fisión de los núcleos investigados en función del parámetro Z^2/A.

Разработка метода регистрации осколков деления с помощью стекол [2], [3] позволила провести измерения внутри камеры синхроциклотрона на различных радиусах и тем самым получить зависимость сечений деления от энергий протонов на ускорителях без вариации энергии. Таким способом на синхроциклотроне ОИЯИ были измерены σ_f в интервале энергий протонов 150–660 Мэв. Точность определения энергии протона ±5 Мэв.

При облучении слой исследуемых элементов касались поверхности стекла. Порог регистрации осколков деления, вообще говоря, зависит как от толщины слоя, так и от распределения осколков по массам и энергиям. Оценки, проведенные согласно данным работ [3–5], показали, что порог регистрации осколков порядка 20–25 Мэв, причем для масс осколков >90 порог регистрации практически не зависит от массы и энергии осколка. Слой исследуемого элемента помещался между двумя стеклами, и число следов определялось в обоих.

Измерения проводились как с толстыми, так и с тонкими (<1 мг/см^2) слоями. Для U^{238}, Bi и Au была получена зависимость эффективности регистрации от толщины слоев. Слои Pt, Re и Ta были толстыми (>пробега осколка в материале слоя). Зависимости эффективности регистрации от толщины, полученные для Bi и Au были проэкстраполированы для Pt, Re и Ta с учетом экспериментально определенных величин пробегов осколков в [5].

Поток протонов мониторировался по измерению числа γ-квантов с энергией 1,38 и 2,76 Мэв, сопровождающих β-распад Na^{24}, возникающего в реакции $Al^{27}(p,3pn)Na^{24}$. Размер алюминиевой пластинки всегда был равен размеру слоя и стекла.

Для определения абсолютных значений сечений всех элементов было использовано как "опорное" сечение деления U^{238}, измеренное Стевенсоном и др. [1]. Согласно их измерениям, $\sigma_f(U^{238})$ в интервале энергий протонов от 50 до 300 Мэв постоянно с точностью ±4%. Нами было принято значение $\sigma_f(U^{238})$ равным $(1,46 \pm 0,06) \cdot 10^{-24}$ см^2 при Ep = 280 Мэв.

Ошибки в сечениях определялись как среднеквадратичные из следующих ошибок:

1. Ошибки в "опорном" сечении ±4%.
2. Статистической ошибки в определении числа зарегистрированных актов деления 3%.
3. Ошибки в определении толщин слоев 2–4%.
4. Ошибки в монтировании потока протонов 1–4%.
5. Ошибки, связанной с определением эффективности регистрации для толстых слоев Pt, Re и Ta 2–5%.

СЕЧЕНИЯ ДЕЛЕНИЯ σ_f ПРОТОНАМИ (10^{-27} см^2)

Энергия протонов, Мэв	Элементы								
	U^{238}	U^{235}	Th^{232}	Bi^{209}	Pb	Au^{197}	Pt	Re	Ta^{181}
150	-	1850 ± 220	950 ± 110	103 ± 12	46 ± 6	16,5 ± 2,5	7,7 ± 1,2	1,7 ± 0,3	-
280	1460 ± 60	-	840 ± 70	166 ± 11	106 ± 11	46 ± 6	25 ± 3	6,9 ± 0,9	2,6 ± 0,4
390	1340 ± 80	1450 ± 150	770 ± 15	170 ± 15	130 ± 15	61 ± 8	32 ± 4	8,1 ± 1,1	4,7 ± 0,7
480	1270 ± 80	1340 ± 134	740 ± 80	214 ± 20	-	74 ± 10	37 ± 5	14,7 ± 2,0	8,3 ± 1,1
564	-	-	-	219 ± 20	-	-	-	14,1 ± 1,9	10,1 ± 1,4
660	1040 ± 75	1340 ± 134	670 ± 70	218 ± 20	121 ± 20	75 ± 9	47 ± 6	20,5 ± 2,8	14,0 ± 1,9

Примечание: Pb, Pt и Re — естественная смесь изотопов.

6. Ошибки, связанной с энергетической зависимостью сечения мониторной реакции 1–4%.

Результаты измерений сведены в таблицу.

Измеренные в настоящей работе σ_f находятся в хорошем согласии с опубликованными в последние годы данными других авторов по сечениям деления Au^{197}, Bi^{209}, Th^{232}.

Заметим, что величина порога регистрации осколков 20–25 Мэв достаточна для уверенной дискриминации актов деления от актов фрагментации ядер с массой ≥ 209, если учесть распределение осколков по массам и энергиям [6]. Для элементов легче свинца определенный вклад в измеренное сечение могут дать продукты фрагментации. Оценки этого эффекта для Та по [7] приводят к сечению фрагментации (0,05–0,15) σ_f.

Измеренные σ_f лишь при энергии 660 Мэв хорошо согласуются с эмпирической зависимостью делимости σ_f/σ_a от Z^2/A, предложенной Н.А. Перфиловым и др.

В заключение авторы считают своим приятным долгом выразить благодарность А.С. Солдатову и В.П. Перелыгину за помощь в освоении методики, и С. Покровскому за абсолютную калибровку счетчика.

ЛИТЕРАТУРА

[1] STEVENSON P.S., HICKS H.G., NERVIK W.E. and NETHAWAY D.R. Phys. Rev. 111 (1958) 886.
[2] FLEISCHER R.L., PRICE P.B. J. Appl. Phys., 34 (1963) 2903.
[3] ПЕРЕЛЫГИН В.П., ТРЕТЬЯКОВА С.П., ЗВАРА И. ПТЭ. 4 (1964) 78, и КАПУСЦИК А. и др. ПТЭ. 5 (1964) 72.
[4] FULMER C.B. Phys. Rev. 108 (1957) 1115.
[5] NORBERT T., PORILE and SUGARMAN NATHAN, Phys. Rev. 107 (1957) 1410.
[6] HALPERN I., Annual Review of Nuclear Science, 9 (1959) 245.
[7] NERVIK W.F., SEABORG G.T., Phys. Rev. 97 (1955) 1092.

LIGHT PARTICLES EMITTED IN FISSION: TERNARY FISSION

(Session IX)

VARIATION OF FISSION-FRAGMENT KINETIC ENERGY DISTRIBUTION, MASS DISTRIBUTION, AND YIELD OF LONG-RANGE ALPHA PARTICLES IN THE RESONANCE-NEUTRON-INDUCED FISSION OF U^{235} AND Pu^{239} *

E. MELKONIAN AND G. K. MEHTA
COLUMBIA UNIVERSITY, NEW YORK, N. Y.
UNITED STATES OF AMERICA

Abstract — Résumé — Аннотация — Resumen

VARIATION OF FISSION-FRAGMENT KINETIC ENERGY DISTRIBUTION, MASS DISTRIBUTION, AND YIELD OF LONG-RANGE ALPHA PARTICLES IN THE RESONANCE-NEUTRON-INDUCED FISSION OF U^{235} AND Pu^{239}. These measurements were undertaken to obtain additional information on the fission process, and to investigate the application of this information to the assignment of J-values to resonance levels, as the usual methods of determining J-values are of limited applicability in the case of fissile isotopes. An earlier study of U^{235} showed that the fission-fragment kinetic energy and the alpha yield varied significantly from level to level, and fell into two groups suggestive of the two possible J-values.

The present paper reports on measurements on Pu^{239}. A study of 19 levels shows 15 levels with high average kinetic energy and 4 levels with low average kinetic energy, the former being assigned J = 1 and the latter J = 0 on the basis of the expected ratio of population of the two spin states and also for maximum compatibility with other determinations. Some variation of relative alpha-particle yield was found. It is concluded that (1) there are definite variations of kinetic energy of the fragments from level to level; (2) the variation in the case of U^{235} is correlated with the relative yield of symmetric fission; (3) there is some indication in the case of Pu^{239} that the variation of fragment energy is correlated with the J-values; and (4) the relative yield of alpha particles varies in an expected fashion.

VARIATION DES DISTRIBUTIONS SELON L'ÉNERGIE CINÉTIQUE ET LA MASSE ET DU RENDEMENT EN PARTICULES ALPHA A LONG PARCOURS DES FRAGMENTS DE LA FISSION DE ^{235}U ET DE ^{239}Pu PAR DES NEUTRONS DE RÉSONANCE. Les mesures dont le mémoire rend compte ont été faites pour obtenir de nouvelles données sur le processus de fission, et pour étudier l'application de ces données à la détermination des valeurs de J relatives aux niveaux de résonance, étant donné que les méthodes habituellement employées pour déterminer les valeurs de J sont d'une utilité limitée dans le cas des produits fissiles. Une étude antérieure des mêmes auteurs sur ^{235}U a montré que l'énergie cinétique des fragments de fission et le rendement en particules alpha variaient sensiblement d'un niveau à l'autre et se répartissaient en deux groupes, ce qui suggère deux valeurs possibles de J.

Le mémoire fait état de mesures portant sur ^{239}Pu. Il ressort de l'étude de 19 niveaux que, pour 15 niveaux, l'énergie cinétique moyenne est élevée et qu'elle est basse pour quatre niveaux, la valeur J = 1 étant assignée à la première et la valeur J = 0 à la seconde sur la base des rapports attendus de population des deux états de spin et en vue d'une comptabilité maximum avec d'autres déterminations. Les auteurs ont constaté que le rendement relatif en particules alpha variait dans une certaine mesure. Ils ont conclu: 1. qu'il y a des variations d'énergie cinétique définies pour les fragments d'un niveau à l'autre; 2. que, dans le cas de ^{235}U, il y a une corrélation entre la variation et le rendement relatif de fission symétrique; 3. que, dans le cas de ^{239}Pu, il semble y avoir des indices d'une corrélation entre la variation de l'énergie des fragments et les valeurs de J; 4. que le rendement relatif en particules alpha varie comme prévu.

* This work was supported by the United States Atomic Energy Commission.

ВАРИАЦИЯ РАСПРЕДЕЛЕНИЯ КИНЕТИЧЕСКОЙ ЭНЕРГИИ ОСКОЛКОВ ДЕЛЕНИЯ, РАСПРЕДЕЛЕНИЯ МАСС И ВЫХОДА АЛЬФА-ЧАСТИЦ БОЛЬШОЙ ДЛИНЫ ПРОБЕГА ПРИ РЕЗОНАНСНОМ ДЕЛЕНИИ УРАНА-235 И ПЛУТОНИЯ-239 ПОД ДЕЙСТВИЕМ НЕЙТРОНОВ.

Измерения были предприняты с целью получения дополнительной информации о процессе деления и для исследования возможности применения полученной информации к определению величины J при резонансных уровнях, поскольку обычные методы определения величины J имеют ограниченное применение в отношении делящихся изотопов. Более раннее исследование по урану-235 показало, что кинетическая энергия осколков деления и выход альфа-частиц значительно менялись в зависимости от уровней и распадались на две группы, что говорит о двух возможных величинах J.

В данном докладе сообщается об измерениях, связанных с плутонием-239. Изучение 19 уровней показывает, что 15 уровней имеют высокую среднюю кинетическую энергию и 4 уровня – низкую среднюю кинетическую энергию; первое объясняется в рамках J = 1, а второе когда J = 0 на основе предполагаемого коэффициента размножения обоих спиновых состояний, а также при максимальной совместимости с другими определениями. Было обнаружено некоторое изменение относительных альфа-частиц. Делается вывод, что 1) имеют место конечные изменения кинетической энергии вместе с осколками от одного уровня к другому, 2) изменение в случае с ураном-235 связано с относительным выходом симметричного деления, 3) имеется определенное указание в случае использования плутония-239, что изменение энергии осколков связано с J-значениями, и 4) относительный выход альфа-частиц изменяется в предполагаемых размерах.

FISION DEL ^{235}U Y DEL ^{239}Pu INDUCIDA POR NEUTRONES DE RESONANCIA: VARIACION DE LA DISTRIBUCION DE LA ENERGIA CINETICA DE LOS FRAGMENTOS DE FISION Y DE LAS MASAS Y RENDIMIENTO DE HELIONES DE GRAN ALCANCE. Las mediciones efectuadas por los autores tenían por objeto proporcionar datos complementarios sobre el proceso de fisión, así como investigar la aplicación de esos datos a la asignación de valores J a los niveles de resonancia, ya que los métodos usuales para la determinación de valores de J son de aplicación limitada en el caso de los isótopos fisionables. Un estudio del ^{235}U realizado previamente puso de manifiesto que la energía cinética de los fragmentos de fisión y el rendimiento alfa variaban considerablemente de un nivel a otro, quedando comprendidos en dos grupos que sugerían los dos valores posibles de J.

En la memoria se exponen las mediciones efectuadas relativas al ^{239}Pu. Se han estudiado 19 niveles, hallándose que la energía cinética media de 15 de ellos es elevada, mientras que la de los cuatro restantes es reducida; cuenta habida de la razón prevista de población de los dos estados de spin, y a fin de facilitar al máximo la compatibilidad con otras determinaciones, se ha asignado a los primeros el valor J = 1, y a los últimos el valor J = 0. Se ha observado cierta variación del rendimiento alfa relativo. Las conclusiones son: a) la energía cinética de los fragmentos varía netamente de un nivel a otro; b) en el caso del ^{235}U, esta variación guarda una correlación con el rendimiento relativo de la fisión simétrica; c) en el caso del ^{239}Pu hay indicios de que la variación de la energía de los fragmentos está correlacionada con los valores J; d) el rendimiento alfa relativo varía conforme a lo previsto.

INTRODUCTION

These measurements are part of a larger programme undertaken to obtain additional detailed information on the fission process. The motivation for the present measurements is the search for methods of determining J-values of resonance levels of the fissile isotopes. All nuclei having non-zero spin (I) can form, with the addition of an S-wave neutron, compound nuclei with two possible values of angular momentum, denoted by $J = I \pm \frac{1}{2}$. For example, U^{235}, with a nuclear spin of $7/2^-$, can form a compound nucleus with $J = 3^-$ or $J = 4^-$, and Pu^{239} with a nuclear spin of $\frac{1}{2}^+$ can form a compound nucleus with $J = 0^+$ or $J = 1^+$. Two basic methods of determining J values have been available: measurement of the total cross-section of polarized nuclei with polarized neutrons; and measurement of the resonance scattering and the total cross-section at the resonance peak. The first is

limited to neutron energies at or near the thermal region. No application of this technique to fissile nuclides has yet been reported. Measurements of neutron resonance scattering have been successfully carried out on Pu^{239} [1], where spins have been assigned to eight levels. Although this method can be applied in principle to any fissile target, in practice the small amount of resonance scattering and large number of fast neutrons produced in fission make it very impractical. Therefore, it was desirable to look for a more practical method.

It was proposed by BOHR [2] that the nucleus at the saddle-point configuration should be cold, as the major part of its energy is bound in potential energy of deformation, and thus has a well-defined nuclear state similar to that of a nucleus at its equilibrium deformation. This would imply that the fission process is a few-channel process rather than the many-channel process that had previously been assumed. Thus, many of the characteristics of fission should be strongly influenced by the specific fission channel through which fission occurs. This proposal was followed by a suggestion from WHEELER [3] that the ratio of asymmetric to symmetric fission yields might depend upon the J-values of the resonances. This suggestion initiated a large number of experiments to study the shape of the mass-yield curve when fission is induced with neutrons of resonance energy. Radiochemical measurements did show differences in the ratio of asymmetric to symmetric fission for the few resonances studied [4], compared with the same ratio for thermal neutrons; the largest by far is a factor of five in the case of the 0.3-eV level of Pu^{239}. This measurement was confirmed by the Oak Ridge group [5] using a back-to-back fission chamber arrangement. For U^{235} the effect was only about 20%. All these measurements were confined to neutron energies of a few electron volts. The only extensive information on mass asymmetry is provided by COWAN et al. [6] for U^{235} from the "spinning-wheel" experiment, utilizing a nuclear bomb explosion as an intense neutron source. A rotating wheel faced with U^{235} was exposed to the neutrons from the explosion 290.5 m away and later analysed radiochemically. In this work a number of resonances were definitely assigned to two groups, one having a smaller and the other having a larger peak-to-valley ratio (asymmetric to symmetric fission ratio) than is observed in thermal fission of U^{235}. This grouping could correspond to two different spin states.

With the advent of solid-state detectors and the availability of high intensity neutron bursts from the Nevis synchrocyclotron, we first thought it might be feasible to observe the mass distribution for a large number of levels in the resonance region, using large arrays of detectors in a back-to-back fission chamber arrangement with the fissile isotope in between. However, it was found subsequently by other groups that solid-state detectors were not adequate for detecting the small changes expected for U^{235}. The reason for this arises from the fact that symmetric fission (which comprises the valley of the double-humped mass-distribution curve) is usually a very small fraction of the total number of events and any experimental distortions of the mass distribution fill in the valley and obscure the effect sought. Our subsequent efforts are based in part on the following considerations.

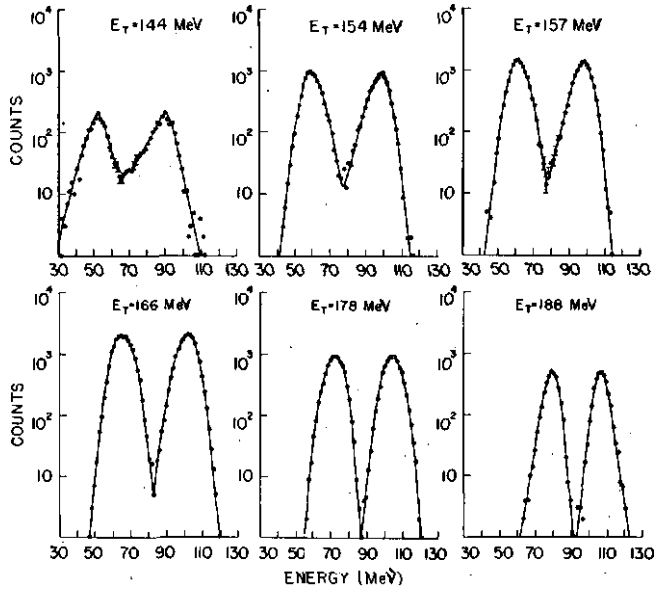

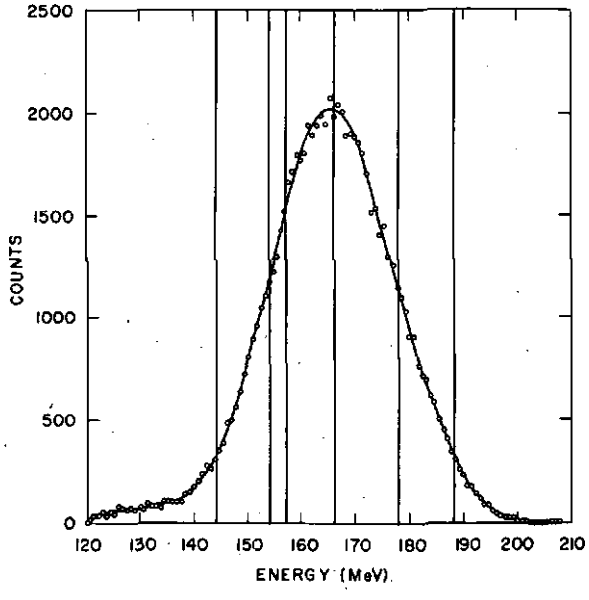

Fig. 1

Lower curve: total kinetic energy distribution of fission fragments from the thermal-neutron fission of U^{235}.
Upper curves: mass distributions of the fission fragments for several values of total fragment energy (E_T).
The abscissa is the fragment energy (E) that is proportional to mass through the relationship Mass = 236 E/E_T.
The data are taken from I. G. Schröder, J. A. Moore and G. F. Safford, Fission Fragment Mass Distribution, Columbia University Pegram Nuclear Physics Lab. Rpt. 208(1960).

Symmetric fission has frequently been considered to be a different mode of fission from asymmetric so that the relative proportion of the two modes may vary with the J-value. An alternative explanation of this variation, at low excitation energies, can be given without postulating two fission modes. If we examine the distribution of total kinetic energy (the sum of the kinetic energies of the two fragments) and the mass distribution of the fragments for various values of total kinetic energy, as shown in Fig. 1, we see that the widths of the mass distribution curves and the relative yield of symmetric fission increase with decreasing total kinetic energy. Thus the relative amount of symmetric fission appears to be correlated with the total kinetic energy distribution of fission fragments. For example, if the total kinetic energy distributions for the different J-values had the same shape but were slightly displaced from each other, the distribution of lower mean energy would have a larger contribution of low-energy fission and hence a higher proportion of symmetric fission. Also, the effects on the total kinetic energy distribution should be reflected in the single fragment kinetic energy distribution. Thus it appears that a measurement of some suitable property associated with the kinetic energy distribution should show a variation from resonance to resonance directly associated with variations in the mass distribution and presumably associated with the J-value of the resonance[1].

Since the change in kinetic energy was expected to be small, the effect was magnified in the earlier measurements [7] by comparing yields of fission fragments from thick with that from thin U^{235} foils. This follows from a consideration of the equation for the yield from a foil of thickness t

$$\text{yield} \sim t\left[1 - \frac{t}{2(R_0 - R_B)}\right]$$

where R_0 is the range of a fission fragment and R_B the range corresponding to the applied bias. For a thin foil, the second term is negligible and the yield is essentially independent of the energy of the fragment. For a thick foil, thicker than the maximum possible value of $(R_0 - R_B)$ the yield becomes

$$\text{yield} \sim (R_0 - R_B),$$

which increases with the increase in fragment energy. Physically, this means that the foil thicknesses are effectively larger for the higher energy fragments since they can come from deeper portions of the foil. Thus, in comparing (thick foil/thin foil) yields for two resonances for which the kinetic energy distributions are different, the ratios will be higher for those resonances with higher effective kinetic energy. This approach thus has the advantages that it enhances the differences in kinetic energy distribution, the use of a thick foil leads to much higher counting-rates, and the detectors do not have to be as good. The only difficulty of this method for U^{235} is that two different time-of-flight spectra have to be compared with the usual difficulty of determining the background. For Pu^{239} there are the additional

[1] These ideas were proposed by one of us (E. M.) at the Washington A. P. S. Meetings of 1963.

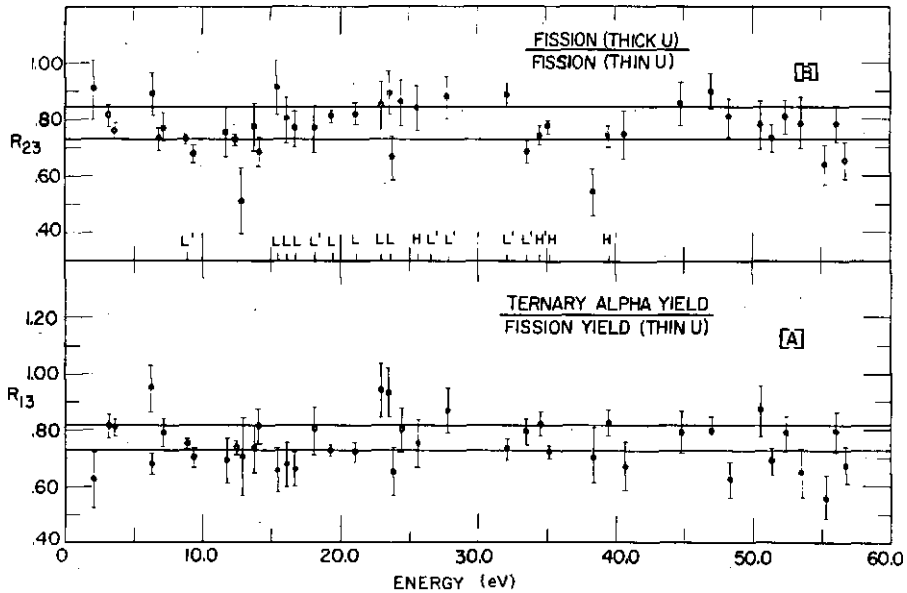

Fig. 2

Ratio of alpha-particle yield to thin uranium-fission yield (A) and the ratio of thick uranium-fission yield to thin uranium-fission yield (B). Both ratios are in arbitrary units. The assignments of COWAN et al. [17] are indicated by vertical lines with the letters H (or L) indicating high (or low) degree of symmetric fission. The primed letters indicate similar assignments with less certainty. The horizontal lines drawn are from a least-square fitting of the data to two ratios.

problems: suitably thick foils are difficult to prepare, and the natural alpha activity (along with that of the contaminants Pu^{240} and Pu^{241} that have much higher specific alpha activities) becomes intolerably high. Thus, in the present measurements, the less sensitive method of using a thin foil to determine average kinetic energies for the various resonances is used for Pu^{239}.

Our earlier (thick/thin) foil data on U^{235} are shown in Fig. 2. The data are incompatible with a single value of the ratio on the basis of a chi-square test, but are so compatible with two values of the ratio ~15% apart.

Comparison is made with the measurements of COWAN et al. [6]. In their results 4 levels showed an increase in symmetry and 13 levels showed a decrease in symmetry when compared with thermal-neutron fission. The assignments of Cowan et al. are marked with letters L and H (L, H meaning low- and high-symmetric fission respectively; primes denote uncertain assignments) in Fig. 2 for comparison. For direct comparison the ratio, R_{23} (= thick uranium yield/ thin uranium yield) and our assignments are also listed in Table II along with Cowan et al. assignments for the resonances studied by them. There are seven levels for which both groups (Cowan's and ours) obtained definite results and for these levels the grouping of levels into two classes is identical. According to the picture discussed in the

introduction, relative yield of symmetric fission increases with decreasing total energy. This effect of decrease in total energy will produce the effect of decrease in yield for thick uranium sample. Thus the increase in symmetric fission corresponds to a lower ratio of thick uranium to thin uranium fission in our case.

This agreement supports our semi-empirical picture in which each value of total kinetic-energy release implies a fairly definite relative symmetric mass yield, so that any variation in over-all relative symmetric mass yield must be related to variations in the total kinetic-energy distribution.

The initial measurements of the relative yield of alpha particles for the various resonances were undertaken in a purely explanatory fashion since no such variation at low energies had been observed. Since the alpha particles yield is low ($\sim$1 in 500 fissions) a thick U^{235} foil was used to get higher count-rates. Significant variations were found, but it was not determinable whether this was caused by an actual variation in yield or by a variation of the kinetic energy distribution of alpha particles, or both. A variation of the kinetic energy distribution would give variations in yield in the same manner as in the case of a thick foil for fission fragments discussed above.

Recent measurements by Schröder, Deruytter and Moore [8] have shown for thermal-neutron fission that with decreasing total fragment kinetic energy the yield of alpha particles increases and the average energy of the alpha particles increases as well. Combining these results with the expected variation of the fission-fragment kinetic energy from level-to-level, it appears that one should observe both a variation of yield from level-to-level as well as a variation of alpha particle kinetic energy. Some indications of the latter were observed in the earlier measurements.

Our earlier data on the relation yield of alpha particles are included in Fig. 2. Again, two groupings are observed, but agreement of assignment of levels to the two groups is in partial agreement only with the assignment made on the basis of (thick/thin) data.

EXPERIMENTAL DETAILS

The Columbia University Synchrocyclotron was used as a pulsed neutron source to make the following measurements as a function of neutron time-of-flight in Aug.-Sep. 1964:

(i) The yield of fission fragments from a thin (200 $\mu g/cm^2$) source of U^{235}, giving a measure of the fission cross-section as well as the kinetic energy distribution of one fission fragment.

(ii) The yield of fission fragments from a thick foil of U^{235} (thicker than the range of fission fragments in uranium), giving when combined with (i) a measure of the variation of the fission-fragment energy distribution from level to level.

(iii) The yield of long-range alpha particles from a 7 mg/cm^2 U^{235} source covered with 6.5 mg/cm^2 Al to absorb the fission fragments and the ordinary alpha particles, giving, when combined with (i) a measure of the variation of the yield of long-range alpha particles from level to level.

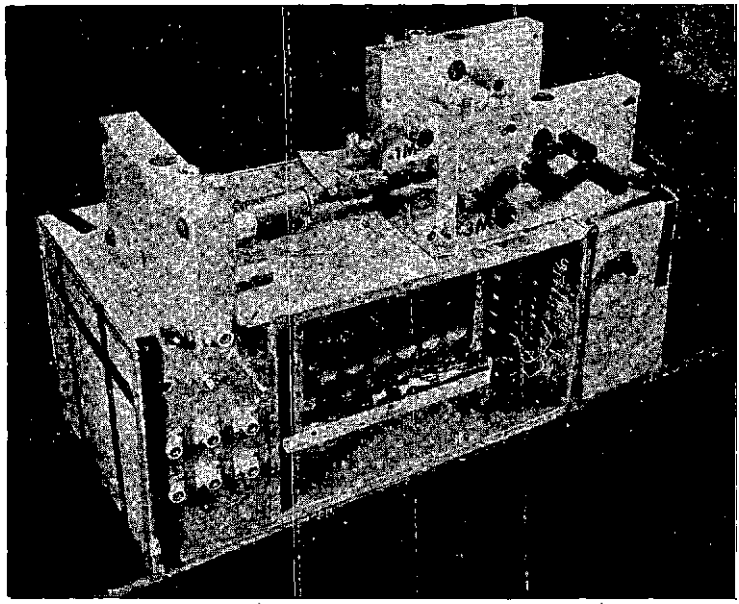

Fig. 3

Photograph of the fission chamber with a detector array mounted inside

(iv) A back-to-back detector arrangement with 50 $\mu g/cm^2$ U^{235} in between, to record the energies of both fission fragments so that mass and total kinetic energy distributions may be determined.

(v) A measurement similar to (i) but with 100 $\mu g/cm^2$ Pu^{239}.

(vi) A measurement similar to (iii) but with 1 mg/cm^2 Pu^{239}.

Figure 3 shows the fission chamber and one bank of 18 solid-state detectors (connected in a series parallel arrangement) feeding into one preamplifier. The experimental setup is shown in Fig. 4. In practice as many as five experiments were run simultaneously, with suitable mixing and identification circuits. After each event is detected and analysed, the information (two pulse heights, one time-of-flight and detector identification) is recorded on an incremental magnetic tape recorder. The resulting tapes are subsequently processed on IBM 1401 and 7094 computers. A total of about 5 000 000 events were recorded.

RESULTS

U^{235}

The new results have been only partially analysed but previous results appear to be generally confirmed in detection of fission fragments. In measurements on alpha emission, a thin foil of U^{225} was used in an attempt to resolve the problem posed by the earlier use of a thick foil. However, considerably less data were obtained during the run than expected, and no sig-

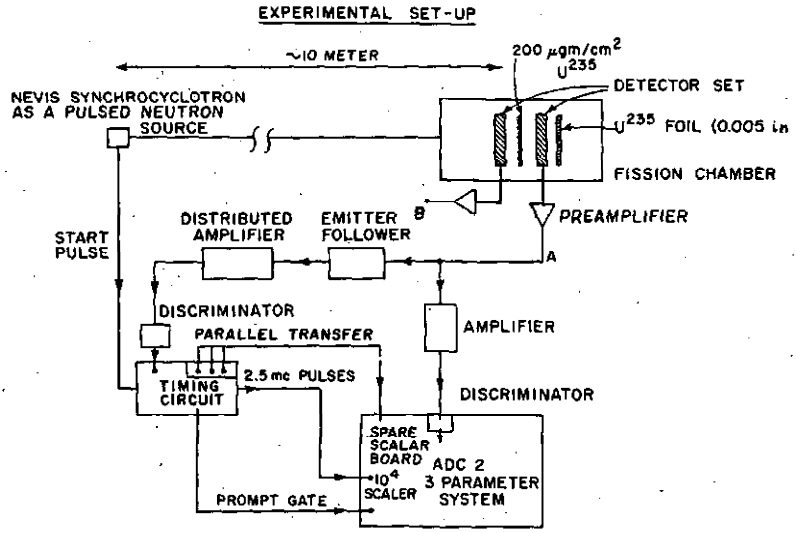

Fig. 4

Block diagram of the experimental setup

nificant variation in yield was observed within the larger statistical errors. The data for determining the possible variation of alpha particle energy have not yet been analysed. The results are given in Table I.

Pu^{239}

The thick/thin foil measurement could not be made, so the energy distribution of fragments from a thin foil was explored. Narrow intervals about the resonances were selected, and average pulse heights computed. These are listed in Table II. Significant variations outside of statistical errors are apparent, and groupings about the two mean values of 310.2 and 312.1 are possible. The lower value is assigned to J = 0 and the higher to J = 1 to get maximum agreement with other determinations, which are also included. Our assignments are thus not absolute except for consistency with the fact that on the basis of a 2J + 1 distribution one would expect three times as many J = 1 levels as J = 0 levels. Considerable agreement is observed for many levels, although there are a number of cases of marked discrepancy.

The alpha emission data were analysed by selecting regions of neutron time-of-flight containing several resonances, assigning errors to the points on the basis of the total count including background, subtracting the background, and making a least-squares curve fit to a sum of Doppler and resolution-broadened Breit-Wigner curves with preselected widths and positions so that only the heights are to be determined. This gives a number proportional to the area under each alpha particle resonance. The thin-foil fission data were similarly treated using the same width and position parameters. The ratio of fission yield to alpha particle yield was then computed for each level.

TABLE I

U^{235} RESULTS

No.	Resonance energy (eV)	Ratio of thick U to thin U	Our assignments of groupings	Cowan et al. assignments
1	8.78	0.730 ± 0.012	H[a]	L'
2	15.40	0.912 ± 0.090	L	L
3	16.09	0.801 ± 0.083	L	L
4	16.67	0.768 ± 0.063	U	L
5	18.05	0.769 ± 0.079	U	L'
6	19.3	0.810 ± 0.022	L	L
7	21.1	0.823 ± 0.039	L	L
8	22.98	0.850 ± 0.084	U	L
9	23.5	0.894 ± 0.081	L	L
10	25.6	0.838 ± 0.081	U	H
11	27.87	0.881 ± 0.077	L	L'
12	32.13	0.886 ± 0.43	L	L'
13	33.6	0.687 ± 0.040	H	L'
14	34.45	0.749 ± 0.034	H	H'
15	35.25	0.758 ± 0.021	H	H
16	39.5	0.740 ± 0.040	H	H

Notation for our assignments:

H → $\langle E \rangle_{Lower}$ → Lower average energy of the fission fragments.

L → $\langle E \rangle_{Higher}$ → Higher average energy of the fission fragments.

U → Uncertain

Notation for Cowan et al. assignments:

L → Low symmetric fission.

H → High symmetric fission.

Primes denote uncertain assignments.

[a] To make the two assignments identical, we have indicated by H the group having lower average energy

TABLE II

Pu^{239} RESULTS

Resonance energy (eV)	Average pulse height	c-J Assignments			
		Present	a	b	c
7.8	4 312.3	1	1		1
11.0	3 312.2	1	1		1
11.9	6 312.0	1	1		1
14.3	6 312.0	1			
14.7	6 311.5	1	0		0
15.5	7 311.6	1		1	0
17.6	6 311.6	1	1		1
22.2	6 312.2	1	0		
26.2	9 311.3	(1)			
32.1	2.0 306.8	0			
41.2	1.2 310.9	(0)	1	(0)	0
44.2	1.6 311.6	(1)	0	(1)	1
47.2	1.0 312.2	1			
49.4	1.0 310.8	(0)			
52.0	1.0 313.9	1		0	1

TABLE II (cont.)

Resonance energy (eV)	Average pulse height	c-J Assignments			
		Present	a	b	c
56.9	7 313.8	1			
58.5	5 311.6	1			
64.8	8 310.0	0		0	
73.6	6 312.1	1		1	

[a] FRASER, J. S. and SCHWARTZ, R. B., Nucl. Phys. 30 (1962) 269

[b] IGNATEV, K. G. and KIRPICHNIKOV, I. V., IAEA Rpt INDSWG/69 (Nov. 1964).

[c] BOLLINGER, L. M., COTE, R. E. and THOMAS, G. E., Proc. 2nd UN Int. Conf. 15 (1958) 127.

Because of the relatively thin Pu^{239} sample used here (1 mg/cm^2), the statistical accuracy of the results is relatively poor, and analysis of some of the smaller levels could not even be attempted. However, two levels, those at 49.4 eV and 64.8 eV, showed a significantly higher yield of alpha particles. On the basis of the above arguments, this implies a lower average kinetic energy of the fission fragments, which in turn implies an assignment of J = 0. This is in agreement with the assignment given in Table II on the basis of kinetic energy measurements.

Mass distribution

The back-to-back chamber data have not yet been analysed, but a brief discussion of possible treatment follows. As indicated above, it is hopeless to look for variations in the symmetric fission. However, inspection of Fig. 1 shows that the fission at low kinetic energy not only has increased symmetric fission, but also increased extremely asymmetric fission, i.e. extremely high and extremely low masses. These regions are not distorted quite as much as the region of symmetric fission, and it is hoped that they will be more amenable to analysis. Also, these data can be used to compute the total kinetic energy distribution. Since this distribution is more closely related to the separation distance at which scission occurs, it may be more sensitive to look for variations in the total kinetic energy distribution than in the energy distribution of the single fragments.

Higher energies

The main interest of these investigations was to study the energy region where resonance levels could be reasonably well separated. However, data up to ~20 keV were recorded. All the properties discussed show considerable statistically significant variation at the higher energies. However, it has not been possible to make background corrections, and it is also possible that instrumental distortions are present.

CONCLUSIONS

Considering both present and earlier data, the following conclusions are reasonably well-established:

(i) There are variations of fission-fragment kinetic energy from level-to-level compatible with two groups. In the case of U^{235}, correlation only with the relative yield of symmetric fission is possible. In the case of Pu^{239}, correlation with J-values is indicated.

(ii) The relative yield of alpha particles behaves similarly, with the occurrence of variation in actual yield as well as in the average energy of the alpha particles.

ACKNOWLEDGEMENTS

The authors thank Professor W. W. Havens, Jr. for his constant interest in these investigations, J. Floyd for assistance in data-taking and calculations, and Dr. John Povelites, of the Los Alamos Scientific Laboratory, for carrying out the evaporation of Pu^{239}.

REFERENCES

[1] FRASER, J. S. and SCHWARTZ, R. B., Nucl. Phys. 30 (1962) 269.
[2] BOHR, A., Proc. UN Int. Conf. PUAE 2 (1956) 151.
[3] WHEELER, J., Physica XXII (1956) 1103.
[4] REGIER, R. B., BURGUS, W. H. and TROMP, R. L., Phys. Rev. 113 (1959) 1589; REGIER, R. B., BURGUS, W. H., TROMP, R. L. and SORENSEN, B. H., Phys. Rev. 119 (1960) 2017.
[5] WALTER, F. J., NEILER, J. H. and SCHMITT, H. W., Bull. Amer. phys. Soc. II, 8 (1963) 369.
[6] COWAN, G. A., BAYHURST, B. P. and PRESTWOOD, R. J., Phys. Rev. 130 (1963) 2380.
[7] MEHTA, G. K., Ph. D. Dissertation, Columbia University (1964).
[8] SCHRÖDER, I. G., Ph. D. Dissertation, Columbia University (1964).

DISCUSSION

M. S. MOORE: I should like to comment on a correlation that we have observed on the symmetric fragment yield, as measured radiochemically, and the long-range heavy-fragment yield, as a function of neutron energy. In these data there is no strong correlation with the resonance structure,

which implies that instead of a spin dependence one can perhaps expect a fission channel dependence, as shown by asymmetries about the resonances in the mass distribution, kinetic energy distribution and relative ternary fission yield.

ALPHA PARTICLE EMISSION IN FISSION*

I. HALPERN
UNIVERSITY OF WASHINGTON, SEATTLE, WASH.,
UNITED STATES OF AMERICA

Abstract — Résumé — Аннотация — Resumen

ALPHA PARTICLE EMISSION IN FISSION. Soon after it was discovered that alpha particles are occasionally emitted in fission, it was concluded, on the basis of the energy and angular distributions of these particles, that they are emitted from the space between the fragments at times close to that of the snapping of the neck that connects them. It is shown that, independent of any (still unknown) dynamic features of the alpha-particle ejection process, the energy required to emit alpha particles from between the fragments at the indicated time is barely available. Presumably the rareness of alpha particles in fission, and the apparent absence of still heavier "third" particles, is associated with the marginal energy supply at the time of actual fragment division. The fact that the total kinetic energy release in so-called ternary fission is roughly equal to that in normal binary fission instead of being about 20 MeV larger is shown to imply that the mean fragment separation at the division time is larger in ternary fission. This is interpreted to indicate that alpha particles are emitted with greatest probability in those fissions where ample energy happens to be provided through the stretching of an abnormally long neck between the fragments before they actually divide. It is suggested that the release of the alpha particles is a sudden rather than adiabatic process.

EMISSION DE PARTICULES ALPHA DANS LA FISSION. Peu après avoir constaté que la fission donne parfois lieu à une émission de particules alpha, on a conclu, en se fondant sur leur distribution selon l'énergie et leur distribution angulaire, que ces particules sont émises dans l'intervalle entre les fragments à des époques proches de celle à laquelle se produit la rupture du col qui relie ces fragments. L'auteur montre qu'indépendamment de tout aspect dynamique (encore inconnu) du processus d'éjection des particules alpha, l'énergie nécessaire pour provoquer l'émission de ces particules dans l'espace entre les fragments à l'époque indiquée n'est guère disponible. La rareté des particules alpha dans une fission et l'absence manifeste de « tierces » particules encore plus lourdes sont probablement dues au fait que la quantité d'énergie n'est que marginale à l'époque où se produit la scission en deux fragments. Le fait que l'énergie cinétique totale libérée dans la fission dite ternaire est à peu près égale à celle qui est produite dans la fission normale, au lieu de la dépasser de 20 MeV, implique, comme le montre l'auteur, qu'en moyenne la distance entre les fragments à l'époque de la scission est plus grande dans une fission ternaire. On peut en conclure que la probabilité d'une émission de particules alpha est la plus grande pour les fissions dans lesquelles un excédent d'énergie est disponible du fait d'un allongement exceptionnel du col entre les fragments avant la scission. L'auteur suppose que la libération des particules alpha est un phénomène instantané et non adiabatique.

АЛЬФА-ИЗЛУЧЕНИЕ ПРИ ДЕЛЕНИИ. Вскоре после того, как было обнаружено, что периодически происходит излучение альфа-частиц при делении, был сделан вывод на основе энергетического и углового распределения этих частиц о том, что они испускаются из пространства между осколками в течение времени, близкого к моменту разрыва перетяжки, соединяющей эти осколки. Показано, что, независимо от каких-либо (все еще не известных) динамических особенностей процесса испускания альфа-частиц, энергия, необходимая для испускания альфа-частиц из пространства между частицами в указанное время, имеется в весьма незначительном количестве. Вероятно, редкое испускание альфа-частиц при делении и очевидное отсутствие еще более тяжелых "третьих" частиц связаны с избыточной поставкой энергии в момент действительного разделения осколков. Тот факт, что общее выделение кинетической энергии при так называемом "делении ядра на три части" приблизительно равно общему выделению энергии при обычном делении ядра на две части вместо того, чтобы быть примерно на 20 Мэв больше, говорит о том, что среднее разделение осколков в течение времени деления больше при делении ядра на три части. Это указывает на то, что

* The work reported here was supported in part by the United States Atomic Energy Commission. Much of this report resembles an earlier version issued at CERN, Geneva (unpublished, 1963).

альфа-частицы испускаются с наибольшей вероятностью при тех делениях, когда избыточная энергия образуется в результате растягивания необычно длинной перетяжки между осколками, прежде чем они действительно разделятся. Предполагается, что выделение альфа-частиц представляет собой скорее внезапный, чем адиабатический процесс.

EMISION DE PARTICULAS ALFA DURANTE LA FISION. Poco después de descubrirse que durante la fisión se emiten ocasionalmente partículas alfa, se dedujo, sobre la base de la distribución energética y angular de dichas partículas, que su emisión se produce desde el espacio existente entre los fragmentos momentos antes de saltar el gollete que los une. Se demuestra que, independientemente de las características dinámicas (aún desconocidas) del proceso de expulsión de las partículas alfa, apenas si existe la energía necesaria para emitir dichas partículas desde el espacio situado entre los fragmentos en el momento indicado. Es probable que el reducido número de partículas alfa emitidas durante la fisión y la aparente ausencia de «terceras» partículas aún más pesadas esté asociada con la energía marginal transferida en el momento de la escisión real en fragmentos. El hecho de que la cantidad total de energía cinética liberada en la fisión denominada ternaria sea comparable a la liberada en la fisión binaria corriente, en lugar de superarla en unos 20 MeV, implica que la separación media de los fragmentos en el momento de la escisión es mayor en la fisión ternaria. De ello se deduce que las partículas alfa son emitidas con una probabilidad mayor en las fisiones en que el estiramiento de un gollete anormalmente largo entre los fragmentos antes de la escisión proporciona energía en cantidad considerable. Se sugiere que la emisión de partículas alfa constituye un proceso repentino y no adiabático.

INTRODUCTION

When a heavy nucleus undergoes fission at low excitation energy it sometimes emits a charged particle during its division. This particle is generally an alpha particle with a broad energy spectrum extending from about 5 to 25 MeV. The angular distribution of the alpha particle with respect to the fission fragments is particularly striking. It is very sharply peaked perpendicular to the fission-fragment direction. Soon after the discovery of the fission alpha particles it was pointed out by TSIEN SAN-TSIANG [1] that this sharp peaking has at least these two important implications: (i) The alpha particle is emitted from a region between the fragments. Its final (observed) direction of motion can then be understood in terms of the effect of the Coulomb field of the two fragments. (ii) The emission takes place while the fragments are still close together. Otherwise the Coulomb field of the fragment actually emitting the alpha particle would play a much stronger role than that of the other fragment. The alpha particle must be produced, then, either during the course of the actual tearing apart of the fragments or very soon after.

Alpha particle emission in fission has not been studied as extensively as some other aspects of fission. The main reason for the neglect is very likely its low probability, typically one alpha particle in several hundred fissions. Nevertheless, because of the time and place at which the alpha particles are emitted, their investigation can be expected to make unique contributions to our understanding of the actual tearing stage (the so-called scission stage) in nuclear fission. This stage is particularly interesting because of the unusual condition of the nuclear matter at scission: it is being stretched to its limit. For obvious reasons, experimental studies of nuclear matter have not been nearly as broad as those of condensed atomic matter. The relatively rare chances that one has to explore unusual conditions of nuclear matter may therefore be particularly valuable.

In what follows an attempt is made to explain some of the most striking features in the observations of fission alpha particles in terms of reasonable assumptions concerning the nature of scission. Most of the considerations will be only semi-quantitative or even qualitative because the state of our knowledge of scission seems still to be inadequate for a very detailed treatment. It will be seen, however, that, independent of detailed assumptions, certain general aspects of the scission process can be deduced from what one already knows about charged particle emission in fission.

The problem of the emission of alpha particles in fission can conveniently be considered in two more or less independent parts, the first referring to the mechanism leading to the release of the alpha particle into the region between the fragments, and the second to the motion of the alpha particle in the Coulomb field of the fragments. Only the first problem will be discussed here; the second is treated elsewhere [2]. A discussion of the release mechanism is given, followed by a comparison of some of the implications of the suggested ejection mechanism with experimental observations.

HOW THE ALPHA PARTICLES ARE RELEASED

The energy requirements for alpha particle emission during fission

The following points lead one to conclude that the alpha particles accompanying fission are not evaporated from the fragments just after scission: (i) A typical evaporation time significantly exceeds the time ($\sim 10^{-21}$ s) that the fragments remain sufficiently close to each other to provide a field strong enough to account for the observed angular distribution of the alpha particles. (ii) If the alpha particles were evaporated, they would tend to be emitted from the outer ends of the fragments rather than into the central region where the Coulomb barrier is much thicker. (iii) The relative evaporation rate compared with that for neutrons would be expected to be much less than the observed rate.

The last two arguments also exclude evaporation from the thin-neck region just before scission. The essential point is that it is energetically very expensive to emit the alpha particle into the region between fragments and, as is well known, the probability for energetically expensive emissions is very small in evaporation. To appreciate the expense in energy, compare the energy of a pair of equal fragments separated by a distance D with a pair from which an alpha particle has been removed and placed midway between fragments. The energy difference between these situations, the removal energy of the alpha particle, is

$$E_R = B_\alpha + \frac{3}{2} V_\alpha \tag{1}$$

where B_α is the average binding energy of an alpha particle to one of the fragments and V_α is the Coulomb potential of the centrally placed alpha particle with respect to one of the fragments. To obtain a rough numerical estimate for U^{236} fission, note that $V_\alpha = 4V_0/Z$ where Z is the charge on

either fragment and V_0 is the Coulomb potential energy between the two fragments. If V_0 is set equal to the observed fragment kinetic energy ($\sim$150 MeV) [3] when alpha particles are produced, $\frac{3}{2}V_\alpha$ is typically about 19 MeV. B_α is about 5 MeV and E_R is therefore roughly 24 MeV. If the alpha particle is emitted with some initial kinetic energy, as it must be, it can be said that it costs at least 25 MeV to release the alpha particle into the region between fragments. This conclusion remains essentially the same if we allow the fragments to be unequal or if we place the alpha particle less symmetrically in the region between fragments. The physical reality of this estimate of 25 MeV is attested by the observation [3, 4] that when alpha particles are produced in fission the (kinetic + internal) energy in the fragment system is reduced from its normal value by roughly this amount.

In the same sense that it costs 25 MeV to release an alpha particle, it costs about 5 MeV, a neutron binding energy, to release a neutron in fission. If both particles are produced by evaporation, the ratio of the number of neutrons to alpha particles produced would be about exp $[\frac{1}{T}(25 - 5)]$ where T is the nuclear temperature in MeV. From observed neutron spectra in low-energy fission, T is known to be no larger and probably rather less than 1 MeV at scission. On this basis, one expects at most e^{-20} or about 10^{-9} alpha particles per neutron in fission. One observes about 10^{-3}. The observed alpha particle yield is therefore much too large to be accounted for by evaporation.

The emission of particles other than alpha particles

Before taking up the question of the mechanism for alpha particle emission, now that evaporation has been rejected, it is worth extending the discussion of emission energetics to other possible particles. In comparing different particles x, one should add to B_x and $\frac{3}{2}V_x$ (see Eq. (1)) an estimated minimum initial kinetic energy, K_x, with which the particles are emitted. The estimate of K_x is somewhat more model dependent than that of the other two quantities. But it is reasonable (and this will be shown in more detail below) to assign to an emitted particle a momentum spread corresponding to the volume v from which it is presumably emitted. The minimum kinetic energy associated with this momentum spread is

$$K_x = \frac{3}{2}\left(\frac{\pi}{v^{\frac{1}{3}}}\right)\frac{h^2}{m_x} \tag{2}$$

where m_x is the mass of the emitted particle. If one takes for the emission volume, the volume of the nuclear neck at scission, containing typically 20 nucleons, then one finds for alpha particles $K_\alpha \cong 4$ MeV. Recent evidence that the emission volume may be even more localized than the neck [5] would suggest that K_α should be increased slightly. One the other hand, the finite duration of the emission process tends to spread the wave train of the emitted particle over a volume larger than that of the original source. All things considered, Eq. (2), with the neck volume for v, probably gives a reasonable rough estimate for K_x. The values for K_x estimated in this way for a number

TABLE I

MINIMUM ENERGIES (MeV) NEEDED FOR THE RELEASE OF PARTICLES INTO THE SPACE BETWEEN FRAGMENTS (FISSION OF U^{236})

Emitted particle	n	p	d	H^3	He^3	α	Li^6	Be^8
B	5	12	15	14	20	5	20	12
$\frac{3}{2}$ V	0	10	10	10	19	19	29	39
K	16	16	8	5	5	4	3	2
Sum (required energy)	21	38	33	29	44	28	52	53

of possible emitted particles are listed in Table I. Also given are the average binding energies of those particles to fission fragments from U^{236} and the average Coulomb energies $\frac{3}{2}V_x$. The former were determined using mass tables [6] and the latter by multiplying the value (19 MeV) estimated above for alpha particles by the ratio Z_x/Z_α. The required energies listed in the table are averages over the mass division in the fission of U^{236}. The spread in values over this distribution can be shown to be small, being generally much less than 10%.

Some of the required energies listed in Table I are rather large and tend to exclude the emission of the particles they refer to, at least by any mechanism that gives angular distributions like those of the alpha particles. A very rough indication of the energy available for the emission of particles during fission is given by the average excitation energy of normal fission fragments. For thermal-neutron fission of U^{235} this energy is 21 MeV. The excitation energy distribution is, however, fairly broad about this mean, 10% of the events giving excitation energies greater than 35 MeV [7]. But excitation energies over 50 MeV lie outside the range normally observed in fission and it is likely that the absence of lithium and heavier fragments in fission [8] is connected with the fact that the release energies needed for these particles (Table I) exceed 50 MeV.

The relative yields of some of the lighter particles listed in Table I have been measured by WEGNER [9] and others [10, 11]. Although Wegner's measurements are for the spontaneous fission of Cf^{252}, the required energies for emission from Cf^{252} are not very different from those for U^{236} (Table I), and it is instructive to compare the tabulated required energies with the measured yields (Table II).

The yield of He^3 is seen to be less than that of H^3 or of He^4, and it is also seen that this observation can be attributed to the very large energy required for the release of He^3. This energy is larger than that for He^4 almost solely because of the difference in the binding energies of the two particles. It is larger than the energy needed to free H^3, partly because of binding energies, but mainly because of the Coulomb energy difference

TABLE II

YIELDS OF CHARGED PARTICLES ACCOMPANYING FISSION (Cf^{252})

Particle	Required energy (computed) (MeV)	Relative yield[a]
He^4	28	100
He^3	44	$< \frac{1}{2}$
H^3	29	6
d	33	$< \frac{1}{2}$
p	38	2.2

[a] From the measurements of WEGNER [9]

(Table I). In any event, it is easy to understand solely on energetic grounds why the He^3 emission probability is very low.

It is not apparent, in terms of considerations involving energy alone, why the alpha particle yield is more than ten times the triton yield and why the proton yield exceeds the deuteron yield. It may be impossible to understand these features without specific reference to the particle release mechanism. Some speculations on these questions are dealt with at the end of the following section where the particle release mechanism is discussed.

The mechanism for charged particle emission during fission

For an alpha particle or other third particle in fission to be able to acquire the very large share of the available energy that it needs to be released between the fragments, this energy must in the meantime be stored in readily convertible form. That is, it must be concentrated on a very few degrees of freedom. Otherwise the large entropy will make improbable reconcentration on the degrees of freedom connected with the escaping particle. In the usual picture of fission most of the energy appearing finally as fragment excitation energy is at the beginning of the process connected with distortion energy, the distortion energy of the stretching nuclear drop or, immediately after scission, the distortion energies of the fragments. The collective degrees of freedom associated with the distortion of the fissioning nucleus can be viewed as the required energy repository. Generally the stored energy is handed on to the distortions of the individual fragments, but on rare occasions it is made available to a third particle, e.g. an alpha particle.

It was noted above that the total energy distributed among the degrees of freedom other than those connected with the fragment motion is on the average insufficient for alpha particle release. Only those events are candidates for alpha particle emission in which there is an abnormally long stretching before scission (and consequently an abnormally small fragment kinetic energy). Moreover, the energy transfer to the alpha particle in these elongated fissions probably takes place through the sudden snap of

the neck stubs after scission. Although the fragments in alpha-accompanied fission make their initial appearance at larger separations than in normal fission, the fragments are less distorted than normal fragments (see below). One should therefore not picture the alpha particle release as a slow thinning of the neck on either side of the alpha particle followed by a slow retraction of the neck stubs into the fragments. There is not enough energy present for the configuration immediately after scission, which this picture implies.

Another way to judge the unlikelihood of a slow, adiabatic abandonment of the alpha particles is in terms of the forces involved. In the neck region, the Coulomb forces are very weak, this region being a saddle of the Coulomb potential surface. If the neck on one side of an alpha particle pinches through, the nuclear forces on the other side have a strong tendency to suck in the alpha particle, since the repulsive Coulomb force of the still-attached fragment is almost exactly nullified by that of the other fragment.

The process of alpha particle release is therefore probably not adiabatic, but rather sudden. The potential that the alpha particle feels is suddenly changed as the neck stubs retract. The potential can be thought to be rapidly displaced as it follows with the retracting nuclear matter. In the non-adiabatic limit the alpha particle in the field of the moving potential will change its potential energy very quickly and its kinetic energy hardly at all. The momentum increase Δp corresponding to a change in potential ΔV is, in one dimension, $-\int \partial V/\partial x \, dt \simeq -\Delta V/u$, where u is the speed with which the potential moves past the particle. For a given ΔV and large enough u, Δp can be made arbitrarily small. Two simple examples of energy transfer through non-adiabatic or sudden potential changes are illustrated in Fig. 1. It is the lower illustration that is meant to correspond to the abandonment

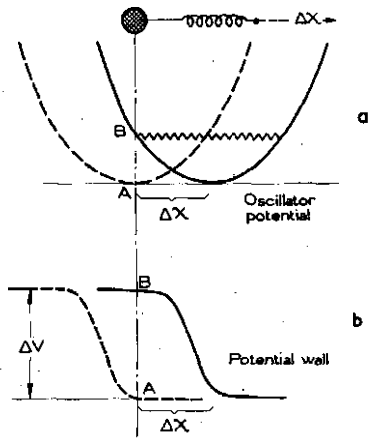

Fig. 1

The effects of sudden potential changes. (a) A spring attached to a particle at rest is suddenly displaced so that the particle finds itself at Δx from equilibrium. Its energy changes from A to B as the potential suddenly changes from the dashed to the solid curve. In the absence of further potential changes, the particle oscillates at level B converting the newly gained potential energy first to kinetic energy, then again to potential energy and so on. (b) If a potential of this shape is suddenly displaced by Δx, a particle initially at rest at A remains at rest at the higher potential B. More generally, its state of motion and position are left unchanged. Only the potential energy changes.

of an alpha particle at scission. The problem of rates of energy transfer in changing potentials has recently been discussed with illuminating examples by FULLER [12] in connection with a problem closely related to the one being considered here, namely that of neutron generation during scission [13].

In discussing the application of the sudden approximation to fission, it is necessary to use a wave-mechanical rather than a classical formulation since the particle wavelengths are of the same order as the system dimensions. In the sudden approximation the wave function remains unchanged [14]. This corresponds to the classical statements that the position and momentum remain the same. Figure 2 shows schematically how the alpha

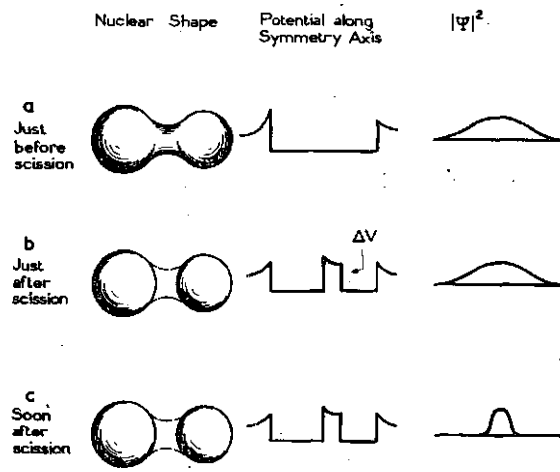

Fig. 2

How a sudden absorption of the neck between two fission fragments can lead to the release of an alpha particle between them. The sudden disappearance of the neck results in the potential change for an alpha particle (row b). If the change is fast enough, there is no change in the wave function. But subsequently the alpha-particle wave function can be reduced in regions occupied by nuclear matter due to absorption (row c). The surviving part of the wave function represents a free alpha particle in the region between fragments.

particle is released in fission according to the sudden approximation. For simplicity it is assumed that the potential changes associated with scission are instantaneous. The figure shows the potential seen by an alpha particle moving along the nuclear symmetry axis. The last column shows how the corresponding part of the alpha particle wave function responds to scission. It does not change during the instant of scission, but after scission the part inside nuclear matter is quickly absorbed leaving only the part originally in the neck of the fissioning nucleus.

No attempt will be made here to carry out calculations, using the sudden approximation, to predict probabilities for alpha particle release during fission. Unfortunately there are too many uncertainties for such calculations to be safe. It must, for example, be stressed that the very use of a completely non-adiabatic description is not easily justifiable for the present problem. In order for the sudden approximation to be valid, the potentials must change in times fast compared to the natural period of motion of the

particles being studied. Although the nuclear surface and hence the nuclear potential can move at speeds approaching those of the fastest nucleons in the nucleus, whereas the centre of mass of an alpha particle cluster moves more slowly, the ratio of these speeds is not as large as 10. Under the circumstances one cannot be sure that a simple application of the sudden approximation would be altogether trustworthy. Another way to appreciate the limitations of the sudden approximation to this problem is to recall that in this approximation there is generally finite probability for arbitrarily large energy transfers. In the present problem the maximum available energy barely exceeds that needed for the phenomenon under investigation.

Another, unrelated problem that stands in the way of a calculation of the alpha particle ejection rate is that of estimating the role of clustering or pre-formation of alpha particles in nuclear matter. One must expect that only those nuclear aggregates will be ejected as alpha particles that, inside the nucleus, happen to have a relative wave-function resembling that of the alpha particle. In short, there appear to be, at present, some uncertainties that stand in the way of a useful estimate of the particle ejection probability at scission. Nevertheless, despite these difficulties, the non-adiabatic limit seems close enough to the truth to be useful for the qualitative and semi-quantitative discussion of the ejection process.

One can speculate about the relatively small probability of triton emission compared with the alpha particle emission in view of the near equality of the estimated release energies (Table I). It may be that the average initial kinetic energy, K, was underestimated for the triton. The chosen K corresponds to a nodeless wave function spanning the nucleus. Since the triton is a fermion, it is subject to the Pauli principle and the mean kinetic energy of intranuclear tritons must exceed the earlier estimate. An increase in K would make triton emission relatively more difficult on energetic grounds. (It would also make the sudden approximation less applicable.) Another possible factor in the smaller triton emission may be a smaller clustering probability for tritons than for alpha particles.

Finally we turn to the fact that the proton yield exceeds the deuteron yield in fission even though proton emission has been estimated to be energetically more costly. Firstly it should be noted that for protons the sudden approximation must be far from valid. For a proton near the fermi surface to leave the nucleus, it must slow down considerably in view of the limited energy available in fission. Certainly the estimated K in Table I is meant to be a minimum initial energy upon ejection, independent of the ejection mechanism. The estimate of 16 MeV for protons is certainly less than the 40 MeV that one would be led to in a strict though inappropriate application of the sudden approximation. But even K = 16 MeV can be an over-estimate. It is based on the assumption that the protons emerge from the neck volume. Since protons are not as strongly absorbed in nuclear matter as the composite particles, the effective emission volume may be larger than that of the neck with the consequence that K is smaller than 16 MeV. Under these circumstances one would expect the angular distribution of the emitted protons (still unmeasured) to be more isotropic than that of the alpha particles.

If one reduces K for protons, one must do the same for neutrons with the implication that a very large yield of scission neutrons is to be expected.

Certainly, on the basis of the energies in Table I, one must expect many more scission neutrons than protons. Unfortunately scission neutrons are hard to observe because of the large background of ordinary fission neutrons evaporated from the fragments. There are, however, indications [15] that there may be as many as one-third scission neutrons per fission. This is roughly 100 times the alpha particle yield and would make the neutron by far the most copious particle ejected at scission.

HOW THE ALPHA PARTICLE PRODUCTION RATE DEPENDS ON OTHER MEASURABLE FEATURES OF THE FISSION PROCESS

Since it is not easy to make a quantitative theory out of the "sudden-snap" picture of alpha particle emission in fission, one can only test the idea by comparing its qualitative implications with a variety of observations. In this section we try to understand some of the observed correlations between the alpha particle emission probability and other physical quantities.

The dependence upon the fissioning species

It follows from the discussion in the preceding section that, other things being equal, the larger the distortion of the two fragments just after scission the larger the probability of the expected alpha particle emission. For example, when the total distortion in both fragments is very small there may not be enough energy present for the ejection of any alpha particles. For fragments with large distortions, the snap-back is more energetic and there is more chance to eject an alpha particle.

In spontaneous fission and slow neutron fission the average value of the total distortion of both fragments at scission is probably well measured by $\bar{\nu}$, the average number of neutrons emitted in the fission. Aside from small corrections for energy lost by radiation, $\bar{\nu}$ certainly measures the excitation energy with which the fragments are produced. It will now be argued that this excitation energy is largely in the form of distortion energy at the moment of scission. That is to say, in low-energy heavy-element fission, the nuclear matter in the newly formed fragments is quite cold. Evidence for this comes from the observed dependence of $\bar{\nu}$ on fragment mass [16] (see Fig. 3).

It is seen from this figure that for, e.g. U^{236}, when the fragment mass ratio is about 1 : 3 or when it is approaching 2 : 0, one member of the mass pair has a small $\bar{\nu}$ and the other a large one. If $\bar{\nu}$ were a measure of the internal excitation or temperature of a fragment at the instant of its formation, it would be expected to be very much the same for both fragments of a pair. The fact that it can be very different indicates, at least for the pairs where it is different, that the temperature at the formation time is low. The observed fragment excitation energies must therefore come from the (unequal) distortions with which the fragments are formed. It is reasonable to suppose that quite generally (i.e. also when $\bar{\nu}$ has roughly the same value for both fragments) $\bar{\nu}$ measures the fragment distortion at the formation time.

If one accepts this conclusion and the implications of the preceding section that the probability of alpha particle production depends upon the total initial distortions of the two fragments just after scission, then one is led to a simple expectation. Those species for which the average $\bar{\nu}$ in low-energy fission is larger, should also have larger values for (α/f), the average number of alpha particles produced per fission. If one examines the available data for (α/f) [17] and for $\bar{\nu}$ [18] one does find such a general trend, especially if one restricts the investigation to species lying close to the stable valley. It is found, however, that proton-rich isotopes tend to have larger values for (α/f) for a given $\bar{\nu}$ than neutron-rich isotopes. This may be taken to indicate that (α/f) depends not only on the snap intensity, or $\bar{\nu}$, but on other physical quantities. The data are unfortunately still too meagre to permit one to deduce the dependence of (α/f) upon more than one variable.

Although it does not deal specifically with the probability ratio, (α/f), the recent work of FRAENKEL and THOMPSON [5] does argue for a connection between alpha particle emission in fission and $\bar{\nu}$. These authors observe that for very asymmetric mass divisions, the alpha particles emitted in fission have angular distributions indicating that they are being released close to the light fragment. For symmetric divisions the alpha particles seem to originate closer to the heavy fragment. FRAENKEL and THOMPSON point out that this observation is consistent with the picture of scission given by WHETSTONE [19] and VLADIMIRSKII [20]. In this picture, the nucleus at scission always has the same standard shape, that of an asymmetric dumb-bell. The mass ratio in a given division is determined by the location of the actual scission cut along the neck between the two unequal dumb-bell ends. For a very asymmetric mass division, the cut occurs at the end of the neck that lies nearer the smaller dumb-bell end. In this situation the heavy fragment is much more distorted than the light one and therefore has a much larger value of $\bar{\nu}$. In fact, the asymmetric-dumb-bell picture accounts in a simple way for the observed saw-tooth dependence of $\bar{\nu}$ upon fragment mass (Fig. 3). According to the sudden-snap picture of alpha particle emission, the peak-of-the-wave function of the released alpha particle should initially be in the neighbourhood of the actual cut. One can therefore understand why, in the very asymmetric fissions, for example, the alpha particle appears to be released close to the light fragment.

The dependence upon the fragment mass

According to the preceding discussion, alpha particles are emitted from otherwise ordinary fission events when four appropriate nucleons in the neck manage to acquire a large share of the available energy. This they rarely do, and the four nucleons involved are therefore normally distributed between the two fragments. Thus when the mass pair (A_L, A_H) appears accompanied by an alpha particle, it has taken the place of one of the pairs $(A_L + 4, A_H)$ $(A_L + 3, A_H + 1)\ldots$ $(A_L, A_H + 4)$ in normal fission. If the mass yield distribution is assumed to vary slowly and smoothly enough with A, one can write for the average yield of the five normal pairs listed above,

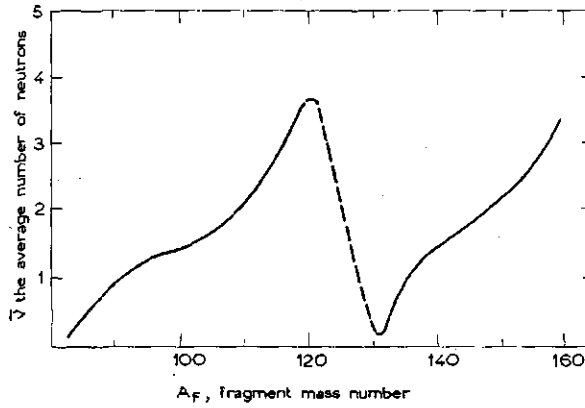

Fig. 3

The average number of neutrons released per fission as a function of fragment mass. This curve has been adapted from the analysis by TERRELL [16] and holds very nearly for all low-energy asymmetric fission.

the yield Y_N (A_L + 2, A_H + 2) of the central pair. The subscript stands for normal fission. If now p is the chance that an alpha particle is emitted during a fission that would usually lead to one of the listed mass pairs, one can write

$$p(A_L) \cong \frac{Y_\alpha(A_L, A_H)}{Y_N(A_L + 2, A_H + 2)}. \tag{3}$$

The subscript α stands for fission accompanied by an alpha particle emission. The fact that p might vary with mass ratio has been explicitly indicated. Figure 4 illustrates how the mass distributions for fission-with-alphas would look under three particular assumptions concerning the nature of $p(A_L)$. In each case only the yield distribution for the light mass numbers, A_L, is shown, since the heavy mass distribution is necessarily complementary. The fission-with-alpha distributions are in each case normalized to the normal distributions at the maxima.

Throughout Fig. 4 the function $p(A_L)$ was assumed to be symmetric about the centre of the mass peak. Under this assumption and the assumption underlying Eq. (3), Y_α is centred two mass units to the left of the normal distribution. In the simplest case, where $p(A_L)$ is a constant, Y_α and Y_N are identical in shape, the only difference being the two unit displacement (Fig. 4a). If $p(A_L)$ has a minimum at the peak of the mass distribution, it follows from Eq. (3) that the mass-distribution, Y_α, for fission-with-alphas will be wider than the normal distribution, Y_N (Fig. 4b). If $p(A_L)$ has a maximum at the mass distribution peak, Y_α is narrower than Y_N (Fig. 4c).

The mass distributions, Y_α and Y_N, have been carefully measured for thermal-neutron fission of U^{235} by SCHMITT and his coworkers [21, 22]. They found that the distribution Y_α is shifted two units to the left of Y_N like the distributions in Fig. 4. They also found that Y_α is slightly narrower

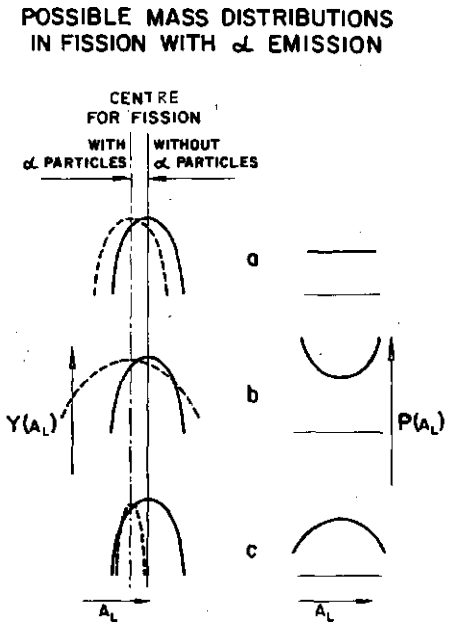

Fig. 4

Idealized representations of $Y_N(A_L)$, the light mass yield distribution for normal fission (——), and of $Y_\alpha(A_L)$, the corresponding distribution for fission with alpha particle emission (– – –). The function $p(A_L)$ gives the chance that an alpha particle is emitted during fission leading to the light mass number A_L. Assuming that on the average, light and heavy fragments contribute equally to form an emitted alpha particle, and further that $p(A_L)$ is symmetric about the maximum of the mass peak, one automatically reproduces the observation [21] that Y_α is centred two mass units below Y_N. Depending on the sign of the second derivative of $p(A_L)$, Y_α can be wider or narrower than Y_N.

than Y_N. In fact the low mass sides of the two distributions virtually overlap. In order to be able to make a numerical estimate, let us characterize this overlap by assuming that both distributions are Gaussian and that, on the low mass side, they have the same abscissa at the half-height point. Since the centre of Y_α is two mass units lower, it follows that the full width at half maximum of this distribution is four mass units narrower than the normal one. Since the normal distribution happens to have a width of about 16 mass units, the distribution with α-particles is about 25% narrower.

Applying Eq. (3), one finds that the value of p at the half-height points is about three-quarters of what it is at the peak of the mass distribution. That is to say, alpha particle emission is only three-quarters as probable for fissions that are heading for mass pairs half way up the curve as it is for fissions that are heading for the most probable mass division. This is not a very great variation, and perhaps the most significant result of the observations of Schmitt is that the probability of alpha particle release is not a very strong function of the mass ratio. The qualitative correctness of this assertion is of course evident from the observation that the mass distribution with alpha particles happens to be very similar to the one without alpha particles. We were led by the fact that Y_α is slightly narrower to conclude that the probability of alpha particle emission is slightly larger

than average at the peak of the mass distribution. If Y_α were very much narrower than Y_N (Fig. 4c) this conclusion would be forced upon us, but a very slight narrowing can be brought about by another effect. In deriving Eq. (3) and in the discussion so far, it has been assumed that the mass pair (A_L, A_H) comes at the expense of normal pairs distributed equally on either side of the pair ($A_L + 2$, $A_H + 2$). But suppose, for example, that on the low side of the A_L distribution (corresponding to the most asymmetric mass divisions) the (A_L, A_H) events are caused mainly by those that would have been (A_L, $A_H + 4$) events had there been no emission of an alpha particle. Suppose further that on the high A_L side of the peak, the corresponding normal mass-pair is instead ($A_L + 4$, A_H). In other words we are assuming that in very asymmetric fission, the alpha particle is released at the expense of the heavy fragment, whereas in the more symmetric fissions, it is the light fragment that loses its alpha particle. Under these assumptions one could qualitatively reproduce Schmitt's observations with an alpha particle emission probability, p, that is constant as a function of mass ratio.

In fact one can reproduce the observations with a great variety of functions $p(A_L)$ (see, e.g. Ref. [22]), depending on the assumptions that one makes for the relative probabilities that the heavy or the light fragment is "giving up" the observed alpha particle. There is no way from observations of Y_α and Y_N to decide about such probabilities, and in fact it is not clear that they are even, in principle, measurable. According to the views of the preceding section, the absorbed parts of the alpha particle wave function are roughly equal on either side of the neck (compare Figs. 2b and 2c). That is, if the alpha particle does not escape, it is as likely to be found in one fragment as the other. Thus the mean fragment mass pair that appears when an alpha particle fails to escape is then always close to ($A_L + 2$, $A_H + 2$), as we have assumed in the derivation of Eq. (3). From this point of view, the essential implications of Schmitt's results are that p is slightly larger for the most popular mass divisions than for the others. According to the picture of WHETSTONE [19] and VLADIMIRSKII [20], it is for these most popular divisions that the cut at scission comes at the centre of the neck. For other divisions it comes closer to one of the fragments. We are thus finally led to the impression that the probability for alpha particle emission is roughly constant as a function of the cut-location along the neck at scission, but that it is somewhat larger for central cuts than for others.

The dependence on the fragment kinetic energy

It is by now well established that the average fragment kinetic energy is smaller in alpha particle accompanied fission than in normal fission [23, 24]. In fact the total kinetic energy including that of the alpha particle is about the same as the total kinetic energy in normal fission. The average energy losses per fragment are unequal, the heavier fragment taking the smaller energy loss. This last observation is the easiest to explain. The fission alpha particles are known to be emitted essentially at 90° to the fragments. They remove virtually no momentum in the fragment direction. Hence, just as in normal fission, the conservation of linear momentum requires for a pair of fragments that $M_L E_L = M_H E_H$.

The reduction of the fragment kinetic energy when alpha particles are emitted in fission implies that the configuration of the fragments at scission is more elongated when alpha particles are emitted than when they are not. To see this, let us imagine that in ordinary fission the fragments are born at rest a distance D apart. Assume also that they are uniformly charged spheres. Then their final total kinetic energy will be Z^2e^2/D where, for simplicity, it has been assumed that the fragments are equally charged. Suppose now that an alpha particle, also at rest, is left behind midway between the fragments at scission. Then the final total kinetic energy of all three particles will be

$$2\,\frac{2(Z-1)e^2}{D/2} + \frac{(Z-1)^2e^2}{D} = \frac{Z^2e^2}{D}\left(1 + \frac{6}{Z} - \frac{7}{Z^2}\right). \tag{4}$$

With $Z = 46$, this represents a 13% increase in kinetic energy in the alpha-accompanied fission. One observes instead essentially no difference in the average total kinetic energy. One must therefore conclude that D happens to be about 13% larger in fissions where alpha particles are released than in normal fission. To be sure, the model of scission used here is a particularly simple one, but it should suffice to make the point that in fission with alpha particles, the scission takes place from fragments at larger than normal separations.

This implication of the observed kinetic energies is in good accord with the sudden-snap picture of scission. One must imagine that as the asymmetric-dumb-bell-shaped nucleus stretches, scission does not always occur at the same elongation. Scission at small elongation gives rise to events of high kinetic and low excitation energy, and vice versa for scissions at large elongation. The distribution in kinetic (or excitation energy) for a given mass pair thus reflects the distributions in elongations at scission. From the earlier discussion, it is clear that only in the long elongations has enough energy been stored to make alpha particle emission possible. One can therefore understand the increased value of D deduced for the alpha-accompanied fissions.

The dependence upon the bombarding energy

The dependence of the alpha particle emission rate upon bombarding energy seems, at present, more difficult to understand than the observed dependences already considered. The ratio of alpha particles produced per fission, (α/f), decreases smoothly with increasing energy from values near 1/300 (for spontaneous fission) to values close to 10^{-3} at 20 MeV [17, 25, 26]. What happens to (α/f) above 20 MeV is, at present, not altogether clear. It either levels off [27] or begins to increase [26]. At any rate, the sharp decrease of the lowest 20 MeV is not maintained.

One can speculate about the reasons for the dramatic decline of (α/f) with energy at low excitations. Suggestions that come to mind include decrease of the clustering probability for nucleons into alpha particles with increasing internal energy, an increase in nuclear viscosity with increased internal energy (when several nucleons are excited above the Fermi

surface, it becomes easier to transfer energy to the nucleons and therefore the relative chances for transfer to an alpha particle become less) and a decrease of the tensile strength of nuclear matter as it gets hotter (this would tend to shorten the mean elongation at scission). These are all interesting possibilities, involving as they do fundamental properties of nuclear matter. Indeed it is largely because fission studies may be in a unique position to illuminate some of these problems that they continue to be of great interest in nuclear physics. We will not, however, attempt here any further exploration of these problems as they are related to alpha particle production in fission.

In conclusion, it should be emphasized that this paper has dealt with only half the problem of the production of alpha particles in fission, i.e. the part relating to the probability for the alpha particle release. The problem of the subsequent history of the emitted alpha particle including its energy and angular distributions can be dealt with separately. It can be shown that as long as the alpha particle is released between the fragments in a distribution reasonably uniform in the available phase space, the details of the release mechanism do not much matter for the observed distributions. The problem of interpreting these distributions has recently been dealt with by a number of authors [2, 28, 29].

REFERENCES

[1] TSIEN SAN-TSIANG, Journal de Physique et le Radium 9 (1948) 6.

[2] HALPERN, I. (to be published).

[3] DMITRIEV, V.N., DRAPCHINSKII, L.V., PETRZHAK, K.A. and ROMANOV, Yu.F., Ž. eksp. teor. Fiz. 39 (1960) 556 (translation: Soviet Phys. - JETP 12 (1961) 390.

[4] APALIN, V.F., DOBRYNIN, Yu.P., ZAKHAROVA, V.P., KUTIKOV, I.E. and MIKAELYAN, L.A., Reactor Sci. Technol. 13 (1961) 86.

[5] FRAENKEL, Z. and THOMPSON, S.G., Phys. Rev. Lett. 13 (1964) 438.

[6] CAMERON, A.G.W., Rpt. AECL 433 (unpublished); SEEGER, P.A., Nucl. Phys. 25 (1961) 1.

[7] MILTON, J.C.D. and FRASER, J.S., Canad. J. Phys. 40 (1962) 1626.

[8] FLYNN, K.F., GLENDENIN, L.E. and STEINBERG, E.P., Phys. Rev. 101 (1956) 1492.

[9] WEGNER, H.E., Bull. Amer. Phys. Soc. II, 6 (1961) 307.

[10] HORROCKS, D.L., Phys. Rev. 134 (1964) B1219.

[11] ANDREEV, V.N. and SIROTKIN, S.M., Ž. eksp. teor. Fiz. 46 (1964) 1178 (translation: Soviet Phys. - JETP 19 (1964) 797).

[12] FULLER, R.W., Phys. Rev. 126 (1962) 684.

[13] STAVINSKII, V.S., Z. eksp. teor. Fiz. 36 (1959) 629 (translation: Soviet Phys. - JETP 9 (1959) 437).

[14] See, e.g. SCHIFF, L.I., in Quantum Mechanics, McGraw-Hill Book Co., New York (1955) 217.

[15] BOWMAN, H.R., THOMPSON, S.G., MILTON, J.C.D. and SWIATECKI, W.J., Phys. Rev. 126 (1962) 2120.

[16] TERRELL, J., Phys. Rev. 127 (1962) 880.

[17] NOBLES, R.A., Phys. Rev. 126 (1962) 1508.

[18] HYDE, E.K., UCRL Rpt. 9036, Univ. Calif. (unpublished).

[19] WHETSTONE, S.L., Jr., Phys. Rev. 114 (1959) 581.

[20] VLADIMIRSKII, V.V., Ž. eksp. teor. Fiz. 32 (1954) 822 (translation: Soviet Phys. - JETP 5 (1957) 673).

[21] SCHMITT, H.W., NEILER, J.H., WALTER, F.J. and CHETHAMSTRODE, A., Phys. Rev. Lett. 9 (1962) 427.

[22] SCHMITT, H.W. and FEATHER, N., Phys. Rev. 134 (1964) B565.

[23] MOSTOVOI, V.I., MOSTOVAYA, T.A., SOVINSKII, M. and SALTYKOV, Yu.S., Reactor Sci. Technol. 13 (1961) 84.
[24] DMITRIEV, V.N., DRAPCHINSKII, L.V., PETRZHAK, K.A. and ROMANOV, Yu.F., Soviet Phys.-Dokl. 4 (1960) 823.
[25] PERFILOV, N.A., SOLOV'EVA, Z.I. and FILOV, R.A., Ž. eksp. teor. Fiz. 41 (1961) 11 (translation: Soviet Phys. - JETP 14 (1962) 7).
[26] COLEMAN, J.A., FAIRHALL, A.W. and HALPERN, I., Phys. Rev. 133 (1964) B724.
[27] LOVELAND, W., private communication.
[28] FRAENKEL, Z., private communication.
[29] GEILIKMAN, B.T. and KHLEBNIKOV, G.I., private communication.

DISCUSSION

M. NÈVE DE MEVERGNIES: Do you think that one can expect any correlation between ternary α-particles and the prompt gamma rays emitted in fission?

I.HALPERN: I have not thought about such a correlation before, but I would think that since the nuclear fragments accompanying α-particles ought to be abnormally round (there being too little energy available for much distortion), one would not tend to excite rotations in the fragments. One might not expect as many soft γ-quanta accompanying fission as one normally sees.

M. SOWINSKI: On the basis of the model presented in your paper, do you think that an α-emission mechanism without fission is possible?

I. HALPERN: The Q-value for the (n,α) reaction in the high barrier for the α-particles is what keeps any α-particles from coming out in great abundance in low-energy neutron bombardments of heavy elements. I do not see how you could get any high-energy α-particles out.

THE EMISSION OF LONG-RANGE ALPHA PARTICLES IN FISSION

N. FEATHER
UNIVERSITY OF EDINBURGH, EDINBURGH,
UNITED KINGDOM

Abstract — Résumé — Аннотация — Resumen

THE EMISSION OF LONG-RANGE ALPHA PARTICLES IN FISSION. Fraenkel and Thompson (1964) have shown that the most probable direction of emission of the long-range alpha particles in the spontaneous fission of californium-252 varies with the ratio of the masses of the residual fission fragments. The angle of emission relative to the direction of motion of the lighter fragment increases significantly as the mass of the lighter fragment decreases. Asssuming that the alpha particle is emitted at the scission point, these authors conclude that the scission point, in ternary fission, occurs progressively nearer to the lighter fragment as the fragment mass ratio is greater. They point out that this is one of the asssumptions underlying the "geometrical" model of mass division of Whetstone (1959) and Vladimirski (1957), and is the feature of that model in terms of which the variation of the average number of neutrons with fragment mass in binary fission is successfully explained. They suggest that these various considerations together indicate that the configuration of the scissioning nucleus at (and before) scission in ternary fission closely resembles the corresponding configuration in binary fission.

Adopting this last hypothesis in relation to the thermal-neutron-induced fission of uranium-235, the writer (1964) has shown that if the liberation of the alpha particle occurs at or just after the moment of scission, so that it may be regarded as emitted from a newly formed, but still deformed, fragment then the probability of emission can be deduced from the experiments of Schmitt et al. (1962), if certain further assumptions are made. On the assumption that the alpha particle is derived from the heavy fragment exclusively, it appears that the probability of release from that fragment correlates directly with the average number of secondary neutrons emitted in in binary fission, and also with the energy available for alpha-particle emission from the undeformed (ground state) fragment. There would be no correlation with the energy available for alpha emission if it were assumed that alpha particles could be derived from light or heavy fragments indiscriminately. Clearly, the writer's point of view and conclusions are not fundamentally antagonistic to those of Fraenkel and Thompson; rather the two approaches are complementary. Discussion of particular points of detail is taken further in the paper.

ÉMISSION DE PARTICULES ALPHA A LONG PARCOURS DANS LA FISSION. Fraenkel et Thompson ont montré (en 1964) que la direction la plus probable d'émission de particules alpha à long parcours lors de la fission spontanée de ^{252}Cf varie en fonction du rapport des masses des fragments de fission résiduels. L'angle d'émission par rapport à la direction du mouvement du fragment léger augmente sensiblement lorsque la masse de ce fragment diminue. En supposant que la particule alpha est émise au point de scission, ces auteurs ont conclu que lors d'une fission ternaire, la scission se produit en un point de plus en plus proche du fragment léger lorsque le rapport des masses des fragments augmente. Ils ont fait observer que c'est là l'une des hypothèses à la base du modèle « géométrique » de la répartition des masses élaboré par Whetstone (1959) et Vladimirski (1957), et la caractéristique du modèle grâce auquel on explique la variation du nombre moyen de neutrons en fonction de la masse des fragments dans la fission normale. A leur avis, l'ensemble de ces diverses considérations indique que la configuration d'un noyau qui subit la scission, à l'époque de la scission (et avant celle-ci), dans une fission ternaire ressemble de très près à la configuration correspondante lors d'une fission normale.

En adoptant cette dernière hypothèse pour la fission de ^{235}U par neutrons thermiques, l'auteur a montré (en 1964) que si les particules alpha sont libérées à l'époque même de la scission ou aussitôt après celle-ci – de sorte qu'elles puissent être considérées comme émises par un fragment nouvellement formé mais encore déformé – on peut déduire la probabilité d'émission à partir des expériences de Schmitt et al. (1962) à condition de faire certaines autres hypothèses. Si l'on suppose que la particule alpha ne provient que du fragment lourd, il se révèle que la probabilité de son émission par ce fragment est en corrélation directe avec le nombre moyen de neutrons secondaires émis dans une fission normale, et aussi avec l'énergie disponible pour l'émission d'une particule alpha par le fragment non déformé (à l'état fondamental). Il n'y aurait aucune corrélation avec l'énergie disponible pour l'émission alpha, si l'on admettait que les particules alpha pourraient provenir in-

différemment du fragment léger ou du fragment lourd. Il est clair que l'opinion et les conclusions de l'auteur ne sont pas en contradiction fondamentale avec celles de Fraenkel et Thompson et que ces deux manières d'envisager le phénomène se complètent. Dans le mémoire, certains points particuliers font l'objet d'un examen détaillé.

ИСПУСКАНИЕ ДЛИННОПРОБЕЖНЫХ АЛЬФА-ЧАСТИЦ ПРИ ДЕЛЕНИИ. Френкель и Томпсон (1964 г) показали, что наиболее вероятное направление испускания длиннопробежных альфа-частиц при спонтанном делении калифорния-252 меняется в зависимости от отношения масс остаточных осколков деления. Угол испускания по отношению к направлению движения более легкого осколка значительно увеличивается по мере уменьшения массы более легкого осколка. Предполагая, что альфа-частица испускается в месте разделения ядра, авторы делают вывод о том, что место разделения ядра при делении на три части прогрессивно приближается к более легкому осколку по мере увеличения отношения масс осколков. Они указывают, что это является одним из предположений, лежащих в основе "геометрической" модели Уэтстона (1959 г) и Владимирского (1957 г), относящейся к разделению массы, а также составляет характерную особенность этой модели, с помощью которой успешно объясняется вариация среднего числа нейтронов с массой осколка при делении на две части. Они считают, что эти различные соображения, взятые вместе, показывают, что конфигурация делящихся ядер в момент (и до) разделения при делении на три части весьма напоминает соответствующую конфигурацию при делении на две части. Принимая эту последнюю гипотезу в отношении деления урана-235 под действием тепловых нейтронов, автор (1964 г) показал, что если испускание альфа-частиц происходит в момент деления или сразу же после него, то его можно рассматривать как излучение из вновь образованного, но все еще деформированного осколка, и, следовательно, вывод о возможности испускания можно сделать на основе экспериментов Шмитта и др. (1962 г), если сделаны определенные дополнительные предположения. При предположении, что альфа-частица испускается исключительно из тяжелого осколка, оказывается, что вероятность испускания из этого осколка непосредственно коррелируется со средним числом вторичных нейтронов, испускаемых при делении на две части, а также с энергией, остающейся на испускание альфа-частиц из недеформированного (в основном состоянии) осколка. Не было бы никакой корреляции с энергией, остающейся на испускание альфа-частиц, если предположить, что альфа-частицы могут испускаться одинаково как из легких, так и из тяжелых осколков. Ясно, что точка зрения автора и выводы в основном не противоречат точке зрения и выводам Френкеля и Томпсона; два подхода скорее дополняют друг друга. Затем в работе конкретно обсуждаются некоторые частные вопросы.

EMISION DE PARTICULAS ALFA DE GRAN ALCANCE EN LA FISION. Fraenkel y Thompson demostraron en 1964 que la dirección más probable de emisión de las partículas alfa de gran alcance, en la fisión espontánea del californio-252, varía según la razón másica de los fragmentos de fisión. El ángulo formado con la dirección de movimiento del fragmento más ligero aumenta sensiblemente a medida que disminuye la masa de dicho fragmento. Suponiendo que el helión es emitido en el punto de escisión, los autores mencionados deducen que en la fisión ternaria dicho punto se desplaza progresivamente hacia el fragmento más ligero a medida que aumenta la razón másica de los fragmentos. Como señalan, es ésta una de las hipótesis en que se basa el modelo "geométrico" de división de la masa propuesto por Whetstone (1959) y Vladimirski (1957); asimismo, es la característica de dicho modelo en función de la cual puede explicarse satisfactoriamente la variación del número medio de neutrones según la masa de los fragmentos en la fisión binaria. Sugieren que de todas estas consideraciones se deduce que la configuración del núcleo en el momento de escindirse (e inmediatamente antes) en la fisión ternaria es muy parecida a la configuración correspondiente en la fisión binaria.

Admitiendo esta última hipótesis para la fisión del uranio-235 inducida por neutrones térmicos, el autor (1964) demuestra que, si la emisión de la partícula alfa se produce en el momento de la escisión o inmediatamente después de la misma, de modo que pueda considerarse como emitida por un fragmento recientemente creado, pero aún deformado, la probabilidad de emisión puede deducirse de los experimentos realizados por Schmitt y col. (1962), a condición de aceptar como válidas algunas otras hipótesis. Suponiendo que la partícula alfa provenga exclusivamente del fragmento pesado, parece que la probabilidad de emisión por este fragmento guarda una relación directa con el número medio de neutrones secundarios emitidos en la fisión binaria, y con la energía disponible para la emisión de partículas alfa por el fragmento no deformado (estado fundamental). Si se supusiera que los heliones pueden ser emitidos indistintamente por los fragmentos ligeros o pesados, dicha probabilidad no guardaría relación alguna con la energía disponible para la emisión de estas

partículas. Por tanto, las apreciaciones y conclusiones del autor no son fundamentalmente opuestas a las de Fraenkel y Thompson; se trata más bien de opiniones complementarias. En la memoria algunas cuestiones de detalle se examinan con más detenimiento.

INTRODUCTION

In June 1964 the present writer suggested [1] that, in relation to the *emission of long-range alpha particles in low-energy fission*, "the hypothesis having the strongest claim to attention is that which assumes that the alpha particles originate in the heavy fragments exclusively, being liberated, very shortly after the instant of scission, with a probability not much less than unity, from fragment nuclei of low yield and small neutron excess" (see also Ref. [2]). Here the reasons supporting that suggestion will be briefly recapitulated, and the suggestion itself will be further examined in the light of more recent publications.

RECAPITULATION

It is taken for granted that the long-range alpha particles in low-energy fission are liberated at an earlier stage than the "prompt" neutrons, indeed that they become free before the fragment nuclei have separated significantly. So much is determined by the characteristic angular distribution of the particles, and by their kinetic energies, which accord well with the assumption that almost all the energy is derived from the electrostatic repulsion of the newly formed fragments. The alpha particles, therefore, must be emitted from the region of the "neck" of the fissioning nucleus, at the moment of scission, or very shortly before, or shortly after, this event. In any case, the alpha particles must be emitted from a system which, in relation to energy, is relatively "cold" (excitation energy not more than a few MeV). In this connection, experiments of APALIN et al [3] on the number of secondary neutrons in ternary fission, and of SCHMITT et al. [4] on the kinetic energies of the fragments in this alpha-particle-associated mode, agree in showing that the initial excitation energy of the fragments is reduced, on the average, by about 6 MeV as a result of alpha particle emission (both experiments refer to the compound nucleus U^{236} formed with 6.43-MeV energy of excitation by thermal-neutron capture).

Because the emitting system is, in any case, relatively cold it is justifiable to compare it, although it is a deformed system, with an undeformed configuration (even with the ground state configuration) of the same constitution. For the hypothesis that the long-range alpha particle is emitted before the instant of scission, the relevant comparison of the emitting system is with the undeformed compound nucleus in its state of initial excitation. For the hypothesis that the alpha particle is emitted from a newly formed fragment shortly after scission has occurred, the relevant comparison of the deformed fragment is with the same fragment undeformed, but possessing such energy of excitation as the fragment actually possesses immediately after scission has taken place.

In the thermal-neutron-induced fission of U^{235}, the excitation of the compound nucleus is such that 11.0 MeV of energy is initially available for alpha disintegration. For an undeformed system the lifetime for this process would be about 10^{-9} s. By contrast, a partial alpha disintegration lifetime of some 10^{-16} s must apply to the deformed compound nucleus if alpha particle emission is to take place with a probability of the order of 10^{-3} during the period of "descent from saddle point to scission" (see FAISSNER and WILDERMUTH [5]). Crudely, there is a discrepancy here of a factor of 10^7 or more; realistically, in the deformed system there will be two opposing effects that will modify this factor. In the first place, the local potential barrier against alpha particle escape will almost certainly be lower in the region of the neck than over the undeformed surface; secondly, the energy immediately available for alpha particle emission will be reduced by the deformation. It is difficult to believe that the first of these effects will so over-compensate the second that an adverse factor of 10^7 can be nullified. For this reason, and others, the hypothesis of pre-scission emission was rejected in the earlier communication [1].

Concerning the alternative hypothesis that the alpha particle in ternary fission is emitted almost immediately after scission from a newly formed fragment, it is necessary, for any comparison, first of all to determine what would be the energy available for alpha disintegration if the fragment were undeformed but possessed the (not very large) energy of excitation characteristic of the fragment at the moment of its formation. This available energy is the sum of the excitation energy and the energy available for alpha disintegration of the fragment species in its ground state configuration. In the earlier paper, therefore, values of Q_α, the ground-state alpha disintegration energy, were first surveyed for all possible fragment species. Using the tabulations of SEEGER [6] for extrapolation, and checking these whenever possible against the experimentally determined nuclear masses as given by KÖNIG et al. [7], it appeared, for the fragments from the low-energy fission of the compound nucleus U^{236}, that (i) there is a fairly sudden increase of approximately 5.5 MeV in Q_α, at some stage, as the mass number of the fragment, A_f, increases through the range 125 to 140 (the change number being adjusted appropriately); (ii) for fragments having the most probable charge for a given mass number, the disintegration energy Q_α does not vary greatly from a mean value of - 7.5 MeV over the range of mass number $90 \leqslant A_f \leqslant 130$, nor greatly from - 2 MeV over the range $140 \leqslant A_f \leqslant 160$; (iii) for fragments having charge number two in excess of the most probable value for a given A_f, the corresponding values of Q_α are - 5.5 MeV ($90 \leqslant A_f \leqslant 125$) and zero ($140 \leqslant A_f \leqslant 160$); and (iv) for a given A_f, and over the significant range of charge number Z, Q_α increases monotonically with Z ($90 \leqslant A_f \leqslant 125$ or $140 \leqslant A_f \leqslant 160$).

In brief, this preliminary survey showed, then, that the hypothesis of alpha particle emission from a newly formed fragment was a priori a credible one if applied to the heavy fragments ($A_f > 130$) in U^{236} fission, but very much less credible if applied to the light fragments. Moreover, in relation to the heavy fragments; the hypothesis was more easily credible for those fragments of small neutron excess than for the fragments of large neutron excess, over the whole range of A_f involved. For that reason it was decided to pursue the investigation on the assumption that only the heavy fragments

are concerned in the process, and to see whether the hypothesis, so modified, made sense in terms of the experimental results of SCHMITT et al [4].

The conclusions deriving from this investigation were first published by SCHMITT and FEATHER [2]. It was shown there that, on the hypothesis that ternary fission is a two-stage process, with the alpha particle emitted from the heavy fragment in all cases, it is possible to derive from a comparison of the primary mass-yield curves for binary and ternary fission [4] unique values of $P_\alpha(A_f)$, the over-all probability of the emission of a long-range alpha particle from an initial fragment of mass number A_f. The values of P_α so derived are reproduced in Fig. 1. The view was taken [1] that the general trend of P_α with A_f therein revealed provided significant support for the hypothesis on which the calculations were based. As is implicit in the hypothesis, the empirical P_α tends to be a very small value as A_f decreases towards the limit $A_f \sim 130$. Insofar as absolute values are concerned, it was emphasized that P_α is an over-all probability referring to the isobaric mixture of primary fission fragments of constant A_f, and the the absolute values represented in the figure are similar to (generally a little less than) the "fractional yield" of a fission fragment having a charge number two units in excess of the most probable value for the given mass number. On this basis the refinement of the two-stage hypothesis to refer particularly to heavy fragments "of low yield and small neutron excess" was seen to be entirely justifiable in the light of the information available. It must be repeated that, by and large, these are effectively the heavy fragments for which the energy available for alpha disintegration (in the undeformed state) is the greatest.

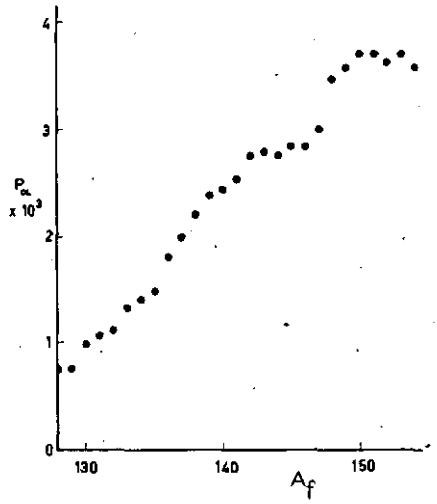

Fig. 1

Probability of long-range alpha particle emission from the heavy fragment as a function of fragment mass number

In evaluating the physical plausibility of the two-stage hypothesis it is appropriate to concentrate attention on the state of affairs in the region of the tip of the collapsing protuberance, which is that portion of the neck of

the compound nucleus belonging to the heavy fragment immediately after scission has taken place. If the hypothesis is to be acceptable, the alpha particle must escape from this region of the deformed fragment within some 10^{-19} s of the instant of scission. This requirement is effectively the requirement of almost instantaneous escape. It can be sustained only if the local potential barrier in the region of the tip of the protuberance is of near-negligible height and thickness; if, moreover, there are both protons and neutrons in the nuclear matter forming the protuberance; and if there is energy available for alpha particle release. The last condition is almost certainly satisfied with the heavy fragments of small neutron excess, as has just been described; the second condition is probably satisfied in general (according to the cluster model of fission [5] the numbers of protons and neutrons available in the initial heavy-fragment protuberance increase with the mass of the fragment); concerning the first condition, if it is satisfied anywhere, it is most likely to be satisfied for near axial emission of particles, at the tips of the opposing protuberances immediately after the two fragments have become separate in the act of scission. It would be difficult to substantiate numerical estimates that would be convincing in this last respect, but over-all it is maintained that the physical plausibility of the two-stage hypothesis is not seriously in doubt.

In the paper of SCHMITT and FEATHER [2] the variation of P_α with A_f was discussed in the same context as the variation of ν_h with A_f (ν_h being the mean number of "prompt" neutrons emitted by the heavy fragment of mass number A_f). Recently, more precise data concerning this latter variation have become available (APALIN et al. [8]). It is strikingly clear that, for the heavy fragments of the thermal-neutron-induced fission of U^{236}, these two variations are very similar indeed. Furthermore, attention has been drawn to the fact that in spontaneous fission the increase of the mean number of "prompt" neutrons with the mass number of the fissioning nucleus almost exactly parallels the increase of the mean probability of long-range alpha particle emission [1]. So long as attention is confined to low-energy fission exclusively, the two phenomena exhibit this close correlation. For higher excitations of the compound nucleus the same cannot be said: the probability of long-range alpha particle emission decreases, whereas the number of secondary neutrons increases as the energy of initial excitation is raised. It is worth while enquiring how these facts may be explained on the basis of the two-stage hypothesis.

The correlation of long-range alpha particle and secondary neutron emission characteristic of low-energy fission is clearly related to the fact that, on this hypothesis, each is determined by the initial deformation of the newly formed fragment [2]. The importance of this deformation for the process of alpha particle emission has been indicated above; in secondary neutron emission, almost the whole of the energy ultimately available for the process is initial-deformation energy. In relation to fission at higher energies the situation is different. The conditions in the collapsing protuberance (initial deformation) remain predominantly important for the former process; for the latter, the increase in the internal energy of excitation of the nascent fragment is primarily responsible for the changed situation. It will be seen that these general considerations already provide considerable scope for a reasonable interpretation of the facts of experiment, but in ad-

dition there is a special consideration that might well be important in the ultimate analysis. By and large, the characteristics of secondary neutron emission are determined by the deformations and initial excitations of the primary fragments of greatest yield for each value of A_f. According to the two-stage hypothesis for ternary fission, as put forward in this paper, the over-all probability of the alpha-particle-associated mode is determined first of all by the fractional yields of the much less abundant primary fragments of small neutron excess. If it should prove to be the case that the degree of charge dispersion among isobaric fragments decreases, even very slightly, as the energy of excitation of the compound nucleus increases, then an entirely adequate explanation would exist for the absolute decrease in the over-all probability of ternary fission that has been observed [9].

FURTHER DISCUSSION

Very recently FRAENKEL and THOMPSON [10] have examined the angular distribution of the long-range alpha particles in the spontaneous fission of Cf^{252}, in its dependence on R, the mass-ratio of the residual fragments. They find that, for a mass ratio between 1.0 and 1.1, the most probable alpha particle direction makes an angle of 72° with the direction of motion of the light fragment; when the mass ratio is greater than 2, the corresponding angle is 99°; for intermediate values of R, intermediate angles apply. They interpret these results as follows: alpha particle emission is incidental to an otherwise normal process of binary fission, the alpha particle becoming free at the scission point at the instant of scission; the division of mass between the fragments is determined by the position of the scission point in the neck of fissioning nucleus, the general configuration of the compound nucleus at scission being asymmetrical; consequently, the nearer the scission point is to the smaller of the two separating "cores" the greater is the mass-ratio R. On this interpretation, for large values of R the electrostatic repulsion of the light fragment, and for small (near unit) values of R the electrostatic repulsion of the heavy fragment, is preponderantly effective in determining the final direction of alpha particle motion.

It will be recognized that the interpretation of Fraenkel and Thompson is based upon the "geometrical" model of mass division in binary fission from VLADIMIRSKI [11] and WHETSTONE [12], and that it is generally consistent with the more sophisticated development of that model in the cluster theory of WILDERMUTH and collaborators [5]. The fact that such an interpretation was possible at all is indeed put forward by Fraenkel and Thompson as providing strong support for the general validity of the model. This is a significant point. Here, however, attention is concentrated on the bearing of the experimental results on the two-stage hypothesis that is our main concern. If the contrary, one-stage, hypothesis is taken literally (the hypothesis that the alpha particle of ternary fission is "left behind" at the instant of scission, and this is the hypothesis that appears to be favoured by Fraenkel and Thompson) inevitably the question must be asked what condition it is that determines (in a small fraction of cases) that the alpha particle is left behind rather than that it coalesces with (or remains part of) one or other of the nascent fragments.. And there is the further question from the standpoint

of this hypothesis: why it is that a composite charged particle, rather than a single proton, is left behind in this way.

In relation to the second question the comment might first be made that if any particle were to be "left behind" at the instant of scission it would be natural to suppose that particle would be a neutron. On this point present experimental evidence is far from conclusive. It may well be that in the low-energy fission of U^{236}, a neutron is so left behind with a probability of about 0.3/fission event [13, 14], and experimental results relating to the spontaneous fission of Cf^{252} would bear a similar interpretation [15, 16], but in relation to long-range proton emission. In the former case, the experimental upper limit is certainly of the order of 10^{-5}/event [17, 18], less by a factor of 100 or more than the probability of long-range alpha particle emission.

It is easy to say that the answers to both questions are to be derived from a consideration of the energetics of the situation. Let it be conceded (in relation to the second question) that a neutron is left behind at scission in 30% of fission events, and that two neutrons are similarly left behind in, e.g. 5% (or even 10%) of such events. Then the formation of a long-range alpha particle might be described as the accession of two protons to this nascent group; the accession of a single proton would provide a long-range triton. According to the experimental evidence [19], the probability of single-proton accession would have to be no more than 5%, or thereabouts, of the probability of two-proton accession (and the probability of single-proton accession to a single neutron smaller still by a factor of nearly 100) if this description were to be valid. Energetically, the possible final products, alpha particle, triton, deuteron, stand in the appropriate order in relation to energy of binding, but it is difficult to accept this essentially statistical description, requiring as it does the greater probability of the (successive) accession of two protons, than of one, to the same system (of two neutrons).

In relation to the first question, an answer based on the energetics of the situation is no more convincing. For an alpha particle to be left behind at scission, it would appear to be necessary that energy should not be released to whichever of the separating fragments the residual alpha particle should attach itself. This situation, according to our earlier considerations, is almost inconceivable; in certain cases energy might not be released if the alpha particle were to attach itself to the heavy fragments, but it would be almost impossible that it should not be liberated if the alpha particle were to attach itself to the light fragment. It is difficult to avoid the conclusion that if there were a preformed alpha cluster in the neck of the fissioning nucleus at the place of imminent scission, then, energetically, this cluster should not go free when scission occurs. Only after scission, when the two fragments have taken on their respective identities, is it naively reasonable to assume that an alpha cluster, newly formed within the collapsing protuberance of a recoiling fragment, might, in suitable circumstances, have sufficient energy to escape through the tip of the protuberance. The distinction between "almost instantaneous escape" from the newly formed fragment (see above) (the requirement of the two-stage hypothesis), and failure to cohere (the assumption of the one-stage hypothesis), may be a slender one, if all that is required is a description of the time sequence of a complex nuclear process (for the distinction turns on a difference of no more than

some 10^{-19} s in time), but, conceptually, it is a real distinction. It is just on this conceptual, interpretative, point that issue is taken with the views put forward by Fraenkel and Thompson.

REFERENCES

[1] FEATHER, N., Proc. Roy. Soc. Edin. 66A (1964) 192.

[2] SCHMITT, H.W. and FEATHER, N., Phys. Rev. 134 (1964) 565.

[3] APALIN, V.F., DOBRYNIN, Yu.P., ZAKHAROVA, V.P., KUTIKOV, I.E. and MIKAELYAN, L.A., Atomnaja Energija 7 (1959) 375; (translation: J. Nucl. Energy 13A (1960) 86).

[4] SCHMITT, H.W., NEILER, J.H., WALTER, F.J. and CHETHAM-STRODE, A., Phys. Rev. Lett. 9 (1962) 427.

[5] FAISSNER, H. and WILDERMUTH, K., Nucl. Phys. 58 (1964) 177.

[6] SEEGER, P.A., Nucl. Phys. 25 (1961) 1.

[7] KÖNIG, L.A., MATTAUCH, J.H.E. and WAPSTRA, A.H., Nucl. Phys. 31 (1962) 18.

[8] APALIN, V.F., GRITSYUK, Yu.N., KUTIKOV, I.E., LEBEDEV, V.I. and MIKAELYAN, L.A., Ž. eksp. teor. Fiz. 46 (1964) 1197; (translation: Soviet Phys. - JETP 19 (1964) 810).

[9] NOBLES, R.A., Phys. Rev. 126 (1962) 1508.

[10] FRAENKEL, Z. and THOMPSON, S.G., Phys. Rev. Lett. 13 (1964) 438.

[11] VLADIMIRSKI, V.V. Ž. eksp. teor. Fiz. 32 (1957) 822; (translation: Soviet Phys. - JETP 5 (1957) 673).

[12] WHETSTONE, S.L., Phys. Rev. 114 (1959) 581.

[13] KAPOOR, S.S., RAMANNA, R. and RAMA RAO, P.N., Phys. Rev. 131 (1963) 283.

[14] SKARSVAG, K. and BERGHEIM, K., Nucl. Phys. 45 (1963) 72.

[15] BOWMAN, H.R., THOMPSON, S.G., MILTON, J.C.D. and SWIATECKI, W.J., Phys. Rev. 126 (1962) 2120.

[16] BOWMAN, H.R., MILTON, J.C.D., THOMPSON, S.G. and SWIATECKI, W.J., Phys. Rev. 129 (1963) 2133.

[17] TITTERTON, E.W., Nature, Lond. 168 (1951) 590.

[18] ANDREEV, V.N. and SIROTKIN, S.M., Ž. eksp. teor. Fiz. 46 (1964) 1178 (translation: Soviet Phys. - JETP 19 (1964) 797).

[19] ALBENESIUS, E.L. and ONDREJCIN, R.S., Nucleonics 18 No. 9 (1960) 100.

LONG-RANGE ALPHA PARTICLE EMISSION IN THE FISSION OF U^{235} BY 3-MeV NEUTRONS

V.A. HATTANGADI, T. METHASIRI*, D.M. NADKARNI, R. RAMANNA AND P.N. RAMA RAO
ATOMIC ENERGY ESTABLISHMENT TROMBAY, BOMBAY, INDIA

Abstract — Résumé — Аннотация — Resumen

LONG-RANGE ALPHA PARTICLE EMISSION IN THE FISSION OF U^{235} BY 3-MeV NEUTRONS. The energy and angular distribution of long-range alpha particles emitted in the fission of U^{235} induced by 3-MeV neutrons have been measured. The alpha particles were detected by solid-state detectors and the fission fragments were detected by a gas scintillation counter. The neutrons were produced by the T (p, n) He^3 reaction using a 5.5-MeV Van de Graaff accelerator. About 3000 fission events accompanied by the emission of a high-energy alpha particle were recorded. The most probable energy of the alpha particles is between 15-16 MeV, and the energy distribution has a full width at half maximum of about 9 MeV, which is the same as observed in thermal-neutron fission.

The angular distribution of the long-range alpha particles with respect to the incident neutron direction was found to be forward-peaked, in agreement with previous work on alpha emission in 14-MeV neutron-induced fission of U^{238}. At angles of 0° and 90° with respect to the incident neutron direction the alpha particles were detected with an angular spread of about ± 25°. The anisotropy [$N_\alpha(0°)/N_\alpha(90°)$] was found to be 1.320 ± 0.12. This value is in agreement with the anisotropy calculated on the basis of statistical evaporation of particles.

The results of the present investigation are consistent with the hypothesis that the emission of long-range alpha particles in fission is an evaporation process. The implications of the results of this work and of other recent investigations on long-range alpha emission are discussed.

ÉMISSION DE PARTICULES ALPHA A LONG PARCOURS DANS LA FISSION DE ^{235}U PAR DES NEUTRONS DE 3 MeV. Les auteurs ont mesuré la distribution selon l'énergie et la distribution angulaire des particules alpha à long parcours émises dans la fission de ^{235}U par des neutrons de 3 MeV. Les particules alpha ont été décelées à l'aide de détecteurs à semi-conducteurs et les fragments de fission par un compteur à scintillateur gazeux. On a obtenu les neutrons par la réaction T (p, n) ^3He en utilisant un accélérateur Van de Graaff de 5,5 MeV. Les auteurs ont enregistré environ 3 000 fissions accompagnées de l'émission d'une particule alpha de haute énergie. L'énergie la plus probable de ces particules se situe entre 15 et 16 MeV et la distribution selon l'énergie accuse une largeur entière d'environ 9 MeV à mi-hauteur du maximum, soit la même que celle qui est observée pour la fission par neutrons thermiques.

Les auteurs ont constaté que la distribution angulaire des particules alpha à long parcours par rapport à la direction des neutrons incidents présentait un pic en avant, ce qui concorde avec les résultats d'une étude faite antérieurement par d'autres chercheurs sur l'émission de particules alpha dans la fission de ^{238}U par neutrons de 14 MeV. A des angles de 0° et 90° par rapport à la direction des neutrons incidents, les particules alpha décelées accusaient une dispersion angulaire de l'ordre de ± 25°. Les auteurs ont trouvé que l'anisotropie [$N_\alpha(0°)/N_\alpha(90°)$] était de 1,320 ± 0,12. Cette valeur est en accord avec l'anisotropie calculée sur la base de l'évaporation statistique des particules.

Les résultats de l'étude qui fait l'objet du mémoire sont compatibles avec l'hypothèse selon laquelle l'émission de particules alpha à long parcours dans la fission est un processus d'évaporation. Les auteurs discutent les incidences de ces résultats et de ceux d'autres recherches récentes sur l'émission de particules alpha.

ИСПУСКАНИЕ ДЛИННОПРОБЕЖНЫХ АЛЬФА-ЧАСТИЦ ПРИ ДЕЛЕНИИ УРАНА-235, ВЫЗВАННОМ НЕЙТРОНАМИ С ЭНЕРГИЕЙ 3 Мэв. Измерено энергетическое и угловое распределение длиннопробежных альфа-частиц, испускаемых при делении урана-235 под действием нейтронов с энергией 3 Мэв. Альфа-частицы были обнаружены с помощью твердых детекторов, а осколки деления — с помощью газового сцинтилляционного счетчика. Нейтроны

* IAEA Fellow on leave of absence from the Office of Thai Atomic Energy, Bangkok.

были получены в результате реакции T (p,n) He^3 с помощью ускорителя Ван де Граафа с энергией 5,5 Мэв. Было зарегистрировано около 3000 актов деления, сопровождавшихся испусканием альфа-частиц большой энергии. Наиболее вероятная энергия альфа-частиц находится в диапазоне 15–16 Мэв, а энергетическое распределение имеет полную ширину на половине высоты порядка 9 Мэв, которая совпадает с наблюдаемой шириной при делении тепловых нейтронов.

Угловое распределение длиннопробежных альфа-частиц по отношению к направлению бомбардирующих нейтронов имеет вид выдвинутого вперед пика, что соответствует предыдущей работе по альфа-излучению при делении урана-238 под действием нейтронов с энергией 14 Мэв. При углах 0° и 90° по отношению к направлению бомбардирующих нейтронов альфа-частицы обнаруживались с угловым расхождением примерно ±25°. Анизотропия [Na (0°)/Na (90°)] составляет 1,320±0,12. Эта величина согласуется с анизотропией, рассчитанной на основе статистического испарения частиц.

Результаты настоящего исследования соответствуют гипотезе о том, что испускание длиннопробежных альфа-частиц при делении представляет собой процесс испарения. Обсуждается значение результатов этой работы, а также других последних исследований по испусканию длиннопробежных альфа-частиц.

EMISION DE HELIONES DE GRAN ALCANCE EN LA FISION DEL ^{235}U POR NEUTRONES DE 3 MeV. Los autores han medido la distribución angular y energética de los heliones de gran alcance emitidos en la fisión del ^{235}U inducida por neutrones de 3 MeV. Los heliones se detectaron mediante dispositivos de estado sólido, y los fragmentos de fisión, con ayuda de un contador de centelleador gaseoso. Los neutrones se produjeron por la reacción T (p, n)^{3}He, empleando un acelerador Van de Graaff de 5,5 MeV. Se registraron unas 3 000 fisiones acompañadas de emisión de heliones de alta energía. La energía más probable de los heliones es del orden de los 15 a 16 MeV, y la distribución energética presenta a la mitad del máximo una anchura total de unos 9 MeV, esto es, un valor que se observó también en la fisión producida por neutrones térmicos.

Se comprobó que el gráfico de la distribución angular de los heliones de gran alcance respecto de la dirección de los neutrones incidentes era del tipo en dientes de sierra, de conformidad con los resultados obtenidos en trabajos anteriores sobre la emisión de heliones en la fisión del ^{238}U inducida por neutrones de 14 MeV. Para ángulos de 0° y de 90° respecto de la dirección de los neutrones incidentes, los heliones se detectaron con una dispersión angular de ±25% aproximadamente. Se comprobó que la anisotropía [N_α (0°)/N_α (90°)] era de 1.320 ± 0,12. Este valor concuerda con el de la anisotropía calculada sobre la base de una evaporación estadística de las partículas.

Los resultados obtenidos por los autores son compatibles con la hipótesis de que la emisión de heliones de gran alcance en la fisión constituye un proceso de evaporación. En la memoria se examinan las posibles consecuencias de los resultados de este trabajo así como de otras investigaciones recientemente realizadas sobre la emisión de heliones de gran alcance.

INTRODUCTION

The mechanism of the emission of charged particles of long range in fission, known as ternary fission, has not been clearly understood. Such emission has been observed in spontaneous fission and fission induced by different projectiles, and in about 95% of the events only alpha particles are emitted. Because it is not likely to occur, there is considerable variation in the reported values of the relative probability of its emission. In the slow neutron fission of U^{235}, the reported values of the relative probabilities of binary to ternary fission range from 200 : 1 to 550 : 1 [1]. For fast neutron fission the reported values are (1050 ± 100) : 1 and 600 : 1 for 14-MeV and 2.5-MeV neutron fission of uranium respectively [2, 3]; and (403 ± 25) : 1, (534 ± 35) : 1 and (446 ± 30) : 1 for 1-MeV neutron-induced fission of Pu^{240}, U^{236} and U^{235} respectively [4].

The energy spectrum of the alpha particles emitted in the slow neutron fission of U^{235} has been investigated by several workers [1]. The spectrum

extends from 7-28 MeV with a peak at about 15-17 MeV and a full width at half maximum of about 10-12 MeV. There is some disagreement in the low-energy part of the spectrum measured by different methods. The spectra observed in fast and thermal-neutron fission of uranium seem to be similar [2]. In view of the importance of the alpha spectrum in high-energy fission and the angular correlation of the emitted alpha particles with the incident neutron direction for understanding the emission process, the spectrum and the angular distribution of alpha particles emitted in the fission of U^{235} by 3-MeV neutrons have been measured. These results confirm the existence of an anisotropy reported earlier in the case of 14-MeV neutron fission of U^{238} using emulsion plate techniques [5]. In the present measurements the alpha particles were detected using solid-state detectors, and the excitation energy of the fissioning nucleus was below the second-chance fission threshold. As the forward peaking of the fragments along the direction of the incident particle observed in the binary fission is not observed in the ternary fission [5], it is essential in measuring the anisotropy of the alpha particles with respect to the neutrons that the distribution is averaged over the actual distribution of the fission fragments.

In the present investigation the relative probability of ternary and binary fission, the energy spectrum of the alpha particles and the anisotropy of the angular distribution with respect to the incident neutron beam in the fission of U^{235} by 3-MeV neutrons have been determined. The 3-MeV neutrons were produced by the $T(p,n)He^3$ reaction using a 5.5 Van de Graaff generator. Solid-state detectors and a gas scintillation counter were used to detect the long-range alpha particles and the fission fragments respectively.

EXPERIMENTAL ARRANGEMENT AND METHOD

Three silicon surface barrier type solid-state detectors were used to detect the long-range alpha particles emitted in coincidence with the fission fragments. The fission fragments were detected by the scintillations produced in the xenon gas, and were observed by a photo-multiplier tube, ensuring that fragments emitted in all directions with respect to the incident neutrons were detected. A schematic diagram of the arrangement of the target and detectors used is shown in Fig. 1. Detector D1 was placed close to the uranium target to detect most of the alpha particles emitted in the backward hemisphere. It had a depletion depth of about 400 μm and hence could detect alpha particles of energy up to about 33 MeV. The active area of the detector was about 200 mm^2, and it was operated with a positive bias of 100 V. Two thin detectors, D2 and D3, were used to detect alpha particles emitted at 0° and 90° with respect to the incident neutron beam direction, and were mounted about 3 cm from the target foil. At 0° and 90° the alpha particles were detected with an angular resolution of about ± 18°. The pressure of the xenon gas used in the chamber was about 2/3 atm, which was sufficient to stop all the fission fragments and natural alpha particles from reaching D2 and D3.

The uranium target used was prepared by electroplating U^{235} on a 10 mg/cm^2 Al backing. The uranium coating was about 1 mg/cm^2. The aluminium foil backing was of sufficient thickness to stop all the fission frag-

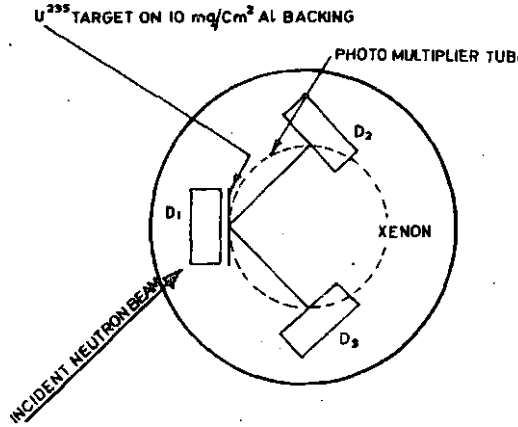

Fig. 1

A schematic diagram of the arrangement of the target and solid-state detectors D1, D2 and D3. The chamber was filled with xenon gas and the dotted circle represents the region seen by the photomultiplier tube.

ments and natural alpha particles, and allow only the long-range alpha particles to reach D1. The maximum energy of the neutron used was about 3.2 MeV with an energy spread of about 200 keV due to the slowing down of protons in the tritium target. The collimated beam spot was about 2-3 mm in diameter. The neutron flux at the uranium target was estimated to be about 10^5 n/cm^2.s.

Three identical low-noise charge-sensitive preamplifier-amplifier systems were used to amplify the pulses from the three solid-state detectors D1, D2 and D3. The alpha-particle spectra from all the three detectors in coincidence with the fission fragments were simultaneously recorded side by side using a 400-channel analyser. The discriminator bias for the fission-fragment counter was so adjusted that all the fission fragments were detected. In the alpha particle detectors there is a background of low-energy charged particles produced in the silicon of the detectors by fast neutrons, and the discriminator level of the detectors was set at a higher level to eliminate accidental coincident events. The bias setting was such as to correspond to an alpha particle energy of about 8 MeV before loss in the aluminium absorber, and the measurements reported here cover an alpha-particle energy range between 8 and 30 MeV only. The calibration was achieved by using a precision mercury pulser previously calibrated, using standard sources of natural alpha particles. The count-rate of the coincident alpha particles was about 12/h at these settings and the ratio of chance to true coincidence rates was found to be negligible. The data were accumulated over 20 runs, and were separately analysed and found to be consistent. During the latter half of the experiment the 0° and the 90° detectors were interchanged and the results for both the arrangements were found to be consistent. Data taken towards the end of the experiments showed that there was a shift of the spectrum towards lower energies. This was attributed to a decrease in the pulse height caused by radiation damage produced in the detectors by the fast neutrons. This part of the data has not been included in the spectrum of alpha particles reported here but has been included for determining

the relative probability of binary and ternary fissions, which was found to be independent of the shift observed.

A similar setup was used to determine the relative probability of binary and ternary fissions in the thermal fission of U^{235} using the thermal column of the reactor APSARA.

EXPERIMENTAL RESULTS

The anisotropy of the angular distribution $[N_\alpha(0°)/N(90°)]$ was obtained by considering the spectrum of alpha particles above 8 MeV in both the 0° and 90° directions. This value was found to be equal to 1.27 ± 0.25 and 1.33 ± 0.13 before and after the interchange of the 0° and 90° detectors respectively, and the average value of the anisotropy was found to be 1.32 ± 0.12. This value of anisotropy is smaller than that observed in the case of 14-MeV neutron-induced fission of U^{238} [5].

The observed energy spectrum of the long-range alpha particles in the 3-MeV neutron fission of U^{235} has been corrected for the loss of energy in the aluminium backing of the target, using the published curves for the energy loss in aluminium [6]. The corrected spectrum is shown in Fig. 2 together with the spectrum of the long-range alpha particles in pile neutron fission of U^{235} as observed by FULMER and COHEN [7]. The two spectra are almost similar and extend over the energy region 8–29 MeV. The maximum energy of the alpha particles observed in the present work was 28.5 MeV. The

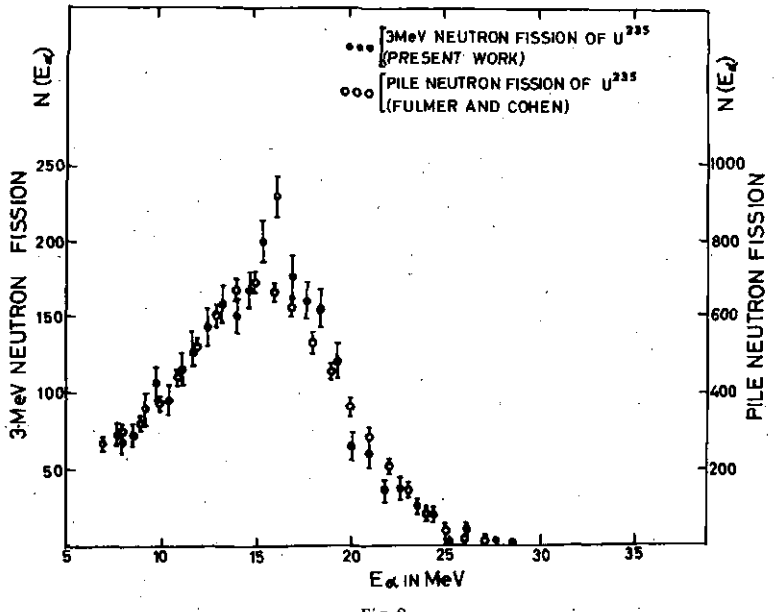

Fig. 2

The spectrum of long-range alpha particles emitted in 3-MeV neutron fission of U^{235}. For comparison the long-range alpha spectrum in pile neutron fission of U^{235} observed by FULMER and COHEN [7] is also shown.

peak of the long-range alpha particles in 3-MeV neutron fission of U^{235} is between 15 and 17 MeV compared with that in the pile neutron fission of U^{235}, which is about 15 MeV. Although the statistical errors are large the shift of the peak to higher energy in fast fission is noticeable. The full width at half maximum of the alpha particle spectrum in 3-MeV neutron fission of U^{235} was found to be equal to about 8.5 MeV, whereas the full width at half maximum of the alpha particle spectrum in pile neutron fission of U^{235} is about 10.5 MeV [7]. PERFILOV et al. do not, however, find any appreciable change in width in 14-MeV neutron-induced fission of U^{238} compared with that in the thermal-neutron fission of U^{235} [2]. However, they find that the width of the alpha particle spectrum in uranium fission is larger than that in plutonium isotopes, the peak of the spectrum in plutonium being at about 17-MeV compared with that of thermal fission of U^{235}, which is at about 15.5 MeV [8].

In the present experiment, about 2760 events of ternary fission were recorded and the probability ratio of binary to ternary fission was found to be $(780 \pm 15):1$. In the thermal fission of U^{235} about 6600 ternary fission events were recorded and the relative probability of binary and ternary fission was estimated to be $(650 \pm 10):1$. The errors quoted are statistical errors only and do not include any possible errors in the corrections made for the geometry employed, which are expected to be higher. A rough estimate would place the maximum possible error due to the latter at about 10%. These measurements indicate, however, that the ratio of binary to ternary fission increases with increasing energy of the incident neutrons.

DISCUSSION

Anisotropy of angular distribution of alpha particles

In the 14-MeV neutron-induced fission of U^{238} the angular distribution of alpha particles with respect to the incident beam direction shows a forward-backward peaked distribution, symmetric about 90°, which is characteristic of the particles evaporated from a compound nucleus having a large angular momentum [5]. The anisotropy is much larger than predicted by the statistical theory of evaporation of particles, and was attributed to neutron emissions from the compound nucleus before alpha emission. In the present experiment for the fission of U^{235}, the excitation energy of the compound nucleus U^{236} is less than the second-chance fission threshold. The measured anisotropy of $32 \pm 12\%$ is in quantitative agreement with the value predicted by the statistical theory of evaporated particles. The angular distribution of the particles evaporated from a compound nucleus having an angular momentum I is given by the statistical theory [9] to be

$$N(\theta) \approx 1 + \frac{\alpha^2 \overline{I^2}\,\overline{I^2}}{2} \cos^2\theta \qquad (1)$$

where $\overline{I^2}$ is the average angular momentum of the evaporated particles, $\overline{I^2}$

is the average angular momentum of the compound nucleus suitably weighted, and

$$\alpha = \hbar^2 / 2JT$$

where J and T are the moment of inertia and temperature respectively of the emitting compound nucleus.

With the use of the sharp cut-off approximation, $\overline{I^2}$ and $\overline{l^2}$ can be computed from the relations

$$\overline{I^2} = \frac{\mu_1 E_1 R_1^2}{\hbar^2} \text{ and } \overline{l^2} = \frac{2\mu_2 T R_2^2}{\hbar^2} \tag{2}$$

where μ_1, E_1, R_1 represent the mass and energy of the incident particle and the interaction radius respectively, and μ_2, R_2 and T represent the mass of the emitted particle interaction radius and the temperature of the emitting nucleus respectively.

The anisotropy calculated using the rigid body moment of inertia is very small compared with the observed values. However, from an analysis of the experimental data on the angular distribution of the fission fragments in the 3-MeV neutron fission of U^{235}, $K_0^2 = JT/\hbar^2$ was found to be equal to about 12 [10]. If this value is used to calculate α^2, the expected anisotropy is about 10-25% depending on the value of γ_0, to which parameter this value is very sensitive. Considering the approximations made in calculating I^2 and l^2 the calculated anisotropy is, therefore, in good agreement with the measured anisotropy of 32 ± 12%. If K_0^2 in the 3-MeV neutron fission of U^{235} and 14-MeV neutron fission of U^{238} is assumed to be nearly of the same value, because of the emission of neutrons prior to fission in the latter case, the value of anisotropy calculated using the formulae (1) and (3) turns out to be in agreement with the value measured in Ref. [5] within the errors of measurement. The anisotropy in the case of 14-MeV neutron fission was obtained by superposing the data for angles below and above 90°. These measurements, therefore, support the hypothesis that the alpha particles in fission are evaporated from a highly deformed compound nucleus before scission.

Spectrum of the long-range alpha particles

According to the statistical theory of evaporation of particles the spectrum of the emitted particles is given by

$$N(E) = \text{Const. } E\, \sigma_c(E)\omega(E^* - E) \tag{3}$$

where $\sigma_c(E)$ is the cross-section for the inverse reaction, E^* is the excitation energy of the compound nucleus, and $\omega(E^*-E)$ is the density of states of the residual nucleus.

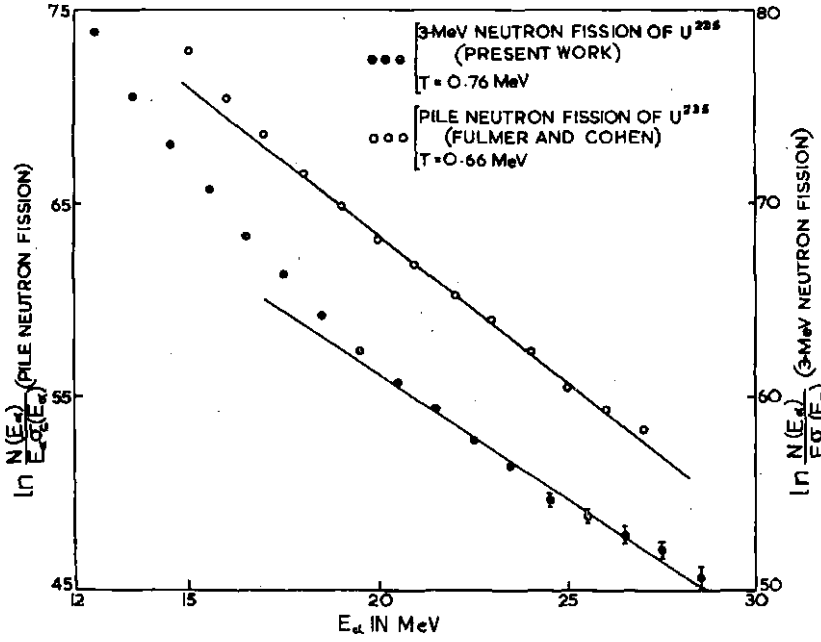

Fig. 3

A plot of $\ln[N(E_\alpha)/E_\alpha\sigma_c(E_\alpha)]$ versus E_α for the long-range alpha particles emitted in 3-MeV neutron and pile neutron fission of U^{235}. $\sigma_c(E_\alpha)$ was computed for a spherical nucleus with $\gamma_0 = 1.2$ fermis.

The nuclear temperature T is defined as

$$\frac{1}{T} = (d/d(E^* - E))\ln \omega(E^* - E) = (-d/dE)[\ln(N(E)/E\sigma(E))] \tag{4}$$

and T can be obtained by plotting $\ln[N(E)/E\sigma_c(E)]$ versus E. Using the numerical calculations of $\sigma_c(E)$ for a spherical nucleus with $\gamma_0 = 1.2$ fermis, it was found that the high-energy part of the alpha spectra corresponds to nuclear temperatures of 0.76 ± 0.04 and 0.66 ± 0.03 MeV in the 3-MeV and pile neutron fission of U^{235} respectively (see Fig. 3). The temperature for the pile neutron fission alpha spectrum in the latter case is in agreement with the temperature T_D in Ref. [5]. The temperature in the case of 3-MeV neutron fission is found to be about 15% higher than that in the case of pile neutron fission of U^{235}. With the assumptions made above this shows that the temperature depends on the excitation energy and in particular increases with the incident energy. The peak of an evaporation spectrum depends on the temperature of the nucleus, and the slight shift of the peak towards higher energy observed in the 3-MeV neutron-fission alpha spectrum compared with that in the pile neutron-fission spectrum is probably caused by the relatively higher temperature in the former case.

It is interesting to correlate the emission of the long-range alpha particles and the pre-scission neutrons emitted in the thermal-neutron fission of U^{235} [11] and in the spontaneous fission of Cf^{252} [12]. It was found that

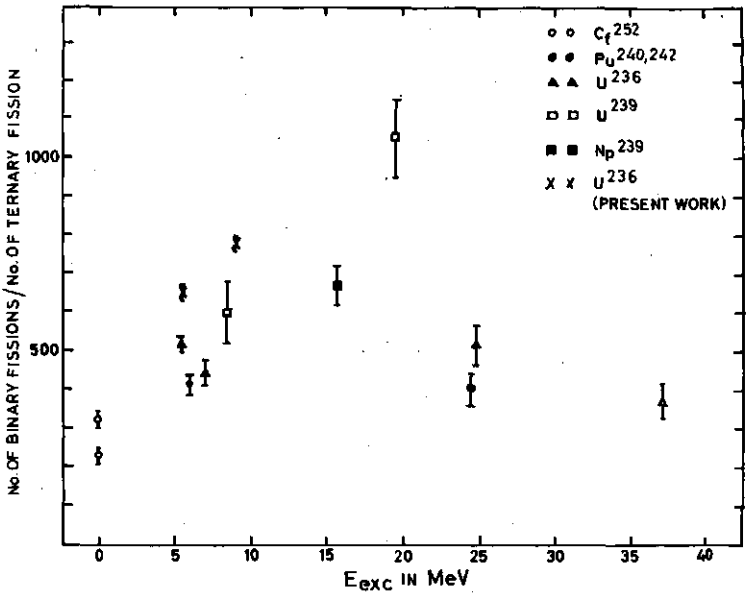

Fig. 4

The ratio of number of binary fissions to the number of ternary fissions versus the excitation energy of the fissioning nucleus. The points refer to the work of various authors [1-4, 13] and the present work.

the pre-scission neutrons have an evaporation-type spectrum with a temperature of about 1.6 MeV indicating that alpha particle and neutron emission are competing modes of de-excitation of the compound fissioning nucleus prior to scission.

Relative probability of ternary and binary fission

The ratio of probabilities of binary and ternary fission in the thermal- and 3-MeV neutron-induced fission of U^{235} shows that the ratio of probabilities increases as the excitation energy of the compound nucleus U^{236} increases. This is in agreement with previous measurements and Fig. 4 gives the variation of this probability with excitation energy. In the region of excitation energy investigated in the present experiment second-chance fissions are energetically not possible, and therefore these results show that for the same compound nucleus the ratio of binary to ternary probability increases with excitation energy. On this basis the ratio should decrease rapidly at those excitation energies where second-chance and higher-chance fissions are energetically possible. The data so far obtained is inconclusive. The ratio, however, increases as the excitation energy is increased to 20 MeV. The increase in the ratio of binary to fission probabilities with the increase of excitation energy of the compound nucleus is probably connected with one of the following processes:

(i) There is some indication, as noted above, that long-range alpha-particle emission and pre-scission neutron emission are competing modes, and a dependence of this competition on the excitation energy of the compound

nucleus could explain the observed dependence of the ratio of binary to ternary fission probabilities on the excitation energy. (ii) The presence of large angular momentum of the compound nucleus in those cases where high-energy incident particles are involved may result in the decrease in the probability of alpha emission [13]. (iii) According to the evaporation theory of alpha emission, the particles are emitted from the neck region where the barrier is depressed. If the probability of occurence of alpha-particle clusters in this region decreases with the excitation energy of the fissioning nucleus, the observed decrease in relative ternary probability with excitation energy follows at once.

In conclusion, the results of the present investigation show that the observed anisotropic angular distribution of the long-range alpha particles with respect to the incident neutron direction, the energy spectra of alpha particles in the pile neutron and 3-MeV neutron fission of U^{235} and the observed increase in the ratio of binary to ternary relative probability with the initial excitation energy can be understood by the mechanism that the alpha particles are evaporated before scission. The low-energy part of the alpha-particle spectrum has been accounted for on the basis of charge polarization in the fissioning nucleus [5], and it can be shown that the recent experimental observations on the angular correlation of the alpha particles and the fission fragments [14] are not inconsistent with the evaporation mechanism discussed above.

ACKNOWLEDGEMENTS

Our thanks are due to B.R. Ballal, S.R.S. Murthy and S.L. Raote for help in carrying out the experiment, and to Dr. S.S. Kapoor for helpful discussions. We also thank R. Rangarajan for computing $\sigma_c(E)$ and the Radiochemistry Division for preparing the uranium foils.

REFERENCES

[1] PERFILOV, N.A., ROMANOV, Yu.F. and SOLOVEVA, Z.I., Soviet Phys. Usp. 3 (1961) 542.
[2] PERFILOV, N.A., SOLOVEVA, Z.I. and FILOV, R.A., Soviet Phys.-JETP 14 (1962) 7.
[3] PERFILOV, N.A. and SOLOVEVA, Z.I., Soviet J. atomic Energy 5 (1958) 175.
[4] NOBLES, R.A., Phys. Rev. 126 (1962) 1508.
[5] RAMANNA, R., NAIR, K.G. and KAPOOR, S.S., Phys. Rev. 129 (1963) 1350.
[6] WHALING, W., Handbuch der Physik, (S. FLUGGE, Ed.) Springer-Verlag, Berlin (1957).
[7] FULMER, C.B. and COHEN, B.L., Phys. Rev. 108 (1957) 370.
[8] PERFILOV, N.A., SOLOVEVA, Z.I., FILOV, R.A. and KHLEZNIKOV, G.I., Soviet Phys.-JETP 17 (1963) 1232.
[9] ERICSON, T. and STRUTINSKI, V., Nucl. Phys. 8 (1958) 284.
[10] SIMMONS, J.E. and HENKEL, R.L., Phys. Rev. 120 (1960) 198.
[11] KAPOOR, S.S., RAMANNA, R. and RAMA RAO, P.N., Phys. Rev. 131 (1963) 283.
[12] BOWMAN, H.R., THOMPSON, S.G., MILTON, J.C.D. and SWIAKECKI, W.J., Phys. Rev. 126 (1962) 2120.
[13] COLEMAN, J.A., FAIRHALL, A.W. and HALPERN, I., Phys. Rev. 133 (1964) B724.
[14] FRAENKEL, Z. and THOMPSON, S.G., Phys. Rev. Lett. 13 (1964) 438.

DISCUSSION

F. NETTER: I understand that no measurements were made on U^{238} + n in these investigations. My impression is that the points on Fig. 4 of the paper are not very coherent. According to our measurements made at the time of the 2nd Geneva Conference (1958)[1], the ratio of binary to ternary fission for U^{238} + 2- or 3-MeV neutrons is clearly higher than indicated in Fig. 4 compared with U^{235} + neutrons of the same energy.

D.M. NADKARNI: Our paper reports only on the 3-MeV fission of U^{235} and not on the fission of U^{238} and so I believe that the points are coherent. In the paper the results are reported for two different excitations of the same compound fissioning nucleus and they are therefore more helpful for the purpose of discussing the variation of the binary/ternary ratio with excitation energy. However, the absolute values are about 10-15% higher than the values obtained by other investigators; the reasons for this are discussed in the paper.

[1] NETTER, F. et al., Proc. 2nd UN Int. Conf. PUAE 15 (1958) 418.

TERNARY FISSION*

M.L. MUGA
DEPARTMENT OF CHEMISTRY AND DEPARTMENT OF PHYSICS,
UNIVERSITY OF FLORIDA, GAINESVILLE, FLA.
UNITED STATES OF AMERICA

Abstract — Résumé — Аннотация — Resumen

TERNARY FISSION. The fission process in which heavy nuclei fragment into three large charged particles, in place of the usual two, has been studied in the case of thermal-neutron-induced fission of U^{235} and the spontaneous fission of Cf^{252}. Solid-state detectors, a fast triple coincidence system and a three-coincident-parameter analyser were used to measure the three fission fragment energies parallel with the detection of each ternary fission event. Experimental evidence is presented supporting the existence of ternary fission by specifically excluding recoil phenomena and accidental events as contributing to the observed three-fold coincidence events.

Mass-energy-angular correlations of ternary fission have been determined and are summarized as follows: The total kinetic energy release in ternary fission appears to be slightly higher (by approximately 10 MeV) than that for binary fission. In the case of the spontaneous ternary fission of Cf^{252}, the frequency of occurrence is observed to be greater than 2.2×10^{-6} ternary fission events per binary fission event. Tripartition of Cf^{252} results preferentially in division into two medium mass particles (one of which has a mass number near 56) and one larger mass. In the case of thermal-neutron-induced fission of U^{235}, the frequency of occurrence is observed to be greater than 1.2×10^{-6} ternary fission events per binary fission event. Ternary fission of U^{236*} results in the formation of one light fragment (near mass 36) and two large fragments or, as in the case of Cf^{252}, two medium fragments and one large one. These results indicate that axially asymmetric distortion modes are possible in the pre-scission configurations of the fissioning nucleus. A description is given of experiments designed to radiochemically detect the light fragment resulting from ternary fission.

FISSION TERNAIRE. Le processus de fission au cours duquel un noyau lourd se scinde en trois grandes particules chargées a été étudié dans le cas de la fission de ^{235}U par neutrons thermiques et dans celui de la fission spontanée de ^{252}Cf. En utilisant des détecteurs à semi-conducteurs, un ensemble rapide à triple coïncidence et un analyseur à trois paramètres coïncidents, l'auteur a procédé à la mesure des énergies des trois fragments de fission parallèlement à la détection de chaque événements de fission ternaire. Il présente des preuves expérimentales qui sont en faveur de l'existence d'une fission ternaire, car elles excluent la possibilité que des phénomènes de recul et des phénomènes fortuits contribuent aux événements à triple coïncidence observés.

L'auteur a déterminé, pour la fission ternaire, les corrélations angle-énergie-masse qui peuvent se résumer comme suit: l'énergie cinétique totale libérée dans une fission ternaire semble être légèrement plus grande (de 10 MeV environ) que dans la fission normale. Dans le cas de la fission ternaire spontanée de ^{252}Cf, la fréquence observée des événements de fission ternaire dépasse $2,2 \cdot 10^{-6}$ par fission normale. La tripartition de ^{252}Cf donne lieu le plus souvent à une répartition des masses entre deux particules de masse moyenne (dont l'une a un nombre de masse voisin de 56) et une autre de masse plus grande. Dans le cas de la fission de ^{235}U par neutrons thermiques, on constate que la fréquence des événements est supérieure à $1,2 \cdot 10^{-6}$ événements de fission ternaire pour un événement de fission normale. La fission ternaire du noyau composé $^{236}U^*$ donne lieu à la formation d'un fragment léger (ayant un nombre de masse voisin de 36) et de deux fragments lourds ou, comme dans le cas de ^{252}Cf, de deux fragments moyens et d'un autre plus grand. Ces résultats indiquent que des modes de distorsion asymétriques par rapport à l'axe peuvent intervenir dans les configurations qui précèdent la scission d'un noyau subissant la fission. L'auteur décrit des expériences conçues pour déceler par voie radiochimique le fragment léger résultant d'une fission ternaire.

ДЕЛЕНИЕ ЯДРА НА ТРИ ЧАСТИ. Процесс деления, при котором тяжелые ядра расщепляются на три крупные заряженные частицы, вместо обычных двух, изучался в отношении

* The work was supported in part by the United States Atomic Energy Commission.

деления урана-235 под действием тепловых нейтронов, а также в отношении спонтанного деления калифорния-252. С помощью кристаллических детекторов, быстрой тройной схемы совпадений и анализатора параметров тройных совпадений измерялась энергия трех осколков деления одновременно с обнаружением каждого акта деления. Представляются экспериментальные данные, которые доказывают существование деления на три части путем специального исключения явлений отдачи и случайных актов, как способствующих наблюдаемым актам тройных совпадений.

Корреляция между массой, энергией и углом для деления на три части определены и полученные результаты суммированы следующим образом: общее выделение кинетической энергии при делении на три части, по-видимому, несколько выше (примерно на 10 Мэв), чем при делении на две части. В отношении спонтанного деления ядра калифорния-252 на три части наблюдаемая частота деления больше, чем $2,2 \cdot 10^{-6}$ актов деления на три части на один акт деления на две части. Результатом деления ядра калифорния-252 на три части является деление на две частицы средней массы (одна из которых имеет массовое число, близкое к 56) и одну частицу с большей массой. В отношении деления ядра урана-235 под действием тепловых нейтронов частота деления больше, чем $1,2 \cdot 10^{-6}$ актов деления на три части на один акт деления на две части. Результатом деления ядра урана-236 на три части является образование одного легкого осколка (близкого к массе 36) и двух крупных осколков или, в отношении калифорния-252, – двух средних осколков и одного большого осколка. Эти результаты говорят о том, что аксиально асимметричные искажения возможны при конфигурациях расщепляющихся ядер перед делением. Описываются эксперименты, которые были проведены для радиохимического обнаружения легкого осколка, образующегося в результате деления ядра на три части.

LA FISION TERNARIA. El proceso de fisión en el que los núcleos pesados se escinden en tres grandes partículas cargadas, en lugar de las dos habituales, se ha estudiado en el caso de la fisión del ^{235}U inducida por neutrones térmicos y de la fisión espontánea del ^{252}Cf. Las energías de los tres fragmentos de fisión se miden, paralelamente a la detección de cada suceso de fisión ternaria, con ayuda de detectores sólidos, un sistema rápido de coincidencia triple y un analizador de parámetros de tricoincidencia. Se presentan pruebas experimentales que confirman la existencia de la fisión ternaria, pues se excluyen específicamente los fenómenos de retroceso y los sucesos fortuitos capaces de contribuir a los sucesos de coincidencia triple observados.

Las correlaciones angulares de masa y energía en la fisión ternaria determinadas por el autor se resumen como sigue: la energía cinética total liberada en la fisión ternaria parece ser ligeramente superior (en unos 10 MeV) a la que corresponde a la fisión binaria. En el caso de la fisión ternaria espontánea del ^{252}Cf, la frecuencia observada es superior a $2,2 \cdot 10^{-6}$ sucesos de fisión ternaria por cada fisión binaria. La escisión del ^{252}Cf en tres fragmentos suele originar dos partículas de masa media (el número másico de una de ellas es del orden de 56), y una tercera de masa mayor. Tratándose de la fisión del ^{235}U inducida por neutrones térmicos, la frecuencia observada es superior a $1,2 \cdot 10^{-6}$ sucesos de fisión ternaria por cada fisión binaria. La fisión ternaria del $^{236}U^*$ da como resultado la formación de un fragmento ligero (número másico 36, aproximadamente) y de dos fragmentos grandes o, como en el caso del ^{252}Cf, de dos fragmentos medios y de uno grande. Estos resultados indican la posibilidad de que existan modos de distorsión axialmente asimétricos en las configuraciones del núcleo previas a la escisión. Se describen experimentos encaminados a identificar por vía radioquímica el fragmento ligero resultante de la fisión ternaria.

INTRODUCTION

The study of the fission process in which heavy nuclei fragment into three large charged particles offers a new approach to gain additional insight into nuclear deformations just before the scission act. Although examples of this process have been previously reported [1 - 5] for fission at low excitation energies, only recently [6] has direct and unambiguous experimental evidence been shown to preclude other nuclear processes (scattering, accidental counts) as responsible for the observed phenomenon. Because the existence of ternary fission has not been generally accepted, the in-

vestigations initiated in this laboratory are planned to achieve the following goals: to establish with confidence the existence of ternary fission, to study the mass-energy-angular correlations of tripartite mass division in the fission process, and to apply these data in developing a model (theory) for better understanding of the binary and ternary fission process. It seems appropriate at this date to present a summary of current results based on a study of the spontaneous ternary fission of Cf^{252} ($Cf^{252} \rightarrow TF$) and the neutron-induced ternary fission of U^{235} ($U^{235} + n_{th} \rightarrow TF$).

The fission process considered in this work (tripartition into three comparable mass fragments) should not be confused with the more frequently occurring and well-established fission process in which a light charged particle (predominently an alpha particle) is simultaneously emitted. Because this latter phenomenon appears to be associated closely with the binary fission process, it is proposed that the term alpha fission (α-fission) be given to this process and the term ternary fission (TF) be reserved for fission into three large charged fragments.

EXPERIMENTAL

A prime requisite of these experiments is the simultaneous detection and energy measurement of the three fragments resulting from tripartition, for only under these conditions can pertinent information (e.g. mass distribution), be derived concerning pre-scission distortion modes in the fission process. The experimental arrangement (Fig. 1) consisted of three solid-state detectors positioned approximately 120° apart in a plane about a fission source. The detectors and source were enclosed in an evacuated aluminium chamber with provisions for externally adjusting the angular position of at least two of the three detectors. The chamber (see Fig. 2) used in the U^{235} experiments was placed in the thermal column (intercepting a flux of approximately 10^9 n/cm^2 · s) of the University of Florida Training Reactor (UFTR). The radial position of the detectors (3.0 and 4.0 cm for Cf^{252}; 1.0 and 1.5 cm for U^{235}; see Fig. 1) corresponded to a range of subtended solid angles from about 0.2 to 0.4 sr. The detectors were of the surface barrier type fabricated from 300 Ωcm silicon with a sensitive area of approximately 4 cm^2 (2.3-cm diam.) as used in the Cf^{252} experiments and 0.25 cm^2 (5 mm × 5 mm squares) as used in the U^{235} experiments. Normally, the detectors were operated at 30-V back-bias voltage and were replaced before the back-bias current exceeded 10 μA.

The Cf^{252} sources were prepared on 70 μg/cm^2 aluminium oxide supporting foil (2×10^5 fissions/min) and on 100 μg/cm^2 beryllium foil (2×10^6 fissions/min) by the self-transfer method. The active deposit was collimated to a 3/8-in diam. circular area.

The U^{235} sources of uniform thickness were prepared by slowly evaporating (in vacuum) $U^{235}F_4$ on to (60 μg/cm^2) nickel foil or (10 μg/cm^2) VYNS [7] film. The uranium (IV) fluoride deposit was confined to a circular area of 3/32-in diam. by a collimating system. Sources ranging up to 300 μg/cm^2 thickness were fabricated.

The schematic of the basic electronic recording system is shown in Fig. 3. The output from each of three solid-state detectors is paralleled

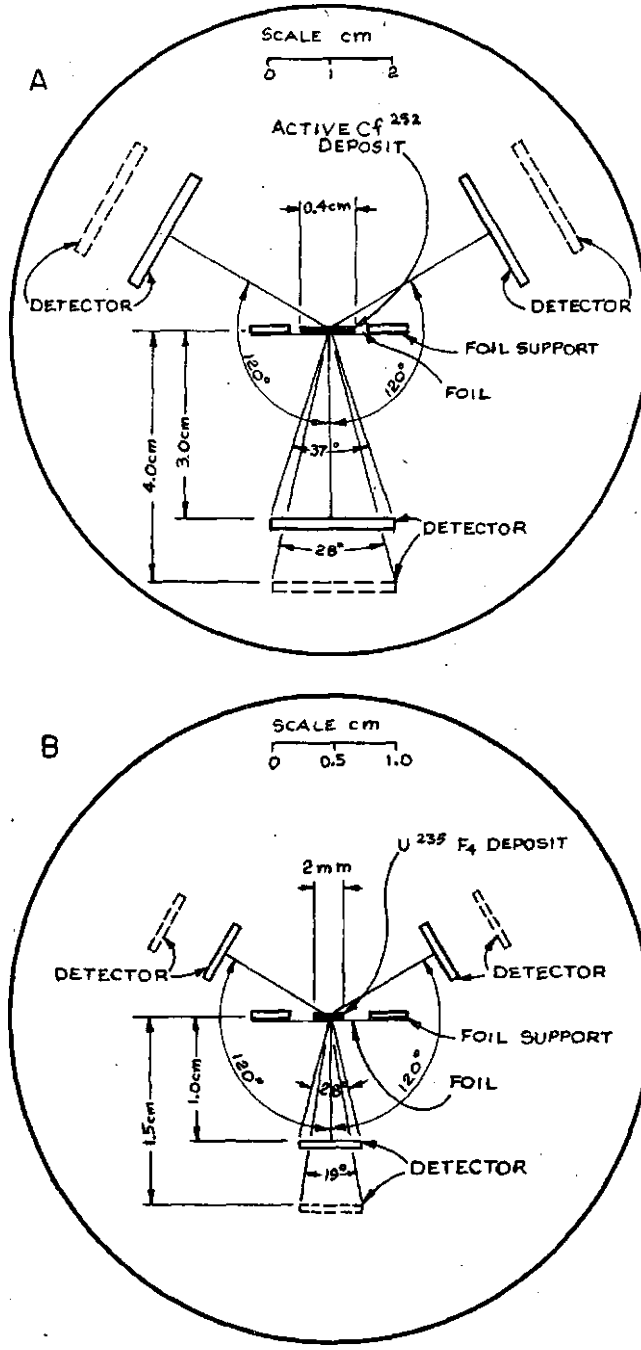

Fig. 1

Scale drawing of the geometrical arrangement of detectors and fission source in the ternary fission of (a) Cf^{252} and (b) $U^{235} + n_{th}$

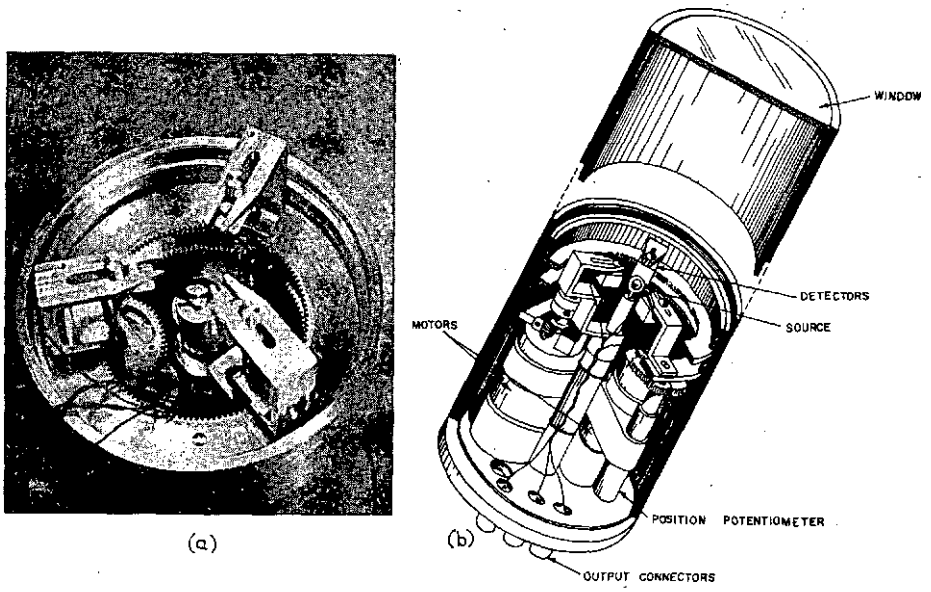

Fig. 2

Ternary-fission chamber used in U^{235} experiments. The chamber is less than 4-in diam. for insertion in the thermal column of the University of Florida Training Reactor (UFTR).
(a) Photograph of top view; detectors are not mounted.
(b) Cut-away diagram of chamber showing motors and gears.
Charge-sensitive "Nuvistor" pre-amplifiers are attached to output connectors.

to two amplifier systems, one of which (linear or slow amplifier) conserves linear response of the detector pulse, the other (fast amplifier) preserves a fast rise time. The leading edge of the latter pulse is used to trigger a 5 - 120 ns pulse that in turn is applied to a three-fold fast coincidence circuit. The coincidence output serves to open three linear gates, allowing the outputs of the three linear amplifiers to pass through for subsequent analysis. One pulse is immediately analysed; the other two pulses are temporarily stored in the buffer storage (pulse stretcher) unit, and are sequentially released and analysed. Upon completion of this three-stage digital conversion, automatic readout on punched paper tape is achieved. The resulting data was subsequently transferred to cards for data reduction using the University of Florida IBM 709 computer and facilities. This instrumentation and the experimental arrangement differ from previously used methods in that nanosecond triple coincidence time resolution is used to distinguish ternary fission events from accidentals, an energy analysis of the three fragment energies is simultaneously conducted in parallel with the detection of the ternary fission events, and the solid angle subtended by each detector is better defined.

Calibration of the detectors was achieved by recording the binary-fission-fragment kinetic energy spectrum at suitable intervals during the experiment. These spectra were compared with that from time-of-flight data [7, 8] and linear extrapolation to lower energies was made using the average light- and heavy-mass energy positions.

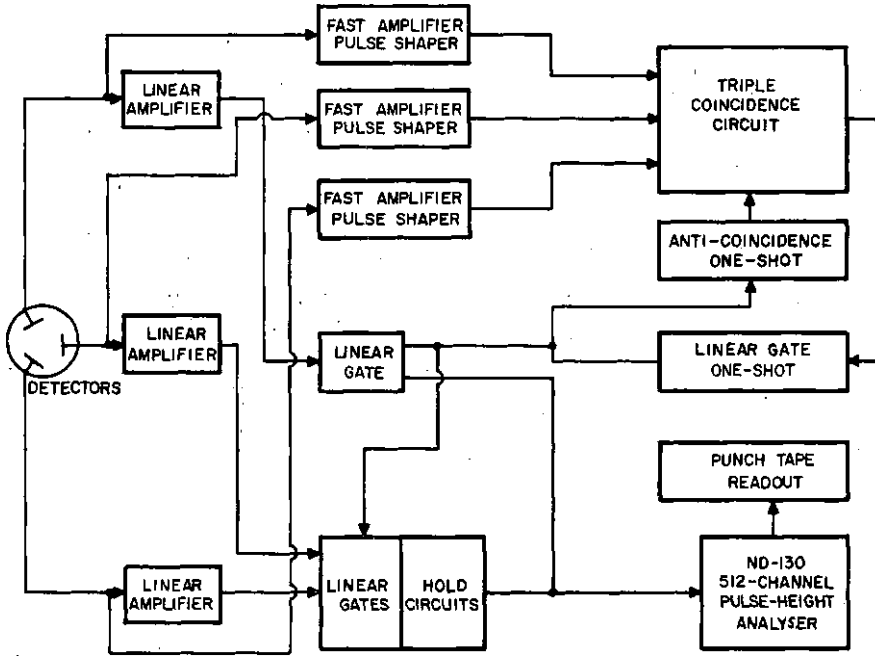

Fig. 3

Simplified block diagram of electronic recording instrumentation. Automatic gain stabilizer units were installed in the linear amplifier channels during the latter portion of these experiments. The basic recording instrument consists of a three-coincident-parameter analyser having 256 x 256 x 256-channel resolution.

The Cf^{252} experiments lasted several months during which four sets of detectors were used. Single count-rates from 250 to 800 counts/s were observed depending on the source strength and radial position of the detectors. A triple coincidence count-rate of about 0.1 - 0.5 counts/h was recorded; approximately 400 ternary-fission events were registered. Daily adjustment of the back-bias voltage across the detectors was necessary to maintain proper amplification and minimum shift in gain. A gain shift of more than 10 channels (~5 MeV) was rarely encountered between successive calibrations; most shifts were less than 6 channels for the light-fragment energy peak; the heavy-fragment energy peak experienced smaller gain shifts.

For the U^{235} experiments, single count-rates were varied from as low as 250 counts/s to a maximum of 18 000 counts/s. Deterioration of the detectors (in the form of pulse-height gain shifts) was quite noticeable for the higher count-rates; typically, however, a single count-rate of 2000 - 3000 fission counts/s was used. In each case the double coincidence count-rate (between any two detectors) was consistent with that expected for independent binary accidental events.

In later stages of these investigations, a zero cross-over technique was used to improve the triple coincidence resolution, and automatic gain stabilizers [9] were used on all three channels to ensure a constant energy

calibration in the linear amplifier systems. Under these conditions, no gain shifts were observed and calibration runs were necessary only at the beginning and end of an experiment.

In the data reduction process, events for which any one detector registered less than 16 channel numbers were discarded. Long-range alpha particles (from the fission process) saturated the detector depletion layer with pulse-heights corresponding to from 8 to 14 channel numbers, and hence their interference was eliminated. Events with channel numbers less than 25 were few.

RESULTS AND DISCUSSION

In the first part of this section results obtained from the Cf^{252} experiments are presented, followed by those from $U^{235} + n_{th}$ experiments, and lastly a discussion.

Spontaneous ternary fission of Cf^{252}

The frequency of occurrence for ternary fission of Cf^{252} was recorded as 1.1×10^{-6} /binary fission event. This value, representing a lower limit, and corrected for geometrical efficiency, is less than the value of four possible events per 120 000 binary events reported [5] using nuclear emulsion techniques.

The total fragment kinetic energy release in ternary fission is of major interest and is shown in Fig. 4. Figure 4a represents data taken with rather poor coincidence resolution (~ 20 ns); Fig. 4b represents data gathered with a resolution of 10 ns. Both sets of data were taken with the 70 $\mu g/cm^2$ Al_2O_3 backed source and with the detectors at 3 cm from the source (see Fig. 1). It is readily seen that the higher-energy (> 240 MeV) component, interpreted as representing accidental counts, is enhanced for the poorer resolution data. These accidental events are most probably caused by the triggering of two detectors by a single binary fission event and the third detector by a single fragment from an independent binary event. These binary coincidences arise from two possibilities. Since the detectors subtend a rather large solid angle, a slight "overlap" of the active area on the source foil will allow single binary events to trigger two detectors. The major contribution, however, arises from physical "carry-over" (self transfer) of the active Cf^{252} on to the surface of the detectors. Following this self transfer, fission of the Cf^{252} will trigger the detector on to which it has been newly deposited; the complementary fragment may then enter one of the other two detectors. That this effect is real, is shown by the gradual increase (in time) of the binary count-rate (between any two detectors) after a new set of detectors has been installed. Accidentals caused by three independent binary fission events are negligible for the single detector count-rates (~ 300 counts/s) observed and is calculated to be of the order of 10^{-8}/s. (Accidental count-rate $R_{123} = 4R_1R_2R_3\tau^2$, where R_1, R_2, R_3 are single count-rates of detectors 1, 2, 3 respectively, and τ is the coincidence resolution time.) The average total kinetic energy release in ternary fission of Cf^{252}

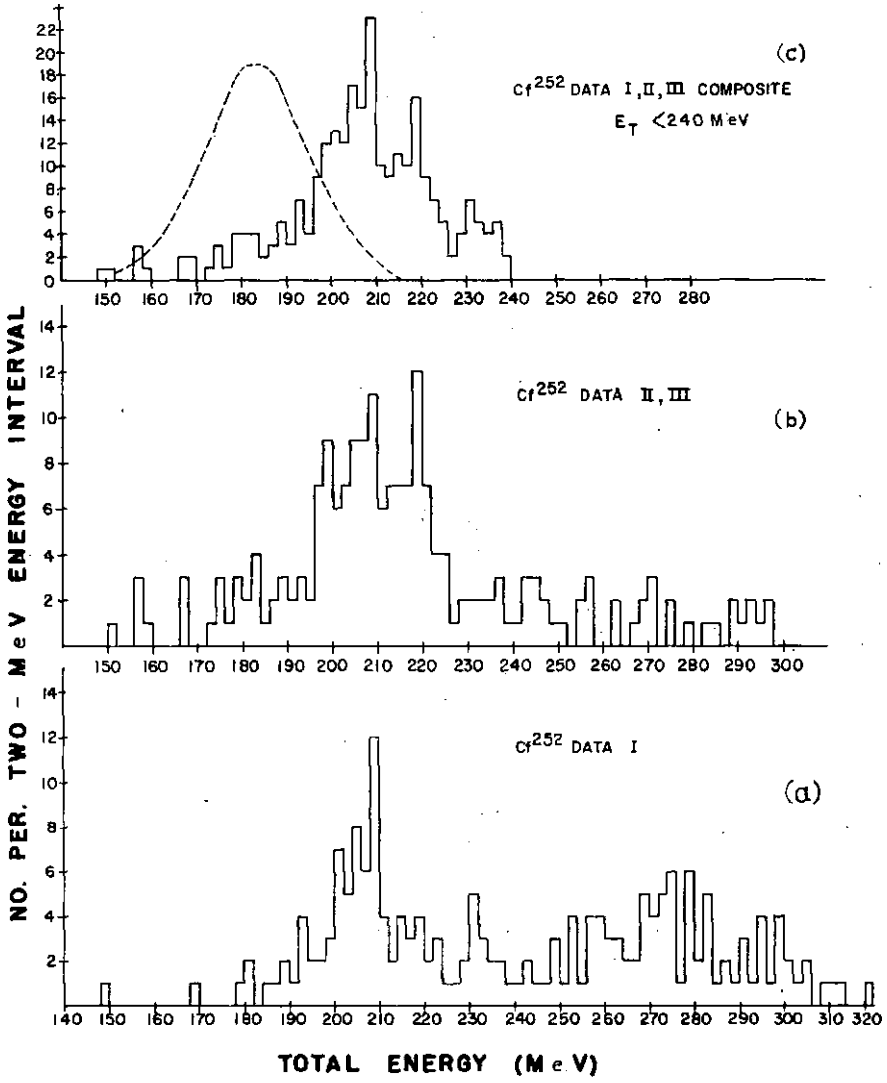

Fig. 4

Total fragment kinetic energy spectrum for triple coincidence events from fission of Cf^{252}.
(a) Data taken with triple coincidence resolution of 20 ns.
(b) Data taken with 10-ns resolution.
(c) Composite of data in (a) and (b) for total fragment kinetic energy less than 240 MeV.
The dashed line represents the total fragment kinetic energy spectrum (arbitrary scale) for binary fission of Cf^{252} as taken from Ref. [8] and as reproduced in these experiments.
The source is mounted on (70 μg/cm²) Al_2O_3 support foil.

is measured as 206 MeV (disregarding all events with total kinetic energy greater than 240 MeV)[1], a value 21 MeV higher than that for binary fission

[1] Events with E_t > 240 MeV are excluded because they appear to originate from accidental counts (Fig. 4a, b), and the mass-energy conversion available does not exceed a value of about 240 MeV.

(Fig. 4c). However, the method of calibration (using the average light- and heavy-mass energy positions) will tend to assign higher energy values [10] to the smaller mass particles formed in ternary fission, hence, these values should be considered as upper limits for the average total kinetic energy release.

The single fragment kinetic energy spectrum (Fig. 5b) is featured by one maximum at about 41 MeV and additional maxima centred at 71 MeV

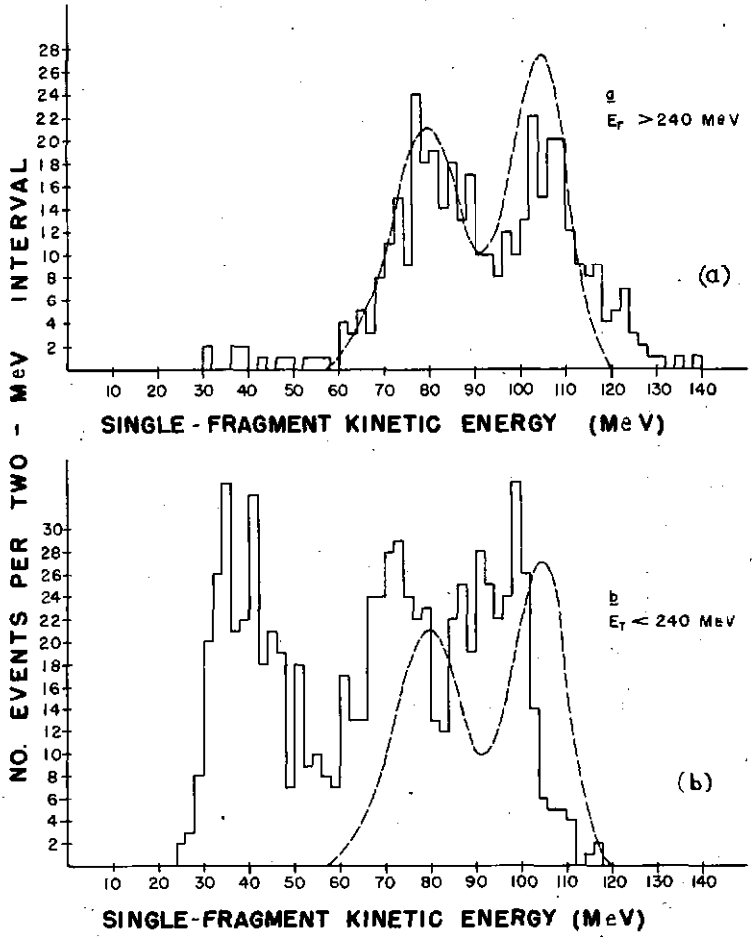

Fig. 5

Single fragment kinetic energy spectrum of triple events for which (a) total kinetic energy E_t > 240 MeV and (b) E_t < 240 MeV.
The dashed line represents the individual binary fission-fragment spectrum (arbitrary scale) as obtained in Ref. [8] and as reproduced in these experiments.
The Cf^{252} source is mounted on (70 μg/cm²) Al_2O_3 support foil.

and 94 MeV. The individual kinetic energy spectrum showing the contribution of the low-, median- and large-energy fragments is presented in Fig. 6. If we assume that scattering by either the light- or heavy-mass fragments

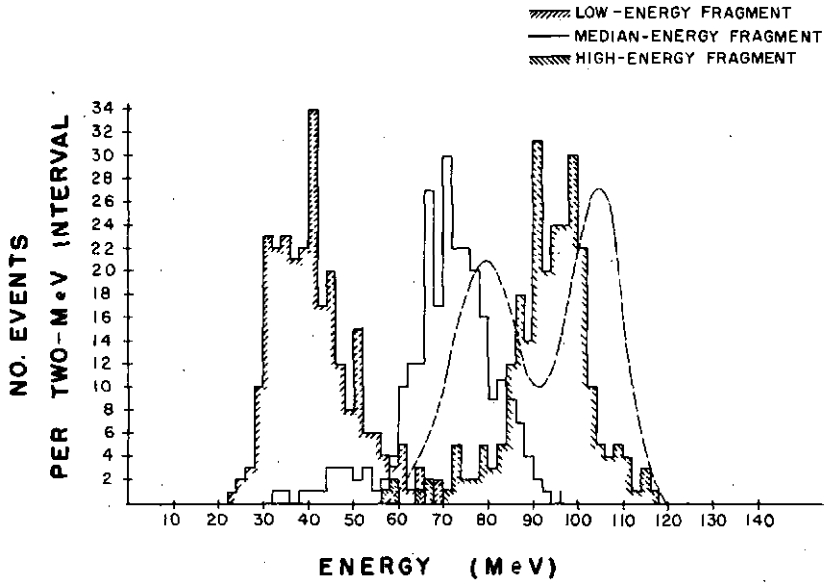

Fig. 6

Individual fragment kinetic energy spectra for ternary fission of Cf^{252}. The dashed line represents the single fragment kinetic energy spectrum (arbitrary scale) for binary fission of Cf^{252} as reported in Ref. [8] and as reproduced in these experiments. The source is mounted on (70 $\mu g/cm^2$) Al_2O_3 support foil.

of binary fission events gives rise to these events, then one should expect either the scattered fragment or recoil nucleus (or both) to have the lower peak energy (centred at 41 MeV); the complementary (unscattered) fission fragment should then be registered with an energy corresponding to a typical heavy- or light-mass fragment from binary fission. Hence, the usual double-peaked binary-fission energy spectrum should be reproduced, distorted slightly in the lower energy region by the scattered fragment spectrum and, also, by a factor reflecting the scattering probability dependence on charge and energy [11] of the scattering fragment. Since Fig. 5b shows very few events corresponding to unscattered heavy-mass fragment energies (typically 80 MeV) and even fewer events corresponding to light-mass fragment energies (105-MeV region), the observed position of the energy peaks indicates that scattering phenomena cannot be responsible for these events. For the foregoing assumption and argument, energy ionization defect effects would be negligible since the fragment energies are calibrated against the average heavy- and light-mass kinetic energy values of binary fission.

As a check on this interpretation, we should expect the single-fragment energy spectrum for accidental events (i.e. those events for which $E_t > 240$ MeV) to reproduce the two peak single-fragment energy spectrum typical of binary fission. Such is the case, as is shown in Fig. 5a. It should be noted that events for which $E_t < 240$ MeV may include a small number of accidental events and/or scattering events. Of more importance is the fact that these binary events (i.e. accidentals, or triple events (with $E_t > 240$ MeV)) serve as an internal calibration to confirm the 9-11-MeV displacement of the average value of the median- and high-energy ternary fission fragments

(71 and 94 MeV respectively) from the typical binary-fission energy maxima (80 and 105 MeV), as is evident by comparing Figs. 5a and 5b. The existence of this displacement (which is quite fortuitous) is essential in the foregoing argument for excluding scattering phenomena as an explanation of these events. Additionally, if these events (E_t <240 MeV) are caused by scattering phenomena, the total energy spectrum should reproduce fairly closely that for binary fission, which it does not, as is evident from Fig. 4c.

Finally, to demonstrate the non-dependency of the measured properties on the material composition of the foil support, a series of experiments was made using a 100 $\mu g/cm^2$ beryllium foil support. The general features of the total energy and individual energy spectra were reproduced as shown in Figs. 7 and 8. The larger ratio of (E_t > 240 MeV) events to (E_t < 240 MeV) events is caused by the longer time resolution (20 ns) and the increased single count-rate from this more active source (2×10^2 fissions/min); both factors cause an increased accidental counting-rate. The shift towards lower energies of the median- and high-energy fragments in ternary fission is still evident, however.

Since we have experimentally precluded the possibility of accidental counts as a major source of triple events for which E_t < 240 MeV (based on Fig. 4a, b), we conclude that most of the observed events of Fig. 4c result indeed from the spontaneous ternary fission of Cf^{252}.

Assuming that the three fragments are emitted at 120° from each other (as indicated by the detector positions about the source) the mass distribution spectrum has been calculated[2] and is plotted in Fig. 9; neutron evaporation effects are neglected. The distribution is quite broad as expected because of the dispersion introduced by the large solid-angle subtended[3]. Nevertheless, it clearly appears that typically two smaller mass fragments (45 to 95 amu) are emitted, accompanied by a larger mass fragment (> 95 amu). For such a combination of three product primary fragments, the typical mass-energy conversion estimated from a semi-empirical mass formula [12] is approximately 240 MeV. Fragmentation into three equal masses appears to be infrequent although such division would produce a larger (~ 260 MeV) mass-energy conversion.

---

[2] The following relation was used:

$$m_i = \frac{M \sin^2 \theta_i}{(E_i/E_1) \sin^2 \theta_1 + (E_i/E_2) \sin^2 \theta_2 + (E_i/E_3) \sin^2 \theta_3}$$

where

m_i = mass of ith fragment, i = 1,2,3
E_i = energy of ith fragment
θ_1 = angle between fragments 2 and 3
θ_2 = angle between fragments 1 and 3
θ_3 = angle between fragments 2 and 1
M = mass of fissioning nucleus.

[3] This mass error (20 amu maximum) was estimated by taking a typical set of data and using the maximum possible angular deviation for one detector to compute the mass distribution, which was then compared to the regular one.

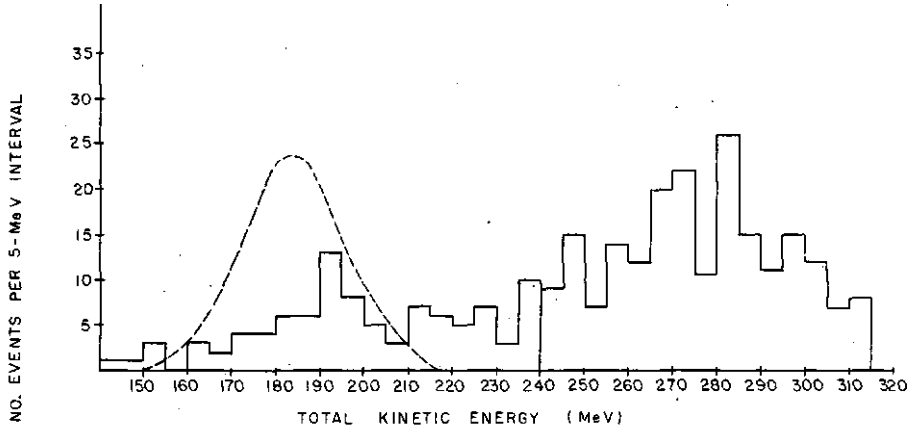

Fig. 7

Total fragment kinetic energy spectrum for triple events from fission of Cf^{252}. The source is mounted on (100 $\mu g/cm^2$) Be foil. The dashed line represents the total fragment kinetic energy spectrum (arbitrary scale) for binary fission of Cf^{252} as taken from Ref. [8] and as reproduced in these experiments.

Ternary fission of U^{235} induced by thermal neutrons

The frequency of ternary fission was measured to be greater than 6×10^{-6}/ binary fission (corrected for geometrical efficiency of the detectors), comparable to the ratio of 6.7×10^{-6} reported previously [2]. In these experiments, a direct measurement of the triple coincidence count-rate was made as a function of the single detector count-rate and also the uranium (IV) fluoride film thickness. Figure 10 demonstrates the non-dependence of the relative frequency of occurrence of ternary fission on the source foil thickness and the square of the single count-rate. The data were collected using a (60 $\mu g/cm^2$) nickel foil support with detectors placed at 1.0 cm from the source. Thus, scattering of binary-fission fragments in the uranium (IV) fluoride source film and accidental (three independent) events is experimentally excluded as causing the triple coincidence count-rate. A straight line plot, passing through the origin, should be obtained if the triple events result from either of these two factors. Accidental events caused by two independent binary-fission events (one of which triggers two detectors) are precluded by the geometry of the experiment (see Fig. 1b). Scattering of binary fission fragments by nickel nuclei in the support foil may be excluded on the basis of the kinetics involved in Rutherford scattering [11]. Scattering phenomena were also excluded through the reproducibility of the experimental data using a VYNS film support instead of the nickel foil.

The total fragment kinetic energy release in ternary fission of U^{236*} is presented in Fig. 11a. An average value of 180 MeV is released, some 12 MeV more than in binary fission. Noticeable is the lack of higher total energy (E_t > 200 MeV) events that are indicative of accidental counts. Figure 11a may be compared with Fig. 4a and b, obtained with Cf^{252} for which accidental events are registered because of physical "carry over" of the active material on to the detector surfaces.

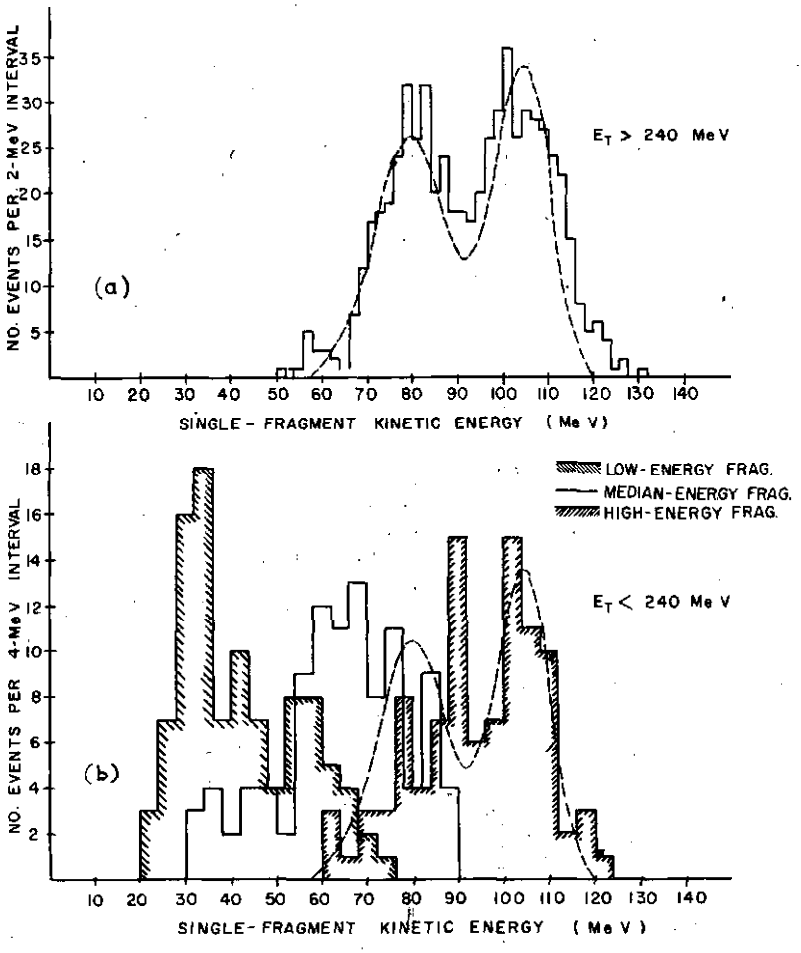

Fig. 8

(a) Single fragment kinetic energy spectrum of triple events for which E_t > 240 MeV.
(b) Individual fragment kinetic energy spectrum of triple events for which E_t < 240 MeV.
The Cf^{252} source is mounted on (100 $\mu g/cm^2$) Be foil. The dashed line represents the individual binary fission fragment spectrum (arbitrary scale) as obtained in Ref. [8] and as reproduced in these experiments.

The single fragment kinetic energy is shown in Fig. 11b. These data were obtained with a (10 $\mu g/cm^2$) VYNS film support and with detectors located at 1.5 cm from the source (see Fig. 1b). It appears that two fragments of low energy (30-50 MeV) are emitted accompanied by a fragment of larger energy.

Because of the better angular resolution (approximately 0.2 sr), conversion of fragment kinetic energies to mass distribution is accompanied by less dispersion than was experienced in the Cf^{252} experiments; therefore the results are more significant. The mass distribution for these events is shown in Fig. 12a; the angles of emission were 120°-120°-120° (Fig. 1b). A range of single fragment masses from 30 to 124 amu was observed, with

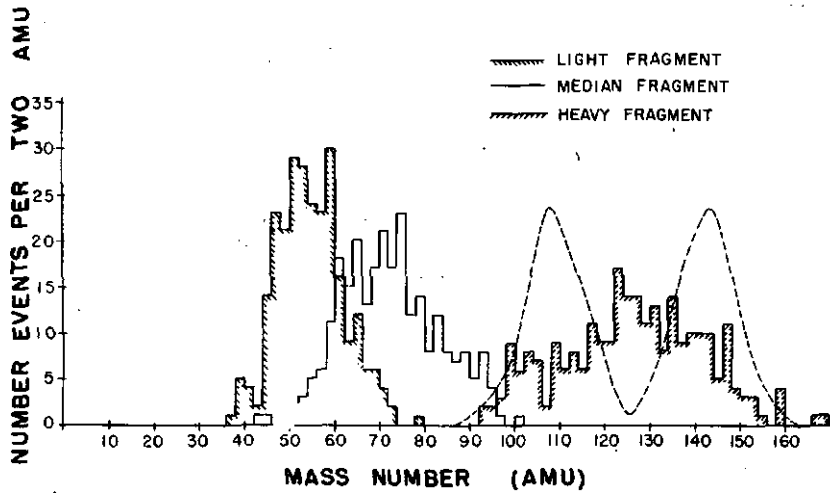

Fig. 9

Approximate mass distribution from ternary fission of Cf^{252} assuming repulsion of tripartite fragments to take place at 120° from each other. Dashed curve represents binary fission mass yield curved (arbitrary scale) as taken from Ref. [8].

evidence for peaks occurring near mass 38 and 56 amu. These events may be divided into two classes as follows:

(i) Type I events are characterized by the formation of two low mass fragments and one heavier fragment. The lowest mass fragment has a mass of approximately 56 amu. The single fragment mass distribution for Type I events is shown in Fig. 12b and is similar (within the deviations expected from statistical errors and mass yield dispersions) to the mass yield curve (Fig. 9) obtained in the ternary fission of Cf^{252}.

(ii) Type II events are characterized by the formation of one light fragment (near mass 38 amu) and two heavier fragments (Fig. 12c). The heavier fragments range in mass from 70 to 124 amu; no fragment of mass near 56 amu is produced.

It is noteworthy that both low mass peaks (38 amu for Type II, 56 amu for Type I) centre in regions of unusual nuclear stability (magic numbers). Furthermore, the full width at half maximum for these peaks is clearly less than that obtained for the light- and heavy-mass peaks of binary fission. Indeed, the light-mass ternary fission peaks may be considerably more narrow, the present spread being caused by the uncertainty in the measurement of the emission angles.

These facts suggest that two distinct modes of division are possible in ternary fission; moreover, underlying shell structure effects are dominant in determining the resulting trifragment mass division.

Discussion of results

Kinetic energy and frequency of occurrence

The average total fragment kinetic energy release in ternary fission is higher than that for binary fission. The percentage increase (from

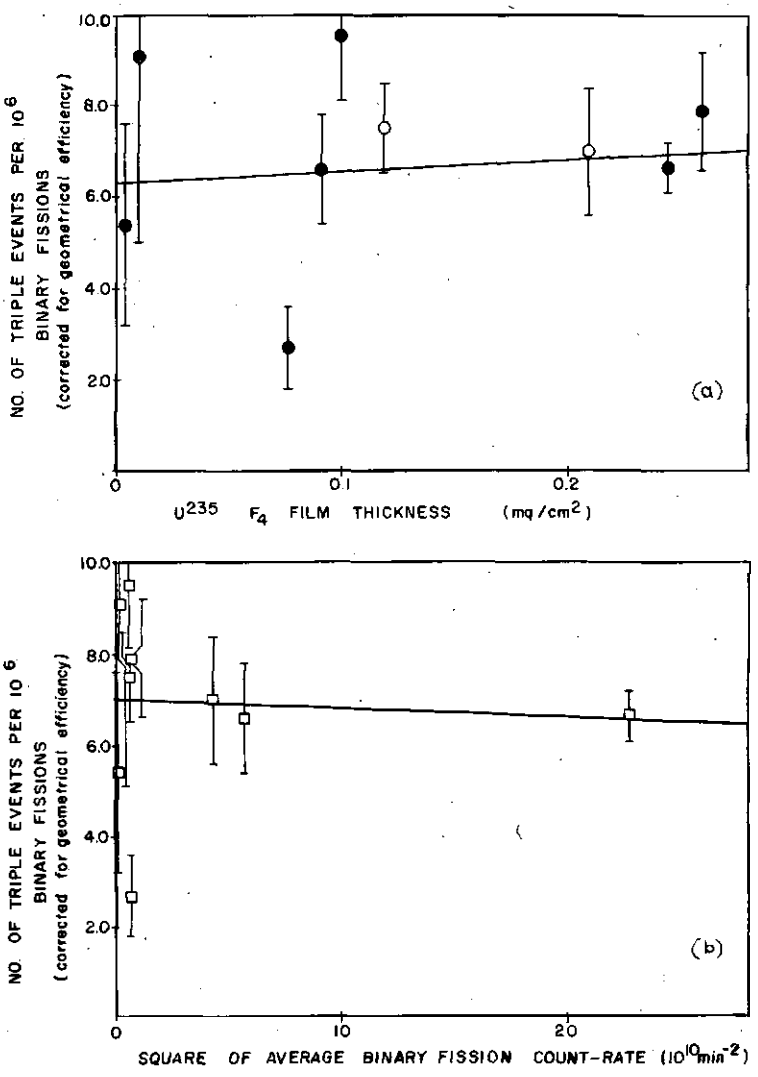

Fig.10

Relative frequency of triple events as a function of (a) $U^{235}F_4$ foil thickness, and (b) square of binary fission count-rate. The straight line is a least-squares fit. Error bars represent statistical errors of counting. In (a) open and closed circles represent data taken with VYNS foil support and nickel foil support respectively.

168 MeV for binary to 180 MeV for ternary fission of U^{236*}; from 185 MeV for binary to 206 MeV for ternary fission of Cf^{252}) is consistent with the corresponding percentage increase in mass-energy conversion realized in ternary fission as opposed to binary fission (as estimated from semi-empirical mass formulae [12]). The full width at half maximum for the total kinetic energy distribution in ternary fission is about the same as for binary fission.

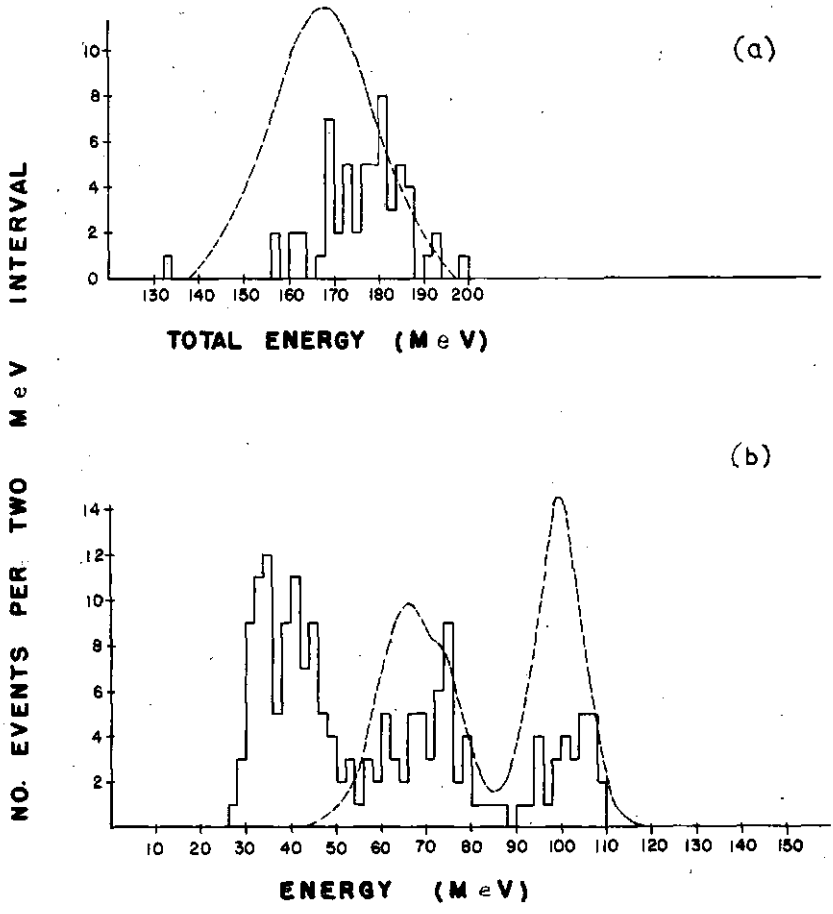

Fig. 11

Ternary fission of U^{235} + neutron. (a) Total kinetic energy spectrum.
(b) Single fragment kinetic energy distribution.
The dashed curves represent the corresponding energy distributions (arbitrary scale) for binary fission as obtained in Ref. [7] and as reproduced in these experiments.

The individual fragment kinetic energy distributions for both fissioning systems are characterized by a low-energy peak ranging from about 30 to 50 MeV.

A lower limit for the frequency of occurrence of ternary fission relative to binary fission was found to be 1.1×10^{-6} for fission of Cf^{252} and 6×10^{-6} for the thermal-neutron induced fission of U^{235}. It appears that tripartition occurs more readily in the fission of U^{236*}, but a determination of the angular dependency of three-fragment emission is necessary to resolve this question.

Mass distribution

Perhaps the most interesting feature of these results is the mass yield distribution (Figs. 9 and 12). Underlying shell structure effects appear to

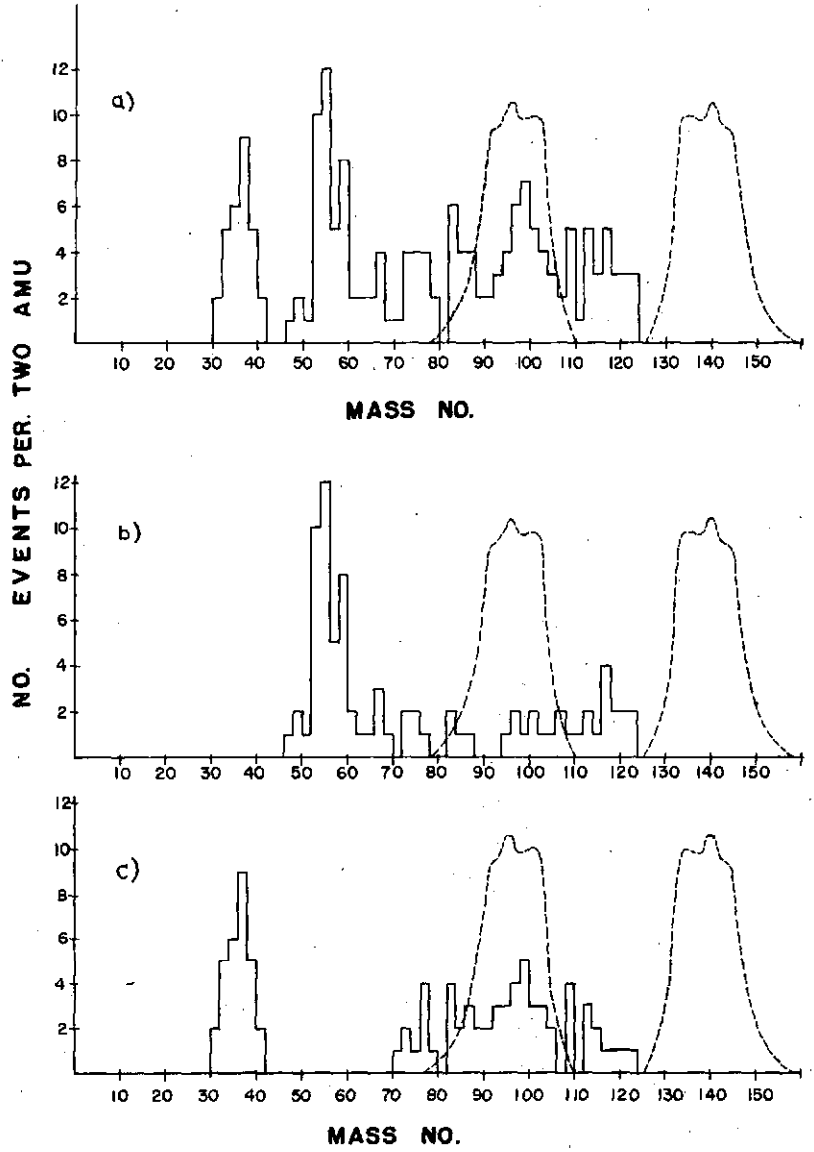

Fig. 12

Mass yield distribution in ternary fission of U^{235} + neutron.
(a) All events. (b) Events of type I (see text). (c) Events of type II (see text).
Dashed curves represent binary fission mass yield distribution (artitrary scale) as taken from Ref. [7].

restrict the choice of resulting fragment masses to two clearly defined types, distinguished by the mass of the lightest fragment produced. Ternary fission of Cf^{252} occurs through Type I for which the light mass fragment is near 56 amu. Ternary fission of U^{236*} proceeds in approximately equal portions through both Type I and Type II mechanisms, the latter of which is featured

by the formation of a light mass fragment near mass 38 amu. Tripartition of nuclei lighter than U^{236*} should proceed to a larger extent through Type II mode; heavier nuclei are expected to trifragment in greater proportion through Type I mode.

The appearance of well-defined mass peaks outside the binary mass yield region, coupled with the observed yield, suggests the possibility of detecting ternary-fission fragments by radiochemical means. In particular, two isotopes appear to be likely candidates; these are Mn^{56} (2.58-h half-life [13]) and S^{38} (2.87-h half-life [14]); both are beta emitters.

The isolation of Mn^{56} as a fission product will have to be done using a fragment recoil technique as outlined in Fig. 13, since this isotope is readily

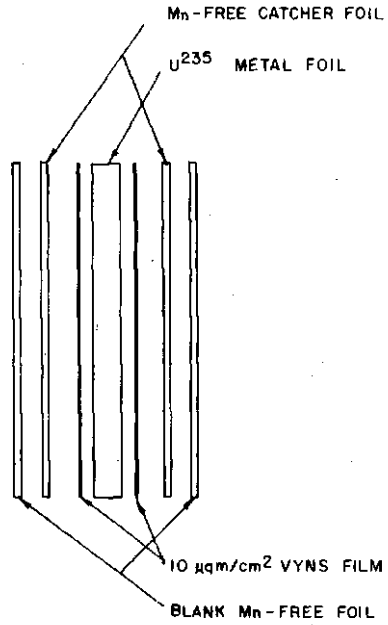

Fig. 13

Proposed experiment for detecting ternary fission fragments by radiochemical means. Neutron irradiation of above assembly causes fission fragments, formed near the surface, to recoil into the adjacent catcher foil. A thin VYNS film between the uranium and catcher foils prevents mechanical carry over of any manganese impurities. A blank catcher foil undergoes identical irradiation in order to account for the effects of impurities present in the catcher foil.

produced by the (n, γ) reaction and, possibly, the (n, p) reaction on manganese and iron impurities respectively. The detection of S^{38} should not be complicated by its formation through side reactions.

Failure to detect these isotopes may result from two causes. If the small fragment is formed from the middle node of a distorted configuration such as depicted in Fig. 14a, then because it is deformed at both ends it will subsequently receive a major portion of the excitation energy imparted to the fragments. Through prompt neutron evaporation, this middle fragment may be moved near to the line of beta stability, bypassing intermediate beta emitters.

Alternately, the mass peak may be considerably more narrow than is shown in Figs. 9 and 12, covering only one or two mass units. This possibility is consistent with the data obtained in this work since the mass peak width can be accounted for by the experimental angular dispersion. Thus, if the low mass peaks centred not on mass 38 or 56 but two mass units on either side, then chemical detection would have to be made of the appropriate mass isotope. The search for these possible isotopes from ternary fission offers an intriguing challenge to the radiochemist.

Fission configurations

The data presented in the foregoing sections are characteristic only of ternary fission for which the trifragment masses are repelled at approximately 120° from each other. It is emphasized that ternary fission in which three large fragments are repelled at approximately 120° from each other implies an off-axial distortion at some stage before the time of scission (Fig. 14a).

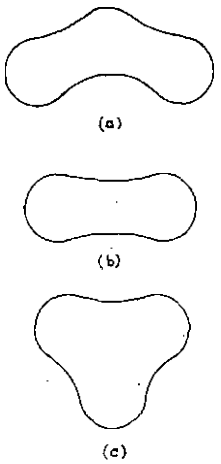

Fig. 14

Diagram showing a possible off-axial static nuclear distortion for the ternary fission process. A configuration such as depicted in (a) is proposed to account for the observed angular emission of three large fragments in the fission process. Such off-axial distortions may also be a contributing factor in the binary fission process for which only axially symmetric distortions as in (b) have heretofore been considered. Three node symmetrical configurations such as in (c) are ruled out because of the higher fission barrier expected, as explained in text.

Symmetrical three-node distortions (Fig. 14c) are excluded from consideration for the following reason. The initial distortion rapidly increases the surface (area) energy without a compensatingly large charge separation and its accompanying decrease in Coulomb energy. As such, the fission barrier is expected to be much higher as energy must be supplied from a source, other than from decreased Coulomb energy, to increase the nuclear surface area.

On the other hand, an initial ellipsoidal elongation provides for a massive charge separation (and decreased Coulomb energy) as well as an increase

in the surface (area) energy. However, fission from a two-node configuration (Fig. 14b) with a subsequent second scission of one of the resultant fragments seems unrealistic in view of the known large fission barriers associated with the medium weight nuclei.

The necessity of a three-nodal configuration indicates a rather large elongation of the nucleus during the transition between the "saddle point" and the time of scission, a view previously suggested [15] on the basis of deformation energy calculations of a charged liquid drop. Such configurations (i.e. those producing three nodes) may be competitive in forming pre-scission shapes leading to binary fission. The additional possibility of axially asymmetric distortions clearly offers a fresh approach to the development of concepts concerning the fission mechanism.

ACKNOWLEDGEMENT

Ray Gatti, Lawrence Radiation Laboratory, fabricated the Cf^{252} sources used in this work. L.D. Butterfield, Jr., UFTR supervisor, ably assisted in the reactor experiments. It is a pleasure to express sincere appreciation to Dr. S.G. Thompson, Lawrence Radiation Laboratory, for his interest and sustained encouragement of this work.

REFERENCES

[1] TSIEN, S., HO, Z., CHASTEL, R. and VIGNERON, L., J. Phys. Radium 8 (1947) 165.
[2] ROSEN, L. and HUDSON, A.M., Phys. Rev. 78 (1950) 533.
[3] CATALA, J., CASANOVA, J. and DOMINGO, V., Nature, Lond. 184 (1959) 1057.
[4] TITTERTON, E.W. and BRINKLEY, T.A., Nature, Lond. 187 (1960) 228.
[5] MUGA, M.L., BOWMAN, H.R. and THOMPSON, S.G., Phys. Rev. 121 (1961) 270.
[6] MUGA, M.L., Phys. Rev. Lett. 11 (1963) 129.
[7] MILTON, J.C.D. and FRASER, J.S., Canad. J. Phys. 40 (1962) 1626.
[8] FRASER, J.S., MILTON, J.C.D., BOWMAN, H.R. and THOMPSON, S.G., Canad. J. Phys. 41 (1963) 2080.
[9] NAKAMURA, M. and REAM, J.E., Lawrence Radiation Laboratory Rpt. UCRL-10624 (1963) 283.
[10] BURNETT, D.S., Lawrence Radiation Laboratory Rpt. UCRL-11006 (1963).
[11] EVANS, R.D., in The Atomic Nucleus, McGraw-Hill Book Co., Inc., New York (1955) 851.
[12] CAMERON, A.G.W., Canad. J. Phys. 35 (1957) 1021.
[13] STROMINGER, D., HOLLANDER, J.M. and SEABORG, G.T., Rev. mod. Phys. 30 (1958) 628.
[14] NETHAWAY, D.R. and CARETTO, A.A., Jr., Phys. Rev. 109 (1958) 504.
[15] SWIATECKI, W.J., Proc. 2nd UN Int. Conf. PUAE 15 (1958) 248.

DISCUSSION

G. FRIEDLANDER: Do you plan to use angles other than 120° in your experiments? Since the ternary fissions you observe are into unequal fragments, it would seem to me that it might be advantageous, from the point of view of counting-rates, to use a different angular arrangement.

L. MUGA: Yes, we do plan to do this because it would be interesting to study the angular correlations and to confirm that scattering phenomena are not present.

VARIATION OF THE BINARY-TO-TERNARY FISSION RATIO FOR U^{235} IN THE THERMAL-NEUTRON-ENERGY REGION

A. J. DERUYTTER AND M. NÈVE de MEVERGNIES
C. E. N. - S. C. K., MOL, BELGIUM

Abstract — Résumé — Аннотация — Resumen

VARIATION OF THE BINARY-TO-TERNARY FISSION RATIO FOR U^{235} IN THE THERMAL-NEUTRON-ENERGY REGION. The slow chopper installed at BR1 was used to make an accurate determination of the binary-to-ternary fission ratio for U^{235} in the neutron-energy range from 0.005 eV to 0.2 eV. Large gold-silicon surface-barrier detectors are used for the consecutive measurement of long-range α-particles (absorber in) and fission fragments (absorber out). The time analysis is done with a 100-channel time-of-flight analyser. A one-metre flight-path and a rotor speed of 50 rev/s is used.

The B/T ratio was also measured with a high statistical accuracy (about 1%) in intense beams with well-defined neutron spectra, i.e. a "cold neutron" beam, a beam extracted from a thermal column and a beam of 0.3-eV neutrons produced by crystal diffraction.

The B/T ratio exhibits a small and smooth variation in the energy range considered. This effect seems to be correlated with measurements of some other fission parameters in the same neutron-energy range.

VARIATION DU RAPPORT ENTRE LES NOMBRES DE FISSIONS NORMALES ET TERNAIRES DE ^{235}U DANS LA GAMME DES ÉNERGIES DES NEUTRONS THERMIQUES. Le hacheur lent dont est muni le réacteur BR1 a été utilisé pour déterminer avec précision le rapport entre les nombres de fissions normales et ternaires de ^{235}U dans la gamme des énergies des neutrons comprises entre 0,005 et 0,2 eV. On a fait appel à de grands détecteurs à barrière de surface Au-Si pour mesurer consécutivement les particules alpha à long parcours (avec absorbeur) et les fragments de fission (sans absorbeur). L'analyse en temps a été faite au moyen d'un analyseur de temps de vol à 100 canaux. On a utilisé une trajectoire de vol de un mètre et, pour le rotor, une vitesse de 50 tours/s.

Le rapport des deux nombres a été également mesuré avec une précision statistique très poussée (de l'ordre de 1%) dans des faisceaux de neutrons intenses à spectres bien définis, à savoir: un faisceau de « neutrons froids » ; un faisceau provenant d'une colonne thermique; un faisceau de neutrons de 0,3 eV produit par diffraction dans un cristal.

Le rapport étudié accuse une variation lente et faible dans la gamme des énergies considérées. Cet effet semble en corrélation avec les mesures d'autres paramètres de fission dans la même gamme d'énergie neutronique.

ВАРИАЦИЯ ОТНОШЕНИЯ ДЕЛЕНИЯ НА ДВЕ ЧАСТИ К ДЕЛЕНИЮ НА ТРИ ЧАСТИ ДЛЯ УРАНА-235 В ОБЛАСТИ ЭНЕРГИИ ТЕПЛОВЫХ НЕЙТРОНОВ. Использовался селектор медленных нейтронов, установленный на реакторе BR1, для точного определения отношения деления на две части к делению на три части для урана-235 в диапазоне энергии нейтронов от 0,005 до 0,2 эв. Большие детекторы с золото-кремниевыми поверхностными барьерами применялись для последовательного измерения длиннопробежных альфа-частиц (поглотитель внутри) и осколков деления (поглотитель снаружи). Временной анализ производился с помощью 100-канального анализатора по времени пролета. Использована 1-метровая траектория пролета и скорость вращения 50 об/сек.

Отношение деления на две части к делению на три части также измерялось с большой статистической точностью (приблизительно 1%) в интенсивных пучках с хорошо определенными спектрами нейтронов, а именно: поток "холодных нейтронов", поток, выведенный из тепловой колонны, и поток нейтронов с энергией 0,3 эв, полученный в результате кристаллической дифракции.

Отношение двойного деления к тройному показывает незначительную гладкую вариацию в рассматриваемом диапазоне энергии. Этот эффект, по-видимому, коррелируется с измерениями некоторых других параметров деления в том же самом диапазоне энергии нейтронов.

VARIACION DE LA RAZON FISIONES BINARIAS/FISIONES TERNARIAS PARA EL ^{235}U EN LA REGION DE LOS NEUTRONES TERMICOS. Los autores utilizaron el interruptor periódico lento instalado en el reactor BR1

con objeto de determinar con precisión la razón fisiones binarias/fisiones ternarias (FB/FT) en el ^{235}U en el intervalo de energía neutrónicas de 0,005 eV a 0,2 eV. Para la medición consecutiva de las partículas α de largo alcance (absorbedor inserto) y de los fragmentos de fisión (absorbedor extraído) emplearon grandes detectores de Au-Si de barrera superficial. El estudio de los tiempos se realizó con un analizador de tiempo de vuelo de 100 canales. Se emplearon trayectorias de 1 m y una velocidad del rotor de 50 rev/s.

También se midió la razón FB/FT con una exactitud estadística elevada (1% aproximadamente) en intensos haces neutrónicos de espectro bien definido; esos haces fueron: un haz de « neutrones fríos », un haz extraído de una columna térmica y un haz de neutrones de 0,3 eV producido por difracción a través de cristal.

La razón FB/FT varía ligera y paulatinamente en el intervalo de energías estudiado. Este efecto parece estar relacionado con los valores medidos de algunos otros parámetros de fisión en el mismo intervalo de energías neutrónicas.

INTRODUCTION

The probability of ternary fission (i.e. fission with emission of two heavy fragments and a long-range alpha particle) is a sensitive test of the shape of the nucleus at the scission point, as the alpha particles originate from the neck joining the two nascent fragments.

As this shape might not be statistically constant for successive neutron resonances (caused by, e.g. a spin effect), it seems interesting to study the constancy of binary-to-ternary fission probabilities as a function of neutron energy.

Instead of selecting a large number of resonances, we have limited ourselves to a more detailed study of the neutron energy range below the first resonance at 0.3 eV. It was expected that the effect would be small, as previous measurements had shown that this ratio is approximately constant [10, 13].

EXPERIMENTAL TECHNIQUES

The slow chopper installed at BR1 was used to measure the ratio of binary-to-ternary fission for U^{235} in a neutron energy range from 0.005 eV to about 0.1 eV. A thick U^{235} target of about 1 mg/cm^2 thick and 8 cm^2 surface, deposited by electrolysis [1] on an aluminium backing (0.1-mm thick) was used. The isotopic composition of the U^{235} target was: 88.35 ± 0.02% U^{235}, 1.202 ± 0.005% U^{234}, 3.756 ± 0.007% U^{236} and 6.69 ± 0.02% U^{238} [1]. A large gold-silicon surface-barrier detector [2] (sensitive surface ≈ 5 cm^2) made from 3000 Ωcm n-type silicon was used for the consecutive measurements of long-range α-particles (absorber in) and fission fragments (absorber out). The long-range α-particles are detected after passage through a 20-μm thick aluminium absorber, sufficient to stop the fission fragments and the natural α-particles from the isotopes present in the foil up to an α-energy of about 5.1 MeV. Consecutive measurements are performed of the ternary α-rate with absorber between target and detector, and of the binary fission rate without absorber. An automatic unit was constructed to move the absorber. Driving motor (outside the neutron beam) with absorber, target and detector, are set up in an evacuated aluminium chamber with

[1] The enriched uranium was supplied by the United States Atomic Energy Commission. The mass-spectrometric measurements were made by Dr. G.H. Debus, CBNM, EURATOM, Geel, Belgium.

thin entrance and exit windows. The neutron time-of-flight analysis is done with a 100-channel TOF analyser. A 1-m flight path and a rotor speed of 50 revolutions/s were used. During the measurements the signals from the detector, after amplification (charge sensitive preamplifier + linear amplifier) are also fed into a multi-channel analyser to register the pulse-height spectrum of the timed pulses. No shifts in the spectra were observed. Another stability check consisted in the registration, between partial measurements, of the natural α-rays from the target (mostly U^{234} α-rays). The importance of shifts in these relative measurements is small because a shift in the spectrum would cause the same change in efficiency over the whole neutron energy range studied.

Background measurements were performed with cadmium filters. These measurements yield the sum of the contributions to the counting-rate caused by signals induced in the semi-conductor detector by epi-cadmium neutrons and gamma rays of the beam, and pulses caused by the neutron background of the room. Both these effects may also cause fission in the target and eventually ternary α-particles. A third eventual contribution included in the background is caused by the possible (n, α) reactions in U^{235} that would yield α-particles above the bias threshold, or α-particles from the target that reach the sensitive surface of the detector after scattering in the chamber, or α-particles from the high-energy α-decay from the daughter nuclei in the target. The background is important in the tail of the Maxwell spectrum ($E_n < 6$ MeV) and for the region ($E_n > 0.05$ eV).

To compare the binary-to-ternary (B/T) ratio for a thermal-neutron beam with a "cold" neutron beam, the same vacuum chamber with absorber system was used as in the experiment described above. However, the much higher neutron intensity in both cases allowed us to use a U^{235} target of only 100 $\mu g/cm^2$ and a diameter of 1 cm. This target was prepared by evaporation under vacuum of UF_4 from a tungsten basket, thus improving the resolution of both the fission-fragment spectra and the ternary α-spectrum. These measurements were performed with a 3000 Ωcm n-type silicon surface barrier detector under 30 V reversed bias.

To make the comparison we used a thermal beam extracted from the thermal column of the BR1 reactor, with an approximately Maxwellian energy spectrum $\varphi(t) = A\,t^{-4} \exp(-t^2/t_0^2)$ with A a scale factor and $t_0 = 428\ \mu s/m$ (t = neutron time-of-flight; t_0 = most probable value of t).

The "cold" neutron beam is obtained through a filter of 30-cm cooled sintered beryllium and 15-cm cooled monocrystalline bismuth and is extracted from the R2 radial beam hole of the BR2 reactor. Its average neutron energy is about 4 MeV.

Again in both cases the ratio of binary-to-ternary fission is obtained by comparing the counting-rates of the solid-state detector with and without absorber between target and detector. Before and after each measurement of the ternary α-particle rate for 100 min a measurement is made of the binary fission rate for 2 min; the natural α-spectrum from the target is also registered as a check of the stability of the detector and electronic circuitry during the run.

The background problem in these measurements is not important, the signal-to-background ratio being much higher.

With the crystal spectrometer installed at the R3 radial beam hole of BR2 we also determined the B/T ratio for two distinct neutron energies, i.e. 0.0668 eV and 0.1376 eV. The beam was diffracted by the $10\bar{1}1$ planes of a beryllium single crystal that yields a low γ-background. The high intensities available allowed us to reach statistical accuracies of 1 to 2% for the B/T ratios within reasonable counting times when using a U^{235} target of about 1 mg/cm^2 UO_2 deposited by electrolysis on aluminium, and with a diameter of 2 cm. As the measuring times involved here were much longer than for the previous measurements, the beam intensity was monitoring during the ternary α-runs with a BF_3 detector.

EXPERIMENTAL RESULTS AND DISCUSSION

The advantage of using a chopper for the first experiment is that the data are registered for all energies during the same run, so that the relative values of the B/T ratio can hardly be influenced by shifts of the fission spectrum or the ternary α-spectrum. The ternary α-spectrum obtained with the detector is shown in Fig. 1. In order to obtain the relative values for the B/T ratio the background is subtracted from binary- and ternary-fission

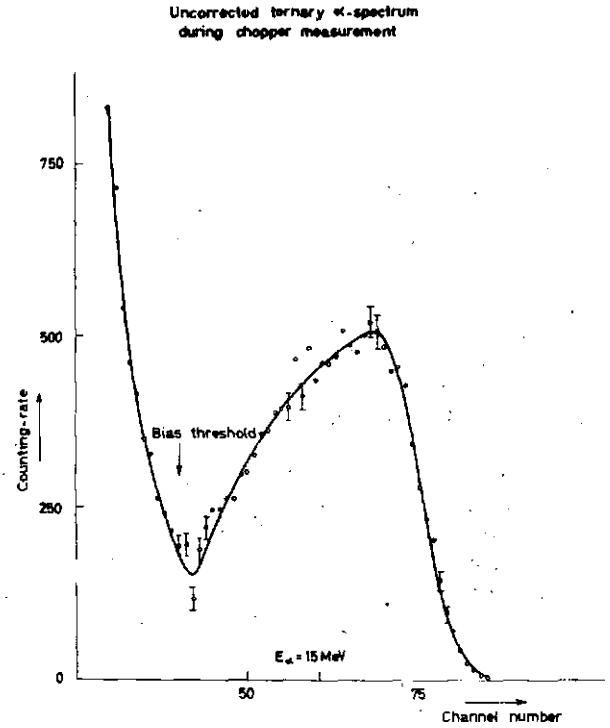

Fig. 1

The uncorrected ternary α-spectrum obtained during the chopper measurements. The shape of the spectrum is distorted at higher energies because of the limited thickness of the depletion layer of the detector.

rates and afterwards all data are normalized to the average value of B/T for the total Maxwellian spectrum taken as unit. The relative values with their errors are summarized in Table I. For $E_n < 6$ MeV and $E_n > 0.05$ eV the background contributes considerably to the error quoted.

These results are shown in Fig. 2. Although the statistical errors are large (5% in the peak of the Maxwellian spectrum) a smooth variation may be present. When we treat all B/T results with the criterion of Birge to find the compatibility with one unique value of this ratio we find a probability of 95% that the measured population is not compatible with a single value.

These data point to a smaller value of B/T for lower-neutron energies, and perhaps to a smaller value in the neighbourhood of the first U^{235} resonance.

The following is a discussion of the measurement made with the "cold"- and "thermal"-neutron beams. Because of the high intensity, the statistical accuracy was about 1%. Typical fission and ternary α-spectra are shown in Fig. 3. Both are very well resolved, so errors caused by discriminator settings are minimized. The relative influence of background is also reduced considerably. The ratio of the B/T values obtained is given by

$$\frac{[R(B/T)]\ \langle E_n \rangle = 28\ \text{MeV}}{[R(B/T)]\ \langle E_n \rangle = 4\ \text{MeV}} = 1.048 \pm 0.017.$$

This difference again points to a lower value of B/T for the "cold" beam, in agreement with the chopper data. The effect observed here is a 5% difference with an error of somewhat less than 2%. If we treat the two B/T values statistically and calculate

$$hx = \frac{R(B/T)_{\langle E_n \rangle = 28\ \text{MeV}} \cdot R(B/T)_{\langle E_n \rangle = 4\ \text{MeV}}}{\sqrt{2\,(\sigma_1^2 + \sigma_2^2)}}$$

we obtain hx = 1.96. This means that the probability of finding a unique value of R(B/T) is smaller than 0.01 (p = 0.0056). In this calculation only statistical errors determined from the counting-rates are considered.

Finally we discuss two measurements made with the BR2 crystal spectrometer, at 0.066 eV and at 0.137 eV respectively.

The value obtained for the ratio of the R(B/T) values is

$$\frac{[R(B/T)]_{E_n} = 0.066\ \text{eV}}{[R(B/T)]_{E_n} = 0.137\ \text{eV}} = 1.03 \pm 0.03.$$

If we calculate again the probability that both results are compatible with one unique value we find for hx

$$hx = \frac{R(B/T)_{0.066\ \text{eV}} - R(B/T)_{0.137\ \text{eV}}}{\sqrt{2\,(\sigma_1^2 + \sigma_2^2)}} = 0.68.$$

TABLE I

RELATIVE VALUES OF BINARY-TO-TERNARY FISSION AS A FUNCTION OF THE NEUTRON ENERGY

E_n (eV)	Relative value of binary-to-ternary fission with statistical error
0.120	0.98 ± 0.27
0.069	0.89 ± 0.09
0.044	0.99 ± 0.06
0.031	1.10 ± 0.06
0.023	1.14 ± 0.07
0.018	1.03 ± 0.07
0.014	0.89 ± 0.06
0.011	1.02 ± 0.11
0.0094	1.11 ± 0.16
0.0079	0.81 ± 0.12
0.0058	0.89 ± 0.14
0.0039	0.67 ± 0.17

This yields a probability of about 0.30, therefore this measurement is not conclusive for a change in the ratio.

CONCLUSION

From this statistical analysis it may be concluded that a small deviation in the B/T ratios is very probable when moving towards lower incident neutron energies, whereas a small deviation in the neighbourhood of the 0.3-eV resonance is not excluded. This decrease of the ratio of binary-to-ternary fission would mean that the relative importance of the ternary fission (fission into two fragments with a long-range α-particle) increases towards lower energies. Comparing our data with the results of FALER and TROMP [3] for the asymmetry ratio, it seems that the small increase in ternary-fission probability is correlated with the decrease of the asymmetry ratio (see Fig. 2). This correlation would mean that a higher symmetric component yields a higher probability for ternary α-emission, in agreement with the model for fission calculated by VANDENBOSCH [4] where for symmetric fission both fragments are rather strongly deformed because they are both far removed from closed shells. SCHMITT and FEATHER [5] have confirmed that the long-range α-particle emission arises mainly from the fragment most removed from a closed neutron shell.

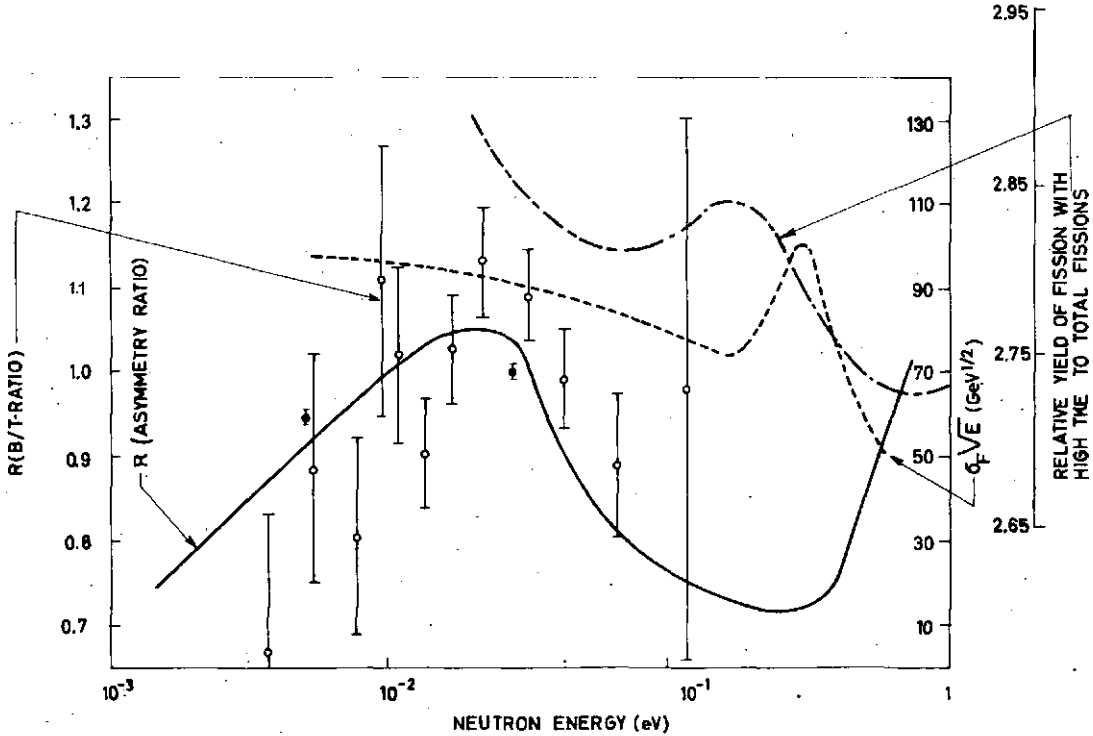

Fig. 2

The open circles with errors are the measured values of the B/T ratio.
The full circles are results for the cold and the thermal neutron beams.
The full line represents the asymmetry ratio as measured by FALER and TROMP [3].
The "dot-dash" line shows the relative yield of fission with high total kinetic energy to total fissions as given by MOORE and MILLER [8]
and the dotted line shows $\sigma_f\sqrt{E_n}$ as a function of E_n, taken from Rpt BNL 325.

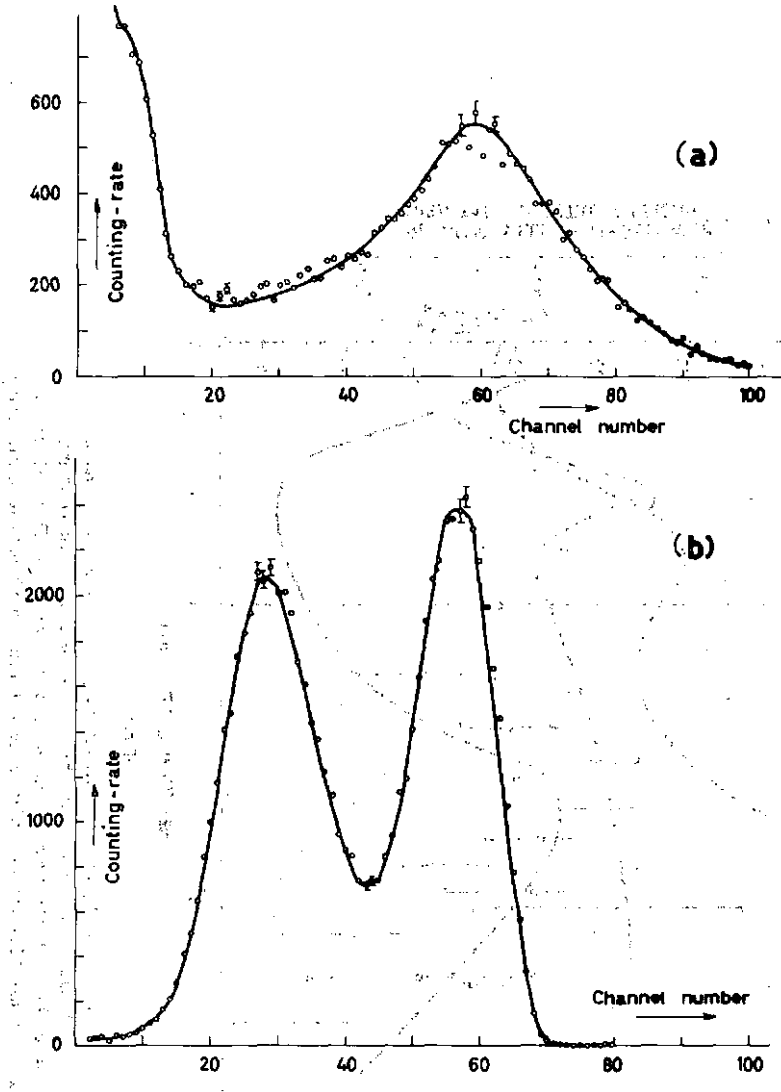

Fig. 3

(a) The uncorrected ternary α-spectrum for a typical ternary α-run at the cold neutron facility
(b) Typical fission spectrum under the same conditions

The variation of the B/T ratio might also be correlated with the spin values of the resonances. This effect has been investigated by MICHAUDON [6] and by MEHTA [7], who both conclude that the ternary-fission probability shows fluctuations from resonance to resonance that are incompatible with a single constant value. In our case, Fig. 2 shows $\sigma_f\sqrt{E_n}$ in the limited energy range studied. An interference mechanism between the 0.3-eV resonance and a negative energy resonance is not excluded. Such a mechanism has been proposed to explain, in the same neutron energy range, the vari-

ation (Fig. 2) of the relative yield of fissions with high total kinetic energies [8] and the change of the angular distribution of fission fragments from aligned nuclei [9]. However, the information on the spin values of these resonances is still very uncertain. This fact, together with the limited statistical significance of our data, does not allow any clear conclusions to be drawn.

ACKNOWLEDGEMENTS

The authors thank Dr. W. Van Dingenen and Dr. S. Hautecler for the use of the cold neutron facility at BR2, Dr. F. Poortmans for the use of the BR2 crystal spectrometer, J. Peeters for assistance in some preliminary chopper runs and Mrs. G. de Corte for calculations.

REFERENCES

[1] DERYUTTER, A. J., Nucl. Instrum. Meth. 7 (1960) 145.
[2] DERUYTTER, A. J., MOORE, J. A. and SCHRÖDER, I. G., Mém. Soc. r. Sci. Liège 28 (1964) 231; CEN Rpt Blg 284.
[3] FALER, K. T. and TROMP, R. L., Phys. Rev. 131 (1963) 1746.
[4] VANDENBOSCH, R., Nucl. Phys. 46 (1963) 129.
[5] SCHMITT, H. W. and FEATHER, N., Phys. Rev. 134 (1964) 565.
[6] MICHAUDON, A., Thèse, Rapport CEA 2552 (1964).
[7] MEHTA, G., Ph. D. Thesis, Columbia University (1963).
[8] MOORE, M. S. and MILLER, L. G., "Channel effects in the kinetic energy of fragments of fission induced by low-energy resonance neutrons", these Proceedings I.
[9] DABBS, J. W. I., WALTER, F. J. and PARKER, G. W., AEC Rpt ORNL 3425 (1964) 82; "Saddle-point rotational states from resonance fission of oriented nuclei", these Proceedings I.
[10] SCHRÖDER, I. G., DERUYTTER, A. J. and MOORE, J. A., Phys. Rev., to be published.
[11] AUCLAIR, J. M., J. Phys. Radium 19 (1958) 68.
[12] GENIN, R., JOLY, R. and RIBRAG, M., J. Phys. Radium 21 (1960) 473.

ТРОЙНОЕ ДЕЛЕНИЕ УРАНА-235 НА РЕЗОНАНСНЫХ НЕЙТРОНАХ

И. КВИТЕК, Ю.П. ПОПОВ и Ю.В. РЯБОВ
ОБЪЕДИНЕННЫЙ ИНСТИТУТ ЯДЕРНЫХ ИССЛЕДОВАНИЙ, ДУБНА
СССР

Abstract — Résumé — Аннотация — Resumen

TERNARY FISSION OF U^{235} BY RESONANCE NEUTRONS. Recently a number of papers have appeared indicating considerable variations in the ratio of the ternary-fission cross-section to the binary-fission cross-section of U^{235} on transition from one neutron resonance to another. However, such variations have not been discovered in U^{233} and Pu^{239}. The paper reports investigations of the ternary fission of U^{235} by neutrons with an energy of 0.1 to 30 eV. Unlike other investigators of the ternary fission of U^{235}, we identified the ternary-fission event by the coincidence of one of the fission fragments with a light long-range particle. This made it possible to separate ternary fissions from the possible contribution of the (n, α) reaction.

The measurements were performed at the fast pulsed reactor of the Joint Institute for Nuclear Research by the time-of-flight method. A flight length of 100 m was used, giving a resolution of 0.6 μs/m.

Gas scintillation counters filled with xenon at a pressure of 2 atm were used to record the fission fragments and the light long-range particle. A layer of enriched U^{235} ~2 mg/cm² thick and ~300 cm² in area was applied to an aluminium foil 20-μm thick. The scintillations from the fission fragments were recorded in the gas volume on one side of the foil and those from the light long-range particles in that on the other.

In order to assess the background (e.g. coincidences of the pulse from a fragment with that from a fission gamma quantum or a proton from the (n, p) reaction in the aluminium foil), a measurement was carried out in which the volume recording the long-range particle was shielded with a supplementary aluminium filter 1-mm thick.

The results obtained indicate the absence of the considerable variations in the ratio between the ternary- and binary- fission cross-sections for U^{235} that have been noted by other authors. Measurements showed no irregularity in the ratio of the cross-sections in the energy range 0.1 to 0.2 eV. The paper discusses the possible effect of the (n, α) reaction on the results obtained in experiments not using the coincidence of a long-range particle with a fission fragment.

FISSION TERNAIRE DE ^{235}U PAR DES NEUTRONS DE RÉSONANCE. On a publié récemment des études dans lesquelles on signale que, lors du passage d'une résonance à une autre, le rapport entre les sections efficaces de fission ternaire et binaire de ^{235}U subit des variations considérables. Or, les auteurs n'ont constaté aucune variation de ce genre ni pour ^{233}U ni pour ^{239}Pu. Le mémoire fait état de recherches sur la fission ternaire de ^{235}U par neutrons de 0,1 à 30 eV. Contrairement à d'autres travaux consacrés à la fission ternaire de ^{235}U, chaque fission ternaire a été identifiée par coïncidence entre l'un des fragments de fission et une particule légère à long parcours. Grâce à ce procédé, les fissions ternaires ont pu être séparées de la contribution qui pourrait être due à la réaction (n, α).

Les mesures ont été faites dans le réacteur à neutrons rapides de l'Institut unifié de recherches nucléaires par la méthode du temps de vol. Les auteurs ont utilisé à cet effet une base de vol de 100 m, ce qui a permis d'obtenir un pouvoir de résolution de 0,6 μs/m.

Pour enregistrer les fragments de fission et la particule légère à long parcours, ils se sont servis de compteurs à scintillateur gazeux remplis de xénon sous une pression de 2 atm. Une couche de ^{235}U enrichi d'environ 300 cm² et de 2 mg/cm² d'épaisseur a été appliquée sur une feuille d'aluminium de 20 μm. Dans le volume de gaz on a enregistré d'un côté de la feuille les scintillations dues aux fragments de fission et, de l'autre côté, celles qui provenaient des particules légères à long parcours.

En vue d'évaluer le bruit de fond (par exemple les coïncidences entre l'impulsion provoquée par un fragment et l'impulsion due à un photon de fission gamma ou un proton provenant de la réaction (n, p) dans la feuille d'aluminium) on a procédé à une mesure pour laquelle le volume où la particule à long parcours était enregistrée se trouvait protégé par un filtre d'aluminium supplémentaire de 1 mm d'épaisseur.

Les résultats de l'expérience montrent que le rapport entre les fissions ternaire et binaire de ^{235}U ne subit pas les fortes variations signalées par d'autres auteurs. Au cours des mesures on n'a constaté aucune irrégularité

dans le rapport entre les sections efficaces pour les énergies de 0,1 à 0,2 eV. Les auteurs du mémoire examinent l'influence éventuelle de la réaction (n, α) sur les résultats des expériences pour lesquelles on n'a pas eu recours à la coïncidence entre particules à long parcours et fragments de fission.

ТРОЙНОЕ ДЕЛЕНИЕ УРАНА-235 НА РЕЗОНАНСНЫХ НЕЙТРОНАХ. В последнее время появились работы, в которых указывалось на существенные колебания отношения сечения тройного деления к сечению двойного деления урана-235 при переходе одного нейтронного резонанса к другому. В то же время для урана-235 и плутония-239 таких колебаний обнаружено не было. В настоящем докладе сообщается об исследованиях тройного деления урана-235 на нейтронах с энергией 0,1 – 30 эв. В отличие от других работ по тройному делению урана-235 акт тройного деления идентифицировался по совпадениям одного из осколков деления с легкой длиннопробежной частицей. Это позволяло отделить тройные деления от возможного вклада реакции (n, α).

Измерения проводились на импульсном быстром реакторе Объединенного института ядерных исследований по методу времени пролета. Использовалась пролетная база длиной 100 м, что обеспечивало разрешение 0,6 мксек/м.

Для регистрации осколков деления и легкой длиннопробежной частицы использовались газовые сцинтилляционные счетчики, наполненные ксеноном до давления 2 атм. Слой обогащенного урана-235 толщиной ~2 мг/см^2 и площадью ~300 см^2 был нанесен на алюминиевую фольгу толщиной 20 микрон. В газовом объеме по одну сторону фольги регистрировались сцинтилляции от осколков деления, по другую – от легких длиннопробежных частиц.

Для оценки фонов (например, совпадения импульса от осколка с импульсом от γ-кванта деления или протона от (n, p) реакции на алюминиевой фольге) проведено измерение, в котором объем, регистрирующий длиннопробежную частицу, экранировался дополнительным алюминиевым фильтром толщиной 1 мм.

Полученные результаты эксперимента указывают на отсутствие существенных колебаний отношения сечений тройного и двойного делений для урана-235, отмечавшихся другими авторами. В измерениях не обнаружено нерегулярности в отношении сечений в области энергий 0,1–0,2 эв. В докладе обсуждается возможное влияние реакции (n, α) на результаты, получаемые в опытах, не использующих совпадений длиннопробежной частицы с осколком деления.

FISIÓN TERNARIA DEL ^{235}U POR NEUTRONES DE RESONANCIA. Recientemente se han publicado varios trabajos acerca de la existencia de una variación considerable en la razón de la sección eficaz de fisión ternaria a la sección eficaz de fisión binaria para el ^{235}U, al pasar de una resonancia neutrónica a otra. Hasta la fecha los autores no han descubierto ninguna variación de esa índole para el ^{233}U ni para el ^{239}Pu. En la presente memoria se presentan los resultados del estudio de la fisión ternaria del ^{235}U inducida por neutrones de 0,1 a 30 eV de energía. A diferencia de otros trabajos sobre fisión ternaria del ^{235}U, el suceso de fisión ternaria se identificó por coincidencia de uno de los fragmentos de fisión con una partícula ligera de largo alcance. Esto permitió separar las fisiones ternarias de la posible contribución de la reacción (n, α).

Las mediciones se efectuaron en el reactor pulsado de neutrones rápidos del Instituto Central de Investigaciones Nucleares, por el método del tiempo de vuelo. La trayectoria de vuelo era de 100 m, lo que permitía lograr un poder de resolución de 0,6 μs/m.

Los fragmentos de fisión y las partículas ligeras de largo alcance se registraron por medio de contadores de centelleo gaseosos, llenos de xenón a 2 atm de presión. La capa de ^{235}U enriquecido, de ~2 mg/cm^2 de espesor y de ~300 cm^2 de superficie, se colocó sobre una lámina de aluminio de 20 μm de espesor. En el volumen gaseoso situado de un lado de la lámina, se registraron los destellos de los fragmentos de fisión, por el otro, los de las partículas ligeras de largo alcance.

Para evaluar la actividad de fondo (por ejemplo, la coincidencia de los impulsos de un fragmento con el impulso de un cuanto gamma de fisión o de un protón procedente de la reacción (n, p) en la lámina de aluminio se efectuaron mediciones en las que el volumen en el que se registraban las partículas de largo alcance, se protegió mediante un filtro de aluminio suplementario de 1 mm de espesor.

Los resultados del experimento indican que la razón entre las fisiones ternarias y binarias del ^{235}U no acusa las fuertes variaciones señaladas por otros autores. En las mediciones no se observó ninguna irregularidad en la razón de las secciones eficaces en el intervalo energético 0,1 - 0,2 eV. En la memoria se discute la posible influencia de la reacción (n, α) sobre los resultados experimentales en los que no se ha recurrido a la coincidencia de las partículas de largo alcance con los fragmentos de fisión.

ВВЕДЕНИЕ

Последнее время исследованию тройного деления (т.е. деления, где, помимо двух тяжелых осколков, вылетает легкая длиннопробежная частица) посвящено значительное количество работ. В ряде экспериментов [1—7], выполненных различными методами, измерялось отношение нейтронных сечений тройного и обычного, двойного, делений изотопов урана и плутония. Результаты оказались противоречивыми. В работах [2, 3] не обнаружено энергетической зависимости отношения тройного и двойного делений на уран-235, в то время как в работах [4, 7] сообщается о существенных колебаниях этого отношения от резонанса к резонансу. По данным Мишадона и др. [1], колебания не превосходят 20—30%. А.А. Панов [5] не обнаружил энергетической зависимости этого отношения для урана-233 и плутония-239.

В качестве одного из объяснений расхождения экспериментальных результатов для урана-235 высказывалось [7] предположение о том, что, кроме тройного деления, α-частицы испускаются в реакции урана-235 (n, α). Однако убедительного экспериментального подтверждения эта точка зрения пока не получила. В то же время вопрос о том, меняется ли отношение тройного и двойного деления от резонанса к резонансу, имеет большое значение для понимания механизма деления ядер. В частности, это связано с определением момента образования длиннопробежной частицы в процессе деления, с выяснением спиновой зависимости каналов, по которым происходит тройное деление.

В связи с изложенным нами было проведено измерение отношения тройного и двойного деления урана-235 монохроматическими нейтронами с энергиями от 0,1 до 50 эв. При этом в отличие от других работ по урану-235 акт тройного деления идентифицировался по совпадениям одного из осколков деления с длиннопробежной α-частицей, что позволило избавиться от возможного влияния на результаты α-частиц от реакций урана-235 (n, α).

МЕТОДИКА И ИЗМЕРЕНИЯ

Измерения проводились на импульсном реакторе ИБР [8] Лаборатории нейтронной физики ОИЯИ методом времени пролета. Пролетное расстояние составляло 100 м, разрешение — 0,6 мксек/м.

Для регистрации α-частиц и осколков деления урана-235 был использован газовый сцинтилляционный детектор. Схема эксперимента приведена на рис. 1. Цилиндрическая камера объемом 8,5 л наполнялась ксеноном до давления 2 атм. Внутренняя поверхность камеры была покрыта тефлоновым отражателем. С торцовых сторон камеры имелись окошки из увиолевого стекла. Объем камеры был разделен на две половины алюминиевой фольгой толщиной 20 мк.

На одной стороне фольги была нанесена мишень из урана-235 толщиной ≈ 2 мг/см^2 и площадью ≈ 300 см^2. Вся внутренняя поверхность камеры, включая алюминиевую фольгу с мишенью и тефлон, покрывалась слоем дифенилстильбена толщиной ≈ 50 мкг/см^2. Дифенилстильбен использовался как сместитель спектра люминесценции ксенона, поскольку этот спектр в основном находится в области ультрафиолета [9]. Загрязнения ксенона

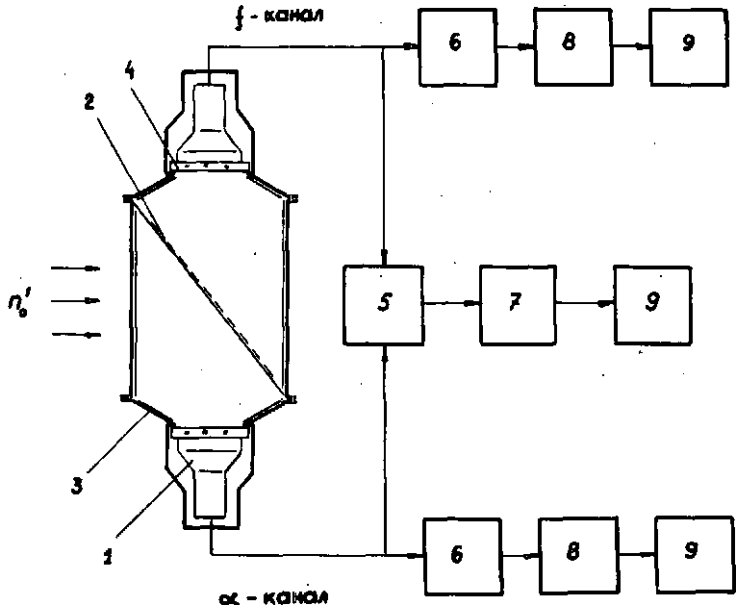

Рис.1

Схема эксперимента по измерению тройного деления:

1 – фотоумножитель; 2 – слой урана-235 на фольге алюминия (20 мк); 3 – камера с тефлоновым отражателем; 4 – увиолевое стекло; 5 – схема совпадений; 6 – усилитель; 7 – катодный повторитель; 8 – дискриминатор; 9 – временной анализатор.

(азот, кислород и др.) периодически устранялись путем откачки остаточных газов над ксеноном, замороженным в жидком азоте.

Каждая половина камеры просматривалась фотоумножителем типа ФЭУ-52. Поскольку алюминиевая фольга являлась непрозрачной для осколков деления и α-частиц естественного распада (газовый сцинтиллятор имеет собственный энергетический порог 0,5 Мэв [10]), то один фотоумножитель регистрировал длиннопробежные α-частицы тройного деления и, возможно, α-частицы урана-235 (n, α) (α-канал), а другой, при более высоком пороге по энергии, – осколки деления (f-канал).

Импульсы с ФЭУ подавались на выходы схемы совпадений с разрешающим временем 0,12 мксек [11], а также на спектрометрический усилитель с дискриминатором. Далее, через катодные повторители по кабелю импульсы поступали в измерительный центр на временные анализаторы. В эксперименте одновременно использовалось два 1024-канальных анализатора с шириной канала 32 мксек. При этом последние 256 каналов ставились в конце временного цикла между вспышками реактора и измеряли постоянную составляющую фона. Первый анализатор регистрировал импульсы от тройного деления, второй – попеременно импульсы с α- или f-канала.

Для уменьшения фона пучок нейтронов коллимировался до диаметра 180 мм, так чтобы прямой пучок от реактора не попадал на фотоумножитель. При регистрации тройного деления схемой совпадений основной фон могли составлять совпадения импульсов от нейтронов и γ-квантов деления в α-

канале с импульсами от осколков деления. Вероятность вклада других эффектов в счет совпадений (регистрация двух γ-квантов от каскада, случайные совпадения и т.д.) значительно ниже. Для оценки фонов была проведена серия измерений, когда со стороны объема, в котором регистрировались α-частицы, вплотную к фольге с ураном ставился экран из алюминия толщиной в 1 мм. При этом счет со схемы совпадений оставался только практически в момент вспышки реактора, а в области измеряемых времен пролета отсутствовал. Экран из алюминия в 50 микрон (поглощались α-частицы с энергией ≤ 12 Мэв) приводил к уменьшению совпадений в два раза.

Эффективность регистрации тройного деления оценивалась из выражения:

$$\frac{N_T}{N_D} = \frac{1}{2}\frac{W_T}{W_D}\frac{\epsilon_T}{\epsilon_D}, \qquad (1)$$

где $\frac{N_T}{N_D}$ – экспериментальное отношение счетов в единицу времени тройного и двойного делений в тепловой области;

ϵ_T и ϵ_D – соответственно эффективность тройного и двойного делений;

$\frac{W_T}{W_D}$ – отношение вероятности соответствующих делений, взятое из работы Ноблеса [12].

Коэффициент 1/2 появляется в результате того, что двойное деление регистрируется в геометрии 4π, а тройное – 2π.

Эффективность регистрации двойного деления определялась по интегральному амплитудному спектру осколков деления от нейтронов Po–Be источника, окруженного парафином. Из интегрального спектра можно было заключить, что при малых порогах дискриминатора эффективность к осколкам деления близка к 100%. Поэтому эффективность регистрации двойного деления при рабочем пороге определялась как отношение счета при рабочем пороге к счету при малом пороге. Эффективность тройного деления, полученная из выражения (1), оценивается в $(85 \pm 15)\%$.

РЕЗУЛЬТАТЫ И ОБСУЖДЕНИЕ

Результаты одной серии измерений счета двойных делений (А) и тройных делений на схеме совпадений (Б) в зависимости от времени пролета нейтронов представлены на рис.2. Кривые получились подобными. Их отношение (по суммам для трех серий измерений) изображено на этом же рисунке (В).

В связи с недостаточной точностью для кривой тройных делений здесь бралось отношение площадей под отдельными резонансами, группами резонансов или между резонансами. Длина горизонтальной черты соответствует временному интервалу, по которому проводилось усреднение. Отношения нормировались на единицу для энергии $\approx 0{,}1$ эв.

Наши экспериментальные данные говорят о том, что колебания отношения вероятностей тройного и двойного делений (если они существуют) могут лежать в пределах $\approx 20\%$. Для нейтронных резонансов с $E_0 < 0$ это отношение можно считать постоянным в пределах статистических ошибок,

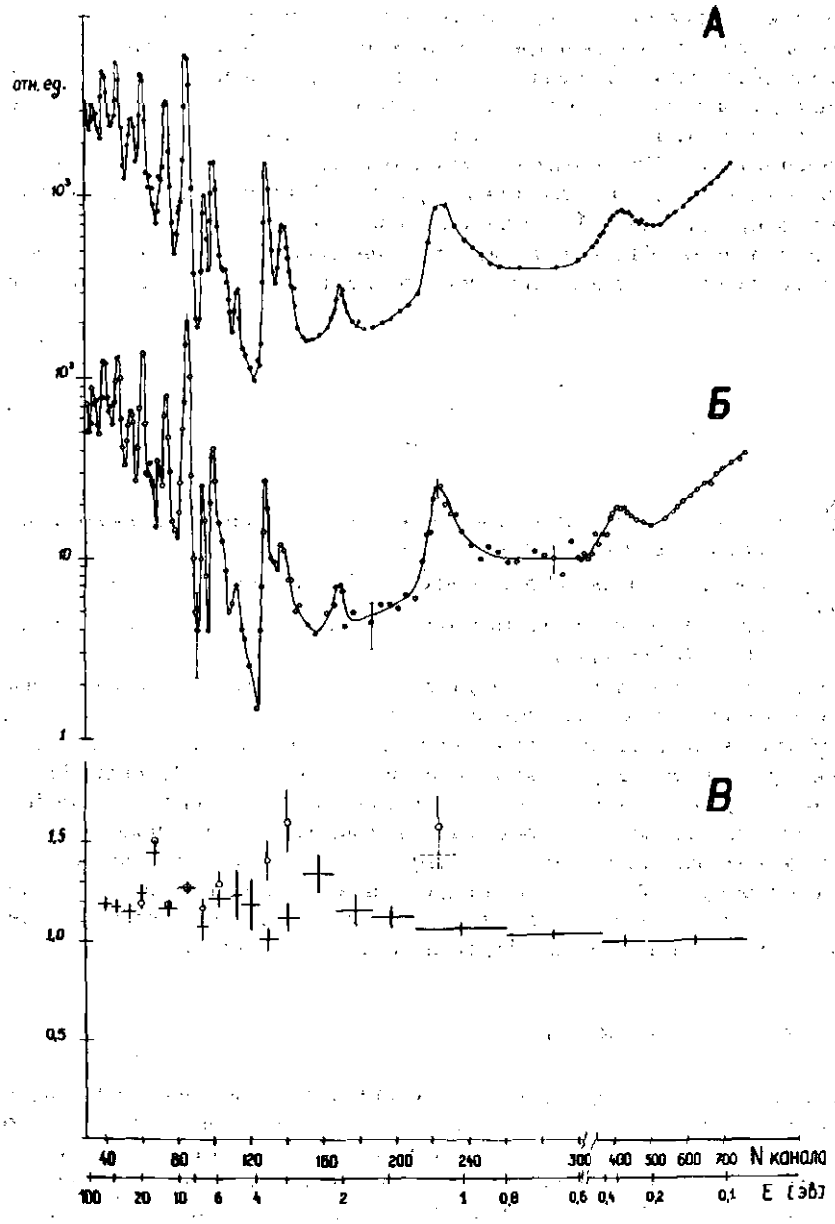

Рис. 2

Зависимость счета f-канала (двойное деление) — А и схемы совпадений (тройное деление) — Б от времени пролета нейтронов. Для кривой Б в области между резонансами точки усреднялись по 2 — 3 каналам.

В — отношение вероятностей тройного и двойного делений, нормированное на единицу по интервалу 0,1 — 0,2 эв. Длина горизонтальной черты соответствует временному интервалу, по которому проводилось усреднение. Вертикальные линии соответствуют величине статистической ошибки. Пунктиром показан результат для резонанса $E_0 = 1,14$ эв за вычетом подножья, обусловленного отрицательным уровнем. Кружками приведены результаты Мишадона и др. [1], нормированные на наши данные по резонансу при 8,8 эв (86-й канал).

указанных на рисунке. Для отрицательного уровня, заметное влияние которого распространяется до ≈ 4 эв, отношение вероятностей деления отличается от среднего для других уровней на 5 ÷ 6 статистических ошибок*.

Здесь же на рис.2 (В) приведены данные Мишадона и др. [1], полученные ими при измерении с алюминиевым экраном (30 мк). Эти результаты нормировались на наши по наиболее сильному резонансу при 8,8 эв. Отношение вероятностей тройного и двойного делений для остальных резонансов (в области энергий, где влиянием отрицательного уровня можно пренебречь) в пределах ошибок измерений совпало с нашими данными. Результат вычитания для резонанса при 1,14 эв вклада, обусловленного отрицательным уровнем (вычитался вклад, интерполированный по счету в 210 и 270 каналах анализаторов) приведен на рисунке 2 (В) пунктиром.

Наши результаты не согласуются с данными работ [4, 7], в которых сообщается о значительных флюктуациях отношения сечений тройного и двойного делений в области резонансных нейтронов. В отношении работы [7] это, по-видимому, связано с недостаточно полным вычитанием фона, что могло привести и к такому эффекту, как сдвиг максимумов в кривой отношения тройного и двойного делений в область между нейтронными резонансами.

В наших измерениях счета с α-канала (без совпадений) получена кривая, в которой резонансы проявились на фоне большого подножья. Отношение счета α-канала к счету f-канала (двойное деление) давало кривую с большими колебаниями, аналогичную приведенной в работе [7]. Однако эти колебания нельзя приписать только вкладу α-частиц от реакции (n, α), поскольку характер кривой существенно не менялся после того, как на пути α-частиц был установлен дополнительный экран — 50 мк алюминия. Такой экран должен был полностью поглотить α-частицы от реакции урана-235 (n, α), так как энергия этих частиц не может превышать 10,9 Мэв.

В заключение авторы выражают свою благодарность Ф.Л. Шапиро за полезные обсуждения. Авторы признательны Я. Фогеловой, М.С. Язвицкой за помощь в проведении эксперимента и Ван Тун-сену за помощь при приготовлении уранового слоя.

ЛИТЕРАТУРА

[1] MICHADON A., LOTTIN A., PAYA D., Доклад на Парижской конференции по ядерной физике, июль 1964 г.
[2] ANCLAIR I.M., Proc. Intern. Conf. on Neutron Ineteraction with Nucleus, New York, Columbia University, Sept. 1957, p.139.
[3] SEPPI E., BAPS, 3 (1958) 227.
[4] METHA Y., MELKONIAN E., 7 (1962) 304.
[5] ПАНОВ А.А., ЖЭТФ, 43 (1962) 851; ЖОТФ, 43 (1962) 1998.
[6] SOWINSKI M., DAKOWSKI M., PIEKARZ H., Phys. Lett., 6 (1963) 321.
[7] МОСТОВАЯ Т.А., МОСТОВОЙ В.И., ЯКОВЛЕВ Г.В., "Атомная энергия", 16 (1964) 3.
[8] БЛОХИН Г.Е. и др., "Атомная энергия", 10 (1961) 437.
[9] ВЯЗЕМСКИЙ В.О. и др., Сцинтилляционный метод в радиометрии, Госатомиздат, 1961.

* Однако необходимо отметить, что величина этого отличия менялась от серии к серии на величину, превышающую статистическую ошибку. По-видимому, это отличие отношения сечений для отрицательного уровня уменьшается с уменьшением энергетического порога в α-канале. Предполагается продолжить эксперименты для выяснения этого обстоятельства.

[10] NOBLES R.A., Rev. Scient. Instr., 27 (1956) 280.
[11] ЖУКОВ Г.П. и др., Препринт ОИЯИ, 602, Дубна, 1960.
[12] NOBLES R.A., Phys. Rev., 126, 4 (1962) 1508.

DISCUSSION

P. RIBON: The variation in the probability of ternary fission as a result of the emission of α-particles in the resonance range is slight and it is rather difficult to study the problem because, unfortunately, it is not possible at present to obtain substantial statistical data. Moreover, experimental details are liable to modify the results. For example, our experiments with U^{235} at Saclay seem to indicate that variations in the ternary/binary fission ratio depend on the thickness of the aluminium screen used, i.e. on the energy of the α-particles.

In the experiment described by Dr. Ryabov, coincidence of the α-particle with a fission fragment has the effect of discriminating against the counting of the α-particles that are emitted almost perpendicularly to the direction of fission. Angular distributions of the different α-particles according to energy might then explain why the results obtained are slightly different from ours.

SUMMARY TALK

J. J. GRIFFIN
LOS ALAMOS SCIENTIFIC LABORATORY,
UNIVERSITY OF CALIFORNIA, LOS ALAMOS, N. MEX.,
UNITED STATES OF AMERICA

I should like to try briefly to summarize some of what we have learned during this Symposium on the Physics and Chemistry of Nuclear Fission. "Summary" is a euphemistic term for any half-hour talk on a solid week of lectures. Actually, one can only try to give his own impressions of the conference and apologize if these seem to involve some mis-emphasis in places.

The survey will divide into three major parts, with headings as follows: (1) Specifics, (2) Energetics and (3) General Theory. By "Specifics" is ment here the growing number of phenomena related to, or discussed in terms of, Bohr's proposed fission barrier collective model and its transition state spectrum. By "Energetics" is meant that broad class of fission phenomena perhaps determined only beyond the fission barrier and about which current theory can at present say rather little of a very specific nature. The label "General Theory" is self-explanatory.

1. SPECIFICS

One unifying theme that has recurred frequently in this Symposium has been the appeal to the transition state spectrum as a means of understanding various observed effects. Perhaps 30% of the papers presented were relevant to this general subject.

For even-even transition state spectra we have seen photofission work (SM-60/81)[1] bearing on the energy difference between $(IK\pi) = (1, 1, -)$ and $(1, 0, -)$ transition states and also, I believe for the first time, on the difference between the $(1, 0, -)$ and $(2, 0, +)$ transition states. (d, pf) data gives evidence for a large energy gap between the "ground" state and two-quasiparticle states. This feature, in conjunction with uninhibited fission through resonance levels of measured spin, seems to require that collective states $(1, 1, -)$ should be lower at the fission barrier shape than at the stable shape (SM-60/4). Such low-lying vibrational states seem likely to be related to the suggestion of Blyumkina[2], cited by Fraser (SM-60/34), that such low-lying collective states in the transition spectrum are related to detailed structure observed in the fragment kinetic energies, and to the "energy gap" discussed by Strutinsky (SM-60/90) in connection with $\bar{\nu}(E)$ (SM-60/44, 46 & 77).

For odd-even nuclei, information on the transition states is beginning to accumulate. Neutron studies (SM-60/7 & /88) now give specific infor-

[1] This number refers to the numbers assigned to the papers presented in the Symposium. These numbers appear in the list of Contents after the titles of the papers.

[2] BLYUMKINA, Yu. A. et al., Nucl. Phys. 52 (1964) 648.

mation on low-lying states in several nuclei. (d, pf) experiments (SM-60/25) indicate an even richer structure.

Here, too, neutron resonance fission impinges. Data on sub-threshold fission (SM-60/15 & /19) have been cited to indicate a possible suppression of s-wave fission resulting from the nature of the low-lying transition states (SM-60/12). Super-threshold resonance fission (SM-60/13, /16 & /17) is also relevant, providing data both on relative fission barriers for different compound nuclear spins and on the channel numbers that play a role in the statistical distribution of fission widths.

In short, there appears to be growing a body of data to play the role that the odd-A ground state spin sequences filled in supporting the Nilsson model of single particle states in nuclei with quadrupole deformations. For an extension of this model to fission barrier shapes, one must expect deformations more complex than the quadrupole. Still, with sufficient data to specify the picture there seems every reason to expect that systematic predictions could be made about the low single particle states at the barrier.

For odd-odd fissioning nuclei the transition state spectrum is still almost a blank canvas. It should be noted, however, that the spontaneously fissioning isomers recently observed in the Soviet Union (SM-60/90) and at Berkeley might very well be involved with this picture. In particular, an excited state of high K-value might be able at the stable shape to exhibit a long life against gamma decay, by virtue of selection rules in the asymptotic Nilsson quantum numbers. In conjunction with a transition state spectrum in which states with high K-values lie especially low, this excited state might exhibit spontaneous fission that was very rapid compared with spontaneous fission from the ground state.

The scope of all these results should soon be expanded considerably by analysis of newly obtained data from such reactions as the (t, ph) (SM-60/21) and (α, α'f) (SM-60/3), and from new techniques for studying resonance fission of oriented nuclei (SM-60/5). One is in fact beginning to treat the transition states as a problem in spectroscopy, a problem whose challenge is not lessened by the fact that the short life of the system requires rather indirect experimentation and oblique inference to solve the problem.

Another question associated with the fission barrier is that of the "two-mode hypothesis". These words mean many things to many people, but here we use them to denote the very specific proposition that the asymmetric fission mode and symmetric fission mode are associated with distinct fission saddle points. Such a situation would suggest different angular distributions for symmetric and asymmetric fission. Several studies (SM-60/25, /39 & /80) reported here agree that such an hypothesis is not supported by the data.

Still other aspects of fission that have been tentatively associated with the transition state spectra include the mass asymmetry (SM-60/26), the fragment kinetic energies (SM-60/10, /34), the long-range alpha particles (SM-60/68, /71 & /75), and the "central neutrons" for which we have heard new evidence this week (SM-60/45). For mass asymmetry there appears to be some evidence suggestive of a correlation between specific resonances and the relative peak-to-valley mass yields. New data to verify or exclude such a connection would be most valuable. The correlation of kinetic energy with the resonance energy seems even less certain at this stage.

Each of these features has also been discussed in the past in terms of properties at the scission point. They emphasize, therefore, perhaps the most important current question concerning the transition state picture: which features of the fission process are closely related to the nature of the transition states, and which are unrelated, or related only indirectly? Only when the answer is obtained can the full weight of all the data be brought to bear reliably on the transition state problem.

2. ENERGETICS

I shall deal now with features of fission not so well embraced by current theory but which involve perhaps the greatest amount of experimental effort. The label "energetics" includes here the problems of mass and charge distribution, fragment kinetic and excitation energies, and post-barrier particle emissions.

For some time a puzzle has existed because nearly mass-symmetric fission exhibits a lower than average fragment kinetic energy. Why this is so is still an unanswered question, but some progress has been made at least on the easier question of how the total energy is released in symmetric fission.

One possibility entertained was that the most probable charges of mass-symmetric fragments might be unequal, leading to a decrease in prompt total energy release for symmetric fission. In this Symposium, however, we have seen evidence from two directions that such a drastic explanation may be unnecessary. On the one hand the number of neutrons emitted in fission is greater for mass-symmetric than for asymmetric fission (SM-60/92). More gamma radiation also appears in the symmetric case (SM-60/54). One concludes, therefore, that at least some of the "missing energy" appears as excitation energy of the fragments. On the other hand new studies (SM-60/22, /29 & /33) of fragment charge including some using X-rays for a direct determination of primary charge (SM-60/31, /57) appear to agree with earlier radiochemical results, and thereby to support the Equal Charge Displacement (ECD) hypothesis. Significant progress has, therefore, been made in determining the experimental facts to answer the missing energy question, at least in its simpler form. However, calculations based on a quasi-static scission configuration (SM-60/11) do not predict the observed ECD charge distribution, so that our "understanding" of this problem remains inadequate.

To describe the division of excitation energy between the two fragments, as indicated by the number of neutrons emitted, it appears necessary now to replace the Vladimirski-Whetstone two-spheres-plus-a-neck picture with a more flexible model. In particular, we have seen this week that the two-spheroid model, when the spheroidal stiffness is parameterized to fit the data on fragment excitation energy, provides a remarkable correlation between the stiffness of a fragment and its shell structure (SM-60/43). It, therefore, suggests a mechanism, even if a very simplified one, for incorporating shell structure into the description of fission.

A less phenomenological path to the same end is indicated by recent attempts of Swiatecki[3] to incorporate deformations and shell effects into semi-empirical mass formulas. This approach will, one hopes, ultimately allow the elimination of most of the free parameters present now in the two-spheroid description in favour of fewer parameters more closely tied to general features of nuclear structure. It might also hold the key to the successful description of mass, charge and kinetic energy distribution in nuclear fission (SM-60/22, /23, /27-/31, /33-/39, /65 & /68).

We have heard about still another feature of fission of which our present understanding is rather slight; viz. the fission alpha particles (SM-60/68, /69, /71 & /75). Dr. Halpern has, in fact, considered various particles that might be snapped out of the nucleus under the impulse of a very non-adiabatic breaking process. This viewpoint emphasizes interesting and still unresolved questions about other features of the fission process. In particular, the possibility of emitting "central neutrons" by such a process has already been discussed theoretically by Fuller[4]. The results call into question the suggested relevance of the transition state spectrum to these neutrons; they raise also a very fundamental question concerning the assumption of equilibrium underlying the two-spheroid model as currently employed: how can the scission process correspond to an equilibrium situation and still exhibit such a non-adiabatic phenomena as alpha emission?

The problem of gross ternary fission (SM-60/73) into three large fragments is one that promises to be even more complex than the problems of the neutrons and the alpha particles. Nonetheless, it is and has long been an interesting question in fission, and one on which data have been, so far, even scarcer than theory.

Finally, in this section on Energetics a few words should be said about the various delayed radiations that follow fission. These ought ultimately to be incorporated into a comprehensive theory of nuclear structure, rather than a theory of fission. Still, they sometimes allow useful inferences regarding fission itself, as in the study of β-decays in mass separated fragments to obtain the primary charge distribution (SM-60/33 & /38). Such results (SM-60/61) and similar studies of delayed neutrons (SM-60/58, /59, /74 & /84) and delayed gamma radiation (SM-60/52) are often of crucial importance in practical applications of the fission process, the most notable case being reactor physics and engineering applications. One cannot turn away from this area of energetics without an explicit recognition of the progress evident this week in experimental techniques. We have heard about many developments here which promise a flood of detailed information on fission.

In particular, the solid-state detectors (SM-60/36 & /40) are rapidly being refined into precise, as well as convenient, tools. Simultaneous velocity and energy measurements (SM-60/23, /35 & /37) now allow the number of neutrons emitted from a fragment to be measured with great ease compared with older methods. Studies of X-rays from fragments give a new method for learning about fragment charge (SM-60/31 & /57). Conversion

[3] SWIATECKI, W.J., Proc. 2nd Int. Conf. on Nuclidic Masses, Vienna (JOHNSON, W.H., Ed.), Springer-Verlag, New York (1964).

[4] FULLER, R.W., Phys. Rev. 126 (1962) 684.

electrons and nuclear gamma rays offer the possibility of detailed nuclear structure studies of fission fragments (SM-60/53). The technique of pulse weighting offers a clear means to improve gross gamma-ray data (SM-60/52 &/54). Mass separation (SM-60/33 & /36) of fragments is a powerful tool for the whole range of delayed radiation, and mica detectors have emerged as a useful means to study small cross-sections (SM-60/64). Finally, at the output stage of any experiment analysers and computers are now able to handle the data conveniently and present them to the experimenter in an appropriate format. There seems, in fact, every reason to believe that total study, fragment by individual fragment, of the whole range of radiations will be possible in the near future.

What does such a development mean for fission physics? One possible result could be a tendency for fission research to move towards a closer unity with nuclear structure studies. These fragments are, in fact, brand new nuclei to the experimental nuclear-structure physicist. It would seem natural that fission physicists who have developed these very elegant techniques might use them to extend the knowledge of nuclear structure into otherwise inaccessible areas.

For the theoretical physicist the impending deluge of data must evoke a mixed response. The theory now embraces in detail only a small fraction of the fission data already available. This situation can only become worse in the near future. Still, a leap forward in empirical knowledge must always be welcomed. There may very well be clues among the detailed data not evident in the (relatively) smooth, averaged and poorly resolved results previously available.

3. GENERAL THEORY

Finally, I would like to say a few words about the state of theory in nuclear fission. It might seem to some as though theory has been the theme throughout this discussion. In a sense this is correct: an attempt has been made to organize the review into conceptually related pieces. In a literal sense it is quite false, since there is no "theory" as yet of nuclear fission. There is a model, sometimes mis-labelled a theory; viz., the liquid drop model. It is a theory for liquid drops, but only a model for nuclear fission, and it generally is of little disturbance to the fission physicist in his assessment of data. Still, it is a very rich model, whose implications have never been adequately studied, even though serious attempts to do so are now in progress (SM-60/1 &/89).

Two main subdivisions of the liquid drop model were noted for us by Dr. Swiatecki (SM-60/1). They describe adiabatic, non-viscous liquids and statistical, viscous liquids. I should like to reiterate the point that nature, by providing a superfluid energy gap, might have allowed nuclei the opportunity to exhibit both kinds of behaviour, the one corresponding to fission through the lowest states that are isolated energetically from the more complex excited states, the other appropriate for "hotter" fission. The new data and the new techniques described this week will doubtless play a role in future examination of this question.

Less comprehensive than the liquid drop model are many other specialized models, some with a great deal of parametric freedom. These and various pictures that we use to help remember complicated data are the only practical conceptual structure currently available for most aspects of nuclear fission. They can be generalized and inter-related, in the hope that they will lead to a unified over-all understanding. But they are only models, and until they have been reinforced by theory based on physical principle, any agreement with experiment may turn out later to have been fortuitous, or (with enough parameters) even inevitable. I should, therefore, like to emphasize that one ought to be very careful not to become mesmerized by success with phenomenology. In particular, any tendency to begin to think about one or other phenomenological description as though it were actually a theory offers the risk of serious disappointment later on and in the meantime may weaken that healthy scepticism that will best promote progress towards complete understanding of the fission process.

SYMPOSIUM ON THE PHYSICS AND CHEMISTRY OF FISSION

HELD IN SALZBURG, 22-26 MARCH 1965

CHAIRMEN OF SESSIONS

Session I	R. JOLY	CEN de Saclay, Gif-sur-Yvette
Session II	N. FEATHER	University of Edinburgh
Session III	L.E. GLENDENIN	Argonne National Laboratory
Session IV	R. RAMANNA	Trombay Atomic Energy Establishment, Bombay
Session V	G. HANNA	Atomic Energy of Canada Ltd.
Session VI	N. STARFELT	AB Atomenergi, Studsvik, Nyköping
Session VII	G. RUDSTAM	CERN, Geneva
Session VIII	N.A. PERFILOV	Radium Institute W.G. Hlopin, Leningrad
Session IX	H. MAIER-LEIBNITZ	Technische Hochschule, Munich

SECRETARIAT OF THE SYMPOSIUM

Scientific Secretaries:	G.R. KEEPIN	Division of Research and Laboratories, IAEA
	G.B. COOK	Division of Research and Laboratories, IAEA
Administrative Secretary:	H.H. STORHAUG	Division of Scientific and Technical Information, IAEA
Editor:	S.M. FREEMAN	Division of Scientific and Technical Information, IAEA
Records Officer:	T.B. DUNNE	Division of Languages, IAEA

LIST OF PARTICIPANTS

Name	Institution	Nominating State or Organization
Aitzetmüller, K.	Atominstitut der Österreichischen Hochschulen, Schüttelstrasse 115, Vienna II	Austria
Alstad, J.	Department of Chemistry, University of Oslo, Oslo 3	Norway
Amiel, S.	Nuclear Chemistry Department, Soreq Nuclear Research Centre, Atomic Energy Commission, Yavne	Israel
Ammentorp-Schmidt, F.	Anorgan.-chem. Laboratorium, Technische Hochschule München, Arcisstrasse 21, 8 Munich 2	Federal Republic of Germany
Andritsopoulos, G.	Reading University, Reading, Berks.	Greece
Armbruster, P.	Kernforschungsanlage Jülich, 517 Jülich	Federal Republic of Germany
Axmann, H.P.	Österreichische Studiengesellschaft für Atomenergie, Lenaugasse 10, Vienna VIII	Austria
Bächmann, K.	Lehrstuhl für Kernchemie, Technische Hochschule, Darmstadt	Federal Republic of Germany
Ballou, N.	United States Naval Radiological Defense Laboratory, San Francisco, Calif. 94135.	United States of America
Barrachina, M.	Junta de Energia Nuclear, Madrid 3	Spain
Bemis, C.	Forskningsinstitutet for Fysik, Stockholm 50, Sweden	United States of America
Bernard, J.	CEA, B.P. No. 511, Paris XVe	France
Bertrand, F.	CEA, B.P. No.511, Paris XVe	France
Blons, J.	CEN de Saclay, B.P. No.2, Gif-sur-Yvette (Seine-et-Oise)	France

Name	Institution	Nominating State or Organization
Boldeman, J. W.	Australian Atomic Energy Commission, Research Establishment, Lucas Heights, Sydney, N. S. W.	Australia
Bowman, H. R.	Lawrence Radiation Laboratory, University of California, Berkeley, Calif.	United States of America
Brandt, R.	CERN, Geneva 23, Switzerland	CERN
Brenner, D.	Universitetets Institut for Teoretisk Fysik, Begdamsvej 17, Copenhagen Ø	Denmark
Caretto, A.	Carnegie Institute of Technology, Pittsburgh	United States of America
Carvalho, H. de	Centro Brasileiro de Pesquisas Fisicas e Commissão Nacional de Energia Nuclear, 71, Venceslau Braz, Rio de Janeiro	Brazil
Chastel, R.	Laboratoire de Physique Nucléaire, 351 Cours de la Libération, Talence (Gironde)	France
Christensen, C. S.	Danish Atomic Energy Commission, Research Establishment Risø, Roskilde	Denmark
Colvin, D.	Centre de Compilation de Données Neutroniques, B. P. 9, Gif-sur-Yvette (Seine-et-Oise)	ENEA
Condé, H.	Research Institute of National Defence, Stockholm 80	Sweden
Cortini, G.	Istituto Nazionale di Fisica Nucleare, Sezione di Napoli, Mostra d'Otromare, Padiglione 19, Naples	Italy
Cowan, G.	Los Alamos Scientific Laboratory, P.O. Box 1663, Los Alamos, N. Mex.	United States of America
Croall, I.	Atomic Energy Research Establishment, Harwell, Didcot, Berks.	United Kingdom
Dabbs, J.	Oak Ridge National Laboratory, Oak Ridge, Tenn.	United States of America
Debeauvais, M.	Centre de Recherches Nucléaires, Laboratoire de Physique Corpusculaire, Strasbourg-Cronenbourg	France

Name	Institution	Nominating State or Organization
Denschlag, H.O.	Institut für Anorganische Chemie und Kernchemie der Universität Mainz, 65 Mainz	Federal Republic of Germany
Dermendjiev, E.	Joint Institute for Nuclear Research, Dubna, USSR	Joint Institute for Nuclear Research
Deruytter, A.	Studiecentrum voor Kernenergie, Boeretang 200, Mol	Belgium
Dickmann, F.	Gesellschaft für Kernforschung mbH, P.O. Box 947, 75 Karlsruhe	Federal Republic of Germany
Droste, G. von	Physikalisch-Technische Bundesanstalt, 33 Braunschweig	Federal Republic of Germany
During, G.	Research Institute of National Defence, Stockholm 80	Sweden
Eastwood, T.A.	Atomic Energy of Canada Ltd., Chalk River, Ont.	Canada
Eccleshall, D.	United Kingdom Atomic Energy Authority, Aldermaston, Berks.	United Kingdom
Eidens, J.	Kernforschungsanlage Jülich, Institut für Neutronenphysik, Postfach 365, 517 Jülich	Federal Republic of Germany
Ekberg, K.	Division of Research and Laboratories, International Atomic Energy Agency, Vienna I	International Atomic Energy Agency
Ewald, H.	II. Physikalisches Institut der Justus Liebig-Universität, 63 Giessen	Federal Republic of Germany
Feather, N.	University of Edinburgh, Edinburgh, Scotland	United Kingdom
Ferguson, A.T.G.	United Kingdom Atomic Energy Authority, Research Group, Atomic Energy Research Establishment, Harwell, Didcot, Berks.	United Kingdom
Fiebiger, N.	Institut für Kernphysik, Am Römerhof 31, 6 Frankfurt/Main	Federal Republic of Germany
Fleck, C.M.	Atominstitut der Österreichischen Hochschulen, Schüttelstrasse 115, Vienna II	Austria

Name	Institution	Nominating State or Organization
Ford, G.	Los Alamos Scientific Laboratory, P.O. Box 1663, Los Alamos, N. Mex.	United States of America
Fraser, J.	Atomic Energy of Canada Ltd., Chalk River, Ont.	Canada
Fraysse, G.	CCR EURATOM, Ispra (Varese), Italy	EURATOM
Friedlander, G.	Brookhaven National Laboratory, Upton, Long Island, N.Y. 11973.	United States of America
Fritze, K.	McMaster University, Hamilton, Ont.	Canada
Gevantman, L.H.	United States Mission to the International Atomic Energy Agency, Schmidgasse 14, Vienna VIII	United States of America
Gibson, W.	Bell Telephone Laboratories, Murray Hill, N.J.	United States of America
Gilboy, W.B.	Gesellschaft für Kernforschung mbH, Kernforschungszentrum, Institut für Angewandte Kernphysik, 75 Karlsruhe	Federal Republic of Germany
Gindler, J.	Argonne National Laboratory, 9700 South Cass Ave., Argonne, Ill.	United States of America
Glendenin, L.E.	Argonne National Laboratory, 9700 South Cass Ave., Argonne, Ill.	United States of America
Gönnenwein, F.	Physikalisches Institut der Universität Tübingen, Gmelinstrasse 6, Tübingen	Federal Republic of Germany
Gordon, G.	Massachusetts Institute of Technology, Cambridge, Mass. 02139	United States of America
Grass, F.	Atominstitut der Österreichischen Hochschulen, Schüttelstrasse 115, Vienna II	Austria
Griffin, J.J.	Los Alamos Scientific Laboratory, P.O. Box 1663, Los Alamos, N. Mex.	United States of America
Hagebø, E.	CERN, Geneva 23, Switzerland	CERN
Halpern, I.	Physics Department, University of Washington, Seattle, Wash.	United States of America

Name	Institution	Nominating State or Organization
Hanna, G.	Atomic Energy of Canada Ltd., Chalk River, Ont.	Canada
Hecht, F.	Analytisches Institut der Universität Wien, Währingerstrasse 38, Vienna IX	Austria
Hemmings, P.J.	Authority Health and Safety Branch, United Kingdom Atomic Energy Authority, Risley, Warrington, Lancs.	United Kingdom
Herrmann, G.	Institut für Anorganische Chemie und Kernchemie, Universität Mainz, 65 Mainz	Federal Republic of Germany
Hicks, H.G.	University of California, Lawrence Radiation Laboratory, P.O. Box 808, Livermore, Calif.	United States of America
Hofmann, D.	Institut für Kernphysik, Am Römerhof 31, 6 Frankfurt/Main	Federal Republic of Germany
Hoffman, D.	Institutt for Atomenergi, Box 40, Kjeller	Norway
Hoffman, M.	Institutt for Atomenergi, Box 40, Kjeller	Norway
Hollstein, M.	Gesellschaft für Kernforschung mbH, 75 Karlsruhe	Federal Republic of Germany
Holmberg, M.	Research Institute of National Defence, Stockholm 80	Sweden
Huizenga, J.R.	Argonne National Laboratory, Argonne, Ill. At present at: Laboratoire Joliot-Curie, University of Paris, Dept. of Nuclear Physics, Orsay (Seine-et-Oise)	United States of America
Ivanov, E.	Institute of Atomic Physics, P.O.B. 35, Bucharest	Romania
James, G.D.	Atomic Energy Research Establishment, Harwell, Didcot, Berks.	United Kingdom
James, M.	United Kingdom Atomic Energy Authority, Atomic Energy Establishment, Winfrith, Dorchester, Dorset	United Kingdom
Joly, R.	CEN de Saclay, B.P. No.2, Gif-sur-Yvette (Seine-et-Oise)	France

Name	Institution	Nominating State or Organization
Józefowicz, E.T.	Institute of Nuclear Research, Swierk, near Warsaw	Poland
Kapoor, S.S.	Trombay Atomic Energy Establishment, Apollo Pier Road, Bombay 1	India
Kashukeev, N.	Institute of Physics, Bulgarian Academy of Sciences, Sofia	Bulgaria
Kiefer, W.	Institut für Anorganische Chemie und Kernchemie, Universität Mainz, 65 Mainz	Federal Republic of Germany
Kjelberg, A.	University of Oslo, Nuclear Chemistry Division, Forskningsvn 1, Blindern	Norway
Kley, W.	CCR EURATOM, Ispra (Varese), Italy	EURATOM
Konecny, E.	II. Physikalisches Institut der Justus-Liebig-Universität, Giessen	Federal Republic of Germany
Kressner, W.	Boeing International Corporation, Maximiliansplatz 12a, 8 Munich 2	United States of America
Kuzminov, B.D.	Institute of Physical Power, Obninsk	USSR
Lamphere, R.	Oak Ridge National Laboratory, P.O. Box X, Oak Ridge, Tenn.	United States of America
Leachman, R.	Los Alamos Scientific Laboratory, P.O. Box 1663, Los Alamos, N. Mex.	United States of America
Lebedev, V.I.	Kurchatov Atomic Institute, Kurchatov	USSR
Leuba, P.	CEA, B.P. No.551, Paris XVe	France
Lindsay, J.E.O.	Ghana Atomic Energy Commission, P.O. Box M.155, Accra	Ghana
Lux, F.	Institut für Radiochemie der Technischen Hochschule München, 8046 Garching	Federal Republic of Germany
Magnuson, D.W.	Division of Research and Laboratories, International Atomic Energy Agency, Vienna I	International Atomic Energy Agency

Name	Institution	Nominating State or Organization
Maier-Leibnitz, H.	Technische Hochschule, Arcisstrasse 21, 8 Munich 2	Federal Republic of Germany
Malý, J.	Nuclear Research Institute of the Czechoslovak Academy of Sciences, Řež, Prague	Czechoslovak Socialist Republic
Marchart, H.	Analytisches Institut der Universität, Währingerstrasse 38, Vienna IX	Austria
Markl, P.	Analytisches Institut der Universität, Währingerstrasse 38, Vienna IX	Austria
Marmol, P. del	CEN, Mol	Belgium
Martalogu, N.	Institute of Atomic Physics, P.O.B. 35, Bucharest	Romania
Marsel, J.	Jožef Stefan Nuclear Institute, Ljubljana	Yugoslavia
Martinot, M.	CEA, B.P. No. 511, Paris XVe	France
Maxia, V.	Laboratorio di Radiochimica dell'Istituto di Chimica Generale dell'Università di Pavia, Viale Taramelli 12, Pavia	Italy
Meister, H.	CCR EURATOM, Ispra (Varese), Italy	EURATOM
Melkonian, E.	Columbia University, Morningside Heights, New York, N.Y. 10027.	United States of America
Meyer, E., Jr.	Instituut voor Kernfysisch Onderzoek, Ooster Ringdijk 18A, Amsterdam-O	United States of America
Michaelis, W.	Gesellschaft für Kernforschung mbH, Weberstrasse 5, 75 Karlsruhe	Federal Republic of Germany
Migneco, E.	Central Bureau of Nuclear Measurements, EURATOM, Geel, Belgium	EURATOM
Milton, J.C.D.	Atomic Energy of Canada Ltd., Chalk River, Ont.	Canada
Moore, M.S.	Phillips Petroleum Co. AED, Box 2067, Idaho Falls, Idaho	United States of America
Moretto, L.	Laboratorio di Radiochimica dell'Istituto di Chimica Generale, Università di Pavia, Viale Taramelli 12, Pavia	Italy

Name	Institution	Nominating State or Organization
Mossop, A.	Reactor Group, United Kingdom Atomic Energy Authority, Windscale, Cumberland	United Kingdom
Moussa, A.	CEN de Grenoble, B.P. No. 269, Grenoble (Isère)	France
Muga, L.	University of Florida, Gainesville, Fla.	United States of America
Müller, P.	Eidg. Militärdepartement, Abt. für Sanität, ABC-Sektion, Wankdorffeldstrasse 102, 3000 Bern 22	Switzerland
Münzel, H.	Gesellschaft für Kernforschung mbH, 75 Karlsruhe	Federal Republic of Germany
Nadkarni, D.M.	Nuclear Physics Division, Trombay Atomic Energy Establishment, Apollo Pier Road, Bombay 1	India
Nagy, L.	Central Research Institute for Physics, B.P. No.49, Budapest 114	Hungary
Neeb, K.H.	Forschungslaboratorium, Siemens-Schuckertwerke AG, G. Scharowskystr. 2, 8520 Erlangen	Federal Republic of Germany
Netter, F.	CEN de Saclay, B.P. No.2, Gif-sur-Yvette (Seine-et-Oise)	France
Nève de Mevergnies, M.	CEN, Mol	Belgium
Nifenecker, H.	CEN de Saclay, B.P. No.2, Gif-sur-Yvette (Seine-et-Oise)	France
Nix, J.R.	Universitetes Institut for Teoretisk Fysik, Blegdamsvej 17, Copenhagen, Denmark	United States of America
Ouvry, F.	CEA, B.P. No.511, Paris XVe	France
Ølgaard, P.L.	Danish Atomic Energy Commission, Risø Research Establishment, Roskilde	Denmark
Patzelt, P.	Institut für Anorganische Chemie und Kernchemie der Universität Mainz, Mainz	Federal Republic of Germany

Name	Institution	Nominating State or Organization
Paya, D.	CEN de Saclay, B.P. No.2, Gif-sur-Yvette, (Seine-et-Oise)	France
Perfilov, N.A.	Radium Institute W.G. Hlopin, Leningrad	USSR
Peter, J.	Laboratoire Joliot-Curie de Physique Nucléaire, B.P. No.1, Orsay, (Seine-et-Oise)	France
Petrascu, M.	Institute of Atomic Physics, P.O.B. 35, Bucharest	Romania
Polak, P.	Instituut voor Kernfysisch Onderzoek, Ooster Ringdijk 18A, Amsterdam-O	Netherlands
Preus, G.	Bundesministerium für Wissenschaftliche Forschung, Luisenstrasse 42, Bad Godesberg	Federal Republic of Germany
Prosdocimi, A.	Association EURATOM - CEA, CEN-Cadarache, B.P. 1, St. Paul-lez-Durance (B. du Rh.)	EURATOM
Pushkov, A.	Division of Nuclear Power and Reactors, International Atomic Energy Agency, Vienna I	International Atomic Energy Agency
Rae, E.R.	Atomic Energy Research Establishment, Harwell, Didcot, Berks.	United Kingdom
Ramanna, R.	Trombay Atomic Energy Establishment, Apollo Pier Road, Bombay 1	India
Ribon, P.	CEN de Saclay, B.P. No.2, Gif-sur-Yvette, (Seine-et-Oise)	France
Ripka, G.	CEN de Saclay, B.P. No.2, Gif-sur-Yvette, (Seine-et-Oise)	France
Rodgers, A.	United Kingdom Atomic Energy Authority, Atomic Weapons Research Establishment, Aldermaston, Berks.	United Kingdom
Roeckl, E.	Kernforschungsanlage Jülich, Institut für Neutronenphysik, Postfach 365, 517 Jülich	Federal Republic of Germany

Name	Institution	Nominating State or Organization
Rohde, G.	Gesellschaft für Kernforschung mbH, 75 Karlsruhe	Federal Republic of Germany
Röper, P.	Institut für Theoretische Physik, Robert-Mayer Str. 6-8, Frankfurt am Main	Federal Republic of Germany
Rudstam, G.	CERN, Geneva 23, Switzerland	CERN
Ryabov, U.V.	Joint Institute for Nuclear Research, Dubna, USSR	Joint Institute for Nuclear Research
Samour, C.	CEN de Saclay, B.P. No.2, Gif-sur-Yvette, (Seine-et-Oise)	France
Sanatani, S.	Division of Nuclear Power and Reactors, International Atomic Energy Agency, Vienna I	International Atomic Energy Agency
Schett, A.	Institut für Theoretische Physik, Innsbruck University, Innsbruck	Austria
Schneeberger, M.	Österreichische Studiengesellschaft für Atomenergie, Lenaugasse 10, Vienna VIII	Austria
Scobie, J.	Scottish Research Reactor Centre, East Kilbride, Scotland	United Kingdom
Segre, G.	CNEN, Via Belisario 15, Rome	Italy
Sekyim-Kwandoh, A.	Ghana Atomic Energy Commission, P.O. Box M.155, Accra	Ghana
Seligman, H.	Deputy Director General, Department of Research and Isotopes, International Atomic Energy Agency, Vienna I	International Atomic Energy Agency
Signarbieux, C.	CEN de Saclay, B.P. No.2, Gif-sur-Yvette, (Seine-et-Oise)	France
Silva, A.G. da	Instituto de Engenharia Nuclear, Ilhado Fundão, Rio de Janeiro	Brazil
Simonoff, G.N.	Laboratoire de Physique Nucléaire, Faculté des Sciences de Bordeaux, Talence (Gironde)	France
Smulek, W.	Institute of Nuclear Research, Swierk, near Warsaw	Poland

Name	Institution	Nominating State or Organization
Soleilhac, M.	CEA, B.P. No. 511, Paris XVe	France
Sowerby, M.	Atomic Energy Research Establishment, Harwell, Didcot, Berks.	United Kingdom
Sowinski, M.	Institute of Nuclear Research, Swierk, near Warsaw	Poland
Sørensen, G.	Physical Institute, University of Aarhus, Aarhus	Denmark
Specht, H.J.	Physik-Department, Teilinstitut Maier-Leibnitz, Technische Hochschule München, Arcisstrasse 21, 8 Munich 2	Federal Republic of Germany
Starfelt, N.	AB Atomenergi, Studsvik, Nyöping	Sweden
Stein, W.	Los Alamos Scientific Laboratory, P.O. Box 1663, Los Alamos, N. Mex.	Federal Republic of Germany
Stephan, C.	Laboratoire Joliot-Curie de Physique Nucléaire, B.P. No. 1, Orsay, (Seine-et-Oise)	France
Stephan, H.	Staatliche Akademie für angewandte Technik, Kesslerstr. 40, 85 Nürnberg	Federal Republic of Germany
Švec, K.	Nuclear Research Institute of the Czechoslovak Academy of Sciences, Řež, Prague	Czechoslovak Socialist Republic
Swiatecki, W.	University of California, Lawrence Radiation Laboratory, Berkeley, Calif.	United States of America
Talât-Erben, M.	Cekmece Nuclear Research and Training Centre, P.O. Box 1, Airport, Istanbul	Turkey
Tchernilin, Y.	Division of Nuclear Power and Reactors, International Atomic Energy Agency, Vienna I	International Atomic Energy Agency
Tépel, J.	South African Atomic Energy Board, Private Bag 256, Pretoria	Republic of South Africa
Terrell, J.	Los Alamos Scientific Laboratory, P.O. Box 1663, Los Alamos, N. Mex.	United States of America
Theobald, J.	Bureau Central de Mesures Nucléaires, Geel, Belgium	EURATOM

Name	Institution	Nominating State or Organization
Thomas, T.D.	Princeton University, Princeton, N.J.	United States of America
Tomlinson, L.	Atomic Energy Research Establishment, Harwell, Didcot, Berks.	United Kingdom
Tornau, R.	INTERATOM, Friedrich Ebert-Str., Bensberg bei Köln	Federal Republic of Germany
Ujlaki, E.	Universität Wien, Vienna IX	Austria
Valentin, M.	CEA, B.P. No.511, Paris XVe	France
Vallis, D.	Atomic Weapons Research Establishment, Aldermaston, Berks.	United Kingdom
Vandenbosch, R.	Chemistry Department, University of Washington, Seattle, Wash.	United States of America
Wagner, S.	Physikalisch-Technische Bundesanstalt, Bundesallee 100, 33 Braunschweig	Federal Republic of Germany
Wahl, A.	Washington Univeristy, St. Louis, Missouri 63130	United States of America
Wahsweiler, H.G.	Institut für Theoretische Physik der Universität, Gartenstrasse 47, 74 Tübingen	Federal Republic of Germany
Weber, M.	Institut für Anorganische Chemie und Kernchemie Mainz, Johann-Joachim-Becker Weg 24, Mainz	Federal Republic of Germany,
Weinzierl, P.	Österreichische Studiengesellschaft für Atomenergie, Lenaugasse 10, Vienna VIII	Austria
Westcott, C.	Division of Research and Laboratories, International Atomic Energy Agency, Vienna I	International Atomic Energy Agency
Westgaard, L.	Universitetets Institut for Teoretisk Fysik, Begdamsvej 17, Copenhagen Ø	Denmark
White, P.	Atomic Weapons Research Establishment, Aldermaston, Berks.	United Kingdom
Wilson, H.W.	Scottish Research Reactor Centre, East Kilbride, Scotland	United Kingdom

Name	Institution	Nominating State or Organization
Wołczek, O.	Institute of Nuclear Research, Swierk, near Warsaw	Poland
Wolf, G.	Lehrstuhl für Radiochemie der Universität Heidelberg, Heidelberg	Federal Republic of Germany
Wölfli, W.	Laboratorium für Kernphysik ETH, Gloriastrasse 35, 8007 Zürich	Switzerland
Wyttenbach, A.	Eidg. Institut für Reaktorforschung, Würenlingen	Switzerland
Yaffe, L.	Director, Division of Research and Laboratories, International Atomic Energy Agency, Vienna 1	International Atomic Energy Agency
Zvára, I.	Joint Institute for Nuclear Research, Dubna, USSR	Joint Institute for Nuclear Research

AUTHOR INDEX

(Including Participants in Discussions)

Roman numerals are volume numbers.
Arabic numerals underlined refer to the first page of a paper by the author concerned.
Other Arabic numerals denote the page numbers of discussion comments.
Literature references are not indexed.

Aiyer, R.N.: I 85
Alves, R.N.: II 343
Amiel, S.: II 171, 221
Andritsopoulos, G.: I 481
Apalin, V.F.: I 587
Aras, N.K.: II 73
Armbruster, P.: I 103, 119, 480; II 54, 113, 143, 170
Atneosen, R.A.: I 385
Ballou, N.E.: I 423
Bayhurst, B.P.: I 347
Bemis, C.: II 221, 241
Benedict, G.: II 197
Blons, J.: I 205, 217
Boldeman, J.W.: II 103
Bowman, H.R.: II 125, 169
Bösch, R.: II 343
Brandt, R.: II 329
Brenner, D.: I 314
Carvalho, H. de: II 315, 343
Colvin, D.W.: II 25
Condé, H.: II 57, 93
Cornell, T.: I 481; II 67
Cortini, G.: II 316
Cowan, G.: I 305, 347, 367
Croall, I.F.: I 355
Dabbs, J.W.T.: I 39, 517, 528, 529, 545
Debeauvais, M.: II 316
Dermendzhiev, E.: I 287
Deruytter, A.J.: II 429
Dubrovina, S.M.: I 157
During, G.: II 93
Dyachenko, P.P.: I 601
Eccleshall, D.: I 77
Eckhardt, W.: II 197
Ewald, H.: I 505
Feather, N.: I 399, 545; II 387
Ferguson, A.T.G.: I 281, 633; II 102
Fiedler, J.: I 197
Flerov, G.N.: I 307
Ford, G.P.: I 333
Fraser, J.S.: I 451; II 39, 109
Fraysse, G.: I 255, 280, 633
Friedlander, G.: II 265, 315 428
Geilikman, B.T.: I 121
Gibson, W.M.: I 385, 465, 531, 545-6, 609-10; II 169
Gilmore, J.S.: I 347
Glendenin, L.E.: I 369; II 169, 170
Gordon, G.E.: I 368, 528; II 73
Göbel, H.: I 401
Graff, G.: II 163
Griffin, H.C.: I 369
Griffin, J.J.: I 23, 37, 76, 218, 559; II 447
Gritsyuk, Yu.N.: I 587
Gunten, H.R. von: I 415
Gursky, J.: I 51
Halpern, I.: II 369, 385
Günther, H.: I 401
Hanna, G.C.: I 621, 632-3; II 37
Hattangadi, V.A.: II 397
Herrmann, G.: II 54-5, 197, 221-2, 243
Hollstein, M.: I 573

Holmberg, M.: I 57
Huizenga, J.R.: I 11, 37, 38, 61, 529, 547
Ishimori, T.: I 573
Ivanov, E.: I 307, 314
Iyer, R.S.: I 439
Jain, H.C.: I 439
James, G.D.: I 217, 235
Joly, R.: I 37
Jousseaume, C.: I 205
Kapitsa, S.P.: I 135
Kapoor, S.S.: I 37, 119, 480, 529, 559; II 23, 54, 125, 170
Keepin, G.R.: II 222-3
Knobeloch, G.W.: I 347
Konecny, E.: I 401, 489, 505
Konshin, V.A.: II 349
Krutikov, I.E.: I 587
Kuzminov, B.D.: I 559, 601, 611
Kvitek, I.: II 439
Lajtai, A.: II 163
Lamphere, R.W.: I 63, 76
Leachman, R.B.: I 51, 61, 333
Lebedev, V.I.: I 76, 587, 598, 599; II 91
Luthardt, G.: II 197
Maier-Leibnitz, H.: II 113, 143, 169
Maksyutenko, B.P.: II 215
Marmol, P. del: II 221, 225
Martalogu, N.: I 307, 314
Maslin, E.E.: II 67
Matusevich, E.S.: II 349
Maurette, M.: II 307
Mehta, G.K.: II 355
Melkonian, E.: II 355
Methasiri, T.: II 397
Michaudon, A.: I 205
Mikaelyan, L.A.: I 587
Miller, L.G.: I 87
Miller, P.D.: I 517
Milton, J.C.D.: I 465, 479-80, 598; II 39, 53, 54, 55
Moore, M.S.: I 87, 101, 279, 304, 367, 559; II 24, 169
Mossop, A.: I 367, 465; II 109, 262
Muga, M.L.: II 409, 428
Münzel, H.: I 573, 586
Nadkarni, D.M.: I 480, II 397, 407
Nagy, L.: II 163, 169
Namboodiri, M.N.: I 439
Neiler, J.H.: I 531
Netter, F.: I 529; II 407
Nève de Mevergnies, M.: I 101, 217, 314; II 23, 225, 385, 429
Nifenecker, H.: I 86, 218, 245, 253
Nix, J.R.: II 315
Opower, H.: I 401, 505
Otroshchenko, G.A.: I 157
Parker, G.W.: I 39
Patzelt, P.: II 197, 243
Pavlinchuk, V.A.: I 127
Perfilov, N.A.: II 283, 315
Perlman, M.L.: I 385
Perrin, G.: I 245
Petrascu, M.: I 84, 279, 632; II 23, 317-22
Pleve, A.A.: I 307
Poenaru, D.: I 307
Polikanov, S.M.: I 307
Popov, Yu.P.: II 439
Pranal, Y.: I 205
Prestwood, R.S.: I 347
Prosdocimi, A.: I 255, 279, 280
Rabotnov, N.S.: I 135
Rae, E.R.: I 37, 187, 217, 218, 305
Rajkishore, M.R.: I 439
Ramaniah, M.V.: I 439, 558
Ramanna, R.: I 85, 86; II 54, 397
Rao, C.L.: I 439
Rao, P.N. Rama: I 397
Rasmussen, J.O.: II 125
Ravindran, N.: I 439
Regchshevsky, V.I.: II 349
Ribon, P.: I 305; II 446
Ribrag, M.: I 561

Ripka, G.: I 560
Rodgers, A.L.: I 481; II 67
Rudstam, G.: II 323
Ryabov, U.V.: I 217-8, 253, 287, 304, 305, 633; II 24, 439
Safford, G.J.: I 467
Saussure, G. de: I 205
Schmitt, H.W.: I 517, 531; II 143
Schüssler, H.D.: II 197
Sergachev, A.I.: I 611
Seyfarth, H.: II 253
Sharma, H.D.: I 439
Shi-di, Van: I 287
Shigin, V.A.: I 157
Signarbieux, C.: I 561
Silva, A.G. da: II 343
Simonoff, G.: I 585-6
Smirenkin, G.N.: I 135
Soldatov, A.S.: I 135
Sowerby, M.G.: II 25, 37
Sowinski, M.: I 545, 546; II 316-7, 385
Specht, H.J.: II 113, 253, 262
Speecke, A.: II 225
Starfelt, N.: I 281
Stein, W.E.: I 491; II 23
Stephan, C.: II 307, 316
Strutinsky, V.M.: I 127, 171
Subramanian, R.: I 85
Swiatecki, W.J.: I 3; II 169, 316
Tâlât-Erben, M.: I 368
Terrell, J.: I 599; II 3, 23, 24, 53
Thomas, T.D.: I 385, 399, 467, 480, 531, 598, 609; II 92, 169-70
Thompson, S.G.: II 125
Tomlinson, L.: II 233, 241
Tsipenyuk, Yu.M.: I 135
Unik, J.P.: I 11, 369, 547
Usachov, L.N.: I 135
Vandenbosch, R.: I 37-8, 399, 547, 558, 559, 560, 598
Vîlcov, N.: I 307
Vorotnikov, P.E.: I 157
Vroey, M. de: I 281
Wahl, A.C.: I 317
Walter, F.J.: I 39, 531
Watson, R.L.: II 125
Weiss, H.V.: I 423
Westcott, C.H.: I 279
White, P.: I 633
Wilkins, B.D.: I 11
Willis, H.H.: I 355
Wölfli, W.: II 343
Wyttenbach, A.: I 415
Yaffe, L.: II 261-2
Yates, M.J.L.: I 77
Yun-chan, Van: I 287

IAEA SALES AGENTS

Orders for Agency publications can be placed with your bookseller or any of our sales agents listed below:

ARGENTINA
Comisión Nacional de
Energía Atómica
Avenida del Libertador
General San Martin 8250
Buenos Aires - Suc. 29

AUSTRALIA
Hunter Publications,
23 McKillop Street
Melbourne, C.1

AUSTRIA
Georg Fromme & Co.
Spengergasse 39
Vienna V

BELGIUM
Office international de librairie
30, avenue Marnix
Brussels 5

BRAZIL
Livraria Kosmos Editora
Rua do Rosario, 135-137
Rio de Janeiro

Agencia Expoente Oscar M. Silva
Rua Xavier de Toledo, 140-1° Andar
(Caixa Postal No. 5.614)
São Paulo

BYELORUSSIAN SOVIET SOCIALIST REPUBLIC
See under USSR

CANADA
The Queen's Printer
Ottawa, Ontario

CHINA (Taiwan)
Books and Scientific Supplies
Service, Ltd.,
P.O. Box 83
Taipei

DENMARK
Ejnar Munjsgaard Ltd.
6 Nörregade
Copenhagen K

FINLAND
Akateeminen Kirjakauppa
Keskuskatu 2
Helsinki

FRANCE
Office international de
documentation et librairie
48, rue Gay-Lussac
Paris 5e

GERMANY, Federal Republic of
R. Oldenbourg
Rosenheimer Strasse 145
8 Munich 8

ISRAEL
Heiliger and Co.
3 Nathan Strauss Street
Jerusalem

ITALY
Agenzia Editoriale Internazionale
Organizzazioni Universali (A.E.I.O.U.)
Via Meravigli 16
Milan

JAPAN
Maruzen Company Ltd.
6, Tori Nichome
Nihonbashi
(P.O. Box 605)
Tokyo Central

MEXICO
Libraria Internacional
Av. Sonora 206
Mexico 11, D.F.

NETHERLANDS
N.V. Martinus Nijhoff
Lange Voorhout 9
The Hague

NEW ZEALAND
Whitcombe & Tombs, Ltd.
G.P.O. Box 1894
Wellington, C.1

NORWAY
Johan Grundt Tanum
Karl Johans gate 43
Oslo

PAKISTAN
Karachi Education Society
Haroon Chambers
South Napier Road
(P.O. Box No. 4866)
Karachi 2

POLAND
Ośrodek Rozpowszechniana
Wydawnictw Naukowych
Polska Akademia Nauk
Pałac Kultury i Nauki
Warsaw

SOUTH AFRICA
Van Schaik's Bookstore (Pty) Ltd.
Libri Building
Church Street
(P.O. Box 724)
Pretoria

SPAIN
Librería Bosch
Ronda de la Universidad 11
Barcelona

SWEDEN
C.E. Fritzes Kungl. Hovbokhandel
Fredsgatan 2
Stockholm 16

SWITZERLAND
Librairie Payot
Rue Grenus 6
1211 Geneva 11

TURKEY
Librairie Hachette
469, Istiklâl Caddesi
Beyoğlu, Istanbul

UKRAINIAN SOVIET SOCIALIST REPUBLIC
See under USSR

UNION OF SOVIET SOCIALIST REPUBLICS
Mezhdunarodnaya Kniga
Smolenskaya-Sennaya 32-34
Moscow G-200

UNITED KINGDOM OF GREAT BRITAIN AND NORTHERN IRELAND
Her Majesty's Stationery Office
P.O. Box 569
London, S.E.1

UNITED STATES OF AMERICA
National Agency for
International Publications, Inc.
317 East 34th Street
New York, N.Y. 10016

VENEZUELA
Sr. Braulio Gabriel Chacares
Gobernador a Candilito 37
Santa Rosalía
(Apartado Postal 8092)
Caracas D.F.

YUGOSLAVIA
Jugoslovenska Knjiga
Terazije 27
Belgrade

IAEA publications can also be purchased retail at the United Nations Bookshop at United Nations Headquarters, New York, at the news-stand at the Agency's Headquarters, Vienna, and at most conferences, symposia and seminars organized by the Agency.

In order to facilitate the distribution of its publications, the Agency is prepared to accept payment in UNESCO coupons or in local currencies.

Orders and inquiries from countries where sales agents have not yet been appointed may be sent to:

Distribution and Sales Unit, International Atomic Energy Agency,
Kärntner Ring 11, Vienna I, Austria

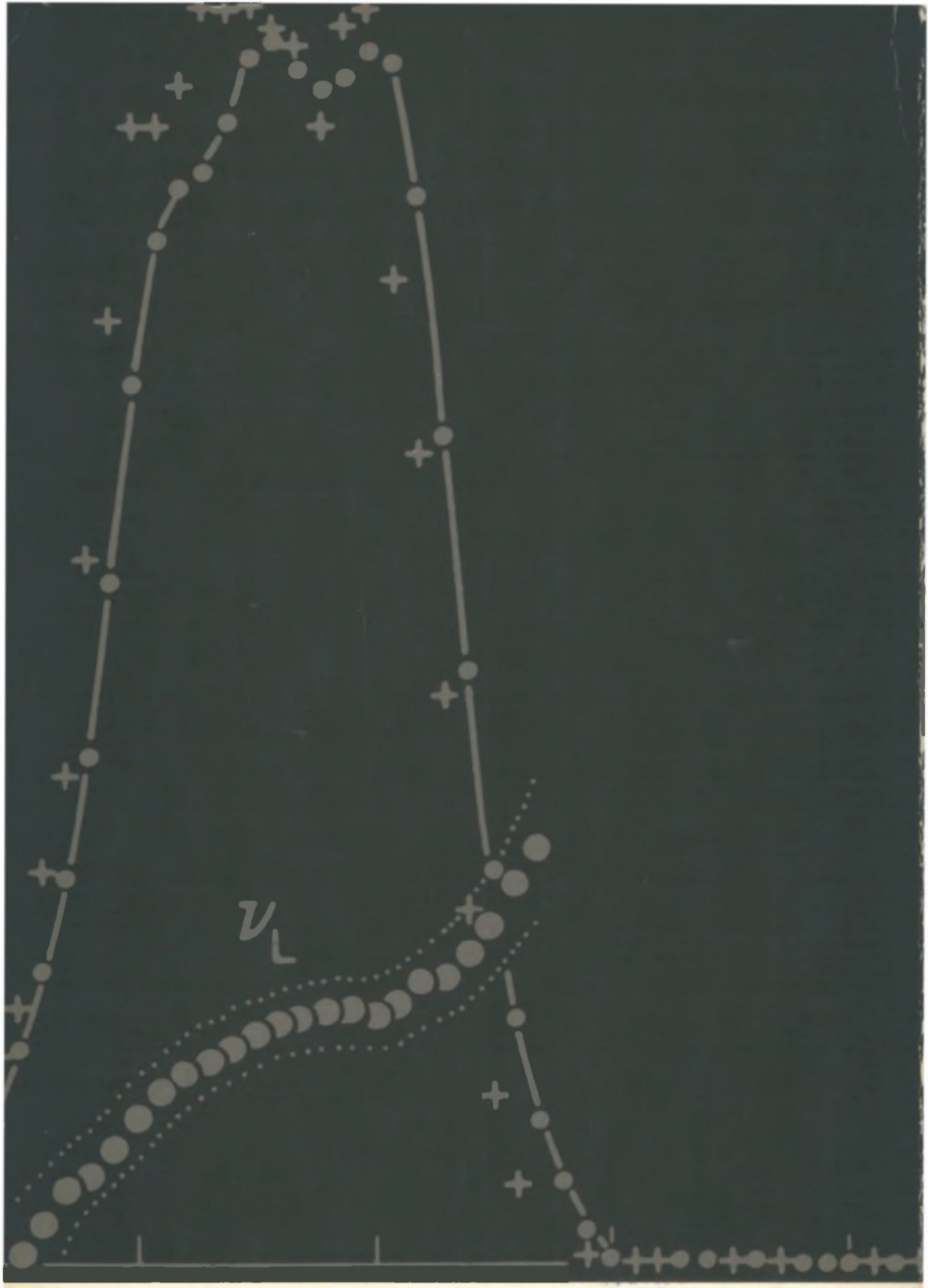

INTERNATIONAL
ATOMIC ENERGY AGENCY,
VIENNA, 1965

PRICE: USA and Canada: US $10.00
Austria and elsewhere: S 210,-
(£3.0.0; F.Fr. 40,-; DM 35,-)